CORALLINE ALGAE: GLOBALLY DISTRIBUTED ECOSYSTEM ENGINEERS

EDITED BY: Laurie Carol Hofmann, Nick Kamenos, João Silva, Nadine Schubert, Paulo Antunes Horta, Julio Aguirre and Kathryn Schoenrock

PUBLISHED IN: Frontiers in Marine Science and Frontiers in Plant Science

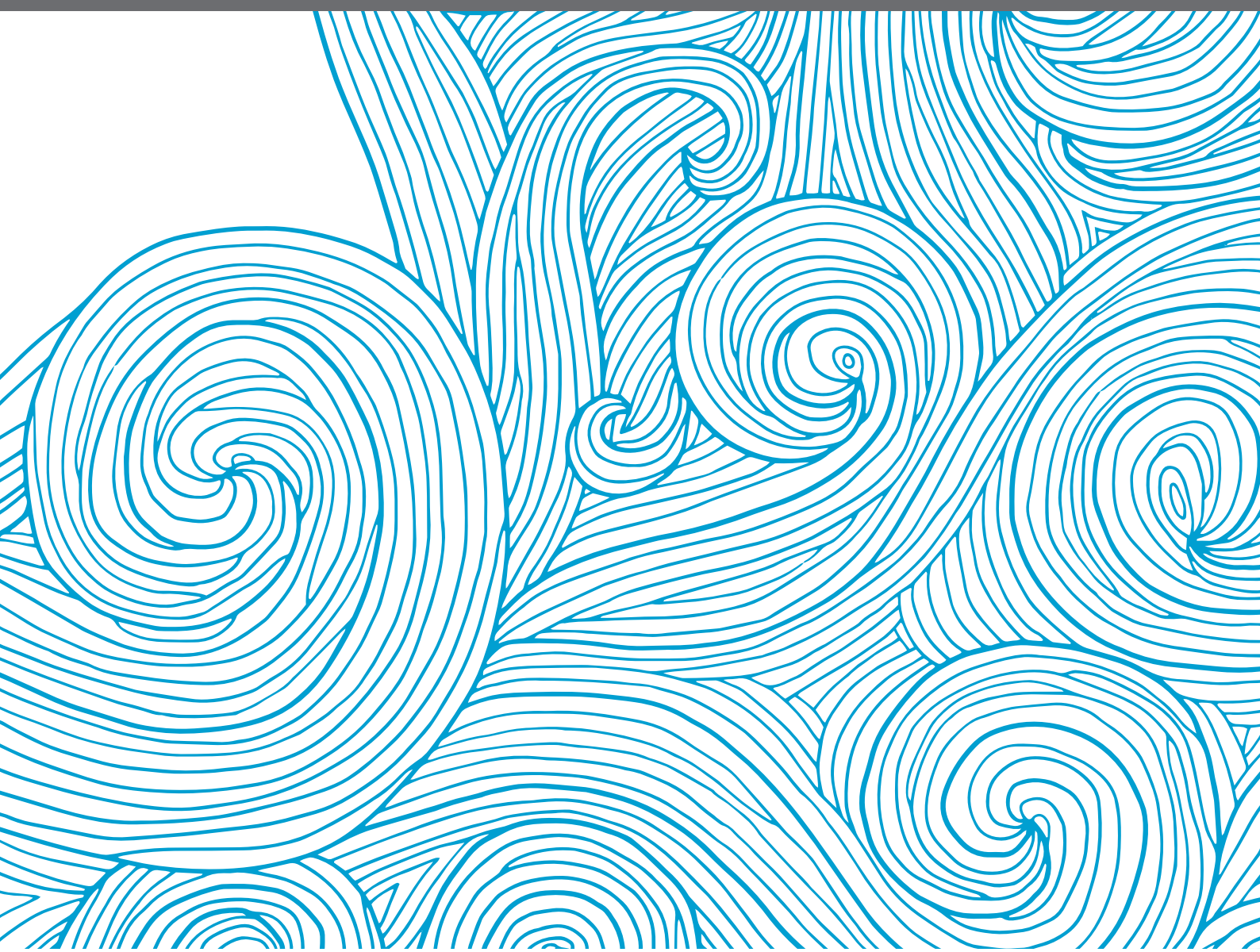

frontiers Research Topics

frontiers

Frontiers eBook Copyright Statement

The copyright in the text of individual articles in this eBook is the property of their respective authors or their respective institutions or funders. The copyright in graphics and images within each article may be subject to copyright of other parties. In both cases this is subject to a license granted to Frontiers.

The compilation of articles constituting this eBook is the property of Frontiers.

Each article within this eBook, and the eBook itself, are published under the most recent version of the Creative Commons CC-BY licence. The version current at the date of publication of this eBook is CC-BY 4.0. If the CC-BY licence is updated, the licence granted by Frontiers is automatically updated to the new version.

When exercising any right under the CC-BY licence, Frontiers must be attributed as the original publisher of the article or eBook, as applicable.

Authors have the responsibility of ensuring that any graphics or other materials which are the property of others may be included in the CC-BY licence, but this should be checked before relying on the CC-BY licence to reproduce those materials. Any copyright notices relating to those materials must be complied with.

Copyright and source acknowledgement notices may not be removed and must be displayed in any copy, derivative work or partial copy which includes the elements in question.

All copyright, and all rights therein, are protected by national and international copyright laws. The above represents a summary only. For further information please read Frontiers' Conditions for Website Use and Copyright Statement, and the applicable CC-BY licence.

ISSN 1664-8714
ISBN 978-2-88963-831-4
DOI 10.3389/978-2-88963-831-4

About Frontiers

Frontiers is more than just an open-access publisher of scholarly articles: it is a pioneering approach to the world of academia, radically improving the way scholarly research is managed. The grand vision of Frontiers is a world where all people have an equal opportunity to seek, share and generate knowledge. Frontiers provides immediate and permanent online open access to all its publications, but this alone is not enough to realize our grand goals.

Frontiers Journal Series

The Frontiers Journal Series is a multi-tier and interdisciplinary set of open-access, online journals, promising a paradigm shift from the current review, selection and dissemination processes in academic publishing. All Frontiers journals are driven by researchers for researchers; therefore, they constitute a service to the scholarly community. At the same time, the Frontiers Journal Series operates on a revolutionary invention, the tiered publishing system, initially addressing specific communities of scholars, and gradually climbing up to broader public understanding, thus serving the interests of the lay society, too.

Dedication to Quality

Each Frontiers article is a landmark of the highest quality, thanks to genuinely collaborative interactions between authors and review editors, who include some of the world's best academicians. Research must be certified by peers before entering a stream of knowledge that may eventually reach the public - and shape society; therefore, Frontiers only applies the most rigorous and unbiased reviews.
Frontiers revolutionizes research publishing by freely delivering the most outstanding research, evaluated with no bias from both the academic and social point of view. By applying the most advanced information technologies, Frontiers is catapulting scholarly publishing into a new generation.

What are Frontiers Research Topics?

Frontiers Research Topics are very popular trademarks of the Frontiers Journals Series: they are collections of at least ten articles, all centered on a particular subject. With their unique mix of varied contributions from Original Research to Review Articles, Frontiers Research Topics unify the most influential researchers, the latest key findings and historical advances in a hot research area! Find out more on how to host your own Frontiers Research Topic or contribute to one as an author by contacting the Frontiers Editorial Office: researchtopics@frontiersin.org

CORALLINE ALGAE: GLOBALLY DISTRIBUTED ECOSYSTEM ENGINEERS

Topic Editors:
Laurie Carol Hofmann, Alfred Wegener Institute Helmholtz Centre for Polar and Marine Research (AWI), Germany
Nick Kamenos, University of Glasgow, United Kingdom
João Silva, University of Algarve, Portugal
Nadine Schubert, University of Algarve, Portugal
Paulo Antunes Horta, Federal University of Santa Catarina, Brazil
Julio Aguirre, University of Granada, Spain
Kathryn Schoenrock, National University of Ireland Galway, Ireland

Citation: Hofmann, L. C., Kamenos, N., Silva, J., Schubert, N., Horta, P. A., Aguirre, J., Schoenrock, K., eds. (2020). Coralline Algae: Globally Distributed Ecosystem Engineers. Lausanne: Frontiers Media SA.
doi: 10.3389/978-2-88963-831-4

Table of Contents

frontiers in Marine Science

EDITORIAL
published: 25 May 2020
doi: 10.3389/fmars.2020.00352

Editorial: Coralline Algae: Globally Distributed Ecosystem Engineers

Nadine Schubert[1], Kathryn M. Schoenrock[2], Julio Aguirre[3], Nicholas A. Kamenos[4], João Silva[1], Paulo A. Horta[5] and Laurie C. Hofmann[6]*

[1] Centre of Marine Sciences, University of Algarve, Faro, Portugal, [2] Department of Zoology, National University of Ireland Galway, Ryan Institute, Galway, Ireland, [3] Department of Stratigraphy and Paleontology, University of Granada, Granada, Spain, [4] School of Geographical and Earth Sciences, University of Glasgow, Glasgow, United Kingdom, [5] Department of Botany, Federal University of Santa Catarina, Florianópolis, Brazil, [6] Alfred Wegener Institute Helmholtz Center for Polar and Marine Research, Bremerhaven, Germany

Keywords: biodiversity, calcification, climate change, coralline algae, genetic and genotypic diversity, photosynthesis

Editorial on the Research Topic

Coralline Algae: Globally Distributed Ecosystem Engineers

From the early days of phycology, coralline algae (CA) have been considered the most formidable and widely distributed algae (Woelkerling, 1988). They compose an abundant and highly diverse group, divided into geniculate (articulated) and non-geniculate species (crusts and rhodolith/maërl forms). CA are present in almost every coastal ecosystem around the world, from the intertidal to mesophotic zones (Johansen et al., 1981; Steneck, 1986; Foster, 2001). They are important ecosystem engineers that provide hard, three-dimensional substrates for a highly diverse fauna and flora (Nelson, 2009), building habitats like the globally distributed rhodolith (or maërl) beds (Foster, 2001), and the large algal bioconstructions that abound in the Mediterranean (coralligenous assemblages, intertidal rims; Ingrosso et al., 2018). In addition, the $CaCO_3$ precipitation within cell walls leads to a high fossilization potential of CA, which are considered the best fossil record among macrobenthic autotrophs since they first appeared in the Lower Cretaceous (Aguirre et al., 2000). It also makes CA major carbonate producers (van der Heijden and Kamenos, 2015), which, considering their abundance and wide distribution, gives them an important role in oceanic carbon cycling and reef building (Adey, 1998; Chisholm, 2003; Martin et al., 2006; Perry et al., 2008) and makes them a group of significant economic interest (Coletti and Frixa, 2017). Like many other marine ecosystems, CA habitats will be negatively affected by future climate change, e.g., due to reduced CA calcification/growth (Martin and Hall-Spencer, 2017; Cornwall et al., 2019) that may eventually lead to ecosystem degradation and reduction of habitat complexity and biodiversity.

Despite the importance of CA and their susceptibility to climate change, the knowledge about these algae is still limited. The nine research articles and one review article in this Research Topic contribute to broadening our understanding of CA across many themes. Genetic variation and reproductive strategy of the European rhodolith species *Phymatolithon calcareum* was studied by Pardo et al. at large to small scales across 15 sites in the North Atlantic, showing that (i) the rhodolith beds are dominated by tetrasporophytes, potentially due to stability of the habitat, and (ii) that these populations exhibit little sexual recombination (few gametophytes) and low dispersal resulting in high genetic structure. Pardo et al. note that the presence of triploid thalli in Northern regions may further explain the wide distribution of this species in Europe.

In the Gulf of Mexico, rhodolith beds represent a vital macroalgal spore repository that may aid in community recovery after environmental disturbance. In this context, Fredericq et al. describe the endolithic phototrophic diversity of rhodoliths, expanding upon original descriptions

OPEN ACCESS

Edited and reviewed by:
Angel Borja, Technological Center Expert in Marine and Food Innovation (AZTI), Spain

****Correspondence:***
Nadine Schubert
nadine_schubert@hotmail.com

Specialty section:
This article was submitted to Marine Ecosystem Ecology, a section of the journal Frontiers in Marine Science

Received: *11 April 2020*
Accepted: *27 April 2020*
Published: *25 May 2020*

Citation:
Schubert N, Schoenrock KM, Aguirre J, Kamenos NA, Silva J, Horta PA and Hofmann LC (2020) Editorial: Coralline Algae: Globally Distributed Ecosystem Engineers. Front. Mar. Sci. 7:352. doi: 10.3389/fmars.2020.00352

of endolithic dinoflagellates and haptophytes (Krayesky-Self et al., 2017). The study validates the microscopic identification of algal and fungal cells within rhodolith skeletons and might set to rest the previous debate regarding their cell entry that apparently occurs through tetrasporangial compartments in the sloughing species *Sporolithon sinusmexicanum*.

Adding to our understanding about the ecological importance of CA, Rindi et al. review CA research in the Mediterranean, beginning with early records and taxonomy, highlighting the importance of these species in geological records and ecosystem functions, and culminating in threats Mediterranean CA face due to climate change. This thorough review identifies knowledge gaps in different fields that should be approached by interdisciplinary research teams spanning the Mediterranean. Regarding the economic importance of CA, Magill et al. experimentally assessed *Corallina officinalis* turf and species assemblage recovery after canopy removal, finding that higher growth rates and sediment accumulation in harvested turfs facilitate a full community recovery within 4–6 months post-harvest.

Studies on CA combining ecological and physiological aspects are increasingly used to understand the prevalence and dominance of certain CA species in specific habitats, but also to infer about their potential responses to climate change. In this context, Tâmega and Figueiredo examine the role of two tropical crustose CA in early colonization and compare their growth and physiological response to irradiance levels in different reef habitats and sites. While the CA are abundant in mature reef communities, they are not among early colonizers, and the higher growth and productivity rates of *Porolithon onkodes* under high irradiance in the reef environment seems to be the driving force behind the species' competitive advantage over *Lithophyllum stictaeforme*. In another study, Sordo et al. assess the effects of seasonal light and temperature variability on the physiology and hence, productivity of the rhodolith *Phymatolithon lusitanicum* in a temperate rhodolith bed, also showing that this species exhibits a high sensitivity to temperature-related climate change scenarios.

At a different scale, the microsensor study of Hofmann et al. gives new mechanistic insights into a strong biological control of Arctic CA over the calcification process, particularly in the dark, which may be a determining factor for predicting their responses to climate change, i.e., ocean acidification (OA). In this context, there is a growing body of evidence on the sensitivity of adult and early life history stages of CA to OA (Martin and Hall-Spencer, 2017), to which the study of Ordoñez et al. contributes by showing that while OA conditions potentially enhance photosynthesis and respiration, they also reduce growth of *Porolithon onkodes* recruits. On the other hand, Johnson et al. report that calcification, but not photosynthetic efficiency of the adult tropical crustose CA *Lithophyllum congestum* is negatively affected by OA, with more pronounced impacts under fluctuating pH regimes. Reduced growth of a CA under OA conditions when combined with increased temperature is also demonstrated by Marchini et al. in the articulated intertidal *Ellisolandia elongata*, a negative effect that is accompanied by shifts from a rich and diverse mobile associated fauna to a more simplified and depauperate community.

In summary, research efforts on CA like those in this special issue should be fostered, as the acceleration of environmental crises related to climate change, widespread coastal pollution, and growing ocean overexploitation represent current and future threats to these organisms and associated ecosystems. Specifically, research should capitalize on increasing our understanding of CA responses to environmental changes and the development of alternative tools to mitigate these impacts.

AUTHOR CONTRIBUTIONS

The editorial was written by NS and KS and edited by JA, NK, JS, PH, and LH.

FUNDING

NS was funded by the European Union's Horizon 2020 research and innovation programme under the Marie Sklodowska-Curie grant agreement (No. 844703). KS was funded by the Environmental Protection Agency in Ireland, and the EU Joint Programming Initiative Thematic Annual Programming on Water (2018-W-MS-35). NS and JS received Portuguese national funds from FCT - Foundation for Science and Technology through project UID/Multi/04326/2019. PH was supported by grants from FINEP/Rede CLIMA (01.13.0353-00) and CNPq-Universal (426215/2016-8). LH was funded by the National Science Foundation Ocean Sciences International Postdoctoral Research Fellow program (Grant No. 1521610).

ACKNOWLEDGMENTS

We thank the contributing authors, reviewers, and the Frontiers in Marine Science Editorial staff for their support in producing this Special Issue.

REFERENCES

Adey, W. H. (1998). Coral reefs: algal structured and mediated ecosystems in shallow, turbulent, alkaline waters. *J. Phycol.* 34, 393–406. doi: 10.1046/j.1529-8817.1998.340393.x

Aguirre, J., Riding, R., and Braga, J. C. (2000). Diversity of coralline red algae: origination and extinction patterns from the Early Cretaceous to the Pleistocene. *Paleobiology* 26, 651–667. doi: 10.1666/0094-8373(2000)026<0651:DOCRAO>2.0.CO;2

Chisholm, J. R. M. (2003). Primary productivity of reef-building crustose coralline algae. *Limnol. Oceanogr.* 48, 1376–1387. doi: 10.4319/lo.2003.48.4.1376

Coletti, G, Basso, D., and Frixa, A. (2017). "Economic importance of Coralline Carbonates," in *Rhodolith/Maërl Beds: A Global Perspective*, eds R. Riosmena-Rodríguez, W. Nelson, and J. Aguirre (Basel: Springer International Publishing), 87–104. doi: 10.1007/978-3-319-29315-8_4

Cornwall, C. E., Diaz-Pulido, G., and Comeau, S. (2019). Impacts of ocean warming on coralline algae: knowledge gaps and key recommendations for future research. *Front. Mar. Sci*. 6:186. doi: 10.3389/fmars.2019.00186

Foster, M. S. (2001). Rhodoliths: between rocks and soft places. *J. Phycol.* 37, 659–667. doi: 10.1046/j.1529-8817.2001.00195.x

Ingrosso, G., Abbiati, M., Badalamenti, F., Bavestrello, G., Belmonte, G., Cannas, R., et al. (2018). Mediterranean bioconstructions along the Italian coast. *Adv. Mar. Biol.* 79, 61–136. doi: 10.1016/bs.amb.2018.05.001

Johansen, H. W. (1981). *Coralline Algae, a First Synthesis, 1st Edn.* Boca Raton, FL: CRC Press, 239.

Krayesky-Self, S., Schmidt, W. E., Phung, D., Henry, C., Sauvage, T., Camacho, O., et al. (2017). Eukaryotic life inhabits rhodolith-forming coralline algae (Hapalidiales, Rhodophyta), remarkable marine benthic microhabitats. *Sci. Rep*. 7:45850. doi: 10.1038/srep45850

Martin, S., Castets, M.-D., and Clavier, J. (2006). Primary production, respiration and calcification of the temperate free-living coralline alga *Lithothamnion corallioides*. *Aquat. Bot.* 85, 121–128. doi: 10.1016/j.aquabot.2006.02.005

Martin, S., and Hall-Spencer, J. M. (2017). "Effects of ocean warming and acidification on rhodolith/maërl beds" in *Rhodolith/Maërl Beds: A Global Perspective*, eds R. Riosmena-Rodríguez, W. Nelson, and J. Aguirre (Basel: Springer International Publishing), 55–85. doi: 10.1007/978-3-319-29315-8_3

Nelson, W. A. (2009). Calcified macroalgae critical to coastal ecosystems and vulnerable to change: a review. *Mar. Freshw. Res.* 60, 787–801. doi: 10.1071/MF08335

Perry, C. T., Spencer, T., and Kench, P. S. (2008). Carbonate budgets and reef production states: a geomorphic perspective on the ecological phase-shift concept. *Coral Reefs* 27, 853–866. doi: 10.1007/s00338-008-0418-z

Steneck, R. S. (1986). The ecology of coralline algal crusts: convergent patterns and adaptive strategies. *Annu. Rev. Ecol. Syst.* 17, 273–303. doi: 10.1146/annurev.es.17.110186.001421

van der Heijden, L. H., and Kamenos, N. A. (2015). Calculating the global contribution of coralline algae to carbon burial. *Biogeosciences* 12, 6429–6441. doi: 10.5194/bg-12-6429-2015

Woelkerling, W. J. (1988). *The Coralline Red Algae: An Analysis of Genera and Subfamilies of Nongeniculate Corallinaceae*. London; Oxford; New York, NY: British Museum (Natural History); Oxford University Press, 268.

Conflict of Interest: The authors declare that the research was conducted in the absence of any commercial or financial relationships that could be construed as a potential conflict of interest.

Copyright © 2020 Schubert, Schoenrock, Aguirre, Kamenos, Silva, Horta and Hofmann. This is an open-access article distributed under the terms of the Creative Commons Attribution License (CC BY). The use, distribution or reproduction in other forums is permitted, provided the original author(s) and the copyright owner(s) are credited and that the original publication in this journal is cited, in accordance with accepted academic practice. No use, distribution or reproduction is permitted which does not comply with these terms.

frontiers in Marine Science

ORIGINAL RESEARCH
published: 06 June 2019
doi: 10.3389/fmars.2019.00285

Sustainable Harvesting of the Ecosystem Engineer *Corallina officinalis* for Biomaterials

Caroline L. Magill[1], Christine A. Maggs[1,2], Mark P. Johnson[1,3] and Nessa O'Connor[1,4]*

[1] School of Biological Sciences, Queen's University Belfast, Belfast, United Kingdom, [2] Joint Nature Conservation Committee, Monkstone House, Peterborough, United Kingdom, [3] Ryan Institute and School of Natural Sciences, National University of Ireland Galway, Galway, Ireland, [4] Department of Zoology, Trinity College Dublin, Dublin, Ireland

Macroalgae are of increasing interest for high-value biotechnological applications, but some seaweeds, such as coralline red algae, cannot be grown in cultivation cost-effectively. Wild harvesting of seaweeds, particularly of those that are ecosystem engineers, must be demonstrably sustainable: here we address the topic of resource sustainability in the context of harvesting *Corallina officinalis* in Ireland for bioceramics. *C. officinalis* provides habitat for a diverse macrofaunal community and the effects of harvesting *C. officinalis* on the associated fauna must be included in any assessment of harvesting sustainability. *Corallina* intertidal turfs subject to experimental harvesting were confirmed, using DNA barcoding with *cox*1, to comprise only *C. officinalis* and not the pseudocryptic species *C. caespitosa*, despite the wide range of morphologies, and they had high genetic diversity. Harvesting of *C. officinalis* was carried out at experimental sites by two techniques (hand cutting and pulling) to test the recovery of the primary resource and the associated macroinvertebrate assemblage. Harvesting the alga by both methods encouraged regrowth: cut and pulled plots had a much higher growth rate than unharvested turfs, regaining their original length within 4–6 months of harvesting, suggesting that turfs of this species may grow to a predetermined length. The structure, richness and evenness of the invertebrate assemblage were not significantly affected by harvesting *C. officinalis* by cutting or pulling, though some organisms within the community showed a response to harvesting. The pattern of recovery of the sediment, an important component of the *C. officinalis* habitat, was consistent with the shorter (harvested) turf trapping more sediment than longer natural turfs. As many of the organisms associated with the habitat use the sediment for food or building materials, this may have ameliorated the effects of harvesting on the community. A period of a year between harvests is recommended to allow the *C. officinalis* biomass to return to baseline levels and unharvested fallow areas should be included in a harvesting plan to allow macroinvertebrates to re-colonize the harvested turf.

Keywords: harvest, Corallinaceae, Ireland, macrofauna, sustainability

OPEN ACCESS

Edited by:
Julio Aguirre,
University of Granada, Spain

Reviewed by:
Alan T. Critchley,
Cape Breton University, Canada
Megan Jane Huggett,
The University of Newcastle, Australia

****Correspondence:***
Caroline L. Magill
cmagill02@qub.ac.uk

Specialty section:
This article was submitted to Marine Ecosystem Ecology, a section of the journal Frontiers in Marine Science

Received: *23 November 2018*
Accepted: *16 May 2019*
Published: *06 June 2019*

Citation:
Magill CL, Maggs CA, Johnson MP and O'Connor N (2019) Sustainable Harvesting of the Ecosystem Engineer Corallina officinalis for Biomaterials. Front. Mar. Sci. 6:285. doi: 10.3389/fmars.2019.00285

INTRODUCTION

Algae are increasingly important as a potentially sustainable resource for biotechnological applications (Kim and Chojnacka, 2015; Rocha et al., 2018). Whilst microalgae are suitable for culture in bioreactors and some macroalgae, or seaweeds, are grown on frames and ropes in the open water (FAO, 2003–2015; Chung et al., 2017), other seaweeds are more efficiently harvested from the wild (McLaughlin et al., 2006; Mac Monagail et al., 2017). Wild algae can be commercially harvested either by hand or mechanically. *Laminaria* spp. (kelp) and other large subtidal canopy-forming algae can be harvested from boats equipped with cutting and raking tools (e.g., the Brittany "scoubidou") (Mesnildrey et al., 2012). Intertidal species with long thalli which float on the surface, such as *Ascophyllum nodosum*, can likewise be harvested mechanically at high tide by shallow-draft paddlewheel or water jet-driven cutters (Meland and Rebours, 2012). However, species with short or delicate thalli are not suitable for mechanical harvesting and must be harvested by hand. Manual (artisanal) harvesting of wild seaweeds has a long history in coastal communities, where they have been collected for food, medicine and as a soil improver (Reed, 1907; Morrissey et al., 2001; Mac Monagail et al., 2017; Yang et al., 2017). Manual harvesting is informed by traditional practices and hand harvesting of seaweeds is largely regarded as sustainable (McLaughlin et al., 2006; O'Toole and Hynes, 2014). However, even with hand harvesting there is a risk of over-exploitation. Unregulated wild harvest can lead to depletion of a species in an area, increasing market value and intensifying harvest efforts on the remaining resources (e.g., *Chondracanthus chamissoi* in Peru: Rebours et al., 2014).

Consequently, before harvesting begins on a commercial scale, sustainability of the resource under probable harvesting regimes must be assessed. An important element of sustainability is genetic diversity, but there are few studies of the genetic effects of harvesting seaweeds. Guillemin et al. (2014) attribute remarkably low diversity in Chilean populations of *Gracilaria chilensis* to a recent genetic bottleneck due to over-exploitation of natural stocks, which has been exacerbated by using genetically depressed populations as stock for aquaculture. In Brittany, France, populations of the economically important kelp *Laminaria digitata* exhibit greater genetic diversity within the Iroise Sea Marine Protected Area than outside it, and act as a source for other regions (Couceiro et al., 2013).

Whilst many commercially valuable algae are collected for their polysaccharides and cellular components (El Gamal, 2011; Kim and Chojnacka, 2015; Mac Monagail et al., 2017), coralline algae contain very little organic material in comparison with more fleshy species, and have been collected traditionally for their calcified skeleton (Wilson et al., 2004). Large quantities of free-living, non-geniculate coralline algae can occur in specific areas as maerl or rhodolith beds, which have traditionally been heavily exploited along the NE Atlantic coastline for low-value applications such as soil conditioning (Blunden et al., 1975). Maerl is also used in higher-value products such as food supplements for humans and domesticated animals (Nielsen et al., 2011; Ryan et al., 2011). However, the growth rate of the most abundant maerl species in Europe, *Phymatolithon calcareum*, is low (less than 2 mm per annum), which precludes sustainable harvesting (Blake and Maggs, 2003). In comparison with maerl, geniculate coralline species have a rapid growth rate and could potentially be considered renewable, whereas maerl is essentially a finite resource. Two species of the geniculate (jointed) coralline genus *Corallina* are currently recognized in the British Isles: *Corallina officinalis* and the semi-cryptic species *C. caespitosa* (Walker et al., 2009; Williamson et al., 2015). Genetic diversity of *Corallina* species is high on European coasts (France and Spain) (Pardo et al., 2015), and samples from southern England included several haplotypes (Walker et al., 2009).

Corallina officinalis occurs on rocky shores around most of the coast of Britain and Ireland, in easily accessible pools and crevices from the sublittoral fringe to the mid-shore (Irvine and Chamberlain, 1994). This widespread distribution could make it a better prospect for coastal communities to exploit on a part-time basis than the low-value fleshy species used for agriculture and food additives. The high-value applications for calcified algae (medical and cosmetic products) could mean a large return from a small amount of biomass collected. For example, *C. officinalis* has been identified as a feedstock for bone substitute materials (Kasperk et al., 1988; Turhani et al., 2005; Clarke et al., 2011) and a novel, low temperature process for the production of high quality material from *C. officinalis* was patented at Queen's University Belfast (Walker et al., 2007; Walsh et al., 2008, 2010, 2011). *C. officinalis* therefore offers a potentially sustainable alternative to the coral-derived bone substitutes that had been used clinically for dental and orthopedic applications, which makes it an attractive prospect for harvesting. Although *Corallina* spp. have traditionally been collected in small quantities in Britain, Ireland and elsewhere in Europe, there is no research underpinning best practice for harvesting (McLaughlin et al., 2006).

Like other geniculate species with similar morphology, *C. officinalis* is known to be a habitat-forming species or ecosystem engineer, which creates a reasonably stable and complex refuge from environmental stressors (Dommasnes, 1968; Bussell, 2003) and predation (Coull and Wells, 1983; Hayakawa et al., 2013), influencing the community structure of the shores on which it occurs (Kelaher, 2002; Nelson, 2009). The dense networks of semi-rigid thalli trap debris, which can be exploited as a food source (Hicks, 1986). *C. officinalis* also supports a community of macro-epiphytes (Munda, 1977; Stewart, 1982; Akioka et al., 1999; Berthelsen and Taylor, 2014) and micro-epiphytes (Perkins et al., 2016) which can be exploited as food. Animals that live amongst *Corallina* use the turf in various ways and exploit different aspects of the habitat. Harvesting the alga will change the habitat structure by affecting the amount of surface area available for settlement, refuge, grazing, and sediment capture – how long these effects persist could be important for resilience of invertebrate assemblages. Important biogenic habitats created by ecosystem engineers have been degraded by exploitation using unsustainable harvesting practices, aimed at the organisms themselves or associated species, e.g., *Ostrea*

edulis (Airoldi and Beck, 2007), *Modiolus modiolus* (Strain et al., 2012) and maerl (Hall-Spencer and Moore, 2000; Hall-Spencer, 2005), and there is increasing awareness that they should be protected from disturbance and overexploitation (Cole et al., 2016). *C. officinalis* is not protected under any conservation legislation and it has not been harvested extensively to date. Therefore, a rare opportunity exists to assess the effects of harvest on the organisms associated with this ecosystem engineer in advance of its possible exploitation.

This study aimed to advance knowledge on harvesting of *C. officinalis* and to determine the feasibility of sustainable harvesting from the Irish coastline, including a preliminary determination of genetic diversity at the proposed harvest site using the DNA barcode marker *cox*1, which is also suitable for molecular identification. Firstly we assessed the regeneration of the alga after differing hand-harvesting methods. In a subsequent experiment, the *a priori* hypothesis that harvesting the *C. officinalis* turf would not change the diversity or structure of the associated invertebrate assemblage was tested. The community of animals living in coralline turf is known to recover rapidly after trampling (Brown and Taylor, 1999; Huff, 2011), therefore it was predicted that harvesting the alga would not have a lasting effect on the invertebrate assemblage. The effect of harvesting on important physical constituents of the habitat i.e., the coralline alga itself and the associated sediment were also tested, and time to recovery was estimated.

MATERIALS AND METHODS

Field Study Sites

Two readily accessible shores with sufficient coralline algal turf cover for experimental manipulation were selected on the north and east coast of Ireland in 2006 as part of the EU project HIPPOCRATES. Sites were chosen to represent exposure to different water bodies: Glashagh Bay, Fanad Head, Co., Donegal, Ireland is on the Northeast Atlantic coast and Killough Bay, Co., Down, Northern Ireland is situated in a bay opening into the Irish Sea (**Figure 1**). Glashagh Bay faces north-west with some shelter from the open Atlantic Ocean provided by offshore rocks and the shallow seabed which is <10 m at 1 km from the shore. It is remote from tourist beaches and the algal turf is therefore at minimal risk of trampling or other anthropogenic damage. Killough Bay faces east into the Irish Sea with some shelter from a point on the north-eastern side of the bay, but it is exposed to waves from the south east. The tidal range for both shores is approximately 5 m. At both sites *Corallina* sp(p) is dominant in the majority of pools from low water of spring tides (LWST) to mean tide level (MTL), forming a turf of varying height. The rock pools support an array of macroalgal species, including filamentous (e.g., *Caradoriella* (formerly *Polysiphonia*) *elongata* and *Ceramium virgatum*) and coarsely branched (e.g., *Osmundea hybrida* and *Gelidium* spp.) red algae; ephemeral (e.g., *Ulva compressa*) and perennial (e.g., *Codium tomentosum*) green algae and brown canopy algae (e.g., *Fucus vesiculosus* and *Halidrys siliquosa*). Encrusting coralline algae covered most of the remaining substratum.

Effect of Harvesting on Growth of *Corallina officinalis* Turf

Following visual surveys of both sites, pools with extensive coverage of *Corallina* sp(p.) were chosen for the first study at Fanad Head (two replicate pools) and Killough (one pool). The pools at Killough (54°14′43.04″N 5°38′15.01″W) and Fanad A (55°15′47.21″N 7°40′45.10″W) were of a similar depth, with rocky substrata throughout. *Corallina* grew in dense foliose clumps throughout the pools, with the only other major algal coverage being *Fucus* spp. Pool B at Fanad (55°15′49.19″N 7°40′37.10″W) was at higher elevation on the shore with a deep area in the center having substantial sedimentation. The *Corallina* in this pool grew in short scrubby clumps mainly around the edges of the pool. Replicate plots (n = 3) of 25 cm × 25 cm to be prepared for three experimental harvesting treatments and comparable unharvested controls (n = 3) were randomly distributed within each of the pools.

To mimic methods used for harvesting other algae, and suitable for large-scale harvesting of *Corallina,* experimental treatments included both cutting and pulling the *C. officinalis* thalli. The treatments were applied as follows: (1) coralline algal turf was cut to ∼30 mm length with scissors; (2) coralline algal turf was cut to ∼10 mm length with scissors; and (3) all coralline algal turf was completely pulled by hand from the basal crustose holdfast, the "pull" treatment, in three replicate quadrats in each pool. With all harvesting methods care was taken to leave the crustose holdfast intact, because in comparison to regeneration of uprights from an existing crustose base, formation of new thalli from spores is slow. The same number of control quadrats of coralline algal turf were left untouched in each pool to estimate ambient algal growth for comparison.

To estimate growth rate and determine when the alga returned to pre-harvested length, thalli were measured in all quadrats: at both pools at Fanad in late February and Killough in early March 2006 (before harvest: month 0) then in August and November 2006 at Fanad (after 6 and 10 months) and in July and November 2006 at Killough (after 4 and 10 months). Ten *C. officinalis* thalli were measured to the nearest mm from base to tip (thallus length = turf height) within each replicate quadrat on each visit; mean thallus length in each quadrat was the basic unit for analysis (see section "Data Analyses"). Increase in thallus length in each quadrat was calculated by subtracting thallus length at one time-point from the next. Thallus length increase was then converted to growth rate in mm mo^{-1} by dividing the length increase by the number of months between measurements.

Molecular Identification and Genetic Diversity of *Corallina officinalis* in Donegal

To ensure the target species was harvested, and to obtain a preliminary assessment of genetic diversity, samples representing the full morphological range of *Corallina* from different habitats (differing in shore height and pool depth) were collected from Glashagh Bay, Fanad Head in January 2009. Thalli from five different individuals, representing the range of morphological variation (**Supplementary Material 1**), were photographed,

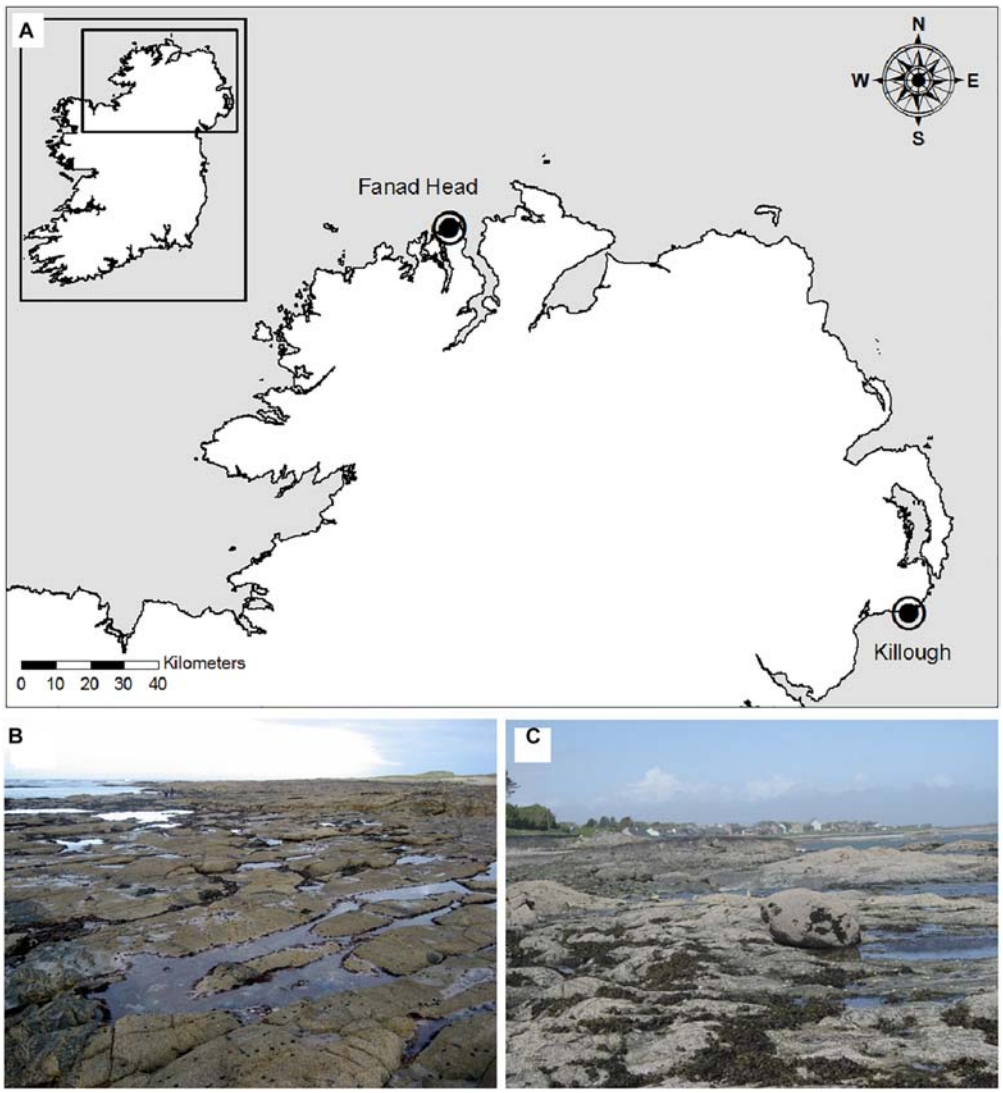

FIGURE 1 | (A) Experimental harvesting sites at Glashagh Bay, Fanad Head, Co., Donegal and Killough, Co., Down and shores where *Corallina officinalis* was harvested in pools at **(B)** Glashagh Bay and **(C)** Killough.

rinsed, picked clean by hand of epiphytes and epifauna, blotted dry and preserved in silica gel prior to DNA extraction. Voucher specimens for the *Corallina* sequences were pressed and deposited in the Natural History Museum, London.

After grinding ∼20 mg of the dried sample with liquid nitrogen in an Eppendorf tube using an autoclaved mini-pestle, DNA was extracted with the Qiagen DNeasy Plant Mini Kit (Qiagen Ltd., W. Sussex, United Kingdom). The variable *cox*1 region was amplified using the primers GazF1 5′ TCAACAAATCATAAAGATATTGG 3′ and GazR1 5′ ACTTCTGGATGTCCAAAAAAYCA 3′ (Saunders, 2005). PCR conditions (Perkin Elmer DNA Thermal Cycler 480; Perkin Elmer Biosystems) were 5 min at 94°C, 35 cycles of 1 min at 94°C, 1.5 min at 51°C (annealing), 2 min at 72°C, and a final extension of 5 min at 72°C. Purification and sequencing of the PCR products were outsourced to Macrogen (Seoul, Korea). New sequences were uploaded to GenBank (**Supplementary Material 2**).

Sequences were edited in Codon Code Aligner version 6.02 (Codon Code Corporation), checking variable nucleotides carefully, and complementary strands were assembled in SeaView version 4 (Gouy et al., 2010). An alignment was constructed with other sequences of members of the tribe Corallineae, mostly *Corallina* spp., selected from GenBank using BLAST searches and relevant publications (Brodie et al., 2013; Pardo et al., 2015). Sequences that were identical to those selected from the same geographical region were ignored. A compressed alignment with all variable sites (**Supplementary Material 2**) was used to assign sequences to haplotypes. The amino acid translation was examined in SeaView. Phylogenetic network estimation using statistical parsimony was carried out with TCS 1.21 (Clement et al., 2000). Using *Corallina vancouveriensis* as

outgroup resulted in too many ambiguities so the network was made with no outgroup.

Effects of Harvesting *Corallina officinalis* on the Diversity of the Invertebrate Community

Glashagh Bay, Fanad Head (**Figure 1**) was chosen for the second study in 2010 as it is representative of sites in the area but has a more extensive coverage of *C. officinalis* than others, making it a potential commercial harvesting site and allowing for a larger scale study. To separate the effects of harvesting on the variability in communities from those caused by shore height (Kelaher et al., 2001; Bussell et al., 2007), a large pool (approximately 0.5–1 m above Chart Datum) that spanned c. 30 m horizontally along the shore but was only c. 5 m max. width, with an estimated ∼80% *Corallina* cover, was chosen as an experimental area (**Figure 2a**). The pool consisted of varying microhabitats, from very shallow sills to deep crevices, and supported a diverse algal community.

A destructive sampling program was designed to avoid repeated measures analysis and maintain independent data among sampling occasions. Five replicates of each experimental treatment, for each sampling month [cut harvesting (n = 30), pull harvesting (n = 30) and no harvesting (n = 35)], were randomly assigned a 25 cm × 25 cm numbered grid square within a 1 m × 1 m alphabetical quadrat area (see **Supplementary Materials 3**, **4** for sample list and grids, respectively). These alphabetical areas were then transferred onto the pool in June 2010 by haphazardly placing a guide quadrat of the same size in 12 (A–L) different parts of the pool with continuous *Corallina* cover and marking their location (**Figure 2b**). Harvesting treatment areas were demarcated when applying the treatments by aligning a quartered 50 × 50 cm quadrat with the outer edges of the 1 × 1 m guide quadrat (**Figure 2c**). Alternate 25 cm × 25 cm grid squares within the smaller quadrat were designated as "fallow" areas to minimize autocorrelation between treatment squares (**Figure 2** inset).

Pre-ordained destructive baseline samples (10 cm × 10 cm; n = 5) were taken in June 2010 before applying the allocated harvesting treatments to all plots. Harvesting treatments were then applied as in the previous harvesting trials, with the modification that only one cut treatment was applied (∼2 cm) (e.g., **Figure 2d**). The unharvested plots underwent the procedure of placing the quadrat, without harvesting. Depth measurements, to be used as co-variates in the analysis, were taken at low tide when all channels draining the pool were empty or still. Nine measurements (**Figure 2f**, gray dots) were taken in each 25 cm × 25 cm grid square with a ruler from the bottom of the pool to the water surface and the mean of these measurements represented the depth for that sample. The mean water depth of the sampled plots was 44 mm (range 0 – 187 mm, **Supplementary Material 5**).

Destructive sampling of a 10 cm × 10 cm portion in the center of the 25 cm × 25 cm plot (to minimize "edge effects" i.e., spatial autocorrelation) of the cut, pulled and unharvested plots commenced 1 month after harvest in July 2010, and continued at months 4 (October 2010), 7 (January 2011), 10 (April 2011), 13 (July 2011), and 16 (October 2011) after harvest treatment (**Figure 2e**). On each sampling occasion, five of the pre-ordained, randomly assigned replicates of cut, pull, and unharvested treatments were collected (see **Supplementary Material 3** for sampling schedule). The 10 cm × 10 cm sample of coralline turf and associated fauna (**Figures 2e,f**) was enclosed in a plastic bag, by pushing the bag down over the sample, removed with a scraper and immediately transferred to a sorting tray. Any large, easily identifiable animals were photographed, logged and returned to the pool. The remaining material was transferred to a Ziploc bag and then preserved in labeled jars with 90% ethanol within 2 h of collection.

The samples composed of coralline turf, sediment, flora and fauna removed from the plots were processed by gently rinsing with running seawater through stacked Endicott sieves of 1 mm, 500 and 63 μm mesh. The 63–500 μm and the >1 mm fraction (*Corallina* and associated fauna) were included in the analyses. The sediment fraction for each plot was transferred to a separate foil tray and oven dried at 60°C in a Gallenkamp oven (Weiss-Gallenkamp, Loughborough, United Kingdom). Prior to weighing, the samples were allowed to cool to room temperature in a desiccator. Samples were then weighed to the nearest 0.1 g with an Ohaus Adventurer AR3130 (Ohaus, Nanikon, Switzerland). Once the associated flora and fauna had been removed, the denuded *C. officinalis* fraction was processed in the same way as the sediment.

The >1 mm fraction of the sample contained coralline algae, epiphytic algae, terete species, epifauna, slow-moving associated fauna and large debris. After removing debris and other free-living algae, the samples were processed under a dissecting microscope. Once the coralline alga had been picked clean, it was dried as detailed previously. Animals were identified using the literature and online material listed in **Supplementary Material 6**, and identification was corroborated by J. Nunn, National Museums Northern Ireland. Free-living annelid worms were not counted as they were most often fragmented and it was impossible to ascertain the number of animals accurately.

Data Analyses

Effect of Harvesting on Growth of *Corallina officinalis* Turf

The basic sampling unit for analysis was the mean thallus length in each quadrat, rather than the individual measurements, as the 10 measurements from each quadrat were considered spatial pseudoreplicates (Millar and Anderson, 2004). Growth rate was used as the response variable in the subsequent analysis rather than thallus length, as *a priori* comparison of thallus lengths at time 0, before harvesting treatments were applied, revealed a significant difference in initial length between treatment plots (p = < 0.001). As sampling at the sites was unbalanced, pools were not nested within site and each pool was treated as a separate entity in the analyses.

To compare overall (10 months) growth rates, univariate ANOVA with Treatment (fixed, four levels) and Pool (random, three levels) as factors was used. *Post hoc* Tukey's HSD test was applied to resolve differences in significant terms. Data were checked for normality and homogeneity of variances with the

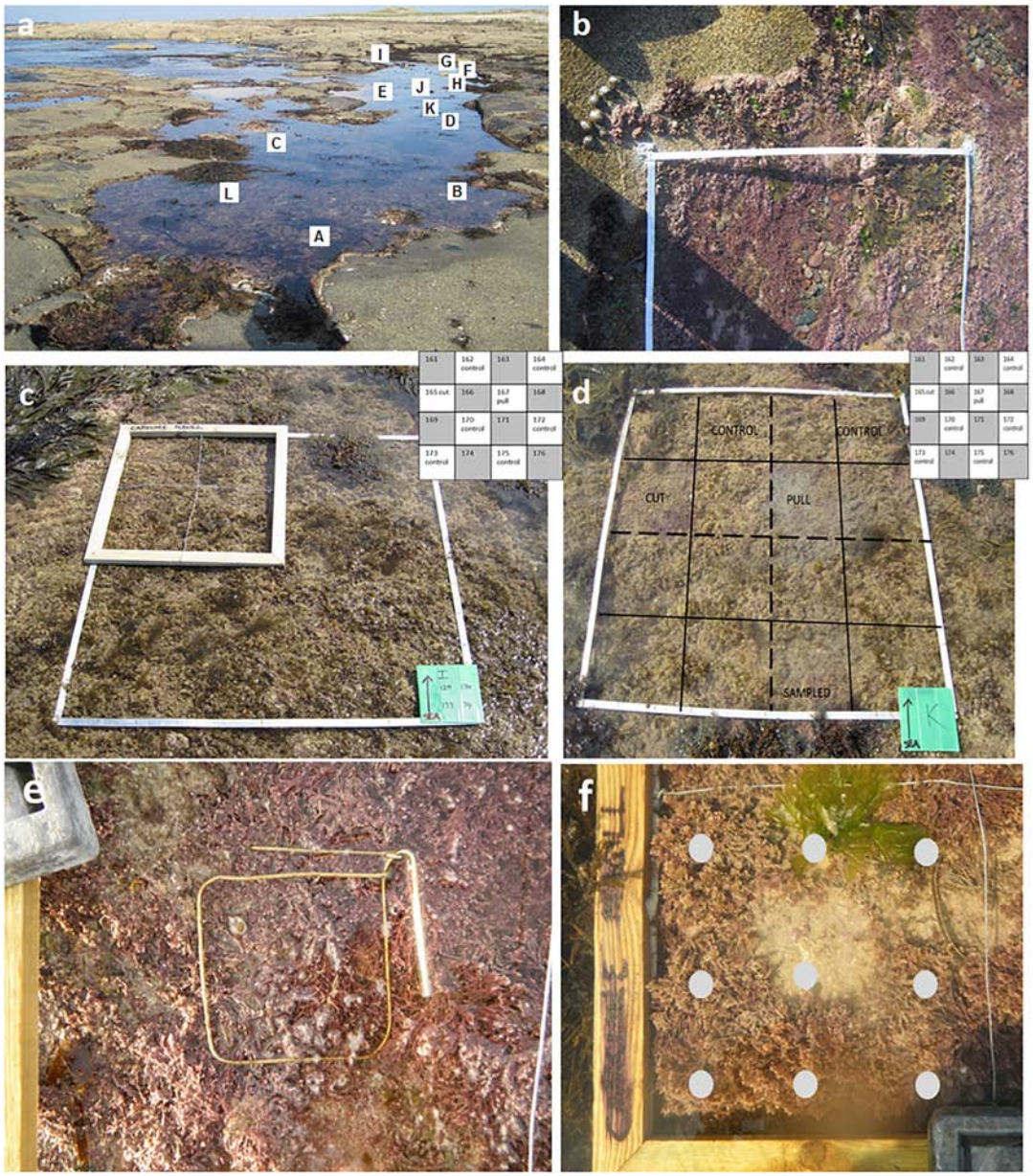

FIGURE 2 | (a) Location of sampling areas in pool. **(b)** Markers drilled to allow exact placement of guide quadrat. **(c)** Example of a harvesting grid and quadrat placement. **(d)** Guide quadrat after applying harvesting treatments on June 2010 [two harvesting treatments applied (cut and pull), five future control samples left untouched (top two control plots marked on picture only) and one baseline control plot sampled]. **(e)** Detail of 10 cm × 10 cm sampling quadrat in place. **(f)** Example of a plot after sampling (dots indicate approximately where depth measurements were taken in each 25 cm × 25 cm quadrat).

Shapiro-Wilk and Cochran's *C* test, respectively. These analyses were conducted in R version 3.1.2 (R Core Team, 2015).

To test for any effect of time of year on the algal growth after harvest, growth rates (mm mo^{-1}) during the two intervals between measurements (spring/summer and autumn/winter) were compared with Permutational multivariate analysis of variance (PERMANOVA+ add-on in PRIMER version 6.1.13; PRIMER-E Ltd., Plymouth, United Kingdom). The univariate PERMANOVA was based on the same model structure as the ANOVA with the addition of Interval as a two level fixed factor. The analysis was performed on a Euclidean distance dissimilarity matrix of untransformed growth rates in mm mo^{-1}. Control data were not considered in this analysis. In one case where a zero growth rate was recorded (possibly due to breakage of the thallus) the value was replaced with a dummy variable of 0.01.

Effects of Harvesting *Corallina officinalis* on the Diversity of the Invertebrate Community

Species were grouped by the lowest taxonomic group practicable to test for difference in diversity and assemblage structure. In

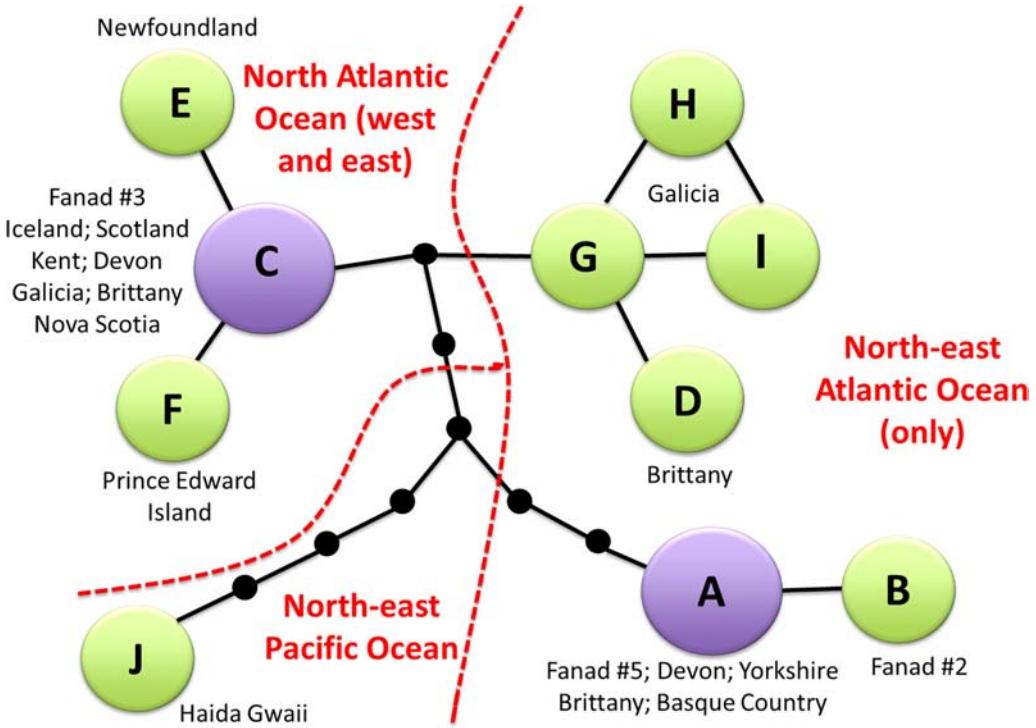

FIGURE 3 | Parsimony network for *cox*1 sequences of *Corallina officinalis* from Fanad sampling site and sequences from GenBank generated in TCS. The compressed alignment is shown in **Supplementary Material 2**. Relationships between haplotypes are depicted with black lines and small black dots indicate missing haplotypes. Haplotypes A and C (purple) are the two commonest and most widespread. An overview of the biogeographical distribution is presented in red.

most cases the taxonomic grouping was by order. In the case of several gastropod species, which have no formally assigned order (WoRMS Editorial Board, 2015), subclass was used as grouping level. Insect larvae, nematodes and ascidians were grouped by phylum (Nematoda only), and class. This method of grouping allowed all invertebrates collected, except for 98 "unidentified tubes," to be included in the analyses.

Analyses were carried out on the "R" statistical computing framework (version 3.1.2, R Core Team, 2015). The *a priori* hypothesis that harvesting *C. officinalis* would have no effect on the sampled invertebrate community was tested using the manyglm function within the R package "mvabund" (Wang et al., 2015). The "manyglm" function was used to fit univariate negative binomial generalized linear models to the abundance of each invertebrate taxon in the community and relate the abundance to a common set of explanatory variables, resulting in a multivariate analysis across taxa (Moorhouse et al., 2014). The "anova" function was then used to generate resampling-based hypothesis tests of the multivariate abundance response. The abundance of invertebrate grouping taxa in each sample was the response variable in the model (90 observations of 26 variables), with harvest treatment (fixed, three levels), and months since treatment (fixed, six levels) as categorical variables (factors). Depth was included in the model as a continuous predictor (covariate). Model assumptions were checked by plotting the residuals to check for normality, i.e., random distribution on the plot (**Supplementary Material 7**). Any correlation between taxa (which would be expected in a community) was accounted for in the resampling method (PIT-trap, Warton et al., 2015).

Taxon richness (number of species in a sample, S) and evenness (relative abundance of different species in a sample, Simpson's, $1-\lambda$) of the associated invertebrates were compared with two-way factorial ANOVAs, with harvest treatment (fixed, three levels), and months since treatment (fixed, six levels) as factors, for the taxonomic groups over the entire study, as a broad-scale measures of effect of harvesting on the invertebrate community.

The structural habitat components, *Corallina* dry biomass and sediment dry mass, were log $x+1$ transformed to normalize the variables then compared by the same method as the richness and evenness to check if and when the *C. officinalis* itself and sediment load within it returned to pre-harvesting levels.

RESULTS

Identification and Genetic Diversity of *Corallina* Samples

Sequence quality of the *cox*1 sequences from five Fanad samples was good except for sample 4 in which only the forward sequence was usable. The alignment was 663 bp in length. Analysis of the *cox*1 sequences, in an alignment with multiple GenBank sequences of *Corallina* spp., indicated that the five Fanad samples were all conspecific. They were identifiable as *C. officinalis*

because some sequences were identical to the *C. officinalis* epitype *cox*1 GenBank accession no. FM180073 from Devon (Brodie et al., 2013), which is also identical to the mitochondrial genome *cox*1 sequence (**Supplementary Material 2**).

The compressed alignment for *C. officinalis* included 16 variable sites, which resulted in ten haplotypes (**Supplementary Material 2**). These separated into two major groups of haplotypes (A + B; C–I), with haplotype J clearly divergent from both groups. There was high genetic variation in the Fanad samples: the five sequences represented three different haplotypes, A, B, and C. Haplotype B, with T rather than C at position 618, was private to Fanad. Parsimony network analysis (**Figure 3**) showed clear phylogeographic structure. It confirmed that Haplotype J, from Haida Gwaii, BC, is the most distant from the other haplotypes, and it differs by four non-synonymous substitutions. Two well-separated Fanad haplotypes had broad geographical distributions: haplotype A was found widely in Europe from Ireland to the Basque Country; haplotype C occurred in the north-east Atlantic, Iceland, and the north-west Atlantic. Haplotypes from Brittany and Galicia form a closely related grouping, with four non-synonymous substitutions in total between this group and the other haplotypes.

Effect of Harvesting on Growth of *Corallina officinalis* Turf

Although growth rates varied amongst the harvested samples, they grew significantly faster than the unharvested controls (**Figure 4** and **Table 1**). The maximum mean growth rate found in this study was 9 mm mo^{-1} for cut harvest (3 cm) and 6.3 mm mo^{-1} for pull harvest (**Supplementary Material 8**). These growth rates are substantially higher than any recorded for *C. officinalis* in the literature (1.4–2.2 mm mo^{-1}; Colthart and Johansen, 1973; Andrake and Johansen, 1980; Blake and Maggs, 2003). ANOVA indicated a significant difference in growth rates between different harvesting methods in the pools (**Figure 4**, letters on bars a–e). There was also a significant Treatment × Pool interaction, which was identified as an isolated difference between the growth rates of the 1 cm cut treatments at Fanad B and Killough. Within the other harvesting treatments there was no significant effect of pool, suggesting that at Fanad A and Killough, two geographically separated sites with similar pool topography and substratum type, the effect of harvesting on growth rate was similar.

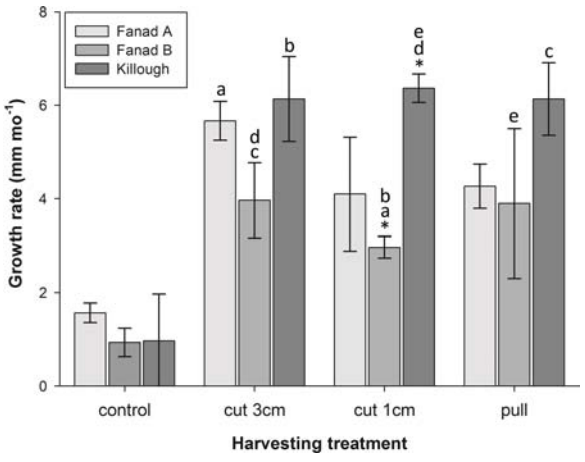

FIGURE 4 | Mean growth rates (mm mo^{-1}, ± SD) of coralline algae harvested by three different methods, and controls in three different pools over the duration of the experiment (10 months). Growth rates of control samples were significantly different from all others. *Indicates isolated difference in growth rate within an experimental harvesting treatment group; letters indicate significant differences between pairs of growth rates across different treatments and pools (*post hoc* Tukey's HSD $p < 0.05$).

TABLE 1 | ANOVA results for the effects of harvesting treatment (cut 3 cm, cut 1 cm, and pull) and pool (Fanad A, Fanad B, and Killough) on growth rate of *Corallina officinalis*.

Source of variation	DF	MS	*F*	*P*
Treatment	3	31.36	48.29	<0.001
Pool	2	11.51	17.72	<0.001
Treatment*pool	6	2.02	3.12	0.020
Residual	24	0.65		

The alga grew at different rates at different sites in the intervals (seasons) (PERMANOVA, Pool × Interval interaction $p = < 0.006$). Comparing the western and eastern sites with each other, Killough had the fastest growing *C. officinalis* in the early part of the year (interval 1, *post hoc* $p = < 0.05$), whilst in the second interval there was no difference between the geographic areas. Within pools across all treatments, Killough and Fanad A grew at similar rates in both intervals, whilst Fanad B grew faster later in the year (*post hoc* $p = < 0.05$; **Figure 5**). The maximum mean growth rates in each interval and in the experiment overall reflect these results (**Supplementary Material 8**). There was no difference between the thallus lengths of the three manipulated plots and the control plot at the sites within any measurement period (*post hoc* $p > 0.05$).

Effect of Harvesting on Invertebrate Assemblage Structure and Diversity

The multivariate test for change in assemblage structure "manyglm" suggested there were effects of harvesting in some months (harvest × month interaction, **Table 2**, $p < 0.05$). When the individual GLM results were examined (**Table 2**), these interaction effects were seen most strongly in six groups of animals (effect size in parentheses): Tanaidacea (*Tanais dulongii*) (Dev = 30.309), Caenogastropoda (*Bittium reticulatum*) (Dev = 26.575), Neogastropoda (*Nucella lapillus*) (Dev = 25.688), Isopoda (*Idotea* spp.) (Dev = 24.77), Sabellidae (*Spirorbis* spp./*Spirorbis corallinae*) (Dev = 23.435) and Nematoda (Dev = 22.742), although none of the effects were statistically significant ($p > 0.05$). The effects were variable and in some cases cutting and pulling the alga seemed to have a positive effect, as the abundances of animals collected from the cut and pulled plots were greater than those from the unharvested plots (see **Figure 6**). In the six taxonomic groups that differed most among experimental harvesting treatments, the effects

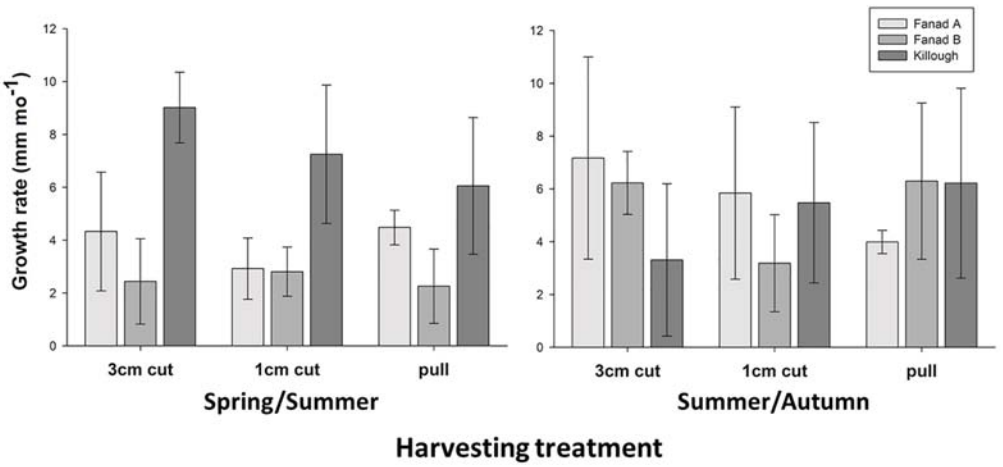

FIGURE 5 | Mean growth rates (mm mo^{-1}, ± SD) of coralline algae harvested by three different methods, in three different pools in interval 1 Spring/Summer (Killough: February–July; Fanad: March–August) and interval 2 Summer/Autumn (Killough: July–November; Fanad: August–November).

of harvesting *C. officinalis* turf were clearly seen in the first month after harvest, July 2010 (**Figure 6**, abundances on harvested alga compared with unharvested), though this only persisted beyond July in Isopoda. For the remainder of the experiment, harvesting the alga did not reduce the abundance of Tanaidacea and Nematoda in general (the pull and cut plots had the highest median abundance, respectively, in the majority of months). Caenogastropoda, Neogastropoda and Sabellidae showed variable abundances, with no discernible pattern. Depth of sample also played a role in the community changes (**Table 2**), though the only individual order on which this had a significant effect was Actinaria (anemones) (Dev = 19.228, $p = 0.002$).

Harvesting *C. officinalis* had no effect on invertebrate species richness (S) or evenness ($1-\lambda$), nor was there any harvest × month interaction (**Supplementary Material 9**). However, there was a significant effect of month on evenness ($p < 0.001$), suggesting strong seasonality in numbers for at least some of the groups of invertebrates.

Effects of Experimental Harvesting Treatments on Structural Components of the Habitat

Corallina officinalis and sediment mass were significantly affected by both harvesting and month (**Supplementary Material 10** and **Figure 7**). Although the *Corallina* biomass in the cut and pull harvested plots differed from the June 2010 unharvested baseline in most months (Tukey's HSD, $p = < 0.05$), the cut samples had recovered to pre-harvesting levels by July 2011 (after 1 year). Furthermore, biomass of the cut and pull harvested samples was not significantly different from the unharvested control plots in the same month at any time after July 2010 (the first month after harvest, at which time only the pull samples were different from the controls, **Figure 7A**; Tukey's HSD $p < 0.001$). This suggests that the unharvested biomass of *Corallina* decreased overall in the winter months and the baseline biomass recorded in June 2010 may have been a maximum.

The sediment mass in all plots in the winter months (October 2010; January 2011; and October 2011), and in the pull harvested samples in July 2010 and April 2011, was significantly different from the June 2010 baseline samples (**Figure 7B**; Tukey's HSD, $p < 0.05$). However, the only time in spring/summer that sediment mass differed between harvested and unharvested control samples within a month was in July 2010, a month after harvest, when the pull samples were significantly different from the controls (Tukey's HSD, $p = 0.001$). This strong influence of time of year on sediment mass in relation to harvested algae was indicated by the significant harvest × month interaction (**Supplementary Material 10**).

DISCUSSION

This study was designed to test the potential for sustainable harvesting of *Corallina officinalis* on Irish shores using three manual methods. Harvesting *C. officinalis* stimulated growth, so it can be argued that it is in principle a renewable resource. Regeneration of thalli was equally rapid after harvesting by both cutting and pulling techniques, and increased significantly relative to unharvested areas. In fact, a cut plot at Killough showed the highest reported growth rate for this species. The meristematic tissues of erect axes of *C. officinalis* are apical, so when the thallus tips are removed lateral branches below the damage continue to grow, in a process resembling apical dominance in plants. Shearing by grazing organisms, which would have a similar effect to cutting in this study, has been found to stimulate growth of *Corallina* sp. in Japan (Akioka et al., 1999). In addition to lateral growth of axes after cut harvesting, the perennial crustose holdfast gives rise to new *C. officinalis* uprights at long as it remains intact. Littler and Kauker (1984) found that complete removal of articulated fronds by pulling stimulated generation of new uprights from the crustose base. This rapid regeneration after upright thalli have been destroyed or truncated is not surprising given that

TABLE 2 | Results of multivariate test of change in assemblage structure followed by individual GLM results identifying taxa with significant or large effects.

Multivariate test

Predictor	Res. Df	Df. Diff	Dev	Pr (>Dev)
(Intercept)	89			
Harvest treatment	87	2	70.0	0.223
Month	82	5	433.4	**0.001***
Depth	81	1	65.7	**0.006***
Harvest × Month	70	10	396.6	**0.005***

Univariate tests

	Isopoda		Veneroida		Anaspidea	
	Dev	**Pr (>Dev)**	**Dev**	**Pr (>Dev)**	**Dev**	**Pr (>Dev)**
Harvest	7.101	0.711	1.601	0.998	3.892	0.980
Month	**55.511**	**0.001***	**49.463**	**0.001***	**38.317**	**0.001***
Depth	4.469	0.575	1.235	0.982	3.203	0.814
Harvest × Month	***24.77***	0.346	14.689	0.966	17.946	0.839
	Decapoda		**Podocopida**		**Nematoda**	
	Dev	**Pr (>Dev)**	**Dev**	**Pr (>Dev)**	**Dev**	**Pr (>Dev)**
Harvest	1.649	0.998	0.202	0.999	4.256	0.961
Month	**31.768**	**0.001***	**23.666**	**0.015***	**22.519**	**0.026***
Depth	0.801	0.996	0.002	0.999	0.535	0.996
Harvest × Month	13.967	0.976	16.258	0.919	***22.742***	0.424
	Actinaria		**Tanaidacea**		**Caenogastropoda**	
	Dev	**Pr (>Dev)**	**Dev**	**Pr (>Dev)**	**Dev**	**Pr (>Dev)**
Harvest	1.778	0.998	1.826	0.998	1.692	0.998
Month	14.898	0.290	13.563	0.388	3.47	0.988
Depth	19.228	**0.002***	5.229	0.457	0.127	0.999
Harvest × Month	12.799	0.994	***30.309***	0.108	***26.575***	0.235
	Neogastropoda		**Sabellidae**			
	Dev	**Pr (>Dev)**	**Dev**	**Pr (>Dev)**		
Harvest	0.501	0.999	2.679	0.994		
Month	4.385	0.988	3.226	0.988		
Depth	1.278	0.982	0.051	0.999		
Harvest × Month	***25.688***	0.286	***23.435***	0.424		

Taxa listed in order of effect size for a particular predictor. Large effects in bold, statistically significant effects in bold with. In the case of the Harvest × Month interaction, non-significant but large effects are in bold italics.*

C. officinalis has evolved in an environment where axes are frequently removed by wave action. It is likely that older heavily epiphytized axes add to the wave drag that results in their selective removal. This could be beneficial to the alga, like the loss of *Chondrus crispus* blades with heavy endophyte loads (Correa and McLachlan, 1992). This dual origin of new algal tissue (from axes and holdfast) means that harvesting *C. officinalis* either by cutting or pulling, methods which would be typical of commercial harvesting, ensures regeneration without the need for recruitment of new individuals. This is in marked contrast to *Laminaria* species, for example, which invariably die if the meristem between the stipe and blade is harvested (Birkett et al., 1998). Sustainable harvesting of these kelps requires expensive hand cutting above the meristem or depends on reliable recruitment of new individuals to bare patches created by mechanical harvesting (Smale et al., 2013).

After harvesting, *C. officinalis* had recovered its original thallus length through rapid regrowth by the date of the first measurement (4–6 months), but the speed of regeneration within this period is unknown. This means that it should be possible to harvest *C. officinalis* every 4–6 months, although growth rates

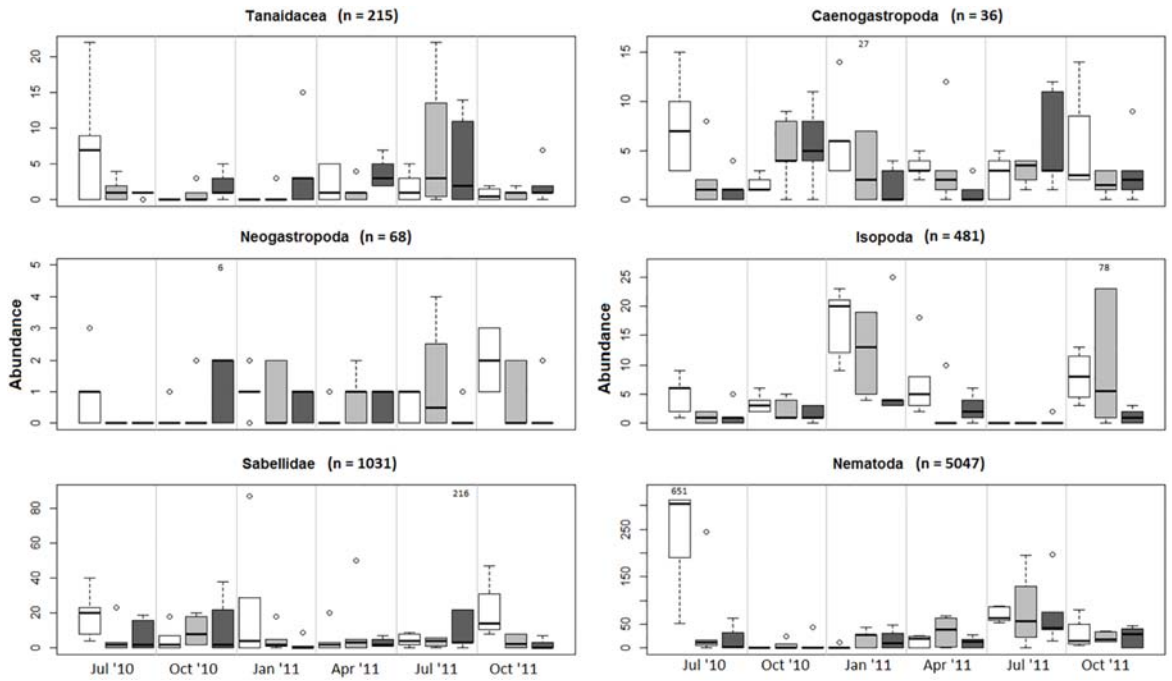

FIGURE 6 | Abundances plotted by harvesting method and month for the six groups with large Harvest × Month interaction effects (Dev = >20, **Table 2**). Effect of harvesting seen in all groups in the first month after harvest (July 2010). Extreme outliers are indicated on the plots. Note differing scales on y axes. Control, unshaded; Cut, light gray; Pull, dark gray. Line, median value; Box, 1st and 3rd quartiles; Whiskers, values falling within 1.5× range of quartiles; outliers are represented by open circles, extreme outlier values are marked.

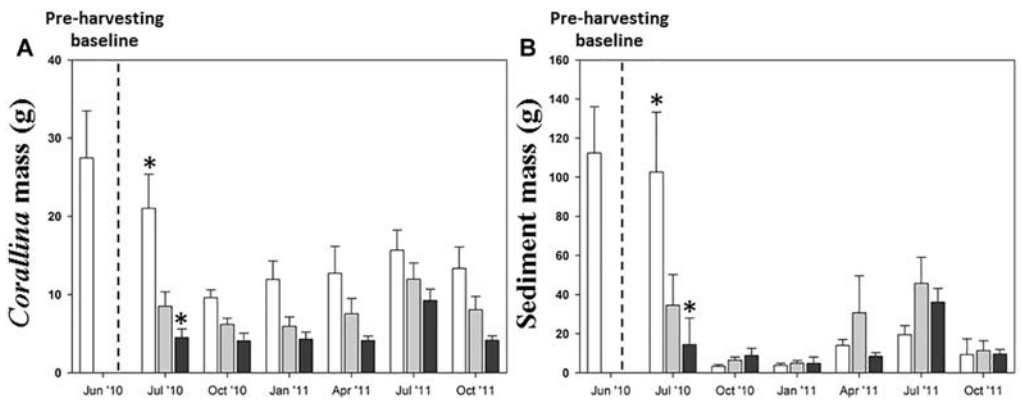

FIGURE 7 | (A) *Corallina* and **(B)** sediment mean mass (±SE) in experimental harvesting treatments (unharvested control, unshaded; cut, light gray; pull, dark gray). *Significant differences between treatments (Tukey's HSD, $p < 0.05$).

will vary with time of year and site. However, it should be noted that the experimentally harvested patches were small and uniform in size, and real harvesters would be more likely to intensively remove the alga from larger areas. The recovery of a system can depend on the size of the perturbation. In areas experimentally cleared of *Ascophyllum nodosum* on a sheltered shore in Maine, larger cleared areas (>2 m) were dominated over time (within 7 years) by either *Fucus vesiculosus* or *Mytilus edulis*, whereas smaller cleared areas returned to *A. nodosum* dominance within the same timeframe (Petraitis et al., 2009). However, as discussed above, regeneration of *C. officinalis* from holdfasts and cut axes does not require recruitment of new individuals, so the process is very different from that taking place after total clearance of fucoids, and it is possible that results would scale up from small quadrats to large patches. Nevertheless, long-term monitoring of the recovery of the *C. officinalis* turf percentage cover would be advisable. Older, larger coralline thalli produce more reproductive structures (conceptacles) than young, smaller thalli (Martone, 2010), and the effect of harvesting on recruitment of new individuals should

be a focus for further work on long-term harvesting effects on size of *C. officinalis* populations.

The complexity of the physical structure created by *C. officinalis* thalli has been shown to have a positive influence on the diversity and abundance of most fauna associated with the alga (Davenport et al., 1999; Kelaher, 2002). Although harvesting reduced the *C. officinalis* biomass, which remained lower than the controls throughout the study, the associated faunal community structure was not significantly affected by harvesting the alga. This suggests, in agreement with previous studies, and with the role of *C. officinalis* as an ecosystem engineer, that the complexity of the habitat, i.e., the amount of physical substratum provided by the algal fronds, was not the sole factor responsible for structuring the associated invertebrate community.

Recovery of the sediment, an important component of the *C. officinalis* habitat, revealed that harvested fronds may have trapped more sediment than unharvested thalli, due to the denser thallus matrix. As many of the organisms associated with the habitat use the sediment for food or building materials, this may have ameliorated the effects of harvesting on the community. *C. officinalis* grows from apices by elongation of meristematic cells (Matty and Johansen, 1981); if the main apices are removed by cutting, growth of branchlets continues. This can result in an increase in lower branching, as was found after shearing of thalli by grazers in Japan (Akioka et al., 1999). Likewise with the pull harvest, the short fronds initiated rapidly from the crustose holdfast (Littler and Kauker, 1984) may have trapped more sediment than long and foliose thalli. In accordance with observations by Bussell et al. (2007), shorter turf in shallower areas retains more sediment than the longer more mobile fronds in deeper areas. Reducing the length of fronds in deeper areas of the pool by harvesting could increase sediment accretion by reducing mobility of the thalli as well as increasing the density of branching. However, the nature of the sediment accreted can also change. After experimental harvesting of *A. nodosum* in Ireland, sediments were coarser, attributed to the change in hydrodynamic conditions with less dampening of turbulence by the long and buoyant fronds (Boaden and Dring, 1980).

Sediment provides construction material for tube-dwelling organisms such as tanaiids. When sediment was elevated in the harvested plots, in comparison with the unharvested, there was a marked increase in abundance of *Tanais dulongii* in comparison with the previous year. Female *T. dulongii* build their tubes from sediment at the base of *C. officinalis* fronds (Johnson and Attramadal, 1982) and the increase in *T. dulongii* on the harvested samples in the year after harvest may relate to the increased amount of sediment available in the plots, as suggested by Bueno et al. (2016) in Brazil. The amount of sediment in coralline algal turfs is positively correlated with the richness and abundance of gastropods (Kelaher et al., 2001; Kelaher and Castilla, 2005), and nematodes are generally found at higher densities in turf algae and sediment (Gibbons and Griffiths, 1986). Two groups of gastropods (Caenogastropoda and Neogastropoda) and nematodes had large effects sizes for the harvest × month interaction in this study. Caenogastropoda was composed of the grazing snail *Bittium reticulatum*, which is associated with sandy bottoms or sediment-rich compact algae (Sánchez-Moyano et al., 2000; Marriner et al., 2005), and Neogastropoda of small numbers of the predatory whelk *Nucella lapillus*, which probably use *C. officinalis* at pool edges as refuge from predatory decapods and desiccation at low tide (Burrows and Hughes, 1991). However, there was no clear pattern of change owing to harvesting in either group, with numbers in the unharvested and harvested plots fluctuating throughout the year. Nematodes mostly remain in the sediment (Armonies, 1988) where they feed by several different modes depending on the species: deposit feeding (including diatoms), predation, and scavenging (Jensen, 1987), and there was a striking similarity between the sediment and nematode abundance throughout the experiment, in terms both of seasonal fluctuation and harvesting treatment differences.

Evaluating the effects of harvesting on the community composition was a critical part of this research. Even immediately after harvesting, the invertebrate community associated with *C. officinalis* turfs was not significantly affected although there were some relatively large non-significant effects on some groups of invertebrates. This information coupled with the rapid regeneration of the resource itself strongly suggests that *C. officinalis* is a sustainable source of biogenic calcium carbonate. Previously, optimal harvesting intervals and methods have been determined for a range of species based only on regeneration time (Baardseth, 1970; Pringle and Sharp, 1980; Keser and Larson, 1984; Ang et al., 1996; Lazo and Chapman, 1997). There are very few examples of investigations of full community effects (e.g., *A. nodosum* in Ireland and New England), which are required for true sustainability studies. Boaden and Dring's (1980) study of communities when cutting *A. nodosum* to 18 cm had good taxonomic coverage (algae and invertebrates) but was limited to a single time period, 2.5 years after the cut. The significant differences they found in algae and some invertebrates were no longer evident 30 years after the harvest (Gregory, 2007). In Maine, United States, comparing the effects on the *A. nodosum* community of cutting at lengths of 18 and 36 cm showed that the community was resilient to a lower intensity disturbance (36 cm cut), recovering within 2 years (Fegley, 2011). Stagnol et al. (2015) reported varying results for species diversity of the communities associated with various harvested seaweed species in Brittany, following the effects for a total of 12 months. Another aspect of sustainability of harvesting natural resources is the effect on genetic diversity of the target species (Guillemin et al., 2014). Here, our preliminary study showed a high genetic diversity in *C. officinalis*, comparable to that in Galicia (Pardo et al., 2015), suggesting a lack of isolation and greater resilience to impacts including anthropogenic disturbance.

Potential new high-value products, ranging from pigments to proteins and polysaccharides, are constantly being developed from species of red seaweeds (Thomas and Kim, 2013). For some of these newly valuable red algae, wild harvests could be a possible source of biomass for extraction of the desired products. Although wild harvests cannot produce a high biomass of seaweeds in Europe, it might be feasible to wild-harvest

sufficient quantities of species that are sources of high-value biotechnological or pharmaceutical products. In order to ensure that commercial harvesting of a macroalgal resource is carried out in a sustainable manner, harvesting trials using different methods should be conducted to assess the effect of those methods on the target species (Vasquez, 1995; McLaughlin et al., 2006). However, *C. officinalis* is a biogenic-habitat-forming organism and ecosystem engineer (Crain and Bertness, 2006) and the communities associated with the *Corallina* turf cannot be omitted from an assessment of sustainability of harvest. Demonstrating the sustainability of harvesting *C. officinalis* in Ireland therefore required a broad approach to understanding the resource and its regeneration after harvesting, as well as the effects of harvesting on the associated invertebrate community.

AUTHOR CONTRIBUTIONS

CLM, CAM, NO'C, and MJ designed the study. CLM conducted the study. CLM and CAM wrote the manuscript.

FUNDING

This work was funded partly under the FP6-funded HIPPOCRATES project (NMP3-CT-2003-505758) and partly by the Department for Employment and Learning Northern Ireland under the Programme for Government initiative.

ACKNOWLEDGMENTS

We thank Dr. Charmaine Beer (DAERA), Prof. Fraser Buchanan (QUB), and Dr. Pamela Walsh (QUB) for their contributions to the fieldwork and work on bioceramics.

SUPPLEMENTARY MATERIAL

The Supplementary Material for this article can be found online at: https://www.frontiersin.org/articles/10.3389/fmars.2019.00285/full#supplementary-material

REFERENCES

Airoldi, L., and Beck, M. W. (2007). Loss, status and trends for coastal marine habitats of Europe. *Oceanogr. Mar. Biol.* 45, 345–405. doi: 10.1201/9781420050943.ch7

Akioka, H., Baba, M., Masaki, T., and Johansen, H. W. (1999). Rocky shore turfs dominated by *Corallina* (Corallinales, Rhodophyta) in northern Japan. *Phycol. Res.* 47, 199–206. doi: 10.1046/j.1440-1835.1999.00164.x

Andrake, W., and Johansen, H. W. (1980). Alizarin red dye as a marker for measuring growth in *Corallina officinalis* L. (Corallinaceae, Rhodophyta). *J. Phycol.* 16, 620–622. doi: 10.1111/j.0022-3646.1980.00620.x

Ang, P. O., Sharp, G. J., and Semple, R. E. (1996). Comparison of the structure of populations of *Ascophyllum nodosum* (Fucales, Phaeophyta) at sites with different harvesting histories. *Hydrobiologia* 326, 179–184. doi: 10.1007/bf00047804

Armonies, W. (1988). Active emergence of meiofauna from intertidal sediment. *Mar. Ecol. Prog. Ser.* 43, 151–159. doi: 10.3354/meps043151

Baardseth, E. (1970). Seasonal variation in *Ascophyllum nodosum* (L.) Le Jol. in the Trondheimsfjord with respect to the absolute live and dry weight and the relative contents of dry matter, ash and fruit bodies. *Bot. Mar.* 13, 13–22.

Berthelsen, A. K., and Taylor, R. B. (2014). Arthropod mesograzers reduce epiphytic overgrowth of subtidal coralline turf. *Mar. Ecol. Prog. Ser.* 515, 123–132. doi: 10.3354/meps11025

Birkett, D. A., Maggs, C. A., Dring, M. J., Boaden, P. J. S., and Seed, R. (1998). *Infralittoral Reef Biotopes with Kelp Species. An Overview of Dynamic and Sensitivity Characteristics for Conservation Management of Marine SACs*, Vol. VII. Oban: Scottish Association of Marine Science.

Blake, C., and Maggs, C. A. (2003). Comparative growth rates and internal banding periodicity of maerl species (Corallinales, Rhodophyta) from northern Europe. *Phycologia* 42, 606–612. doi: 10.2216/i0031-8884-42-6-606.1

Blunden, G., Binns, W. W., and Perks, F. (1975). Commercial collection and utilisation of maerl. *Econ. Bot.* 29, 141–145. doi: 10.1007/bf02863313

Boaden, P. J., and Dring, M. T. (1980). A quantitative evaluation of the effects of *Ascophyllum* harvesting on the littoral ecosystem. *Helgol. Meeresuntersuchungen* 33, 700–710. doi: 10.1007/bf02414790

Brodie, J., Walker, R. H., Williamson, C. J., and Irvine, L. M. (2013). Epitypification and redescription of *Corallina officinalis* L., the type of the genus, and *C. elongata* Ellis *et* Solander (Corallinales, Rhodophyta). *Cryptogam. Algol.* 34, 49–56. doi: 10.7872/crya.v34.iss1.2013.49

Brown, P. J., and Taylor, R. B. (1999). Effects of trampling by humans on animals inhabiting coralline algal turf in the rocky intertidal. *J. Exp. Mar. Biol. Ecol.* 235, 45–53. doi: 10.1016/s0022-0981(98)00186-5

Bueno, M., Dena-Silva, S. A., Flores, A. A. V., and Leite, F. P. P. (2016). Effects of wave exposure on the abundance and composition of amphipod and tanaidacean assemblages inhabiting intertidal coralline algae. *J. Mar. Biol. Assoc. U.K.* 96, 761–767.

Burrows, M. T., and Hughes, R. N. (1991). Variation in foraging behaviour among individuals and populations of dogwhelks, *Nucella lapillus*: natural constraints on energy intake. *J. Anim. Ecol.* 60, 497–514.

Bussell, J. A. (2003). *Biodiversity of the Invertebrate Community Associated with the Turf-forming Red Alga Corallina officinalis in Tide Pools*. Doctoral dissertation. Bangor: University of Wales.

Bussell, J. A., Lucas, I. A., and Seed, R. (2007). Patterns in the invertebrate assemblage associated with *Corallina officinalis* in tide pools. *J. Mar. Biol. Assoc. U.K.* 87, 383–388. doi: 10.1017/s0025315407055385

Chung, I. K., Sondak, C. F. A., and Beardall, J. (2017). The future of seaweed aquaculture in a rapidly changing world. *Eur. J. Phycol.* 52, 495–505. doi: 10.1080/09670262.2017.1359678

Clarke, S. A., Walsh, P., Maggs, C. A., and Buchanan, F. (2011). Designs from the deep: marine organisms for bone tissue engineering. *Biotechnol. Adv.* 29, 610–617. doi: 10.1016/j.biotechadv.2011.04.003

Clement, M., Posada, D., and Crandall, K. (2000). TCS: a computer program to estimate gene genealogies. *Mol. Ecol.* 9, 1657–1660.

Cole, V. J., Hutchings, P. A., and Ross, P. M. (2016). Predicting biodiversity changes due to loss of bioengineers from an intertidal landscape, a case study from Sydney Harbour. *Aust. Zool.* 39, 194–206. doi: 10.7882/AZ.2015.034

Colthart, B. J., and Johansen, H. W. (1973). Growth rates of *Corallina officinalis* (Rhodophyta) at different temperatures. *Mar. Biol.* 18, 46–49. doi: 10.1007/bf00347919

Correa, J. A., and McLachlan, J. L. (1992). Endophytic algae of *Chondrus crispus* (Rhodophyta). IV. Effects on the host following infections by *Acrochaete operculata* and *A. heteroclada* (Chlorophyta). *Mar. Ecol. Prog. Ser.* 81, 73–87. doi: 10.3354/meps081073

Couceiro, L., Robuchon, M., Destombe, C., and Valero, M. (2013). Management and conservation of the kelp species *Laminaria digitata*: using genetic tools to explore the potential exporting role of the MPA "*Parc naturel marin d'Iroise*". *Aqu. Living Resour.* 26, 197–205. doi: 10.1051/alr/2012027

Coull, B. C., and Wells, J. B. J. (1983). Refuges from fish predation: experiments with phytal meiofauna from the New Zealand rocky intertidal. *Ecology* 64, 1599–1609. doi: 10.2307/1937513

Crain, C. M., and Bertness, M. D. (2006). Ecosystem engineering across environmental gradients: implications for conservation and management. *Bioscience* 56, 211–218. doi: 10.1002/ece3.5040

Davenport, J., Butler, A., and Cheshire, A. (1999). Epifaunal composition and fractal dimensions of marine plants in relation to emersion. *J. Mar. Biol. Assoc. U.K.* 79, 351–355. doi: 10.1017/s0025315498000393

Dommasnes, A. (1968). Variations in the meiofauna of *Corallina officinalis* L. with wave exposure. *Sarsia* 34, 117–124. doi: 10.1080/00364827.1968.10413376

El Gamal, A. A. (2011). "Biological importance of marine algae," in *Handbook of Marine Macroalgae: Biotechnology and Applied Phycology*, ed. S. K. Kim (Hoboken, NJ: John Wiley and Sons), 3–27.

FAO (2003–2015). *Fisheries and Aquaculture topics. Ecosystems. Topics Fact Sheets*. Rome: FAO Fisheries and Aquaculture Department.

Fegley, J. C. (2001). *Ecological Implications of Rockweed, Ascophyllum nodosum* (L.) Le Jolis, harvesting. Ph.D. Thesis. Orono, ME: University of Maine.

Gibbons, M. J., and Griffiths, C. L. (1986). A comparison of macrofaunal and meiofaunal distribution and standing stock across a rocky shore, with an estimate of their productivities. *Mar. Biol.* 93, 181–188. doi: 10.1007/bf00508255

Gouy, M., Guindon, S., and Gascuel, O. (2010). SeaView version 4: a multiplatform graphical user interface for sequence alignment and phylogenetic tree building. *Mol. Biol. Evol.* 27, 221–224. doi: 10.1093/molbev/msp259

Gregory, L. (2007). *Assessments of Recovery 30 years After Algal (Ascophyllum nodosum) Harvesting at Rathcunningham Quay, Co. Down, Northern Ireland.* Belfast: Queen's University Belfast.

Guillemin, M. L., Valero, M., Faugeron, S., Nelson, W., and Destombe, C. (2014). Tracing the trans-Pacific evolutionary history of a domesticated seaweed (*Gracilaria chilensis*) with archaeological and genetic data. *PLoS One* 9:e114039. doi: 10.1371/journal.pone.0114039

Hall-Spencer, J. M. (2005). Ban on maerl extraction. *Mar. Pollut. Bull.* 50, 121–124.

Hall-Spencer, J. M., and Moore, P. G. (2000). Scallop dredging has profound, long-term impacts on maerl habitats. *ICES J. Mar. Sci.* 57, 1407–1415. doi: 10.1006/jmsc.2000.0918

Hayakawa, J., Kawamura, T., Kurogi, H., and Watanabe, Y. (2013). Shelter effects of coralline algal turfs: protection for *Turbo cornutus* juveniles from predation by a predatory gastropod and wrasse. *Fish. Sci.* 79, 15–20. doi: 10.1007/s12562-012-0569-2

Hicks, G. R. F. (1986). "Meiofauna associated with rocky shore algae," in *The Ecology of Rocky Coasts*, eds P. G. Moore and R. Seed (New York, NY: Columbia University Press), 36–56.

Huff, T. M. (2011). Effects of human trampling on macro-and meiofauna communities associated with intertidal algal turfs and implications for management of protected areas on rocky shores (Southern California). *Mar. Ecol.* 32, 335–345. doi: 10.1111/j.1439-0485.2011.00467.x

Irvine, L. M., and Chamberlain, Y. M. (eds) (1994). "Seaweeds of the British Isles Vol 1: Rhodophyta; Part 2B," *Corallinales, Hildenbrandiales* (London: HMSO).

Jensen, P. (1987). Feeding ecology of free-living aquatic nematodes. *Mar. Ecol. Prog. Ser.* 35, 187–196. doi: 10.1186/s13071-017-2030-y

Johnson, S. B., and Attramadal, Y. G. (1982). Reproductive behaviour and larval development of *Tanais cavolinii* (Crustacea: Tanaidacea). *Mar. Biol.* 71, 11–16. doi: 10.1007/bf00396987

Kasperk, C., Ewers, R., Simons, B., and Kasperk, R. (1988). Algae-derived (phycogene) hydroxylapatite: a comparative histological study. *Int. J. Oral Maxillofac. Surg.* 17, 319–324. doi: 10.1016/s0901-5027(88)80012-2

Kelaher, B. P. (2002). Influence of physical characteristics of coralline turf on associated macrofaunal assemblages. *Mar. Ecol. Prog. Ser.* 232, 141–148. doi: 10.3354/meps232141

Kelaher, B. P., and Castilla, J. C. (2005). Habitat characteristics influence macrofaunal communities in coralline turf more than mesoscale coastal upwelling on the coast of Northern Chile. *Estuar. Coast. Shelf Sci.* 63, 155–165. doi: 10.1016/j.ecss.2004.10.017

Kelaher, B. P., Chapman, M. G., and Underwood, A. J. (2001). Spatial patterns of diverse macrofaunal assemblages in coralline turf and their associations with environmental variables. *J. Mar. Biol. Assoc. U.K.* 81, 917–930. doi: 10.1017/s0025315401004842

Keser, M., and Larson, B. R. (1984). Colonization and growth of *Ascophyllum nodosum* (Phaeophyta) in Maine. *J. Phycol.* 20, 83–87. doi: 10.1111/j.0022-3646.1984.00083.x

Kim, S. K., and Chojnacka, K. (eds) (2015). *Marine Algae Extracts: Processes, Products, and Applications*, Vol. 2. Hoboken, NJ: John Wiley and Sons.

Lazo, L., and Chapman, A. R. O. (1997). Effects of harvesting on *Ascophyllum nodosum* (L.) Le Jol. (Fucales, Phaeophyta): a demographic approach. *Oceanogr. Literat. Rev.* 4:385.

Littler, M. M., and Kauker, B. J. (1984). Heterotrichy and survival strategies in the red alga *Corallina officinalis* L. *Bot. Mar.* 27, 37–44.

Mac Monagail, M., Cornish, L., Morrison, L., Araújo, R., and Critchley, A. T. (2017). Sustainable harvesting of wild seaweed resources. *Eur. J. Phycol.* 52, 371–390. doi: 10.1080/09670262.2017.1365273

Marriner, N., Morhange, C., Boudagher-Fadel, M., Bourcier, M., and Carbonel, P. (2005). Geoarchaeology of Tyre's ancient northern harbour, Phoenicia. *J. Archaeol. Sci.* 32, 1302–1327. doi: 10.1016/j.jas.2005.03.019

Martone, P. T. (2010). Quantifying growth and calcium carbonate deposition of *Calliarthron cheilosporioides* (Corallinales, Rhodophyta) in the field using a persistent vital stain. *J. Phycol.* 46, 13–17. doi: 10.1111/j.1529-8817.2009.00770.x

Matty, P. J., and Johansen, H. W. (1981). A histochemical study of *Corallina officinalis* (Rhodophyta, Corallinaceae). *Phycologia* 20, 46–55. doi: 10.2216/i0031-8884-20-1-46.1

McLaughlin, E., Kelly, J., Birkett, D., Maggs, C., and Dring, M. (2006). *Assessment of the Effects of Commercial Seaweed Harvesting on Intertidal and Subtidal Ecology in Northern Ireland*. Environment and Heritage Service Research and Development Series, 1–90.

Meland, M., and Rebours, C. (2012). Introduction to the management and regulation of Norwegian seaweed industry. *Bioforsk Fokus* 7, 275–277.

Mesnildrey, L., Jacob, C., Frangoudes, K., Reunavot, M., and Lesueur, M. (2012). *Seaweed Industry in France. Report Interreg Program NETALGAE*. Rennes: Agrocampus Ouest. 34.

Millar, R. B., and Anderson, M. J. (2004). Remedies for pseudoreplication. *Fish. Res.* 70, 397–407. doi: 10.1016/j.fishres.2004.08.016

Moorhouse, T. P., Poole, A. E., Evans, L. C., Bradley, D. C., and Macdonald, D. W. (2014). Intensive removal of signal crayfish (*Pacifastacus leniusculus*) from rivers increases numbers and taxon richness of macroinvertebrate species. *Ecol. Evol.* 4, 494–504. doi: 10.1002/ece3.903

Morrissey, J., Kraan, S., and Guiry, M. (2001). *A Guide to Commercially Important Seaweeds on the Irish Coast*. Dublin: Bord Iascaigh Mhara.

Munda, I. (1977). A comparison of the north- and south-European associations of *Corallina officinalis*. *Hydrobiologia* 52, 73–87. doi: 10.1007/bf02658084

Nelson, W. A. (2009). Calcified macroalgae–critical to coastal ecosystems and vulnerable to change: a review. *Mar. Freshw. Res.* 60, 787–801.

Nielsen, B. D., Ryan, E. C., and O'Connor-Robison, C. I. (2011). "A marine mineral supplement for Aquacid^{TM}," in *Applied Equine Nutrition and Training*, ed. A. Lindner (Wageningen: Wageningen Academic Publishers).

O'Toole, E., and Hynes, S. (2014). "An Economic Analysis of the Seaweed Industry," in *Proceedings of the SEMRU Working Paper*, (Galway).

Pardo, C., Pena, V., Barreiro, R., and Bárbara, I. (2015). A molecular study of *Corallina* sensu lato (Corallinales, Rhodophyta) in the Atlantic Iberian Peninsula. *Cryptogam. Algol.* 36, 31–54. doi: 10.7872/crya.v36.iss1.2015.31

Perkins, R. G., Williamson, C. J., Brodie, J., Barillé, L., Lavaud, J., Yallop, M. L., et al. (2016). Microspatial variability in community structure and photophysiology of calcified macroalgal microbiomes revealed by coupling of hyperspectral and high-resolution fluorescence imaging. *Sci. Rep.* 6:22343. doi: 10.1038/srep22343

Petraitis, P. S., Methratta, E. T., Rhile, E. C., Vidargas, N. A., and Dudgeon, S. R. (2009). Experimental confirmation of multiple community states in a marine ecosystem. *Oecologia* 161, 139–148. doi: 10.1007/s00442-009-1350-9

Pringle, J. D., and Sharp, G. J. (1980). Multispecies resource management of economically important marine plant communities of eastern Canada. *Helgol. Meersunters* 33, 711–720. doi: 10.1007/bf02414791

R Core Team (2015). *R: A Language and Environment for Statistical Computing*. Vienna: R Foundation for Statistical Computing.

Rebours, C., Marinho-Soriano, E., Zertuche-González, J. A., Hayashi, L., Vásquez, J. A., Kradolfer, P., et al. (2014). Seaweeds: an opportunity for wealth and sustainable livelihood for coastal communities. *J. Appl. Phycol.* 26, 1939–1951. doi: 10.1007/s10811-014-0304-8

Reed, M. S. (1907). *The Economic Seaweeds of Hawaii and their Food Value*. Washington, DC: US Government Printing Office.

Rocha, D., Seca, A., and Pinto, D. (2018). Seaweed secondary metabolites in vitro and in vivo anticancer activity. *Mar. Drugs* 16, 410. doi: 10.3390/md16110410

Ryan, S., O'Gorman, D. M., and Nolan, Y. M. (2011). Evidence that the marine-derived multi-mineral Aquamin has anti-inflammatory effects on cortical glial-enriched cultures. *Phytother. Res.* 25, 765–767. doi: 10.1002/ptr.3309

Sánchez-Moyano, J. E., Estacio, F. J., García-Adiego, E. M., and García-Gómez, J. C. (2000). The molluscan epifauna of the alga *Halopteris scoparia* in Southern Spain as a bioindicator of coastal environmental conditions. *J. Molluscan Stud.* 66, 431–448. doi: 10.1093/mollus/66.4.431

Saunders, G. W. (2005). Applying DNA barcoding to red macroalgae: a preliminary appraisal holds promise for future applications. *Philos. Trans. R. Soc. B* 360, 1879–2188.

Smale, D. A., Burrows, M. T., Moore, P., O'Connor, N., and Hawkins, S. J. (2013). Threats and knowledge gaps for ecosystem services provided by kelp forests: a northeast Atlantic perspective. *Ecol. Evol.* 3, 4016–4038. doi: 10.1002/ece3.774

Stagnol, D., Renaud, M., and Davoult, D. (2015). Unravelling the impact of harvesting pressure on canopy-forming macroalgae. *Mar. Freshw. Res.* 67, 153–161.

Stewart, J. G. (1982). Anchor species and epiphytes in intertidal algal turf. *Pac. Sci.* 36, 45–59.

Strain, E. M. A., Allcock, A. L., Goodwin, C. E., Maggs, C. A., Picton, B. E., and Roberts, D. (2012). The long-term impacts of fisheries on epifaunal assemblage function and structure, in a special area of conservation. *J. Sea Res.* 67, 58–68. doi: 10.1016/j.seares.2011.10.001

Thomas, N., and Kim, S. K. (2013). Beneficial effects of marine algal compounds in cosmeceuticals. *Mar. Drugs* 11, 146–164. doi: 10.3390/md11010146

Turhani, D., Cvikl, B., Watzinger, E., Weissenbock, M., Yerit, K., Thurnher, D., et al. (2005). In vitro growth and differentiation of osteoblast-like cells on hydroxyapatite ceramic granule calcified from red algae. *J. Oral Maxillofac. Surg.* 63, 793–799. doi: 10.1016/j.joms.2005.02.015

Vasquez, J. A. (1995). Ecological effects of brown seaweed harvesting. *Bot. Mar.* 38, 251–258.

Walker, G., Buchanan, F., Walsh, P., Dring, M., and Maggs, C. (2007). International patent application no. "PCT/GB2007/001844.

Walker, R. H., Brodie, J., Russell, S., Irvine, L. M., and Orfanidis, S. (2009). Biodiversity of coralline algae in the northeastern Atlantic including *Corallina caespitosa* sp. nov. (Corallinoideae, Rhodophyta). *J. Phycol.* 45, 287–297. doi: 10.1111/j.1529-8817.2008.00637.x

Walsh, P. J., Buchanan, F. J., Dring, M., Maggs, C., Bell, S., and Walker, G. M. (2008). Low-pressure synthesis and characterisation of hydroxyapatite derived from mineralised red algae. *Chem. Eng. J.* 137, 173–179. doi: 10.1016/j.cej.2007.10.016

Walsh, P. J., Walker, G. M., Maggs, C. A., and Buchanan, F. J. (2010). Thermal preparation of highly porous calcium phosphate bone filler. *J. Mater. Sci.* 21, 2281–2286. doi: 10.1007/s10856-010-4056-y

Walsh, P. J., Walker, G. M., Maggs, C. A., and Buchanan, F. J. (2011). A study of the relationship between process conditions and mechanical strength of mineralised red algae in the preparation of a marine-derived bone void filler. *Proc. Instit. Mech. Eng. Part H* 225, 563–574. doi: 10.1177/0954411910396306

Wang, Y., Naumann, U., Wright, S., and Warton, D. (2015). *mvabund: Statistical Methods for Analysing Multivariate Abundance Data. R package version 3.10.4*. Available at: http://CRAN.R-project.org/package=mvabund

Warton, D. I., Foster, S. D., De'ath, G., Stoklosa, J., and Dunstan, P. K. (2015). Model-based thinking for community ecology. *Plant Ecol.* 216, 669–682. doi: 10.1007/s11258-014-0366-3

Williamson, C. J., Walker, R. H., Robba, L., Yesson, C., Russell, S., Irvine, L. M., et al. (2015). Toward resolution of species diversity and distribution in the calcified red algal genera *Corallina* and *Ellisolandia* (Corallinales, Rhodophyta). *Phycologia* 54, 2–11. doi: 10.2216/14-024.1

Wilson, S., Blake, C., Berges, J. A., and Maggs, C. A. (2004). Environmental tolerances of free-living coralline algae (maerl): implications for European conservation. *Biol. Conserv.* 120, 283–293.

WoRMS Editorial Board (2015). *World Register of Marine Species*. Available at: http://www.marinespecies.org at VLIZ. (accessed November 15, 2016)

Yang, L.-E., Lu, Q.-Q., and Brodie, J. (2017). A review of the bladed Bangiales (Rhodophyta) in China: history, culture and taxonomy. *Eur. J. Phycol.* 52, 251–263. doi: 10.1080/09670262.2017.1309689

Conflict of Interest Statement: The authors declare that the research was conducted in the absence of any commercial or financial relationships that could be construed as a potential conflict of interest.

Copyright © 2019 Magill, Maggs, Johnson and O'Connor. This is an open-access article distributed under the terms of the Creative Commons Attribution License (CC BY). The use, distribution or reproduction in other forums is permitted, provided the original author(s) and the copyright owner(s) are credited and that the original publication in this journal is cited, in accordance with accepted academic practice. No use, distribution or reproduction is permitted which does not comply with these terms.

frontiers in Marine Science

ORIGINAL RESEARCH
published: 26 March 2019
doi: 10.3389/fmars.2019.00150

pH Variability Exacerbates Effects of Ocean Acidification on a Caribbean Crustose Coralline Alga

Maggie D. Johnson[1,2,3], Lucia M. Rodriguez Bravo[1], Shevonne E. O'Connor[4], Nicholas F. Varley[5] and Andrew H. Altieri[1,6]*

[1] Smithsonian Tropical Research Institute, Panama City, Panama, [2] Smithsonian Marine Station, Fort Pierce, FL, United States, [3] Tennenbaum Marine Observatories Network, Smithsonian Institution, Edgewater, MD, United States, [4] Mount Holyoke College, South Hadley, MA, United States, [5] Department of the Geophysical Sciences, University of Chicago, Chicago, IL, United States, [6] Department of Environmental Engineering Sciences, University of Florida, Gainesville, FL, United States

Crustose coralline algae (CCA) are among the most sensitive marine taxa to the pH changes predicted with ocean acidification (OA). However, many CCA exist in habitats where diel cycles in pH can surpass near-future OA projections. The prevailing theory that natural variability increases the tolerance of calcifiers to OA has not been widely tested with tropical CCA. Here, we assess the response of the reef-building species *Lithophyllum congestum* to stable and variable pH treatments, including an ambient control (amb/stable). The amb/variable treatment simulated an ambient diel cycle in pH (7.65–7.95), OA/stable simulated constant low pH reflecting worst-case year 2100 predictions (7.7), and OA/variable combined diel cycling with lower mean pH (7.45–7.75). We monitored the effects of pH on total calcification rate and photophysiology (maximum quantum yield) over 16 weeks. To assess the potential for acclimatization, we also quantified calcification rates during the first (0–8 weeks), and second (8–16 weeks) halves of the experiment. Calcification rates were lower in all pH treatments relative to ambient controls and photophysiology was unaffected. At the end of the 16-week experiment, total calcification rates were similarly low in the amb/variable and OA/stable treatment (27–29%), whereas rates declined by double in the OA/variable treatment (60%). When comparing the first and second halves of the experiment, there was no acclimatization in stable treatments as calcification rates remained unchanged in both the amb/stable and OA/stable treatments. In contrast, calcification rates deteriorated between periods in the variable treatments: from a 16–47% reduction in the amb/variable treatment to a 49–79% reduction in the OA/variable treatment, relative to controls. Our findings provide compelling evidence that pH variability can heighten CCA sensitivity to reductions in pH. Moreover, the decline in calcification rate over time directly contrasts prevailing theory that variability inherently increases organismal tolerances to low pH, and suggests that mechanisms of tolerance may become limited with increasing time of exposure. The significant role of diel pH cycling in CCA responses to OA indicates that organisms in habitats with diel variability could respond more severely to rapid changes in ocean pH associated with OA than predicted by experiments conducted under static conditions.

Keywords: calcification, diel variability, global change, *Lithophyllum congestum*, pH, photophysiology

OPEN ACCESS

Edited by:
Nick Kamenos, University of Glasgow, United Kingdom

Reviewed by:
Heidi L. Burdett, The Lyell Centre, United Kingdom
Sophie J. McCoy, Florida State University, United States

****Correspondence:***
Maggie D. Johnson
johnsonmd4@si.edu

Specialty section:
This article was submitted to Marine Ecosystem Ecology, a section of the journal Frontiers in Marine Science

Received: *17 November 2018*
Accepted: *08 March 2019*
Published: *26 March 2019*

Citation:
Johnson MD, Rodriguez Bravo LM, O'Connor SE, Varley NF and Altieri AH (2019) pH Variability Exacerbates Effects of Ocean Acidification on a Caribbean Crustose Coralline Alga. Front. Mar. Sci. 6:150. doi: 10.3389/fmars.2019.00150

INTRODUCTION

Ocean acidification (OA) is a leading global threat to the persistence of coral reefs and other calcifier-dominated marine habitats (Hoegh-Guldberg et al., 2007). Calcification by foundational taxa is essential to healthy habitat structure and ecosystem function (Vargas-Angel et al., 2015; Edmunds et al., 2016; Smith et al., 2016), but decreasing ocean pH, and the associated changes in seawater carbon chemistry, impair calcification of reef-building corals and algae (Kroeker et al., 2010). Crustose coralline algae (CCA) are important ecosystem engineers in a variety of nearshore marine habitats (McCoy and Kamenos, 2015), including coral reefs, where they help build the three-dimensional carbonate framework of the reef, and stabilize the reef matrix via calcification (Bosence, 1985; Adey, 1998). However, they also secrete the most soluble polymorph of $CaCO_3$ (high-Mg calcite) and are highly vulnerable to changes in carbonate chemistry associated with OA (McCoy and Kamenos, 2015). Negative effects of OA that result in decreased calcification rates or increased dissolution of CCA jeopardize the reef habitat framework and affiliated species (Eyre et al., 2014; Comeau et al., 2016).

Near-future OA models are based on the open ocean (Duarte et al., 2013), where rates of change in environmental conditions are relatively gradual and invariable over time (Hofmann et al., 2011). Until recently, the majority of perturbation experiments have used this as a basis for simulating OA with constant low pH treatments. However, many benthic organisms, including tropical CCA, inhabit nearshore ecosystems where environmental conditions, including pH, fluctuate over multiple temporal scales (Takeshita et al., 2018). In these habitats, biophysical coupling between metabolism (e.g., photosynthesis and respiration) and physical properties of the water column can cause pH to fluctuate on a diel cycle (Kleypas et al., 2011). Photosynthetic depletion of CO_2 increases pH during the day, release of CO_2 through respiration decreases pH at night, and the magnitude of this cycle can be shaped by water residence time and community biomass (Duarte et al., 2013). In ecosystems dominated by photosynthetic organisms (e.g., coral reefs and seagrass meadows), the range of diel changes in pH can exceed the difference between current conditions and end-of-century OA projections for the open ocean (Hofmann et al., 2011; Duarte et al., 2013). *In situ* pH manipulations, such as free ocean carbon enrichment (FOCE) experiments (Kline et al., 2012) and studies using natural gradients in pH (e.g., CO_2 vents and tide pools), have shed light the potential for natural variability to influence organismal and community-scale responses to pH reductions (Kroeker et al., 2013; Noisette et al., 2013; Stark et al., 2019). These experiments demonstrate how pH variability can influence the structure and trajectory of calcifier-dominated ecosystems (Kroeker et al., 2013) and can mediate the response of calcifiers to changes in mean pH (Georgiou et al., 2015). Applying this approach to manipulative experiments, by incorporating local-scale pH variability into pH treatments, is a necessary step toward improving the predictive power and ecological relevance of laboratory perturbation experiments to nearshore ecosystems (Rivest et al., 2017; Vargas et al., 2017).

Exposure to environmental variability can increase organismal tolerances to subsequent environmental stress (Boyd et al., 2016) by facilitating phenotypic plasticity (i.e., acclimatization) or genotypic variation (i.e., adaptation) (van Oppen et al., 2015). An example of this environmental variability-stress acclimatization theory includes corals exposed to thermal variability that bleach less when faced with subsequent exposure to temperature extremes (Mayfield et al., 2012). pH variability is likewise proposed to increase organismal tolerances to OA (Anthony et al., 2011; Duarte et al., 2013; Vargas et al., 2017). If pH variability leads to enhanced tolerance to acidified conditions, it would have important implications for the response of sensitive taxa, such as CCA, and the functioning of marine communities, to near-future OA. However, this hypothesis has not yet been widely tested with tropical calcified algae (except see Johnson et al., 2014a; Cornwall et al., 2018). Alternatively, organisms from high variability habitats that are already surviving at their upper physiological limits may be less resilient to further environmental stress. While our knowledge of environmental drivers of genetic and phenotypic adaptation is relatively advanced for tropical corals (Palumbi et al., 2014), we know little about whether there is similar potential for CCA to acclimatize or adapt to environmental stress. Quantifying how environmental variability shapes organismal responses to OA is essential for understanding the effects of OA in an ecologically relevant context, to elucidating the environmental factors that influence species and habitat-specific sensitivities to OA, and to improving our ability to predict ecosystem trajectories in response to OA.

Results from a handful of studies demonstrate that tropical CCA have the potential to acclimatize to past and present exposure to pH stress following exposure to pH variability. For example, a temperate CCA from a high variability site was resistant to subsequent exposure to stable low pH (Padilla-Gamiño et al., 2016). Likewise, tropical corallines with a history of exposure to high pH variability calcified more under moderate pH variability (simulating ambient pH variability) than corallines with a history of exposure to low pH variability (Johnson et al., 2014a; Cornwall et al., 2018). These two studies found that prior exposure to pH variability did not increase calcification under stable OA conditions, thus support for the hypothesis that pH variability increases tolerance to OA is mixed, at best, for tropical CCA. Conversely, some temperate coralline algae from tide pools with a highly variable pH regime were not more tolerant to OA than those from a stable pH regime (Noisette et al., 2013). Moreover, CCA may be more sensitive to pH variability, in the context of rapid and acute pH reductions that simulate upwelling or carbon capture and release, than to chronic low pH exposure (Kamenos et al., 2013). Collectively, these studies demonstrate that some corallines possess the potential to acclimatize to environmental conditions, that pH variability influences CCA calcification, and that prior exposure to variability may facilitate acclimatization. They also indicate that variability does not inherently increase tolerances to mean reductions in pH. The limited number of studies and conflicting results make it difficult to disentangle the role of exposure to pH variability in shaping CCA responses to OA. As a result, it is unclear if tropical CCA fit the environmental variability-stress

acclimatization theory that pH variability increases tolerances to OA (Anthony et al., 2011).

Though we have a cursory understanding of potential effects of pH variability on coralline calcification, less is known about potential interactions of OA with diel pH cycling. Only one study, to date, has tested the combined effects of lower mean pH (OA) with simultaneous exposure to diel pH variability in tropical CCA (Cornwall et al., 2018). This study found that variability superimposed on OA had no negative effects on net calcification in the tropical coralline *Hydrolithon reinboldii*, despite the increased time spent at extreme low pH. Corallines can demonstrate species-specific responses to OA (Johnson et al., 2014b; Comeau et al., 2018) that could be linked to physiological control over calcification (Cornwall et al., 2018). Though some CCA appear to control intracellular carbonate chemistry at the site of calcification (Cornwall et al., 2017), the degree of control may influence their calcification response to OA and may vary by species (Comeau et al., 2018; Cornwall et al., 2018). The potential interactions of OA, diel variability, and species-specific susceptibilities to changing pH, among other confounding factors, are highly complex. More work is needed to understand the potential effects of OA on tropical CCA in habitats with diel pH cycling.

To address these gaps, we exposed a common reef-building CCA (*Lithophyllum congestum*) to a combination of stable and variable pH treatments. We tested the hypotheses that exposure to pH variability increases the tolerance of a tropical CCA to OA and that OA combined with pH variability synergistically decreases CCA calcification. We quantified the effects of stable and variable pH on coralline net calcification rates and photophysiology after 16 weeks of exposure to these treatments. Additionally, we quantified calcification rates in the first and second 8-weeks of this period to explore the potential for acclimatization to different pH regimes. This approach allowed us to partition calcification rates into a total net response (0–16 weeks), an initial response (0–8 weeks), and a potential acclimatization response (8–16 weeks). By incorporating diel pH variability into an OA framework, we increase the relevance of our results to nearshore, environmentally variable ecosystems, and provide insight into the potential compounding effects of diel pH cycling and OA on a reef-builder with critical importance to coral reef ecosystems.

MATERIALS AND METHODS

Specimen Collection

Lithophyllum congestum is a heavily calcified crustose coralline alga that produces stout, blunt branches (**Figure 1**), and is an abundant framework builder on shallow coral reefs throughout the Caribbean (Adey, 1978). Fragments of *L. congestum* were collected at 3 m in Bahía Almirante in the Bocas del Toro archipelago off the Caribbean coast of Panamá. Specimens were collected with diagonal cutters and returned to the Smithsonian Tropical Research Institute (STRI), where they were maintained under ambient light and flow-through seawater until the start of the experiment. Fragments were cleaned of epiphytes with tweezers and attached to plastic Vexar bases with underwater epoxy (Aquamend), oriented with branch tips facing up. Exposed non-living carbonate underneath and around the base of fragments was coated with epoxy to prevent dissolution in acidification treatments. Specimens were allowed to recover from collection for 4 days in ambient light (282 $\pm$ 6 μmol photon m^{-2} s^{-1}) and flow-through seawater (29.0 $\pm$ 0.5°C). Fragments were monitored for epiphytic growth every 3 days for the duration of the experiment and, when necessary, cleaned with a soft-bristle brush and tweezers.

Experimental Design

Our experiment was conducted in the temperature controlled aquarium facilities at STRI's Bocas del Toro Research Station (BRS) in Panamá from June – September 2017. *L. congestum* fragments were exposed to one of the following 4 pH treatments for the 16-week experiment: ambient/stable (amb/stable), ambient/variable (amb/variable), OA/stable, and OA/variable. The amb/stable treatment consisted of seawater pumped from a depth of 3 m near the STRI dock and passed through a 50 μm filter in the BRS seawater line. The variable treatments simulated a 0.3 unit diel cycle in pH, with highest pH during peak daylight hours, and lowest pH at the end of the night. This represents daily changes in pH due to photosynthesis during the day and respiration during the night (Rivest et al., 2017; Takeshita et al., 2018). In the amb/variable treatment, pH ranged from 7.65 to 7.95 over 24 h, simulating a moderate diel cycle in pH that is characteristic on some shallow coral reefs (Hofmann et al., 2011; Price et al., 2012; Guadayol et al., 2014). Further, these conditions approximate the pH regime at the collection site, where daily mean (±SE) pH is 7.98 $\pm$ 0.006, minimum is 7.88, and maximum is 8.03 (Johnson, unpublished data). In the OA/stable treatment, pH was maintained at ∼7.70, simulating conditions projected in representative concentration pathway (RCP) 8.5 for the year 2100 (Hartin et al., 2016). pH ranged from 7.45 to 7.75 in the OA/variable treatment, superimposing the 0.3 unit diel cycle in pH over a lower mean pH and simulating potential conditions in nearshore habitats if reductions in pH associated with OA are overlaid with natural diel pH cycles. At the start of the experiment pH was gradually decreased by 0.05 units per day until treatment levels were reached, in order to minimize shock of rapid environmental change.

Experimental replicates were 2.8 L plastic tanks containing 3 *L. congestum* fragments, with 6 replicate tanks per treatment. Each tank received a continuous supply of ambient or treatment seawater at 15.7 mL min^{-1}. Ambient seawater was plumbed from the BRS seawater line into each amb/stable tank. The pH of treatment seawater was manipulated in one of three reservoir tanks and then pumped into respective treatment tanks. Water was circulated in each tank with a small aquarium pump (300 L hr^{-1}). Treatments were assigned randomly to tanks and tanks were shuffled haphazardly every 2–3 days to reduce the potential for positional effects (due to lighting or other unforeseen positional factors).

Temperature was maintained by controlling the ambient air temperature of the experimental room, set to 28°C. Lighting was provided by 8, 7-color LED lights (Hydra52, AquaIllumination).

FIGURE 1 | Fragments of *Lithophyllum congestum*, a common reef-building crustose coralline alga on Caribbean coral reefs, were collected from a shallow coral reef in Bocas del Toro, Panamá and exposed to a combination of stable and variable pH treatments for 16-weeks. Though a coral is pictured alongside the CCA *in situ*, the fragments used in the experiment were comprised solely of *L. congestum*.

Lights were programmed to a 12:12 h photoperiod (0600–1800). Lights ramped up to maximum intensity over 4 h starting with sunrise and then ramped down starting 4 h before sunset. Peak midday irradiance mirrored photosynthetically active radiation (PAR) measured at the collection site and depth (∼270 μmol photon m^{-2} s^{-1}). *In situ* irradiance was measured over one peak period on a sunny day with a LiCor meter (Li1400) and underwater cosine sensor (Li-193). During the experiment, light levels were measured between 1000 and 1400 (period of maximum intensity). Though light levels remained constant for the duration of the experiment, we measured light every 2–3 days when tanks were repositioned to avoid potential effects of tank position in relation to light sources.

pH Manipulation and Carbonate Chemistry

Treatment pH was manipulated in 75-L reservoir tanks with pure CO_2 and a pH feedback system. Each reservoir received a continuous supply of filtered, ambient seawater, with flow controlled by an automated float valve. pH was measured every minute in each reservoir with a lab-grade pH probe (Neptune), calibrated weekly with NBS buffers (7, 10) following factory protocol. Probes were connected to an Apex aquacontroller (Neptune) and solenoid valves, set to maintain pH within 0.1 of a target value. When pH increased above the set value, the solenoid valve opened and released pure CO_2 until pH decreased to the set value. Diffusion of CO_2 in each reservoir was facilitated by an aquarium pump (1600 L hr^{-1}) fitted with a venturi injector. Treatment water was pumped from each reservoir into respective treatment tanks with a separate aquarium pump. pH measurements from Neptune probes were cross-calibrated with daily, discrete pH measurements (described below). Settings were adjusted to maintain target pH conditions on the total scale (pH_T). pH variability was established by programming the aquacontroller with incremental changes in the target values over a diel cycle. pH_T in the variable treatments fluctuated by ∼0.3 units over a diel cycle throughout the experiment, while pH_T in the amb/stable and OA/stable treatments was held constant at ∼8.04 and ∼7.70, respectively (**Figure 2**).

Tank conditions were monitored daily between 0930 and 1030. pH was measured in each tank with a glass triode (Ross Ultra) connected to a pH meter (Orion Star) and calibrated with certified Tris buffer in synthetic seawater (Batch T30, A. Dickson). Temperature measurements were taken simultaneously with a traceable digital thermometer (Thomas Traceable Kangaroo). Salinity was measured every 2–3 days in reservoir tanks with a handheld YSI (YSI-63). Salinity of treatment tanks matched salinity of reservoir tanks due to high flow rates from the reservoir.

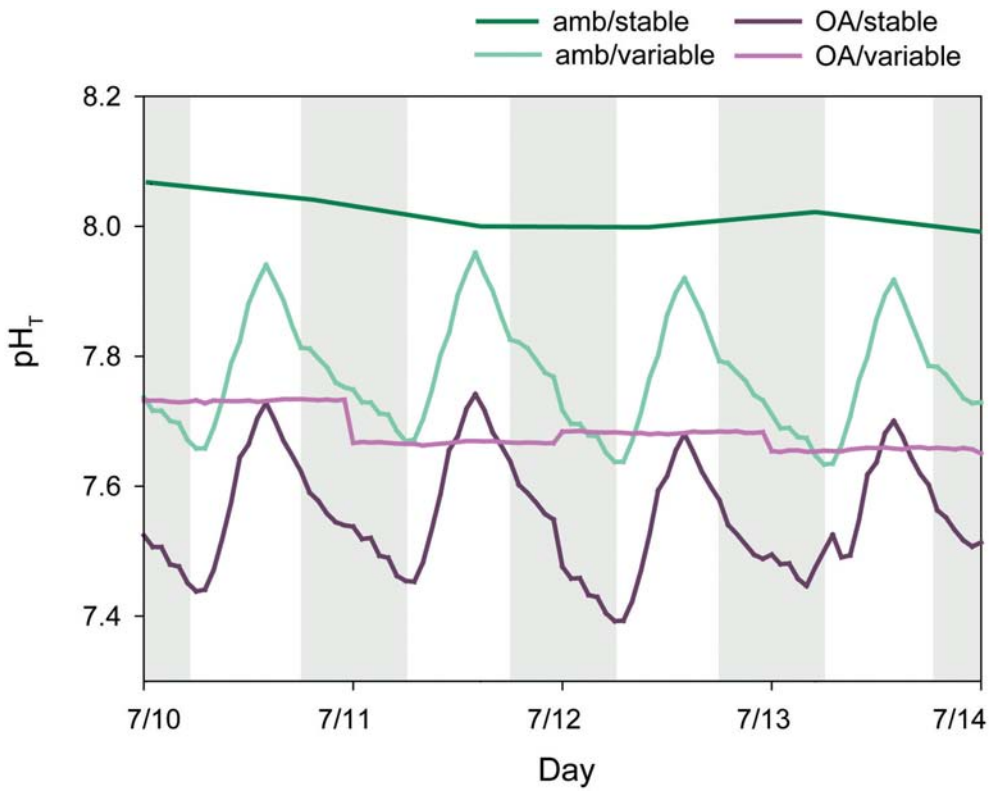

FIGURE 2 | Mean hourly pH_T (total scale) from treatment reservoir tanks and daily pH_T from discrete measurements of ambient tanks. Shaded areas indicate nighttime.

Water samples were collected from reservoir tanks, a subset of treatment tanks, and the ambient seawater line each week for total alkalinity (A_T) determinations. Samples were either titrated within 12-h of collection or poisoned with 200 μL of a saturated mercuric chloride solution for later processing. A_T was determined with modified open-cell potentiometric titrations at room temperature using an automated titrator (Mettler Toledo DL15) fit with a glass pH electrode (Mettler Toledo DG115-SC). The pH probe was calibrated with NBS buffers (4, 7, and 10) at the start of each day of titrations. Titrations followed standard operating protocol (SOP) 3b (Dickson et al., 2007), and used certified titrant (A. Dickson). Accuracy of A_T determinations was evaluated by titrating certified reference material (Batch 158, Reference Material for Oceanic CO_2 measurements, A. Dickson) at the start of titrations, after every 10 titrations, and again at the end of each day of titrations. A_T determinations were accurate to 0.86% of reference values (n = 25). The full carbonate system in seawater was calculated from measured pH_T, A_T, temperature, and salinity with the R package *seacarb* (Lavigne et al., 2014).

All treatment parameters, including the average daily minimum and maximum pH_T from reservoir tanks, are presented in **Table 1**.

Response Variables

Lithophyllum congestum fragments were buoyant weighed at the start of the experiment, after 8 weeks, and again after 16 weeks to determine net calcification rates (Davies, 1989). Buoyant weights were converted to dry weights based on the density of calcite. Calcification rates were normalized to initial fragment weight, and are expressed as mg $CaCO_3$ mg^{-1} day^{-1}. Total net calcification rates were calculated over the full duration of the experiment (0–16 weeks). Calcification rates were also calculated for the first (0–8 weeks) and second (8–16 weeks) halves of the experiment, to assess the potential for acclimatization to treatment conditions.

Instantaneous photophysiology was assessed with a blue light pulse-amplitude modulated fluorometer (Junior-PAM, Walz) at the start and end of the experiment. Maximum quantum yield (F_v/F_m) measurements were taken on fragments that were dark adapted for at least 1 h following sunset. One measurement was taken from three different tips of each *L. congestum* fragment (n = 3 measurements per fragment), with the probe held ∼1 mm away from the tissue surface at a constant angle. Settings were optimized to yield initial fluorescence measurements of F_0 = 300–500 units. Measuring light intensity was minimized to reduce actinic effects and gain was minimized to avoid amplifying noise (Fitt et al., 2001). The same settings were used for all measurements (saturation intensity = 12, saturation pulse width = 0.8, measuring light intensity = 8, frequency = 2, and gain = 1). Maximum quantum yield provides a useful proxy for photosynthetic efficiency because it is proportional to the rate of electron transport, and it provides a non-invasive and

TABLE 1 | Mean (±SE) physical conditions of treatments calculated from daily discrete measurements and weekly water samples.

Treatment	pH_T	Diel min pH_T	Diel max pH_T	Diel Δ pH_T	Temp	Salinity	A_T	pCO_2	C_T	Ω_C
amb/stable	8.04 (0.004)	7.92 (0.007)	8.05 (0.006)	0.13	29.2 (0.08)	32.2 (0.16)	2134 (11)	386 (4)	1841 (3)	5.21 (0.06)
amb/variable	7.76 (0.005)	7.67 (0.005)	7.94 (0.004)	0.27	28.9 (0.07)	32.2 (0.16)	2126 (13)	815 (10)	1967 (5)	3.02 (0.03)
OA/stable	7.70 (0.004)	7.68 (0.004)	7.72 (0.005)	0.04	29.0 (0.07)	32.2 (0.16)	2132 (15)	918 (6)	1990 (6)	2.68 (0.03)
OA/variable	7.58 ± 0.006	7.45 (0.009)	7.75 (0.010)	0.30	28.8 (0.07)	32.2 (0.16)	2128 (14)	1241 (12)	2022 (5)	2.09 (0.03)

Total scale pH (pH_T), temperature (°C), salinity, and total alkalinity (A_T, $\mu mol\ kg^{-1}$) were used to derive pCO_2 (μatm), total carbon (C_T, $\mu mol\ kg^{-1}$), and the saturation state of calcite (Ω_C) using the R package seacarb (Lavigne et al., 2014). Diel minimum (min), maximum (max), and range (Δ) in pH_T were calculated from hourly means of reservoir tanks and discrete measurements of ambient seawater.

instantaneous estimate of the performance of the photosynthetic machinery in algae (Kolber and Falkowski, 1993; Hader and Figueroa, 1997).

Statistics

Experimental parameters are presented as treatment averages, calculated from the daily means of replicate tanks within each treatment. For maximum quantum yield, the three measurements for a given fragment were averaged and the fragment mean was used in subsequent analyses.

All statistical analyses were performed in R version 3.4.2 with the untransformed data. Each response variable was evaluated with a separate linear mixed-effects models using the package *lme4* (Bates et al., 2015). For total calcification rate and photophysiology, the full model included treatment as a fixed factor and tank as a random factor nested within treatment. We chose to keep the random tank factor in all models to account for potential pseudoreplication issues from having multiple fragments within a tank. To evaluate calcification rates over time, the full model also included time period (0–8 or 8–16 weeks) as a fixed factor and individual as a random factor. Models were fit with maximum likelihood and the significance of fixed factors was evaluated with type II ANOVA tables using Satterthwaite's method. Significant differences between treatments were determined with Tukey's *post hoc* pairwise comparisons using the package *emmeans* (Lenth, 2018).

RESULTS

Total Net Calcification Rate

Total net calcification rates of *L. congestum* over the full duration of the experiment (0–16 weeks) were significantly lower in all pH treatments relative to the ambient control (amb/stable) ($F_{3,24}$ = 15.62, $p < 0.001$). Total calcification rates were 27 and 29% lower in the amb/variable and OA/stable treatment than in the ambient controls. Corallines in the OA/variable treatment demonstrated the most severe calcification response, with a 60% reduction in calcification rates relative to ambient controls (**Figure 3A**).

Net Calcification Rate Over Time

There was a significant interactive effect of treatment and time ($F_{3,67}$ = 5.06, p = 0.003) on *L. congestum* calcification when rates were partitioned into the first and second halves of the experiment. Calcification rates remained unchanged between the first and second half of the experiment in the OA/stable treatment (p = 0.481) and amb/stable control (p = 0.307), but magnified over time in both of the variable treatments with rates decreasing from the first to second half of the experiment ($p < 0.001$ for both amb/variable and OA/variable treatments) (**Figure 3B**). After 0–8 weeks of exposure, CCA calcification rates in the amb/variable treatment were 16% lower than ambient controls, and from 8 to 16 weeks calcification rates were 47% lower than the respective ambient controls. In the OA/variable treatment, the reduction in calcification rates relative to ambient controls was

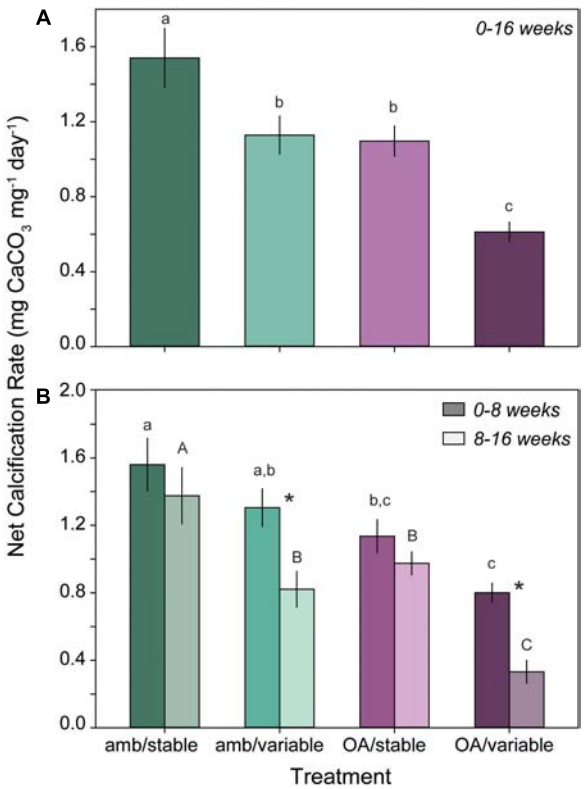

FIGURE 3 | (A) Mean (±SE) total calcification rate of *L. congestum* over the full duration of the experiment (0–16 weeks) (n = 6) and **(B)** during the first (0–8 weeks, dark shade) and second (8–16 weeks, light shade) halves of the experiment (n = 6). Treatments with different letters are significantly different at α = 0.05, case denotes statistical differences within a time point. Asterisk indicates a significant difference within a treatment between time points.

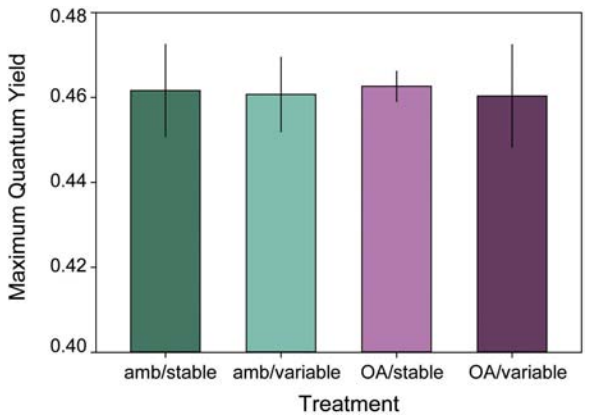

FIGURE 4 | Mean (±SE) maximum quantum yield of *L. congestum* after 16 weeks of exposure to treatment conditions ($n = 6$). There were no significant effects of treatment on maximum quantum yield.

49 and 79% from 0 to 8 and 8–16 weeks, respectively. Conversely, calcification rates in the OA/stable treatment ranged from 27 to 37% lower than controls, but did not differ significantly between time points (**Figure 3B**).

Maximum Quantum Yield

Initial maximum quantum yield was the same for *L. congestum* fragments randomly assigned to each treatment ($F_{3,24} = 0.50$, $p = 0.683$). Mean (±SE) initial yields by treatment were 0.48 ± 0.01 (amb/stable, amb/var), 0.46 ± 0.02 (stable/OA), and 0.47 ± 0.004 (OA/var). There were no differences among treatments in maximum quantum yield at the end of the 16-week experiment (**Figure 4**) ($F_{3,24} = 0.01$, $p = 0.998$), and no significant change in yield over time ($F_{1,43} = 2.58$, $p = 0.113$).

DISCUSSION

Here, we demonstrate that exposure to diel pH cycling influenced the response of a common reef-building CCA to OA, and that pH variability and OA synergistically decreased calcification. Instead of increasing tolerances to low pH, as predicted by environmental variability-stress acclimatization theory (Boyd et al., 2016), variability exacerbated the negative effects of OA on coralline net calcification. Notably, the magnitude of treatment responses changed over time, with both variable treatments having stronger negative effects with longer duration of exposure. In contrast to the calcification response, photophysiology was unaffected by pH treatment, which indicates that the effects of pH treatment on calcification were independent of photosynthetic processes. Our results show that pH variability does not inherently increase the tolerance of tropical CCA to OA, and suggests that both pH variability and exposure time could be important factors underlying differential responses to OA. Moreover, our findings indicate that OA combined with diel pH cycling can have synergistic and extreme negative effects.

When we normalized the net calcification response of *L. congestum* over the full duration of the experiment (0–16 weeks), the amb/variable and OA/stable treatment decreased calcification rates by the same magnitude relative to ambient controls (amb/stable). This is notable because corallines in the amb/variable treatment were exposed to low pH conditions for roughly half the amount of time as the corallines in the OA/stable treatment. Further, pH variability combined with OA (i.e., OA/variable) had the most extreme effect on calcification, decreasing rates by 60% relative to ambient controls. These results are intriguing because they suggest that, overall, ambient pH variability (amb/variable) incurred the same cost to calcification as the OA/stable treatment. Moreover, simultaneous exposure to lower pH and variability exacerbated the negative effects of OA.

Exposure to variability can influence physiological responses to environmental stress, independent of environmental history. A complete discussion of the role of environmental history in the response of tropical coralline algae to OA, and potential mechanisms underpinning acclimatization, are reviewed in Rivest et al., 2017. Here, we considered only the effect of continued exposure to pH variability on the tropical CCA *L. congestum*, with no change in regime (i.e., treatment) over the course of the experiment.

Diel pH variability could increase CCA tolerances to OA by providing periods of reprieve from low pH (Rivest et al., 2017). For example, higher pH during the day could provide a favorable timeframe for active calcification, compensating for decreased calcification during periods of lower pH at night (Comeau et al., 2013a; Cornwall et al., 2018). Alternatively, low pH at night could drive dissolution and counteract any benefits of high pH during the day (Cornwall et al., 2013). Furthermore, the rate of change in pH can elicit stronger negative responses than exposure to stable low pH. For example, calcification and skeletal structure of the temperate CCA *Lithothamnion glaciale* was more sensitive to rapid decreases in pH, simulating pH changes associated with upwelling or carbon capture and release, than chronic exposure to stable, low pH (Kamenos et al., 2013). This suggests that daily exposure to rapid pH changes could have long-term negative consequences for calcification in tropical CCA. Thus, the switch between these alternative scenarios could depend on both the magnitude and rate of change over the course of the diel cycle. Our results support the latter, indicating that cyclic exposure to low pH has net detrimental effects on CCA calcification. This could be due to a non-linear relationship between pH and calcification, or some lag in resumption of calcification after pH returns to favorable levels.

Our total calcification responses concur with Cornwall et al. (2013), which found that ambient variable pH decreased relative growth of the temperate articulated coralline *Arthrocardia corymbosa* by the same amount as stable OA. Coralline recruits from the same study responded, similarly (Roleda et al., 2015). As with our results, they found that fluctuating pH combined with OA had the most extreme effects and synergistically decreased growth of adults and recruits (Cornwall et al., 2013; Roleda et al., 2015). Johnson et al. (2014a) also found similar results for the tropical CCA *Porolithon onkodes*, where calcification rates

were lower in variable pH conditions than ambient controls. Our results conflict with those of Cornwall et al. (2018), which found the tropical CCA *H. reinboldii* was unaffected by exposure to either pH variability, OA, or the combination of both. Our results contribute to a growing body of studies that demonstrate pH variability generally decreases calcification in tropical CCA, and suggests that the results with *H. reinboldii* in the Cornwall et al. (2018) study may be an exception worthy of further examination.

Comparing overall net calcification responses across experiments is difficult due to species-specific physiology and differences in duration of experiments ranging from 14 days (Johnson et al., 2014a) and 40 days (Cornwall et al., 2013) to 100–112 days (Cornwall et al., 2018, present study). Given the similarities in design (e.g., treatments and duration) between our study and Cornwall et al. (2018), we might expect to see similar responses. However, Cornwall et al. (2018) found no response to pH variability or OA, and hypothesized that the lack of response in *H. reinboldii* was a result of physiological control over calcification. They further concluded that physiological control may be species-specific. While intracellular control over calcification has been recognized as a potential underlying mechanism for species-specific tolerances to OA in corals (Comeau et al., 2013b), it has only recently been identified as a potential mechanism for CCA (Cornwall et al., 2017). Thus, differences between these studies may be related to taxa-specific calcification mechanisms. While *L. congestum* and *H. reinboldii* are morphologically similar in their production of blunt branches, they may be fundamentally different with respect to calcification physiology. Future work should take a comparative approach to elucidating mechanisms of calcification across coralline species, as we know little about interspecific variation in calcification physiology.

Time is a critical component for organismal acclimatization, especially given that compensatory changes in cellular machinery take time to manifest following the onset of stressful conditions (Comeau et al., 2018). However, the negative effects of prolonged exposure to stressful conditions can also compound over time. For example, repeated exposure to thermal stress can increase bleaching susceptibility in corals (Schoepf et al., 2015). When we partitioned net calcification into the first and second halves of the experiment, calcification responses to the variable treatments, but not stable OA, changed with longer duration of exposure. Instead of facilitating acclimatization to pH conditions, pH variability increased the sensitivity of *L. congestum* over time. For example, the magnitude of decrease in calcification in the amb/variable and OA/variable treatments relative to ambient controls doubled between 0–8 weeks and 8–16 weeks. Conversely, the magnitude of the OA/stable treatment effect stayed the same between time points. These are the first results to explore a temporal component to tropical CCA responses to pH regimes in the lab. The temperate CCA *L. glaciale* showed some temporal variation in response to simulated OA and warming throughout a 1-year experiment, but overall showed no clear trend toward acclimatization or compounding negative effects over time (Martin and Gattuso, 2009).

Though discerning the mechanisms underlying the increased sensitivity of *L. congestum* to pH variability over time is beyond the scope of this study, we propose a few potential mechanisms that could explain this response. First, dissolution under low pH at night may have counteracted any benefits to calcification of higher pH during the day (Rivest et al., 2017). Part of this may be that these CCA may already be living below their optimal pH range and additional fluctuations push them beyond their tolerance threshold. Second, constant exposure to low pH (as in the OA/stable treatment) may have initiated the up- or downregulation of cellular machinery necessary for regulating internal pH (Comeau et al., 2018). Furthermore, exposure to fluctuating conditions may have been insufficient to trigger initiation of the physiological mechanisms underlying phenotypic plasticity or may have outright inhibited it. Importantly, alterations in gene expression take time to manifest, and fluctuating pH regimes may have inhibited the changes in expression that underly acclimatization. Third, the species used in this study, *L. congestum*, may not have the same capacity for internal pH control, or other mechanisms that facilitate calcification under fluctuating pH, that was recently documented in other corallines (Cornwall et al., 2017). Future experiments should explore if other tropical CCA species demonstrate similar sensitivities to variability and OA over time and identify the underlying mechanisms.

An important caveat to the present study is that the experiment took place over the course of 16 weeks (120 days), whereas the changes in pH associated with OA are occurring over decades-to-centuries. Thus, scaling the results of this relatively short-term laboratory experiment to the long-term effects of OA is limited by our inability to fully simulate the rate of pH change occurring with OA. In nature, the response of tropical CCA to OA will be shaped by a multitude of interacting biotic and abiotic factors accumulating over time. Given the significant role of pH variability in shaping CCA responses to mean reductions in pH documented here, natural variation will likely mediate *in situ* responses to the longer-term reductions in pH due to OA.

Though *L. congestum* showed a distinct calcification response to pH, photophysiology (i.e., maximum quantum yield) was unaffected. The yield values we measured are relatively low, and this may be due to where on the algal thallus we took the readings. Quantum yield from branching CCA morphologies, like *L. congestum*, can vary depending on if the measurements is taken from a branch tip or near the base (Burdett et al., 2012). Our measurements were taken from branch tips, where tissues were more lightly pigmented. Indeed, our average yield is similar to those measured from the upward facing branch tips of a CCA in the Red Sea (*L. kotschyanum*) (Burdett et al., 2014). Quantum yield was measured the same across all treatments, and though yield values were lower than expected, we would still expect to detect treatment effects if they were present.

Calcification and photosynthesis are tightly coupled, where photosynthesis provides the energy for calcification and can increase internal pH at the site of calcification (Borowitzka, 1981). Understanding how each process is affected by OA provides insight into potential physiological mechanisms underlying the response of calcification to changes in pH. The lack of response

in maximum quantum yield across our experimental treatments suggests that the response of calcification to variation in pH was independent of any changes to photosynthesis. However, these results should be interpreted cautiously, because quantum yield is only a proxy for photosynthesis and it may not be as accurate for algae with abundant accessory pigments. CCA are red algae that possess phycobilin pigments (Kursar and Alberte, 1983). Any change in phycobilin pigment content or contribution to higher photosynthetic rates may not have been detected. Other studies have found mixed effects of OA on algal photophysiology (Koch et al., 2013). For example, photosynthetic rates and pigment content in tropical CCA are sometimes enhanced by lower pH (Johnson and Carpenter, 2018), but in other cases they are negatively impacted (Anthony et al., 2008) or not affected (Johnson et al., 2014b). More accurate techniques, such as oxygen evolution incubations, should be used to accurately assess the effects of OA on photosynthesis in CCA (Hurd et al., 2009).

CONCLUSION

Here, we provide evidence that negative effects of pH variability on calcification of a tropical CCA intensified over time and increased sensitivity to OA. This is among the first studies to quantify a temporal component to CCA response to pH variability and OA, and sheds light on the dynamic nature of organismal responses to environmental stress over time. Moreover, our findings illustrate the potential synergistic effects of OA and diel pH variability, which has important implications for nearshore ecosystems where environmental conditions fluctuate over a diel cycle. Notably, our findings do not support the theory that variability inherently increases calcifier tolerances to OA stress. These results imply that environmentally variable nearshore habitats may not provide a refuge from environmental stress associated with global change, but may in fact be the most vulnerable ecosystems due to heightened sensitivity of calcifiers to predicted OA.

DATA AVAILABILITY

The datasets generated for this study are available on request to the corresponding author.

AUTHOR CONTRIBUTIONS

MJ conceived and designed the experiments and analyzed the data. MJ, LRB, NV, and SO implemented the experiments. MJ and AA interpreted the data, wrote the manuscript, and secured the financial support. All authors edited the manuscript and approved the final submission.

FUNDING

This work was supported by Smithsonian Institution Marine Global Earth Observatory (MarineGEO) and Smithsonian Tropical Research Institute (STRI) postdoctoral fellowships to MJ, and by STRI funds to AA. NV received internship support from STRI Academic Programs and the University of Chicago International Experience Grant. SO received internship support from the Miller Worly Center for the Environment at Mount Holyoke College. Research permits were provided by the Autoridad Nacional del Ambiente de Panamá.

ACKNOWLEDGMENTS

We thank Rachel Collin for facilities support at the Bocas del Toro Research Station, Plinio Gondola, and the research station staff for logistical support. We are grateful to the lab and field assistance from Nicte-Ha Muñoz, Manuel Rodriguez Bravo, and William Wied, and for critical feedback from Mike Fox. We also thank Sophie McCoy and Heidi Burdett for their constructive feedback. This is contribution 36 from the Smithsonian's MarineGEO network.

REFERENCES

Adey, W. H. (1978). Algal rides of the Caribbean and West-Indies. *Phycologia* 17, 361–367. doi: 10.2216/i0031-8884-17-4-361.1

Adey, W. H. (1998). Coral reefs: algal structured and mediated ecosystems in shallow, turbulent, alkaline waters. *J. Phycol.* 34, 393–406. doi: 10.1046/j.1529-8817.1998.340393.x

Anthony, K. R. N., Kleypas, J. A., and Gattuso, J. P. (2011). Coral reefs modify their seawater carbon chemistry - implications for impacts of ocean acidification. *Glob. Chang. Biol.* 17, 3655–3666. doi: 10.1111/j.1365-2486.2011.02510.x

Anthony, K. R. N., Kline, D. I., Diaz-Pulido, G., Dove, S., and Hoegh-Guldberg, O. (2008). Ocean acidification causes bleaching and productivity loss in coral reef builders. *Proc. Natl. Acad. Sci. U.S.A.* 105, 17442–17446. doi: 10.1073/pnas.0804478105

Bates, D., Maechler, M., Bolker, B., and Walker, S. (2015). Fitting linear mixed-effects models using lme4. *J. Stat. Softw.* 67, 1–48. doi: 10.18637/jss.v067.i01

Borowitzka, M. A. (1981). Photosynthesis and calcification in the articulated coralline red algae *Amphiroa anceps* and *Amphiroa foliacea*. *Mar. Biol.* 62, 17–23. doi: 10.1007/BF00396947

Bosence, D. W. J. (1985). The morhology and ecology of a mound-building coralline alga (*Neogoniolithon strictum*) from the Florida Keys. *Palaeontology* 28, 189–206.

Boyd, P. W., Cornwall, C. E., Davison, A., Doney, S. C., Fourquez, M., Hurd, C. L., et al. (2016). Biological responses to environmental heterogeneity under future ocean conditions. *Glob. Chang. Biol.* 22, 2633–2650. doi: 10.1111/gcb.13287

Burdett, H. L., Hennige, S. J., Francis, F. T. Y., and Kamenos, N. A. (2012). The photosynthetic characteristics of red coralline algae, determined using pulse amplitude modulation (PAM) fluorometry. *Botanica Marina* 55, 499–509. doi: 10.1515/bot-2012-0135

Burdett, H. L., Keddie, V., MacArthur, N., McDowall, L., McLeish, J., Spielvogel, E., et al. (2014). Dynamic photoinhibition exhibited by red coralline algae in the red sea. *BMC Plant Biol.* 14:139. doi: 10.1186/1471-2229-14-139

Comeau, S., Carpenter, R. C., and Edmunds, P. J. (2013a). Coral reef calcifiers buffer their response to ocean acidification using both bicarbonate and carbonate. *Proc. R. Soc. B Biol. Sci.* 280:20122374. doi: 10.1098/rspb.2012.2374

Comeau, S., Edmunds, P. J., Spindel, N. B., and Carpenter, R. C. (2013b). The responses of eight coral reef calcifiers to increasing partial pressure of CO2 do not exhibit a tipping point. *Limnol. Oceanogr.* 58, 388–398. doi: 10.4319/lo.2013.58.1.0388

Comeau, S., Cornwall, C. E., DeCarlo, T. M., Krieger, E., and McCulloch, M. T. (2018). Similar controls on calcification under ocean acidification across unrelated coral reef taxa. *Glob. Chang. Biol.* 24, 4857–4868. doi: 10.1111/gcb.14379

Comeau, S., Lantz, C. A., Edmunds, P. J., and Carpenter, R. C. (2016). Framework of barrier reefs threatened by ocean acidification. *Glob. Chang. Biol.* 22, 1225–1234. doi: 10.1111/gcb.13023

Cornwall, C. E., Comeau, S., DeCarlo, T. M., Moore, B., D'Alexis, Q., and McCulloch, M. T. (2018). Resistance of corals and coralline algae to ocean acidification: physiological control of calcification under natural pH variability. *Proc. R. Soc. B Biol. Sci.* 285:20181168. doi: 10.1098/rspb.2018.1168

Cornwall, C. E., Comeau, S., and McCulloch, M. T. (2017). Coralline algae elevate pH at the site of calcification under ocean acidification. *Glob. Chang. Biol.* 23, 4245–4256. doi: 10.1111/gcb.13673

Cornwall, C. E., Hepburn, C. D., McGraw, C. M., Currie, K. I., Pilditch, C. A., Hunter, K. A., et al. (2013). Diurnal fluctuations in seawater pH influence the response of a calcifying macroalga to ocean acidification. *Proc. Biol. Sci.* 280:20132201. doi: 10.1098/rspb.2013.2201

Davies, P. S. (1989). Short-term growth measurements of corals using an accurate buoyant weighing technique. *Mar. Biol.* 101, 389–395. doi: 10.1007/BF00428135

Dickson, A. G., Sabine, C. L., and Christian, J. R. (2007). *Guide to Best Practices for Ocean CO2 Measurements*. Sidney: North Pacific Marine Science Organization.

Duarte, C. M., Hendriks, I. E., Moore, T. S., Olsen, Y. S., Steckbauer, A., Ramajo, L., et al. (2013). Is ocean acidification an open-ocean syndrome? Understanding anthropogenic impacts on seawater pH. *Estuaries Coasts* 36, 221–236. doi: 10.1007/s12237-013-9594-3

Edmunds, P. J., Comeau, S., Lantz, C., Andersson, A., Briggs, C., Cohen, A., et al. (2016). Integrating the effects of ocean acidification across functional Scales on tropical coral reefs. *Bioscience* 66, 350–362. doi: 10.1093/biosci/biw023

Eyre, B. D., Andersson, A. J., and Cyronak, T. (2014). Benthic coral reef calcium carbonate dissolution in an acidifying ocean. *Nat. Clim. Change* 4, 969–976. doi: 10.1038/nclimate2380

Fitt, W. K., Brown, B. E., Warner, M. E., and Dunne, R. P. (2001). Coral bleaching: interpretation of thermal tolerance limits and thermal thresholds in tropical corals. *Coral Reefs* 20, 51–65. doi: 10.1007/s003380100146

Georgiou, L., Falter, J., Trotter, J., Kline, D. I., Holcomb, M., Dove, S. G., et al. (2015). pH homeostasis during coral calcification in a free ocean CO2 enrichment (FOCE) experiment, Heron Island reef flat, Great Barrier Reef. *Proc. Natl. Acad. Sci. U.S.A.* 112, 13219–13224. doi: 10.1073/pnas.1505586112

Guadayol, Ò, Silbiger, N. J., Donahue, M. J., and Thomas, F. I. (2014). Patterns in temporal variability of temperature, oxygen and pH along an environmental gradient in a coral reef. *PLoS One* 9:e85213. doi: 10.1371/journal.pone.0085213

Hader, D. P., and Figueroa, F. L. (1997). Photoecophysiology of marine macroalgae. *Photochem. Photobiol.* 66, 1–14. doi: 10.1016/j.marenvres.2014.07.012

Hartin, C., Bond-Lamberty, B., Patel, P., and Mundra, A. (2016). Ocean acidification over the next three centuries using a simple global climate carbon-cycle model: projections and sensitivities. *Biogeosciences* 13, 4329–4342. doi: 10.5194/bg-13-4329-2016

Hoegh-Guldberg, O., Mumby, P. J., Hooten, A. J., Steneck, R. S., Greenfield, P., Gomez, E., et al. (2007). Coral reefs under rapid climate change and ocean acidification. *Science* 318, 1737–1742. doi: 10.1126/science.1152509

Hofmann, G. E., Smith, J. E., Johnson, K. S., Send, U., Levin, L. A., Micheli, F., et al. (2011). High-frequency dynamics of ocean pH: a multi-ecosystem comparison. *PLoS One* 6:e28983. doi: 10.1371/journal.pone.0028983

Hurd, C. L., Hepburn, C. D., Currie, K. I., Raven, J. A., and Hunter, K. A. (2009). Testing the effects of ocean acidification on algal metabolism: considerations for experimental designs. *J. Phycol.* 45, 1236–1251. doi: 10.1111/j.1529-8817.2009.00768.x

Johnson, M. D., and Carpenter, R. C. (2018). Nitrogen enrichment offsets direct negative effects of ocean acidification on a reef-building crustose coralline alga. *Biol. Lett.* 14:20180371. doi: 10.1098/rsbl.2018.0371

Johnson, M. D., Moriarty, V. W., and Carpenter, R. C. (2014a). Acclimatization of the crustose coralline alga *Porolithon onkodes* to variable pCO2. *PLoS One* 9:e87678. doi: 10.1371/journal.pone.0087678

Johnson, M. D., Price, N. N., and Smith, J. E. (2014b). Contrasting effects of ocean acidification on tropical fleshy and calcareous algae. *PeerJ* 2:E411. doi: 10.7717/peerj.411

Kamenos, N. A., Burdett, H. L., Aloisio, E., Findlay, H. S., Martin, S., Longbone, C., et al. (2013). Coralline algal structure is more sensitive to rate, rather than the magnitude, of ocean acidification. *Glob. Chang. Biol.* 19, 3621–3628. doi: 10.1111/gcb.12351

Kleypas, J. A., Anthony, K. R. N., and Gattuso, J. P. (2011). Coral reefs modify their seawater carbon chemistry - case study from a barrier reef (Moorea, French Polynesia). *Glob. Chang. Biol.* 17, 3667–3678. doi: 10.1111/j.1365-2486.2011.02530.x

Kline, D. I., Teneva, L., Schneider, K., Miard, T., Chai, A., Marker, M., et al. (2012). A short term in situ CO2 enrichment experiment on Heron Island (GBR). *Sci. Rep.* 2:413. doi: 10.1038/srep00413

Koch, M., Bowes, G., Ross, C., and Zhang, X.-H. (2013). Climate change and ocean acidification effects on seagrasses and marine macroalgae. *Glob. Chang. Biol.* 19, 103–132. doi: 10.1111/j.1365-2486.2012.02791.x

Kolber, Z., and Falkowski, P. G. (1993). Use of active fluorescence to estimate phytoplankton photosynthesis in situ. *Limnol. Oceanogr.* 38, 1646–1665. doi: 10.4319/lo.1993.38.8.1646

Kroeker, K. J., Kordas, R. L., Crim, R. N., and Singh, G. G. (2010). Meta-analysis reveals negative yet variable effects of ocean acidification on marine organisms. *Ecol. Lett.* 13, 1419–1434. doi: 10.1111/j.1461-0248.2010.01518.x

Kroeker, K. J., Micheli, F., and Gambi, M. C. (2013). Ocean acidification causes ecosystem shifts via altered competitive interactions. *Nat. Clim. Change* 3:156. doi: 10.1038/nclimate1680

Kursar, T. A., and Alberte, R. S. (1983). Photosynthetic unit organization in a red alga- relationships between light-harvesting pigmetns and reaction centers. *Plant Physiol.* 72, 409–414. doi: 10.1104/pp.72.2.409

Lavigne, H., Epitalon, J.-M., and Gattuso, J.-P. (2014). *seacarb: Seawater Carbonate Chemistry with R. R Package Version 3.0*. Available at: https://cran.r-project.org/package=seacarb.

Lenth, R. (2018). *Emmeans: Estimated Marginal Means, Aka Least-Squares Means. R Package Version 1.2*. Available at: https://mran.microsoft.com/snapshot/2018-03-30/web/packages/emmeans/index.html.

Martin, S., and Gattuso, J. P. (2009). Response of Mediterranean coralline algae to ocean acidification and elevated temperature. *Glob. Chang. Biol.* 15, 2089–2100. doi: 10.1002/ece3.475

Mayfield, A. B., Chan, P. H., Putnam, H. M., Chen, C. S., and Fan, T. Y. (2012). The effects of a variable temperature regime on the physiology of the reef-building coral *Seriatopora hystrix*: results from a laboratory-based reciprocal transplant. *J. Exp. Biol.* 215, 4183–4195. doi: 10.1242/jeb.071688

McCoy, S. J., and Kamenos, N. A. (2015). Coralline algae (Rhodophyta) in a changing world: integrating ecological, physiological, and geochemical responses to global change. *J. Phycol.* 51, 6–24. doi: 10.1111/jpy.12262

Noisette, F., Egilsdottir, H., Davoult, D., and Martin, S. (2013). Physiological responses of three temperate coralline algae from contrasting habitats to near-future ocean acidification. *J. Exp. Mar. Biol. Ecol.* 448, 179–187. doi: 10.1016/j.jembe.2013.07.006

Padilla-Gamiño, J. L., Gaitán-Espitia, J. D., Kelly, M. W., and Hofmann, G. E. (2016). Physiological plasticity and local adaptation to elevated pCO2 in calcareous algae: an ontogenetic and geographic approach. *Evol. Appl.* 9, 1043–1053. doi: 10.1111/eva.12411

Palumbi, S. R., Barshis, D. J., Traylor-Knowles, N., and Bay, R. A. (2014). Mechanisms of reef coral resistance to future climate change. *Science* 344, 895–898. doi: 10.1126/science.1251336

Price, N. N., Martz, T. R., Brainard, R. E., and Smith, J. E. (2012). Diel variability in seawater pH relates to calcification and benthic community structure on coral reefs. *PLoS One* 7:e43843. doi: 10.1371/journal.pone.0043843

Rivest, E. B., Comeau, S., and Cornwall, C. E. (2017). The role of natural variability in shaping the response of coral reef organisms to climate change. *Curr. Clim. Chang. Rep.* 3, 271–281. doi: 10.1007/s40641-017-0082-x

Roleda, M. Y., Cornwall, C. E., Feng, Y., McGraw, C. M., Smith, A. M., and Hurd, C. L. (2015). Effect of ocean acidification and pH fluctuations on the growth and development of coralline algal recruits, and an associated benthic algal assemblage. *PLoS One*, 10:e0140394. doi: 10.1371/journal.pone.0140394

Schoepf, V., Stat, M., Falter, J. L., and McCulloch, M. T. (2015). Limits to the thermal tolerance of corals adapted to a highly fluctuating, naturally extreme temperature environment. *Sci. Rep.* 5:17639. doi: 10.1038/srep17639

Smith, J. E., Brainard, R., Carter, A., Grillo, S., Edwards, C., Harris, J., et al. (2016). Re-evaluating the health of coral reef communities: baselines and evidence for

human impacts across the central Pacific. *Proc. R. Soc. B. Biol. Sci.* 283:20151985. doi: 10.1098/rspb.2015.1985

Stark, J. S., Peltzer, E. T., Kline, D. I., Queirós, A. M., Cox, T. E., Headley, K., et al. (2019). Free ocean CO2 enrichment (FOCE) experiments: scientific and technical recommendations for future in situ ocean acidification projects. *Prog. Oceanogr.* 172, 89–107. doi: 10.1016/j.pocean.2019.01.006

Takeshita, Y., Cyronak, T., Martz, T. R., Kindeberg, T., and Andersson, A. J. (2018). Coral reef carbonate chemistry variability at different functional scales. *Front. Mar. Sci.* 5:175. doi: 10.3389/fmars.2018.00175

van Oppen, M. J., Oliver, J. K., Putnam, H. M., and Gates, R. D. (2015). Building coral reef resilience through assisted evolution. *Proc. Natl. Acad. Sci. U.S.A.* 112, 2307–2313. doi: 10.1073/pnas.1422301112

Vargas, C. A., Lagos, N. A., Lardies, M. A., Duarte, C., Manriquez, P. H., Aguilera, V. M., et al. (2017). Species-specific responses to ocean acidification should account for local adaptation and adaptive plasticity. *Nat. Ecol. Evol.* 1:0084. doi: 10.1038/s41559-017-0084

Vargas-Angel, B., Richards, C. L., Vroom, P. S., Price, N. N., Schils, T., Young, C. W., et al. (2015). Baseline assessment of net calcium carbonate accretion rates on US Pacific reefs. *PLoS One* 10:e0142196. doi: 10.1371/journal.pone.0142196

Conflict of Interest Statement: The authors declare that the research was conducted in the absence of any commercial or financial relationships that could be construed as a potential conflict of interest.

Copyright © 2019 Johnson, Rodriguez Bravo, O'Connor, Varley and Altieri. This is an open-access article distributed under the terms of the Creative Commons Attribution License (CC BY). The use, distribution or reproduction in other forums is permitted, provided the original author(s) and the copyright owner(s) are credited and that the original publication in this journal is cited, in accordance with accepted academic practice. No use, distribution or reproduction is permitted which does not comply with these terms.

frontiers in Marine Science

ORIGINAL RESEARCH
published: 29 March 2019
doi: 10.3389/fmars.2019.00149

Local Coastal Configuration Rather Than Latitudinal Gradient Shape Clonal Diversity and Genetic Structure of *Phymatolithon calcareum* Maerl Beds in North European Atlantic

Cristina Pardo[1†], Marie-Laure Guillemin[2,3†], Viviana Peña[1], Ignacio Bárbara[1], Myriam Valero[3] and Rodolfo Barreiro[1]*

[1] BioCost Research Group, Departamento de Bioloxía, Facultade de Ciencias, Universidade da Coruña, A Coruña, Spain, [2] Instituto de Ciencias Ambientales y Evolutivas, Facultad de Ciencias, Universidad Austral de Chile, Valdivia, Chile, [3] UMI EBEA 3614, Evolutionary Biology and Ecology of Algae, CNRS, PUCCh, UACH, Station Biologique de Roscoff, Sorbonne Université, Roscoff, France

OPEN ACCESS

Edited by:
Kathryn Schoenrock, National University of Ireland Galway, Ireland

Reviewed by:
Anne Chenuil, Centre National de la Recherche Scientifique (CNRS), France
Stacy Krueger, University of Alabama at Birmingham, United States

***Correspondence:**
Marie-Laure Guillemin
marielaure.guillemin@gmail.com

[†]These authors have contributed equally to this work

Specialty section:
This article was submitted to Marine Ecosystem Ecology, a section of the journal Frontiers in Marine Science

Received: *01 November 2018*
Accepted: *08 March 2019*
Published: *29 March 2019*

Citation:
Pardo C, Guillemin M-L, Peña V, Bárbara I, Valero M and Barreiro R (2019) Local Coastal Configuration Rather Than Latitudinal Gradient Shape Clonal Diversity and Genetic Structure of Phymatolithon calcareum Maerl Beds in North European Atlantic. Front. Mar. Sci. 6:149. doi: 10.3389/fmars.2019.00149

Maerl beds are one of the world's key coastal ecosystems and are threatened by human activities and global change. In this study, the genetic diversity and structure of one of the major European maerl-forming species, *Phymatolithon calcareum*, was studied using eight microsatellite markers. Two sampling scales (global: North East Atlantic and regional: Galicia) were investigated and fifteen maerl beds from Atlantic Europe were sampled. At the regional-scale the location of sites outside and within four estuaries allowed to test for the influence of coastal configuration on population connectivity and genetic diversity. Results suggested that clonal reproduction plays an important role in the population dynamics of *P. calcareum* maerl beds. Clonality was variable among populations, even within the same region. At the European scale, these differences in clonality cannot be explained by the geographic or latitudinal distribution of the populations studied. A significant genetic differentiation was found among almost all population pairs and a positive correlation between geographic and genetic distances showed the limited dispersal capacity of *P. calcareum*. Moreover, a very clear pattern of genetic structure was revealed at the regional scale between populations located within and at the mouth of the estuaries. Genetic differentiation among estuaries was less marked for the sites located in outer-zones compared to those located in the inner-zones. In addition, variation in level of clonality linked to seascape was also observed: populations situated in the outer-zones of the estuaries were less clonal than those in the inner-zones. Finally, populations from the same estuary generally shared one or several mutilocus genotypes.

Keywords: coralline red algae, conservation, ecosystem engineer, genetic and genotypic diversity, mating system, microsatellite, North European Atlantic, rhodolith

INTRODUCTION

The majority of plants involve both sexual and asexual/clonal reproduction (Halkett et al., 2005; Vallejo-Marín et al., 2010). The balance between the two modes of reproduction varies widely between species and even between populations of the same species, highly influencing demography and genetic structure (Eckert, 2002; Halkett et al., 2005). Most asexual reproductive modes, such as vegetative propagation, bypass meiosis and do not involve recombination. In this case, asexual offspring (ramets) are exact genetic copies of the parent genotypes (produced by sexual reproduction) with exceptions linked to somatic mutations (Harper, 1981; Eckert, 2002; Vallejo-Marín et al., 2010). All ramets produced clonally, as well as the original parental individual, are part of the same genetic unit also called a genet (Vallejo-Marín et al., 2010). In dense populations inhabiting stable environments, extensive clonal spread has been observed (Arnaud-Haond et al., 2010). Within these populations, increasing competition among genets for space or resources through time could lead to an overwhelming dominance of one or a few clonal lineages: the more ecologically competent excluding the less fit lineage (Eriksson, 1993; Arnaud-Haond et al., 2010; Becheler et al., 2014). By combining both sexual and clonal mode of reproduction, partially asexual organisms can potentially generate new recombinant genets at each generation avoiding then the accumulation of deleterious mutations while being able to maintain the best performing genotypes over time scales far exceeding sexual generation times (Otto and Lenormand, 2002; Arnaud-Haond et al., 2012). Asexual reproduction has been reported to be more important at the limit of the species range distribution, where adverse environmental conditions can limit sexual reproduction referred to as geographic parthenogenesis in Kearney (2005). In brown, red, and green macroalgae, ramets constitute free-living forms after thallus fragmentation (Fucus: Johannesson et al., 2011; *Agarophyton,* previously known as Gracilaria: Guillemin et al., 2008; and Caulerpa: Ceccherelli and Cinelli, 1999). These drifting fragments (mature or vegetative) are considered as the major mechanism for long distance dispersal in macroalgae (review in Macaya et al., 2016).

Traits linked to the reproductive system and migration ultimately generate the spatial pattern of genotype distributions, hence influencing the intraspecific competition for resources utilization and the species capacity to buffer negative impacts of stochastic environmental changes. Estimating the rate of sex is central in predicting the resilience of partially asexual organisms since different evolutionary consequences are expected in asexual and sexual populations after large perturbations (Hörandl, 2006). Resilience of asexual populations could be favored on the short term since large clones have a higher probability to survive bottlenecks and high clonality may somewhat buffer the loss of variation linked to severe population size reduction (Diaz-Almela et al., 2008). On the contrary, sexual populations in which genetic diversity could be quickly replenished, could show better resilience on a long term scale than asexual ones (Hörandl, 2006). Information about genetic diversity, population connectivity, and the impact of the reproductive system on genotype assemblages is then a prerequisite to assess population resilience to climatic changes or the direct impact of human activities and design effective management plans for keystone species (Gaines et al., 2010; Segelbacher et al., 2010). The use of genetic data has been shown to be of paramount importance in defining optimal number and size of Nature Reserves (Soulé and Simberloff, 1986) and establish long term management practices and ecological restoration programs (Schwartz et al., 2007).

In the marine realm, the maerl beds (also known as rhodolith beds) function as autogenic ecosystem engineers (Barbera et al., 2003). The complex nature of the three-dimensional calcified habitat structure generated by the maerl forming species host a large variety of organisms, the associated communities presenting an exceptional biological and functional diversity (Foster, 2001; Barbera et al., 2003; Grall et al., 2006; Peña et al., 2014a). Maerl beds provide a unique habitat to many commercially important crustacean, bivalve and fish species (Grall and Hall-Spencer, 2003; Grall et al., 2006) and can be seen as one of largest stores of carbon in the biosphere (Birkett et al., 1998). Worldwide, maerl-forming species are threatened due to anthropogenic disturbances (e.g., large-scale extraction, dredging, destructive fishing, and fish and mussel farming) as well as global climatic changes (e.g., ocean warming and acidification; Barbera et al., 2003; Grall and Hall-Spencer, 2003; Peña and Bárbara, 2008; Nelson, 2009; Brodie et al., 2014). Rhodolith beds regression would presumably result in more unfavorable conditions for many benthic organisms due to the loss of habitat and food resources (Airoldi et al., 2008; Cloern et al., 2016). Maerl-forming species are partially asexual organisms that combine the characteristic complex sexual life cycle of haploid-diploid red algae with vegetative fragmentation (see **Figure 1**). The importance of sexual vs. asexual reproduction varies between species and even between regions within species; and some authors proposed that for the most common species forming maerl beds along the temperate coast of North European (NE) Atlantic, asexual reproduction by fragmentation is the main mechanism of population renewal and maintenance (Bosence, 1976; Irvine and Chamberlain, 1994; Peña et al., 2014b; Pardo et al., 2017). Maerl lifespan can reach hundreds of years (i.e., living rhodolith's age estimated between a few hundred years up to thousand years, depending on the species and methodology used; Littler et al., 1991; Foster, 2001; Goldberg, 2006; McConnico et al., 2014) and populations of secular clones could exhibit low resilience to disturbances (McConnico et al., 2014). Despite their ecological significance, the maerl bed's dynamics of recruitment, maintenance, and main mechanisms of dispersion and colonization are not well understood. In particular, knowledge on the impact of clonal propagation, scales of dispersal, and gene flow on spatial genetic diversity of these habitat-forming algae is required to develop relevant management strategies. Moreover, habitat differences such as those found between estuarine and open sea habitats may also be important features shaping the pattern of genetic differentiation at a local scale (as for example in a fucoid alga: Coleman et al., 2018).

Among the NE Atlantic maerl beds, recent assessments using molecular approaches detected up to ten maerl-forming species (Peña et al., 2011, 2015; Pardo et al., 2014a, 2017; Hernández-Kantún et al., 2015). Most species show a restrained geographic

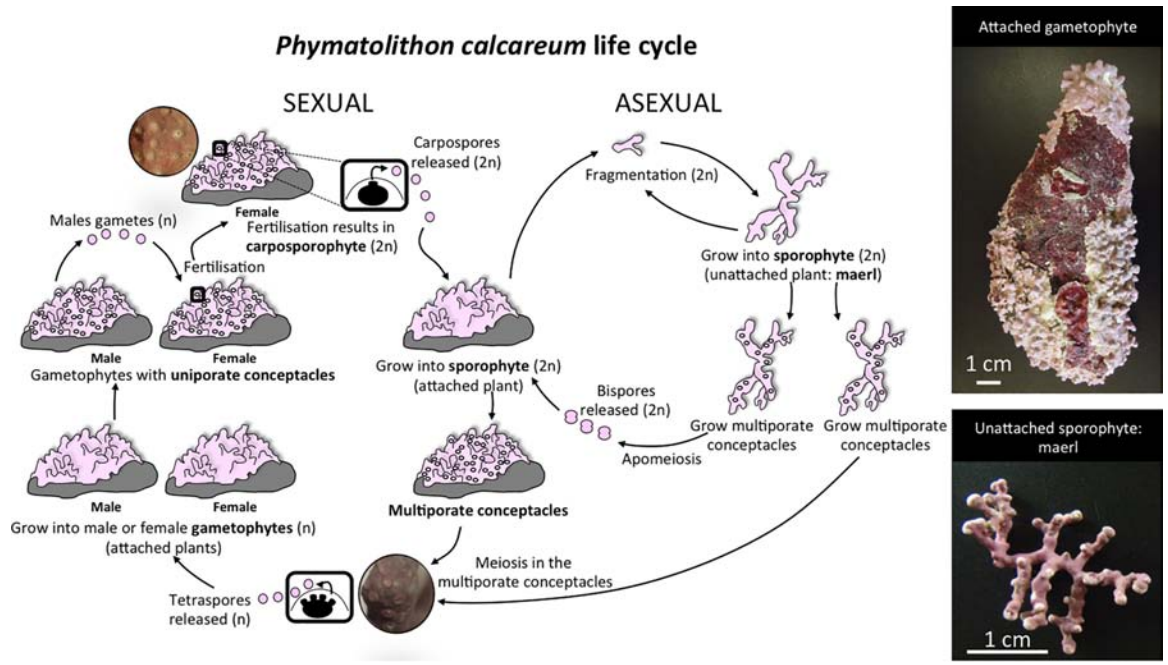

FIGURE 1 | The typical life cycle of maerl-forming species, including *Phymatolithon calcareum*. Sexual reproduction typically involves an alternation between diploid sporophytes and haploid male and female gametophytes. Regardless of their phase or sex, all spore recruits grow into encrusting-forms. The sporophyte (2n) produces, through meiosis, tetraspores (n) that are released and further develop as gametophytes. Male gametophytes (n) produce gametes by mitosis that are released and fertilize the gametes of female gametophytes (n) produced in uniporate conceptacles. Fertilization results in the formation of a zygote, which undergoes a complex series of changes that ultimately result in a diploid carposporophyte, retained on the female thallus. Carposphorophyte produces carpospores (2n) mitotically, which develop as sporophytes when they are released, completing the sexual cycle. Branches of encrusting growth-forms can break and grow into large unattached thalli that characterize the maerl (generally only reports of sporophytic maerl plants, Cabioch, 1969, 1970; Mendoza and Cabioch, 1998; Pardo et al., 2017). Fragmentation of branches from free-living maerl thalli can also occur enhancing the sporophyte vegetative reproduction (Bosence, 1976; Peña et al., 2014b; Pardo et al., 2017). Attached and unattached sporophyte thalli can also reproduce asexually by apomeiotic uninucleate bispores (Irvine and Chamberlain, 1994). Photos of an attached gametophyte (specimen with sexual uniporate conceptacles from Molène Archipelago described in Pardo et al., 2017, photograph by Cristina Pardo) and an unattached sporophyte (specimen with sexual multiporate conceptacles from Morlaix used in our study, photograph by Ignacio Bárbara) are given in the upper right hand corner and the lower right hand corner, respectively. Close-up from sexual uniporate conceptacles and multiporate conceptacles are given in circular inserts within the sexual life cycle. Please note that sporophytes of red algae producing tetraspores are commonly named tetrasporophytes in the literature.

distribution, while *Phymatolithon calcareum* (Pallas) W. H. Adey and D. L. McKibbin is confirmed as one of the most widespread builder of maerl beds in the temperate waters of this area (from Norway to the Iberian Peninsula, Carro et al., 2014; Pardo et al., 2014a). The existence of cryptic species within the same maerl bed (e.g., Carro et al., 2014) and the lack of genetic markers available for these non-model plants have, to date, restrained our capacity to develop population genetic studies. The main objective of our work was to determine the impact of clonal propagation on diversity and genotypic assemblage in *P. calcareum* populations sampled from fifteen sites along the temperate NE Atlantic coast, using eight microsatellites developed by Pardo et al. (2014b). In species with haploid-diploid life cycle, high rate of asexual reproduction can lead to an overdominance of one of the phases (Guillemin et al., 2008; Krueger-Hadfield et al., 2016). The level of clonality of *P. calcareum* populations was estimated by combining direct observations of reproductive structures, appraisal of the sporophytes / gametophytes ratio and classical estimates of genetic and genotypic diversity (Eckert, 2002; Arnaud-Haond et al., 2007). Our sampling covers the main distribution area of this maerl-forming species, from the British Isles to the Iberian Peninsula. In this study, we aim to answer the following questions: (i) what is the level of clonality of *P. calcareum* populations and its variation among populations?; (ii) what is the effect of clonality on the genetic diversity and the genotypic assemblage at a large scale, and is there any geographical trend linked to latitude?; (iii) at the local scale of the NW Iberian Peninsula (Galicia), how is the seascape shaping the patterns of genetic and genotypic differentiation within and among estuaries?

MATERIALS AND METHODS

Model Species

Phymatolithon calcareum is a non-geniculate coralline red alga encountered along the coast of the North Atlantic (from Norway to Atlantic Iberian Peninsula) and Mediterranean Sea. It is further considered one of the major maerl species, forming vast beds in temperate/cold waters within its distribution range (Pardo et al., 2014a) and is also listed as species whose

exploitation requires management (in Annex V of Eriksson and Fröborg, 1996). The species' complex sexual life cycle involves an alternation between two types of independent functional individuals: the diploid sporophyte and haploid, dioicious gametophytes (**Figure 1**). *Phymatolithon calcareum* is also able to reproduce asexually via vegetative fragmentation as well as more rarely by apomeiotic uninucleate bispores (**Figure 1**). All spores (haploids or diploids) grow into encrusting-forms (**Figure 1**) and even though the formation of bispores has also been reported in maerl-forming species, the presence of crusts has generally been associated with the occurrence of sexual reproduction in this species (Cabioch, 1969, 1970; Mendoza and Cabioch, 1998). While there are reports of fertile plants (both gametophytes and sporophytes) in the Mediterranean (Bressan and Babbini, 2003; Wolf et al., 2016), along the North European Atlantic (NE Atlantic), crustose forms of *P. calcareum* are very rare and have so far almost exclusively been observed in the French region of Brittany, growing as small epilithic crusts on pebbles or dead maerl (Mendoza and Cabioch, 1998; Peña et al., 2014b; Pardo et al., 2017). North European Atlantic maerl beds of *P. calcareum* are typically composed of free-living diploid sporophyte thalli that originated from broken branches initially growing on tetrasporophyte crusts (**Figure 1**). Maerl plants continue to grow, fragment, and multiply during their life with occasional production of tetrasporangial conceptacles (Cabioch, 1969, 1970; Bosence, 1976; Irvine and Chamberlain, 1994; Mendoza and Cabioch, 1998; Peña et al., 2014b; Pardo et al., 2017) (**Figure 1**). Further, the low abundance of encrusting individuals or free-living rhodoliths bearing reproductive organs have led to the conclusion that *P. calcareum* rhodolith beds were highly clonal and asexual reproduction by fragmentation of the own free-living maerl plants has been proposed as the main mechanism of their population renewal and maintenance (Bosence, 1976; Irvine and Chamberlain, 1994; Peña et al., 2014b; Pardo et al., 2017).

Sampling, DNA Extraction, Molecular-Based Species Detection and Genotyping

Maerl samples were collected along the NE Atlantic coasts between February and July 2011 in fifteen maerl beds distributed from the British Isles to Southern Portugal; eight of them located within protected areas (e.g., Natura 2000[1]) (**Supplementary Table S1**). To assess the pattern of genetic and genotypic diversity at different spatial scales, a hierarchical sampling design was applied. At the scale of the North Atlantic, four different geographic regions were defined according to the principal biogeographic provinces delimited in Spalding et al. (2007): the British Isles, Atlantic France, Atlantic Spain, and Southern Portugal (**Supplementary Table S1**). Except for South Portugal, three to four areas were sampled within each region: three areas in the British Isles (Northern Ireland, Wales, and England), three areas in Atlantic France (Northern Brittany, Western Brittany, and Southern Brittany), and four areas in Atlantic Spain (Ría de Muros e Noia, Ría de Arousa, Ría de Pontevedra, and Ría de Vigo) (**Supplementary Table S1** and **Figure 2**). Southwards, maerl beds composed of *P. calcareum* are found in the Algarve region, where only one bed could be sampled (Carro et al., 2014; Pardo et al., 2014a) (**Supplementary Table S1** and **Figure 2**). At the regional scale of Galicia, sampling was performed in the outermost zone (hereafter referred to as "outer-zone") and the middle sector (hereafter referred to as "inner-zone") of four estuaries (**Figure 2**). In our study, the sampled outer-zones were San Francisco, Barbafeita, Illa de Ons, and Illas Cíes; and the sampled inner-zones were Bornalle, Benencia, Tulla and Con de Pego (in Ría de Muros e Noia, Ría de Arousa, Ría de Pontevedra, and Ría de Vigo, respectively; **Figure 2** and **Supplementary Table S1**).

Maerl samples were collected by scuba diving at 3.9–20 m of depth. At each site, the sampling design consisted of 12–16 sampling points separated by 1–3 m along a linear transect in the maerl bed (i.e., a total transect length of 14–50 m). In each sampling point of the linear transect, three to six samples were collected randomly. The number of maerl samples collected per transect varied depending on the maerl bed's density. Once in the laboratory, specimens were air-dried and stored in silica for later observation and DNA extraction. Each individual was observed under a stereomicroscope and the presence of uniporate and multiporate conceptacles was used to define the phase (i.e., haploid gametophyte or diploid sporophyte; **Figure 1**). Genomic DNA extraction was performed using the NucleoSpin 96 Tissue kit (Macherey-Nagel, Düren, Germany) following the manufacturer's protocol. For all samples, a fragment of 950 base pairs (bp) of the plastidial gene photosystem II reaction center protein D1 (*psb*A) was amplified using the primers *psb*A-F1 and *psb*A-R2 from Yoon et al. (2002). Additionally, in some specimens, a fragment of 664 bp of the 5′ end of the mitochondrial gene cytochrome oxidase I (COI-5P) was amplified using the primers GazF1 and GazR1 or GCorR3 (Saunders, 2005; Pardo et al., 2014a). PCR conditions and thermal profiles followed those in Saunders and McDevit (2012) and Pardo et al. (2014a). Comparisons of the *psb*A and COI-5P sequences to the DNA barcodes available for the neotype specimen (voucher BM000712373, Pardo et al., 2014a; Peña et al., 2014b) were used to identify *P calcareum* samples.

Eight microsatellite loci developed by Pardo et al. (2014b) were amplified in two multiplex reactions for all samples identified as *P. calcareum*. Multiplexed PCR products were genotyped on an Applied Biosystems 3730XL DNA analyzer at Macrogen (Seoul, Korea) and scored using the GeneMarker® v1.7.0 software (SoftGenetics, State College, PA, United States). The raw data supporting the conclusions of this manuscript are available in **Supplementary Table S2** and can also be downloaded from Dryad (doi: 10.5061/dryad.ds2714g). Prior to analyses, raw data were checked for null alleles using a maximum-likelihood estimator with the software ML-NULLFREQ (Kalinowski and Taper, 2006).

Clonal Diversity

First, in order to assess the capacity of the eight microsatellite loci genotyped to discriminate all possible distinct MultiLocus Genotypes (MLGs) in each site, a jackknife resampling of loci

[1]http://ec.europa.eu/environment/nature/natura2000/index_en.htm

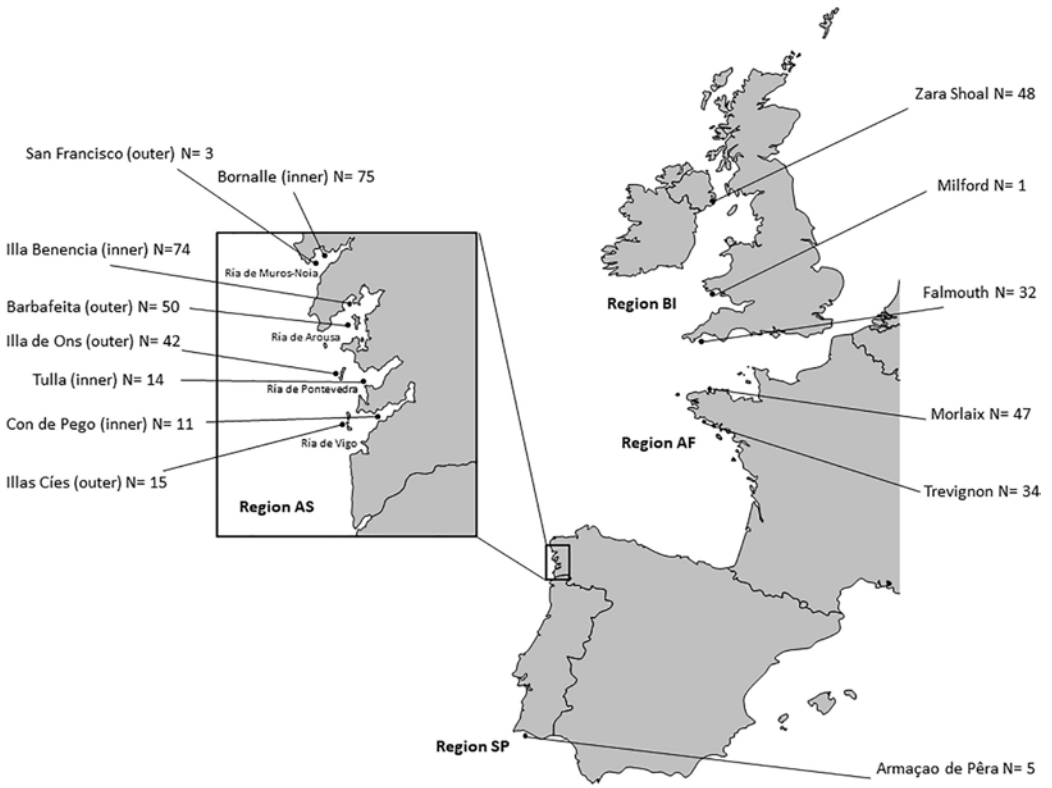

FIGURE 2 | Studied maerl beds, where *Phymatolithon calcareum* samples were collected and successfully scored for eight microsatellite markers (N, number of samples).

(1000 permutations) was used to estimate the average number of distinct MLGs that can be detected using the GENECLONE v.2.0 software (Arnaud-Haond and Belkhir, 2007). Herewith, the accumulation curve of the clonal diversity (*R*; genotypic diversity index; calculated as $R = (G - 1)/(N - 1)$, with G being the number of MLGs detected in the population and N the total number of individuals sampled; Dorken and Eckert, 2001) given the number of loci genotyped was plotted. The level of clonality within each site was estimated by calculating the number of MLGs and their *Psex* using the GENECLONE v.2.0 software (Arnaud-Haond and Belkhir, 2007), where *P*sex is the probability that a given MLG detected in N samples derived from distinct sexual reproductive events (i.e., thus actually belonging to different genets) (Arnaud-Haond et al., 2007). In order to limit overestimation of events of asexual reproduction in the investigated maerl beds, identical MLGs were considered as ramets of the same genet only when *P*sex fell below a threshold value fixed at 0.05. Indeed, for molecular markers with limited polymorphism and low statistical power, some distinct lineages could falsely appear identical (Arnaud-Haond et al., 2007). The genotypic diversity (R_{genets}) was calculated only taking into accounts the different genets as $R_{genets} = (G_{genets} - 1)/(N - 1)$, with G_{genets} being the number of genets detected in the population (including all repeated MLGs with *P*sex > 0.05) and N the total number of individuals sampled (Dorken and Eckert, 2001). Additionally, the effectiveness of our sampling effort to properly estimate the genotypic diversity in *P. calcareum* beds was tested using a resampling procedure where R values were estimated for multiple random combination of sampling units, for sample sizes ranging from 1 to N (N being equal to 75, the maximum sampling size within the data set; Bornalle, **Table 1**). The rate of change in R with increasing sampling size $N\left(i.e., \frac{dR}{dN}\right)$ was then plotted to estimate the number of sampled individuals required to yield R values approaching the asymptote (Arnaud-Haond and Belkhir, 2007).

Genetic Diversity and Structure

Note that all analyses of genetic diversity and structure were only carried out for sites with $N \geq 10$ *P. calcareum* (11 sites, **Table 1**) and that the site of Falmouth was not included since specimens sampled in this site were possibly triploids (more details are given at the beginning of the results section). Two data sets were constituted: a first a data set including all the sampled individuals (hereafter named "ramets") and a second one where repeated MLGs with *P*sex lower than 0.05 were removed (hereafter named "genets"). The following analyses were implemented using both, the "ramets" and the "genets" data sets.

For each site, number of alleles (*Na*), number of private alleles (*Nap*), observed heterozygosity (*Ho*), and unbiased expected heterozygosity (*He*) were computed for each locus and over all

TABLE 1 | Measures of clonal identity of *Phymatolithon calcareum* along the European Atlantic coast.

Region	Site	*N*	*MLGs*	*Genets*	*R*	R_{genets}
BI	Zara Shoal	48	33	33	0.681	0.681
	Milford Haven	1	1	–	–	–
	Falmouth[$]	32	2	–	0.032	–
AF	Morlaix	44	14	17	0.302	0.372
	Trevignon	34	10	13	0.273	0.364
AS	San Francisco (outer)	3	3	3	1	1
	Bornalle (inner)	75	19	20	0.243	0.257
	Barbafeita (outer)	50	6	8	0.102	0.143
	Benencia (inner)	74	4	21	0.041	0.274
	Illa de Ons (outer)	42	27	27	0.634	0.634
	Tulla (inner)	14	4	4	0.231	0.231
	Illas Cíes (outer)	15	6	6	0.357	0.357
	Con de Pego (inner)	11	4	5	0.300	0.400
SP	Armaçao de Pêra	4	4	4	1	1

[$]*Note that in Falmouth, all 32 sporophytes were triploids. BI, British Isles; AF, Atlantic France; AS, Atlantic Spain; SP, Southern Portugal; (outer), outer-zone of the Ría; (inner): inner-zone of the Ría. N, number of samples successfully scored. MLGs, number of MultiLocus Genotypes. Genets, number of genets detected (i.e., number of individuals produced by sexual reproduction; including repeated MLGs with Psex > 0.05). R, genotypic diversity index.* R_{genets}*, genotypic diversity index taking into accounts only the different genets.*

loci using GenAlEx v.6.501 (Peakall and Smouse, 2012). Allelic richness (*AR*) was estimated with a rarefaction approach using the software HP-RARE v.1 (Kalinowski, 2005). Estimations of AR were calculated standardizing the sample size to $N = 11$ for the "ramets" and $N = 4$ for the "genets" data set.

For each population, linkage disequilibrium (*LD*) was assessed using the association index $\bar{r}_d$ in MultiLocus v.1.2. (Agapow and Burt, 2001). To test departure from random associations between loci, the observed dataset was compared with 1000 simulated datasets, in which recombination was imposed by randomly reshuffling the alleles, independently for each locus, among individuals (Agapow and Burt, 2001). Tests for departure from Hardy-Weinberg equilibrium were performed using FSTAT v.2.9.3.2 (Goudet, 1995). F_{IS} was calculated for each locus and over all loci according to Weir and Cockerham (1984) and significance was tested by running 1000 permutations of alleles, among individuals, within samples. To investigate population differentiation, Weir and Cockerham's unbiased measure of F_{ST} was estimated over all loci using FSTAT v.2.9.3.2 (Goudet, 1995). To test isolation by distance (IBD) a Mantel test was carried out using 999 permutations in GenAlEx v.6.501 (Peakall and Smouse, 2012). As suggested by Rousset (1997) for sampling schemes undertaken in at a two-dimensional scale, F_{ST} / (1- F_{ST}) was plotted against the logarithm of the geographical distance between each populations pair.

At the regional scale of Galicia, a nested analysis of molecular variance (AMOVA) was implemented using ARLEQUIN v.3.1 (Excoffier et al., 2005) to test for the partition of genetic variance within sites, between sites within estuaries, and among estuaries. In addition, differences between sites located in the outer, and inner-zone of the estuaries were tested for several genetic measures (*R*, *AR*, *Ho*, *He*, and F_{IS}) using non-parametric Mann–Whitney tests with STATGRAPHICS[2].

RESULTS

Of the 1142 maerl plants sequenced, 455 samples were identified as *P. calcareum*. The percentage of *P. calcareum* observed was very variable depending on the site under study, ranging from 96% in Benencia (Galicia) to 0% in Brest (Western Brittany) (**Supplementary Table S1**).

Most of the *P. calcareum* plants were vegetative even if some sporophytes (44 over the 455 studied, 10%, **Supplementary Table S2**) were identified thanks to the occurrence of sexual structures (i.e., presence of multiporate conceptacles, see **Figure 1**). No mature gametophytes, characterized by uniporate conceptacles (**Figure 1**), were detected. Of the 455 *P. calcareum* individuals, 447 were successfully scored for the eight microsatellite loci (**Table 1**) and diploid individuals (i.e., sporophytes) were defined as individuals showing a heterozygous genotype for at least one locus (Guillemin et al., 2008; Krueger-Hadfield et al., 2016). Non-mature plants were all characterized by genotypes showing at least one heterozygous locus and were classified as sporophytes (**Supplementary Table S2**). All populations, except Falmouth, were composed exclusively of diploid sporophytes. All specimens collected in Falmouth (32 plants, **Table 1** and **Supplementary Table S1**) displayed a triploid profile in three of the eight loci scored (PC-2, PC-3, and PC-7, Pardo et al., 2014b) and were considered as possible triploid sporophytes. In Falmouth, clonal diversity (*G* and *R*) was estimated by directly using the triploid data set (Menken et al., 1995).

Missing Data and Power of Clone Detection of the Eight Microsatellites Genotyped

Of all the individuals genotyped, only four did not amplify at all eight microsatellite loci and were not included in our analyses (**Table 1**). One individual did not amplify for the locus PC-8 while three individuals did not amplify for the locus PC-6 (**Supplementary Table S2**). When only considering the individuals scored at every locus, results from ML-NULLFREQ (Kalinowski and Taper, 2006) showed evidence of null alleles at the loci PC-6 (null allele frequency = 20.58%) and PC-8 (null allele frequency = 24.41%). Even if missing data can have an impact on the estimation of genotypic frequencies (Gourraud et al., 2004), we chose to keep all loci in the subsequent analyses since (i) our capacity to detect distinct MLGs was limited at some sites, even when all eight microsatellite loci were included (see **Supplementary Figure S1**), and (ii) it has been demonstrated that including loci with low to moderate frequencies of null alleles (i.e., <20–30%) does not profoundly affect classical and Bayesian population genetic analyses of population structure (Séré et al., 2014).

[2]http://www.statgraphics.net/

The power of the eight microsatellite loci genotyped to discriminate all possible distinct MLG was sufficient at five sites of the study area (Zara Shoal, Illa de Ons, Illas Cies, Tulla, and Bornalle; **Supplementary Figure S1**), as the accumulation curve of the clonal diversity reached a plateau at values lower than eight. In contrast, the curve obtained for three sites (Barbafeita, Benencia, and Falmouth; **Supplementary Figure S1**) did not show the typical asymptotic growth nor a plateau. Likewise, in Con de Pego, Morlaix, and Trevignon (**Supplementary Figure S1**) the accumulation curve did not reach a plateau even when using the eight loci available. Therefore, it is possible that our estimation of clonal diversity in these last six sites may be less accurate.

In sites where more than ten maerl plants of *P. calcareum* were sampled (11 sites), the number of MLGs varied from two (Falmouth, 32 samples) to 33 (Zara Shoal, 48 samples) (**Table 1**). For most repeated MLGs, *Psex* values were lower than 0.05, suggesting that a high number of them were ramets of the same genet (**Supplementary Table S2**). However, in the six sites where the power of the eight microsatellites genotyped for MLG distinction was low (Barbafeita, Benencia, Falmouth, Con de Pego, Morlaix, and Trevignon; **Supplementary Figure S1**), some repeated MLGs had *Psex* values higher than 0.05 and were considered as the possible outcome of sexual reproduction and kept as different genets (**Table 1** and **Supplementary Table S1**). Except for Benencia, within the aforementioned sites, only a few repeated MLGs show $Psex > 0.05$, and our estimation of clonal diversity is likely unaffected (**Table 1**). In Benencia, 17 copies of repeated MLGs could not be considered to come from asexual reproduction (**Table 1**).

Clonal Identity

In two sites where less than ten maerl plants of *P. calcareum* were sampled (Armaçao de Pêra in South Portugal and San Francisco in Galicia), all samples belonged to distinct MLGs (**Table 1**). In the eleven sites where more than ten *P. calcareum* were sampled, a typical signature of clonality was observed with a number of genets much lower than the total number of samples (**Table 1**). Zara Shoal and Illa de Ons showed a relatively high clonal diversity ($R = R_{genets} = 0.681$ and 0.634, respectively), while the site of Falmouth was the less clonally diverse, with a R of only 0.032 (**Table 1**). Because of the lack of power of our markers, in Benencia, its clonal diversity was more difficult to estimate and the value of R_{genets} was six times higher (0.274) than the value of R (0.041) (**Table 1**). Clonal diversity was highly variable within regions and even within estuaries (for example, in Ría de Pontevedra, R_{genets} from Illa de Ons is three times higher than from Tulla, **Table 1**).

Interestingly, our study revealed that in seven cases two MLGs within the same site were differentiated by a single mutational step and that in three cases these pairs of MLGs belonged each to one rare genotype and one frequent one (**Supplementary Table S2**). In Falmouth, the difference between the rare MLG ($N = 1$) and the frequent MLG ($N = 31$) occurred at a locus where three alleles were detected (PC-3; **Supplementary Table S2**).

Most MLGs, were private to one sampling site (**Figure 3**). Only four MLGs were shared between sites and generally these were only encountered among close by sampling sites located in Galicia (**Figure 3**). MLG015 was the most commonly sampled genotype (sampled 103 times, equivalent to 23% of all genotyped *P. calcareum* individuals) and the only MLG encountered in two biogeographic provinces: Atlantic Spain and Atlantic France (**Figures 2**, **3**).

Genetic Diversity and Structure of the Maerl Beds at the Two Spatial Scales Studied

All data on multilocus genetic diversity estimates are given in **Table 2**. No clear patterns of latitudinal variation of genetic and genotypic diversity were observed at the scale of the NE Atlantic. The mean number of alleles varied between 1.63 and 3.50, and the highest values ($Na > 3.00$) were found in Trevignon, Illa de Ons and Illas Cíes (**Table 2**). The higher values of allelic richness (AR) were observed in Illa de Ons and Illas Cíes, when all individuals were included in the analyses ("ramets" data set; $AR > 3.00$, **Table 2**). Levels of observed heterozygosity (Ho) were usually higher than unbiased expected heterozygosity (He) and the highest values of Ho were detected in Galicia, in the populations from Tulla and Illas Cíes (**Table 2**). Significant excess of heterozygotes was indeed detected in five sites when all individuals were included in the analyses ("ramets" data set; Trevignon, Barbafeita, Benencia, Tulla, and Con de Pego; **Table 2**). If only genets were taken into account, F_{IS} values retrieved were higher than those for the "ramets" data set at all sites, and significant excess of heterozygotes was detected in Trevignon and Benencia ("genets" data set; **Table 2**). Among ramets, LD values were significant for all sites except Benencia, while among genets, roughly half of the study sites showed significant LD ($\bar{r}_d$; **Table 2**). When all these analyses were performed without the two loci with a non-negligible frequency of null alleles (PC-6 and PC-8), the results did not change substantially except for the fact that all F_{IS} were negative and significant, and all $\bar{r}_d$ values were significant among the ramets data set (data not shown).

Private alleles were encountered in all regions except in Atlantic France and the percentage of private alleles was very high in Southern Portugal (12.5% of private allele; **Supplementary Table S3**). For the "ramets" data set, all pairwise F_{ST} values calculated among sites were significantly different from zero, and ranged from 0.11 to 0.61 (**Supplementary Table S4A**). Similarly, F_{ST} values calculated among sites using the "genets" data set were all positive and significant, except among some sites sampled in Galicia and between Tulla and Trevignon (**Supplementary Table S4B**). Concerning the relationship between genetic and geographical distance, significant patterns of IBD were observed for both, the "ramets" (Mantel test, $P = 0.01$) and the "genets" data set (Mantel test, $P = 0.0001$) (**Supplementary Figures S2A,B**).

At the local scale of Galicia, clear differences in genetic diversity and structure were observed between sites located in the outer and in inner-zones of the estuaries (**Table 2** and **Figure 4**). First, for both data sets, parametric Mann–Whitney tests ($P < 0.05$) showed a significantly higher allelic richness in the outer-zones ("ramets" $AR = 2.838 \pm 0.211$;

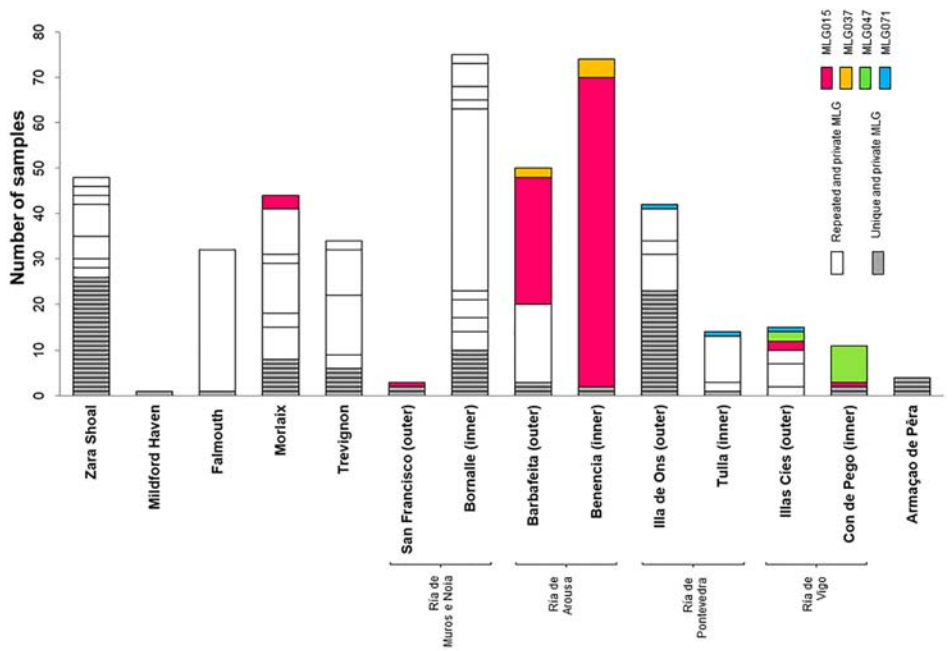

FIGURE 3 | MultiLocus Genotypes (MLGs) observed for eight microsatellite markers in *Phymatolithon calcareum* from fourteen study sites. Private and unique MLGs are shown in gray while private repeated MLGs and are shown in white. The different colors represent MLGs shared between sites.

"genets" $AR = 2.663 \pm 0.175$), than in the inner-zones of the estuaries ("ramets" $AR = 1.975 \pm 0.156$; "genets" $AR = 2.008 \pm 0.168$). Expected heterozygosity (*He*) was also significantly higher (Mann-Whitney test, $P < 0.05$) in the outer than in the inner-zones of the estuaries for both data sets ("ramets" $He = 0.497 \pm 0.043$ and 0.330 ± 0.052; "genets" $He = 0.534 \pm 0.043$ and 0.395 ± 0.057; results given for the outer and inner-zones, respectively). The F_{IS} values showed a clear excess of heterozygotes only in the inner-zones (inner-zones: "ramets" $F_{IS} = -0.396 \pm 0.168$, "genets" $F_{IS} = -0.227 \pm 0.158$; outer-zones: "ramets" $F_{IS} = 0.021 \pm 0.116$, "genets" $F_{IS} = 0.070 \pm 0.111$), and differences between the outer and inner-zones were significant in both data sets (Mann–Whitney test, $P < 0.05$). The mean F_{ST} values between sites from the same estuary and between outer estuarine sites were low ($F_{ST} < 0.176$; **Figure 4**). On the other hand, F_{ST} values between inner estuarine sites were much higher ($F_{ST} = 0.456$; **Figure 4**). The results of the AMOVA showed that genetic variation among estuaries (≈19 and 16%; "ramets" and "genets" data set, respectively) is slightly higher than among sites within estuaries (≈14 and 7%; "ramets" and "genets" data set, respectively) whatever the data set under study (**Supplementary Tables S5A,B**).

DISCUSSION

Because of the existence of various cryptic species in the maerl beds of the NE Atlantic (Pardo et al., 2014a), *Phymatolithon calcareum* specimens cannot be identified using taxonomical criteria based on morphology. This limits the ability to plan a homogeneous population genetic sampling strategy and, indeed, only a few to no specimens of *P. calcareum* could be collected at four of the fifteen sampled sites. Notwithstanding this limitation, our results show clear signature of clonality affecting both the maerl beds population dynamics (i.e., all beds dominated by the tetrasporophytic phase of the life cycle) as well as genetic diversity and structure. High levels of genetic differentiation suggest that recruitment occurs mostly locally with dispersal being limited by geographic distance but also by coastal configuration and water dynamics. Nevertheless, some rare long-distance dispersal events may have spread clones of *P. calcareum* over larger areas (e.g., one clone located in two biogeographic regions). We propose a complex interplay between the outcomes of sexual/asexual reproduction, mutation, and hybridization as a possible explanation to the pattern of genetic and genotypic diversity in this maerl forming species.

Slow Accumulation of Genotypic Diversity in a Long-Lived Clonal Maerl Forming Species

The low genotypic diversity, complete absence of gametophytes, and low number of samples producing spores revealed in this study confirms that *Phymatolithon calcareum* propagates primarily via clonal fragmentation. The pattern of genotypic diversity was highly variable among populations confirming previous reports of geographical variation of phenotypic occurrence of sexual *P. calcareum* thalli (reports of fertile sporangial maerl plants or small crustose gametophytes: Cabioch, 1969, 1970; Mendoza and Cabioch, 1998; Peña et al., 2014b; Pardo

TABLE 2 | Genetic diversity estimates, inbreeding coefficient and linkage disequilibrium calculated for eight polymorphic microsatellite markers in ten sites where *Phymatolithon calcareum* were sampled along the Atlantic coasts of Europe.

			Mean over 8 loci (ramets)					
Region	***Population***	***N***	***Na ± SD***	***AR ± SD***	***Ho ± SD***	***He ± SD***	F_{IS}	$\bar{r}_d$
BI	Zara Shoal	48	2.75 ± 1.83	2.23 ± 0.81	0.414 ± 0.293	0.454 ± 0.186	0.089	0.070*
	Milford Haven	1	—	—	—	—	—	—
	Falmouth[$]	32	—	—	—	—	—	—
AF	Morlaix	44	2.13 ± 0.35	2.07 ± 0.37	0.375 ± 0.354	0.361 ± 0.162	−0.038	0.099*
	Trevignon	34	3.13 ± 2.03	2.52 ± 1.13	0.493 ± 0.483	0.358 ± 0.257	−0.384*	0.610*
AS	San Francisco (outer)	3	—	—	—	—	—	—
	Bornalle (inner)	75	2.88 ± 0.64	2.52 ± 0.57	0.418 ± 0.368	0.426 ± 0.163	0.018	0.397*
	Barbafeita (outer)	50	2.25 ± 1.04	2.05 ± 0.80	0.420 ± 0.406	0.353 ± 0.247	−0.193*	0.940*
	Benencia (inner)	74	1.63 ± 0.74	1.41 ± 0.53	0.370 ± 0.507	0.191 ± 0.260	−0.948*	−0.030
	Illa de Ons (outer)	42	3.13 ± 0.83	3.02 ± 0.74	0.458 ± 0.314	0.558 ± 0.147	0.180	0.146*
	Tulla (inner)	14	2.75 ± 0.71	2.61 ± 0.63	0.705 ± 0.426	0.455 ± 0.220	−0.584*	0.386*
	Illas Cíes (outer)	15	3.50 ± 1.07	3.46 ± 1.04	0.558 ± 0.387	0.581 ± 0.161	0.040	0.447*
	Con de Pego (inner)	11	1.88 ± 0.64	1.88 ± 0.64	0.466 ± 0.501	0.343 ± 0.247	−0.385*	0.490*
SP	Armaçao de Pêra	4	—	—	—	—	—	—
			Mean over 8 loci (genets)					
Region	**Population**	***Genets***	***Na ± SD***	***AR ± SD***	***Ho ± SD***	***He ± SD***	F_{IS}	$\bar{r}_d$
BI	Zara Shoal	33	2.75 ± 1.83	2.03 ± 0.52	0.413 ± 0.277	0.459 ± 0.189	0.102	0.015
	Milford Haven	1	—	—	—	—	—	—
	Falmouth[$]	3	—	—	—	—	—	—
AF	Morlaix	17	2.13 ± 0.35	1.82 ± 0.32	0.301 ± 0.282	0.316 ± 0.158	0.047	0.003
	Trevignon	13	3.13 ± 2.03	2.18 ± 0.98	0.500 ± 0.478	0.377 ± 0.274	−0.346*	0.514*
AS	San Francisco (outer)	3	—	—	—	—	—	—
	Bornalle (inner)	20	2.88 ± 0.64	2.38 ± 0.50	0.456 ± 0.321	0.508 ± 0.169	0.104	0.047*
	Barbafeita (outer)	8	2.25 ± 1.04	2.08 ± 0.84	0.406 ± 0.332	0.393 ± 0.271	−0.037	0.795*
	Benencia (inner)	21	1.63 ± 0.74	1.42 ± 0.53	0.357 ± 0.484	0.199 ± 0.262	−0.829*	−0.103
	Illa de Ons (outer)	27	3.13 ± 0.83	2.74 ± 0.59	0.477 ± 0.293	0.582 ± 0.120	0.183	0.034*
	Tulla (inner)	4	2.75 ± 0.71	2.75 ± 0.71	0.656 ± 0.421	0.594 ± 0.178	−0.125	0.127
	Illas Cíes (outer)	6	3.50 ± 1.07	3.17 ± 0.84	0.563 ± 0.377	0.627 ± 0.143	0.112	0.223*
	Con de Pego (inner)	5	1.88 ± 0.64	1.87 ± 0.63	0.425 ± 0.471	0.392 ± 0.259	−0.097	0.088
SP	Armaçao de Pêra	4	—	—	—	—	—	—

Only sites where more than ten individuals of P. calcareum were sampled were taken into account. All calculations were performed using both the "ramets" and "genets" data set. [$]*Note that in Falmouth, all 32 sporophytes were triploids. BI, British Isles; AF, Atlantic France; AS, Atlantic Spain; SP, Southern Portugal; (outer), outer-zone of the Ría; (inner), inner-zone of the Ría. N, number of samples successfully scored (ramets, i.e. morphological individuals). Genets, number of genets detected (i.e., number of individuals produced by sexual reproduction). Na, number of alleles. AR, allelic richness recalculated using a rarefaction method with 11 and 4 samples for the "ramets" and "genets" data sets, respectively. SD, standard deviation. Ho, observed heterozygosity. He, unbiased expected heterozygosity.* F_{IS}*, inbreeding coefficient.* $\bar{r}_d$*, coefficient of Multilocus Linkage Disequilibrium. *P < 0.05.*

et al., 2017). However, the genetic estimates of sexual/asexual reproduction provided by the current study do not vary accordingly to the frequency of sexual phenotypes reported previously. Indeed, sexually mature thalli have never been reported in some well-studied maerl beds of Galicia (Peña et al., 2014b, 2015; Pardo et al., 2017) or the British Isles (Irvine and Chamberlain, 1994); while there are few reports of phenotypic occurrence of sexual reproduction from Brittany (Cabioch, 1969, 1970; Mendoza and Cabioch, 1998; Peña et al., 2014b; Pardo et al., 2017) and these are common in the Mediterranean (Bressan and Babbini, 2003; Wolf et al., 2016). In our study, values of genotypic diversity detected in Brittany (Morlaix and Trevignon) were generally similar or lower to those measured in Galicia, a result opposite to the one expected based on direct observation of mature thalli (see Pardo et al., 2017). Maerl beds, ten meters thick, can extend over several square-kilometers. This indicates great temporal stability, lasting probably over thousands of years (e.g., Brittany; Grall and Hall-Spencer, 2003). Such temporal scale may explain why neither production of sexual structures nor sporelings recruitments has ever been observed in some maerl beds. Even if extremely uncommon, successful recruitment of new genets generated by sexual reproduction may have considerable implications on population genotypic diversity in such long-lived sexual/asexual organisms (terrestrial plants: Eriksson and Fröborg, 1996; Stehlik and Holderegger, 2000; seagrasses: Alberto et al., 2005; Arnaud-Haond et al., 2012, 2014;

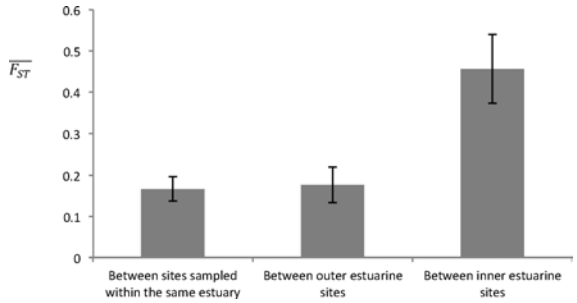

FIGURE 4 | Mean (and SE) F_{ST} values calculated between sites within the same estuary, between outer estuarine sites, and between inner estuarine sites in Galicia using eight microsatellite loci. The two populations from the Ría de Muros e Noia, San Francisco and Bornalle, were not included since only three specimens of *Phymatolithon calcareum* were sampled in San Francisco (i.e., outer-zone, see **Figure 2**). F_{ST} values correspond to the ones calculated using the whole data set (i.e., the "ramets" data set).

soft coral: McFadden, 1997). As stated by Hurst and Peck (1996), "a little sex may go a long way" and very low rates of recruitment have been shown to produce high genetic variation in long-lived clonal plant (Eriksson and Fröborg, 1996; Stehlik and Holderegger, 2000). Thus, the maintenance of substantial numbers of different genotypes in some population could be explained by the combined effects of large population size and slow renewal of the populations.

Except in Falmouth, where *P. calcareum* thalli were recognized as putative triploids, all samples from this species were diploid in the maerl beds studied. Moreover, six of the ten beds dominated by diploid tetrasporophytes displayed strong heterozygote excess. An uncoupling of the complex haploid-diploid life cycle and an overdominance of one of the phases (generally dominance of the diploid tetrasporophytes over the haploid gametophytes) has previously been recorded in clonal populations of red algae (Sosa et al., 1998; Guillemin et al., 2008; Kamiya and West, 2010; Krueger-Hadfield et al., 2016). In those algal populations as in other plant and animal species (Balloux et al., 2003), heterozygote excess was also detected. Even if recent theoretical studies have shown that neutral dynamics of genotype frequencies in partially clonal organism may explain transient negative values of F_{IS} (Reichel et al., 2016), heterozygote excess in clonal organisms has classically been related to either passive accumulation of somatic mutations over time (Klekowski, 1997; Ally et al., 2008; Ardehed et al., 2015) or advantage related to heterozygosity (Balloux et al., 2003; Guillemin et al., 2008; Krueger-Hadfield et al., 2016). These three explanations (i.e., neutral transient dynamics of the F_{IS}, accumulation of somatic mutations and heterozygote advantage) may account for the excess of heterozygotes observed in *P. calcareum*.

The Special Case of Triploid Clones in the *Phymatolithon calcareum* Bed From Falmouth

Hybridization and introgression events could be leading to changes in reproductive mode, producing new, generally obligate, asexual genotypes (Gastony, 1986; Tucker et al., 2013). Supporting this idea, in algae, hybrids of genetically distinct entities have been repeatedly associated with the formation of asexual lineages (in red algae: Kamiya and West, 2008; Kamiya et al., 2011, 2017; in green algae: Ogawa et al., 2015; and in brown algae: Coyer et al., 2006) and with sterility linked to changes in ploidy level (e.g., polyploidy and aneuploidy; Coyer et al., 2006; Montecinos et al., 2017b). Interestingly, the *P. calcareum* bed from Falmouth populated by putative triploids is also the population presenting the lowest genotypic diversity and of the only two genotypes identified there, one seems to have arisen from mutations and not from sexual reproduction and recombination. We, thus, propose that in *P. calcareum*, genetic variation results mostly from successful settlement of sexually produced genotypes and accumulation of new somatic mutations in long-lived clones but that rare events of past hybridization and introgression could have been at the origin of some obligate asexual lineages. The identification of the second potential parental species could not be deduced from our data set. In Falmouth, only two species were detected in the maerl beds, *P. calcareum*, and *Lithothamnion corallioides* (Carro et al., 2014; Pardo et al., 2017). However, other species of *Phymatolithon*, such as *P. lamii* or *P. laevigatum*, have also been reported in the area (Pardo et al., 2017). Resequencing of regional maerl specimens from the British Isles and Atlantic France for several unlinked genetic markers and the search for incongruence between them could be a first step to test for the existence of hybridization in Falmouth and identify the second parental species (Montecinos et al., 2017a).

Large-Scale Distribution of Genetic Diversity: Restricted Dispersal but No Clear Influence of Latitude or Historical Climatic Oscillations

At the large European scale, a significant pattern of isolation by distance was detected in *P. calcareum*, confirming the limited dispersal capacity of spores and gametes observed in various sexually reproducing macroalgae (Durrant et al., 2014). It seems that even low levels of gene flow, probably more through movement of small rhodoliths or detached branches than through spore recruitments, have been able to connect populations over the whole *P. calcareum* distribution area. Maerl beds appear to be quite patchy nowadays, but rhodolith dominated benthic communities have reached much more extensive development in the past, colonizing most of the temperate platforms (e.g., during late Miocene; Halfar and Mutti, 2005), and it is possible that stepping-stone migration between large beds could have been more common in the past.

In the NE Atlantic, *P. calcareum* is steadily replaced by other rhodolith forming species in both the north of the British Isles region and south of Galicia (Carro et al., 2014; Pardo et al., 2014a; Peña et al., 2015) and the most southern and northern sampling sites in the present study are located at the species distribution edges. However, we did not detect any significant

pattern of variation of genotypic or genetic diversity with latitude that could be explained by geographic parthenogenesis (Eckert, 2002) or rapid poleward recolonization after the Last Glacial Maximum from genetically rich, lower latitude refugia (Maggs et al., 2008; Neiva et al., 2016). Nonetheless in macroalgae, shifts toward asexual reproduction have been detected in populations living in highly stressful environments such as in brackish waters of the Baltic Sea (Bergström et al., 2003) and at high intertidal limits and/or at range edges (Suneson, 1982; Fierst et al., 2010; Krueger-Hadfield et al., 2013; Oppliger et al., 2014). Other hypotheses, as the intermediate disturbance theory, further attempt to explain changes in genetic and genotypic diversity along species ranges (e.g., in the seagrass *Zostera muelleri*, Macreadie et al., 2014). Genotypic diversity is expected to be higher in habitats with intermediate disturbance levels where recurrent opening of accessible space allows for the recruitment of new seedlings. In the NE Atlantic, differences in recurrence intervals of hurricane-strength storms or surge-events (Hickey, 2011) may explain in part the high variability in genotypic diversity among our sampling sites.

Successive expansion and contraction events occurring during the Pleistocene have led to a gradient in genetic diversity among most marine species distributed along the NE Atlantic coasts, with high genetic diversity and distinctiveness characterizing populations at the rear edge (i.e., Iberian Peninsula and Algarve) and high genetic homogeneity at the leading edge (i.e., British Isles) (Maggs et al., 2008; Neiva et al., 2016). The sampling site of Armaçao de Pêra, located in Algarve and corresponding to the southernmost edge of *P. calcareum*'s distribution in the Atlantic (Carro et al., 2014; Pardo et al., 2014a), presented high genotypic diversity and high numbers of private alleles. This result may be related to long-term stability and isolation of the maerl beds located in South Portugal (the potential rear edge) during the past glacial and interglacial climatic oscillations. However, no latitudinal gradient of genetic diversity could be identified in *P. calcareum* since most northern beds did not have reduced genetic diversity when compared to the ones from the Iberian Peninsula.

Processes Driving Clonal Distribution at Small Scales: Coastal Configuration, Currents, and Storm Incidence

Most of the clones observed in the present study were restricted to one site. This aggregated distribution of clones supports direct observations made by Cabioch (1970) in Brittany proposing that ramets coming from fragments of overgrown rhodoliths mostly accumulate locally and are not necessarily rapidly swept away from their parental plants by currents. Field observations and experimentations have shown that rhodoliths are easily moved over scales of tens of centimeters by wind-propagated waves or disturbances due to bioturbation caused by fish and invertebrates, and can even be transported over meters by swell generated by strong winds (Marrack, 1999 and references therein). Anthropogenic activities such as bivalve dredging are known to alter the structure complexity of maerl beds in the NE Atlantic (Barbera et al., 2003) and could also facilitate the local spread of rhodoliths (but see Hall-Spencer et al., 2003).

At the regional scale, coastal topography and hydrodynamics (waves, tides, and currents) seem to control the rate of recruitment of new sexual or asexual propagules and the gene flow between estuarian and coastal populations. The more protected inner-zones of estuaries were characterized by lower genetic and genotypic diversity than coastal outer-zones. This pattern could be linked to a lower rate of recruitment of sexual seedlings in the inner-zones of the estuaries and is indeed concordant with the higher excess of heterozygotes detected in these populations (expected for predominantly asexual populations; Balloux et al., 2003). In the region of Rías Baixas, connectivity along the coast was reduced between populations located in the inner zone compared to those of the outer-zone. Strikingly similar results have been reported in a brown alga living both inside and outside estuaries along the Australian coast (*Hormosira banksii*, Coleman et al., 2018). In *H. banksii*, patterns of connectivity were linked to coastal topography and water exchange between estuaries and the open coast, where populations inside estuaries acted as sinks of migrants. Inner-zones sampled in our study present a combination of estuarine and marine characteristics while the outer-zones' hydrodynamics are governed by open-ocean water movement (deCastro et al., 2000; García-Gil et al., 2000; Iglesias and Carballo, 2009; Bernabeu et al., 2012). The geographical limit of each zone varies depending on the seasonal upwelling-downwelling sequences that define the patterns of circulation in the estuaries (Torres and Barton, 2007). Strong waves and swell affect the outer-zones of Rías Baixas (Bernabeu et al., 2012) and frequent disturbances could enhance recruitment of new genotypes that can be flush inside the Rías by powerful scouring bottom currents during the upwelling season (Iglesias and Carballo, 2009). Once trapped in the estuaries inner-zones, rhodoliths seem to mostly reproduce asexually. Similarly, a higher rate of asexual reproduction of *H. banksia* has been measured within estuaries when compared to areas along the open coast (Coleman et al., 2018). Authors further proposed that estuarine populations could have originated from floating thalli, teared off from neighboring open coast populations after large-scale storms.

Mirroring the results obtained with estimates of population divergence (F_{ST}), a few MLGs were shared between geographically close populations located in the estuaries outer-zones and those from the inner-zone and the mouth of estuaries. However, one MLG was extremely common in Galicia and spread over the whole sampled region of the Rías Baixas. Since ramets constitute free-living forms after thallus fragmentation in *P. calcareum*, the geographical range colonized by a single MLG cannot be used to estimate the age of clones (as for example, in the case of *Posidonia oceanica*, a clonal seagrass reproducing asexually via stolon growth; Arnaud-Haond et al., 2012). Growth rate of rhodoliths is considered as extremely low (as low as ∼1 mm per year for *P. calcareum* maerl; Adey and McKibbin, 1970; Blake and Maggs, 2003) and even ramets lifespan can reach hundreds of years (Foster, 2001; Goldberg, 2006). Speed of formation of new maerl beds have never been

estimated. However, the radio carbon age of surface maerl thalli sampled near Trevignon was estimated to be of more than 1000 years BP (Before Present) while thalli sampled deeper in the same maerl bed reached almost 6000 years BP (Grall and Hall-Spencer, 2003). These results have leaded to the hypothesis that the maerl beds observed in Brittany have accumulated slowly during the las 10.000 years (i.e., since the end of the last glaciation; Grall and Hall-Spencer, 2003). Interestingly, the estuaries of the Rías Baixas have also reached their current coast lines and bathymetry 11.000 years ago (Méndez and Vilas, 2005). Because of these antecedents, we propose that the huge spatial and numerical dominance of the MLG015 genet can only have been established over a very long period of time and that extended distribution of some genotypes probably correspond to very old genets that have slowly spread over time to adjacent beds and even over whole region due to episodic large-scale disturbance such as hurricane-like storms. Extreme longevity of genets has been reported in other slow growing clonal organisms and genets age reach tens of thousands of years in the quaking aspen (Kemperman and Barnes, 1976) and in the seagrass *P. oceanica* (Arnaud-Haond et al., 2012).

Consequences for the Management and Conservation of *Phymatolithon calcareum*

Maerl beds are categorized as "vulnerable" in the European Red List of Habitats (Gubbay et al., 2016) and as threatened and/or declining habitats in the OSPAR list (Hall-Spencer et al., 2010), while *P. calcareum* is only listed in Annex V of the European Community Habitats Directive 1992[3] as a species whose exploitation requires management. Our study reveals that some clones of *P. calcareum* might be very old and that its genenotypic diversity has been accumulated over large temporal scales. We therefore question the long term impact of the exploitation of this species and advocate that maerl beds of the NE Atlantic should be considered a non-renewable resource with extremely poor recovery potential (see also Barbera et al., 2003; Hall-Spencer et al., 2010).

Eight of the 15 maerl beds studied were located in areas with legal protection status. However, strong genetic structure and the generally highly restricted distribution of clones (and alleles) stress the necessity for broader scale protection network, involving all countries with a NE Atlantic shoreline. Maerl beds lack any conservation status in some regions such as South Portugal. Likewise, results obtained at the regional scale indicate that the current protection measures, which are mainly restricted to two maerl beds located within a National Park (Illa Ons and Illas Cíes), may not be enough to preserve the high genetic diversity and complex structure found in Galicia. Galician maerl beds are located in areas characterized by high human population density, critically impacted by agriculture and industrial activities, and a reduction of areas colonized by rhodoliths have been observed during the last decades in the Rías Baixas (Peña and Bárbara, 2008). Negative impact of ocean acidification on maerl beds have also been postulated (Brodie et al., 2014) and, under the current scenario of global changes, maerl beds of high latitudes in the NE Atlantic could decline and particular attention should be given to beds located in Brittany and the British Isles, especially regarding their huge ecological and economical relevance.

[3]http://ec.europa.eu/environment/nature/legislation/habitatsdirective/index_en.htm#enlargement

DATA AVAILABILITY

This manuscript contains previously unpublished data. GENBANK accession numbers of psbA and COI-5P sequences are given in the text (i.e., legend of the **Supplementary Table S1**) and the genotype profile of the 455 samples of the maerl bed forming red algae *Phymatolithon calcareum* scored for eight microsatellite markers are available in **Supplementary Table S2** and can also be downloaded from Dryad (doi: 10.5061/dryad.ds2714g).

AUTHOR CONTRIBUTIONS

RB designed the study. CP, VP, IB, and RB conducted the field work. CP generated the data. CP, M-LG, and MV performed the data analyses. CP, MV, and M-LG wrote the manuscript. All authors read, commented, and agreed on the manuscript.

FUNDING

This research was supported by Spain's Ministerio de Economía y Competitividad (CTM2010-18787) and Xunta de Galicia (10MMA103003PR). ASSEMBLE (grant agreement no. 227799) provided support for sampling in Brittany. CP acknowledges support by Xunta de Galicia (Axudas á etapa predoutoral do Plan I2C 2011) and Spain's Ministerio de Educación (Programa FPU 2010; Programa FPU-Estancias Breves 2013). VP acknowledges support by Universidade da Coruña Universidade da Coruña (Programa Campus Industrial de Ferrol). ML and M-LG acknowledge support from Clonix and Clonix2 (France: ANR11-BSV7-00704 and ANR-18-CE32-0001-05).

ACKNOWLEDGMENTS

We are grateful to Belén Carro for her help in the Laboratory, to Sophie Martin, Philippe Potin, and Thierry Comtet for the discussions on maerl beds growth rate and radiocarbon dating and to the three reviewers for their constructive comments.

SUPPLEMENTARY MATERIAL

The Supplementary Material for this article can be found online at: https://www.frontiersin.org/articles/10.3389/fmars.2019.00149/full#supplementary-material

REFERENCES

Adey, W. H., and McKibbin, D. L. (1970). Studies on the maerl species *Phymatolithon calcareum* (pallas) nov. comb. and *Lithothamnium coralloides* crouan in the ría de vigo. *Bot. Mar.* 13, 100–106. doi: 10.1515/botm.1970.13.2.100

Agapow, P. M., and Burt, A. (2001). Indices of multilocus linkage disequilibrium. *Mol. Ecol. Notes* 1, 101–102. doi: 10.1046/j.1471-8278.2000.00014.x

Airoldi, L., Balata, D., and Beck, M. W. (2008). The gray zone: relationships between habitat loss and marine diversity and their applications in conservation. *J. Exp. Mar. Biol. Ecol.* 366, 8–15. doi: 10.1016/j.jembe.2008.07.034

Alberto, F., Gouveia, L., Arnaud-Haond, S., Pérez-Lloréns, J. L., Duarte, C. M., and Serrao, E. A. (2005). Within-population spatial genetic structure, neighbourhood size and clonal subrange in the seagrass *Cymodocea nodosa*. *Mol. Ecol.* 14, 2669–2681. doi: 10.1111/j.1365-294X.2005.02640.x

Ally, D., Ritland, K., and Otto, S. P. (2008). Can clone size serve as a proxy for clone age? An exploration using microsatellite divergence in *Populus tremuloides*. *Mol. Ecol.* 17, 4897–4911. doi: 10.1111/j.1365-294X.2008.03962.x

Ardehed, A., Johansson, D., Schagerström, E., Kautsky, L., Johannesson, K., and Pereyra, R. T. (2015). Complex spatial clonal structure in the macroalgae *Fucus radicans* with both sexual and asexual recruitment. *Ecol. Evol.* 5, 4233–4245. doi: 10.1002/ece3.1629

Arnaud-Haond, S., and Belkhir, K. (2007). GENCLONE: a computer program to analyse genotypic data, test for clonality and describe spatial clonal organization. *Mol. Ecol. Notes* 7, 15–17. doi: 10.1111/j.1471-8286.2006.01522.x

Arnaud-Haond, S., Duarte, C. M., Alberto, F., and Serrão, E. A. (2007). Standardizing methods to address clonality in population studies. *Mol. Ecol.* 16, 5115–5139. doi: 10.1111/j.1365-294X.2007.03535.x

Arnaud-Haond, S., Duarte, C. M., Diaz-Almela, E., Marbà, N., Sintes, T., and Serrão, E. A. (2012). Implications of extreme life span in clonal organisms: millenary clones in meadows of the threatened seagrass *Posidonia oceanica*. *PLoS One* 7:e30454. doi: 10.1371/journal.pone.0030454

Arnaud-Haond, S., Marbà, N., Diaz-Almela, E., Serrão, E. A., and Duarte, C. M. (2010). Comparative analysis of stability-genetic diversity in seagrass (*Posidonia oceanica*) meadows yields unexpected results. *Estuar. Coast.* 33, 878–889. doi: 10.1007/s12237-009-9238-9

Arnaud-Haond, S., Moalic, Y., Hernández-García, E., Eguiluz, V. M., Alberto, F., Serrño, E. A., et al. (2014). Disentangling the influence of mutation and migration in clonal seagrasses using the genetic diversity spectrum for microsatellites. *J. Hered.* 105, 532–541. doi: 10.1093/jhered/esu015

Balloux, F., Lehmann, L., and de Meeûs, T. (2003). The population genetics of clonal and partially clonal diploids. *Genetics* 164, 1635–1644.

Barbera, C., Bordehore, C., Borg, J. A., Glemarec, M., Grall, J., Hall-Spencer, J. M., et al. (2003). Conservation and management of northeast atlantic and mediterranean maerl beds. *Aquat. Conserv.* 13, S65–S76. doi: 10.1002/aqc.569

Becheler, R., Benkara, E., Moalic, Y., Hily, C., and Arnaud-Haond, S. (2014). Scaling of processes shaping the clonal dynamics and genetic mosaic of seagrasses through temporal genetic monitoring. *Heredity* 112, 114–121. doi: 10.1038/hdy.2013.82

Bergström, L., Bruno, E., Eklund, B., and Kautsky, L. (2003). Reproductive strategies of *Ceramium tenuicorne* near its inner limit in the brackish Baltic Sea. *Bot. Mar.* 46, 125–131. doi: 10.1515/BOT.2003.013

Bernabeu, A. M., Lersundi-Kanpistegi, A. V., and Vilas, F. (2012). Gradation from oceanic to estuarine beaches in a ría environment: a case study in the ría de vigo. *Estuar. Coast. Shelf Sci.* 102, 60–69. doi: 10.1016/j.ecss.2012.03.001

Birkett, D. A., Maggs, C., and Dring, M. J. (1998). *MAERL: an Overview of Dynamics and Sensitivity Characteristics for Conservation Management of Marine SACs*. scottish association for marine science: UK Marine SACs Project.

Blake, C., and Maggs, C. A. (2003). Comparative growth rates and internal banding periodicity of maerl species (*Corallinales, Rhodophyta*) from northern Europe. *Phycologia* 42, 606–612. doi: 10.2216/i0031-8884-42-6-606.1

Bosence, D. W. (1976). Ecological studies on two unattached coralline algae from western ireland. *Palaeontology* 19, 365–395.

Bressan, G., and Babbini, L. (2003). Biodiversità marina delle coste italiane: corallinales del mar mediterraneo: guida alla determinazione. *Biol. Mar. Medit.* 10, 1–237.

Brodie, J., Williamson, C. J., Smale, D. A., Kamenos, N. A., Mieszkowska, N., Santos, R., et al. (2014). The future of the northeast atlantic benthic flora in a high CO2 world. *Ecol. Evol.* 4, 2787–2798. doi: 10.1002/ece3.1105

Cabioch, J. (1969). Les fonds de maërl de la baie de morlaix et leur peuplement végétal. *Cah. Biol. Mar.* 10, 139–161.

Cabioch, J. (1970). Le maërl des côtes de bretagne et le problème de sa survie. *Penn Ar Bed* 7, 421–429.

Carro, B., Lopez, L., Peña, V., Bárbara, I., and Barreiro, R. (2014). DNA barcoding allows the accurate assessment of European maerl diversity: a proof-of-concept study. *Phytotaxa* 190, 176–189. doi: 10.11646/phytotaxa.190.1.12

Ceccherelli, G., and Cinelli, F. (1999). The role of vegetative fragmentation in dispersal of the invasive alga *Caulerpa taxifolia* in the Mediterranean. *Mar. Ecol. Prog. Ser.* 182, 299–303. doi: 10.3354/meps182299

Cloern, J. E., Abreu, P. C., Carstensen, J., Chauvaud, L., Elmgren, R., Grall, J., et al. (2016). Human activities and climate variability drive fast-paced change across the world's estuarine–coastal ecosystems. *Glob. Chang. Biol.* 22, 513–529. doi: 10.1111/gcb.13059

Coleman, M. A., Clark, J. S., Doblin, M. A., Bishop, M. J., and Kelaher, B. P. (2018). Genetic differentiation between estuarine and open coast ecotypes of a dominant ecosystem engineer. *Mar. Freshwater Res.* doi: 10.1071/MF17392

Coyer, J. A., Hoarau, G., Pearson, G. A., Serrao, E. A., Stam, W. T., and Olsen, J. L. (2006). Convergent adaptation to a marginal habitat by homoploid hybrids and polyploid ecads in the seaweed genus *Fucus*. *Biol. Lett.* 2, 405–408. doi: 10.1098/rsbl.2006.0489

deCastro, M., Gómez-Gesteira, M., Prego, R., Taboada, J. J., Montero, P., Herbello, P., et al. (2000). Wind and tidal influence on water circulation in a galician ria (NW Spain). *Estuar. Coast. Shelf Sci.* 51, 161–176. doi: 10.1006/ecss.2000.0619

Diaz-Almela, E., Marba, N., Alvarez, E., Santiago, R., Holmer, M., Grau, A., et al. (2008). Benthic input rates predict seagrass (*Posidonia oceanica*) fish farm-induced decline. *Mar. Pollut. Bull.* 56, 1332–1342. doi: 10.1016/j.marpolbul.2008.03.022

Dorken, M. E., and Eckert, C. G. (2001). Severely reduced sexual reproduction in northern populations of a clonal plant, *Decodon verticillatus* (*Lythraceae*). *J. Ecol.* 89, 339–350. doi: 10.1046/j.1365-2745.2001.00558.x

Durrant, H. M., Burridge, C. P., Kelaher, B. P., Barrett, N. S., Edgar, G. J., and Coleman, M. A. (2014). Implications of macroalgal isolation by distance for networks of marine protected areas. *Conserv. Biol.* 28, 438–445. doi: 10.1111/cobi.12203

Eckert, C. G. (2002). The loss of sex in clonal plants. *Evol. Ecol.* 15, 501–520. doi: 10.1023/A:1016005519651

Eriksson, O. (1993). Dynamics of genets in clonal plants. *Trends Ecol. Evol.* 8, 313–316. doi: 10.1016/0169-5347(93)90237-J

Eriksson, O., and Fröborg, H. (1996). "Windows of opportunity" for recruitment in long-lived clonal plants: experimental studies of seedling establishment in *Vaccinium* shrubs. *Can. J. Bot.* 74, 1369–1374. doi: 10.1139/b96-166

Excoffier, L., Laval, G., and Schneider, S. (2005). Arlequin ver. 3.0: an integrated software package for population genetics data analysis. *Evol. Bioinform.* 1, 47–50. doi: 10.1177/117693430500100003

Fierst, J. L., Kübler, J. E., and Dudgeon, S. R. (2010). Spatial distribution and reproductive phenology of sexual and asexual *Mastocarpus papillatus* (*Rhodophyta*). *Phycologia* 49, 274–282. doi: 10.2216/PH09-41.1

Foster, M. (2001). Rhodoliths: between rocks and soft places. *J. Phycol.* 37, 659–667. doi: 10.1046/j.1529-8817.2001.00195.x

Gaines, S. D., White, C., Carr, M. H., and Palumbi, S. R. (2010). Designing marine reserve networks for both conservation and fisheries management. *Proc. Natl. Acad. Sci. U.S.A.* 107, 18286–18293. doi: 10.1073/pnas.0906473107

García-Gil, S., Durán, R., and Vilas, F. (2000). Side scan sonar image and geologic interpretation of the ría de Pontevedra seafloor (Galicia, NW Spain). *Sci. Mar.* 64, 393–402. doi: 10.3989/scimar.2000.64n4393

Gastony, G. J. (1986). Electrophoretic evidence for the origin of fern species by unreduced spores. *Am. J. Bot.* 73, 1563–1569. doi: 10.1002/j.1537-2197.1986.tb10907.x

Goldberg, N. (2006). Age estimates and description of rhodoliths from Esperance Bay, Western Australia. *J. Mar. Biol. Assoc. U.K.* 86, 1291–1296. doi: 10.1017/S0025315406014317

Goudet, J. (1995). FSTAT (version 1.2): a computer program to calculate F-statistics. *J. Hered.* 86, 485–486. doi: 10.1093/oxfordjournals.jhered.a111627

Gourraud, P.-A., Génin, E., and Cambon-Thomsen, A. (2004). Handling missing values in population data: consequences for maximum likelihood estimation of haplotype frequencies. *Eur. J. Hum. Genet.* 12, 805–812. doi: 10.1038/sj.ejhg.5201233

Grall, J., and Hall-Spencer, J. M. (2003). Problems facing maerl conservation in Brittany. *Aquat. Conserv.* 13, S55–S64. doi: 10.1002/aqc.568

Grall, J., Le Loc'h, F., Guyonnet, B., and Riera, P. (2006). Community structure and food web based on stable isotopes (δ15N and δ13C) analysis of a North Eastern Atlantic maerl bed. *J. Exp. Mar. Biol. Ecol.* 338, 1–15. doi: 10.1016/j.jembe.2006.06.013

Gubbay, S., Sanders, N., Haynes, T., Janssen, J. A. M., Rodwell, J. R., Nieto, A., et al. (2016). *European Red List of Habitats. Part 1: Marine Habitats*. Luxembourg: European Union,

Guillemin, M.-L., Faugeron, S., Destombe, C., Viard, F., Correa, J. A., and Valero, M. (2008). Genetic variation in wild and cultivated populations of the haploid- diploid red alga *Gracilaria chilensis*: how farming practices favor asexual reproduction and heterozygosity. *Evolution* 62, 1500–1519. doi: 10.1111/j.1558-5646.2008.00373.x

Halfar, J., and Mutti, M. (2005). Global dominance of coralline red-algal facies: a response to miocene oceanographic events. *Geology* 33, 481–484. doi: 10.1130/G21462.1

Halkett, F., Simon, J.-C., and Balloux, F. (2005). Tackling the population genetics of clonal and partially clonal organisms. *Trends Ecol. Evol.* 20, 194–201. doi: 10.1016/j.tree.2005.01.001

Hall-Spencer, J., Grall, J., Moore, P. G., and Atkinson, R. J. A. (2003). Bivalve fishing and maerl-bed conservation in France and the UK- retrospect and prospect. *Aquat. Conserv.* 13, 33–41. doi: 10.1002/aqc.566

Hall-Spencer, J. M., Kelly, J., and Maggs, C. A. (2010). *Background Document for Maërl Beds," in OSPAR Commission Report 491/201036pp*. Available at:http://qsr2010.ospar.org/media/assessments/Species/P00491_maerl.pdf

Harper, J. L. (1981). "The concept of population in modular organisms," in *Theoretical Ecology*, ed. R. M. May (Oxford: Blackwell), 53–77.

Hernández-Kantún, J. J., Rindi, F., Adey, W. H., Heesch, S., Peña, V., Le Gall, L., et al. (2015). Sequencing type material resolves the identity and distribution of the generitype *Lithophyllum incrustans*, and related European species *L. hibernicum* and *L. bathyporum* (*Corallinales. Rhodophyta*). *J. Phycol.* 51, 791–807. doi: 10.1111/jpy.12319

Hickey, K. (2011). *The Impact of Hurricanes on the Weather of Western Europe, Recent Hurricane Research - Climate, Dynamics, and Societal Impacts*. Available at: https://www.intechopen.com/books/recent-hurricane-research-climate-dynamics-and-societal-impacts/the-impact-of-hurricanes-on-the-weather-of-western-europe

Hörandl, E. (2006). The complex causality of geographical parthenogenesis. *New Phytol.* 171, 525–538. doi: 10.1111/j.1469-8137.2006.01769.x

Hurst, L. D., and Peck, J. R. (1996). Recent advances in understanding of the evolution and maintenance of sex. *Trends Ecol. Evol.* 11, 46–52. doi: 10.1016/0169-5347(96)81041-X

Iglesias, G., and Carballo, R. (2009). Seasonality of the circulation in the ría de muros (NW Spain). *J. Mar. Syst.* 78, 94–108. doi: 10.1016/j.jmarsys.2009.04.002

Irvine, L. M., and Chamberlain, Y. M. (1994). *Seaweeds of the British Isles Vol. 1: Rhodophyta, Part 2B Corallinales, Hildenbrandiales*. London: The Natural History Museum.

Johannesson, K., Johansson, D., Larsson, K. H., Huenchuñir, C. J., Perus, J., Forslund, H., et al. (2011). Frequent clonality in fucoids (*Fucus radicans* and *Fucus vesiculosus*; *Fucales, Phaeophyceae*) in the Baltic Sea. *J. Phycol.* 47, 990–998. doi: 10.1111/j.1529-8817.2011.01032.x

Kalinowski, S. (2005). HP-RARE 1.0: a computer program for performing rarefaction on measures of allelic richness. *Mol. Ecol. Notes* 5, 187–189. doi: 10.1111/j.1471-8286.2004.00845.x

Kalinowski, S., and Taper, M. (2006). Maximum likelihood estimation of the frequency of null alleles at microsatellite loci. *Conserv. Genet.* 7, 991–995. doi: 10.1017/S0016672312000341

Kamiya, M., Saba, E., and West, J. A. (2017). Marginal distribution and high heterozygosity of asexual *Caloglossa vieillardii* (*Delesseriaceae, Rhodophyta*) along the Australian coasts. *J. Phycol.* 53, 1283–1293. doi: 10.1111/jpy.12580

Kamiya, M., and West, J. A. (2008). Origin of apomictic red algae: outcrossing studies of different strains in *Caloglossa monosticha* (*Ceramiales, Rhodophyta*). *J. Phycol.* 44, 977–984. doi: 10.1111/j.1529-8817.2008.00551.x

Kamiya, M., and West, J. A. (2010). "Investigations on reproductive affinities in red algae," in *Red Algae in the Genomic Age*, eds J. Seckbach and D. J. Chapman (Dordrecht: Springer), 77–109. doi: 10.1007/978-90-481-3795-4_5

Kamiya, M., West, J. A., and Hara, Y. (2011). Induction of apomixis by outcrossing between genetically divergent entities of *Caloglossa leprieurii* (*Ceramiales, Rhodophyta*) and evidence of hybrid apomicts in nature. *J. Phycol.* 47, 753–762. doi: 10.1111/j.1529-8817.2011.01016.x

Kearney, M. (2005). Hybridization, glaciation and geographical parthenogenesis. *Trends Ecol. Evol.* 20, 495–502. doi: 10.1016/j.tree.2005.06.005

Kemperman, J. A., and Barnes, B. V. (1976). Clone size in American aspens. *Can. J. Bot.* 54, 2603–2607. doi: 10.1139/b76-280

Klekowski, E. J. (1997). "Somatic mutation theory of clonality," in *The Ecology and Evolution of Clonal Plants*, eds H. De Kroon and J. Van Groenendael (Leiden: Backhuys Publishers), 227–241.

Krueger-Hadfield, S. A., Kollars, N. M., Byers, J. E., Greig, T. W., Hammann, M., Murray, D. C., et al. (2016). Invasion of novel habitats uncouples haplo-diplontic life cycles. *Mol. Ecol.* 25, 3801–3816. doi: 10.1111/mec.13718

Krueger-Hadfield, S. A., Kübler, J. E., and Dudgeon, S. R. (2013). Reproductive effort of Mastocarpus papillatus (Rhodophyta) along the California coast1. *J.Phycol.* 49, 271–281. doi: 10.1111/jpy.12034

Littler, M. M., Littler, D. S., and Hanisak, M. D. (1991). Deep-water rhodolith distribution, productivity, and growth history at sites of formation and subsequent degradation. *J. Exp. Mar. Biol. Ecol.* 150, 163–182. doi: 10.1016/0022-0981(91)90066-6

Macaya, E. C., López, B., Tala, F., Tellier, F., and Thiel, M. (2016). "Float and raft: role of buoyant seaweeds in the phylogeography and genetic structure of non-buoyant associated for a," in *Seaweed Phylogeography*, eds Z. M. Hu and C. I. Fraser (Dordrecht: Springer), 97–130.

Macreadie, P. I., York, P. H., and Sherman, C. D. (2014). Resilience of *Zostera muelleri* seagrass to small-scale disturbances: the relative importance of asexual versus sexual recovery. *Ecol. Evol.* 4, 450–461. doi: 10.1002/ece3.933

Maggs, C. A., Castilho, R., Foltz, D., Henzler, C., Jolly, M. T., Kelly, J., et al. (2008). Evaluating signatures of glacial refugia for North Atlantic benthic marine taxa. *Ecology* 89, S108–S122. doi: 10.1890/08-0257.1

Marrack, E. C. (1999). The relationship between water motion and living rhodolith beds in the southwestern Gulf of California, Mexico. *Palaios* 14, 159–171. doi: 10.2307/3515371

McConnico, L. A., Foster, M. S., Steller, D. L., and Riosmena-Rodríguez, R. (2014). Population biology of a long-lived rhodolith: the consequences of becoming old and large. *Mar. Ecol. Prog. Ser.* 504, 109–118. doi: 10.3354/meps10780

McFadden, C. S. (1997). Contributions of sexual and asexual reproduction to population structure in the clonal soft coral, *Alcyonium rudyi*. *Evolution* 51, 112–126. doi: 10.1111/j.1558-5646.1997.tb02393.x

Méndez, G., and Vilas, F. (2005). Geological antecedents of the rias baixas (galicia, northwest iberian peninsula). *J. Mar. Syst.* 54, 195–207. doi: 10.1016/j.jmarsys.2004.07.012

Mendoza, M. L., and Cabioch, J. (1998). Étude comparée de la reproduction de *Phymatolithon calcareum* (pallas) adey & mcKibbin et *Lithothamnion corallioides* (P. & H. Crouan) P. & H. Crouan (*Corallinales, Rhodophyta*), et reconsidérations sur le définition des genres. *Can. J. Bot.* 76, 1433–1445. doi: 10.1139/b98-116

Menken, S. B., Smit, E., and Nijs, H. J. (1995). Genetical population structure in plants: gene flow between diploid sexual and triploid asexual dandelions (*Taraxacum* section ruderalia). *Evolution* 49, 1108–1118. doi: 10.1111/j.1558-5646.1995.tb04437.x

Montecinos, A. E., Couceiro, L., Peters, A. F., Desrut, A., Valero, M., and Guillemin, M.-L. (2017a). Species delimitation and phylogeographic analyses in the *Ectocarpus* subgroup siliculosi (*Ectocarpales, Phaeophyceae*). *J. Phycol.* 53, 17–31. doi: 10.1111/jpy.12452

Montecinos, A. E., Guillemin, M.-L., Couceiro, L., Peters, A. F., Stoeckel, S., and Valero, M. (2017b). Hybridization between two cryptic filamentous brown seaweeds along the shore: analysing pre- and post-zygotic barriers in

populations of individuals with varying ploidy levels. *Mol. Ecol.* 26, 3497–3512. doi: 10.1111/mec.14098

Neiva, J., Serrão, E. A., Assis, J., Pearson, G. A., Coyer, J. A., Olsen, J. L., et al. (2016). "Climate oscillations, range shifts and phylogeographic patterns of North Atlantic Fucaceae," in *Seaweed Phylogeography*, eds Z. M. Hu and C. I. Fraser (Dordrecht: Springer), 279–308.

Nelson, W. A. (2009). Calcified macroalgae - critical to coastal ecosystems and vulnerable to change: a review. *Mar. Freshwater Res.* 60, 787–801. doi: 10.1071/MF08335

Ogawa, T., Ohki, K., and Kamiya, M. (2015). High heterozygosity and phenotypic variation of zoids in apomictic *Ulva prolifera* (*Ulvophyceae*) from brackish environments. *Aquat. Bot.* 120, 185–192. doi: 10.1016/j.aquabot.2014.05.015

Oppliger, L. V., Von Dassow, P., Bouchemousse, S., Robuchon, M., Valero, M., Correa, J. A., et al. (2014). Alteration of sexual reproduction and genetic diversity in the kelp species *Laminaria digitata* at the southern limit of its range. *PLoS One* 9:e102518. doi: 10.1371/journal.pone.0102518

Otto, S. P., and Lenormand, T. (2002). Resolving the paradox of sex and recombination. *Nat. Rev. Genet.* 3, 252–261. doi: 10.1038/nrg761

Pardo, C., Bárbara, I., Barreiro, R., and Peña, V. (2017). Insights into species diversity of associated crustose coralline algae (*Corallinophycidae, Rhodophyta*) with atlantic european maerl beds using DNA barcoding. *An. Jardín Bot. Mad.* 74:e059. doi: 10.3989/ajbm.2459

Pardo, C., Lopez, L., Peña, V., Hernández-Kantún, J., Le Gall, L., Bárbara, I., et al. (2014a). A multilocus species delimitation reveals a striking number of species of coralline algae forming maerl in the OSPAR maritime area. *PLoS One* 9:e104073. doi: 10.1371/journal.pone.0104073

Pardo, C., Peña, V., Bárbara, I., Valero, M., and Barreiro, R. (2014b). Development and multiplexing of the first microsatellite markers in a coralline red alga (*Phymatolithon calcareum*, *Rhodophyta*). *Phycologia* 53, 474–479. doi: 10.2216/14-031.1

Peakall, R., and Smouse, P. (2012). GenAlEx 6.5: genetic analysis in excel. population genetic software for teaching and research-an update. *Bioinformatics* 28, 2537–2539. doi: 10.1093/bioinformatics/bts460

Peña, V., Adey, W. H., Riosmena-Rodríguez, R., Jung, M.-Y., Choi, H. G., Afonso Carrillo, J., et al. (2011). *Mesophyllum sphaericum* sp. nov (*Corallinales, Rhodophyta*): a new maërl-forming species from the northeast Atlantic. *J. Phycol.* 47, 911–927. doi: 10.1111/j.1529-8817.2011.01015.x

Peña, V., and Bárbara, I. (2008). Maërl community in the north-western Iberian peninsula: a review of floristic studies and long-term changes. *Aquat. Conserv.* 18, 339–366. doi: 10.1002/aqc.847

Peña, V., Barbara, I., Grall, J., Maggs, C. A., and Hall-Spencer, J. M. (2014a). The diversity of seaweeds on maerl in the NE Atlantic. *Mar. Biodiv.* 44, 533–551. doi: 10.1007/s12526-014-0214-7

Peña, V., Hernández-Kantún, J. J., Grall, J., Pardo, C., López, L., Bárbara, I., et al. (2014b). Detection of gametophytes in the maerl-forming species *Phymatolithon calcareum* (*Melobesioideae, Corallinales*) assessed by DNA barcoding. *Cryptog. Algol.* 35, 15–25. doi: 10.7872/crya.v35.iss1.2014.15

Peña, V., Pardo, C., López, L., Carro, B., Hernández-Kantún, J., Adey, W. H., et al. (2015). *Phymatolithon lusitanicum* sp. nov. (*Hapalidiales, Rhodophyta*): the third most abundant maerl-forming species in the atlantic iberian peninsula. *Cryptog. Algol.* 36, 1–31.

Reichel, K., Masson, J.-P., Malrieu, F., Arnaud-Haond, S., and Stoeckel, S. (2016). Rare sex or out of reach equilibrium? The dynamics of fis in partially clonal organisms. *BMC Genet.* 17:76. doi: 10.1186/s12863-016-0388-z

Rousset, F. (1997). Genetic differentiation and estimation of gene flow from F-statistics under isolation by distance. *Gene. Mol. Biol.* 145, 1219–1228.

Saunders, G. W. (2005). Applying DNA barcoding to red macroalgae: a preliminary appraisal holds promise for future applications. *Philos. T. R. Soc. B* 360, 1879–1888. doi: 10.1098/rstb.2005.1719

Saunders, G. W., and McDevit, D. C. (2012). "Methods for DNA barcoding photosynthetic protists emphasizing the macroalgae and diatoms," in *DNA Barcodes: Methods and Protocols*, eds W. J. Kress and D. L. Erickson (Totowa, NJ: Humana Press), 207–222.

Schwartz, M. K., Luikart, G., and Waples, R. S. (2007). Genetic monitoring as a promising tool for conservation and management. *Trends Ecol. Evol.* 22, 25–33. doi: 10.1016/j.tree.2006.08.009

Segelbacher, G., Cushman, S. A., Epperson, B. K., Fortin, M.-J., Francois, O., Hardy, O. J., et al. (2010). Applications of landscape genetics in conservation biology: concepts and challenges. *Conserv. Genet.* 11, 375–385. doi: 10.1007/s10592-009-0044-5

Séré, M., Kaboré, J., Jamonneau, V., Belem, A. M. G., Ayala, F. J., and De Meeûs, T. (2014). Null allele, allelic dropouts or rare sex detection in clonal organisms: simulations and application to real data sets of pathogenic microbes. *Parasite. Vector.* 7, 331–344. doi: 10.1186/1756-3305-7-331

Sosa, P., Valero, M., Batista, F., and Gonzalez-Perez, M. (1998). Genetic structure of natural populations of *Gelidium* species: a re-evaluation of results. *J. Appl. Phycol.* 10, 279–284. doi: 10.1023/A:1008092023549

Soulé, M. E., and Simberloff, D. (1986). What do genetics and ecology tell us about the design of nature reserves? *Biol. Cons.* 35, 19–40. doi: 10.1016/0006-3207(86)90025-X

Spalding, M. D., Fox, H. E., Allen, G. R., Davidson, N., Ferdaña, Z. A., Finlayson, M. A. X., et al. (2007). Marine ecoregions of the world: a bioregionalization of coastal and shelf areas. *BioScience* 57, 573–583. doi: 10.1641/B570707

Stehlik, I., and Holderegger, R. (2000). Spatial genetic structure and clonal diversity of *Anemone nemorosa* in late successional deciduous woodlands of central europe. *J. Ecol.* 88, 424–435. doi: 10.1046/j.1365-2745.2000.00458.x

Suneson, S. (1982). The culture of bisporangial plants of *Dermatolithon litorale* (suneson) hamel et lemoine (*Rhodophyta, Corallinaceae*). *Br. Phycol. J.* 17, 107–116. doi: 10.1080/00071618200650121

Torres, R., and Barton, E. D. (2007). Onset of the Iberian upwelling along the Galician coast. *Cont. Shelf Res.* 27, 1759–1778. doi: 10.1016/j.csr.2007.02.005

Tucker, A. E., Ackerman, M. S., Eads, B. D., Xu, S., and Lynch, M. (2013). Population-genomic insights into the evolutionary origin and fate of obligately asexual *Daphnia pulex*. *Proc. Natl. Acad. Sci. U.S.A.* 110, 15740–15745. doi: 10.1073/pnas.1313388110

Vallejo-Marín, M., Dorken, M. E., and Barrett, S. C. H. (2010). The ecological and evolutionary consequences of clonality for plant mating. *Annu. Rev. Ecol. Evol. Sci.* 41, 193–213. doi: 10.1146/annurev.ecolsys.110308.120258

Weir, B. S., and Cockerham, C. C. (1984). Estimating F-statistics for the analysis of population structure. *Evolution* 38, 1358–1370.

Wolf, M. A., Falace, A., Kaleb, S., and Moro, I. (2016). Molecular data confirm the existence of attached crustose tetrasporangial thalli in *Phymatolithon calcareum* (*Melobesioideae, Hapalidiaceae, Rhodophyta*) from the mediterranean Sea. *Aquat. Bot.* 134, 75–81. doi: 10.1016/j.aquabot.2016.07.006

Yoon, H. S., Hackett, J. D., and Bhattacharya, D. (2002). A single origin of the peridinin- and fucoxanthin- containing plastids in dinoflagellates through tertiary endosymbiosis. *Proc. Natl. Acad. Sci. U.S.A.* 99, 11724–11729. doi: 10.1073/pnas.172234799

Conflict of Interest Statement: The authors declare that the research was conducted in the absence of any commercial or financial relationships that could be construed as a potential conflict of interest.

The reviewer SK declared a past co-authorship with several of the authors to the handling Editor.

Copyright © 2019 Pardo, Guillemin, Peña, Bárbara, Valero and Barreiro. This is an open-access article distributed under the terms of the Creative Commons Attribution License (CC BY). The use, distribution or reproduction in other forums is permitted, provided the original author(s) and the copyright owner(s) are credited and that the original publication in this journal is cited, in accordance with accepted academic practice. No use, distribution or reproduction is permitted which does not comply with these terms.

frontiers in Marine Science

ORIGINAL RESEARCH
published: 19 March 2020
doi: 10.3389/fmars.2020.00136

Seasonal Photosynthesis, Respiration, and Calcification of a Temperate Maërl Bed in Southern Portugal

Laura Sordo[1,2], Rui Santos[1], Isabel Barrote[1], Cátia Freitas[1] and João Silva[1]**

[1] CCMAR—Centre of Marine Sciences, University of Algarve, Faro, Portugal, [2] Portuguese Institute for the Ocean and Atmosphere (IPMA), DivRP, Olhão, Portugal

Rhodolith (maërl) beds are biodiversity hotspots with a worldwide distribution. Maërl is the general term for free-living non-geniculate rhodoliths or coralline red algae. In southern Portugal, maërl beds are mainly composed of *Phymatolithon lusitanicum*, recently identified as a new species and commonly misidentified as *Phymatolithon calcareum*. Photosynthesis, respiration, and growth rates of the algae were measured seasonally, as well as the photosynthetic pigment composition. To characterize the seasonal and interannual patterns of key abiotic conditions in the largest described maërl bed of the Portuguese coast, temperature, irradiance, and dissolved oxygen were continuously monitored over a 2-year period. At the bed depth (22 m), temperature ranged between 14°C in winter and 24°C in summer, irradiance varied from 5 to 75 μmol m^{-2} s^{-1}, and dissolved oxygen from 5.8 to 7.25 mg O_2 L^{-1}. We found a strong linear relationship (r^2 = 0.95) between gross primary production (GPP) and relative electron transport rates (rETRs). Both methods led to similar results and an average molar ratio of 0.24. Photosynthesis and respiration increased in summer and decreased in autumn and winter. In the summer of 2013, the growth rates were twofold higher (1.34 μmol $CaCO_3$ g^{-1} day^{-1}) than in the other seasons. In winter and spring, to compensate for light deprivation and low temperature, algae increased their chlorophyll *a* and carotenoid concentrations while also decreasing their phycobilin concentration, in this case probably due to nutrient limitation. To isolate the role of temperature on the algae's metabolism, the photosynthetic and respiration rates of individual thalli were measured at eight different temperatures in the laboratory (from 12°C to 26°C). *Phymatolithon lusitanicum* photosynthesis increased twofold after a threshold of 18°C (from 2.2 at 18°C to 3.87 μmol O_2 m^{-2} s^{-1} at 20°C), whereas respiration increased fourfold with temperature after a threshold of 22°C (from −0.38 at 18°C to −1.81 μmol O_2 m^{-2} s^{-1} at 24°C). The significant increases on respiration, photosynthetic rates, and maximum growth with temperature reveal that the metabolic rates of *P. lusitanicum* are highly sensitive to ocean warming.

Keywords: coralline algae (maërl), photosynthesis, respiration, calcification, photosynthetic pigments, temperature, irradiance

OPEN ACCESS

Edited by:
Christos Dimitrios Arvanitidis, Hellenic Centre for Marine Research (HCMR), Greece

Reviewed by:
Figueroa L. Felix, University of Málaga, Spain
José M. Rico, University of Oviedo, Spain

****Correspondence:***
Laura Sordo
laura.sordo@ipma.pt;
l.sordodelasnieves@hotmail.com
João Silva
jmsilva@ualg.pt

Specialty section:
This article was submitted to Marine Ecosystem Ecology, a section of the journal Frontiers in Marine Science

Received: *31 October 2018*
Accepted: *20 February 2020*
Published: *19 March 2020*

Citation:
Sordo L, Santos R, Barrote I, Freitas C and Silva J (2020) Seasonal Photosynthesis, Respiration, and Calcification of a Temperate Maërl Bed in Southern Portugal. Front. Mar. Sci. 7:136. doi: 10.3389/fmars.2020.00136

INTRODUCTION

Rhodolith beds are biodiversity spots, globally distributed from the poles to the tropics (Foster et al., 2013). Maërl is a type of rhodolith and the general term used for free-living non-geniculate coralline algae (Bosence, 1976). Rhodolith beds support complex trophic chains and are important carbonate deposits (Steller and Cáceres-Martinez, 2009; van der Heijden and Kamenos, 2015; Hernandez-Kantun et al., 2017; Schoenrock K. et al., 2018). However, research on maërl ecosystems is globally scarce, and the full range of maërl forming species is yet to be listed, which hampers the protection of these habitats (Barberá et al., 2003). In the northeast Atlantic, a few maërl beds are protected and, over the next decade, declines due to fishing activities, mariculture, and commercial extraction will increase (Hall-Spencer et al., 2010). While information on the metabolism of northern beds already exists for Canada (Halfar et al., 2013), Greenland (Schoenrock K. et al., 2018), and France (e.g., Martin et al., 2006, 2007), very little is known about Portuguese maërl beds (Hall-Spencer et al., 2010; Peña and Bárbara, 2013; Brodie et al., 2014; Carro et al., 2014), and only one publication reports the effects of temperature and irradiance on the maërl community (Peña and Bárbara, 2010).

Temperature and irradiance exert determinant effects on the primary production and calcification of maërl (Martin et al., 2006; Peña and Bárbara, 2010; Halfar et al., 2013). Studies on these effects have been conducted elsewhere (e.g., Freiwald and Henrich, 1994 in Norway; Blake and Maggs, 2003 in Ireland; Martin et al., 2006, 2007 in France; Steller et al., 2007 in Baja California; Amado-Filho et al., 2012 in Brazil; Burdett et al., 2012 in Scotland; Adey et al., 2015 in Canada; Schoenrock K.M. et al., 2018 in Greenland), but not yet in southern Europe. The most common methods to assess the metabolism and physiology of maërl beds are *in situ* benthic incubations (e.g., Martin et al., 2007) and PAM fluorescence (e.g., Burdett et al., 2012; Schoenrock K.M. et al., 2018). In addition, Attard et al. (2015) reported one case where the eddy covariance technique was used to measure the benthic oxygen fluxes in a maërl bed. Seasonal changes in temperature and irradiance regulate the photosynthesis, respiration, and calcification of coralline algae (Martin et al., 2006, 2007, 2013a; Halfar et al., 2013; Egilsdottir et al., 2016; Schoenrock K.M. et al., 2018), but there is scarce information on the interannual variability of environmental factors or on that of biological indicators such as photosynthetic pigments. Because of their annual growth increments and cycling of Mg content with temperature, coralline algae hold a potential to become a high-resolution climate archive that will enhance our understanding of climatic variation (Adey et al., 2015).

Under increasing acidity and temperature, maërl beds are expected to suffer severe impacts worldwide (Hall-Spencer et al., 2010; Foster et al., 2013; Martin and Hall−Spencer, 2017). However, the diversity in results among different experimental studies with positive, negative, and parabolic metabolic responses to ocean acidification (OA) and warming (Martin et al., 2013b) makes it difficult to predict the future outcome of these habitats. Divergences in results may be species specific or related to the interaction with other environmental variables such as temperature (Vásquez-Elizondo and Enríquez, 2016) and irradiance (Gao and Zheng, 2010) that modify the effect of OA on coralline algae (see Martin et al., 2013b for a review). Even if it is essential to apply realistic environmental conditions on OA assays, most experiments are not accompanied by a monitoring of the natural communities on the field, and there is an important gap of information on community-scale studies (McCoy and Kamenos, 2015).

Ocean acidification and warming will negatively affect the maërl beds from the northeastern Atlantic first, as aragonite saturation decreases, while Lusitanian maërl beds are expected to persist (Brodie et al., 2014). In Algarve, maërl beds are primarily composed of the unattached and non-geniculate coralline red algae *Phymatolithon lusitanicum*, recently described as a new species and commonly misidentified as *Phymatolithon calcareum* (Peña et al., 2015). *Lithothamnion corallioides* and *P. calcareum* are also present in the maërl beds from Algarve, but their occurrence is uncommon (Carro et al., 2014; Peña et al., 2015). Both species are abundant in Brittany and the British Isles, but they are being replaced by *P. lusitanicum* in Galicia (NW Spain) (Carro et al., 2014). In the Iberian Peninsula, *P. lusitanicum* is abundant in Galicia (4–13 m) and Algarve (15–25 m). The largest *P. lusitanicum* individuals with the thickest morphology in the Iberian Peninsula have been found in Algarve (Carro et al., 2014; *P. lusitanicum* is referred to as *Phymatolithon* sp3 in Peña et al., 2015). This species has also been identified in Northern Ireland (from the intertidal to 4 m), the Alborán Sea (40–48 m), and in the Balearic Islands (54–64 m) (Peña et al., 2015).

The information currently available on *P. lusitanicum* is restricted to descriptive studies of its morphology and the composition of the beds (Carro et al., 2014; Peña et al., 2015), associated flora (Peña and Bárbara, 2010, 2013), and the effect of high CO_2 and warming on the photosynthesis, calcification, and respiration (Sordo et al., 2016, 2018, 2019). Despite the recognized importance of the habitat, there is no information on the environmental conditions under which these algae live or on the key abiotic variables that regulate the metabolic rates of *P. lusitanicum* under natural conditions or increasing temperatures. The objectives of this study are 1) to determine the seasonal variations in the photosynthesis, calcification, respiration, and pigment concentration of *P. lusitanicum* and also 2) to investigate the effects of increasing temperature on the photosynthetic performance and respiration of the algae. This information is deemed essential to understand how climate change might impact maërl beds in southern Europe, and to establish a baseline for a proper management and protection of this poorly understood ecosystem.

MATERIALS AND METHODS

Environmental Description

The southwest area off the Iberian Peninsula (SWIP, NE Atlantic) is classified as a vulnerable area to climate change because it is a transition zone between temperate and subtropical waters. Phytoplankton abundance in all SWIP

regions presents a significant seasonal pattern, increasing during the late winter/early spring period (Krug et al., 2017). However, some strong coastal–oceanic differences in phytoplankton seasonality (chlorophyll-*a*) were found and especially accentuated in the coastal zone. These differences are probably related to an increase in nutrient concentration due to riverine discharges, mostly during winter, and upwelling induced by zonal westerly winds, stronger during summer (Krug et al., 2017).

The studied maërl bed is located at 4.7 nautical miles offshore in Armação de Pêra, in the region of Algarve, Southern Portugal (N 37°011′.650″/W −8°19′.034″) (**Figure 1**). This maërl bed has an estimated area of 3 km^2 and extends from 13- to 25-m depth. The study site has a sandy bottom where maërl thalli accumulate on the depressions of the ripple marks. The thickness of the maërl bed can reach 5 cm, and most thalli present a discoidal shape. In the summer of 2013, an area of the maërl bed at 22-m depth was delimited to install environmental sensors and a translucent box with tagged algae for growth measurements.

Sensors for temperature (HOBO temperature loggers Onset Company, United States), irradiance (Odyssey Integrating cosine corrected PAR Sensor; Dataflow Systems Limited, New Zealand), and dissolved oxygen (miniDOT oxygen logger; Precision Measurement Engineering, Inc., PME, United States) were attached to a concrete block at 22-m depth, ∼30 cm above the seabed, and left to record in a continuous basis (every 15 min) from July 2013 to May 2015. Every 3 to 4 months, the sensors were removed from the field, the data were downloaded, and then the sensors were brought back to the field. It was not possible to deploy sensors in the field from December 2013 to February 2014, or from October to November of 2014, due to adverse weather conditions. The mean monthly values (± SE) of the maximum and minimum values recorded daily are represented in **Figure 2**.

Photosynthesis and Respiration

Using a pulse-amplitude-modulated (PAM) fluorometer (Diving-PAM, Heinz Walz, Effeltrich, Germany), effective quantum yield (YII) and relative electron transport rates (rETR) (Schreiber et al., 1995) were seasonally determined *in situ* as:

$$YII = (F'm - Ft) \times (F'm)^{-1}$$

where F'm is the maximum chlorophyll fluorescence in the light-adapted thalli, and Ft is the steady-state level of fluorescence under non-saturating illumination (Genty et al., 1989) and

$$rETR = YII \times EPAR \times 0.5$$

where EPAR is the irradiance, and 0.5 is the fraction of chlorophyll associated to PSII (FII), assuming that PSI and PSII absorb equal amounts of incoming photons (Beer et al., 1998). Several authors (e.g., Grzymski et al., 1997) have pointed out that specific Chl-*a* absorption coefficients should be used for red algae (see Discussion section), but in the absence of a consensual value, we used the theoretical standard 0.5.

Rapid light curves (RLCs) were also generated *in situ* (n = 9) using 8 to 12 different light levels ranging from 10 to 655 μmol m^{-2} s^{-1}. The saturating light pulse applied after 20-s exposure at each light level lasted for 0.8 s.

Seasonal P–E and dark-respiration curves were generated using a Clark-type oxygen electrode following the methodology described in Silva and Santos (2004). Rhodoliths were collected once every season by SCUBA diving (n = 10). Thalli were gently cleaned of epiphytes and biofilm with a soft brush and transferred to a walk-in chamber. Algae were kept under the same light and temperature conditions than those found in the field for 1 day prior to measurements. For each measurement, an individual was held vertically inside an incubation chamber (15 ml volume) coupled to a Clark-type oxygen electrode (DW3/CB1; Hansatech, Norfolk, United Kingdom) and filled with GF/F filtered seawater, which was changed after every three measurements. Actinic light was provided by a slide projector (Pradovit 150; Leica, Germany) equipped with a halogen lamp (Osram Xenophot 150 W). P–E curves were obtained by sequentially applying light levels ranging from 8 to 1,460 μmol m^{-2} s^{-1}. Neutral density filters mounted on slide frames were used to obtain the different light

FIGURE 1 | Study site location (SW Iberian Peninsula) in Armação de Pêra Bay, southern Portugal. The maërl bed (20- to 23-m depth) is located 4.7 nautical miles offshore (black dot). Figure modified from source: http://geoportal.lneg.pt/.

intensities. Dark respiration was measured after turning off the light source and covering the incubation chambers with a black opaque plastic. Each light level (including darkness) was applied for ca. 10 min, the necessary time to reach steady-state oxygen evolution. A magnetic stirrer was used for water homogenization (Model A1/2; Hansatech Instruments, Norfolk, United Kingdom) (see Silva and Santos, 2004).

A thermostatic bath with a recirculation system (Julabo HC, Julabo LabortechnIk, Seelbach, Germany) was used to maintain the desired temperatures in the incubation chambers. Photosynthetic and dark-respiration rates (oxygen evolution/consumption) were calculated on a dry-weight (seasonal P–E curves) or area basis (P–E curves at different temperatures) using the following formula:

$$A = [O_2] \times 10^{-3} \times 15 \times {C_1}^{-1} \times tg\alpha \times p \times U^{-1} \times Exp^{-1}$$

where A is the oxygen evolution rate per unit of area or weight (mg O_2 s^{-1} cm^{-2} or g^{-1}); $[O_2]$ is the O_2 saturation concentration at the given temperature and salinity conditions (mg L^{-1}); C_1 is the corresponding calibration height (cm) of O_2-saturated water in the plotter's paper; $tg\alpha$ is the angle of the slope of the oxygen evolution/consumption line; p is the plotter speed (cm s^{-1}); U is the area (cm^2) or weight (g) of the sample, and Exp. is the signal amplification. At the end of the measurements, the fresh weight or the maximum length and width of the thalli were recorded. For the calculations of the seasonal P–E curves, each individual was placed in an open aluminum foil envelope (to avoid water condensation) and left to dry in the oven at 60°C and weighted 1 week later (dry weight). In order to enable a correlation between these results and the fluorescence data, gross photosynthesis was expressed in μmol O_2 m^{-2} s^{-1}.

In a separate experiment, P–E curves and dark-respiration rates of *P. lusitanicum* were also determined at eight different temperatures (n = 6): 12°C, 14°C, 16°C, 18°C, 20°C, 22°C, 24°C, and 26°C using a Clark-type oxygen electrode. Algae were collected and maintained under the conditions found in the field (16°C) for 2 weeks. Before the measurements, thalli were left to acclimate for 48 h, at each tested temperature in a walk-in chamber. All the measurements were carried out during 4 weeks as previously described.

To investigate the relationship between the relative electron transport rate (rETR) (μmol e^- m^{-2} s^{-1}) and the gross photosynthesis (μmol O_2 m^{-2} s^{-1}), chlorophyll fluorescence measurements were carried out using a pulse–amplitude-modulated (PAM) fluorometer (Diving-PAM; red light; Heinz Walz, Effeltrich, Germany) coupled to the oxygen electrode (n = 8) (see Silva and Santos, 2004 for further details). The relative electron-transport rate (rETR), the maximum photosynthetic rate (P_{max}), the ascending slopes at limiting irradiances (α), and the half-saturation irradiances (E_k) were calculated. Both light-response curves (O_2 and fluorescence derived) were fitted with the models of Smith (1936) and Talling (1957):

$$P = P_m[\alpha EPAR/(P^2m + (\alpha EPAR)^2)^{1/2}]$$

in which P_m is the maximum photosynthetic rate (or the maximum electron transport rate), α is the ascending slope at limiting irradiances, and EPAR is the irradiance.

Curve fitting was done using the software package SigmaPlot (Systat Software 2008, Inc., Germany). The simultaneous use of both methods allowed us to establish the coupling degree between oxygen production and rETR, expressed by the molar ratio $rETR/O_2$ (Silva and Santos, 2004). Measurements were done with algae incubated under experimental conditions at a temperature of ∼16°C.

Photosynthetic Pigments

Photosynthetic pigment concentrations were analyzed in autumn and summer 2013, winter and spring 2014, and summer 2015 (n = 5). Maërl thalli were sampled seasonally in the field and kept under −80°C until analyses. The thalli were ground in liquid nitrogen, before extraction in acetone (chlorophylls and total carotenoids) or in phosphate buffer (phycoerythrin and phycocyanin), and the extracts were then centrifuged. The absorbances of all pigment extracts were measured with a spectrophotometer (Beckman Coulter; DU-650; United States) in a 1-cm glass cuvette. The pigment concentrations were expressed in mg gFW^{-1}.

Chlorophyll *d* (Chl *d*) was extracted from 1.5 g of fresh thalli in 5 ml of 90% acetone. The extract was then centrifuged (Heraeus Megafuge 16R; Thermo scientific, MA, United States) for 5 min at 2,000 × *g* and 4°C. The absorbance of the supernatant was read at 630, 647, 664, and 691 nm. Chl *d* concentration was calculated according to Ritchie (2008):

$$\text{Chlorophyll } d = -0.5881A_{630} + 0.0902A_{647} - 0.1564A_{664} - 11.0473A_{691}$$

Total carotenoids and chlorophyll *a* (Chl *a*) were extracted from 1.5 g of fresh thalli in 5 ml of 100% acetone. The extract was then centrifuged (Heraeus Megafuge 16R; Thermo scientific, MA, United States) for 5 min at 2,000 × *g* and 4°C, and the supernatant absorbance was read at 470 and 661.6 nm. The pigment concentrations were calculated using the equations of Torres et al. (2014) adapted from Lichtenthaler and Buschmann (2001) for red algae:

$$\text{Chlorophyll } a = 10.82 \times A_{661.6}$$

$$\text{Carotenoids} = (1,000 \times A_{470} - 1.90 \times \text{Chl } a)/214$$

The phycobilins phycoerythrin (PE) and phycocyanin (PC) were extracted from 1 g of fresh weight in 2 ml of phosphate buffer (pH 6.5) at 4°C. The extract was centrifuged (Heraeus Megafuge 16R; Thermo Scientific, United States) at 4,696 × *g* for 40 min, and absorbance was read at 564, 618, and 730 nm. The concentrations of phycobilins were determined using the equations of Sampath-Wiley and Neefus (2007):

$$\text{Phycocyanin (PC)} = 0.154(A_{618} - A_{730})$$

$$\text{Phycoerythrin (PE)} = 0.1247[(A_{564} - A_{730}) - 0.4583(A_{618} - A_{730})]$$

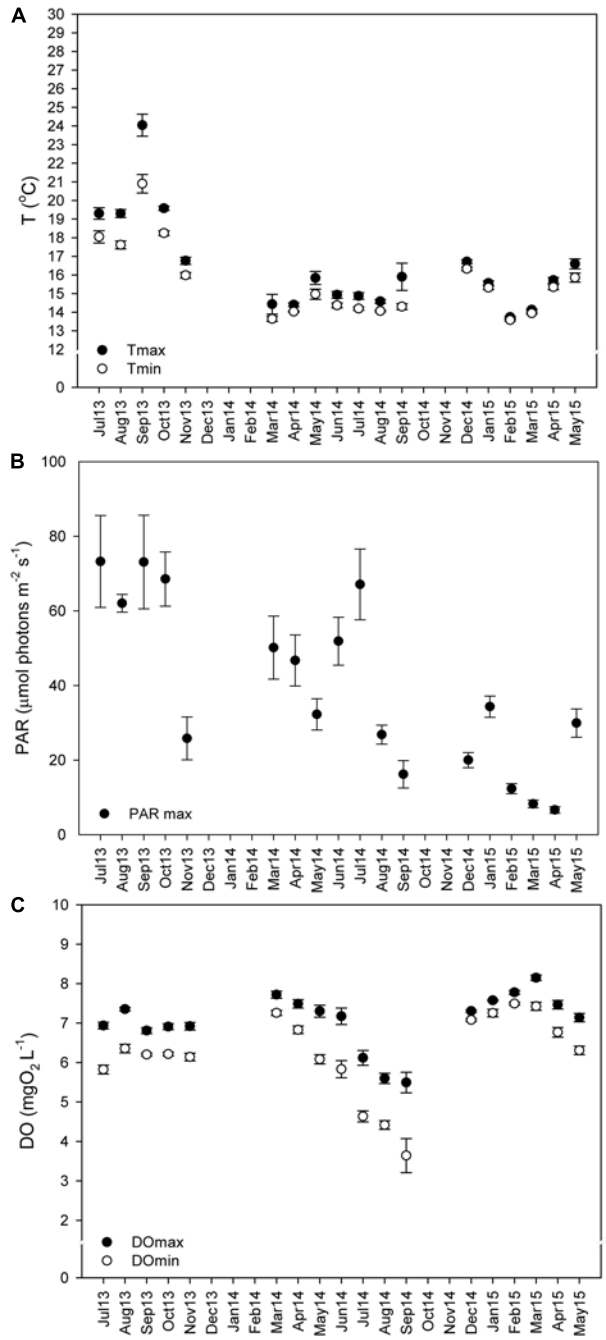

FIGURE 2 | Monthly average of daily maximum and minimum temperatures (**A**,°C), photosynthetically active radiation (PAR) (**B**, µmol m^{-2} s^{-1}), and dissolved oxygen (DO) concentrations (**C**, mg L^{-1}). Values from summer 2013 (Jul 13–Aug 13), autumn 2013 (Sep 13–Nov 13), winter 2013–2014 (Dec 13–Feb 14), spring 2014 (Mar 14–May 14), summer 2014 (Jun 14–Aug 14), autumn 2014 (Sep 14–Nov 14), winter 2014–2015 (Dec 14–Feb 15), and spring of 2015 (Mar 15–May 15) depicted as mean ± standard error.

Growth

The growth of the thalli was followed *in situ* under natural conditions for 695 days (from summer 2013 to spring 2016). A total of 160 individuals were tagged with small plastic labels attached with nylon wire and placed in a translucent hard plastic box covered with a plastic mesh with uniform holes of about ∼3 cm in all of its surface. Because of this, the water flow and irradiance conditions inside the box were identical to its surroundings (previously assessed in laboratory). The box was fixed with chains and weights to a concrete block at 22-m depth.

Every 2 months, the tagged algae were removed from the box and taken to the laboratory. The excess of epiphytes was gently cleaned, and the rhodoliths' individual growth was measured using the buoyant weight (BW) technique. Once measured, the tagged individuals were returned to the field. According to Steller et al. (2007), the buoyant weight technique assumes that the skeleton of the algae is mainly composed of calcium carbonate. Because the density of the organic tissue equals that of seawater, any increment on the buoyant weight is assumed to be an increment of $CaCO_3$ deposition or calcification. Prior to the experiment, the $CaCO_3$ composition of *P. lusitanicum* was determined by eliminating $CaCO_3$ through acidification. After drying and weighing, 24 thalli were placed individually in 25 ml of 5% HCl. The thalli were submerged into the acid solution until all $CaCO_3$ was dissolved. The HCl solution was changed every 24 h. After total decalcification, samples were rinsed in distilled water and allowed to dry to constant weight in an oven at 60°C. Finally, the $CaCO_3$ content was determined by subtracting the dry weight from the pre-acidified weight (Steller et al., 2007).

To determine the individual weight of the thalli, these were suspended by a nylon string attached to an electronic balance (Sartorius 0.1 mg, Germany) in a beaker filled with filtered seawater. The algae were weighted and the water temperature (Roth digital thermometer, Hanna, EU) and salinity (CO310 conductivity meter; VWR, United States) measured to calculate the seawater density. Then, the buoyant weight of the algae was calculated using the equation described in Steller et al. (2007):

$$Wcc = Wb\,[Dcc\,(Dcc - Dw)^{-1}]$$

where Wcc is the dry weight of the $CaCO_3$, Wb is the buoyant weight of the thalli, Dcc is the density of $CaCO_3$ (2.71 g cm^{-3}), and Dw is the density of seawater displaced by the sample (1.03 g cm^{-3}). The following equation is obtained after substituting the density of seawater and $CaCO_3$:

$$Wcc = 1.61Wb$$

In order to be able to compare the growth of tagged algae of different sizes, we use the relative growth rate (RGR) as it allows more equitable comparisons (Hunt, 1990) than the absolute growth rate. The mean value of the RGR is the increase in weight per unit of pre-existing weight (W) over the interval t_1 to t_2:

$$RGR = (\log W_2 - \log W_1) \times (t_2 - t_1)^{-1}$$

Statistical Analyses

The software package SigmaPlot version 11.0 (Systat Software 2008, Inc., Germany) was used to perform all statistical analyses. Monthly or seasonal differences among the abiotic

variables (temperature, dissolved oxygen, and PAR), respiration, calcification (repeated growth measures of tagged algae), photosynthesis, pigment concentration and, the comparison between the relative electron transport rate (rETR) and gross photosynthesis were analyzed using one-way ANOVA tests. A *post hoc* test (Student–Newman–Keuls, SNK) was applied to explore differences between treatments when significant differences were found. When data presented equal variance, but did not meet the assumption of normal distribution (Kolmogorov–Smirnov test) even after square root or log transformation, an ANOVA on ranks (Kruskal–Wallis analyses of variance) was applied.

RESULTS

Environmental Variables

Maërl beds in southern Portugal are exposed to low light and temperature conditions all year round (**Figure 2**). Still, an important inter-annual temperature variability (one-way ANOVA on ranks; H = 392.509; $P \leq 0.001$) was observed, with maximum temperatures in summer 2013 (24°C) being 8° higher than those observed in summer of 2014 (16°C) at 22-m depth.

The maximum and minimum mean daily values for each month were calculated (mean ± SE) (see **Figure 2**). In autumn and summer of 2013 were recorded the highest temperatures (17 ± 0.21 to 24 ± 0.59°C) and PAR irradiances levels (62 ± 2.36 to 73 ± 12.31 μmol m^{-2} s^{-1}), and high dissolved oxygen concentrations (6.8 ± 0.40 to 7.3 ± 0.23 mg O_2 L^{-1}). In spring and early summer of 2014, the PAR irradiances were high (32 ± 4.17 to 67 ± 9.47 μmol m^{-2} s^{-1}) and so was the dissolved oxygen (7.5 ± 0.16 to 7.7 ± 0.09 mg O_2 L^{-1}). By the end of the summer of 2014, irradiance decreased by about 41 μmol m^{-2} s^{-1}, to 26.8 ± 2.54 μmol m^{-2} s^{-1}, and dissolved oxygen reached the minimum values (3.64 ± 1.29 mg O_2 L^{-1}), while temperature remained unaltered (∼15.9 ± 2.18°C). The minimum temperatures (13.6 ± 0.04°C) and irradiances (6.6 ± 0.87 μmol m^{-2} s^{-1}) were recorded from winter to spring of 2015, as did the maximum DO concentrations (8.1 ± 0.07 mg O_2 L^{-1}). The low PAR and temperature values and the increase in DO during this period were related to agitated seas due to continued rough weather conditions (*personal observations*) (see **Figures 2A–C**).

Photosynthesis and Respiration

The highest relative electron transport rates (rETR) were recorded in summer and the lowest in winter (**Figures 3B,D** and **Supplementary Table S1**). There were significant differences among seasons (one-way ANOVA; F = 183.928; $P \leq 0.001$) but no differences between spring and autumn ($P = 0.797$) (**Figures 3A,C**). The ascending slope at limiting irradiance (α) also changed seasonally (one-way ANOVA; F = 13.710; $P \leq 0.001$), being higher in winter and autumn and lower in spring and summer, but with no differences between autumn and summer ($P = 0.507$). The E_k was lower in winter (one-way ANOVA; F = 13.889; $P \leq 0.001$), and did not differ between summer and autumn ($P = 0.180$) or spring ($P = 0.187$).

The maximum photosynthetic rates (P_{max}) (one-way ANOVA; F = 98.293; $P \leq 0.001$), and the ascending slope at limiting irradiance (α) of the oxygen evolution curve also changed seasonally (one-way ANOVA; F = 17.87; $P \leq 0.001$) reaching the highest values in summer and spring (**Figures 4B,A**) and the lowest in autumn and winter (**Figures 4C,D**; see **Supplementary Table S2**). In contrast, there were no significant seasonal differences in E_k (one-way ANOVA; F = 0.509; $P = 0.681$). We found a linear relationship ($r^2 = 0.95$) between gross primary production (GPP) and relative electron transport rates (rETRs), with an average molar ratio of 0.24 (∼1/4) (**Figures 5A,B**).

Dark respiration also changed seasonally with the highest respiration rates in summer and spring and the lowest in winter and autumn (**Figure 5C**). Significant differences were observed only between winter and summer (one-way ANOVA; F = 4.166; $P = 0.023$).

Relative Growth Rate (RGR) *in situ* (Buoyant Weight Technique)

In this study, we estimated through HCl acidification that *P. lusitanicum* is composed of ∼96% $CaCO_3$. After more than 695 days in the field, the relative growth rate changed with time (ANOVA on ranks; H = 34.011; $P \leq 0.001$) (**Figure 5D**). These differences were due to the high RGR observed from September to November of 2013 (1.34 μmol $CaCO_3$ g^{-1} day^{-1}). In the rest of the periods, the growth rates were constant, and from November 2014 to May 2016, they went from 0.77 to 0.66 μmol $CaCO_3$ g^{-1} day^{-1}. The lowest RGR was observed from November 2013 to November of 2014 (0.23–0.28 μmol $CaCO_3$ $g^{-1}day^{-1}$).

Photosynthetic Pigments

Chlorophyll *a* concentration changed seasonally (one-way ANOVA; F = 8.230; $P \leq 0.001$), being higher in winter and spring of 2014 and lower in autumn and summer of 2013 (**Figure 6A**). These differences were mostly due to the high values observed in winter 2014 with respect to summer 2013 ($P < 0.001$), summer 2015 ($P < 0.004$), autumn 2013 ($P < 0.001$), and spring 2014 ($P = 0.021$). Carotenoid concentration also varied seasonally (One-way ANOVA; F = 5.623; $P = 0.003$), being higher in winter and spring and lower in autumn and summer (**Figure 6A**). Once again, these differences were due to the high values observed in winter of 2014 with respect to autumn 2013 ($P = 0.003$), summer 2013 ($P = 0.008$), summer 2015 ($P = 0.013$), and spring 2014 ($P = 0.043$).

During all periods, *P. lusitanicum* presented higher concentrations (mg gFW^{-1}) of phycoerythrin (0.188 ± 0.067) than phycocyanin (0.01 ± 0.004). Phycocyanin (one-way ANOVA; F = 5.959; $P = 0.003$) and phycoerythrin (one-way ANOVA; F = 9.766; $P \leq 0.001$) concentrations changed seasonally, being higher in autumn and summer and lower in

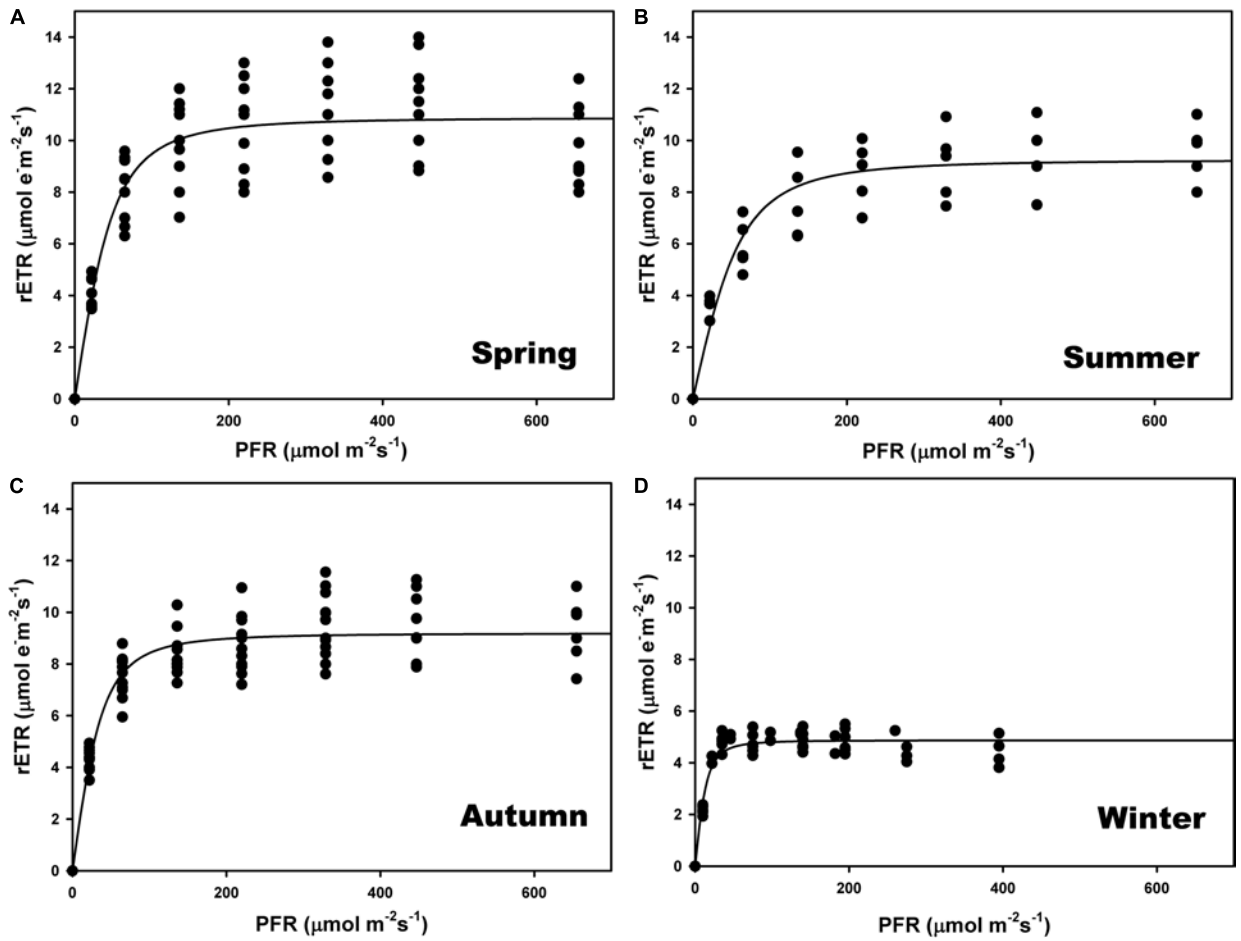

FIGURE 3 | Seasonal rapid light curves (RLC) during spring **(A)**, summer **(B)**, autumn **(C)**, and winter **(D)**. Data generated *in situ* at a maërl bed of *Phymatolithon lusitanicum* (∼22-m depth) using a Diving PAM fluorometer. Curves represent the adjustment of the model equation of Smith (1936) and Talling (1957) to the observed values (n = 9).

winter and spring (**Figure 6B**). Phycocyanin concentrations were significantly lower in winter 2014 with respect to autumn 2013 (P = 0.003) and summer 2015 (P = 0.007). Phycoerythrin concentrations in winter 2014 were significantly lower with respect to autumn 2013 ($P < 0.001$), summer 2013 (P = 0.002), and also spring of 2014 (P = 0.014) (*post hoc* test Student–Newman–Keuls, SNK).

Effects of Temperature on Respiration and Photosynthesis

The dark respiration rates of *P. lusitanicum* increased with temperature (**Figure 7A**) and were significantly higher at 24°C and 26°C (one-way ANOVA; F = 9.392; $P \leq 0.001$). The maximum photosynthetic rates (P_{max}) were observed at 24°C (**Figure 7B**) (one-way ANOVA; F = 16.618; $P \leq 0.001$). The E_k values (µmol m^{-2} s^{-1}) tended to increase from 18°C to 20°C and decreased under high temperatures (24°–26°C) but with no statistical differences (one-way ANOVA; F = 0.993; P = 0.450) (**Table 1**), the same occurring for the ascending slope at limiting irradiances (α) (one-way ANOVA; F = 1.311; P = 0.271).

DISCUSSION

Both the maximum electron transport rates measured on the field and the gross photosynthetic rates of *P. lusitanicum* measured in the laboratory increased in summer and spring and decreased in autumn and winter. This corroborates the results from previous studies where the net production of *Lithothamnion corallioides* (Martin et al., 2006) and the gross production of *Ellisolandia elongata* (Egilsdottir et al., 2016) were, respectively, two- and threefold higher in summer than in winter. Martin et al. (2007) also found that the gross community production of maërl beds in the Bay of Brest displayed a seasonal variability, being 3.5-fold higher in summer than in winter.

Previous studies have assessed the photosynthetic activity of non-geniculate coralline algae using the non-invasive chlorophyll-a fluorometry technique (e.g., Wilson et al., 2004;

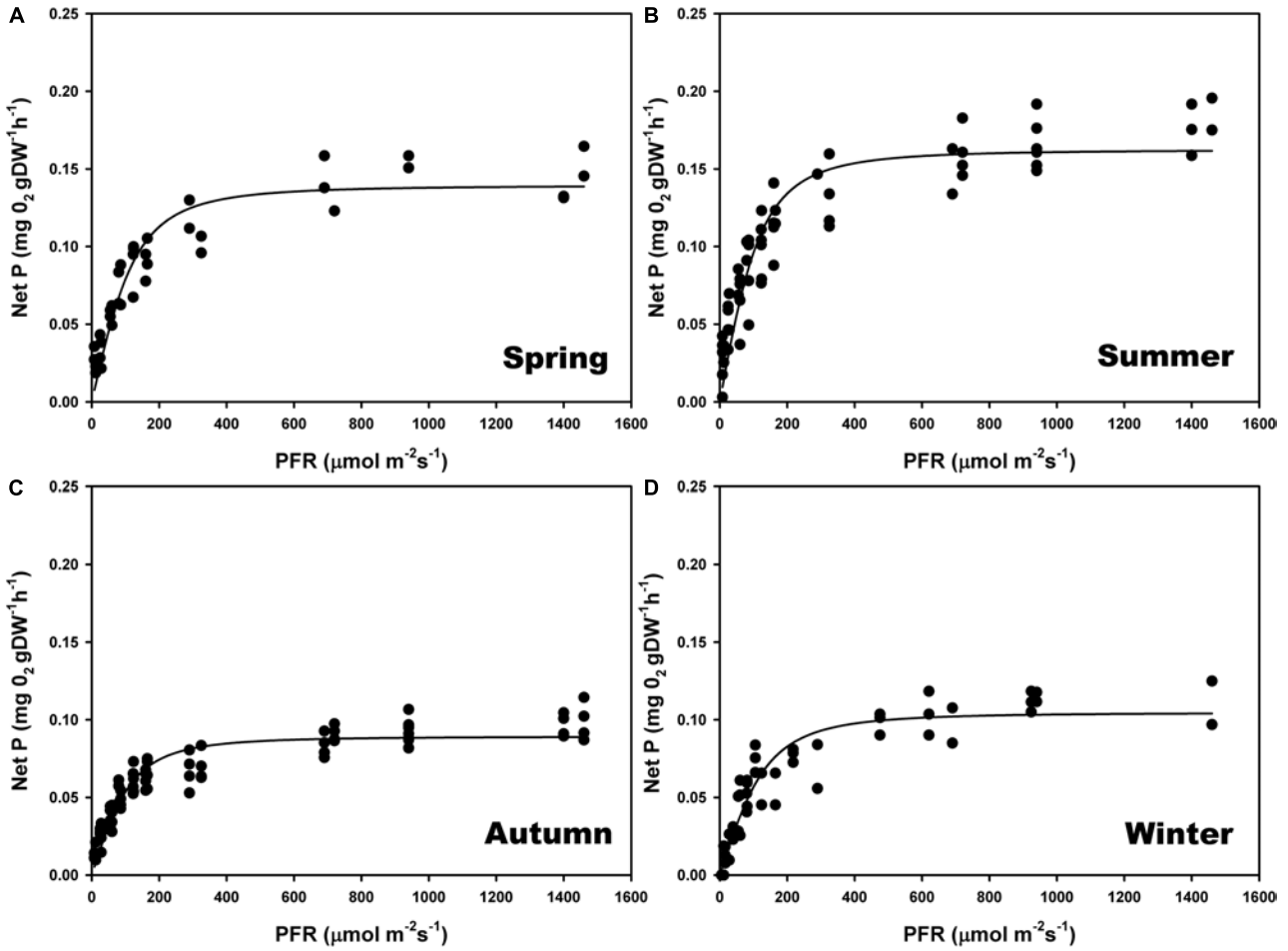

FIGURE 4 | Seasonal photosynthesis–irradiance (P–E) curves, determined on individual thalli of *P. lusitanicum* in the laboratory using an oxygen Clark-type electrode (n = 5) during spring **(A)**, summer **(B)**, autumn **(C)**, and winter **(D)**. Curves represent the adjustment of the model equation of Smith (1936) and Talling (1957) to the observed values.

Burdett et al., 2012; Schoenrock K.M. et al., 2018). In this study, the seasonal measurements carried out both *in situ* (PAM fluorescence) and in the laboratory (O_2 Clark electrode) revealed that there is a seasonality in the photosynthetic activity of maërl beds from southern Portugal. We speculate that the lower slope (α) and higher E_k values of the oxygen evolution P–E curves with respect to the values observed for the RLCs was probably related to differences in the light quality and to the acclimation of experimental algae to higher light conditions in the laboratory than those observed under natural conditions in the field. Figueroa et al. (2003) measured the ETR and oxygen evolution of different algal species under different light conditions and also found that the ETR-based α was higher than the O_2-based α in all species. The authors pointed out that the quantity and quality of light was a decisive factor on the results and that the absorbed quanta of algae cultivated long term under experimental conditions decreased as a consequence of photoacclimation.

When directly compared in a separate laboratorial assay, the two methods yielded comparable results between them, revealing a very strong correlation and an average molar ratio close to 1/4 between gross photosynthesis and electron transport rates. Figueroa et al. (2003) also found that the calculated O_2/ETR

TABLE 1 | Parameters from photosynthesis–irradiance (P–E) curves at different temperatures (12–26°C): maximum photosynthetic rates (P_{max}), ascending slope at limiting irradiances (α), and half-saturation irradiation (E_k).

T	P_{max}	α	E_k
(°C)	(μmol O_2 m^{-2} s^{-1})	(μmol O_2 μmol photons^{-1})	(μmol photons m^{-2} s^{-1})
12	1.66 ± 0.07*c*	0.06 ± 0.01	26.84 ± 5.37
14	3.60 ± 0.22*b*	0.10 ± 0.03	35.81 ± 9.18
16	2.42 ± 0.11*c*	0.06 ± 0.01	39.64 ± 7.60
18	2.22 ± 0.09*c*	0.03 ± 001	64.19 ± 9.67
20	3.87 ± 0.35*b*	0.06 ± 0.02	67.44 ± 22.47
22	3.20 ± 0.28*b*	0.05 ± 0.02	64.57 ± 21.50
24	4.82 ± 0.26*a*	0.09 ± 0.03	53.70 ± 15.38
26	3.67 ± 0.33*b*	0.07 ± 0.02	52.25 ± 18.31

Different letters indicate significant differences. Mean values ± standard error.

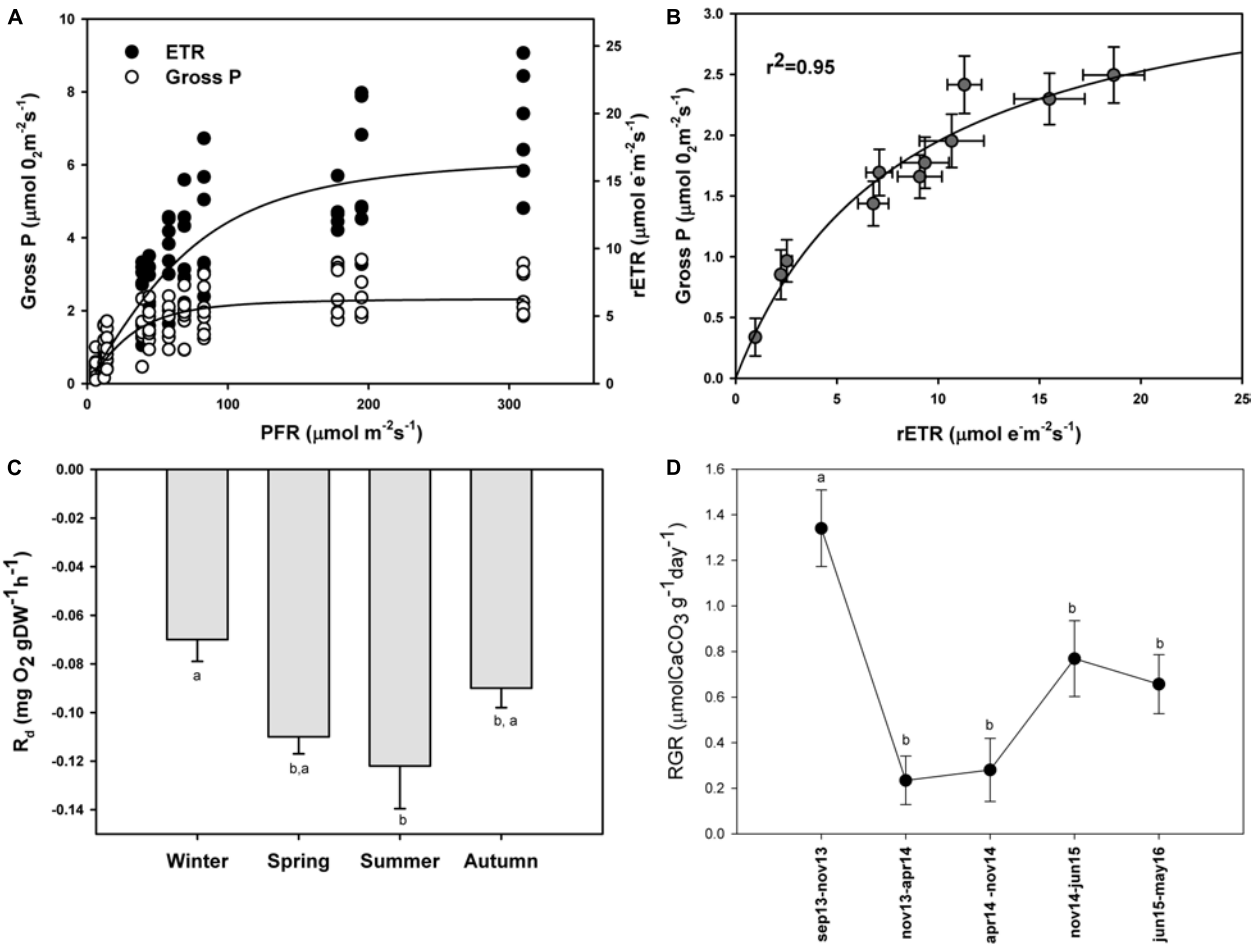

FIGURE 5 | Simultaneous measurements of oxygen evolution (Gross P.; μmol O_2 m^{-2} s^{-1}) and relative electron transport rates (rETR; μmol e^- m^{-2} s^{-1}) in *P. lusitanicum* **(A)**. Gross photosynthesis vs. rETR relationship **(B)** (n = 8). Seasonal variation of dark respiration rates of *P. lusitanicum* (R_d, mg O_2 gDW^{-1} h^{-1}) measured in the laboratory (n = 10). **(C)** Relative growth rate of *P. lusitanicum* (RGR) from September 2013 (Sep 13) to May 2016 (May 16) determined on marked individuals on the field (n = 160) **(D)**. Mean values ± standard error. Different letters indicate significant differences.

molar ratios were close to 0.25 for the red algae *Porphyra leucosticta*. However, for this particular species, the Gross P was associated to the estimated ETR only at high irradiances, when algae were pre-incubated under 500–1,000 μmol m^{-2} s^{-1}. Herein, we found that at lower irradiances, the relation between GP and ETR is close to four electrons per 1 mol of oxygen produced. However, this value increased to 8 at the saturating irradiance of 200 μmol m^{-2} s^{-1}. At saturating irradiances, the uncoupling between water splitting activity in PSII and PSI strongly reduces the plastoquinone pool and enhancing the ETR (Prasil et al., 1996). In cases where the xanthophyll cycle activity is limited, this mechanism could be essential for protecting shade-adapted species to saturating irradiance levels (see Figueroa et al., 2003). More extensive research is needed to verify if it is possible to make a generalized extrapolation between Gross P and rETR for the species *P. lusitanicum*. Additionally, there is a controversy on the value of the FII constant used to calculate rETR for red algae. In most studies, the constant commonly used to calculate the fraction of chlorophyll associated with PSII (FII) in algae is 0.5 (e.g., Beer et al., 1998). However, Grzymski et al. (1997) developed specific Chl-*a* absorption coefficients for brown and red algae. Because of this, it is worth mentioning that the FII of 0.5 may be more adequate for green algae, while for red algae FII, it is probably closer to 0.15, and for brown algae would be around 0.8 (Grzymski et al., 1997; Figueroa et al., 2014). However, in the absence of a consensual value, we used an FII of 0.5 in our calculations of ETR.

The saturating irradiances for *P. lusitanicum* in the field were high when compared with other subtidal red calcareous species from temperate latitudes. The E_k values derived from the RLCs ranged from 17 to 44 μmol m^{-2} s^{-1} in winter and autumn, and from 56 to 70 μmol m^{-2} s^{-1} in summer and spring. These values are higher than the E_k values observed in May and March for the low-light adapted maërl species *Lithothamnion glaciale* (4.45–54.6 μmol m^{-2} s^{-1}) (Burdett et al., 2012), for the Arctic species *Phymatolithon foecundum* and also for *Phymatolithon tenue* (7 and 17 μmol m^{-2} s^{-1}) (Roberts et al., 2002), but lower than the values recorded for the tropical *Porolithon* sp. (∼700 μmol

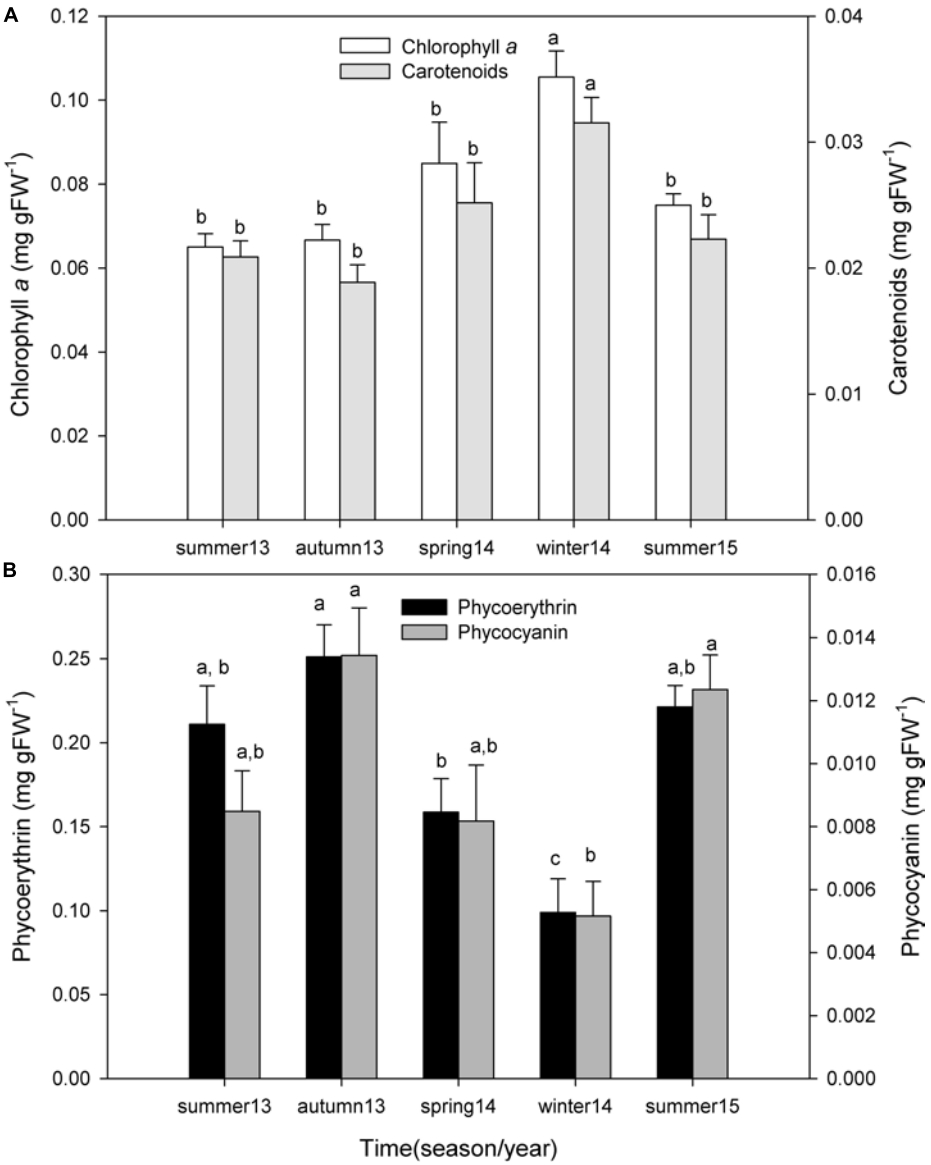

FIGURE 6 | Seasonal variation of chlorophyll *a* and carotenoid pigment concentration **(A)**, and phycoerythrin and phycocyanin pigment concentration **(B)** of *P. lusitanicum* (mg gFW^{-1}). Different letters indicate significant differences between seasons for each photosynthetic pigment. Mean values ± standard error (n = 5).

m^{-2} s^{-1} at 12:00) (Burdett et al., 2014). Under experimental conditions, the high E_k values observed in a wide range of temperatures suggest that *P. lusitanicum*, like *P. calcareum*, can tolerate high temperatures, which explains the wide distribution of these two species (Wilson et al., 2004). While other factors, such as hydrodynamics, can determine the presence or absence of maërl species, light and temperature are the main factors that control the depth and geographical distribution of crustose and unattached corallines (Bosence, 1976).

Respiration was almost twofold higher in summer than in winter. This agrees with previous studies where the respiration rates of the non-geniculate *Lithothamnion corallioides* (Martin et al., 2006) and the geniculate *Ellisolandia elongata* (Egilsdottir et al., 2016) were, respectively, three- and 10-fold higher in summer than in winter. Also, Martin et al. (2007) found that in the Bay of Brest (France), the maërl community respiration exhibited a strong seasonality with the greatest rates in summer (August) and the lowest in winter (February).

In more northern maërl beds of the Iberian Peninsula, the maërl community is tightly correlated with temperature, and irradiance increases (Peña and Bárbara, 2010), and seasonality in the flora associated was observed during this study but not quantified. Under a global change scenario, the increase in the abundance of the epiflora during high temperature and irradiance periods could favor calcification by increasing the

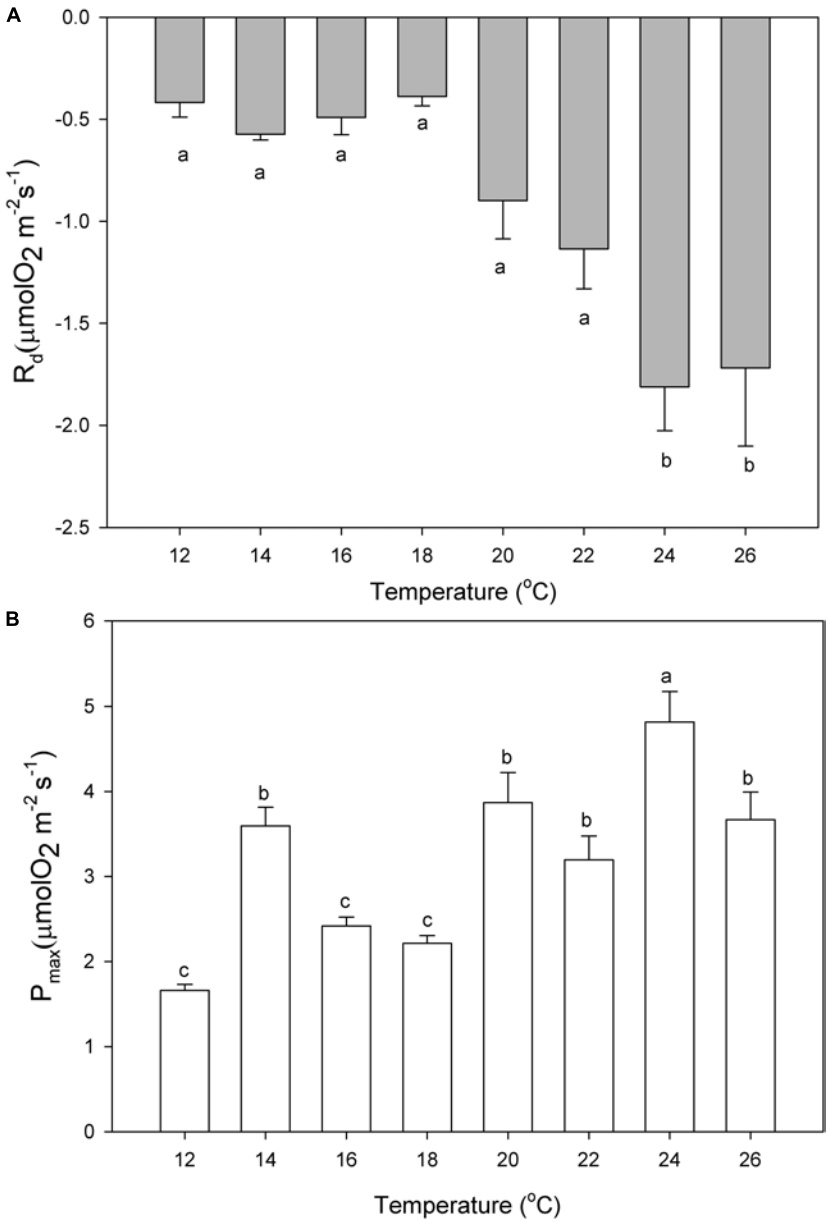

FIGURE 7 | Dark respiration (R_d, **A**) and maximum photosynthetic rates (P_{max}, **B**) of *P. lusitanicum* (μmol O_2 m^{-2} s^{-1}) as a function of temperature. Different letters indicate significant differences. Mean values ± standard error (n = 6).

pH as a consequence of the photosynthetic activity of the non-calcareous algae (Short et al., 2015). Algal cover can also protect the maërl beds from the detrimental effect of high irradiance (Figueiredo et al., 2000). Since the community response to global change is complex, to be able predict the future response of marine communities, it is important to understand the effect of environmental changes on species interactions (Short et al., 2015). Therefore, the seasonal flora associated to the maërl bed is an important factor to consider because it plays a major role in the gross community production (Martin et al., 2007). Also, it is important to understand how environmental changes affect species interactions to determine the effect that global change will have on the maërl community (Legrand et al., 2017).

This is the first study to assess how environmental factors affect the concentration of photosynthetic pigments in *P. lusitanicum*. Chlorophyll *a* and carotenoids increased in winter of 2014–2015 and decreased in summer of 2013 and 2015. In this study, algae compensated the light deprivation during winter of 2014–2015 by increasing their photosynthetic pigments. In contrast, under experimental conditions, Noisette et al. (2013) found that the chlorophyll *a* concentration of the temperate rhodolith algae *Lithothamnion corallioides* was unaffected by

temperature, while carotenoid concentration decreased with temperature. The interaction of environmental variables such as irradiance, nutrients (Lin and Stekoll, 2011), and temperature (Kim et al., 2007), has an effect on pigment production. However, previous studies have found that the biochemical response to these variables is highly species specific (see Kim et al., 2007; Lin and Stekoll, 2011; Stengel et al., 2014).

The lowest phycocyanin and phycoerythrin concentrations were also observed in winter of 2014–2015, and in spring of 2014, when the temperatures were low, but these pigments increased during the warmer seasons (summer and autumn of 2013, and summer of 2015). The phycobilins phycoerythrin and phycocyanin are the main light-harvesting pigments in marine red algae (Beer and Eshel, 1985; Lin and Stekoll, 2011). Also, when nitrogen supply becomes limiting, phycobilin pigments may be used as nitrogen reserves for growth and other physiological processes (Lin and Stekoll, 2011). The phycoerythrin concentrations of *P. lusitanicum* were in the same order of magnitude as the phycobilin concentrations recorded for the temperate coralline red algae *Lithothamnion glaciale* (see Donohue, 2015). Donohue (2015) found that the phycoerythrin concentration of low-light adapted *Lithothamnion glaciale* increased in winter to compensate for the decrease in irradiance. However, this author also found that under experimentally increased temperature and CO_2 conditions, phycoerythrin concentrations decreased in winter, probably due to a reallocation of resources (i.e., nitrogen) for other physiological processes. During the warmer months, a higher availability of nutrients can be expected at the studied area because of the upwelling induced in the southwestern area of the Iberian Peninsula by zonal westerly winds, stronger during summer (Krug et al., 2017). Because there are no light limitations during summer, the increase in phycobilin concentrations might be related to a high nutrient availability. In contrast, during low light and temperature periods when there is less primary production and less nutrients available, *P. lusitanicum* might be using the stored nitrogen in their phycobilin pigments.

Previous studies have found that phycobiliproteins also have a nutrient storage function (Kim et al., 2007; Lin and Stekoll, 2011) and might decline due to a lack of sufficient inorganic nitrogen for continued synthesis of new pigments (Kim et al., 2007). In a short-term experiment, Stengel et al. (2014) observed that the phycobilin content of the intertidal red algae *Ellisolandia elongata* was unaffected by temperature, nutrients, or irradiance (Stengel et al., 2014). In contrast, in a field study, Pereira et al. (2012) observed that the pigment and protein concentrations of the red algae *Gracilaria dominguensis* increased with decreasing sunlight and increasing nutrients, and gradually decreased with increasing irradiance and decreasing nutrient concentration. The variability of responses among algal species highlights the importance of further long-term field studies to assess the effect that different environmental conditions exert on the acclimation of algae and concentration of their biochemical components (Pereira et al., 2012; Stengel et al., 2014).

Our results show that calcification in *P. lusitanicum* is more temperature controlled and not as dependent on light as photosynthesis. In a previous experiment where the effect of temperature and high CO_2 in the net production and calcification of *P. lusitanicum* was assessed, we also found that calcification increases with temperature, and this effect is more pronounced under high CO_2 (Sordo et al., 2019). The highest relative growth rates were observed from September to November of 2013 when we recorded the highest temperature and irradiance conditions. According to NOAA (2013), the global temperatures across the world's ocean surfaces in July of 2013 were higher than the average, and this was the sixth warmest July since records started in 1880. In nearby Spain, July 2013 was the warmest July since 1961. The same pattern was corroborated by data from the fixed monitoring station SIMPATICO (integrated system for *in situ* multiparametric monitoring in coastal areas), moored offshore from the lower Guadiana Estuary (see Garel and Ferreira, 2015) in southern Portugal (37°11.300N, 7°24.670W), which recorded unusually high temperatures during summer of 2013.

These results suggest that during this period, calcification in the field increased with temperature and irradiance. In a long-term study, Halfar et al. (2013) found that the growth and Mg/Ca ratios of crustose coralline algal buildups in the Arctic were sensitive to changes in both temperature and solar radiation. This agrees with previous studies where the calcification of *Lithothamnion corallioides* (Martin et al., 2006), *Lithothamnion glaciale* (Schoenrock K.M. et al., 2018), and *Ellisolandia elongata* (Egilsdottir et al., 2016) increased with temperature and irradiance in summer and decreased in winter. Also, Martin et al. (2007) found that maërl community calcification was sixfold higher in summer than in winter. From November of 2013 to April of 2014, the temperatures went down and also did the calcification rates. In contrast, from November 2014 to June 2015, the temperatures increased, and despite the low light conditions, algae increased their calcification rates. Many coralline algae species are low-light adapted and can even survive sporadic burial events. According to Wilson et al. (2004), the non-geniculate species *P. calcareum* showed little stress after spending 4 weeks in the dark. The authors suggested that probably this maërl species is able to survive several months in the darkness without showing deleterious effects. In this study, we found that *P. lusitanicum* is able to maintain relatively constant growth rates despite low light and temperature conditions.

In the lab assays, dark respiration increased with temperature from 20°C to 24°C but started to decrease at 26°C. The measurements at different temperatures confirmed that respiration of *P. lusitanicum* increased gradually with temperature. It is widely known that respiration of coralline algae increases with temperature until their thermal tolerance limit is exceeded (see Martin et al., 2013b; Martin and Hall−Spencer, 2017 for a review). In a previous experiment with *P. lusitanicum*, Sordo et al. (2016) found that respiration was unaffected by CO_2 but positively affected by temperature. This increase was significant only from 24°C but decreased under 26°C. Even if not significant, this might indicate that the thermal limit for *P. lusitanicum* is above 26°C, a higher value than the temperatures observed under natural conditions. In contrast, the lowest respiration rates were observed at the lowest temperatures. This might constitute an algae's mechanism to avoid excessive loss of carbon through the liberation of CO_2 (Martin et al., 2006).

Even though there were no statistical differences with temperature, we observed the highest E_k values at 18°C and above (>50 μmol m^{-2} s^{-1}), with the exception at 14°C, where the maximum net photosynthetic rates were reached at irradiances of about 35.8 μmol m^{-2} s^{-1}, resulting in an α slightly higher than the α obtained at 24°C. At low light intensities and temperatures (12°C and 16°C), the P_{max} observed was inferior to 3 μmol O_2 m^{-2} s^{-1} with α values of 0.06 μmol O_2 m^{-2} s^{-1}. When irradiance increases, the adaptation of these algae to low light makes them more susceptible to photoinhibition, especially if this increase is accompanied by temperatures lower or higher than the optimum range for the organism (Kalituho et al., 2003). Because of this, the E_k values found in this study (26-67 μmol m^{-2} s^{-1}) were lower than the E_k registered by Egilsdottir et al. (2016) for the intertidal red algae *Ellisolandia elongata* (30.5 in summer and 82.6 μmol m^{-2} s^{-1} in summer), but higher than the E_k registered by Figueiredo et al. (2012) for deeper rhodolith communities dominated by the species *Mesophyllum engelhartii* (12 to 30 μmol m^{-2} s^{-1}).

Low temperature may decrease the fluidity of the membrane, negatively interfering with the electron transport chain, which, in these conditions, loses electrons for O_2 leading to the formation of reactive oxygen species or ROS (Reis et al., 2011; Goh et al., 2012). This could explain the low P_{max} values observed in this study for *P. lusitanicum* at 12°C. Even if temperature was the main factor regulating the photosynthetic activity, irradiance intensified the negative effects on the net production at 26°C. Our results suggest that a decrease in the net production at a high temperature is more evident under high irradiance. Therefore, both temperature and irradiance have a main role on the regulation of the photosynthetic rates in the red algae *P. lusitanicum*. From 20°C to 26°C, the algae reached the highest P_{max}, but also at 14°C (a temperature close to the values observed at the field in winter). Our results suggest that even with lower photosynthetic rates, *P. lusitanicum* will be able to maintain some growth at low temperatures if the light intensity does not exceed the saturation light intensity for those temperatures (Kalituho et al., 2003).

CONCLUSION

Despite the relatively stable environmental conditions recorded in the studied area, the photosynthetic rates and pigment concentrations of *P. lusitanicum* are regulated by temperature and irradiance, while respiration is regulated solely by temperature. Calcification/growth is influenced by irradiance but is more strongly dependent on temperature changes. Both photosynthesis and respiration increased in summer and decreased in autumn and winter, while growth did not change seasonally.

This is the first study to identify and measure the main environmental variables that regulate the metabolism of Lusitanian maërl beds. This information is essential to assess the impacts that global warming and ocean acidification will have on the valuable ecological services these maërl beds provide. Under a global warming scenario, temperature and irradiance will have a positive effect on the photosynthetic rates of maërl beds from southern Portugal, and respiration and calcification will also increase with temperature. In a drastic scenario, above 26°C, respiration and calcification (as CO_2 sources) could eventually surpass photosynthetic carbon uptake, rendering the system heterotrophic. In such case, calcium carbonate dissolution could also surpass deposition, with an important negative effect on the maërl community and on the carbon cycle. Cornwall et al. (2020) found that crustose coralline algae (CCA) can gain tolerance to OA after six generations of exposure. However, in shallow areas, the negative effect of OA on the photochemical efficiency of coralline algae is expected to increase with light, constraining CCA species to a narrower range of light environments (Briggs and Carpenter, 2019). Maërl beds from southern Portugal, on the other hand, are located between 13- and 25-m depth, with most of its area below 22 m, where PAR is low and temperature conditions are relatively stable, except for sporadic heat waves. In the projected climate change scenarios, these conditions have the potential to become natural refuges for these algae.

AUTHOR CONTRIBUTIONS

LS designed the experiments, carried out the research, analyzed the data, and wrote the manuscript. RS and IB contributed to the experimental design, interpretation of data, and revision of the manuscript. CF participated in the research, analysis, and interpretation of data. JS designed the experiments, helped with the research, analysis of data, and revision of the manuscript. The submitted version was approved by all the authors.

FUNDING

This study received Portuguese national funds from FCT—Foundation for Science and Technology through projects PTDC/MAR/115789/2009 and UIDB/04326/2020. The first author (LS) was funded by the FCT doctoral grant SFRH/BD/76762/2011.

ACKNOWLEDGMENTS

We deeply thank Miguel Rodrigues from Divespot, and Rogerio Nuno Ferreira for their help during the fieldwork. We will like to thank four reviewers for their constructive comments on the manuscript.

SUPPLEMENTARY MATERIAL

The Supplementary Material for this article can be found online at: https://www.frontiersin.org/articles/10.3389/fmars.2020.00136/full#supplementary-material

REFERENCES

Adey, W., Halfar, J., Humphreys, A., Suskiewicz, T., Belanger, D., Gagnon, P., et al. (2015). Subarctic rhodolith beds promote longevity of crustose coralline algal buildups and their climate archiving potential. *Palaios* 30, 281–293. doi: 10.2110/palo.2014.075

Amado-Filho, G. M., Moura, R. L., Bastos, A. C., Salgado, L. T., Sumida, P. Y., Guth, A. Z., et al. (2012). Rhodolith beds are major CaCO3 bio-factories in the tropical south west atlantic. *PLoS One* 7:e35171. doi: 10.1371/journal.pone.0035171

Attard, K. M., Stahl, H., Kamenos, N. A., Turner, G., Burdett, H. L., and Glud, R. N. (2015). Benthic oxygen exchange in a live coralline algal bed and an adjacent sandy habitat: an eddy covariance study. *Mar. Ecol. Prog. Ser.* 535, 99–115. doi: 10.3354/meps11413

Barberá, C., Bordehore, C., Borg, J. A., Glémarec, M., Grall, J., Hall-Spencer, J. M., et al. (2003). Conservation and management of northeast Atlantic and Mediterranean maërl beds. *Aquat. Conserv.* 13, 65–76. doi: 10.1002/aqc.569

Beer, S., and Eshel, A. (1985). Determining phycoerythrin and phycocyanin concentrations in aqueous crude extracts of red algae. *Aust. J. Mar. Freshw. Res.* 36, 785–792. doi: 10.1071/MF9850785

Beer, S., Vilenkin, B., Weil, A., Veste, M., Susel, L., and Eshel, A. (1998). Measuring photosynthetic rates in seagrass by pulse amplitude modulated (PAM) fluorometry. *Mar. Ecol. Prog. Ser.* 174, 293–300. doi: 10.3354/meps174293

Blake, C., and Maggs, C. A. (2003). Comparative growth rates and internal banding periodicity of maerl species (Corallinales, Rhodophyta) from northern Europe. *Phycologia* 42, 606–612. doi: 10.2216/i0031-8884-42-6-606.1

Bosence, D. W. (1976). Ecological studies on two unattached coralline algae from western Ireland. *Palaeontology* 19, 365–395.

Briggs, A. A., and Carpenter, R. C. (2019). Contrasting responses of photosynthesis and photochemical efficiency to ocean acidification under different light environments in a calcifying alga. *Sci. Rep.* 9:3986. doi: 10.1038/s41598-019-40620-8

Brodie, J., Williamson, C. J., Smale, D. A., Kamenos, N. A., Mieszkowska, N., Santos, R., et al. (2014). The future of the northeast Atlantic benthic flora in a high CO2 world. *Ecol. Evol.* 4, 2787–2798. doi: 10.1002/ece3.1105

Burdett, H. L., Hennige, S. J., Francis, F. T. Y., and Kamenos, N. A. (2012). The photosynthetic characteristics of red coralline algae, determined using pulse amplitude modulation (PAM) fluorometry. *Bot. Mar.* 55, 499–509. doi: 10.1515/bot-2012-0135

Burdett, H. L., Keddie, V., MacArthur, N., McDowall, L., McLeish, J., Spielvogel, E., et al. (2014). Dynamic photoinhibition exhibited by red coralline algae in the red sea. *BMC Plant Biol.* 14:139. doi: 10.1186/1471-2229-14-139

Carro, B., López, L., Peña, V., Bárbara, I., and Barreiro, R. (2014). DNA barcoding allows the accurate assessment of European maerl diversity : a Proof-of-Concept study. *Phytotaxa* 190, 176–189. doi: 10.11646/phytotaxa.190.1.12

Cornwall, C. E., Comeau, S., DeCarlo, T. M., Larcombe, E., Moore, B., Giltrow, K., et al. (2020). A coralline alga gains tolerance to ocean acidification over multiple generations of exposure. *Nat. Clim. Change* 10, 149–146. doi: 10.1038/s41558-019-0681-8

Donohue, P. J. C. (2015). *The Effects of Acidification and Warming on Marine Calcifying Biota*. Ph.D. thesis, University of Glasgow, Scotland, 256.

Egilsdottir, H., Olafsson, J., and Martin, S. (2016). Photosynthesis and calcification in the articulated coralline alga *Ellisolandia elongata* (Corallinales, Rhodophyta) from intertidal rock pools. *Eur. J. Phycol.* 51, 59–70. doi: 10.1080/09670262.2015.1101165

Figueiredo, M. A. O., Coutinho, R., Villas-Boas, A. B., Tâmega, F. T. S., and Mariath, R. (2012). Deep-water rhodolith productivity and growth in the southwestern Atlantic. *J. Appl. Phycol.* 24, 487–493. doi: 10.1007/s10811-012-9802-8

Figueiredo, M. A. O., Kain, J. M., and Norton, T. A. (2000). Responses of crustose corallines to epiphyte and canopy cover. *J. Phycol.* 36, 17–24. doi: 10.1046/j.1529-8817.2000.98208.x

Figueroa, F. L., Conde-Álvarez, R., and Gómez, I. (2003). Relations between electron transport rates determined by pulse amplitude modulated chlorophyll fluorescence and oxygen evolution in macroalgae under different light conditions. *Photosynth. Res.* 75, 259–275. doi: 10.1023/A:1023936313544

Figueroa, F. L., Domínguez-González, B., and Korbee, N. (2014). Vulnerability and acclimation to increased UVB radiation in three intertidal macroalgae of different morpho-functional groups. *Mar. Environ. Res.* 97, 30–38. doi: 10.1016/j.marenvres.2014.01.009

Foster, M. S., Amado-Filho, G. M., Kamenos, N. A., Riosmena-Rodriguez, R., and Steller, D. L. (2013). "Rhodoliths and rhodolith beds," in *Research and Discoveries: The Revolution of Science Through SCUBA*, eds M. A. Lang, R. L. Marinelli, S. J. Roberts, and P. R. Taylor, (Washington, DC: Smithsonian Contributions to the Marine Sciences), 143–155.

Freiwald, A., and Henrich, R. (1994). Reefal coralline algal build-ups within the Arctic Circle: morphology and sedimentary dynamics under extreme environmental seasonality. *Sedimentology* 41, 963–984. doi: 10.1111/j.1365-3091.1994.tb01435.x

Gao, K., and Zheng, Y. (2010). Combined effects of ocean acidification and solar UV radiation on photosynthesis, growth, pigmentation and calcification of the coralline alga *Corallina sessilis* (Rhodophyta). *Glob. Change Biol.* 16, 2388–2398. doi: 10.1111/j.1365-2486.2009.02113.x

Garel, E., and Ferreira, Ó (2015). Multi-year high-frequency physical and environmental observations at the Guadiana Estuary. *Earth Syst. Sci. Data* 7, 299–309. doi: 10.5194/essd-7-1-2015

Genty, B., Briantais, J., and Baker, N. (1989). The relationship between the quantum yield of photosynthetic electron transport and quenching of chlorophyll fluorescence. *Biochim. Biophys. Acta* 990, 87–92. doi: 10.1016/S0304-4165(89)80016-9

Goh, C. H., Ko, S. M., Koh, S., Kim, Y. J., and Bae, H. J. (2012). Photosynthesis and environments: photoinhibition and repair mechanisms in plants. *J. Plant Biol.* 55, 93–101. doi: 10.1007/s12374-011-9195-2

Grzymski, J., Johnsen, G., and Sakshaug, E. (1997). The significance of intracellular self-shading on the bio optical properties of brown, red and green macroalgae. *J. Phycol.* 33, 408–414. doi: 10.1111/j.0022-3646.1997.00408.x

Halfar, J., Adey, W. H., Kronz, A., Hetzinger, S., Edinger, E., and Fitzhugh, W. W. (2013). Arctic sea−ice decline archived by multicentury annual−resolution record from crustose coralline algal proxy. *Proc. Natl. Acad. Sci. U.S.A.* 110, 19737–19741. doi: 10.1073/pnas.1313775110

Hall-Spencer, J. M., Kelly, J., and Maggs, C. A. (2010). *Background Document for Maerl*. London: OSPAR Commission.

Hernandez-Kantun, J. J., Hall-Spencer, J. M., Grall, J., Adey, W., Rindi, F., Maggs, C. A., et al. (2017). "North Atlantic rhodolith/maërl beds," in *Rhodolith/Maërl Beds: A Global Perspective. Coastal Research Library*, eds R. Riosmena-Rodriguez, W. Nelson, and J. Aguirre, (Cham: Springer), 265–279. doi: 10.1007/978-3-319-29315-8_10

Hunt, R. (1990). "Relative growth rates," in *Basic Growth Analysis*, eds G. E. Wickens, J. R. Goodin, and D. V. Field, (London: Unwin Hyman), 25–34. doi: 10.1007/978-94-010-9117-6_3

Kalituho, L. N., Pshybytko, N. L., Kabashnikova, L. F., and Jahns, P. (2003). Photosynthetic apparatus and high temperature: role of light. *Bulg. J. Plant Physiol.* 29, 281–289.

Kim, J. K., Kraemer, G. P., Neefus, C. D., Chung, I. K., and Yarish, C. (2007). Effects of temperature and ammonium on growth, pigment production and nitrogen uptake by four species of *Porphyra* (Bangiales, Rhodophyta) native to the New England coast. *J. Appl. Phycol.* 19, 431–440. doi: 10.1007/s10811-006-9150-7

Krug, L. A., Platt, T., Sathyendranath, S., and Barbosa, A. B. (2017). Unravelling region-specific environmental drivers of phytoplankton across a complex marine domain (off SW Iberia). *Remote Sens. Environ.* 203, 162–184. doi: 10.1016/j.rse.2017.05.029

Legrand, E., Riera, P., Lutier, M., Coudret, J., Grall, J., and Martin, S. (2017). Species interactions can shift the response of a maërl bed community to ocean acidification and warming. *Biogeosciences* 14, 5359–5376. doi: 10.5194/bg-14-5359-2017

Lichtenthaler, H. K., and Buschmann, C. (2001). "Chlorophylls and carotenoids: measurement and characterization by UV-VIS spectroscopy," in *Current Protocols in Food Analytical Chemistry (CPFA)*, eds R. E. Wrolstad, T. E. Acree, H. An, E. A. Decker, M. H. Penner, D. S. Reid, et al. (New York, NY: John Wiley and Sons). F4.3.1–F4.3.8.

Lin, R., and Stekoll, M. S. (2011). Phycobilin content of the conchocelis phase of Alaskan *Porphyra* (bangiales, rhodophyta) species: responses to environmental variables. *J. Phycol.* 47, 208–214. doi: 10.1111/j.1529-8817.2010.00933.x

Martin, S., Castets, M.-D., and Clavier, J. (2006). Primary production, respiration and calcification of the temperate free-living coralline alga *Lithothamnion*

corallioides. *Aquat. Bot.* 85, 121–128. doi: 10.1016/j.aquabot.2006.02.005

Martin, S., Charnoz, A., and Gattuso, J. P. (2013a). Photosynthesis, respiration and calcification in the Mediterranean crustose coralline alga *Lithophyllum cabiochae* (Corallinales, Rhodophyta). *Eur. J. Phycol.* 48, 163–172.

Martin, S., Clavier, J., Chauvaud, L., and Thouzeau, G. (2007). Community metabolism in temperate maërl beds. I. Carbon and carbonate fluxes. *Mar. Ecol. Prog. Ser.* 335, 19–29. doi: 10.3354/meps335019

Martin, S., Cohu, S., Vignot, C., Zimmerman, G., and Gattuso, J.-P. (2013b). One-year experiment on the physiological response of the Mediterranean crustose coralline alga, *Lithophyllum cabiochae*, to elevated *p*CO2 and temperature. *Ecol. Evol.* 3, 676–693. doi: 10.1002/ece3.475

Martin, S., and Hall−Spencer, J. M. (2017). "Effects of ocean warming and acidification on rhodolith/maërl beds," in *Rhodolith/Maërl Beds: A Global Perspective. Coastal Research Library*, eds R. Riosmena−Rodríguez, W. Nelson, and J. Aguirre, (Cham: Springer), 55–85. . doi: 10.1007/978-3-319-29315-8_3

McCoy, S. J., and Kamenos, N. A. (2015). Coralline algae in a changing world: integrating ecological, physiological, and geochemical responses to global change. *J. Phycol.* 51, 6–24. doi: 10.1111/jpy.12262

NOAA, (2013). *National Centers for Environmental Information, State of the Climate: Global Climate Report for July 2013, Published Online August 2013*. Available online at: https://www.ncdc.noaa.gov/sotc/global/201307 (accessed February 4, 2019).

Noisette, F., Duong, G., Six, C., Davoult, D., and Martin, S. (2013). Effects of elevated *p*CO2 on the metabolism of a temperate rhodolith *Lithothamnion corallioides* grown under different temperatures. *J. Phycol.* 49, 746–757. doi: 10.1111/jpy.12085

Peña, V., and Bárbara, I. (2010). Seasonal patterns in the maërl community of shallow European Atlantic beds and their use as a baseline for monitoring studies. *Eur. J. Phycol.* 45, 327–342. doi: 10.1080/09670261003586938

Peña, V., and Bárbara, I. (2013). Non-coralline crustose algae associated with maërl beds in Portugal: a reappraisal of their diversity in the Atlantic Iberian beds. *Bot. Mar.* 55, 481–493. doi: 10.1515/bot-2013-0083

Peña, V., Pardo, C., López, L., Carro, B., Hernandez-Kantun, J., Adey, W. H., et al. (2015). Phymatolithon lusitanicum sp. nov. (Hapalidiales, Rhodophyta): the third most abundant maërl-forming species in the Atlantic Iberian Peninsula. *Crypt. Algol.* 36, 429–459. doi: 10.7872/crya/v36.iss4.2015.429

Pereira, D. C., Trigueiro, T. G., Colepicolo, P., and Marinho-Soriano, E. (2012). Seasonal changes in the pigment composition of natural population of *Gracilaria domingensis* (Gracilariales. Rhodophyta). *Rev. Bras. Farmacogn.* 22, 874–880. doi: 10.1590/S0102-695X2012005000075

Prasil, O., Kolber, Z., Berry, J. A., and Falkowski, P. G. (1996). Cyclic electron flow around Photosystem II *in vivo*. *Photosynth. Res.* 48, 395–410. doi: 10.1007/BF00029472

Reis, M. O., Necchi, O., Pio, C., and Marcelo, B. (2011). Co-stressors chilling and high light increase photooxidative stress in diuron-treated red alga *Kappaphycus alvarezii* but with lower involvement of H2O2. *Pest. Biochem. Physiol.* 99, 7–15. doi: 10.1016/j.pestbp.2010.09.003

Ritchie, R. J. (2008). Universal chlorophyll equations for estimating chlorophylls *a*, *b*, *c* and *d* and total chlorophylls in natural assemblages of photosynthetic organisms using acetone, methanol or ethanol solvents. *Photosynthetica* 46, 115–126. doi: 10.1007/s11099-008-0019-7

Roberts, R. D., Kühl, M., Glud, R. N., and Rysgaard, S. (2002). Primary production of crustose coralline red algae in a high arctic fjord. *J. Phycol.* 38, 273–283. doi: 10.1046/j.1529-8817.2002.01104.x

Sampath-Wiley, P., and Neefus, C. (2007). An improved method for estimating R-phycoerythrin and R-phycocyanin contents from crude aqueous extracts of Porphyra (Bangiales, Rhodophyta). *J. Appl. Phycol.* 19, 123–129. doi: 10.1007/s10811-006-9118-7

Schoenrock, K., Vad, J., Muth, A., Pearce, D., Rea, B., Schofield, J., et al. (2018). Biodiversity of Kelp Forests and Coralline Algae Habitats in Southwestern Greenland. *Diversity* 10:117. doi: 10.3390/d10040117

Schoenrock, K. M., Bacquet, M., Pearce, D., Rea, B. R., Schofield, J. E., Lea, J., et al. (2018). Influences of salinity on the physiology and distribution of the arctic coralline algae, *Lithothamnion glaciale* (Corallinales, Rhodophyta). *J. Phycol.* 54, 690–702. doi: 10.1111/jpy.12774

Schreiber, U., Bilger, W., and Neubauer, C. (1995). "Chlorophyll fluorescence as a nonintrusive indicator for rapid assessment of *in vivo* photosynthesis," in *Ecophysiology of Photosynthesis*, eds E. D. Schulze, and M. M. Caldwell, (Berlin: Springer-Verlag), 49–70. doi: 10.1007/978-3-642-79354-7_3

Short, J. A., Pedersen, O., and Kendrick, G. A. (2015). Turf algal epiphytes metabolically induce local pH increase, with implications for underlying coralline algae under ocean acidification. *Estuar. Coast. Shelf. Sci.* 164, 463–470. doi: 10.1016/j.ecss.2015.08.006

Silva, J., and Santos, R. (2004). Can chlorophyll fluorescence be used to estimate photosynthetic production in the seagrass *Zostera noltii*? *J. Exp. Mar. Biol. Ecol.* 307, 207–216. doi: 10.1016/j.jembe.2004.02.009

Smith, E. L. (1936). Photosynthesis in relation to light and carbon dioxide. *Proc. Natl. Acad. Sci. U.S.A.* 22, 504–511. doi: 10.1073/pnas.22.8.504

Sordo, L., Santos, R., Barrote, I., and Silva, J. (2018). High CO2 decreases the long-term resilience of the free-living coralline algae *Phymatolithon lusitanicum*. *Ecol. Evol.* 8, 4781–4792. doi: 10.1002/ece3.4020

Sordo, L., Santos, R., Barrote, I., and Silva, J. (2019). Temperature amplifies the effect of high CO2 on the photosynthesis, respiration, and calcification of the coralline algae *Phymatolithon lusitanicum*. *Ecol. Evol.* 9, 11000–11009. doi: 10.1002/ece3.5560

Sordo, L., Santos, R., Reis, J., Shulika, A., and Silva, J. (2016). A direct CO2 control system for ocean acidification experiments: testing effects on the coralline red algae *Phymatolithon lusitanicum*. *PeerJ* 4:e2503. doi: 10.7717/peerj.2503

Steller, D. L., and Cáceres-Martinez, C. (2009). Coralline algal rhodoliths enhance larval settlement and early growth of the Pacific calico scallop *Argopecten ventricosus*. *Mar. Ecol. Prog. Ser.* 396, 49–60. doi: 10.3354/meps08261

Steller, D. L., Hernandez-Ayon, J. M., Riosmena-Rodriguez, R., and Cabello-Pasini, A. (2007). Effect of temperature on photosynthesis, growth and calcification rates of the free-living coralline alga *Lithophyllum margaritae*. *Cienc. Mar.* 33, 441–456. doi: 10.7773/cm.v33i4.1255

Stengel, D. B., Conde-Álvarez, R., Connan, S., Nitschke, U., Arenas, F., Abreu, H., et al. (2014). Short-term effects of CO2, nutrients and temperature on three marine macroalgae under solar radiation. *Aquat. Biol.* 22, 159–176. doi: 10.3354/ab00576

Talling, J. F. (1957). Photosynthetic characteristics of some freshwater plankton diatoms in relation to underwater radiation. *New Phytol.* 56, 29–50. doi: 10.1111/j.1469-8137.1957.tb07447.x

Torres, P. B., Chow, F., Furlan, C. M., Mandelli, F., Mercadante, A., and Santos, D. Y. A. C. (2014). Standardization of a protocol to extract and analyze chlorophyll a and carotenoids in *Gracilaria tenuistipitata* Var. Liui. Zhang and Xia (Rhodophyta). *Braz. J. Oceanogr.* 62, 57–63. doi: 10.1590/s1679-87592014068106201

van der Heijden, L. H., and Kamenos, N. A. (2015). Calculating the global contribution of coralline algae to carbon burial. *Biogeosci. Discuss.* 12, 7845–7877. doi: 10.5194/bgd-12-7845-2015

Vásquez-Elizondo, R. M., and Enríquez, S. (2016). Coralline algal physiology is more adversely affected by elevated temperature than reduced pH. *Sci. Rep.* 6:19030. doi: 10.1038/srep19030

Wilson, S., Blake, C., Berges, J. A., and Maggs, C. A. (2004). Environmental tolerances of free-living coralline algae (maërl): implications for European marine conservation. *Biol. Cons.* 120, 283–293. doi: 10.1016/j.biocon.2004.03.001

Conflict of Interest: The authors declare that the research was conducted in the absence of any commercial or financial relationships that could be construed as a potential conflict of interest.

Copyright © 2020 Sordo, Santos, Barrote, Freitas and Silva. This is an open-access article distributed under the terms of the Creative Commons Attribution License (CC BY). The use, distribution or reproduction in other forums is permitted, provided the original author(s) and the copyright owner(s) are credited and that the original publication in this journal is cited, in accordance with accepted academic practice. No use, distribution or reproduction is permitted which does not comply with these terms.

frontiers in Marine Science

ORIGINAL RESEARCH
published: 08 January 2019
doi: 10.3389/fmars.2018.00502

The Critical Importance of Rhodoliths in the Life Cycle Completion of Both Macro- and Microalgae, and as Holobionts for the Establishment and Maintenance of Marine Biodiversity

Suzanne Fredericq[1], Sherry Krayesky-Self[1], Thomas Sauvage[2], Joseph Richards[1], Ronald Kittle[1], Natalia Arakaki[3], Emma Hickerson[4] and William E. Schmidt[1]*

[1] Department of Biology, University of Louisiana at Lafayette, Lafayette, LA, United States, [2] Smithsonian Marine Station, Fort Pierce, FL, United States, [3] Instituto del Mar del Perú, Banco de Germoplasma de Organismos Acuáticos, Area Funcional de Investigaciones en Acuicultura, Callao, Peru, [4] Flower Garden Banks National Marine Sanctuary, Galveston, TX, United States

OPEN ACCESS

Edited by:
Julio Aguirre, University of Granada, Spain

Reviewed by:
Christine Maggs, Queen's University Belfast, United Kingdom
Adela Harvey, La Trobe University, Australia

***Correspondence:**
Suzanne Fredericq
slf9209@louisiana.edu

Specialty section:
This article was submitted to Marine Ecosystem Ecology, a section of the journal Frontiers in Marine Science

Received: *31 October 2018*
Accepted: *14 December 2018*
Published: *08 January 2019*

Citation:
Fredericq S, Krayesky-Self S, Sauvage T, Richards J, Kittle R, Arakaki N, Hickerson E and Schmidt WE (2019) The Critical Importance of Rhodoliths in the Life Cycle Completion of Both Macro- and Microalgae, and as Holobionts for the Establishment and Maintenance of Marine Biodiversity. Front. Mar. Sci. 5:502. doi: 10.3389/fmars.2018.00502

Rhodoliths are the main hard substrata for the attachment of benthic macroalgae in the NW Gulf of Mexico rubble habitats that are associated with salt domes, unique deep bank habitats at ~50–90 m depth on the continental shelf offshore Louisiana and Texas. With the advent of additional sequencing technologies, methodologies for biodiversity assessments are now rapidly shifting to DNA metabarcoding, i.e., High Throughput Sequencing (HTS) of environmental DNA mixtures with standardized molecular markers, such as 16S V4, for rapid, cost-effective biodiversity measurement. We newly tested 16S V4 metabarcoding on endolithic portions of mesophtic rhodoliths exhibiting low phototroph colonization that revealed a hidden, cryptic algal diversity targeting spores, propagules, and unsuspected life history stages. We explored cryo-SEM as a potentially more informative method than regular SEM to minimize artifacts of sample preparation in the study of endolithic cell inclusions which brought to light a suite of microalgal stages. We were able to differentiate floridean starch from cellular inclusions. We associated the effect of anatomical growth pattern on presence or absence of cellular inclusions in biogenic rhodoliths. Analyses of combined 16S V4 metabarcodes and 16S Sanger sequences of two red algal orders, the Halymeniales and Bonnemaisoniales, increased the established record of diversity in the region. We view rhodoliths as marine biodiversity hotspots that may function as seedbanks, temporary reservoirs for life history stages of ecologically important eukaryotic microalgae, and macroalgae or as refugia for ecosystem resilience following environmental stress.

Keywords: CCA, coralline algae, Gulf of Mexico, marine biodiversity, mesophotic, metabarcoding, rhodoliths

INTRODUCTION

This paper focuses on rhodoliths from mesophotic rhodolith beds occurring in the northwestern Gulf of Mexico (NWGMx) on the continental shelf offshore Louisiana and Texas (USA) at ~45–90 m depth (**Figures 1–3**). It is to be viewed as a conceptual primer to address insights and working hypotheses on the dynamic role of rhodoliths as marine biodiversity hotspots and seedbanks for macroalgae and microalgae in maintaining the health of marine ecosystems.

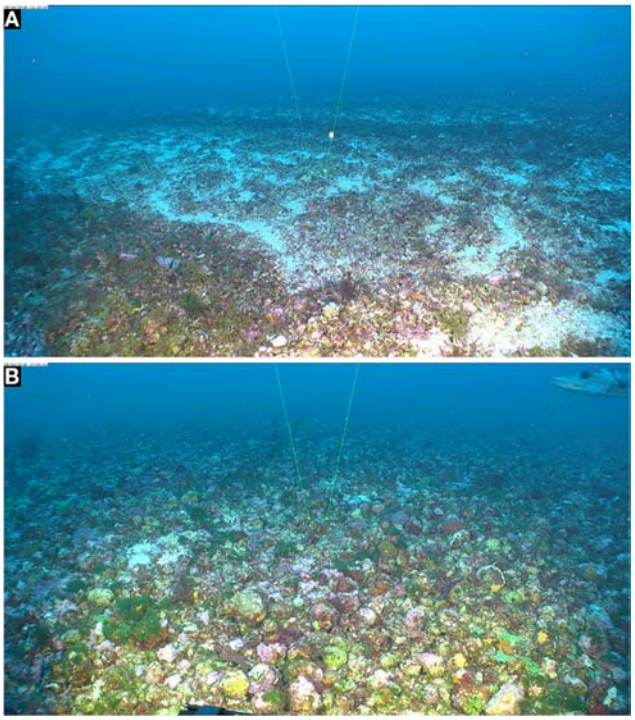

FIGURE 1 | Extensive rhodolith beds in East Flower Garden Bank, FGBNMS. Mohawk ROV photos taken on 24 Sept. 2018. **(A)** 27°56'22.2288"N, 93°36'1.3068"W, 53 m (Dive 701_0905_111338). **(B)** 27°54'4.6182" N; 93°36'40.2732" W, 52.9m (Dive 703_0603_172042). Space between spot lasers = 10 cm.

FIGURE 2 | Rhodoliths form the substratum for attached fleshy and crustose red, brown, and green seaweeds. Mohawk ROV photos taken on 25 Sept. 2018 in West Flower Garden Bank, FGBNMS. **(A)** 27°52'7.2732"N, 93°51'34.4088"W, 58.8 m depth (Dive 706_0238_122144). The visible macroscopic seaweed is the green alga *Codium isthmocladum* Vickers (Codiaceae, Bryopsidales). **(B)** 27°52' 7.1682"N, 93°51'34.185"W, 58.8 m depth (Dive 706_0268_123120). The visible fleshy macroscopic red algal blades are the red alga *Anatheca* sp. (Areschougiaceae, Gigartinales). Space between spot lasers = 10 cm.

Rhodoliths are unattached, marine, benthic algal nodules of various sizes, and origins that are predominantly accreted by non-geniculate (crustose) coralline red algae (CCA) precipitating $CaCO_3$ within their cell walls (Foster, 2001). Bioturbation or water motion is critical for rhodoliths to grow and remain unburied by sediments, and it also limits fouling by enabling their periodic rotation to allow light exposure on all sides (Steneck, 1986; Hinojosa-Arango et al., 2009). Rhodolith beds are common constituents of modern and fossil marine environments worldwide, especially in clear tropical waters with beds up to 10 m thick (Littler et al., 1985; Amado-Filho et al., 2007, 2012; Pereira-Filho et al., 2011, 2012; Harvey et al., 2017). The taxonomic composition of mesophotic algae (Spalding et al., 2019) associated with rhodolith beds at 45–90 m depth in the NWGMx typically encompasses fleshy and crustose species limited to those low light habitats and includes some taxa from very deep branches of the algal Tree of Life (e.g., the recently erected Class Palmophyllophyceae, Leliaert et al., 2016).

Representative species of three orders of coralline algae (Corallinophycidae) that grow as rhodoliths, i.e., Hapalidiales, Corallinales, and Sporolithales, are found in the NWGMx. On the basis of comparative DNA sequence analysis and anatomy, Richards et al. (2016) recognized eight species of *Lithothamnion* (Hapalidiales) rhodoliths in the Gulf of Mexico where only a total of three taxa were previously reported. Also discovered were a wealth of other taxa, including, so far, 3 species of *Harveylithon,* and at least 3 species of *Lithophyllum* and "*Titanoderma*" (Corallinales) (Richards et al., 2014, Richards, unpubl. data), as well as two new species of *Sporolithon* (Sporolithales) (Richards and Fredericq, 2018, and Richards, unpubl. data). Cryptic or pseudocryptic species of CCA (crustose coralline algae) forming rhodoliths abound in the NWGMx because they do not appear that different from one another based on superficial characters and external morphology alone. Likewise, internal morpho-anatomy can be very similar between different species. Overall, it is not unreasonable to assume that the true diversity of rhodoliths species in the NWGMx is much greater than is currently recognized.

Rhodoliths represent an important and understudied component of marine diversity that contributes to major ecosystem functions. They are important ecosystem engineers (Foster et al., 2007; Cavalcanti et al., 2014) providing structurally complex habitats harboring high biodiversity (Nelson et al., 2014; Teigert, 2014; Riosmena-Rodríguez et al., 2017), including many microhabitats for diverse assemblages of algae, invertebrates and other macroscopic taxa (Cabioch, 1969; Hinojosa-Arango and Riosmena-Rodríguez, 2004). For instance, the sand tilefish *Malacanthus plumieri* (Bloch) further increases habitat

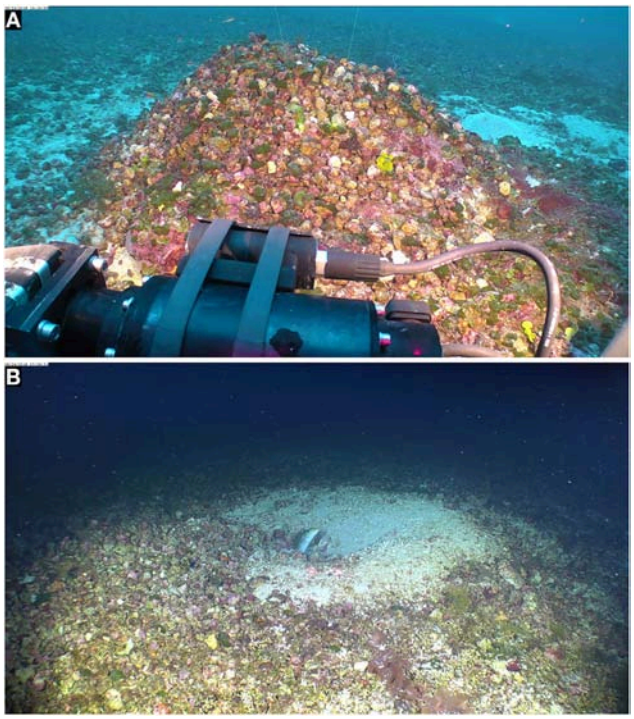

FIGURE 3 | Mound of rhodoliths with attached fleshy and crustose red, brown, and green seaweeds, built by sand tilefish (*Malacanthus plumieri* Bloch 1786, Malacanthidae). Mohawk ROV photos taken on 24 Sept. 2018 in East Flower Garden Bank (FGBNMS). **(A)** (27°55'22.1334"N, 93°35'31.8048"W, 51.2 m (Dive 702_0063_131400). **(B)** Sand tilefish at entry of its rhodolith mound, 27°56'20.7132"N, 93°36'1.1052"W, 51.8 m (Dive 700_0040_075832). Space between spot lasers = 10 cm.

complexity provided by the rhodoliths by building mounds that coalesce in more solid structures and may constitute an early successional stage in the formation of large coralline reefs on SW Atlantic tropical shelves (Pereira-Filho et al., 2011). Pereira-Filho et al. (2015) summarize that the purpose of the rhodolith mounds in the Fernando de Noronha Archipelago, Brazil, is yet undetermined and may provide an orientation reference for the tilefish during foraging, a refuge from predation, a nutritional source, and/or are important for social organization.

As primary producers, rhodoliths and their associated macroalgae are crucial components of the photosynthetic community that produces O_2, provides food and shelter for invertebrates and vertebrates, and induces settlement and metamorphosis of some invertebrate larvae (Heyward and Negri, 1999; Hadfield and Paul, 2001; Riosmena-Rodríguez and Medina-Lopez, 2011); these processes may also be linked to co-habiting microbial communities. Rhodoliths also fulfill an important function in biogeochemical cycling. For example, they exude organic matter (Smith et al., 2006) that is utilized by co-residing prokaryotes, which in turn cycle key biogeochemical elements necessary for these primary producers and other eukaryotic rhodolith colonizers. Corallines are one of the major producers of dimethylsulfoniopropionate (DMSP) (Kamenos et al., 2008), which, upon being metabolized by algal-associated bacteria, produces volatile compounds such as dimethyl sulfide (DMS) that has direct effects on the global sulfur cycle and global climate change (Burdett et al., 2015; Wang et al., 2018). Yet, integrated baseline data on the rhodoliths' microbiome (microbiota) composition and gene expression in relation to biogeochemical cycling are sorely needed to better understand the functions of these nodules within the marine ecosystem.

$CaCO_3$ provides various advantages such as skeletal strength, protection from grazers and borers, and enhanced survivorship by increasing resistance to wave action (Borowitzka and Larkum, 1987; Foster et al., 2007). The deposition of $CaCO_3$ by rhodoliths and other calcifying marine algae is an essential process in the global carbon cycle (Vecsei, 2004; McCoy and Kamenos, 2015), and rhodoliths are recognized as foremost carbonate builders when they form extensive beds. The modulation of $CaCO_3$ deposition by the corallines and its dissolution is receiving much attention because ocean acidification and rising global sea surface temperatures represent major threats to calcifying marine organisms and their associated microbes (Anthony et al., 2008; Webster et al., 2016). They are highly sensitive to variations in temperature (Adey et al., 2013; Halfar et al., 2013) and are mostly composed of high-Mg biogenic calcite, the most sensitive $CaCO_3$ polymorph to decreases in ocean pH (Kamenos et al., 2013; Webster et al., 2013; Krayesky-Self et al., 2016; Ragazzola et al., 2016). They may be the first indicators of ocean acidification by dissolution (Morse et al., 2006; Andersson et al., 2007; Ragazzola et al., 2012), with ensuing negative effects on a variety of biotic interactions, such as larval settlement reduction of spawning corals (Anthony et al., 2008; Doropoulos et al., 2012; Webster et al., 2013).

Prior to the April 2010 Macondo Well Blowout (04/2010, 28°44'12.01"N, 88°23'13.78"W) and resulting Deepwater Horizon oil spill (DWH) offshore Louisiana (Paris et al., 2012; Rabalais, 2014), mesophotic rhodolith beds occurring throughout the NWGMx, such as Ewing Bank, harbored diversity-rich, lush assemblages of red, green, and brown seaweeds. In contrast, post-DWH, macroalgae in Ewing Bank rhodolith beds in the vicinity of the Macondo Well blowout disappeared, and most rhodoliths themselves appeared bleached, and fully or partially bare of surface macroalgae (Felder et al., 2014; Fredericq et al., 2014), a situation that has persisted in the field as of May 2018, our last expedition to Ewing Bank. These post-DWH impacts appear long-lasting, with little macroalgal growth recovery in the field, for reasons still unknown. Since rhodoliths and their associated macroalgae are ecologically important phototrophs at the base of the oxygen-based food chain, their continued, apparent drastic die-off may have important consequences for the health and recovery of the marine mesophotic bank ecosystem in the NWGMx. The full extent, reasons and ecological consequences of the disappearance of healthy rhodoliths and associated macroalgae on Ewing Bank post-DWH, and the potential link of this decline to consumers is currently unknown. This requires an ecosystem-wide investigation that must include the less visible component of primary producers, such as endolithic algae growing within $CaCO_3$-lined cells of the rhodoliths, resting spores, and carbonate dwellers, heteromorphic life history stages,

and their interaction with bacterial communities involved in elemental cycling within the rhodoliths.

Two major rhodolith categories can be found in the NWGMx, i.e., *biogenic* and *autogenic* rhodoliths. *Biogenic* rhodoliths (**Figures 4A–C,F**, **5**) are formed by the non-geniculate crustose coralline algae (CAA) themselves, e.g., *Lithothamnion* spp. (Hapalidiales) and *Sporolithon sinusmexicanum* (Sporolithales). In contrast, *autogenic* rhodoliths (**Figures 4D–F**) are derived from already existing calcium carbonate rubble established by differential erosion processes of the caprock (Gore, 1992), with the rubble becoming secondarily covered by various encrusting and fleshy algae (Felder et al., 2014; Fredericq et al., 2014; Richards et al., 2014, 2016; Krayesky-Self et al., 2017; Schmidt et al., 2017). We view the autogenic rhodoliths as a specific type of nucleated rhodoliths (*sensu* Freiwald and Henrich, 1994) in which the core derives from calcium carbonate rubble as opposed to other materials. These two categories of rhodoliths co-inhabit the same rhodolith beds but the internal (endolithic) microbiome of each category differs with regard to the number and diversity of taxa (biogenic: Krayesky-Self et al., 2017, and autogenic: Sauvage et al., 2016). Even though corallines belong in the Supergroup Plants (Yang et al., 2016), the calcium carbonate-encrusted cell lumina are hard and "stony," and the endophytic ("inside plant") nature of algal inclusions can be interpreted as endolithic ("inside stone").

Post-DWH observations that prompted us to explore algal diversity *within* and on the *surface* of rhodoliths include the fact that **(1)** Bare, denuded, and "apparently dead" rhodoliths collected at Ewing and Sackett Banks offshore Louisiana were brought back to the laboratory and placed into 75 liter microcosms. After a few weeks, diverse macroalgal growth started to emerge from the rhodoliths' surface, reflecting macroalgal community present prior to the DWH oil spill (Arakaki et al., 2014; Felder et al., 2014; Fredericq et al., 2014), with many taxa reaching sexual maturity and completing their life life cycle. **(2)** Presence of algal propagules and spores, bacteria, fungal hyphae, and diatoms, dinoflagellates, were shown on the surface (*epilithic*) or inside (*endolithic*) autogenic rhodoliths with SEM and epifluorescence microscopy (Felder et al., 2014; Fredericq et al., 2014). Furthermore, SEM, TEM, and Fluorescence microscopy documented previously unrecognized benthic life history stages of bloom-forming microalgae such as the dinoflagellate *Prorocentrum lima* and the haptophyte *Ochrosphaera verrucosa* (Krayesky-Self et al., 2017) residing endolithically *inside* calcium carbonate-lined cell lumina of *biogenic* CCA rhodoliths *(Lithothamnion* sp., Hapalidiales). **(3)** Metabarcoding (amplicon environmental sequencing) of *endolithic* DNAs from within an Ewing Bank *autogenic* rhodolith with degenerate primers for plastid *tuf* A (elongation factor EF-T*tu*) (Sauvage et al., 2016) recovered a wide microbiotal diversity of photosynthetic prokaryotic (cyanobacteria) and eukaryotic algae, including red algae (Florideophyceae, Rhodophyta), green algae (Ulvophyceae, Chlorophyta), and Haptophyta. In addition, sequencing of observed single cell inclusion within live CCA cells of biogenic rhodoliths also confirmed their microalgal identity (Krayesky-Self et al., 2017) and remains understudied.

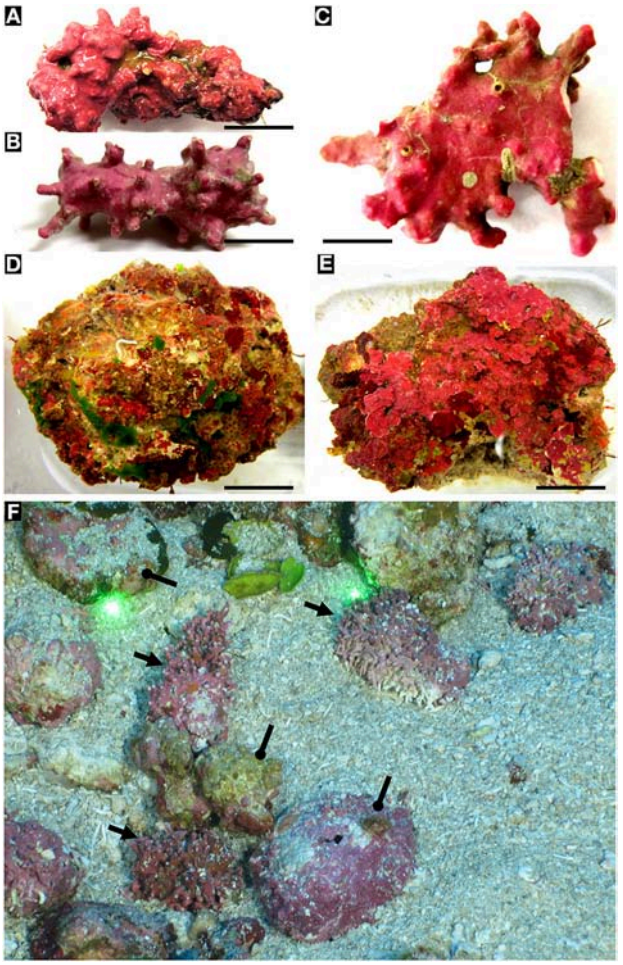

FIGURE 4 | Biogenic and autogenic rhodoliths. **(A)** biogenic rhodoliths. **(A,B)** *Lithothamnion* spp. (Hapalidiales). Scale bars: 0.8 cm; 0.5 cm. **(C)** *Sporolithon sinumexicanum* (Sporolithales) collected from the central cavity of a sponge. Scale bar: 0.5 cm. **(D,E)** Examples of NWGMx autogenic rhodoliths. Scale bars: 1.5 cm; 2 cm. **(F)** Mohawk ROV photo taken on 24 Sept. 2018 of biogenic (arrows) and autogenic rhodoliths (circle pointers) in East Flower Garden Bank (FGBNMS), 27°55' 21.9612"N, 93°35'31.6674"W, 50.9 depth (Dive 702_0007_131247). Space between spot lasers = 10 cm.

In this paper we expanded upon our previous work by testing 16S V4 for recovering phototrophic diversity of mesophotic rhodoliths exhibiting low phototroph colonization. We also tested cryo-SEM as a potentially a more informative method than regular SEM to minimize artifacts of sample preparation in the study endolithic cell inclusions, and utilized staining techniques to differentiate floridean starch from cellular inclusions. We associated the effect of anatomical growth pattern on presence or absence of cellular inclusions in biogenic rhodoliths.

MATERIALS AND METHODS

Study Area

Rhodolith beds offshore Louisiana and Texas in the NW Gulf of Mexico (NWGMx, **Supplementary Figure S1**) are associated with salt domes (diapirs), unique mesophotic bank habitats on

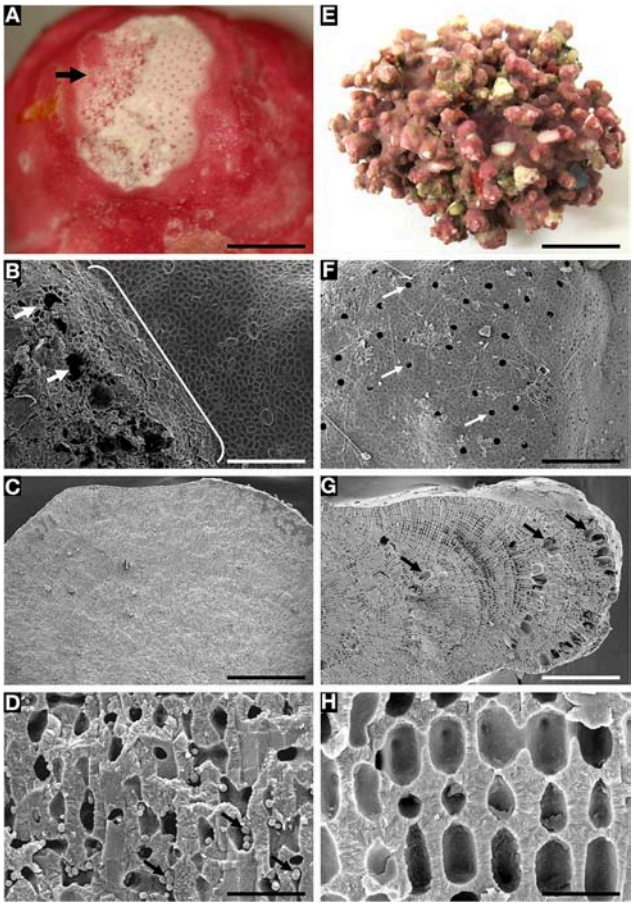

FIGURE 5 | Rhodolith species with sloughed tetrasporangial sori and epithallial layers showing endolithic cells **(A–D)**, and species with non-sloughed tetrasporangial sori **(E–H)** lacking endolithic cells. **(A–D)** *Sporolithon sinusmexicanum* (**A,C,D** = specimen LAF6970B from Dry Tortugas vicinity [24° 31.494'N, 83°19.793'W, 69 m]; B = specimen LAF6956A from Sackett Bank, LA [28° 38.0'N, 89°33.028'W, 69 m]). **(A)** Thallus surface showing tetrasporangial sorus (arrow) in the process of sloughing. Scale bar = 500 μm. **(B)** Disintegrating tetrasporangial sorus showing exposed tetrasporangial compartments (arrows) and sloughing epithallial cells (bracket). Scale bar = 160 μm. **(C)** Longitudinal fracture of rhodolith protuberance showing lack of buried tetrasporangial compartments. Scale bar = 720 μm. **(D)** Perithallial cells with putative endolithic cell stages (arrows). Scale bar = 32 μm. **(E–H)** *Sporolithon* sp. nov. (LAF7260). **(E)** Thallus habit. Scale bar = 1.1 cm. **(F)** Thallus surface with tetrasporangial sorus showing lack of sloughing and pores of intact tetrasporangial compartments. Scale bar = 176 μm. **(G)** Longitudinal fracture of rhodolith protuberance showing layers of unshed and buried tetrasporangial compartments (arrows). Scale bar = 400 μm. **(H)** Perithallial cells lacking endolithic cell stages. Scale bar = 22 μm.

the continental shelf (Rezak et al., 1985; Felder and Camp, 2009) that are peculiar to that part of the NW Gulf, at ∼45–90 m depth (**Figures 1**, **2**). By virtue of their geological history, especially in that they often surmount salt domes where strata trap hydrocarbons, many of the rhodolith habitats are located in or immediately adjacent to areas of intensive oil and gas exploration, production, and transportation (Felder and Camp, 2009). The composite sedimentary overlayer of $CaCO_3$, gypsum, and anhydrite above a salt dome is geologically known as caprock. Anaerobic bacteria obtain the carbon necessary to reduce anhydrite to limestone from petroleum hydrocarbons accumulating in pockets along the edge of the salt dome banks (Gore, 1992), and it is the caprock slopes and peaks that are covered by rhodolith (algal nodule) beds (Minnery et al., 1985; Minnery, 1990; Fredericq et al., 2009, 2014; Felder et al., 2014; Richards et al., 2014, 2016). Offshore Louisiana and Texas (**Figures 1**, **2**), the majority of benthic fleshy, erect, decumbent and crust-forming red, green, and brown seaweeds grow attached to the surface of rhodoliths (**Figures 3**, **4**). In the NWGMX, the continuous and extended rhodolith bed facies may become spatially discontinuous by sandy or silty patches forming scattered mounds of rhodoliths (**Figure 3**) built by sand tilefish (*Malacanthus plumieri* Bloch) (Rezak et al., 1985; Tom Bright, pers. comm.; also shown in multiple Flower Garden Banks National Marine Sanctuary (FGBNMS) annotations, photographs, and videos at FGBNMS, a true ecosystem engineer!

Extensive rhodolith beds occur also at the edge of thriving coral reefs in the FGBNMS on the outer continental shelf about 170 km south of the Texas-Louisiana border (Scanlon et al., 2003; Gardner and Beaudoin, 2005; Slowey et al., 2008) but these rhodolith beds (**Figures 1**–**3**) are only found below the hermatypic coral zone. These coral reefs are an important natural laboratory for interdisciplinary studies, and we contend the same holds true for their associated rhodolith beds. The FGBNMS has a web page that shows a series of mapped deep banks throughout Louisiana and Texas, with a discussion of continental slope and carbonate bank sedimentary processes, high-resolution seismic stratigraphy, and physical properties of marine sediments in the Gulf of Mexico (sanctuaries.noaa.gov/about/pdfs/se_gom.pdf). Hickerson et al. (2008) provided an in-depth habitat characterization scheme that identifies the CCA zone which includes the rhodolith (algal nodule) zone.

Sample Collection

Mesophotic rhodolith collections used in this study were collected at Ewing Bank (vicinity of 28°05.7′N, 91°01.2′W) during August 2008 (Pre-DWH), October 2013, and May 2018 (Post-DWH) cruises aboard the R/V *Pelican*. Rhodoliths were retrieved using an Hourglass-design box dredge (Joyce and Williams, 1969) with minimum tows (usually 10 min or less) at depths ranging from 50–110 m. Water samples and environmental data were collected *in situ* using a CTD/Rosette system with sensors and Niskin bottles aboard ship. Samples were initially stored on-site by location in containers filled with seawater collected *in situ* from the same depth and site of the sampled rhodoliths using the onboard CTD water sampling rosette. Samples were kept aerated aboard ship for the duration of the trip (2–4 days) and transferred into microcosms, filled with *in situ* collected seawater, located in our laboratory at UL Lafayette. Subsamples of rhodoliths were also immediately upon retrieval placed in Ziploc bags filled with the desiccant silica gel for long-term preservation for subsequent DNA analysis and microscopy studies. Pre-and post-DWH-collected rhodoliths from Ewing Bank are housed at the University of Louisiana at Lafayette Herbarium (LAF). Images and samples collected by a Mohawk ROV of rhodolith beds in the West and East Flower

Garden Banks were taken at ∼55 m depth aboard the R/V *Manta* in September 2018. An extensive library of images collected during ROV surveys since 2001 throughout the reefs and banks of the northwestern Gulf of Mexico are held by the Flower Garden Banks National Marine Sanctuary, and will be assessed in the future.

Metabarcoding

Metabarcoding of 16S ribosomal RNA (rRNA) gene with the V4 region (Caporaso et al., 2011) was conducted on three pre- and three post-DWH-collected autogenic rhodoliths from Ewing Bank selected from previous collections desiccated in silica gel (see above). 16S V4 was selected to explore bacterial profiles from these rhodoliths as well as test its viability as an easily amplifiable marker to recover eukaryotic algae in mesophotic rhodolith samples exhibiting relatively low density of endolithic phototrophs. Moreover, our laboratory has previously used the 16S marker in phylogenetic studies of red algae via Sanger sequencing (Olsen et al., 2004; Hommersand et al., 2006; Rodríguez-Prieto et al., 2013). Succinctly, the sampling of endolithic communities consisted in drilling non-encrusted patches (with a drill, $n = 5$–6 patches per rhodolith) adjacent to CCA or peyssonnelioid crusts, i.e., "bare" substratum with a sterile 1.6 mm (1/16") bit (Sauvage et al., 2016). DNA extraction was then carried with a PowerSoil DNA Isolation kit (MO BIO Laboratories, Carlsbad, CA, USA. DNA extracts were shipped to MRDNA, where they were amplified with the HotStarTaq Plus Master Mix Kit (Qiagen, USA) with indexed primer for the 16S rRNA V4 region (515F and 806R, Caporaso et al., 2011). Paired-end reads (2 × 250 bp) of the V4 amplicons were generated on the Illumina MiSeq Next-Generation Sequencing platform at MRDNA (www.mrdnalab.com, Shallowater, TX, USA).

OTUs

Demultiplexed FASTQ files (NCBI SRA accession PRJNA508570) were processed with the DADA2 pipeline (Callahan et al., 2016) to produce RDP-annotated (Cole et al., 2014) 16S V4 OTUs denoised and devoid of chimeras. OTUs as "Chloroplast" and Cyanobacteria were extracted for further taxonomic investigation. We first merge this OTU file with the PhytoREF (Decelle et al., 2015) and built an exploratory tree to visualize without ambiguity the different classes retrieved from the rhodoliths (note that percent identity thresholds to be used with 16S for accurate classification have not been worked out for phototrophs, and thus the tree method provided a much less ambiguous alternative). We then used TREE2FASTA (Sauvage et al., 2018) to rapidly segregate OTUs belonging to the Rhodophyta to a separate file. These were then used for BLASTn search against Genbank's nt to find their closest matches and retrieve contextual sequences for tree building and determine their best identification (ordinal level) (see below and results).

Sanger Sequencing

We generated plastid 16S Sanger sequences of pertinent species of Halymeniaceae (Halymeniales) and Bonnemaisoniales, including many taxa from throughout the Gulf of Mexico, following the primer and sequencing protocols listed in Hommersand et al. (2006).

Tree Building

OTUs, Genbank matches, and Sanger sequences (see **Supplementary Table S1**) were merged, multiple-aligned and run with RAxML (Stamatakis, 2014) with a GTR+ G model of evolution rooted with early-branching Rhodophyta to display Florideophycean taxa found within the sampled endolithic communities (the best ML tree out of 1,000 restarts was kept and branch support assessed with 1,000 bootstrap replicates, full tree not shown). To showcase the phylogenetic representation of OTUs present within endolithic communities or as epilithic spores, we display trees for the Halymeniales, and Bonnemaisoniales.

Scanning Electron Microscopy (SEM)

SEM was used to document coralline morpho-anatomy and endolithic life history stages inside perithallial cells of biogenic rhodoliths. Portions of biogenic rhodoliths from silica gel-dried specimens were removed using a single-edged razor blade and forceps, or live rhodoliths of interest were placed into a folded sheet of paper and underwent short bursts of directed force with a hammer and resulting fragments subsequently preserved in silica gel. Vertical fractures were performed on crustose portions whereas protuberances were sectioned longitudinally using a new razor blade for each fracture. Sections were mounted using conductive adhesive tape or liquid graphite and coated with 5–16.5 nm of gold. Specimens were viewed using a Hitachi S-3000N SEM at a voltage of 15 or 20 kV, or a JEOL field emission scanning electron microscope (FESEM), both housed in the Microscopy Center at UL Lafayette (Richards et al., 2016; Krayesky-Self et al., 2017).

Live rhodoliths for the Cryo-SEM study were taken from the microcosm and immediately placed in liquid nitrogen for 1–2 min. Portions were moved to a Cryo-modified stub that held small amounts of liquid nitrogen. The Cryo-SEM stub was placed into a Hitachi S-3000N SEM at a voltage of 15V. Backscatter electrons were collected for viewing and imaging purposes. The backscatter electron detector was set to either composition mode or to topographic mode. Sublimation was allowed to occur for 2 h under a high vacuum in some cases. Each sublimated sample was sputter-coated with 10–13 nm gold and viewed on a JEOL SEM microscope following the procedure of Pesacreta and Hasenstein (2018).

Light Microscopy

Microcosm rhodoliths collected from Ewing Bank in May 2018 (**Figures 8A,B**) and 2013 (**Figure 8C**) were cut into small sections using a new razor blade for each sample. The hand sections were done on a glass slide covered by seawater. Seawater was then removed using a narrow-tipped transfer pipette. A 2% iodine solution (Carolina Biological Supply, CAT#869093) was added to the sections to test for the presence of floridean starch, and allowed to react for 5 min. The same samples were then rinsed with seawater, viewed with an Olympus SZX7 microscope and photographed using the True Chrome IIS digital system.

RESULTS

SEM Microscopy

Sporolithon sinusmexicanum, a biogenic rhodolith species that sloughs its tetrasporangial sori and epithallial layers, showed putative endolithic cell stages within perithallial cell lumina (**Figures 5A–D**). In contrast, *Sporolithon* sp. nov., a species with non-sloughed tetrasporangial sori and epithallial layers, lacked endolithic cell stages (**Figures 5E–H**) within perithallial cell lumina. At sites where tetrasporangial sori underwent sloughing from the rhodolith surface (**Figure 5B**), exposed openings into the rhodolith interior were observed that are larger than the pores of the tetrasporangial compartments which are not sloughed (**Figure 5F**).

SEM documented a variety of presumed microalgae residing endolithically *inside* calcium carbonate-lined cell

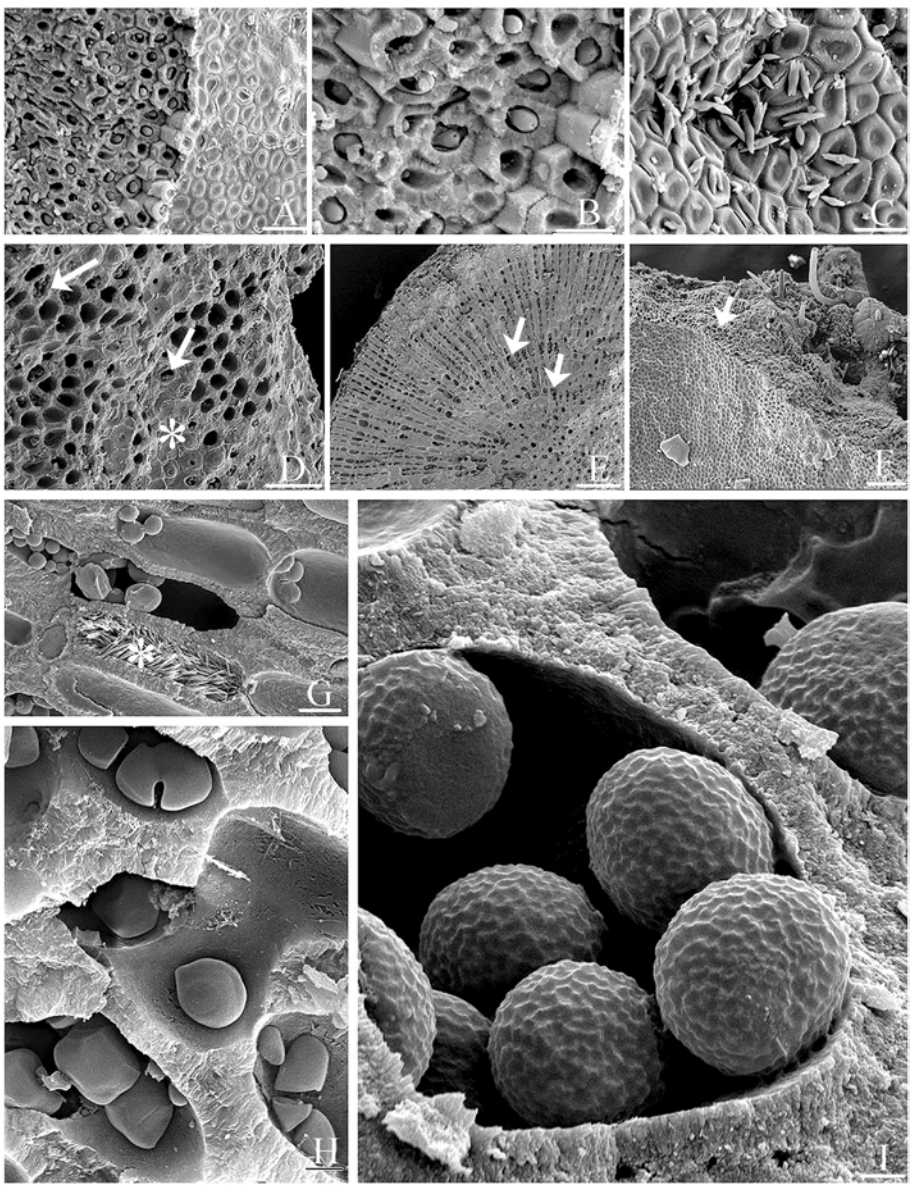

FIGURE 6 | Epilithic microalgae and various endolithic cellular inclusions of unknown taxonomic identity in biogenic rhodoliths. **(A)** Biogenic rhodolith surface (epithallus, at right) revealing underlying perithallus (at left) with endolithic cellular inclusions within calcium carbonate-enclosed cell lumina. Scale bar = 10 μm. **(B)** Close-up of **(A)** Scale bar = 20 μm. **(C)** Free-living microalgae on rhodolith surface Scale bar = 14 μm. **(D)** Surface cells (asterisk), and underlying exposed perithallial cells. Epithallial cells (asterisk) have been partly removed exposing endolithic cellular inclusions (arrows) in some perithallial cells. Scale bar = 5 μm. **(E)** Transverse view of rhodolith nodule showing endolithic cellular inclusions (arrows) within perithallial cells. Scale bar = 200 μm. **(F)** Surface (epithallus, at left) and fractured perithallus (in center, arrow) with cellular inclusions, and with burrowing taxa (at top). Scale bar = 300 μm. **(G)** Perithallial cells filled with aragonite crystals (asterisk), or endolithic cells. Scale bar = 20 μm. **(H)** Perithallial cells filled with endolithic cells. Some endolithic cells reside in perithallial fusion cells. Scale bar = 0.5 μm. **(I)** Endolithic cells showing surface ornamentation within perithallial cells. Scale bar = 0.7 μm.

lumina of biogenic *Lithothamnion* (Hapalidiales) rhodoliths (**Figures 6A–I**). The identity of many of these microalgal stages still needs to be confirmed. Micrographs reveal rhodolith surfaces (epithallus) with underlying perithallus enclosing endolithic cellular inclusions within their calcium carbonate-enclosed cell lumina (**Figures 6**, **7**). Often, free-living microalgae were also seen on the rhodolith surface (**Figure 6C**). Burrowing taxa were also observed (**Figure 6F**). Perithallial cells can also be filled with aragonite crystals (**Figure 6G**) next to perithallial cells containing endolithic cells. There is a great variety of shape and surface ornamentation on endolithic cells (**Figures 6H,I**). Some of the endolithic cells reside in perithallial fusion cells (**Figure 6H**)

Cryo-SEM micrographs (**Figures 7A–C**) showed copious amounts of clusters of endolithic cells within perithallial cells and validate the use of this method as a better approach when live material is available to better document endolithic cells. In samples that have been frozen, sublimation, and gold-coating bypass traditional fixation and dehydration protocols (**Figure 7A**) resulting in micrographs that include larger numbers of endolithic cells since they were not lost during the fixation and dehydration process. Furthermore, frozen samples can be viewed using backscatter electrons collected with the detector mode set to topographic (**Figure 7B**) or composition mode (**Figure 7C**). The composition mode is sensitive to variance in atomic number contrast, while topographic mode is sensitive to contrast between depths.

When rhodolith sections were exposed to iodine (**Figure 8**), floridean starch granules inside some rhodolith cells turned purple, indicating that these represented the floridean starch intrinsic to the coralline cells. Some areas contained brownish

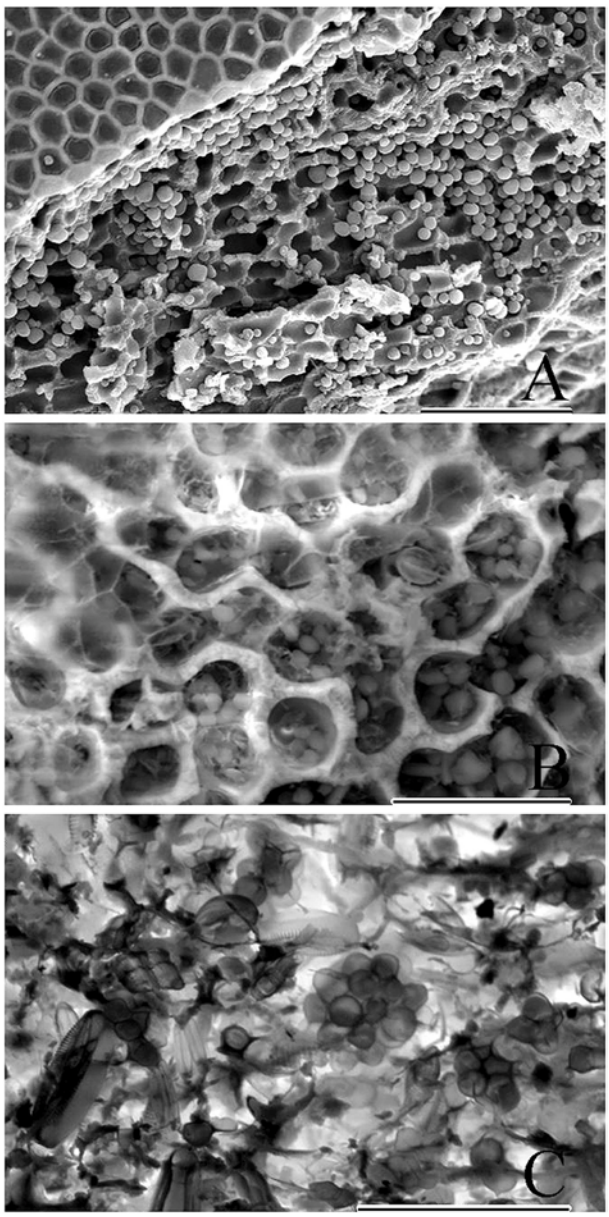

FIGURE 7 | Cryo-SEM micrographs showing copious amounts of endolithic cells**. (A)** Epithallus (at left) of a biogenic rhodolith, and clusters of endolithic cells viewed following sublimation and gold-coating. Scale bar = 100 μm. **(B)** Exposed perithalial cells enclosing endolithic cells. Micrograph produced using backscatter electrons collected with the detector mode set to topographic. Scale bar = 30 μm. **(C)** Micrograph showing clusters of endolithic cells, produced using backscatter electrons with the detector set to composition mode. Scale bar = 30 μm.

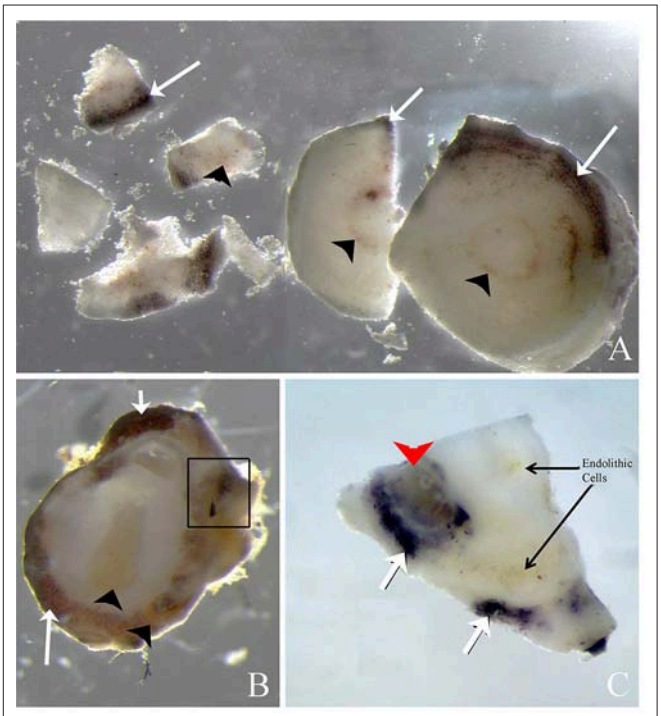

FIGURE 8 | Rhodolith sections exposed to 2% iodine solution. **(A,B)** Cross sections of rhodolith protuberance that has been exposed to iodine resulting in purple staining of floridean starch (arrows) present in the coralline cells. Brownish endolithic cells (arrowheads) do not stain purple after exposure to iodine. Some areas contain perithalial cells with and without purple stain, indicating that endolithic cells may have consumed floridean starch (in box, **B**). **(C)** Periclinal section of rhodolith nodule showing darkly staining floridean starch, brownish endolithic cells, and areas where both floridean starch and endolithic cells co-occur (arrowhead).

cellular inclusions but tested negative for floridean starch, whereas other regions contained a mixture of starch and cellular inclusions (**Figures 8A–C**, box).

Metabarcoding

Metabarcoding of 16S V4 rRNA recovered a large proportion of bacterial taxa (heterotrophs) as compared to phototrophs (Cyanobacteria and eukaryotic algae) in terms of richness (number of OTUs per phylum) and abundance (total read number per phylum) (see C/C annotation for "Cyanobacteria/Chloroplast" on **Figures 9 A,B** bar graphs) (**Table 1**). The most abundant prokaryotes consisted of 10 phyla of Bacteria and 1 phylum of Archaea (Thaumarchaeota). Sequencing depth strongly varied (see total read number per sample, **Figure 9B** and **Table 1**) with ENV14 (pre-DWH) and ENV10 (post-DWH) being the most sampled. Among these two samples, ENV10 exhibited higher richness (i.e., more OTUs) than ENV14 in spite of the latter larger sequencing depth (compare bar height in **Figures 9A,B**. Because of their more adequate sampling (sequencing depth), ENV10 and ENV14 may reflect phyletic profiles of the endolithic community within a mesophotic rhodolith more accurately as compared to the other samples, which mostly harbored the most abundant bacterial phyla (Proteobacteria, Firmicutes, Actinobacteria). A total of 55 phototrophic OTUs were found aside 1,321 heterotrophic OTUs in 4 phyla (Cyanophyta, Chlorophyta, Rhodophyta, Ochrophyta) (**Figures 9C,D**). Phototrophic OTUs represented <5% of total OTUs per sample (range 0.8 to 4.7%), and <4% of total read abundance per sample (range 0.2 to 3.4%) (**Table 1**, **Figure 9**). As for heterotrophic profiles, the post-DWH ENV10 exhibited greater richness and abundance than the pre-DWH ENV14 and may highly likely represent an exceptionally rich endolithic community rather than an effect of the DWH-spill since other samples (ENV11 and ENV12) exhibited very few phototrophs comparable to other pre-DWH samples (ENV04 and ENV13). Overall, the phototrophic OTU profiles may be extremely skewed because of the unequal sequencing depth of the samples and their relative low proportion in 16S data.

Phototrophic Diversity

Using tree methods with PhytoREF coupled with Genbank Blastn search (not shown), phototrophic OTUs obtained from the rhodoliths $CaCO_3$ could be identified in seven classes. These included "Bacillariophyceae" (5 OTUs), Cyanophyceae (7 OTUs), Florideophyceae (20 OTUs), Pedinophyceae (1 OTU), Phaeophyceae (4 OTUs), Pinguiophyceae (1 OTU), and Ulvophyceae (16 OTUs). Interestingly, the Ulvophyceae and the Florideophyceae were the diversity-richest classes. The Ulvophyceae included primarily euendoliths, such as *Ostreobium* and related unresolved Bryopsidales with 16S V4. The Florideophyceae represented spores or alternative filamentous life stages of otherwise epilithic/epiphytic fleshy macroalgae from several orders, i.e., the Bonnemaisoniales, Gracilariales, Gelidales, Gigartinales, Dumontiaceae-complex, Halymeniales, Nemaliales, and Sebdeniales. A few crustose members of Florideophytes, e.g., Corallinophycidae, and Peyssonneliales were also detected representing filaments or contaminants introduced from accidental drilling during sample preparation prior to DNA extraction. The Phaeophyceae represented primarily members of the order Ectocarpales. Phylogenetic trees showcasing Halymeniales and Bonnemaisoniales (**Figure 10**) and retrieved OTUs belonging to these orders showed 100% identity to a previously unrecorded genus for the Gulf of Mexico, *Reticulocaulis* (Naccariaceae, Bonnemaisoniales), and a *Halymenia* sp. (Halymeniaceae, Halymeniales) previously sequenced in our laboratory rom thalli collected during collecting cruises.

DISCUSSION

Considering Rhodoliths as Seedbanks for Macroalgae

Based on our previous research, the fact that post-DWH-collected macroalgae were not conspicuously visible at Ewing Bank *in situ* at their corresponding pre-DWH-collecting depths, sites and dates, but subsequently appeared in microcosms, suggested that rhodoliths play an important role as seedbank reservoirs of dormant microscopic stages of macroalgae (Fredericq et al., 2014; Sauvage et al., 2016; Krayesky-Self et al., 2017) to persist through adverse environmental conditions. Hitherto unknown cryptic, microscopic life history stages (e.g., small sporophytes) of macroalgae that are part of the rhodolith microbiota can now be linked with their macroscopic thalli using environmental sequencing. Our previous metabarcoding investigations of *tuf* A, which included a rhodolith from the Gulf of Mexico (ENV14, Sauvage et al., 2016) and newly presented 16S V4 data (herein), coupled with the above observations of newly emerging taxa in our microcosms, reveal that the interior of rhodoliths contained previously unknown life history stages of macroalgae, some of which we described taxonomically earlier (Arakaki et al., 2014). Additional linking of microscopic sporophytic stages with their macroscopic female/male gametophytes using multi-marker metabarcoding, Sanger sequencing, and various microscopy tools are needed to better ascertain the true biodiversity of the NWGMx's phototrophic component. Other calcareous substrata are well-known to be essential for life cycle completion of some seaweeds in which the heteromorphic stage of the sporophyte individual (in which meiosis occurs) is often a small crust, disk or aggregation of creeping filaments that does not resemble the larger gametophyte individual (e.g., Drew, 1949; Guiry, 1990; Hawkes, 1990; Hommersand and Fredericq, 1990).

Considering Rhodoliths as Seedbanks for Microalgae

Many planktonic microalgae, such as dinoflagellates (Dale, 1983; Steidinger and Garcés, 2006; Steidinger, 2010; Bravo and Figueroa, 2014), are known to possess benthic stages (i.e., cysts). Our previous work on rhodolith-associated microalgae (Krayesky-Self et al., 2017) demonstrated that common coastal bloom-forming microalgae may also be endolithically associated *within* biogenic rhodolith cells for part of their life cycle and we hypothesized that this phenomenon is common and widespread

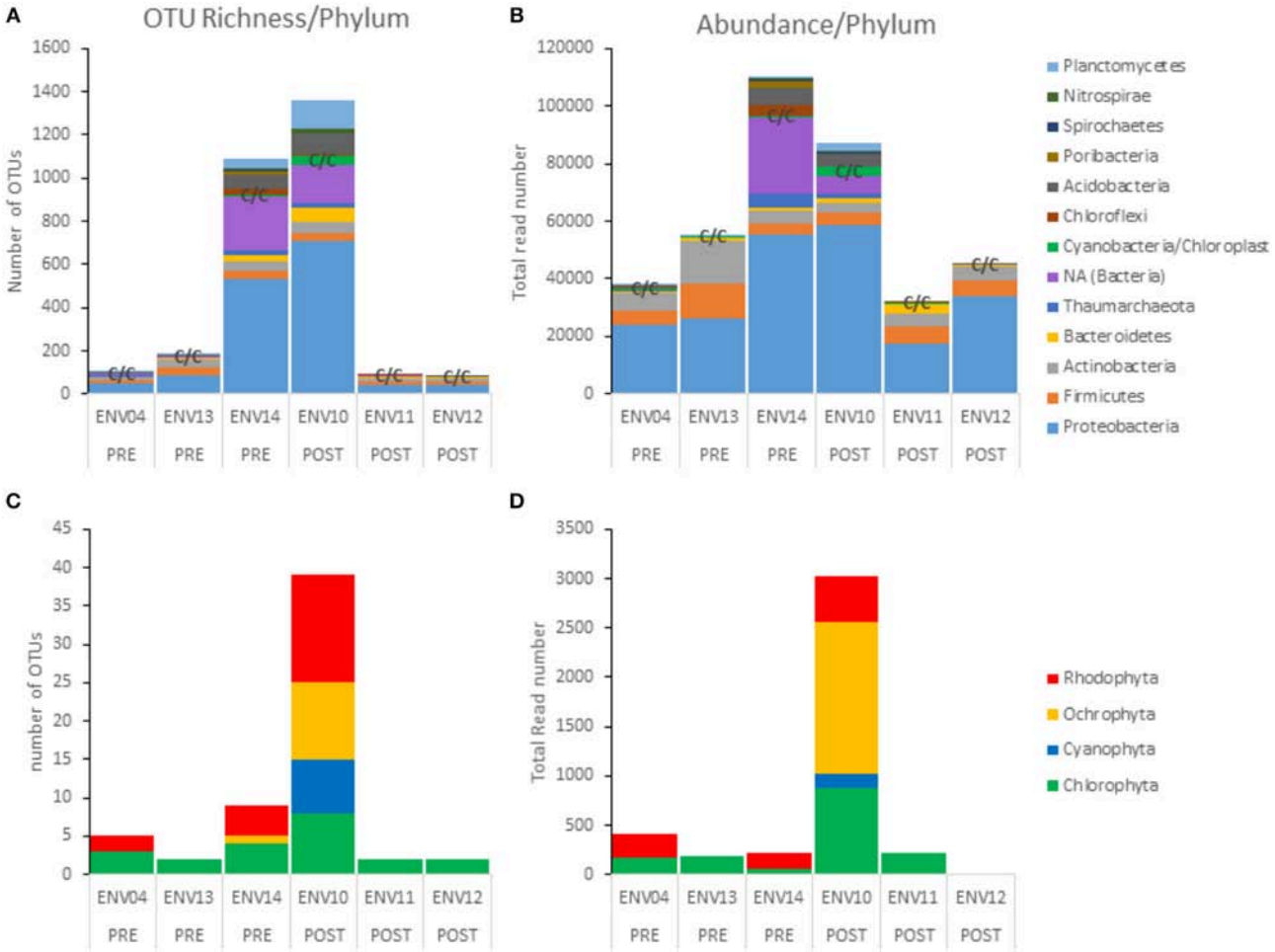

FIGURE 9 | Phototroph richness (OTU number) and abundance (read counts) retrieved with 16S V4 rDNA from pre- and post-DWH rhodolith endolithic communities. **(A,B)** All phyla. **(C,D)** Phototrophic phyla only. Note the relatively small number of OTUs and abundance of phototrophic OTUs (C/C for Cyanobacteria/Chloroplast) as compared to heterotrophic phyla.

TABLE 1 | Heterotrophic and phototrophic abundance (OTUs read counts) and richness (OTU number).

		Pre-DWH			Post-DWH		
		ENV4	**ENV13**	**ENV14**	**ENV10**	**ENV11**	**ENV12**
Abundance	All	38,072	55,252	110,761	87,439	31,946	45,790
	Heterotrophic	37,667	55,061	110,538	84,422	31,729	45,779
	Phototrophic	405	191	223	3017	217	11
	% Heterotrophs	98.9	99.7	99.8	96.5	99.3	100.0
	% Phototrophs	1.1	0.3	0.2	3.5	0.7	0.0
Richness	All	106	186	1,105	1,376	88	82
	Heterotrophic	101	184	1,096	1,337	86	80
	Phototrophic	5	2	9	39	2	2
	% Heterotrophs	95.3	98.9	99.2	97.2	97.7	97.6
	% Phototrophs	4.7	1.1	0.8	2.8	2.3	2.4

Note variation in sequencing depth across the sample and overall low proportion of phototrophic OTUs in the 16S V4 assays.

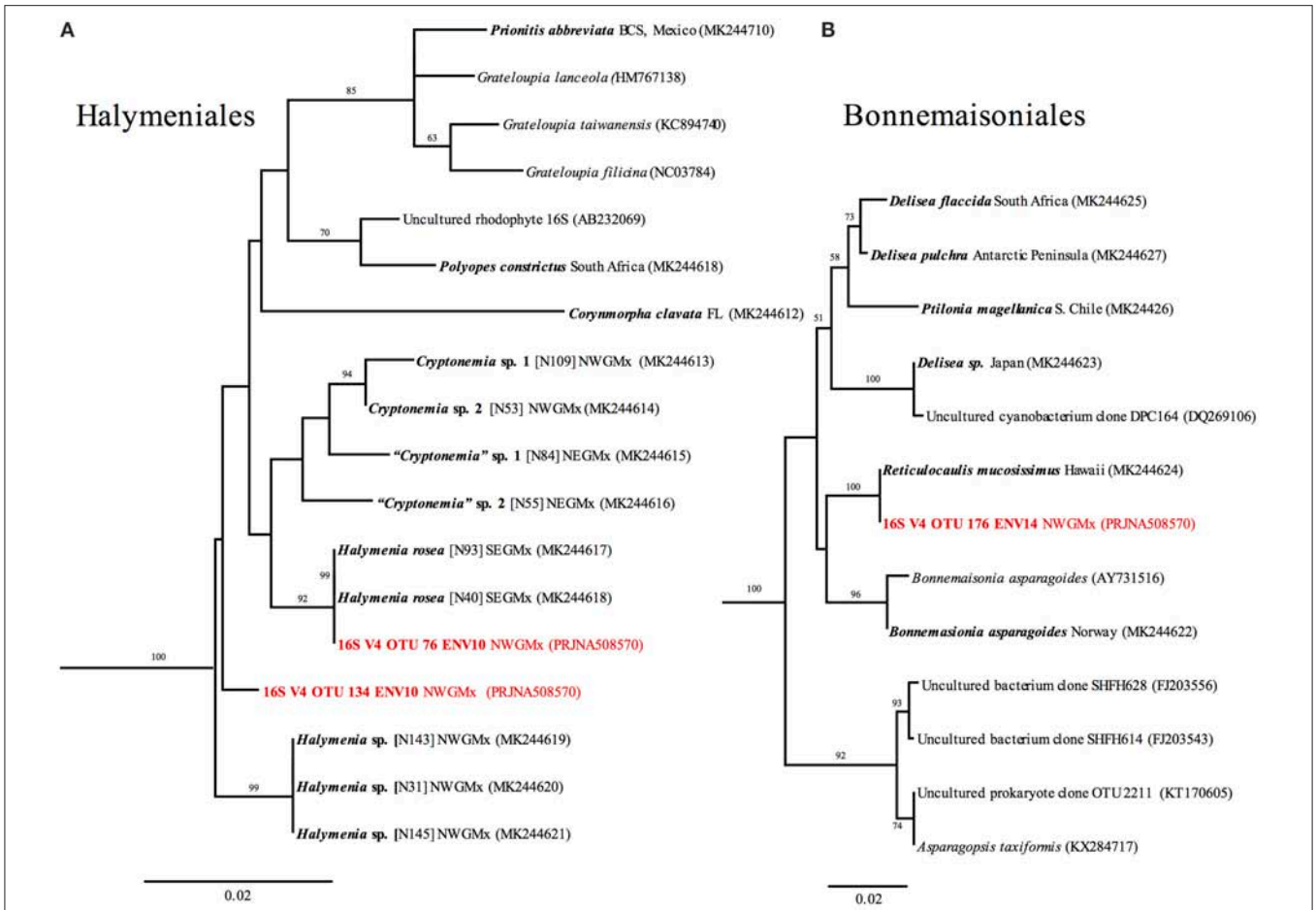

FIGURE 10 | RaxML trees of **(A)** Halymeniaceae and **(B)** Bonnemaisoniales based on 16S sequences, and 16S V4 metabarcodes (in red). Newly generated sequences are shown in bold. Branch numbers indicate bootstrap values >50 out of 1,000 replicates.

in the marine environment. For instance, our previous *tuf*A metabarcoding analysis pointed out that there was a large proportion of *Ochrosphaera verrucosa* Schussnig sequences originating from endolithic cells *inside* calcareous substrata (Sauvage et al., 2016). Krayesky-Self et al. (2017) were able to extract this species from Ewing Bank rhodoliths using single cell genome amplification. *O. verrucosa* is a common haptophyte in coastal waters worldwide and a taxon of which all the stages in its proposed haplo-diplontic cycle have not yet been observed (Fresnel and Probert, 2005) and may have been overlooked in the endolithic niche. Here, 16S V4 retrieved limited microalgae that we attribute to inadequate sequencing depth. In ENV10, an autogenic rhodolith showing the most phototrophic diversity, we retrieved an OTU identified as a Pinguiophyceae (*Pinguiococcus pyrenoidosus*), whose cyst is unknown (Andersen et al., 2002), and like *O. verrucosa*, may also occur in the endolithic niche. With deeper sequencing on a larger number of samples, we expect that more microalgae will be documented. Overall, we contend that numerous other microalgae use the calcareous niche for part of their life cycle and that the discovery of unsuspected endolithic stages may reveal important implications for understanding and predicting the onset of phytoplankton blooms, including those that form harmful algal blooms (HABs, Faust and Gulledge, 2002). Further research may help resolve incomplete life histories and enable one to link previously unknown endolithic stages of bloom-forming microalgae with their free-living stages, a current "hot" topic of great interest to HAB research (e.g., Steidinger and Garcés, 2006; Steidinger, 2010).

Critical Importance of Rhodoliths in Life Cycle Completion of Macro- and Microalgae

Our observations of thalli newly emerging in laboratory microcosms revealed that rhodoliths housed previously unknown life history stages of red (e.g., Halarachnion louisianensis, Arakaki et al., 2014; Schmitzia sp., unpubl. data), brown (e.g.,*"Syringoderma" floridana*, Camacho et al., 2018, 2019), and green algae (Sauvage et al., 2016). However, when excluding the rhodolith substratum, the culturing of these taxa prevented their life cycle completion, thus corroborating the

critical importance of $CaCO_3$ substrata in the life cycle of many macroalgae.

Using 16S V4 metabarcoding, we were able to link the taxonomic identity of the "invisible," cryptic parts of a macroalga *inside* a rhodolith with their corresponding "visible" macroscopic thalli through Sanger sequencing of plastid 16S-generated reference sequences from the NWGMx. Whereas 16S V4 is already an established metabarcode for all prokaryotes, we will continue to show that it can resolve phototrophic diversity (i.e., cyanobacteria, eukaryotes) as well. The macroalgal component will thus vastly improve with our preliminary 16S reference database and greatly increase our understanding of general phototrophic biodiversity in rhodolith beds and other marine communities. Our research answers the call by Yoon et al. (2016) that efforts should be made to update 23S and 16S sequences in databases. A 16S framework will allow the scientific community at large to re-examine their 16S datasets and accurately resolve their phototrophic component (e.g.,. 16S sequences labeled "uncultured cyanobacterium" in Genbank actually refer to specific species of *Delisea* and *Asparagopsis* (Bonnemaisoniales, **Figure 10B**). Thus, grossly unexplored biodiversity, new species discovery, and information relevant at both the barcode and phylogenetic level will improve with 16S V4 metabarcoding, as with other metabarcodes, and will greatly contribute to viewing both biogenic and autogenic rhodoliths as overlooked major marine diversity hotspots.

Dynamics of Endolithic Microalgal Cells in Biogenic Rhodoliths

The point of entry into the interior of biogenic rhodoliths (those fully accreted by corallines as opposed to secondarily colonizing nodules, i.e., autogenic rhodoliths) and later exit of life history stages of micro- and macroalgae are currently unresolved and purely speculative at this time. Corallines have the capacity to slough off their external (epithallial) cell layers (Wegeberg and Pueschel, 2002), including parts of their conceptacles (reproductive structures), that can become replenished with a unique type of intercalary meristem. It is possible that the roundish cellular inclusions (=microalgal life history stages) present within individual calcium carbonate-lined coralline cell lumina may passively become surrounded by new coralline surface cell layer growth, or perhaps enter/exit via the large pit connections that approximate the cell width of the endolithic stages, or via cell fusions (Krayesky-Self et al., 2017). There is no consensus about the nature of such cellular inclusions that have either been referred to as floridean starch (Viola et al., 2001), chloroplasts (Kunkel, 2005-2013), or bacteria (Garbary and Veltkamp, 1980; Kazmierczak and Iryu, 1999; Roh and Sim, 2012). The hypothesis that these inclusions were floridean starch was quickly rejected when iodine starch reaction turned negative for the inclusions (**Figure 8**). Likewise, the large size of the cellular inclusions excluded the concentric structures from being chloroplasts or bacteria (O'Reilly et al., 2012). Because we observed some coralline cells containing starch grains, and others which did not, we speculate that some of the cellular inclusions in biogenic rhodoliths are heterotrophic, consuming starch granules within perithallial cells of a rhodolith for their required maintenance. It is interesting that, from what we have observed so far, the biogenic rhodoliths that include the cellular inclusions also slough off their tetrasporangial sori and surface layers, e.g., *Sporolithon sinusmexicanum* (**Figures 5A–D**). In contrast, the species that does not slough off tetrasporangial sori layers does not include cellular inclusions, e.g., *Sporolithon* sp. nov. (**Figures 5E–H**). The larger openings formed by sloughing off of the tetrasporangial sori may provide a larger and more direct route for life history stages of microalgae to enter the rhodolith. Observing larger sample sizes of rhodoliths in future studies may shed light on whether this phenomenon is consistent throughout the populations of these two species and if similar phenomena occur in other species.

Our Cryo-SEM studies have shown us that the number of endolithic cells (**Figure 7**) is greater than revealed by traditional SEM. Furthermore, the variation of the surface ornamentation of the endolithic cells is more variable than previously observed with SEM and FESEM (Krayesky-Self et al., 2017).

We speculate that the majority of microalgal endolithic populations (aside from euendolithic taxa such as *Ostreobium*) within biogenic rhodoliths may not be permanent residents of these rhodoliths but are transient life history stages (potentially resting stages) that may form blooms once released in the water column from the rhodolith's interior following abrasion or sloughing off of the coralline's surface cell layers. Alternatively, micro- and macro-borers could also be responsible for releasing these cellular inclusions by opening burrows to the water column. This is a fascinating aspect of bentho-planktonic coupling of microalgal species and their association with CCA that we hope will get resolved in the future. Euendolithic taxa and filaments of alternate life stages of macroalgae may possibly enter biogenic rhodoliths via such mechansism. For comparison, in autogenic rhodoliths (those secondarily colonized from initially inert $CaCO_3$), patches of "open" substratum adjacent to encrusting red algae may function as a direct port of entry to the endolithic niche.

Use of 16S V4 Metabarcode Marker

Metabarcoding of 16S V4 rRNA recovered abundant Bacteria, some Archaea and limited phototrophic diversity, i.e., cyanobacteria and eukaryotic algae (**Figure 9**). Sequencing depth seemed grossly insufficient in order to comprehensively enumerate the biodiversity present in 4 of the samples (ENV04, ENV11, ENV12, ENV13). Nonetheless, while sequencing depth is important, it did not always equate to greater richness (i.e., compare ENV10 vs. ENV14). Overall, based on our analyses, we recommend that exploration of mesophotic rhodolith biodiversity via 16S V4 should be done with depth of >100,000 to 200,000 paired-end reads (possibly more) to stabilize prokaryotic profiles and better access their phototrophic fraction. Indeed, because of the extremely conserved nature of V4's priming region in the chloroplast of algae, which is derived from prokaryotic ancestors, and the inherent overabundance of bacterial taxa in any environmental samples, the latter tend to strongly "mask" phototrophs. For instance in a recent study of phytoplankton communities, the use of 16S for

metabarcoding still only resulted in 3–9% of phototrophic reads (Bennke et al., 2018), about twice more than obtained here (<5%). In this context, additional or alternative markers better targeting phototrophic diversity may be considered. For instance, UPA, the Universal Plastid Amplicon (Sherwood and Presting, 2007) should amplify as easily as 16S V4 and retrieve a much larger phototrophic component because of its greater specificity to chloroplasts, but it may not amplify some Chlorophyta that harbor introns in this region (T. Sauvage, pers. obs.). The chloroplast gene *tuf* A is another alternative to retrieve phototrophs in higher relative abundance (Sauvage et al., 2016). While we had successfully amplified *tuf* A at UL Lafayette, MRDNA failed to produce PCR products using fusion primers (containing Illumina adapters), except for the ENV14 rhodolith (see Sauvage et al., 2016, sample labeled GM14). We recognize that *tuf* A, while a very high quality metabarcode for its phylogenetic informativeness across numerous algal phyla, can be more difficult to amplify because of the high degeneracy of the environmental primers. Samples with low phototroph density, such as those of mesophotic rhodoliths here, can be more challenging to optimize and thus successful amplicons should rely on alternative library preparation than fusion primers. Regardless, *tuf* A and 16S V4 metabarcodes seemed to retrieve the same 3 phyla for ENV14 (see Figure 13b in Sauvage et al., 2016, and **Figure 9**), but further database curation and referencing of specimens than presently available in the 16S PhytoREF (Decelle et al., 2015) will be needed for finer scale identification of 16S OTUs at lower taxonomic rank (Edgar, 2018).

A display of OTUs' topological relationships with our newly generated Sanger data for reference specimens in the Halymeniales and Bonnemaisoniales (**Figure 10**) illustrates the power of metabarcoding to track alternate life stages (filaments/spores) of macroalgae. These trees, showcasing these two orders, demonstrated the presence of a previously unknown record of *Reticulocaulis mucosissimus* (Naccariaceae, Bonnemaisoniales) for the Gulf of Mexico, whose OTU exhibited a 100% identity match with our 16S reference collections from Hawaii. *Reticulocaulis* started to emerge from the surface of pre-DWH rhodoliths in our laboratory micoscosms. Since we never collected it in the field, it may be either ephemeral, rare, or not expressed in its macroalgal stage in the NWGMx. A *Halymenia* sp. OTU (Halymeniaceae, Halymeniales), also exhibited 100% identity to previously sequenced specimens in our laboratory on the basis of macroalgae dredged during previous cruises or emerging in our laboratory microcosms. A second OTU represented an unknown member of the Halymeniales that was also present but for which we could not yet produce a matching 16S sequence. Both Halymeniales OTUs originated from ENV10, a post-DWH sample, and while grown thalli were not observed in the field, were present endolithically.

Impact of the Deepwater Horizon Oil Spill

Because of the 2010 DWH oil spill offshore Louisiana (see **Supplementary Figure S1** for site of the Deepwater Horizon Macondo Well Blowout) and disappearance of mesophotic macroalgae at Ewing Bank, NWGMx, prompted us to look at rhodoliths endolithically following observation of regeneration of macroalgae in microcosms (Felder et al., 2014; Fredericq et al., 2014; Krayesky-Self et al., 2017), it opened many doors for new research directions and paradigms. One such direction made clear that further research is needed to link the eukaryotic component of the rhodolith holobiont ("total organism") with its co-occurring prokaryotic component. Great taxon diversity implies great genetic diversity, hence more gene families that will be expressed, and hence more modes of metabolism that will be directly related to biogeochemical cycles, among others. The biogeochemical cycles, in turn, provide the nutrients to support the high taxon diversity of the rhodolith holobiont. If any part of this described sequence is disturbed, the integration of the entire system falls apart and may take years to recover. This is what we believe happened in the NWGMx following the 2010 DWH oil spill: a biogeochemical upheaval post-DWH may have caused a shift in nutrients which led to a change in both the gene expression of the prokaryotic component and a shift in prokaryotic and eukaryotic taxon diversity (i.e., algal die-off) externally, on the *surface* of the rhodoliths. In contrast, the cryptic microbiotal component *inside* the rhodolith post-DWH acted as a stable buffer zone resilient to outside anthropogenic disturbances potentially allowing for regeneration. This is the reason macroalgae have emerged from "apparently dead" rhodoliths in our microcosms, while their growth, for reasons still unknown (e.g., herbivory, residual contaminants?), is still suppressed in the field (Ewing Bank). There is an obvious need to continue going back to monitor Ewing Bank to track the fate of the rhodolith beds. Additional research will shed light about ecosystem resilience and the extent rhodoliths play in biogeochemical and biodiversity cycling in their respective ecosystems. To address this, quantitative biogeochemical and transcriptomics data (both metatranscriptomics and qPCR) will need to be compared with the phylogenetic diversity of algal, prokaryotic, viral, and fungal communities and their role in biological succession following a disturbance using statistical models.

To inform us about the entire community composition associated with a rhodolith, deep metagenomic (non-amplicon environmental sequencing) studies will need to be conducted on rhodoliths worldwide. Metagenomes will allow us to recover viruses, fungi, metazoans, and other taxa that were not captured by our selected metabarcodes, but some of which were seen in our micrographs. Metagenomics will also allow us to evaluate the total rhodolith holobiont regardless of metabarcode bias. Cavalcanti et al. (2014) conducted metagenomic studies on rhodoliths from the Abrolhos Bank, Brazil, but the focus was on prokaryotes and they did not differentiate between the rhodolith *interior* (endolithic) and *surface* (epilithic) and whether the rhodoliths were biogenic or autogenic. It is especially timely to define the dynamics of the essential biogeochemical cycles associated with rhodolith beds in the NWGMx considering the recent disappearance of conspicuous macroalgae at Ewing Bank since the DWH oil spill (April 2010) with no visible sign of their recovery as of May 2018, our last collecting cruise date.

CONCLUSION

The fact that phototrophic OTUs could be obtained from within pre- and post-DWH rhodoliths suggests that although currently not visible in the field, seaweeds are still present in the NWGMx as "resting" microscopic stages (e.g., spores) *within* the rhodolith $CaCO_3$. Additional research on rhodoliths from different NWGMx areas is needed. Further exploration worldwide is also essential to confirm our findings that rhodoliths are marine biodiversity hotspots for unsuspected eukaryotic life and to ascertain whether the rhodolith interior functions as seedbanks for algal stages, as temporary reservoirs for life history stages of algal bloom-forming species, or as refugia for ecosystem resilience following environmental stress. Such studies will allow detection of community changes (including bioinvasions) in the face of possible re-colonization after catastrophic events. The study may have major implications for the prediction of microalgal blooms, shifts in the benthic primary-producer rhodolith community that followed the 2010 Deepwater Horizon Oil Spill in the NW Gulf of Mexico, and the possible effects of global warming and ocean acidification on the calcifying rhodoliths and their microbiota.

AUTHOR CONTRIBUTIONS

SF, TS, SK-S, JR, and WS conceived the study; SF, SK-S, WS, TS, NA, RK, and JR collected the samples; TS, SK-S, JR, WS, and NA conducted the laboratory work; TS, SK-S, and WS performed the data analyses. SF and TS wrote the manuscript with contributions from WS, SK-S, JR, NA, EH, and RK. All authors edited the manuscript before submission.

FUNDING

This work was funded by NSF DEB-1754504.

ACKNOWLEDGMENTS

We greatly acknowledge the support from NSF research grants DEB-0315995, and DEB1754504, and thank the crew of the R/V *Pelican* for their help with sampling protocols aboard ship and close research collaborators Darryl L. Felder, James N. Norris, Olga Camacho, Dago Venera-Ponton, Daniela Gabriel and D. Wilson Freshwater. We thank the FGBNMS, R/V *Manta* crew and Jason White and Eric Glidden from the University of North Carolina-Undersea Vehicle Program (WUNCW-UVP) for the ROV-collections and images taken at the East and West Flower Garden Banks. We also thank Brooke Bocklud for her work with the light microscopy, and the UL Lafayette Microscopy Center for their interest.

SUPPLEMENTARY MATERIAL

The Supplementary Material for this article can be found online at: https://www.frontiersin.org/articles/10.3389/fmars.2018.00502/full#supplementary-material

Supplementary Figure 1 | Map of the Gulf of Mexico showing collection locality data (●). From left to right: West Flower Garden Bank (WFG), East Flower Garden Bank (EFG), Ewing Bank (EB), Sackett Bank (SB), and vicinity of the Dry Tortugas, Florida (DT), and site of the Deepwater Horizon Macondo Well Blowout (◌).

Supplementary Table 1 | Taxon and collection data of plastid 16S reference sequences and GenBank accession numbers (including newly generated sequences shown in **boldface**) and 16 V4 sequences of Halymeniaceae (Halymeniales) and Bonnemaisoniales. Newly generated 16 V4 OTUs are shown in red (NCBI SRA). SF, Suzanne Fredericq; DWF, Wilson Freshwater; MHH, Max H. Hommersand; JR, Jan Rueness.

REFERENCES

Adey, W. J., Halfar, J., and Williams, B. (2013). The coralline genus *Clathromorphum* Foslie emend. Adey; biological, physiological and ecological factors controlling carbonate production in an Arctic/Subarctic climate archive. *Smithsonian Contr. Mar. Sc.* 40, 1–83. doi: 10.5479/si.1943667X.40.1

Amado-Filho, G. M., Maneveldt, G., Marins, B., Manso, R. C. C., Pacheco, M. R., and Guimarães, S. P. B. (2007). Structure of rhodolith beds from 4 to 55 meters deep along the southern coast of Espírito Santo State, Brazil. *Cienc. Mar.* 33, 399–410. doi: 10.7773/cm.v33i4.1148

Amado-Filho, G. M., Moura, R. L., Bastos, A. C., Salgado, L. T., Sumida, P. Y., Guth, A. Z., et al. (2012). Rhodolith beds are major $CaCO_3$ bio-factories in the tropical South West Atlantic. *PLoS ONE* 7:e35171. doi: 10.1371/journal.pone.0035171

Andersen, R. A., Potter, D., and Bailey, J. C. (2002). *Pinguiococcus pyrenoidosus* gen. et sp. nov. (Pinguiophyceae), a new marine coccoid alga. *Phycol. Res.* 50, 57–66. doi: 10.1111/j.1440-1835.2002.tb00136.x

Andersson, A. J., Bates, N. R., and Mackenzie, F. T. (2007). Dissolution of carbonate sediments under rising pCO_2 and ocean acidification: observations from Devil's Hole, Bermuda. *Aquat. Geochem.* 13, 237–264. doi: 10.1007/s10498-007-9018-8

Anthony, K. R. , Kline, D. I., Diaz-Pulido, G., Dove, S., and Hoegh-Guldberg, O. (2008). Ocean acidification causes bleaching and productivity loss in coral reef builders. *Proc. Natl. Acad. Sci. U.S.A.* 105, 17442–17446. doi: 10.1073/pnas.0804478105

Arakaki, N., M., Suzuki, M., and Fredericq, S. (2014). *Halarachnion* (Furcellariaceae, Rhodophyta), a newly reported genus for the Gulf of Mexico, with the description of *H. louisianensis*, sp. nov. *Phycol. Res.* 62, 306–315. doi: 10.1111/pre.12065

Bennke, C. M., Pollehne, F., Müller, A., Hansen, R., Kreikemeyer, B., and Labrenz, M. (2018). The distribution of phytoplankton in the Baltic Sea assessed by a prokaryotic 16S rRNA gene primer system. *J. Plankton Res.* 40, 244–254. doi: 10.1093/plankt/fby008

Borowitzka, M. A., and Larkum, A. W. D. (1987). Calcification in algae: mechanisms and the role of metabolism. *Crit. Rev. Plant Sci.* 6, 1–45. doi: 10.1080/07352688709382246

Bravo, I., and Figueroa, R. I. (2014). Towards and ecological understanding of dinoflagellate cyst functions. *Microorganisms* 2, 11–32. doi: 10.3390/microorganisms2010011

Burdett, J. L., Hatton, A. D., and Kamenos, N. A. (2015). Coralline algae as a globally significant pool of marine dimethylated sulfur. *Glob. Biogeochem. Cycl.* 29, 1845–1853. doi: 10.1002/2015GB005274

Cabioch, J. (1969). Les fonds de maërl de la baie de Morlaix et leur peuplement végétal. *Cah. Biol. Mar.* 10, 139–161.

Callahan, B. J., McMurdie, P. J., Rosen, M. J., Han, A. W., Johnson, A. J., and Holmes, S. P. (2016). DADA2: high-resolution sample inference from Illumina amplicon data. *Nat. Methods* 13, 581–583. doi: 10.1038/nmeth.3869

Camacho, O., Fernández-García, C., Vieira, C., Gurgel, C. F. D., Norris, J. N., Freshwater, D. W., et al. (2019). The genus *Lobophora* (Dictyotales,

Phaeophyceae) in the western Atlantic and eastern Pacific oceans with the description of eight new species. *J. Phycol.*

Camacho, O., Sauvage, T., and Fredericq, S. (2018). Taxonomic transfer of syringoderma to microzonia (Syringodermataceae, Syringodermatales), including the new record M. *floridana (E.C.Henry*) comb. nov. in the Gulf of Mexico. *Phycologia* 57, 413–421. doi: 10.2216/17-51.1

Caporaso, J. G., Lauber, C. L., Walters, W. A., Berg-Lyons, D., Lozupone, C. A., Turnbaugh, P. J., et al. (2011). Global patterns of 16S rRNA diversity at a depth of millions of sequences per sample. *PNAS* 108 (Suppl. 1), 4516–4522. doi: 10.1073/pnas.1000080107

Cavalcanti, G. S., Gregoracci, G. B., dos Santos, E. O., C. B., Silveira, C. B., Meirelles, P. M., Longo, L.,et al. (2014). Physiologic and metagenomic attributes of the rhodoliths forming the largest $CaCO_3$ bed in the South Atlantic Ocean. *ISME J.* 8, 52–62. doi: 10.1038/ismej.2013.133

Cole, J. R., Wang, Q., Fish, J. A., Chai, B., McGarrell, D. M., Sun, Y., et al. (2014). Ribosomal database project: data and tools for high throughput rRNA analysis. *Nucl. Acids Res.* 42, D633–D642. doi: 10.1093/nar/gkt1244

Dale, D. (1983). "Dinoflagellate resting cysts: "benthic plankton" in *Survival Strategies of the Algae*, ed G. A. Fryxell (New York, NY: Cambridge University Press), 69–136.

Decelle, J., Romac, S., Stern, R. F., Bendif, E. M., Zingone, A., Audic, S., et al. (2015). PhytoREF: a reference database of the plastidial 16S rRNA gene of photosynthetic eukaryotes with curated taxonomy. *Mol. Ecol. Res*. 5, 1435–1445. doi: 10.1111/1755-0998.12401

Doropoulos, C., Ward, S., Diaz-Pulido, G., Hoegh-Guldberg, O., and Mumby, P. J. (2012). Ocean acidification reduces coral recruitment by disrupting intimate larval-algal settlement interactions. *Ecol. Lett*. 15, 338–346. doi: 10.1111/j.1461-0248.2012.01743.x

Drew, K. M. (1949). Conchocelis-phase in the life-history of *Porphyra umbilicalis* (L.) Kütz. *Nature* 164, 748–749. doi: 10.1038/164748a0

Edgar, R. (2018). Taxonomy annotation and guide tree errors in 16S rRNA databases. *PeerJ* 6:e5030. doi: 10.7717/peerj.5030

Faust, M. A., and Gulledge, R. A. (2002). Identifying harmful marine dinoflagellates. *Contr. U.S. Natl. Herbarium* 42, 1–144.

Felder, D. L., and Camp, D. K. (Eds) (2009). *Gulf of Mexico Origin, Waters and Bioota, Biodiversity. Vol*. 1. College Station, TX: A & M University Press.

Felder, D. L., Thoma, B. P., Schmidt, W. E., Sauvage, T., Self-Krayesky, S., Chistoserdov, A., et al. (2014). Seaweeds and decapod crustaceans on Gulf deep banks after the Macondo Oil Spill. *Bioscience* 64, 808–819. doi: 10.1093/biosci/biu119

Foster, M. S. (2001). Rhodoliths: between rocks and soft places—minireview. *J. Phycol*. 37, 659–667. doi: 10.1046/j.1529-8817.2001.00195.x

Foster, M. S., McConnico, L. M., Lundsten, L., Wadsworth, T., Kimball, T., Brooks, L. B., et al. (2007). Diversity and natural history of a *Lithothamnion muelleri-Sargassum horridum* community in the Gulf of California. *Cienc. Mar*. 33, 367–384. doi: 10.7773/cm.v33i4.1174

Fredericq, S., Arakaki, N., Camacho, O., Gabriel, D., Krayesky, D., Self-Krayesky, S., et al. (2014). A dynamic approach to the study of rhodoliths: a case study for the Northwestern Gulf of Mexico. *Crypt. Algol*. 35, 77–98. doi: 10.7872/crya.v35.iss1.2014.77

Fredericq, S., Cho, T. O., Earle, S. A., Gurgel, C. F., Krayesky, D. M., Mateo Cid, L. E., et al. (2009). "Seaweeds of the Gulf of Mexico," in *Gulf of Mexico: Its Origins, Waters, and Biota. I. Biodiversity*, eds D. L. Felder and D. K. Camp (College Station: Texas A&M Univ. Press), 187–259.

Freiwald, A., and Henrich, R. (1994). Reefal coralline algal build-ups within the Arctic Circle: morphology and sedimentary dynamics under extreme environmental seasonality. *Sediment* 41, 963–984. doi: 10.1111/j.1365-3091.1994.tb01435.x

Fresnel, J., and Probert, I. (2005). The ultrastructure and life cycle of the coastal coccolithophorid *Ochrosphaera neapolitana* (Prymnesiophyceae). *Eur. J. Phycol*. 40, 105–122. doi: 10.1080/09670260400024659

Garbary, D., and Veltkamp, C. J. (1980). Observations on *Mesophyllum lichenoides* (Corallinaceae, Rhodophyta) with the scannning electron microscope. *Phycologia* 19, 49–53. doi: 10.2216/i0031-8884-19-1-49.1

Gardner, J. V., and Beaudoin, J. (2005). High-resolution multibeam bathymetry and acoustic backscatter of selected northwestern Gulf of Mexico outer shelf banks. *Gulf Mexico Sci*. 1, 5–29. doi: 10.18785/goms.2301.03

Gore, R. H. (1992). *The Gulf of Mexico*. Sarasota, FL: Pineapple Press. 384.

Guiry, M. D. (1990). "Sporangia and spores," in *Biology of the Red Algae,* eds K. M. Cole and R. G. Sheath (Cambridge: Cambridge Univ. Press), 347–376.

Hadfield, M. J., and Paul, V. J. (2001). "Natural chemical cues for settlement and metamorphosis of marine invertebrate larvae," in *Marine Chemical Ecology*, eds J. B. Clintock and B. J. Baker (Boca Raton: CRC Press), pp. 431–461

Halfar, J., Adey, W. H., Kronz, A., Hetzinger, S., Edinger, E., and Fitzhugh, W. (2013). Arctic sea ice decline archived by multicentury annual-resolution crustose coralline algal proxy. *Proc. Natl. Acad. Sci*. 110, 19737–19741. doi: 10.1073/pnas.1313775110

Harvey, A. S., Harvey, R. M., and Merton, E. (2017). The distribution, significance and vulnerability of Australian rhodolith beds: a review. *Mar. Freshw. Res*. 68, 411–428. doi: 10.1071/MF15434

Hawkes, M. W. (1990). "Reproductive strategies," in *Biology of the Red Algae,* eds K. M. Cole and R. G. Sheath (Cambridge: Cambridge Univ. Press), 455–476.

Heyward, A. J., and Negri, A. P. (1999). Natural inducers for coral larval metamorphosis. *Coral Reefs* 18, 273–279. doi: 10.1007/s003380050193

Hickerson, E. L., Schmahl, G. P., Robart, M., Precht, W. E., and Caldow, C. (2008). "The state of coral reef ecosystems of the Flower Garden Banks, Stetson Bank, and other banks in the northwestern Gulf of Mexico," in: *The State of Coral Reef Ecosystems of Flower Garden Banks*, 190–218. Available online at: https://nmsflowergarden.blob.core.windows.net/flowergarden-prod/media/archive/document_library/scidocs/stateofcoralfgbnms08.pdf

Hinojosa-Arango, G., Maggs, C. A., and Johnson, M. P. (2009). Like a rolling stone: the mobility of maerl (Corallinaceae) and the neutrality of the associated assemblages. *Ecology* 90, 517–528. doi: 10.1890/07-2110.1

Hinojosa-Arango, G., and Riosmena-Rodríguez, R. (2004). Influence of rhodolith-forming species and growth-form on associated fauna of rhodolith beds in the central-west Gulf of California, México. *Mar. Ecol*. 25, 109–127. doi: 10.1111/j.1439-0485.2004.00019.x

Hommersand, M. H., and Fredericq, S. (1990). "Sexual reproduction and cystocarp development," in *Biology of the Red Algae,* eds K. M. Cole and R. G. Sheath (Cambridge: Cambridge Univ. Press) 305–45.

Hommersand, M. H., Freshwater, D. W., Lopez Bautista, J., and Fredericq, S. (2006). Proposal of the Euptiloteae Hommersand and Fredericq, Trib. Nov., and transfer of some Southern Hemisphere Ptiloteae to the Callithamnieae (Rhodophyta). *J. Phycol*. 42, 203–225. doi: 10.1111/j.1529-8817.2006.00175.x

Joyce, A. E., and Williams, J. (1969). Rationale and pertinent data. *Mem. Hourglass Cruises* 1, 11–50.

Kamenos, N. A., Burdett, H. L., Aloisio, E., Findlay, H. S., Martin, S., Longbone, C., et al. (2013). Coralline algal structure is more sensitive to rate, rather than the magnitude, of ocean acidification. *Glob. Change Biol*. 19, 3621–3628. doi: 10.1111/gcb.12351

Kamenos, N. A., Strong, S. C., Shenoy, D. M., Wilson, S. T., Hatton, A. D., and Moore, P. G. (2008). Red coralline algae as a source of marine biogenic dimethylsulphonio-propionate. *Mar. Ecol. Progr. Ser*. 372, 61–66. doi: 10.3354/meps07687

Kazmierczak, J., and Iryu, Y. (1999). Cyanobacterial origin of microcrystalline cements from Pleistocene rhodoliths and coralline algal crusts of Okierabu-jima, Japan. *Acta Palaeont. Polon*. 44, 117–130.

Krayesky-Self, S., Richards, J. L., Rahmatian, M., and Fredericq, S. (2016). Aragonite infill in overgrown conceptacles of coralline *Lithothamnion spp*. (Hapalidiaceae, Hapalidiales, Rhodophyta): new insights in biomineralization and phylomineralogy. *J. Phycol*. 52, 161–173. doi: 10.1111/jpy.12392

Krayesky-Self, S., Schmidt, W. E., Phung, D., Henry, C., Sauvage, T., Camacho, O., et al. (2017). Eukaryotic life inhabits rhodolith-forming coralline algae (Hapalidiales, Rhodophyta), remarkable marine benthic microhabitats. *Sc. Rep*. 7:45850. doi: 10.1038/srep45850

Kunkel, D. (2005-2013). *Dennis Kunkel Microscopy, Inc.* Available online at: https://pixels.com/featured/1-coralline-red-alga-dennis-kunkel-microscopyscience-photo-library.html

Leliaert, F., Tronholm, A., Lemieux, C., Turmel, M., DePriest, M. S., Bhattacharya, D., et al. (2016). Chloroplast phylogenomic analyses reveal the deepest-branching lineage of the Chlorophyta, Palmophyllophyceae class. nov. *Sci. Rep*. 6:25367. doi: 10.1038/srep25367

Littler, M. M., Littler, D. S., Blair, S. M., and Norris, J. N. (1985). Deepest known plant life discovered on an unchartered seamount. *Science* 227, 57–59. doi: 10.1126/science.227.4682.57

McCoy, S. J., and Kamenos, N. A. (2015). Coralline algae (Rhodophyta) in a changing world: integrating ecological, physiological, and geochemical responses to global change. *J. Phycol.* 51, 6–24. doi: 10.1111/jpy.12262

Minnery, G. A. (1990). Crustose coralline algae from the Flower Garden Banks, Northwestern Gulf of Mexico - controls on distribution and growth-morphology. *J. Sedim. Petrol.* 60, 992–1007.

Minnery, G. A., Rezak, R., and Bright, T. J. (1985). "Chapter 18: Depth zonation and growth form of crustose coralline algae: Flower Garden Banks, northwestern Gulf of Mexico," in *Paleoalgology: Contemporary Research and Applications* eds. D. F. Toomey and M. H. Titecki (Berlin; Heidelberg: Springer-Verlag), 238–246.

Morse, J. W., Andersson, A. J., and Mackenzie, F. T. (2006). Initial responses of carbonate-rich shelf sediments to rising atmospheric pCO_2 and "ocean acidification": Role of high Mg-calcites. Geochim. *Cosmochim. Acta* 70, 5814–3580. doi: 10.1016/j.gca.2006.08.017

Nelson, W., D'Arcino, R., Neill, K., and Farr, T. (2014). Macroalgal diversity associated with rhodolith beds in northern New Zealand. *Cryptogam Algol* 35, 27–47. doi: 10.7872/crya.v35.iss1.2014.27

Olsen, K. N., Melton, R. D., Yaudes, K. M., Norwood, K. G., and Freshwater, D. W. (2004). Characteristics and utility of plastid-encoded 16S rRNA gene sequence data in phylogenetic studies of red algae. *J. North Carolina Acad. Sc.* 120, 143–151.

O'Reilly, S., Jurley, S., Coleman, N., Monteys, X., Szpak, M., O'Dwyer, T., et al. (2012). Chemical and physical features of living and non-living maerl rhodoliths. *Aquat. Biol.* 15, 215–224. doi: 10.3354/ab00431

Paris, C. B., Hénaff, M. L., Aman, Z. M., Subramaniam, A., Helgers, J., Wang, D. P., et al. (2012). Evolution of the Macondo well blowout: simulating the effects of the circulation and synthetic dispersants on the subsea oil transport. *Env. Sc. Technol.* 46, 13293–13302, doi: 10.1021/es303197h

Pereira-Filho, G. H., Amado-Filho, G. M., de Moura, R. L., Bastos, A. C., Guimarães, S. M. P. B., Salgado, L. T., et al. (2012). Extensive rhodolith beds cover the summits of southwesten Atlantic Ocean seamounts. *J. Coast. Res.* 28, 261–269. doi: 10.2112/11T-00007.1

Pereira-Filho, G. H., Amado-Filho, G. M., Guimarães, S. M., Moura, R. L., Sumida, P. Y., Abrantes, D. P., et al. (2011). Reef fish and benthic assemblages of the Trindade and Martin Vaz island group, southwestern Atlantic. *Braz. J. Oceanogr.* 59, 201–212. doi: 10.1590/S1679-87592011000300001

Pereira-Filho, G. H., Veras, P., de, C., Francini-Filho, R. B., Moura, R. L. de, Pinheiro, H. T., Gibran, F. Z., et al. M (2015). Effects of the sand tilefish Malacanthus plumieri on the structure and dynamics of a rhodolith bed in the Fernando de Noronha Archipelago, tropical West Atlantic. *MEPS* 541, 65–73. doi: 10.3354/meps11569

Pesacreta, T. C., and Hasenstein, K. H. (2018). Tissue accumulation patterns and concentrations of potassium, phosphorus, and carboxyfluorescein translocated from pine seed to the root. *Planta* 248, 393–407. doi: 10.1007/s00425-018-2897-7

Rabalais, N. (2014). Assessing early looks at biological responses to the Macondo Event. *BioScience* 64, 757–759. doi: 10.1093/biosci/biu132

Ragazzola, F., Foster, L. C., Form, A., Anderson, P. S. L., Hansteen, T. H., and Fietzke, J. (2012). Ocean acidification weakens the structural integrity of coralline algae. *Glob. Change Biol.* 18, 2804–2812. doi: 10.1111/j.1365-2486.2012.02756.x

Ragazzola, F., Foster, L. C., Jones, J. J., Scott, T. B., Fietzke, J., Kilburn, M. R., et al. (2016). Impact of high CO2 on the geochemistry of the coralline algae *Lithothamnion glaciale*. *Sci. Rep.* 6:20572. doi: 10.1038/srep20572

Rezak, R., Bright, T. J., and McGrail, D. W. (1985). *Reefs and Banks of the Northwestern Gulf of Mexico: Their Geological, Biological, and Physical Dynamics*. New York,NY: Wiley. 259.

Richards, J. L., and Fredericq, S. (2018). *Sporolithon sinusmexicanum* sp. nov. (Sporolithales, Rhodophyta): a new rhodolith-forming coralline species from deepwater rhodolith beds in the Gulf of Mexico. *Phytotaxa* 350, 135–146. doi: 10.11646/phytotaxa.350.2.2

Richards, J. L., Gabrielson, P. W., and Fredericq, S. (2014). New insights into the genus *Lithophyllum* (Lithophylloideae, Corallinaceae, Corallinales) from offshore the NW Gulf of Mexico. *Phytotaxa* 190, 162–175. doi: 10.11646/phytotaxa.190.1.11

Richards, J. L., Vieira-Pinto, T., Schmidt, W. E., Sauvage, T., Gabrielson, P. W., Oliveira, M. C., et al. (2016). Molecular and morphological diversity of *Lithothamnion* spp. rhodoliths (Hapalidiaceae, Hapalidiales) from deepwater rhodolith beds in the northwestern Gulf of Mexico. *Phytotaxa* 278, 81–114. doi: 10.11646/phytotaxa.278.2.1

Riosmena-Rodríguez, R., and Medina-Lopez, M. (2011). "The role of rhodolith beds in the recruitment of invertebrate species in the Southwestern Gulf of Mexico," in: *All Flesh is Green, Plant-Animal Interrelationships. Cellular Origin, Life in Extreme Habitats and Astrobiology Vol. 16*, eds J. Seckbach and Z. Dubinsky (New York, NY: Springer), 417–428.

Riosmena-Rodríguez, R., Nelson, W., and Aguirre, J. (Eds) (2017). *Rhodolith/Maërl Beds: A Global Perspective*. Switzerland: Springer International Publishing. 368.

Rodríguez-Prieto, C., Freshwater, D. W., and Hommersand, M. H. (2013). Vegetative and reproductive development of Mediterranean *Gulsonia nodulosa* (Ceramiales, Rhodophyta) and its genetic affinities. *Phycologia* 52, 357–367. doi: 10.2216/13-132.1

Roh, E., and Sim, J. (2012). "Biomineralization of carbonate minerals: implications for rhodolith formation," in *Proceeding 2nd International Conference on Environment and BioScience Vol 44* (Singapore), 48–53.

Sauvage, T., Plouviez, S., Schmidt, W. E., and Fredericq, S. (2018). TREE2FASTA: a flexible Perl script for batch extraction of FASTA sequences from exploratory phylogenetic trees. *BMC Res. Notes* 11:164. doi: 10.1186/s13104-018-3268-y

Sauvage, T., Schmidt, W. E., Suda, S., and Fredericq, S. (2016). A metabarcoding framework for facilitated survey of coral reef and rhodolith endolithic communities with *tufA*. *BMC Ecol.* 16:8. doi: 10.1186/s12898-016-0068-x

Scanlon, K. M., Ackerman, S. D., and Rozycki, J. E. (2003). *Texture, Carbonate Content, and Preliminary Maps of Surficial Sediments, Flower Garden Banks Area, Northwest Gulf of Mexico outer shelf*. U.S. Geol. Surv. Open File Report 03–002.

Schmidt, W. E., Lozada-Troche, C., Ballantine, D. L., Arakaki, N., Norris, J. N., Gabriel, D., et al. (2017). Taxonomic transfer of *Chrysymenia enteromorpha* and *C. wrightii* to *Botryocladia* (Rhodymeniaceae, Rhodymeniales, Rhodophyta). *Phytotaxa* 324, 122–138. doi: 10.11646/phytotaxa.324.2.2

Sherwood, A. R., and Presting, G. G. (2007). Universal primers amplify a 23S rDNA plastid marker in eukaryotic algae and cyanobacteria. *J. Phycol.* 43, 605–608. doi: 10.1111/j.1529-8817.2007.00341.x

Slowey, N., Holcombe, T., Betts, M., and Bryant, W. (2008). "Habitat islands along the shelf edge of the northwestern Gulf of Mexico," in *A Scientific Forum on the Gulf of Mexico: The Islands in the Stream Concept, Marine Sanctuaries Conservation Series*, eds K. B. Ritchie and B. Keller (Silver Spring: NOAA), 19–24.

Smith, J. E., Shaw, M., Edwards, R. A., Obura, D., Pantos, O., Sala, E., et al. (2006). Indirect effects of algae on coral: algae-mediated, microbe-induced coral mortality. *Ecol. Lett.* 9, 835–845. doi: 10.1111/j.1461-0248.2006.00937.x

Spalding, H. L., Amado-Filho, G. M., Bahia, R. G., Ballantine, D. L., Fredericq, S., Leichter, J. J., et al. (2019). "Macroalgae," In: *Mesophotic Coral Ecosystems*, eds Y. Loya, K. A. Puglise, and T. C. L. Bridge (New York, NY: Springer).

Stamatakis, A. (2014). RAxML version 8: a tool for phylogenetic analysis and post-analysis of large phylogenies. *Bioinformatics* 30, 1312–1313. doi: 10.1093/bioinformatics/btu033

Steidinger, K. A. (2010). Research on the life cycles of harmful algae: A commentary. *Deep Sea Res. II* 57, 162–165. doi: 10.1016/j.dsr2.2009.09.001

Steidinger, K. A., and Garcés, E. (2006). "Importance of life cycles in the ecology of harmful microalgae," in: *Ecology of Harmful Algae*, eds E. Granéli and, J. T. Turner (Berlin: Springer), 37–49.

Steneck, R. S. (1986). The ecology of coralline algal crusts: convergent patterns and adaptive strategies. *Ann. Rev. Ecol. Syst.* 17, 273–303. doi: 10.1146/annurev.es.17.110186.001421

Teigert, S. (2014). Hollow rhodoliths increase Svalbard's shelf biodiversity. *Sci. Rep.* 4:6972. doi: 10.1038/srep06972

Vecsei, A. (2004). A new estimate of global reefal carbonate production including the fore-reefs. *Global Planet. Change* 43, 1–18. doi: 10.1016/j.gloplacha.2003.12.002

Viola, R., Nyvall, P., and Pedersen, M. (2001). The unique features of starch metabolism in red algae. *Proc. Biol. Sc.* 268, 1417–1422. doi: 10.1098/rspb.2001.1644

Wang, S., Maltrud, M., Elliott, S., Cameron-Smith, O., and Jonko, A. (2018). Influence of dimethyl sulfide on the carbon cycle and biological production. *Biogeochem* 138, 49–68. doi: 10.1007/s10533-018-0430-5

Webster, N. S., Negri, A. P., Botté, E. S., Laffy, P. W., Flores, F., Nooonan, S., et al. (2016). (2016). Host-associated coral reef microbes respond to the cumulative pressures of ocean warming and ocean acidification. *Sci. Rep*. 6:19324. doi: 10.1038/srep19324

Webster, N. S., Uthicke, S., Botte, E. S., Flores, F., and Negri, A. P. (2013). Ocean acidification reduces induction of coral settlement by crustose coralline algae. *Glob. Change Biol*. 19, 303–315. doi: 10.1111/gcb.12008

Wegeberg, S., and Pueschel, C. M. (2002). Epithallial and initial cell fine structure in species of *Lithothamnion* and *Phymatolithon* (Corallinales, Rhodophyta). *Phycologia* 41, 228–244. doi: 10.2216/i0031-8884-41-3-228.1

Yang, E. C., Boo, S. M., Bhattacharya, D., Saunders, G. W., Knoll, A. H., Fredericq, S., et al. (2016). Divergence time estimates and evolution of major lineages in the florideophyte red algae. *Sci. Rep*. 6:21361. doi: 10.1038/srep21361

Yoon, T.-H., Kang, H.-E., Kang, C.-K., Lee, S. H., Ahn, D.-H., Park, H., et al. (2016). Development of a cost-effective metabarcoding strategy for analysis of the marine phytoplankton community. *Peer J*. 4:e2115. doi: 10.7717/peerj.2115

Conflict of Interest Statement: The authors declare that the research was conducted in the absence of any commercial or financial relationships that could be construed as a potential conflict of interest.

Copyright © 2019 Fredericq, Krayesky-Self, Sauvage, Richards, Kittle, Arakaki, Hickerson and Schmidt. This is an open-access article distributed under the terms of the Creative Commons Attribution License (CC BY). The use, distribution or reproduction in other forums is permitted, provided the original author(s) and the copyright owner(s) are credited and that the original publication in this journal is cited, in accordance with accepted academic practice. No use, distribution or reproduction is permitted which does not comply with these terms.

frontiers in Marine Science

REVIEW
published: 29 November 2019
doi: 10.3389/fmars.2019.00723

Coralline Algae in a Changing Mediterranean Sea: How Can We Predict Their Future, if We Do Not Know Their Present?

Fabio Rindi[1]*, *Juan C. Braga*[2], *Sophie Martin*[3], *Viviana Peña*[4], *Line Le Gall*[5], *Annalisa Caragnano*[1] and *Julio Aguirre*[2]

[1] Dipartimento di Scienze della Vita e dell'Ambiente, Università Politecnica delle Marche, Ancona, Italy, [2] Departamento de Estratigrafía y Paleontología, Universidad de Granada, Granada, Spain, [3] Équipe Écogéochimie et Fonctionnement des Écosystèmes Benthiques, Laboratoire Adaptation et Diversité en Milieu Marin, Station Biologique de Roscoff, Roscoff, France, [4] Grupo BioCost, Departamento de Bioloxía, Universidade da Coruña, A Coruña, Spain, [5] Institut Systématique Evolution Biodiversité (ISYEB), Muséum National d'Histoire Naturelle, CNRS, Sorbonne Université, Paris, France

OPEN ACCESS

Edited by:
Susana Carvalho,
King Abdullah University of Science and Technology, Saudi Arabia

Reviewed by:
Steeve Comeau,
UMR7093 Laboratoire d'océanographie de Villefranche (LOV), France
Anne Chenuil,
Centre National de la Recherche Scientifique (CNRS), France

***Correspondence:**
Fabio Rindi
f.rindi@univpm.it

Specialty section:
This article was submitted to Marine Ecosystem Ecology, a section of the journal Frontiers in Marine Science

Received: 30 October 2018
Accepted: 08 November 2019
Published: 29 November 2019

Citation:
Rindi F, Braga JC, Martin S, Peña V, Le Gall L, Caragnano A and Aguirre J (2019) Coralline Algae in a Changing Mediterranean Sea: How Can We Predict Their Future, if We Do Not Know Their Present? Front. Mar. Sci. 6:723. doi: 10.3389/fmars.2019.00723

In this review we assess the state of knowledge for the coralline algae of the Mediterranean Sea, a group of calcareous seaweeds imperfectly known and considered highly vulnerable to long-term climate change. Corallines have occurred in the Mediterranean area for ∼140 My and are well-represented in the subsequent fossil record; for some species currently common the fossil documentation dates back to the Oligocene, with a major role in the sedimentary record of some areas. Some Mediterranean corallines are key ecosystem engineers that produce or consolidate biogenic habitats (e.g., coralligenous concretions, *Lithophyllum byssoides* rims, rims of articulated corallines, maerl/rhodolith beds). Although bioconstructions built by corallines exist virtually in every sea, in the Mediterranean they reach a particularly high spatial and bathymetric extent (coralligenous concretions alone are estimated to exceed 2,700 km^2 in surface). Overall, composition, dynamics and responses to human disturbances of coralline-dominated communities have been well-studied; except for a few species, however, the biology of Mediterranean corallines is poorly known. In terms of diversity, 60 species of corallines are currently reported from the Mediterranean. This number, however, is based on morphological assessments and recent studies incorporating molecular data suggest that the correct estimate is probably much higher. The responses of Mediterranean corallines to climate change have been the subject of several recent studies that documented their tolerance/sensitivity to elevated temperatures and pCO_2. These investigations have focused on a few species and should be extended to a wider taxonomic set. Phylogeography, genomics, transcriptomics, and associated microbiomes are fields in which the information for Mediterranean corallines is very limited. We suggest that future work on Mediterranean corallines should be based on a multidisciplinary perspective combining different approaches, and that it should consist of large-scale efforts by scientists based both in western and eastern Mediterranean areas.

Keywords: climate change, Corallinales, ecosystem engineers, Hapalidiales, marine bioconstructions, paleontological records, Sporolithales, taxonomy

INTRODUCTION

The Mediterranean is the largest (2,969,000 km^2) and deepest (average 1,460 m, maximum 5,267 m) enclosed sea on Earth (Coll et al., 2010). Although it represents only 0.82% in surface area and 0.32% in volume of the world oceans (Bianchi and Morri, 2000), it is a well-known hotspot of marine biodiversity, with not <20,000 species recorded (Pascual et al., 2017). Such diversity originates from its complex paleoceanographic history and changes in its paleogeographic configurations (particularly through the Cenozoic) and from the current diversity of oceanographic conditions among different regions of the basin (Bianchi and Morri, 2000). The events that characterized the geological history of the Mediterranean in the last 15 My produced a high number of endemic species (which led Bianchi and Morri, 2000 to define the Mediterranean "a factory designed to produce endemics").

The Mediterranean, however, is also highly impacted and threatened. Climatic models predict that the Mediterranean basin will be one of the regions most affected by the ongoing warming trend and by an increase in extreme events (Lejeusne et al., 2010; Galli et al., 2017). These predictions are supported by climatological data: the average maximum summer seawater temperature has risen by 1°C in 20 years in some areas of the western Mediterranean (Marbà and Duarte, 2010) and a 0.4°C warming per decade since 1986 was reported for the entire Mediterranean Sea by Sakalli (2017). Seasonal and depth-related warming trends were documented by Nykjaer (2009) and Coma et al. (2009), respectively. Studies that measured and modeled pH changes since preindustrial times in the Mediterranean (Hassoun et al., 2015; Goyet et al., 2016) provided evidence of acidification related to excessive increase of atmospheric CO_2. The mean surface pH has decreased by ∼0.002 units per year from 1994 to 2006 in the northwestern Mediterranean (Howes et al., 2015; Kapsenberg et al., 2017) and by 0.004 units at the Strait of Gibraltar (Flecha et al., 2015). These trends are projected to continue throughout the twenty-first century.

The impact of climate change on Mediterranean marine biota is expected to be strong, because it will interact with anthropogenic disturbances operating at local scales (e.g., chemical pollution, eutrophication, increase in sediment load, habitat degradation caused by trawling). Mediterranean coastal ecosystems have been exploited by humans for millennia, and have been therefore altered in many ways. Nowadays Mediterranean shores are heavily urbanized and support a high population density; impacts of human activities are proportionally stronger in the Mediterranean than in any other sea of the world (Coll et al., 2010). Habitat loss, degradation and pollution, overexploitation of marine resources and invasions of alien species are the main drivers of change, which in future decades will overlap and interact with climate-related changes.

Coralline algae have existed in the Mediterranean (or in the area corresponding to the present Mediterranean) for ∼140 My (Chatalov et al., 2015) and are ubiquitous on modern Mediterranean rocky shores. They are key components in some of the most common Mediterranean benthic communities, such as coralligenous concretions (**Figure 1A**), *Lithophyllum byssoides* rims (**Figure 1B**), maerl/rhodolith beds (**Figure 1C**), barrens formed at sites subjected to heavy grazing (**Figure 1D**), rims of *Ellisolandia elongata* and other articulated corallines (**Figure 1E**), and the epiphytic assemblage of the seagrass *Posidonia oceanica* (**Figure 1F**). In these communities coralline species often play a key role as ecosystem engineers: the accumulation of their calcareous thalli produces bioconstructions that modify the tridimensional structure of the substratum and profoundly influence ecosystem functioning (Bressan et al., 2009; Ingrosso et al., 2018). Mediterranean bioconstructions built by corallines are known as major repositories of biodiversity (e.g., coralligenous communities host not <1,700 animal and algal species; Ballesteros, 2006) and carbonate-producing ecosystems (Cebrián et al., 2000; El Haikali et al., 2004; Canals and Ballesteros, 2007; Bracchi and Basso, 2012). Furthermore, although bioconstructions formed by corallines exist in every sea, in the Mediterranean they reach a particularly high spatial and bathymetric extent (coralligenous concretions alone are estimated to exceed 2,700 km^2 in surface; Martin et al., 2014). There is evidence that some of these bioconstructions are undergoing substantial degradation and that the corallines that produce them are suffering a loss of vitality (Laborel et al., 1993; Blanfuné, 2016); in general, observations of bleaching and necroses in Mediterranean corallines have become increasingly common in recent years (Hereu and Kersting, 2016; Basso et al., 2018; Quéré et al., 2019; **Figure 2**).

The need of a deep understanding of the biology of Mediterranean corallines is therefore more important than ever. Mediterranean corallines have a long history of study and in the last few decades have attracted great interest from marine biologists. Despite of this, many aspects of their biology are still poorly or insufficiently known. It is also noteworthy that detailed information is available for relatively few species (mainly those shown in **Figure 3**). It is thus timely to summarize the state of knowledge for these seaweeds and highlight gaps on which future research should concentrate, which we aim to do in this review. This review focuses strictly on the biology of coralline species and does not deal with Mediterranean communities/habitats built or dominated by corallines, for which detailed summaries are already available (coralligenous communities: Ballesteros, 2006; rhodolith beds: Basso et al., 2017; Bracchi et al., 2019a; *Lithophyllum byssoides* rims: Laborel, 1987; Bressan et al., 2009; Verlaque, 2010; *Ellisolandia elongata* rims: Laborel, 1987; Ballesteros, 1988; Bressan et al., 2009; epiphytic community of *Posidonia oceanica*: Piazzi et al., 2015).

HISTORICAL SUMMARY

Being unusual among algae, corallines have long intrigued scientists. If detailed observations were provided in the eighteenth century, corallines were often studied together with other calcified organisms currently classified among animals. Calcareous algae in the Mediterranean were first described more than two centuries ago, and some species of the genus *Corallina* with distribution encompassing the

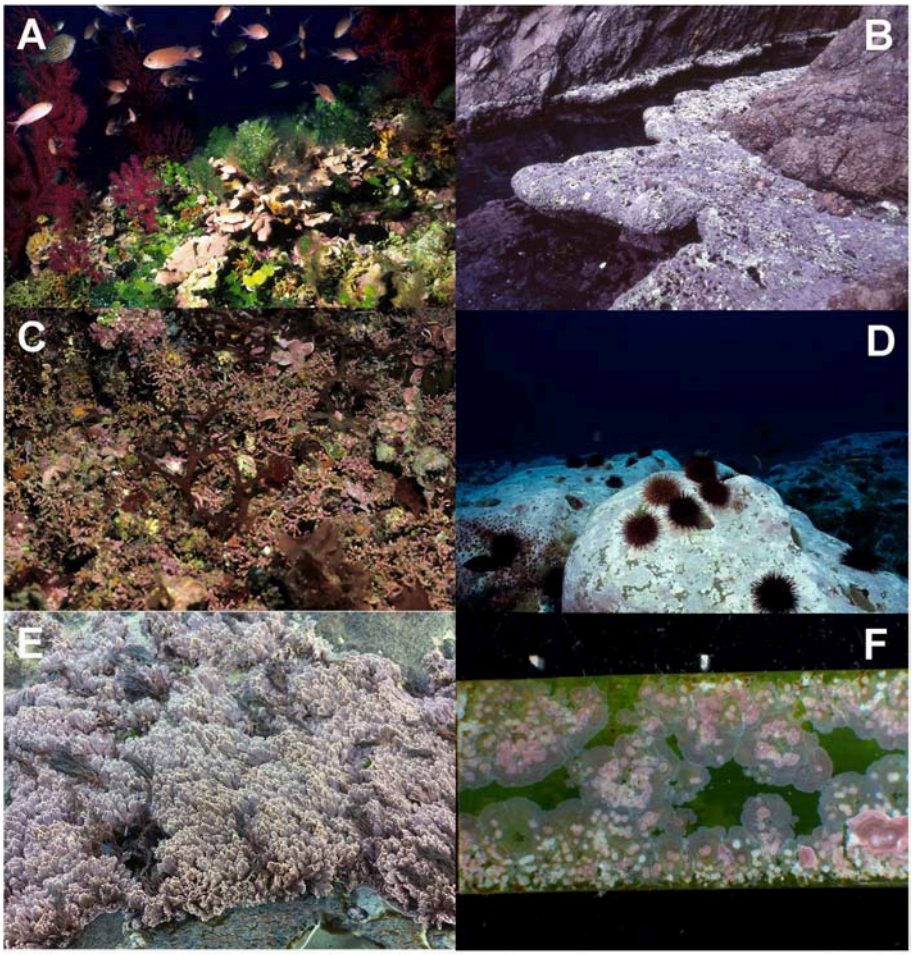

FIGURE 1 | Examples of coralline-dominated habitats in the Mediterranean. **(A)** A coralligenous community (Islas Columbretes, Spain); copyright: Enric Ballesteros (kike@ceab.csic.es). **(B)** A *Lithophyllum byssoides* rim (Cala Litizia, Scandola Nature Reserve, Corsica, France); copyright: Marc Verlaque (marc.verlaque@mio.osupytheas.fr). **(C)** Detail of a maerl bed (Islas Columbretes, Spain); copyright: Enric Ballesteros (kike@ceab.csic.es). **(D)** A barren ground dominated by encrusting corallines on a bottom heavily grazed by sea urchins (Alboran Island, Spain); copyright: Enric Ballesteros (kike@ceab.csic.es). **(E)** An intertidal rim of articulated corallines (Passetto di Ancona, Italy). **(F)** Detail of a leaf of the seagrass *Posidonia oceanica* covered by epiphytic encrusting corallines (Ischia Island, Italy); copyright: Maria Cristina Gambi (gambimc@gmail.com). All pictures were provided by the copyright owners and reproduced with their permission.

FIGURE 2 | Examples of necroses in Mediterranean corallines. **(A)** *Lithophyllum cabiochae*, close-up view of a specimen largely bleached. **(B)** Encrusting corallines showing incipient bleaching at the edges (Piscinetta del Passetto, Ancona, Italy).

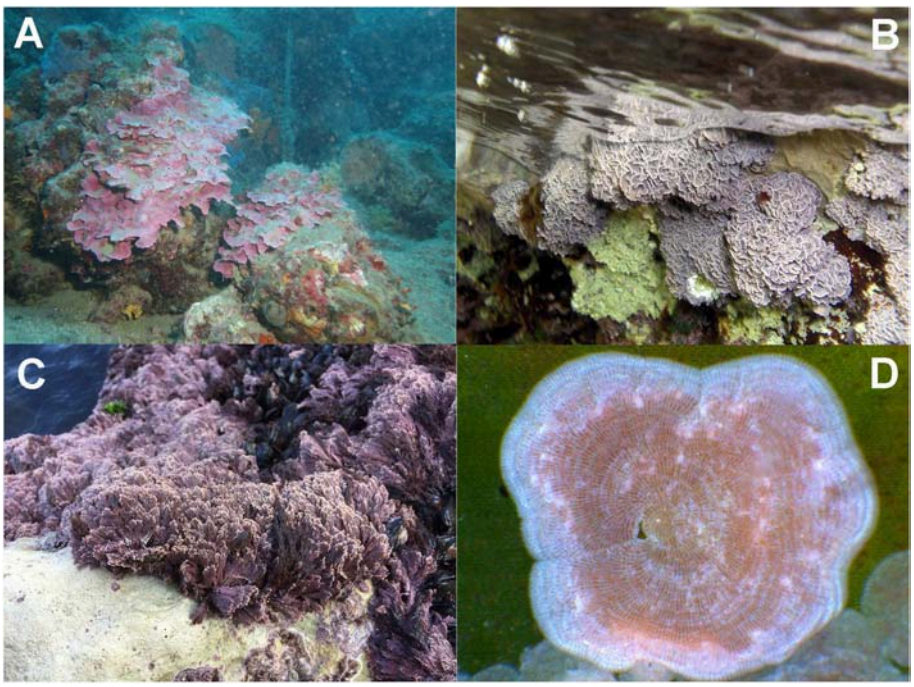

FIGURE 3 | Examples of Mediterranean corallines that have been subject of many studies. **(A)** *Lithophyllum stictiforme*, bioconstructor species of coralligenous concretions (reported in many studies as *Lithophyllum cabiochae*); copyright: Carlo Cerrano (c.cerrano@univpm.it). **(B)** *Lithophyllum byssoides* forms biogenic rims ("trottoirs") in the intertidal zone; copyright: Sara Kaleb (sara.kaleb@gmail.com). **(C)** Articulated corallines (usually identified as *Ellisolandia elongata*) are common in the Mediterranean low intertidal and shallow subtidal zones. **(D)** *Pneophyllum fragile*, a common epiphyte on the leaves of the seagrass *Posidonia oceanica*; copyright: Maria Cristina Gambi (gambimc@gmail.com). All pictures were provided by the copyright owners and reproduced with their permission.

Mediterranean were among the first seaweeds described with Latin binomials in the Linnaean system (Linnaeus, 1758). Many species that are common in the Mediterranean were described in the late eighteenth and early nineteenth centuries (Ellis, 1768; Ellis and Solander, 1786; Esper, 1796; de Lamarck, 1801; Bory de Saint-Vincent, 1832). The subsequent work carried out until the 70s−80s of the twentieth century consisted mainly of paleontological studies, floristic inventories, traditional taxonomy based on morphology, and descriptive distributional and ecological studies (Bressan, 1974; Bressan and Babbini, 1995, and references therein). Most ecological studies had in fact a general perspective and concerned coralline-dominated habitats (mainly coralligenous concretions and *Lithophyllum byssoides* rims), rather than coralline biology itself.

A critical review of the literature concerning Mediterranean corallines (results summarized in **Figure 4**; the list of references used is reported in the **File SM1**) shows that in the last decades paleontological record, taxonomy and phylogenetic diversity, responses to climate change and physiology are the main aspects on which research has focused. So, in this review we discuss primarily the state of knowledge in these fields. Remarkably, phylogeography, genomics, transcriptomics, study of associated microbial communities and mineralization are fields in which the information for Mediterranean corallines is still very limited.

GEOLOGICAL HISTORY OF THE MEDITERRANEAN AND PALEONTOLOGICAL RECORD OF MEDITERRANEAN CORALLINES

The present-day configuration of the Mediterranean Sea is the result of a complex geological history. The evolutionary history of Mediterranean corallines has taken place in a changing environment with long-term but major changes in paleogeography, climate and oceanography since the early Lower Cretaceous, for about 140 My. The paleogeographic evolution of the Mediterranean is part of the progressive closing and partitioning of the Tethys, the ancient circumtropical ocean, due to the convergence of Southern Hemisphere crustal plates with the northern ones (Scotese, 2014a; **Figure 5**). The global trends of ocean temperatures during such a long period show an initial rise up to the mid-Cretaceous climate maximum (some 95 Mya) and, since then, temperature has been declining with frequent and sometimes large reversals (Zachos et al., 2001; Friedrich et al., 2012; O'Brien et al., 2017).

A critical review of hundreds of publications on fossil corallines shows that 359 species have been reported in Cretaceous to Pleistocene deposits in different regions of the Mediterranean (**File SM2,** list of references in **File SM6**). These can be attributed to the orders Sporolithales (80 species, **File SM3**), Hapalidiales (159 species, **File SM4**), and Corallinales

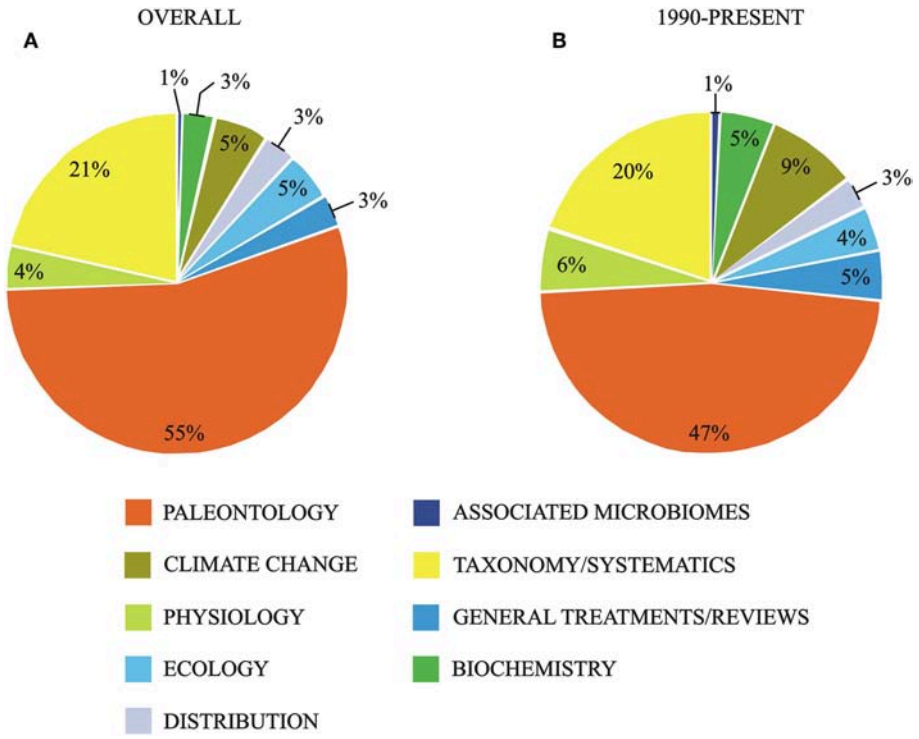

FIGURE 4 | Summary of the literature for Mediterranean corallines based on a critical bibliographic review and subdivided in research fields. **(A)** Overall information. **(B)** Information for the period 1990-present. The list of references used for the preparation of the figure (and details about the criteria used for the compilation of the list) is presented in the **File SM1**.

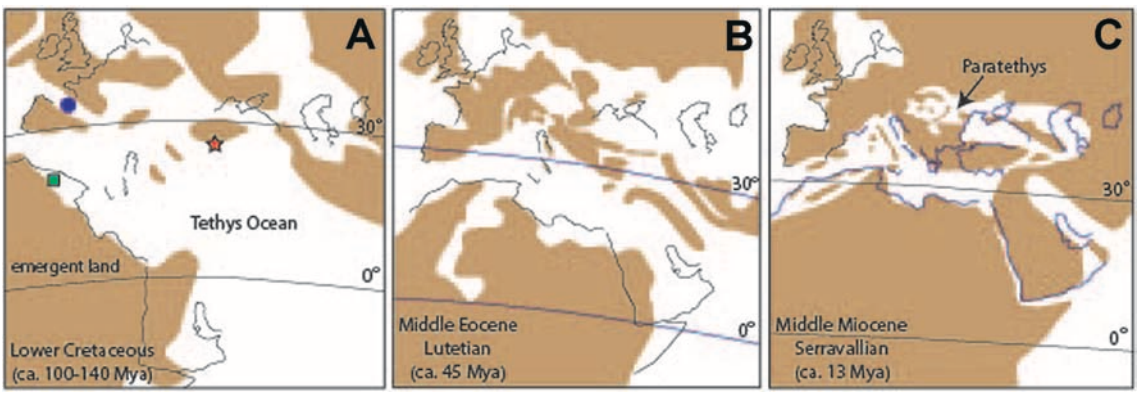

FIGURE 5 | Paleogeographical sketches of the Mediterranean region at three time intervals in the last 140 My. Brown areas: emergent land; white areas: ocean/seas. Black lines: present-day shorelines for geographic reference. Position of Equator (0°) and parallel 30° N at each time. **(A,B)** The northward movement of Southern Hemisphere crustal plates converging with the Eurasian plates, progressively narrowed and divided the circumtropical Tethys Ocean (modified from Barrier et al., 2018). **(C)** By the Middle Miocene, the Mediterranean Sea became isolated from the Indo-Pacific and remained connected to the open ocean only at its western end (modified from Rögl, 1998). Location of the first records of Spolithales (red star), Hapalidiales (green square), and Corallinales (blue circle).

(120 species, **File SM5**). The oldest known fossil corallines attributable to extant orders occur in the Lower Cretaceous (Valanginian, 137 Mya) in northern Greece. They are scarce specimens of *Sporolithon* that lived on a carbonate platform surrounding an island at the northern margin of the Tethys (Chatalov et al., 2015; **Figure 5A**). For millions of years, the only recorded corallines are rare encrusting *Sporolithon* associated to coral reefs (Conrad and Masse, 1989; Arias et al., 1995; Tomás et al., 2007; Bucur, 2008; Woelkerling et al., 2014). In the late Barremian-Aptian (126–113 Mya), the Sporolithales became more frequent and diverse with several extinct genera (*Agardhiellopsis, Kymalithon, Paraphyllum*) (Moussavian, 1993).

In this time interval, there are also poorly contrasted reports of Hapalidiales (*Lithothamnion*) at the southern margin of the Tethys (Algeria, Lemoine, 1939) and Corallinales (*Lithoporella* and Corallinoideae) in the marine passage that corresponds to the present-day Pyrenees (Poignant, 1968; Lemoine, 1970). In the Albian (113–100 Mya), the morpho-species diversity of Sporolithales increases and locally they are common components of carbonate rocks (Lemoine, 1970; Moussavian, 1993; Bucur, 1994; Rosales, 1995; Lopez-Horgue et al., 2009). Reports of Hapalidiales (as *Lithothamnion* and *Melobesia*) are scarce and inconclusive (Lemoine, 1970; Poignant, 1981). Few scattered records might correspond to geniculate Corallinoideae (Maslov, 1956; Lemoine, 1970). For most of the Upper Cretaceous (Cenomanian-Campanian, 100–72 Mya) coralline algae continue to be generally scarce components of carbonate platforms. The relatively few records scattered all over the region indicate an increase in Sporolithales (mainly of *Sporolithon*) with the appearance of a new genus in this order, *Hemiphyllum*, now extinct. Reports of Hapalidiales, both *Lithothamnion* and *Mesophyllum* (Lemoine, 1970; Poignant, 1981), are poorly illustrated and remain doubtful. Within Corallinales, the first occurrence in the region of reliable representatives of Neogoniolithoideae sensu Rösler et al. (2016) is recorded (*Spongites* as *Lithophyllum*, Bucur and Baltres, 2002). In the Maastrichtian (72–66 Mya), the last stage of the Cretaceous, the number of Hapalidiales increases (Poignant, 1978, 1981). The oldest-known Hydrolithoideae (*Karpathia*, Bassi et al., 2005 and references therein) also appear in this time interval, together with a few more Corallinales (Rösler et al., 2017).

The Tethys narrowed during the Cretaceous in its western end with the progressive convergence of African and European plates, but in the Paleocene (66–56 Mya) an uninterrupted marine connection continued to exist at low latitudes around the globe. The partial emergence of the Pyrenees and large areas of western Europe reduced the passages from the Tethys to the Atlantic. Two-thirds of the coralline species disappeared during the Cretaceous mass extinction (Aguirre et al., 2000a,b), but the number of recognized morpho-species recovered and substantially increased during the Paleocene (Aguirre et al., 2000a,b, 2007). This recovery was mainly due to the increase in Hapalidiales (*Lithothamnion, Mesophyllum*, and *Phymatolithon*) and Corallinales, whilst the Sporolithales started a decrease that continued throughout the Cenozoic with minor reversals. All genera of Sporolithales other than *Sporolithon* recorded in Cretaceous rocks disappeared before the Paleocene. Corallines from this epoch occur in coral-bearing carbonates, either *in situ* in shallow-water paleoenvironments (e.g., Moussavian, 1993; Aguirre et al., 2007) or re-deposited in deeper settings (Stockar, 2000).

As a marked reversal of the general global cooling trend initiated in the mid-Cretaceous, during the Early and Middle Eocene epochs (56–38 Mya) global temperatures were higher than in older and younger Cenozoic times (Zachos et al., 2001, 2008; Anagnostou et al., 2016). During this warm interval, large coral reefs disappeared from low latitudes (Scheibner and Speijer, 2008; Kiessling, 2010; Perrin and Kiessling, 2010). The global sea level was several tens of meters higher than in the modern ocean (Miller et al., 2011), favoring the development of extensive carbonate platforms dominated by larger benthic foraminifers and algae (Nebelsick et al., 2005; Scheibner and Speijer, 2008; Norris et al., 2013). The emergence of the antecedent reliefs of the Alpine mountain belts (Alps, Carpatian mountains) as many small islands caused a complex paleogeography of the northern margin of the Tethys, which extended north of the modern Black and Caspian seas (Scotese, 2014b; **Figure 5B**). Coralline algae occurred in rhodolith beds and in bioclastic facies in platform deposits or in deep-water, re-worked sediments (e.g., Aroldi and Bucur, 2002; Nebelsick et al., 2005). Numbers of reported species and relative proportions of coralline orders did not change throughout this interval (Aguirre et al., 2000a).

In the Late Eocene (38–34 Mya) global temperatures and sea level progressively decreased (Zachos et al., 2001; Miller et al., 2011). In addition to rhodolith beds (and maerl) and bioclastic facies, coralline algae of this age occurred associated with corals in shallow water carbonates (Bassi, 1998; Rasser, 2000; Nebelsick et al., 2005; Barattolo et al., 2007) at both margins of the Tethys in the Mediterranean region. The number of reported morpho-species of Hapalidiales and Corallinales slightly increased, whereas Sporolithales resumed their diversity decline after a long interval of stability.

The most dramatic global cooling of the Cenozoic era took place at the Eocene–Oligocene transition (at 34 Mya). Development of Antartic ice sheets and onset of glaciation marked the beginning of the modern icehouse world (Zachos et al., 2001). A significant sea-level drop was coeval of these processes. The continued rising of Alpine belts led to the separation of the Paratethys, a large marine body extending to the north of the Alps, from the Rhône Basin over eastern Europe to the east of the modern Caspian Sea (Popov et al., 2004). Since the Oligocene (34–23 Mya) the Paratethys was an individual paleobiogeographic province with connections to the Tethys/Mediterranean Sea during most of its paleogeographic evolution (Harzhauser and Piller, 2007). The marine connections remained continuous from the present-day Indo-Pacific to the North Atlantic oceans (Rögl, 1998).

In the majority of localities, Oligocene corallines occur in coral reef deposits or in laterally associated sediments as rhodoliths, coralline debris, or as crusts directly growing on the soft sea floor (Fravega et al., 1987; Brandano, 2017). Occasionally, rhodoliths and algal debris have also contributed as important carbonate producers in late Oligocene homoclinal carbonate ramps in the western Tethys (Bover-Arnal et al., 2017). They also occur in deep-water, re-deposited carbonates (Rasser and Nebelsick, 2003). Most reports of Oligocene coralline algae derive from the northern margin of the Western Tethys, especially from the Piedmont and Ligurian basins, and the circumalpine area (north-eastern Italy, northern Slovenia, Austria and southern Bavaria) (Nebelsick et al., 2005). Hundreds of species of Oligocene corallines were described in these areas in the last century (Airoldi, 1932; Conti, 1950; Mastrorilli, 1968; Fravega et al., 1987; further references in Braga et al., 2010). Long species lists were also reported from the Balkan and Carpatian mountains (Lemoine, 1977; Bucur et al., 1989). Oligocene corallines were also described from Algeria at the southern margin of the

Western Tethys (Lemoine, 1939) and from ancient islands in the Tethys, such as Maltese Islands (Brandano, 2017), Salento Peninsula, southern Italy (Bosellini and Russo, 1992), and the Malaguide Complex in southern Spain (Braga and Bassi, 2011). *Titanoderma pustulatum* occurred in the early Oligocene from NW Iran (Basso et al., 2019), an area connecting the Indian Ocean and the Tethys before its final closure in the middle Miocene. This new finding places the oldest record of the *Titanoderma/Lithophyllum pustulatum* group in this area rather than in the late Oligocene from the Central Pacific as previously recorded (Bassi et al., 2009). Reported diversity of morpho-species of Corallinales and Hapalidiales continued the rise initiated in the late Eocene. By contrast, the number of species of *Sporolithon* decreased (Aguirre et al., 2000a).

Continued convergence of African and European plates and emergence of Alpine mountain belts led to significant palaeoceanographic changes during the Miocene (23–5.3 Mya). The long-lasting circum-tropical ocean was partitioned by land masses, changing the global geography and major current patterns. The connections of the Mediterranean to the Indian Ocean were interrupted in the middle Miocene (at about 14 Mya, Rögl, 1998) by the emergence of the Middle East reliefs. The Paratethys was strongly isolated during the late Miocene and its European sub-basins became continental (Rögl, 1998; Popov et al., 2004; Harzhauser and Piller, 2007). At the western end of the Mediterranean, uplift of the Betic-Rifean reliefs gradually closed the seaways to the Atlantic Ocean. The connections were temporarily interrupted during the Messinian Salinity Crisis at about 5.5 Mya (Hsü et al., 1977). The opening of the Gibraltar Straits established the present-day configuration of Mediterranean Sea as a partially isolated, evaporitic water body, which needs inflow from the Atlantic Ocean to maintain its level (Mariotti et al., 2002). A global warm phase, the Mid-Miocene Climatic Optimum (about 15 Mya), took place after a brief glaciation interval in the earliest Miocene. Since that phase, the Earth's climate has been cooling with reversals (Zachos et al., 2001). The Northern Hemisphere ice-sheets started growing in the late Miocene. During the Miocene, global sea-level fluctuations of 50–60 m on the million-year scale and superimposed oscillations controlled by orbital obliquity (41,000 year cycles) did not show a marked ascending or descending trend (Miller et al., 2011).

Rhodolith beds were widespread in Miocene platform carbonate and siliciclastic deposits in the Mediterranean and Paratethys (Halfar and Mutti, 2005; Braga, 2017). They were most common in carbonate ramps together with small coral buildups, and locally they occurred in reef-rimmed shelf deposits (Hrabovský et al., 2016; Braga, 2017). Coralline biostromes (*coralligène de plateau*) were reported in the Maltese Islands (Bosence and Pedley, 1982). Rhodoliths and coralline debris also occur as deep re-deposited sediments (Bassi et al., 2017).

The number of fossil non-geniculate coralline species reported in the literature reached its maximum in the early Miocene and then decreased with small reversals (Aguirre et al., 2000a). Some available modern accounts based on comparable diagnostic characters seem to confirm a morphospecies richness reduction throughout the Miocene. While Checconi (2006) describes 35 species in the early Miocene (Burdigalian) of the Southern Apennines (Italy), only 21 morphospecies were found in the late Miocene (Messinian) reefs in Salento and Sorbas Basin together (Braga et al., 2009). The reduction is even more marked within some genera, such as *Spongites*, encompassing 13 species during the Burdigalian (Checconi, 2006) and only 5 during the Messinian in southern Italy (Braga et al., 2009). *Lithophyllum* (and *Lithophyllum* gr. *pustulatum* –*Titanoderma*, Bassi et al., 2009) is first recorded in the Mediterranean region in the early Miocene from SE France (Burdigalian; Coletti et al., 2018a). In the Miocene, for the first time in the evolutionary history of corallines, Mediterranean assemblages differ from their pantropical counterparts at the genus level (Braga et al., 2010). *Spongites*, *Neogoniolithon*, and *Lithophyllum* are the main components in shallow-water Miocene Mediterranean paleoenvironments, including coral reefs. *Porolithon*, *Hydrolithon* gr. *boergesenii,* and *Aethesolithon* J.H. Johnson, which occur with those genera in coral reefs in low latitudes, are absent in the Mediterranean basins. This biogeographical differentiation was probably due to the isolation of the Mediterranean from the Indian Ocean, complete by the middle Miocene (Rögl, 1998; **Figure 5C**). Although coral reefs persisted in the Mediterranean until the latest Miocene, after its eastern closure the coral diversity decreased (Bosellini and Perrin, 2008). The strong decline of species number of *Sporolithon*, a genus of tropical affinity, after the middle Miocene, might also be due to the isolation from the Indian Ocean (Braga and Bassi, 2007).

The general configuration of the modern Mediterranean was established in the Pliocene (5.3–2.6 Mya). Paleogeography within the basin, however, changed substantially due to the uplift of modern reliefs, with a progressive reduction of the areas invaded by the sea. Global temperatures continued the decrease initiated in the middle Miocene (Zachos et al., 2001) and sea level followed a falling trend modulated by oscillations with amplitude of several tens of meters (Miller et al., 2011).

Rhodolith beds are scarcer than in Miocene rocks but have been reported in southern Spain (Aguirre, 1998; Aguirre and Jiménez, 1998; Aguirre et al., 2012) and northern Italy (Vannucci et al., 1996; Checconi et al., 2007). Corallines also occur in vermetid reefs in early Pliocene deposits of northeastern Spain (Aguirre et al., 2014). Here, *Spongites fruticulosus* is the main coralline, differently from modern Mediterranean vermetid reefs, in which *Neogoniolithon brassica-florida* is the dominant species (Boudouresque, 2004; Langar et al., 2011). The Pliocene coralline morphospecies in the few published accounts are similar to those of the present-day Mediterranean. More than 90% of the 19–20 species identified in early Pliocene in southern Spain (Aguirre et al., 2012) and 88% of the 8 reported in the late Pliocene of Tuscany (Italy) (Checconi et al., 2007) are living in the Mediterranean and Lusitanian provinces.

Except in areas with intense recent uplift such as Sicily, the Quaternary (last 2.6 My) shorelines of the Mediterranean at high sea levels were close to the present-day situation. The few Pleistocene and Holocene inventories suggest that Mediterranean Quaternary corallines were not different from the modern ones. They occurred in build-ups (*coralligène de plateau*) (Nalin et al.,

2006; Coletti et al., 2018b; Bracchi et al., 2019b), in rhodolith beds, and in rhodoliths and debris dispersed in siliciclastic deposits (Di Geronimo, 1998; Coletti et al., 2018b). The dramatic global climatic and sea level changes that took place repeatedly during the Pleistocene (e.g., Rohling et al., 2014) did not substantially affect coralline assemblages in the Mediterranean, although a few species might have migrated into the Mediterranean from the North Atlantic in the colder periods (Di Geronimo, 1998).

FLORISTIC DIVERSITY

Due to the long history of taxonomic studies, it is not surprising that a plethora of names (both species and intraspecific taxa) has accumulated for Mediterranean corallines. The nomenclatural history of these algae is very complicated and would be impossible to summarize in a concise form. A comprehensive summary of the names available and information about their taxonomic validity can be found in the account of Cormaci et al. (2017) and in AlgaeBase (Guiry and Guiry, 2019). Here we follow primarily the taxonomy of Cormaci et al. (2017). These authors reported for the Mediterranean 57 species; with the addition of *Lithophyllum yessoense* (recorded by Verlaque, 2001), *Pneophyllum cetinanensis* (freshwater species described by Žuljević et al., 2016) and *Lithophyllum nitorum* (recorded by Peña et al., 2018), the Mediterranean coralline flora as currently known consists of 60 species (**Table 1**). The genus *Lithophyllum* is the species-richest (16 species), followed by *Mesophyllum* (6 species), and *Amphiroa*, *Jania,* and *Lithothamnion* (5 species each). Twenty-seven species were originally described based on Mediterranean material (see type localities in **Table 1**). For details of morphology and habitat for each species, see Irvine and Chamberlain (1994), Bressan and Babbini (2003), and Cormaci et al. (2017).

MOLECULAR STUDIES OF MEDITERRANEAN CORALLINES

Taxonomy, Phylogeny, and Geographical Distribution

There are well-founded reasons to believe that the current estimate of 60 species is an underestimation of the real species number. The taxonomy of Mediterranean corallines so far has been based almost entirely on morphological data. Species circumscriptions have been based on gross morphology and morpho-anatomical characters observed in light and electron microscopy (Hamel and Lemoine, 1953; Huvé, 1962; Bressan, 1974; Bressan et al., 1977; Boudouresque and Verlaque, 1978; Woelkerling, 1983, 1985; Woelkerling et al., 1985; Athanasiadis, 1989, 1995, 1997, 1999a,b; Basso, 1995; Bressan and Babbini, 1995; Basso et al., 1996, 2004, 2011; Furnari et al., 1996; Chamberlain, 1997; Cabioch and Mendoza, 1998, 2003; Bressan and Cabioch, 2004; Basso and Rodondi, 2006; Athanasiadis and Neto, 2010; Kaleb et al., 2011, 2012; Cormaci et al., 2017).

In recent decades, DNA sequence data have become a widespread tool in coralline taxonomy and have plaid an increasingly important role in species circumscriptions. After the first studies published around the end of the last century (Bailey and Chapman, 1996, 1998), the last decade has seen an exponential increase of DNA-based phylogenetic and taxonomic studies. Investigations of molecular-assisted alpha taxonomy (MAAT) have now become the normality in coralline taxonomy and systematics. This approach uses molecular markers to assign collections to genetic groups followed by detailed morphological observations (Hind et al., 2014). Such new information has revolutionized our understanding of coralline diversity and evolution (Nelson et al., 2015) and has drawn a new scenario in which some points are now well-established. First, coralline algae are characterized by high levels of cryptic diversity. The genetic diversity of these organisms unraveled by DNA sequence data is much higher than indicated by morpho-anatomical data, both in geniculate and non-geniculate species. Cryptic diversity has been shown to abound in marine macroalgae (De Clerck et al., 2013; Verbruggen, 2014); although corallines have a morpho-anatomical structure that offers more characters for species discrimination compared to other red seaweeds, they are perhaps the group of rhodophytes in which this situation is most pervasive (Pezzolesi et al., 2019). Second, many morpho-anatomical features traditionally used to identify corallines are not reliable for identification purposes. Therefore, a taxonomy based entirely or mostly on these characters (as it is the case for the Mediterranean) is likely to be misleading, with substantial risk of misidentifications and underestimation of species numbers (e.g., for the genus *Lithophyllum* Hernandez-Kantun et al. (2016) estimated a species diversity likely two to four times greater than currently estimated in each geographic region). Third, special care must be used in the application of species names. When cryptic diversity is demonstrated and a morphospecies turns to represent a complex of cryptic species, it may be very difficult to decide to which cryptic species the Linnaean binomial is correctly assigned. This may create great confusion when different cryptic species have different geographical distributions. Considering this problem, in absence of molecular data the practice of identifying specimens from a certain geographical region with names of species described from widely separated regions should be abandoned (Pezzolesi et al., 2019).

The first study presenting molecular data for Mediterranean corallines was published by Walker et al. (2009). These authors presented *cox*1 and SSU rRNA sequences for 2 samples of *Corallina ferreyrae* (as *Corallina elongata*) from northern Greece in their taxonomic study of European articulated corallines. At present, there are in GenBank 1153 sequences obtained from Mediterranean corallines, which were produced in 18 different studies (among which De Jode et al., 2019 provided the largest contribution, 812 sequences; **Table S1**). These sequences were generated by PCR amplification and Sanger sequencing of selected markers. The plastid gene of the photosystem II protein D1 (*psb*A), the mitochondrial COI-5P fragment of the cytochrome c oxydase I gene, the mitochondrial *cox*2,3 spacer, and the nuclear genes of the small subunit (SSU) and large subunit (LSU) of the ribosomal RNA have been the main markers used (**Table S1**). To date, the transcriptomic data presented by De Jode et al. (2019) are the

TABLE 1 | Species of coralline algae reported for the Mediterranean Sea and currently regarded as taxonomically valid.

Species	Synonyms frequently used in the mediterranean literature	Habit	Type locality	Known distribution in the mediterranean	Important references
Amphiroa beauvoisii J.V. Lamouroux		Geniculate	Portugal	Widespread. SP, FR, IT, MA, CR, TK, CY, SY, IL, TU, AG, MO	Cormaci et al., 2017
Amphiroa cryptarthrodia Zanardini		Geniculate	Trieste (Italy), Istria and Dalmatia (Croatia)	Reported as widespread, but in need of reassessment due to previous confusion with *A. rubra*. SP, FR, IT, MA, SL, CR, AL, GR, TK, CY, SY, LE, IL, LI, TU, AG, MO	Rosas-Alquicira et al., 2010; Cormaci et al., 2017
Amphiroa fragilissima (Linnaeus) J. V. Lamouroux		Geniculate	"*In Indiis*" (probably Jamaica)	Poorly-known species, reported only from some areas in the western and central Mediterranean. SP, FR, IT, AG	Cormaci et al., 2017
Amphiroa rigida J.V. Lamouroux		Geniculate	Mediterranean Sea	Widespread. SP, FR, IT, MA, CR, AL, GR, TK, CY, SY, LE, IL, EG, LI, TU, AG, MO	Cormaci et al., 2017
Amphiroa rubra (Philippi) Woelkerling		Geniculate	Sicily	Rarely recorded. IT, TK.	Cormaci et al., 2017
Boreolithon vanheurckii (Chalon) A.S. Harvey et Woelkerling	*Melobesia vanheurckii* (Heydrich) De Toni	Encrusting	St. Brelade, Jersey, Channels Islands, U.K.	Rarely recorded. SP, IT	Irvine and Chamberlain, 1994
Choreonema thuretii (Bornet) Schmitz		Filamentous endophytic	Pointe de Querqueville, France	Widespread, more common in the western and central Mediterranean than in the eastern. SP, FR, IT, MA, SL, CR, AL, GR, TK, CY, AG, MO	Hamel and Lemoine, 1953; Irvine and Chamberlain, 1994
Corallina ferreyrae E. Y. Dawson, Acleto et Foldvik	*Corallina caespitosa* Walker, Brodie et L.M. Irvine	Geniculate	Pucusana, Peru	All records as *C. caespitosa*. Rarely reported, but probably much more common than the current records suggest. SP, FR, IT, GR	Walker et al., 2009; Pardo et al., 2015; Williamson et al., 2015; Bustamante et al., 2019
Corallina officinalis Linnaeus		Geniculate	"*Hab. O. Eur*." (European seas)	Widespread. SP, FR, IT, MA, SL, CR, AL, GR, TK, CY, SY, IL, EG, LI, TU, AG, MO	Brodie et al., 2013; Pardo et al., 2015; Williamson et al., 2015
Ellisolandia elongata (J. Ellis et Solander) K. Hind et G.W. Saunders	*Corallina elongata* J. Ellis et Solander; *Corallina mediterranea* Areschoug	Geniculate	Cornwall, U.K.	Widespread. SP, FR, IT, MA, CR, AL, GR, TK, CY, SY, LE, IL, EG, LI, TU, AG, MO	Irvine and Chamberlain, 1994; Brodie et al., 2013; Pardo et al., 2015
Harveylithon rupestre A. Rösler, Perfectti, V. Peña et J. Braga	*Hydrolithon rupestre* (Foslie) Penrose	Encrusting	Ocean Beach, Phillip Island, Victoria, Australia	In the Mediterranean known only from Vis Island, Croatia. Considered an introduction from tropical regions of the southern hemisphere	Wolf et al., 2015
Hydrolithon boreale (Foslie) Y.M. Chamberlain	*Fosliella farinosa* var. *solmsiana* (Falkenberg) W.R. Taylor	Encrusting	Roundstone, Co. Galway, Ireland	Reported mostly from the western and central Mediterranean, rarely from the eastern. SP, FR, IT, CR, GR, TU	Irvine and Chamberlain, 1994
Hydrolithon cruciatum (Bressan) Y.M. Chamberlain	*Fosliella cruciata* Bressan	Encrusting	Gulf of Trieste, Adriatic Sea	Reported mostly from the western and central Mediterranean, rarely from the eastern. SP, FR, IT, MA, SL, GR, CY	Irvine and Chamberlain, 1994; Bressan and Babbini, 2003
Hydrolithon farinosum (J.V. Lamouroux) Penrose et Y.M. Chamberlain	*Fosliella farinosa* (J.V. Lamouroux) M. Howe	Encrusting	Mediterranean Sea	Widespread. SP, FR, IT, MA, SL, CR, AL, GR, TK, CY, SY, LE, IL, EG, LI, TU, AG, MO	Irvine and Chamberlain, 1994; Cormaci et al., 2017
Jania adhaerens J.V. Lamouroux		Geniculate	Mediterrranean Sea	Widespread. SP, FR, IT, GR, CY, IL, EG, TU, AG, MO	Cormaci et al., 2017
Jania longifurca Zanardini ex Zanardini		Geniculate	Harbor of Zadar, Croatia	Widespread. SP, FR, IT, MA, CR, GR, TK, CY, SY, IL, EG, LI, TU, AG, MO	Cormaci et al., 2017

(Continued)

TABLE 1 | Continued

Species	Synonyms frequently used in the mediterranean literature	Habit	Type locality	Known distribution in the mediterranean	Important references
Jania rubens (Linnaeus) J.V. Lamouroux		Geniculate	"*In Oceano Europaeo*" (European seas)	Widespread. SP, FR, IT, MA, SL, CR, AL, GR, TK, CY, SY, LE, IL, EG, LI, TU, AG, MO	Irvine and Chamberlain, 1994; Cormaci et al., 2017
Jania squamata (Linnaeus) J.H. Kim, Guiry et H.G. Choi	*Haliptilon squamatum* (Linnaeus) H.W. Johansen, L.M. Irvine et A. Webster	Geniculate	"*In O. Europaeo*" (European seas)	Widely reported but many records in need of reassessment, due to possible confusion with *Corallina officinalis* and *Elisolandia elongata*. FR, IT, GR, TK, CY, TU	Irvine and Chamberlain, 1994; Cormaci et al., 2017
Jania virgata (Zanardini) Montagne	*Corallina granifera* J. Ellis et Solander; *Haliptilon virgatum* (Zanardini) Garbary et H.W. Johansen	Geniculate	Not designated in the protologue, but the original material was collected from the Adriatic Sea	Widespread. SP, FR, IT, MA, SL, CR, AL, GR, TK, SY, LE, IL, EG, LI, TU, AG, MO	Bressan and Babbini, 2003; Cormaci et al., 2017
Lithophyllum byssoides (Lamarck) Foslie	*Lithophyllum lichenoides* Philippi; *Goniolithon byssoides* (Lamarck) Foslie	Encrusting.	Effectively unknown ("La Manche"; see Pezzolesi et al., 2017)	Common in the western and central Mediterranean, rare in the eastern Mediterranean. SP, FR, IT, MA, CR, AL, GR, TK, IL, EG, TU, AG, MO	Chamberlain, 1997; Verlaque, 2010; Pezzolesi et al., 2017
Lithophyllum corallinae (P.L. et H.M. Crouan) Heydrich	*Titanoderma corallinae* (P.L. et H.M. Crouan) Woelkerling, Y.M. Chamberlain et P.C. Silva	Encrusting.	Banc du Chateau and Baie de La Ninon, Brest, France	Widespread. SP, FR, IT, SL, CR, GR, TK, CY, LI, TU	Irvine and Chamberlain, 1994
Lithophyllum cystoseirae (Hauck) Heydrich	*Titanoderma cystoseirae* (Hauck) Woelkerling, Y.M. Chamberlain et P.C. Silva	Encrusting	Adriatic Sea	Widespread. SP, FR, IT, MA, SL, CR, GR, TK, CY, IL, LI, TU, AG, MO	Bressan and Babbini, 2003; Cormaci et al., 2017
Lithophyllum decussatum (J. Ellis et Solander) Philippi		Encrusting	Coast of Portugal	Rare, known only from the western and central Mediterranean. SP, FR, IT, LI, MO.	Cormaci et al., 2017
Lithophyllum dentatum (Kützing) Foslie		Encrusting, or unattached forming rhodoliths	Naples, Italy	Common in the western and central Mediterranean, rare in the eastern Mediterranean. SP, FR, IT, MA, CR, AL, GR, TU, AG, MO	Woelkerling, 1985; Bressan and Babbini, 2003
Lithophyllum hibernicum Foslie		Encrusting	Fahy Bay, Ballynakill Harbor, Co. Galway, Ireland	Presence in the Mediterranean demonstrated by DNA sequence data. Currently documented for SP and FR, but probably more widely distributed	Hernandez-Kantun et al., 2015a
Lithophyllum incrustans Philippi		Encrusting, or unattached forming rhodoliths	Sicily	Widespread, but many records should be reassessed based on DNA sequence data. SP, FR, IT, MA, SL, CR, AL, GR, TK, SY, LE, EG, LI, TU, AG, MO	Hernandez-Kantun et al., 2015a
Lithophyllum nitorum		Encrusting	Port Erin Harbor, Isle of Man, U.K.	Presence in the Mediterranean demonstrated by DNA sequence data. Currently documented for SP, but probably more widely distributed	Irvine and Chamberlain, 1994; Peña et al., 2018
Lithophyllum orbiculatum (Foslie) Foslie		Encrusting	Kristiansund, Norway	Uncommon, reported mostly from the western and central Mediterranean, rarely from the eastern. SP, FR, IT, GR, TK, AG, TU	Irvine and Chamberlain, 1994
Lithophyllum papillosum (Zanardini ex Hauck) Foslie	*Dermatolithon papillosum* (Zanardini ex Hauck) Foslie; *Goniolithon papillosum* (Zanardini ex Hauck) Foslie	Encrusting	West coast of Susak Island, Croatia	Reported mostly from the western and central Mediterranean, rarely from the eastern. SP, FR, IT, CR, GR, TK, AG, MO	Cormaci et al., 2017

(Continued)

TABLE 1 | Continued

Species	Synonyms frequently used in the mediterranean literature	Habit	Type locality	Known distribution in the mediterranean	Important references
Lithophyllum pustulatum (J.V. Lamouroux) Foslie	*Dermatolithon pustulatum* (J.V. Lamouroux) Foslie; *Titanoderma pustulatum* (J.V. Lamouroux) Nägeli	Encrusting	France	Widespread. SP, FR, IT, MA, SL, CR, GR, TK, CY, SY, LE, EG, LI, TU, AG, MO	Irvine and Chamberlain, 1994; Cormaci et al., 2017
Lithophyllum racemus (Lamarck) Foslie		Unattached, forming rhodoliths/maërl	Capri, Gulf of Naples, Italy	Reported mostly from the central Mediterranean. SP, FR, IT, MA, SL, CR, AL, GR, LI, TU, AG	Basso et al., 1996; Cormaci et al., 2017
Lithophyllum stictiforme (Areschoug) Hauck	*Pseudolithophyllum expansum* (Philippi) Me. Lemoine; *Pseudolithophyllum cabiochae* Boudouresque et Verlaque; *Lithophyllum cabiochae* (Boudouresque et Verlaque) Athanasiadis; *Lithophyllum frondosum* (Dufour) Furnari, Cormaci et Alongi	Encrusting	Mediterranean Sea	Widespread. SP, FR, IT, MA, SL, CR, AL, GR, TK, SY, IL, EG, LI, TU, AG, MO	Athanasiadis, 1999a
Lithophyllum trochanter (Bory) Huvé ex Woelkerling	*Titanoderma trochanter* (Bory) Benhissoune, Boudouresque, Perret-Boudouresque et Verlaque	Encrusting	Greece	Warmer parts of the Mediterranean. Most common in the eastern Mediterranean, probably absent in the western; records from France and Algeria probably refer to *L. woelkerlingii*. FR, IT, CR, AL, GR, CY, SY, IL, LI	Bressan and Cabioch, 2004; Cormaci et al., 2017
Lithophyllum woelkerlingii Alongi, Cormaci et Furnari	*Titanoderma ramosissimum* (Heydrich) Bressan et Cabioch	Encrusting	Algeria	SP, FR, AG. Distribution in need of reassessment due to the previous confusion with *L. trochanter*	Bressan and Cabioch, 2004; Cormaci et al., 2017
Lithophyllum yessoense Foslie		Encrusting	Yoichi, Shiribeshi Province, Hokkaido, Japan	FR. Known only from the Thau Lagoon, where it was introduced with Asian oysters and is now well-established	Verlaque, 2001
Lithothamnion corallioides (P.L. et H.M. Crouan) P.L. et H.M. Crouan		Unattached, forming rhodoliths/maërl	Rade de Brest, France	Widespread. SP, FR, IT, MA, CR, GR, CY, LI, TU	Irvine and Chamberlain, 1994
Lithothamnion crispatum Hauck		Encrusting, or unattached forming rhodoliths/maërl	Rovinj, Croatia	Widespread, in general more common in the western and central Mediterranean than in the eastern. SP, FR, IT, CR, GR, TK, LI, AG	Basso et al., 2011; Cormaci et al., 2017
Lithothamnion minervae Basso		Unattached, forming rhodoliths/maërl	Pontian Islands, Italy.	Central Mediterranean; FR, IT, MA. Possibly underrecorded due to the deep subtidal habitat	Basso, 1995; Basso et al., 2004; Cormaci et al., 2017
Lithothamnion sonderi Hauck		Encrusting	Helgoland, Germany	Not common in the Mediterranean, but reported with wide distribution. SP, FR, IT, GR, IL, TU	Irvine and Chamberlain, 1994
Lithothamnion valens Foslie		Unattached, forming rhodoliths/maërl	Probably Adriatic Sea, see Woelkerling et al. (2005)	Western and central Mediterranean; SP, FR, IT, CR, TU. Possibly underrecorded due to the deep subtidal habitat	Basso, 1995, Woelkerling et al., 2005
Melobesia membranacea (Esper) J.V. Lamouroux	*Epilithon membranaceum* (Esper) Heydrich	Encrusting	West coast of France	Widespread. SP, FR, IT, SL, CR, GR, TK, CY, SY, IL, TU, AG, MO	Chamberlain, 1985; Irvine and Chamberlain, 1994
Mesophyllum expansum (Philippi) Cabioch et Mendoza		Encrusting	Sicily	SP, FR, IT, GR. Records of this species for other countries require reassessment; most are probably incorrect and should be referred to *Lithophyllum stictiforme*	Athanasiadis and Neto, 2010; Peña et al., 2015a

(Continued)

TABLE 1 | Continued

Species	Synonyms frequently used in the mediterranean literature	Habit	Type locality	Known distribution in the mediterranean	Important references
Mesophyllum lichenoides (J. Ellis) M.me Lemoine		Encrusting, occasionally unattached	Cornwall, U.K.	Reported as widespread, but all Mediterranean records of this species need reassessment based on DNA sequence data. SP, FR, IT, CR, AL, GR, TK, CY, LE, LI, TU, AG, MO	Irvine and Chamberlain, 1994; Peña et al., 2015a
Mesophyllum macedonis Athanasiadis		Encrusting	Pigeon Cave, Sithonia Peninsula, Greece	Known only from the type locality. GR	Athanasiadis, 1999b
Mesophyllum macroblastum (Foslie) W.H. Adey		Encrusting	Gulf of Naples, Italy	Western and central Mediterranean. SP, FR, IT	Kaleb et al., 2011; Peña et al., 2015a
Mesophyllum philippii (Foslie) W.H. Adey	*Lithothamnion philippii* Foslie	Encrusting, or unattached forming rhodoliths/maërl	Banyuls-sur-Mer, France	Reported mostly from the western and central Mediterranean, rarely from the eastern. SP, FR, IT, CR, GR, CY, LI, AG, MO	Cormaci et al., 2017
Mesophyllum sphaericum V. Peña, Bárbara, W.H. Adey, Riosmena-Rodríguez et Choi		Unattached, forming rhodoliths/maërl; occasionally encrusting	Benencia Island, Ria de Arousa, Galicia, Spain	SP, IT. Presence in the Mediterranean demonstrated using DNA sequence data; distribution probably much wider than currently known	Peña et al., 2015a
Neogoniolithon brassica-florida (Harvey) Setchell et R.L. Mason	*Neogoniolithon mamillosum* (Hauck) Setchell et Mason *nom. illeg*., is a species widely cited in the Mediterranean literature, for which the distinction from *N. brassica-florida* is unclear. Cormaci et al. (2017) consider it a species of uncertain identity, in need of taxonomic reassessment	Encrusting, or unattached forming rhodoliths/maërl	Algoa Bay, Cape Province, South Africa.	Widely recorded, but Mediterranean records of this species in need of reassessment based on DNA sequence data. SP, FR, IT, CR, AL, GR, TK, CY, SY, LE, IL, TU, AG, MO	Bressan and Babbini, 2003; Cormaci et al., 2017
Phymatolithon calcareum (Pallas) W.H. Adey et D.L. McKibbin ex Woelkerling et L.M. Irvine		Unattached, forming rhodoliths/maërl; occasionally encrusting	Falmouth Harbor, Cornwall, U.K.	Widespread. SP, FR, IT, MA, CR, GR, LE, IL, LI, TU, AG, MO	Irvine and Chamberlain, 1994; Wolf et al., 2016
Phymatolithon lamii (M.me Lemoine) Y.M. Chamberlain		Encrusting	Pointe de Cancaval, Rance, France	Reported in the Mediterranean only from the Gulf of Trieste (northern Adriatic Sea). IT	Irvine and Chamberlain, 1994; Kaleb et al., 2012
Phymatolithon lenormandii (Areschoug) W.H. Adey	*Lithothamnion lenormandii* (Areschoug) Foslie	Encrusting	Arromanches-le-Bains, Calvados, France	Widespread. SP, FR, IT, MA, SL, CR, GR, TK, SY, LE, EG, LI, AG, MO	Irvine and Chamberlain, 1994; Cormaci et al., 2017
Phymatolithon lusitanicum V. Peña		Unattached, forming rhodoliths/maërl	Con de Pego, Ria de Vigo, Galicia, Spain	This recently described species is known from the Alboran Sea and the Balearic Islands, but its distribution in the Mediterranean is probably wider. SP	Peña et al., 2015b
Pneophyllum cetinanensis Kaleb, Žuljević, et V. Peña		Encrusting	River Cetina, Croatia	Freshwater species, known only from the type locality. CR	Žuljević et al., 2016
Pneophyllum confervicola (Kützing) Y.M. Chamberlain		Encrusting	Trieste, Italy	Widespread. SP, FR, IT, SL, CR, GR, TK, TU	Irvine and Chamberlain, 1994
Pneophyllum coronatum (Rosanoff) Penrose	*Pneophyllum caulerpae* (Foslie) P.L. Jones et Woelkerling	Encrusting	Port Phillip Bay, Victoria, Australia	Western and central Mediterranean. SP, FR, IT, MA, LI, TU, AG	Irvine and Chamberlain, 1994; Cormaci et al., 2017
Pneophyllum fragile Kützing	*Fosliella lejolisii* (Rosanoff) M. Howe	Encrusting	Mediterranean Sea	Widespread. SP, FR, IT, MA, SL, CR, GR, TK, CY, SY, LE, TU, AG, MO	Irvine and Chamberlain, 1994; Cormaci et al., 2017

(Continued)

TABLE 1 | Continued

Species	Synonyms frequently used in the mediterranean literature	Habit	Type locality	Known distribution in the mediterranean	Important references
Pneophyllum zonale (P. Crouan et H. Crouan) Y.M. Chamberlain	*Fosliella zonalis* (P. Crouan et H. Crouan) J. Feldmann; *Melobesia zonalis* P. Crouan et H. Crouan) Foslie	Encrusting	Rade de Camaret, Brest, France	Species of uncertain taxonomic identity. SP, FR, IT, MAL, GR, TU	Feldmann, 1939; Cormaci et al., 2017
Spongites fruticulosus Kützing		Encrusting, or unattached forming rhodoliths/maërl	Mediterranean Sea	Widespread. SP, FR, IT, SL, CR, GR, TK, CY, LI, TU, AG, MO	Woelkerling, 1985; Basso and Rodondi, 2006; Rösler et al., 2016
Sporolithon ptychoides Heydrich		Encrusting, occasionally unattached	Sinai Peninsula, Egypt	Western and central Mediterranean. SP, FR, IT, MA	Cormaci et al., 2017; Richards et al., 2017
Tenarea tortuosa (Esper) M.me Lemoine	*Lithophyllum tortuosum* (Esper) Foslie	Encrusting	Mediterranean Sea	Central and eastern Mediterranean. Records of this species from the western Mediterranean are most probably misidentifications of *Lithophyllum byssoides*. IT, CR, AL, GR, TK, CY, SY, LE	Woelkerling et al., 1985; Bressan and Babbini, 2003; Cormaci et al., 2017

For details of basionyms and taxonomic synonymies see Cormaci et al. (2017) and Guiry and Guiry (2019). Codes for countries: SP, Spain; FR, France; IT, Italy; MA, Malta; SL, Slovenia; CR, Croatia; AL, Albania; GR, Greece; TK, Turkey; CY, Cyprus; SY, Syria; LE, Lebanon; IL, Israel; EG, Egypt; LI, Libya; TU, Tunisia; AG, Algeria; MO, Morocco. Distribution information based on Bressan and Babbini (2003) and Guiry and Guiry (2019, and references therein). Herein we define western Mediterranean as the part of the basin extending from the Strait of Gibraltar to the western coasts of Corsica and Sardinia; eastern Mediterranean the part extending from the line Cape Matapan (Greece)-Benghazi (Libya) to the Levant States (Syria, Lebanon, Israel); and central Mediterranean the part comprised between western and eastern Mediterranean.

only molecular data other than Sanger sequences produced from Mediterranean corallines.

Of the 18 studies, only 8 focused totally or mainly on Mediterranean taxa: Hernandez-Kantun et al. (2015a), Peña et al. (2015a), Wolf et al. (2015, 2016), Žuljević et al. (2016), Pezzolesi et al. (2017, 2019), and De Jode et al. (2019). Five of these (Peña et al., 2015a; Žuljević et al., 2016; Pezzolesi et al., 2017, 2019; De Jode et al., 2019) provided most of the DNA sequence data available (**Table S1**) and have particularly contributed to our current understanding of the genetic diversity of Mediterranean corallines.

The integrative study of Peña et al. (2015a) on the genus *Mesophyllum*, based on molecular (COI-5P, *psb*A) and morphological data redefined the distribution of four species in Atlantic Europe and the Mediterranean. *M. expansum, M. macroblastum,* and *M. sphaericum* were detected in the Mediterranean. The results suggested that *M. expansum* is a major contributor to bioconstruction of coralligenous concretions and occurs also in the Atlantic Iberian Peninsula and Macaronesia. This species was found from the intertidal to −50 m, with a positive correlation between depth and the maximum sea surface temperature, suggesting that this species may mitigate future consequences of global warming by changes in depth profile. By contrast, *M. macroblastum* appears to be restricted to the Mediterranean. Two *Mesophyllum* species reported in the Mediterranean literature (*M. lichenoides* and *M. alternans*) were not recorded and their presence in the Mediterranean requires confirmation based on molecular data. The Atlantic Iberian *M. sphaericum* was first reported in the Mediterranean, under two different growth-forms (rhodolith and crustose).

The study of Pezzolesi et al. (2017) on the intertidal bioconstructor *Lithophyllum byssoides* was the first phylogeographic investigation of a Mediterranean coralline. Using *psb*A and *cox*2,3 sequences, these authors unraveled a high haplotypic diversity and detected 7 lineages, whose geographical distribution did not follow the main biogeographical boundaries recognized in the central Mediterranean. For several lineages the distribution was restricted to one or few sites. The results also showed a clear genetic differentiation between Mediterranean and Atlantic *Lithophyllum byssoides*, suggesting a likely separation at species level (which could not be confirmed due to insufficient data from the Atlantic).

The two recent studies of Pezzolesi et al. (2019) and De Jode et al. (2019) unraveled a striking case of cryptic diversity: the *Lithophyllum stictiforme* complex. *Lithophyllum stictiforme* and *Lithophyllum cabiochiae* have been long known as common species in the Mediterranean subtidal, where they are major contributors to the formation of coralligenous concretions (Athanasiadis, 1999a; see also Boudouresque and Verlaque, 1978; Furnari et al., 1996). Whereas some authors have separated these species, others (Cormaci et al., 2017; Guiry and Guiry, 2019) consider *L. cabiochiae* and *L. stictiforme* conspecific. Pezzolesi et al. (2019), sequencing three markers (*cox*2,3, *psb*A, *rbc*L) in samples collected from many sites in the western and central Mediterranean, concluded that *Lithophyllum stictiforme* represents a complex of at minimum 13 cryptic species. De Jode et al. (2019), combining Sanger sequencing (COI, *psb*A, LSU) and transcriptomics, reached very similar conclusions, showing

that on the French coasts specimens with the *L. stictiforme/L. cabiochiae* morphology represent a complex of 8 cryptic species. De Jode et al. (2019) demonstrated also the reproductive isolation of these species and documented differences in their depth range. Both Pezzolesi et al. (2019) and De Jode et al. (2019) noted that for several cryptic species the geographical distribution appears restricted to one particular area or site.

Pezzolesi et al. (2017, 2019) interpreted the patterns observed for *L. byssoides* and the *L. stictiforme* complex as consequences of past hydrogeological and climatic events, in combination with modern oceanographic features. The fossil documentation suggests that these algae have existed in the Mediterranean, respectively, since the Messinian (7.3–5.3 Mya, Braga and Aguirre, 2001; Braga et al., 2009) and the late Langhian (14.5 Mya, Hrabovský et al., 2016). Spatial fragmentation of populations that took place during the Messinian Salinity Crisis (5.96–5.33 Mya) may have stimulated genetic differentiation, and, in the case of the *Lithophyllum stictiforme* complex, allopatric speciation. Subsequent climatic events such as the Quaternary glaciations (2.6 Mya to present), which also altered the Mediterranean coastline and partially separated different sectors, probably further contributed to shape the current distribution of these algae.

The relevance of past climatic events in the diversification of Mediterranean corallines is highlighted by a discovery of particular interest made in recent years, i.e., the first known freshwater coralline alga: *Pneophyllum cetinaensis*, endemic to the Cetina River, Croatia (Žuljević et al., 2016). This species, which is fully adapted to freshwater conditions, descends from an ancestor that was preadapted to changes in water salinity produced in landlocking events such as the last glaciation (120,000–20,000 years ago). In addition, molecular data obtained in this study exclude a close phylogenetic relationship between the freshwater *P. cetinaensis* and other Mediterranean and Atlantic *Pneophyllum* species.

Among other studies, Hernandez-Kantun et al. (2015a) reassessed the taxonomic identity of the generytype species *Lithophyllum incrustans* using a partial *rbc*L sequence obtained from the lectotype specimen (epizoic on a sea snail shell, collected in Sicily). The results re-defined the distribution of *L. incrustans* and highlighted that this is mainly a subtidal species. The presence in the Mediterranean of *Lithophyllum hibernicum* was also demonstrated. Additional data were provided by Bittner et al. (2011), who sequenced 9 unidentified samples of Mediterranean corallines in their phylogenetic assessment of the order Corallinales (*psb*A and, in part, COI-5P). Rösler et al. (2016) published 21 new sequences for Mediterranean collections, including one for a specimen therein designated as epitype of *Spongites fruticulosus*. Additional data produced new records for the Mediterranean flora: *Harveylithon rupestre* (as *Hydrolithon rupestre*, Wolf et al., 2015); *Phymatolithon lusitanicum* (Peña et al., 2015b); the attached encrusting form of the maerl-forming *Phymatolithon calcareum* (Wolf et al., 2016); and *Lithophyllum nitorum* (Peña et al., 2018). Finally, some sequences of Mediterranean fossil corallines were published by Hughey et al. (2008).

Molecular Data and Application of Taxonomic Names in Mediterranean Corallines

In situations where cryptic diversity is discovered, the only definitive solution for a correct application of Linnaean names is to obtain sequences from the type specimen, the only one to which a species name is unambiguously attached. In this way, the type specimen can be linked to one of the lineages recovered in molecular phylogenies, and the species name will therefore be attached to that lineage. Fortunately, in the case of coralline algae this approach has generally worked. In air-dried coralline specimens, DNA is preserved in a form that is often adequate to obtain partial sequences for one or more markers (either by high-throughput sequencing methods or by nested PCR performed with adequate equipment). Sequences of sufficient quality have been produced from many type specimens, allowing an accurate assessment of many species (e.g., Adey et al., 2015; Hernandez-Kantun et al., 2015a, 2016; Hind et al., 2016; Richards et al., 2017, 2018; Gabrielson et al., 2018; Peña et al., 2018). Conversely, for some species to obtain sequences from type specimens is impossible (either because the type material is in very limited amount, or because it is formol-preserved). In these cases, a different specimen should be sequenced and used as molecular reference for the species. Such specimen should be collected at the type locality, and the details of its morphology and habitat should be in agreement with the protologue of the original description. If the nature of the original type is ambiguous, this specimen can be designated as epitype following the article 9.9 of the ICN (Turland et al., 2018).

For corallines occurring in the Mediterranean, an assessment based on sequences generated from type specimens has been made for 11 species. Sequences were obtained from holotypes, lectotypes, or isotypes for *Corallina ferreyrae* (Bustamante et al., 2019; previously reported in the Mediterranean as *Corallina caespitosa*, Walker et al., 2009), *Lithophyllum incrustans* (Hernandez-Kantun et al., 2015a), *Lithophyllum nitorum* (Peña et al., 2018), *Lithophyllum stictiforme* (Pezzolesi et al., 2019), *Mesophyllum sphaericum* (Peña et al., 2011), *Phymatolithon lusitanicum* (Peña et al., 2015b), and *Pneophyllum cetinanensis* (Žuljević et al., 2016). For *Spongites fruticulosus*, Rösler et al. (2016) generated SSU, LSU, COI, and 23S sequences from the epitype specimen. For *Corallina officinalis* and *Ellisolandia elongata*, Brodie et al. (2013) designated epitype specimens, from which they obtained *cox*1 and *rbc*L sequences. Finally, Hernandez-Kantun et al. (2015b) produced SSU and *psb*A sequences from the neotype of *Phymatolithon calcareum* (designated by Woelkerling and Irvine, 1986).

PRESENT-DAY DISTRIBUTION AND BIOGEOGRAPHY

Our knowledge of the distribution of Mediterranean corallines is largely based on records derived from morpho-anatomical identifications (see Bressan and Babbini-Benussi, 1996, for a synthesis of the information available until the late 90s of the last century). Six species were recorded in recent

years based on molecular data: *Corallina ferreyrae,* reported as the heterotypic synonym *C. caespitosa* (Walker et al., 2009), *Harveylithon rupestre* (Wolf et al., 2015), *Lithophyllum hibernicum* (Hernandez-Kantun et al., 2015a), *Lithophyllum nitorum* (Peña et al., 2018), *Mesophyllum sphaericum* (Peña et al., 2015a), and *Phymatolithon lusitanicum* (Peña et al., 2015b).

Based on the present knowledge, 7 species are Mediterranean endemics (*Amphiroa rubra*, *Lithophyllum trochanter*, *L. woelkerlingii*, *Lithothamnion minervae*, *L. valens*, *Mesophyllum macedonis*, *Pneophyllum cetinaensis*) (**Table 1**). In terms of distribution, it is possible to recognize three main groups. Some species are clearly widespread throughout the Mediterranean, having been recorded in all regions of the basin. This group includes 27–28 species, which usually also occur on Atlantic European coasts and in Macaronesia; examples are *Ellisolandia elongata*, *Hydrolithon farinosum*, *Jania rubens*, *Lithophyllum incrustans,* and *Pneophyllum fragile*. A smaller number of species (16–17) occurs only in the western and central Mediterranean, or is much more common there than in the eastern Mediterranean. Examples are *Choreonema thuretii*, *Mesophyllum macroblastum*, *Lithophyllum byssoides*, *L. dentatum,* and *Lithothamnion valens*. Finally, two species (*Lithophyllum trochanter* and *Tenarea tortuosa*) are clearly associated with the warmer parts of the basin and reliable records refer mostly to the eastern Mediterranean. At present, two species are considered introduced. *Lithophyllum yessoense* was recorded by Verlaque (2001) from the Lagune de Thau (Hérault, France), a well-known hotspot of introduction of alien species; the species was probably introduced from the North Pacific by transfer of Asian oysters. *Harveylithon rupestre* was recorded by Wolf et al. (2015) from Vis Island (Croatia) (as *Hydrolithon rupestre*). These authors believed that the species was probably introduced in the area by shellfish aquaculture activities.

It can be expected, however, that future studies incorporating molecular data will lead to geographical reassessments for many species. The main change that we expect is an increase in the number of endemic species. This expectation is based on theoretical grounds (the hydrogeological history of the Mediterranean in the last 15 My and the high number of endemics in many animal groups) and on the results of some recent studies. For the *Lithophyllum stictiforme* complex, De Jode et al. (2019) and Pezzolesi et al. (2019) discovered numerous cryptic species for which the present known distribution is restricted to the Mediterranean. Although some of these species surely will be shown to occur in neighboring Atlantic regions, we feel that almost certainly several others will turn to be real Mediterranean endemics. *Lithophyllum byssoides* is another candidate for Mediterranean endemicity: Pezzolesi et al. (2017) showed that Mediterranean samples of this species are genetically distinct from Atlantic samples to an extent that may justify separation at species level. If future studies incorporating additional extra-Mediterranean samples confirm this separation, the Mediterranean population will have to be considered an endemic species. The same situation applies to *Mesophyllum macroblastum*: Peña et al. (2015a) noted that extra-European specimens identified with this name were resolved in molecular analyses as different species from Mediterranean specimens (which can be considered the real *M. macroblastum*: the type locality is the Gulf of Naples, Italy); thus, the occurrence of this species out of the Mediterranean has to be definitively demonstrated yet. Pardo et al. (2015), in a taxonomic investigation focusing on *Corallina* and *Ellisolandia* of the Atlantic Iberian Peninsula, discovered a species of *Corallina* with distribution encompassing Atlantic and Mediterranean shores (for which they did not provide a formal description and named it *Corallina* sp.2). Pardo et al. (2015) remarked that Atlantic and Mediterranean forms of this species showed clear morphological differences and had different COI-5P haplotypes. It cannot be discounted that future studies will lead to separation at species level between the two forms; in that case, the Mediterranean form would probably be an endemic Mediterranean. Based on these examples we suggest that, for all species originally described from the Mediterranean, the distribution should be reassessed using DNA sequence data produced from the whole geographic range.

REPRODUCTIVE BIOLOGY

The life histories of Mediterranean corallines have not been investigated in detail using culture studies. Evidence based on observation of field-collected material suggests that these algae have the triphasic life history typical of later-divergent florideophytes, with one haploid generation reproducing sexually (the gametophyte) and two diploid generations reproducing asexually by spores (the carposporophyte and the tetrasporophyte) (Graham et al., 2018).

Nearly all information available on the reproductive biology of Mediterranean coralline is based on observation of reproductive specimens in the field and in the laboratory. The only information based on molecular evidence has been provided by De Jode et al. (2019). Analyzing their multilocus genotypes for clonality, these authors documented sexual reproduction in the *Lithophyllum stictiforme/cabiochiae* complex and demonstrated sexual isolation among the 8 cryptic species occurring on French shores. This is to date the only study providing robust support for the biological species concept in a taxon of Mediterranean corallines.

In general, observations of reproductive specimens/structures in Mediterranean corallines are not infrequent. Bressan and Babbini (2003) provided general information about the reproductive periods for many species (i.e., reported the months in which a species is reproductive); however, they did not specify the source of this information and if they referred to sexual or asexual phases. Most observations of reproduction available in the literature have been published as records of reproductive specimens in field investigations, reporting the reproductive structures observed (spermatangia, carposporangia, tetrasporangia, bisporangia; or sexual vs. asexual conceptacles) (Feldmann, 1939; Cecere et al., 1996; Cormaci et al., 1997, 2000; Catra et al., 2006; Falace et al., 2011).

Most records are based on observations made in a limited timespan. Investigations over extended periods are more useful to define temporal patterns and understand the environmental factors influencing reproduction, but unfortunately are less

frequent. Vatova (1948) summarized the reports of fertility available for the seaweeds of the area of Rovinj (Croatia). Gómez-Garreta et al. (1982) studied for 2 years the phenology of the most common seaweeds, including several coralline species, in four benthic communities in the Balearic Islands. Soto and Conde (1989) made similar observations over a 5 years period at several sites in southeastern Spain. Overall, inconsistent patterns were found in these studies, i.e., different reproductive periods were reported for the same species in the different areas considered. A common aspect, however, is that reproductive specimens were more frequently recorded in articulated species (*Amphiroa* spp., *Jania* spp., *Ellisolandia elongata*) than in encrusting species (possibly because observation of conceptacles in encrusting forms is generally more difficult, especially in the field). Another common feature (remarked by Soto and Conde, 1989) is that asexual structures were much more frequent than sexual (i.e., sporangial conceptacles were more frequently observed than gametangial conceptacles). This has been reported in many field studies of red seaweeds, even Mediterranean (Rindi and Cinelli, 2000) and is considered related to the presumed low rate of fertilization due to absence of flagellate gametes in red algae.

Additional information on reproductive phenology has been reported separately for few species (usually ecologically important). For *Lithophyllum byssoides*, the reproduction of tetrasporophytes has been reported in March-July at Marseilles and in February-December in the Balearic Islands; the reproduction of gametophytes only in autumn (October) (Verlaque, 2010, based on Huvé, 1956a,b; Gómez-Garreta, 1981; Chamberlain, 1997). The main period of recruitment for this species appears to be the autumn (Verlaque, 2010, according to Huvé, 1954, 1970).

The most detailed studies of reproduction in Mediterranean corallines focused on forms of coralligenous habitats (Garrabou and Ballesteros, 2000; Rodriguez-Prieto, 2016). Garrabou and Ballesteros (2000) studied populations of *Lithophyllum* and *Mesophyllum* (identified as *L. frondosum* and *M. alternans*, respectively) in a coralligenous community in Catalonia for 2 years. By photographic sampling, they estimated the percentage of reproductive specimens throughout the study period (by observation of mature conceptacles in their images). They found no seasonal trends in *Mesophyllum*, for which ∼25% of the specimens had mature conceptacles in each sampling date. Conversely, in *Lithophyllum* the percentage of thalli with mature conceptacles was significantly higher in early autumn in both years. Based on these differences and differences in growth patterns, Garrabou and Ballesteros (2000) remarked the ecological differences between the two species, concluding that *Mesophyllum* has a more opportunistic life strategy, whereas *Lithophyllum* has a more conservative strategy. Rodriguez-Prieto (2016) carried out experiments in controlled conditions (temperature, daylength and photon irradiance) on *Lithophyllum stictiforme* from Catalonia. She concluded that an irradiance of 20 μmol photons m^{-2} s^{-1} combined with 10–12°C and a 8:16 h light:dark regime was the most favorable condition for the species. In culture, the conceptacles matured in conditions simulating late summer-early autumn, in agreement with the behavior of field specimens. Rodriguez-Prieto (2016) noted that, in culture, maturation and release of reproductive cells are rare events, since no development of new conceptacles was observed after the release of reproductive cells.

Information on reproduction by vegetative propagules or thallus fragmentation in Mediterranean corallines is very limited. Coppejans (1978) documented multicellular vegetative propagules in *Hydrolithon farinosum* (as *Fosliella farinosa*) from Corsica, describing their development and release (previously reported only by Solms-Laubach, 1881). Additional records of these structures in the same species were provided by Cormaci and Furnari (1988). Thallus fragmentation is frequent in maerl/rhodolith-forming species, especially branched species with thin branches such as *Lithothamnion corallioides* and *Phymatolithon calcareum* (Bosence, 1976; Peña et al., 2014). It can be expected that this type of reproduction plays an important role in Mediterranean rhodolith beds, but there are no experimental studies or genetic data that allow generalizations about its relative contribution compared to reproduction by spores.

No direct information is available about the dispersal of Mediterranean corallines. Some indirect information can be inferred from the genomic data of De Jode et al. (2019) for the most common cryptic species of the *Lithophyllum stictiforme/cabiochiae* complex of the French shores. These authors detected genetic differences at population level that suggested limited gene flow (and, indirectly, limited dispersal) even at distances of a few km. Conversely, no significant genetic differentiation was found between populations occurring in two different depth ranges (24–31 m and 37–46 m), suggesting that depth is not a barrier to dispersal. These conclusions are consistent with theoretical prediction of a generally limited dispersal in coralline algae. As for all other rhodophytes, the principal mean of dispersal is represented by non-flagellate spores (bispores, carpospores, and tetraspores). These are small-sized cells with very limited active movement, which are able to settle only on hard substrata and remain viable for relatively short periods (Guiry, 1990; Pickett-Heaps et al., 2001). Although the magnitude of water flow greatly influences their dispersal (Norton, 1992), it is generally believed that they do not disperse over long distances. It is likely that long-distance dispersal may take place in small-sized species (*Hydrolithon* spp., *Pneophyllum* spp., *Melobesia membranacea*) that grow as epiphytes on drifting leaves of *Posidonia oceanica* or larger seaweeds. This theoretical prediction, however, needs to be corroborated by population genetic data.

MICROBIOMES OF MEDITERRANEAN CORALLINES

Marine macroalgae host a wide range of microbial organisms, among which bacteria are typically the dominant group. Bacterial communities associated with seaweeds establish strict biochemical interactions with their algal hosts and differ significantly from those found in the surrounding seawater (Brodie et al., 2016). Epiphytic bacterial communities have been reported as essential for normal morphological development of the algal host, and bacteria with antifouling properties are

thought to protect chemically undefended macroalgae from detrimental, secondary colonization by other epibionts (Egan et al., 2012). In the case of some tropical corallines associated with coral reefs, the microbiome also facilitates the larval settlement of multiple species of corals (Sneed et al., 2015).

Studies concerning the microbiomes of corallines highlighted a great diversity of these assemblages (Cavalcanti et al., 2014; Sneed et al., 2015; Brodie et al., 2016) and suggested that the associated bacterial communities contribute to biomineralization and host fitness (Cavalcanti et al., 2014). Microbiomes are therefore likely to play an important role in the responses of corallines to long-term climatic changes. Studies focusing on microbial communities, however, have mostly concerned encrusting tropical species associated with coral reefs (*Porolithon* spp., *Hydrolithon* spp., *Neogoniolithon* spp.). Limited information is available for temperate species and, to date, only the studies of Ismail-Ben Ali et al. (2012) and Quéré et al. (2019) considered the microbiomes of Mediterranean corallines. Ismail-Ben Ali et al. (2012), in a study with pharmacological focus, isolated 19 bacterial strains from the surface of *Jania rubens*. Their results revealed that the main bacterial groups were Alphaproteobacteria, Gammaproteobacteria, Bacteroidetes and Firmicutes, and that 36% of the isolates produced antibiotics effective against Gram + and Gram – bacteria and the yeast *Candida albicans*. Quéré et al. (2019), compared the microbiome of *Neogoniolithon brassica-florida* affected by white-band syndrome with that of healthy specimens; they could not identify a potential causative agent of the disease, but characterized several opportunistic bacteria colonizing diseased tissues.

BIOCHEMISTRY AND PHYSIOLOGY

Research on Mediterranean corallines in these fields is relatively recent. Excluding work focusing on responses to climate change and ocean acidification, biochemical and physiological research has considered very few species, mainly articulate. For easiness of sampling due to its intertidal/shallow subtidal habitat, *Ellisolandia elongata* has been a favored target for this type of investigations.

Early work on this species examined photosynthetic performances (Häder et al., 1996, 1997), synthesis of chlorophylls and phycobiliproteins in response to light composition (López-Figueroa et al., 1989; López-Figueroa and Niell, 1990) and effects of red and blue light on the N-metabolism (Figueroa, 1993). Estimates of productivity and calcification rates were provided by El Haikali et al. (2004) for French populations. Overall, these studies depicted *Ellisolandia elongata* as a versatile species, capable to regulate its pigment content and metabolism based on quantity and quality of the light irradiation available. It should be noted, however, that these studies were performed before the description of *Corallina caespitosa* (Walker et al., 2009), a species morphologically similar to *Ellisolandia elongata* (now considered a synonym of *C. ferreyrae*, Bustamante et al., 2019). So, the taxonomic identity of the material used in these studies should be reassessed (especially for Häder et al., 1997: these authors distinguished two morphotypes, sun- and shade-adapted, which might represent different species).

More recent studies investigated populations of *Ellisolandia elongata* from the Alboran Sea, highlighting several metabolic features that make this alga well-adapted to withstand the environmental stresses typical of its interidal habitat (Celis-Plá et al., 2014; Figueroa et al., 2014a; Korbee et al., 2014; Parages et al., 2014; Stengel et al., 2014). This alga is able to improve its photoprotective capacity by regulating its content in mycosporine-like aminoacids (MAAs, compounds well-known for their photoprotective role in numerous algae) in response to environmental conditions (Celis-Plá et al., 2014; Korbee et al., 2014). Stengel et al. (2014) demonstrated a reduction in the effective photosystem II quantum efficiency in the central hours of the day, and showed that the highest phycocyanin content occurred in the evening; Parages et al. (2014) performed proteomic studies on the same samples and concluded that mitogen-activated protein kinase (MAPK)-like proteins are involved in the response of this species to environmental stress. Figueroa et al. (2014b) argued that the species is resistant to UVB-radiation thanks to the high reflectance of its calcareous thallus.

Jania rubens has been another common subject for biochemical work. Biochemical data for samples identified with this name were provided in several studies performed mainly by northern African investigators. These examined the content of chemical contaminants in environmental monitoring (Al-Masri et al., 2003; Abdallah and Abdallah, 2008; Olgunoglu and Polat, 2008; Hernández et al., 2011; Laib and Legouchi, 2012), biological activities of algal extracts (Abd-Elnaby, 2010; Khairy and El-Sheikh, 2015) and biochemical composition in relation to nutritional value (Polat and Ozogul, 2009, 2013) or for biodiesel production (El Maghraby and Fakhry, 2015; Soliman et al., 2018).

RESPONSES OF MEDITERRANEAN CORALLINES TO CLIMATE CHANGE AND OCEAN ACIDIFICATION

Approaches Used in the Study of the Responses of Coralline Algae to Climate Change and Acidification

Coralline algae are sensitive to changes in temperature and CO_2 conditions and identified as being among the most vulnerable organisms to ocean acidification, because of the solubility of their high-magnesium (high-Mg) calcite skeleton (McCoy and Kamenos, 2015; Martin and Hall-Spencer, 2017). The responses of Mediterranean corallines to climate change and ocean acidification have been the subject of several studies that documented their tolerance or sensitivity to elevated temperatures and CO_2. The effects of elevated CO_2 on Mediterranean coralline algae were studied on single species (Martin and Gattuso, 2009; Martin et al., 2013a,b), in association with a small group of taxa (Asnaghi et al., 2013) and at the community scale (Porzio et al., 2011; Kroeker et al., 2012; Cox et al., 2015, 2017a,b; Marchini et al., 2019). These investigations have focused on a few species, mainly restricted to the group

of (non-geniculate) crustose coralline algae (CCA), including epiphytic (on seagrass leaves) and engineering (coralligenous bio-constructors) species. Their response to ocean acidification and/or warming was studied through a variety of different approaches, including laboratory and field experiments, *in situ* observations in natural volcanic CO_2 vent sites, and *in situ* manipulations using a Free Ocean Carbon dioxide Enrichment (FOCE) system. This variety of approaches provides critical insights in the effects of climate-related stressors on corallines isolated from their surrounding environment and in more complex ecosystems or naturally variable environments.

Impacts of Current Warming on the Health and Survival of Mediterranean Coralline Algae

Although some corallines can adapt to their local environment and acclimatize to a novel thermal regime, as recently suggested for some tropical species able to cope with thermal stress (Siboni et al., 2015), Mediterranean corallines appear particularly sensitive to warming. Several observations have been reported in different localities of the northwestern Mediterranean after summer seasons characterized by positive thermal anomalies. CCA mortality was reported at down to 30 m depth in late summer 1999, when seawater temperature was higher than normal by 2–4°C (Cerrano et al., 2000). In the laboratory, long exposure to elevated temperature (25°C) during summer was the cause of increased frequency of tissue necroses and mortality in *Lithophyllum stictiforme* (as *L. cabiochae*, Martin and Gattuso, 2009). Diseases of corallines described as white band syndrome or white patch disease (**Figure 2**) have recently been reported associated with high seawater temperature in the northwestern Mediterranean (Hereu and Kersting, 2016). These diseases affected the encrusting *Lithophyllum incrustans*, *Mesophyllum alternans*, and *Neogoniolithon* sp., and the geniculate *Ellisolandia elongata*, *Jania rubens* and *Amphiroa rigida* at shallow depths. The emergence of these thermo-dependent diseases is one of the most serious threats to Mediterranean coralline-dominated communities in the context of climate change.

Physiological Response of Mediterranean Coralline Algae to Climate Change and Ocean Acidification

Temperature directly affects enzymatic processes and is a dominant factor in determining physiological rates in corallines (Lüning, 1990). Rising temperature, within the range of temperature experienced in natural habitats, is beneficial for coralline algae with an increase in photosynthetic and calcification rates (Martin et al., 2006, 2013a), but increased temperature above these levels is detrimental. For example, a +3°C increase in seawater temperature was beneficial to calcification in *Lithophyllum stictiforme* (as *L. cabiochae*) in winter, when temperature is lowest, but a +3°C above maximum summer temperature caused increased frequency of necroses and mortality, and subsequent net calcification drop and further dissolution (Martin and Gattuso, 2009).

Effects of thermal stress were studied by Nannini et al. (2015) in populations of *Ellisolandia elongata* from western Italy and by Guy-Haim et al. (2016) in populations from Israel. Nannini et al. (2015) compared growth and calcification in field specimens with specimens cultured at different temperatures. They reported that thallus extension was higher in culture than in the field; the carbonate mass in the field was higher than in cultured material after 2 and 4 months, but decreased after 6 months. Guy-Haim et al. (2016) measured primary production, respiration and calcification of *Ellisolandia elongata* in the temperature range 15–35°C. In the population examined, the alga consists of the typical frondose form at temperatures <23°C; above this temperature, it switches to a reduced crustose form with short erect axes, but photosynthesis and calcification occur optimally in the interval 15–31°C. Above 31°C there is a metabolic breakdown, with bleaching and tissue necrosis. The authors argued that in the eastern Mediterranean, with continued warming, the species will experience a westward range contraction with phenological shifts, performance, and reproduction declines, population decreases and possible local extinctions.

Decreasing pH in the sea surface will cause major shifts in seawater chemistry over the course of this century, with changes in the relative proportion of the three forms of dissolved inorganic carbon (DIC) species (HCO_3^-, CO_3^{2-}, and CO_2). These changes are likely to affect photosynthesis and calcification, since these physiological processes use DIC as substrate. Increase in CO_2 may be beneficial for photosynthesis in some primary producers but the decrease in pH and CO_3^{2-} may be detrimental for the precipitation of $CaCO_3$ in calcifiers (Koch et al., 2013). Most of the studies on coralline algae showed that calcification is negatively affected under elevated pCO_2 (Martin and Hall-Spencer, 2017) and that this effect is exacerbated by warming (Anthony et al., 2008). However, some work shows a significant pCO_2 effect on calcification only when this is combined with an increase in temperature (Martin and Gattuso, 2009). The physiological response of coralline algae to increased pCO_2 is variable among species (Martin and Hall-Spencer, 2017) and very few studies have focused on Mediterranean species. For *Lithophyllum stictiforme* (as *L. cabiochae*) Martin and Gattuso (2009) and Martin et al. (2013a) provided evidence of the ability to maintain or even enhance rate of calcification at near future levels of pCO_2 (700 ppm). Such response may be related to the ability of this species to maintain an elevated pH at the site of calcification, despite reduced external pH that would favor $CaCO_3$ precipitation (Cornwall et al., 2017).

The combination of ocean warming and acidification may cause a much greater effect on corallines. In healthy specimens of *L. stictiforme*, sensitivity of photosynthesis and calcification to high temperature increased in summer when combined with elevated pCO_2 (Martin et al., 2013a). In the geniculate *Ellisolandia elongata*, such combined changes in pH and temperature can impair algal growth (Marchini et al., 2019). The combined effects of ocean warming and acidification can also make corallines more sensitive to other environmental stressors as shown by Fine et al. (2017), who studied thermal tolerance and resilience to low pH, high

light intensity and desiccation in *Neogoniolithon brassica-florida*, an encrusting species acting as consolidator of vermetid reefs. This species resulted sensitive to increased light intensity, particularly in conditions of elevated temperature and low pH, with substantial decrease in photosynthetic performances; calcification was significantly impaired at lower pH. The authors concluded that this species is likely to lose its role of reef consolidator in future, mutated climatic conditions.

Effects of Climate Change and Ocean Acidification on the Mineralogy of Mediterranean Coralline Algae

Different forms of biogenic $CaCO_3$ have different solubilities in seawater (aragonite > calcite). In calcite, the replacement of some Ca^{2+} by Mg^{2+} increases solubility. High-Mg calcite (>8–12 mol% $MgCO_3$) is the most soluble $CaCO_3$ form (Morse et al., 2007) and coralline algae skeletons composed of 8–29 mol% $MgCO_3$ (Kamenos et al., 2013) are considered highly susceptible to dissolution in the context of ocean acidification. However, potential resilience of coralline algae may occur through changes in skeletal mineralogy, either by producing calcite with lower Mg content (Agegian, 1985; Egilsdottir et al., 2013) or by favoring accumulation of carbonate forms with lower solubility such as dolomite (Diaz-Pulido et al., 2014). However, recent studies on Mg incorporation in the skeleton of Mediterranean coralline algae found no pCO_2 effect. Acidification did not drive any significant change in the Mg content of *Lithophyllum stictiforme* grown experimentally at 700 ppm (Nash et al., 2016). Similarly, no pCO_2 effect was found on the Mg carbonate composition of *Posidonia oceanica* coralline epiphytes exposed to a decrease of 0.3 pH unit by using a FOCE system (Cox et al., 2017b). Kamenos et al. (2016) also found that CCA recruited on tiles had similar Mg content in ambient and low pH (7.8) sites in CO_2 vents off Ischia Island (Italy). This lack of a pCO_2 effect is consistent with findings suggesting that skeletal mineralogy may be under biological control (Nash et al., 2015). The high total alkalinity of Mediterranean waters (Palmiéri et al., 2015) may also have a potential role in buffering the effect of ocean acidification.

The Mg content in coralline algae is also known to vary as function of seawater temperature (Kamenos et al., 2008; Ragazzola et al., 2019). This has been confirmed in Mediterranean *Lithophyllum stictiforme*, for which the mineralogy is primarily controlled by temperature as shown experimentally with an increase of Mg incorporation of 1 mol% $MgCO_3$ for an increase of 3°C (Nash et al., 2016). The high vulnerability of Mediterranean CCA skeleton to dissolution was already shown by Martin et al. (2008) and Cox et al. (2015) near and below pH_T 7.7. Under experimental conditions of elevated temperature (+3°C) and elevated pCO_2 (700 ppm), the percentage of death for Mediterranean *Lithophyllum stictiforme* was 2- to 3-fold higher and was accompanied by a rate of dissolution of dead algal thalli 2- to 4- times higher (Martin and Gattuso, 2009), suggesting that net dissolution is likely to exceed net calcification in *L. stictiforme* by the end of this century.

Effects of Climate Change and Ocean Acidification on Early Life Stages of Mediterranean Coralline Algae

Early life stages of corallines are particularly vulnerable to ocean acidification. The first studies were conducted on tropical species and showed that recruitment was drastically reduced under elevated pCO_2 (Agegian, 1985; Kuffner et al., 2008).

In the Mediterranean, several studies were performed in CO_2 vents of Ischia (Italy), where pH decreases naturally along a gradient from ambient (pH_T 8.1) to very low pH (<7), in a range greater than expected under future climate scenarios. At these sites, the decrease in coralline cover with decreasing pH may be due to changes in physiological and competitive ability of these algae, but also to lowered reproduction (Porzio et al., 2011) or lowered recruitment (Kroeker et al., 2012). Decreased reproductive capacity has been reported for some coralline species. Cumani et al. (2010) showed in an artificial culture that CCA spore production and growth are inhibited by ocean acidification with an increase in the mortality of germination disks. Reduction in reproductive structures was also observed in the geniculate *Jania rubens* at pH 7.8 in CO_2 vents of Ischia (Porzio et al., 2011). Since these vents are open systems, the negative effects due to the lower capacity of reproduction may be masked in these sites due to the import of spores and zygotes from external or control nearby sites. In the CO_2 vents of Ischia, the recruitment of CCA appears to be inhibited at low pH. Changes in the succession of algae with a replacement of corallines by fleshy seaweeds were observed on settlement tiles at low pH (Porzio et al., 2011, 2013; Kroeker et al., 2012). The lowest pH (pH_T < 7.2) caused failure in coralline algal recruitment but the genera *Hydrolithon* and *Corallina* were still recruited under medium pH (pH_T 7.8; Porzio et al., 2013), suggesting that some species of corallines may be able to persist at pH levels expected for the end of this century. However, the high pH variability observed in the medium pH sites means that pH rises to/close to current pH levels regularly and may lead to an underestimation of the impact of acidification, as these sites are not remaining constantly under low pH conditions (Porzio et al., 2013). In the same area, Kamenos et al. (2016) observed that the largest individuals of CCA recruited on tiles maintained growth and were of similar size in low (7.8) and ambient (8.0–8.1) pH zones. The ability of some thalli to continue growing in lower pH suggests acclimation/adaptation to low pH conditions and ability to provide recruits for populations adapted to survive in lower pH environment in the future. Through *in situ* pH manipulation using a FOCE system in a *Posidonia oceanica* meadow, Cox et al. (2017a) also found that early stages of CCA are sensitive to decreased pH, with lower coverage of CCA on recruitment tiles placed in a pH-manipulated enclosure (−0.3 pH unit offset) compared to an un-manipulated enclosure (ambient pH). Although previous studies suggested post-settlement competition between fleshy and calcareous algae (Porzio et al., 2011; Kroeker et al., 2012; Kamenos et al., 2016), Cox et al. (2017a) suggested that losses of CCA were driven by taxa sensitivity, because the other taxa were also reduced by the lower pH conditions and there was still bare space available for colonization.

Field Assessment of the Impacts of Ocean Acidification on Mediterranean Coralline Algae

The responses of coralline algae to acidification can be altered by biotic (e.g., competition for space and resource or herbivory) and abiotic (e.g., irradiance or nutrient supply) interactions. Although most investigations on corallines were conducted in the laboratory with single taxa or relatively small groups of taxa isolated from the surroundings, some studies in the Mediterranean used whole ecosystem approaches (CO_2 vents or FOCE system) that allow to consider these interactions. These studies focused mostly on the epiphytic CCA in seagrass meadows. *In situ* observations near CO_2 vents reported clear reductions or losses of corallines where the pH is naturally lower (Hall-Spencer et al., 2008; Martin et al., 2008; Porzio et al., 2011; Kroeker et al., 2012; Baggini et al., 2014; Donnarumma et al., 2014). In the CO_2 vents of Ischia, Martin et al. (2008) showed a complete disappearance of epiphytic CCA on *Posidonia oceanica* at an average pH_T of 7.7, consistent with pH expected for the end of this century, but with large temporal pH variations from <7 to >8.1. Vent systems are not perfect predictors of future ocean ecology, due to the high pH variability in space and time that makes difficult to identify threshold or tipping points (Hall-Spencer et al., 2008; Kerrison et al., 2011). Recently, some studies reached conclusions in contrast with previous findings on ocean acidification projections. Cox et al. (2017b) found no pH effect on epiphytic CCA on *Posidonia oceanica* exposed to a decrease of −0.3 pH unit in a pH-manipulated enclosure using a FOCE system. Additional insights into community-level effects of warming and ocean acidification are beginning to emerge from longer-term multispecies laboratory experiments (Hale et al., 2011; Legrand et al., 2017). Similarly, Asnaghi et al. (2013) demonstrated that grazing activity exacerbated the effects of pCO_2 on corallines with higher weight loss in the geniculate *Ellisolandia elongata* under elevated pCO_2 in the presence of urchins. It is clear that the impact of global changes on corallines will depend on the combined influence of direct environmental effects on individual species and indirect effects mediated by changes in interspecific interactions (Harley et al., 2012). Long-term multispecies experiments combining warming and ocean acidification appear essential to improve our future understanding of Mediterranean coralline algae.

CONCLUSIONS AND DIRECTIONS FOR FUTURE WORK

The present summary shows that there are still substantial gaps in our knowledge of Mediterranean corallines, despite of the large amount of information available for some coralline-dominated habitats (particularly coralligenous). Giving the ecological importance of these algae and their sensitivity to climate change, the body of information available should be now substantially expanded.

As general recommendation, we suggest that future work on Mediterranean corallines should be based on a multidisciplinary perspective combining different approaches. So far, work on these algae has consisted mostly of separate efforts/projects, carried out by researchers working in different fields and interested in different aspects. The integration of different approaches will be essential, in particular, to address major large-scale and long-term issues, such as the responses of individual species and populations to future, mutated climatic scenarios. We also note that most of the information currently available for Mediterranean corallines has been produced by scientists based in a relatively small number of countries (mainly France, Italy and Spain). As consequence, the body of information available for the western Mediterranean is currently much larger than for the eastern Mediterranean. This represents a major limit for the interpretation of general patterns, especially for coralline species with distribution extending to the whole Mediterranean. Within a same species, populations from the western Mediterranean (especially northwestern) and from the eastern Mediterranean are presumably characterized by different ecophysiological traits and therefore are likely to respond differently to future climatic changes. Therefore, we suggest that future research on basic aspects of the biology of Mediterranean corallines should involve many scientists with different backgrounds, based in several countries, both in the western and eastern Mediterranean.

More specifically, there are some tasks that we identify as prioritary for each of the main fields of investigation:

1) Further paleontological investigations, focusing on identification of morpho-anatomical species groups with paleoecological and/or paleobiogeographical meanings, study of the evolution of Mediterranean coralline assemblages in the context of important paleogeographic changes, and how global environmental parameters such as sea-level, ocean acidification, and global temperature affected in the past the evolution of Mediterranean species.
2) An accurate taxonomic reassessment of the Mediterranean coralline flora based on a modern combination of molecular, morphoanatomical and ecological data. This is also a critical requirement for an accurate biogeographic reassessment. Taxa surrounded by taxonomic uncertainty or for which molecular data are lacking should receive priority; among these, we suggest:
   - *Neogoniolithon*, a genus for which the only species *N. brassica-florida* is currently recognized in the Mediterranean, but in which species circumscription is unclear (Kato et al., 2013).
   - Members of Sporolithales, for which there are no molecular data from Mediterranean collections.
   - Maerl/rhodolith-forming species for which no sequences are available (*Lithothamnion minervae*, *L. valens*), or for which conspecifity with Atlantic counterparts should be verified (*Lithothamnion corallioides*).
   - *Lithophyllum* of intertidal and shallow subtidal zones; these algae in the Mediterranean have been usually identified as *L. incrustans*, but the data of Hernandez-Kantun et al. (2015a) highlighted that this is mainly a subtidal species, suggesting that the identity of intertidal specimens requires reassessment.

- *Lithophyllum trochanter* and *L. woelkerlingii*, two species separated by Bressan and Cabioch (2004) based on subtle characters.

3) Studies of reproductive biology combining observations in the field and experiments in the laboratory with molecular and biochemical studies aiming to elucidate the mechanisms triggering fertility and release of reproductive cells.
4) Transcriptomic studies and characterization of associated microbiomes, starting from species important as bioconstructors or habitat-formers (*Lithophyllum stictiforme*, *L. byssoides*, *Ellisolandia elongata*). Investigations of this type are necessary for a deep understanding of the molecular and biochemical processes determining responses to environmental disturbances, and for early detection of stress in populations of ecologically important species.
5) Extending studies on the effects of climate change and acidification to a wider set of species, and expanding them to long-term experimental investigations. We suggest that *Mesophyllum* species contributing to coralligenous concretions, maerl/rhodolith-forming species (*Lithophyllum racemus*, *Lithothamnion corallioides*, *L. minervae*, *L. valens*, *Phymatolithon calcareum*) and bioconstructor species of the intertidal/shallow subtidal zone (*Lithophyllum byssoides*, *L. trochanter*) are natural candidates for such studies. New studies focusing on the main aspects (physiology, mineralogy, vitality of early life stages) in which Mediterranean corallines may be affected by climate change and ocean acidification will represent valuable contributions.
6) Basic studies on mineralization. The complete lack of information for Mediterranean species is striking, considering the importance of this aspect for growth, carbonate formation, and bioconstruction activity of these algae.
7) Accurate phylogeographic studies based on high-resolution genetic methods, such as microsatellites, Single Nucleotide Polymorphisms (SNPs) or sequencing of Restriction Site Associated DNA markers (RAD), starting from ecologically significant species (*Lithophyllum stictiforme*, *L. byssoides*, *Mesophyllum expansum*, *Ellisolandia elongata*, *Lithothamnion corallioides*). Data of this type are essential to draw effective conservation measures for marine species. It is striking that in general studies of this type are in great shortage for Mediterranean seaweeds (ironically, from this point of view some introduced taxa have been so far the best-studied seaweeds in the Mediterranean). This is even more surprising considering that, in contrast, the amount of similar studies concerning Mediterranean fishes and invertebrates is ponderous (see Patarnello et al., 2007; Pascual et al., 2017).

We remark that these tasks can be best tackled by integrating the work in each specific field with other types of data/approaches. The integration of basic ecological, physiological and biochemical work with genomics, taxonomy and molecular phylogeny will be especially important to predict both changes in distribution and abundance of individual coralline species, and shifts in the structure of Mediterranean ecosystems built or dominated by corallines. This will be mandatory when the corallines studied turn to be complexes of cryptic species that differ in ecological and physiological traits, as recently stressed by De Jode et al. (2019). In general, cryptic diversity in corallines is an aspect that in the future will require much more attention from Mediterranean marine biologists. Neglecting it might lead to erroneous interpretations of the results of studies in many different fields. At ecosystem level, changes in diversity of coralline assemblages, if undetected due to the cryptic nature of the species involved, may lead to shifts in ecosystem structure and functioning (Hind et al., 2019).

Even for this reason, we recommend that all future studies on Mediterranean corallines (of any type, not just taxonomic) should base their identifications on DNA sequence data and take care to deposit voucher specimens in herbaria or other permanent collections. This will give the possibility to verify the correctness of the identifications, which will be a critically important requirement for comparison of the results of different studies.

AUTHOR CONTRIBUTIONS

FR led the conceptual design of the paper, contributed to the writing of the sections Introduction, Historical Summary, Floristic Diversity, Molecular Studies of Mediterranean Corallines, Present-Day Distribution and Biogeography, Reproductive Biology, Microbiomes of Mediterranean Corallines, Biochemistry and Physiology, and Conclusions and Directions for Future Work, assembled the first version of the manuscript, and prepared the **Table 1**, the **Figures 1**, **2**, and **3**, and the **File SM1**. JA and JB wrote the section Geological History of the Mediterranean and Paleontological Record of Mediterranean Corallines, and prepared the **Figure 5** and the **Files SM2** – **SM6**. SM wrote the section Responses of Mediterranean Corallines to Climate Change and Ocean Acidification. VP, LG, and AC contributed to the writing of the sections Introduction, Historical Summary, Floristic Diversity, Molecular Studies of Mediterranean Corallines, Present-Day Distribution and Biogeography, and Conclusions and Directions for Future Work. AC prepared the **Figure 4**. VP prepared the **Table S1**.

ACKNOWLEDGMENTS

We are grateful to Enric Ballesteros, Marc Verlaque, Carlo Cerrano, Maria Cristina Gambi, and Sara Kaleb for kindly allowing use of pictures. The ideas presented in this article are partially based on results produced in a P.R.I.N. 2010–2011 project (Coastal bioconstructions: structure, function and management), for which FR acknowledges financial support from the Italian Ministry for Education, Universities and Research. VP acknowledges support from the Universidade da Coruña (Programa Campus Industrial de Ferrol).

SUPPLEMENTARY MATERIAL

The Supplementary Material for this article can be found online at: https://www.frontiersin.org/articles/10.3389/fmars.2019.00723/full#supplementary-material

Table S1 | Detail of DNA sequence data obtained from Mediterranean corallines.

File SM1 | List of references used for the compilation of the bibliographic summary of Mediterranean corallines.

File SM2 | List of fossil corallines reported from the Mediterranean area.

File SM3 | Records of fossil Sporolithales reported for the Mediterranean area.

File SM4 | Records of fossil Hapalidiales reported for the Mediterranean area.

File SM5 | Records of fossil Corallinales reported for the Mediterranean area.

File SM6 | List of references for supplementary files SM2, SM3, SM4, and SM5.

REFERENCES

Abdallah, M. A. M., and Abdallah, A. M. A. (2008). Biomonitoring study of heavy metals in biota and sediments in the South Eastern coast of Mediterranean Sea, Egypt. *Environ. Monitor. Assess.* 146, 139–145. doi: 10.1007/s10661-007-0066-8

Abd-Elnaby, H. (2010). Bacteria-algae interactions in Abu-Qir marine ecosystem and some applied aspects of algal extracts. *J. Appl. Sci. Res.* 6, 345–357.

Adey, W. H., Hernandez-Kantun, J. J., Johnson, G., and Gabrielson, P. W. (2015). DNA sequencing, anatomy, and calcification patterns support a monophyletic, subarctic, carbonate reef-forming *Clathromorphum* (Hapalidiaceae, Corallinales, Rhodophyta). *J. Phycol.* 51, 189–203. doi: 10.1111/jpy.12266

Agegian, C. R. (1985). *The biogeochemical ecology of porolithon gardineri (Foslie)* (Ph.D. thesis). University of Hawaii, Honolulu, Hawaii.

Aguirre, J. (1998). El Plioceno marino del SE de la Península Ibérica (provincia de Almería). Síntesis estratigráfica, sedimentaria, bioestratigráfica y paleogeográfica. *Rev. Soc. Geol. España* 11, 297–315.

Aguirre, J., Baceta, J. I., and Braga, J. C. (2007). Recovery of primary marine producers after the Cretaceous-Tertiary mass extinction: paleocene calcareous red algae from the Iberian Peninsula. *Palaeogeog. Palaeoclimatol. Palaeoecol.* 249, 393–411. doi: 10.1016/j.palaeo.2007.02.009

Aguirre, J., Belaústegui, Z., Domènech, R., Gibert, J. M., and de Martinell, J. (2014). Snapshot of a lower pliocene dendropoma reef from sant onofre (Baix Ebre Basin, Tarragona, NE Spain). *Palaeogeog. Palaeoclimatol. Palaeoecol.* 395, 9–20. doi: 10.1016/j.palaeo.2013.12.011

Aguirre, J., Braga, J. C., Martín, J. M., and Betzler, C. (2012). Palaeoenvironmental and stratigraphic significance of Pliocene rhodolith beds and coralline algal bioconstructions from the Carboneras Basin (SE Spain). *Geodiversitas* 34, 115–136. doi: 10.5252/g2012n1a7

Aguirre, J., and Jiménez, A. P. (1998). Analogues of present-day *Cladocora caespitosa* coral banks; sedimentary setting, dwelling community, and taphonomy (late Pliocene, W Mediterranean). *Coral Reefs* 17, 203–213. doi: 10.1007/s003380050119

Aguirre, J., Riding, R., and Braga, J. C. (2000a). Diversity of coralline red algae: origination and extinction patterns from the early cretaceous to the pleistocene. *Paleobiology* 26, 651–667. doi: 10.1666/0094-8373(2000)026<0651:DOCRAO>2.0.CO;2

Aguirre, J., Riding, R., and Braga, J. C. (2000b). Late Cretaceous incident light reduction: evidence from benthic algae. *Lethaia* 33, 205–213. doi: 10.1080/00241160025100062

Airoldi, M. (1932). Contributo allo studio delle corallinacee del terziario italiano. 1. Le Corallinacee dell'Oligocene Ligure-Piemontese. Palaeontogr. *Ital., Mem. Paleont.* 33, 55–83.

Al-Masri, M. S., Mamish, S., and Budier, Y. (2003). Radionuclides and trace metals in eastern Mediterranean Sea algae. *J. Environ. Riadioactiv.* 67, 157–168. doi: 10.1016/S0265-931X(02)00177-7

Anagnostou, E., John, E., Edgar, K., Foster, G., Ridgwell, A., Inglis, G., et al. (2016). Changing atmospheric CO_2 concentration was the primary driver of early Cenozoic climate. *Nature* 533, 380–384. doi: 10.1038/nature17423

Anthony, K. R. N., Kline, D. I., Diaz-Pulido, G., Dove, S., and Hoegh-Guldberg, O. (2008). Ocean acidification causes bleaching and productivity loss in coral reef builders. *Proc. Nat. Acad. Sci. U.S. A.* 105, 17442–17446. doi: 10.1073/pnas.0804478105

Arias, C., Masse, J. P., and Vilas,. L. (1995). Hauterivian shallow marine calcareous biogenic mounds: S. E. Spain. *Palaeogeog. Palaeoclimatol. Palaeoecol.* 119, 3–17. doi: 10.1016/0031-0182(95)00056-9

Aroldi, C., and Bucur, I. I. (2002). Palaeogene microfacies in some calcareous blocks of the Roaia Formation (Wildflysch Nappe – Maramures). *Stud. Univ. Babes-Bolyai Geol. Ep. Issue* 1, 13–30.

Asnaghi, V., Chiantore, M., Mangialajo, L., Gazeau, F., Francour, P., Alliouane, S., et al. (2013). Cascading effects of ocean acidification in a rocky subtidal community. *PLoS ONE* 8:e61978. doi: 10.1371/journal.pone.0061978

Athanasiadis, A. (1989). North Aegean marine algae. III. Structure and development of the encrusting coralline *Titanoderma cystoseirae* (Rhodophyta, Lithophylloideae). *Nord. J. Bot.* 9, 435–441. doi: 10.1111/j.1756-1051.1989.tb01023.x

Athanasiadis, A. (1995). Morphology, anatomy and reproduction of the eastern Mediterranean coralline *Tenarea tortuosa* and its relationship to members of the Lithophylloideae and Mastophoroideae (Rhodophyta, Corallinales). *Nord. J. Bot.* 15, 655–663. doi: 10.1111/j.1756-1051.1995.tb02136.x

Athanasiadis, A. (1997). On the typification and taxonomic status of *Melobesia notarisii* Dufour (Rhodophyta, Corallinales). *Phycologia* 36, 410–415. doi: 10.2216/i0031-8884-36-5-410.1

Athanasiadis, A. (1999a). The taxonomic status of *Lithophyllum stictaeforme* (Rhodophyta, Corallinales) and its generic position in light of phylogenetic considerations. *Nord. J. Bot.* 19, 735–745. doi: 10.1111/j.1756-1051.1999.tb00682.x

Athanasiadis, A. (1999b). *Mesophyllum macedonis*, nov. sp. (Rhodophyta, Corallinales), a putative Tethyan relic in the North Aegean Sea. *Eur. J. Phycol.* 34, 239–252. doi: 10.1017/S0967026299002103

Athanasiadis, A., and Neto, A. I. (2010). On the occurrence of *Mesophyllum expansum* (Philippi) Cabioch et Mendoza (Melobesioideae, Corallinales, Rhodophyta) in the Mediterranean Sea, the Canary Isles and the Azores. *Bot. Mar.* 53, 333–341. doi: 10.1515/BOT.2010.042

Baggini, C., Salomidi, M., Voutsinas, E., Bray, L., Krasakopoulou, E., and Hall-Spencer, J. M. (2014). Seasonaility affects macroalgal community response to increases in pCO_2. *PLoS ONE* 9:e106520. doi: 10.1371/journal.pone.0106520

Bailey, J. C., and Chapman, R. L. (1996). "Evolutionary relationships among coralline red algae (Corallinaceae, Rhodophyta) determined by 18S rRNA gene sequence analysis", in *Cytology, Genetics and Molecular Biology of Algae,* eds B. R. Chaudhary and S. B. Agrawal (Amsterdam: SPB Academic Publishing), 363–376.

Bailey, J. C., and Chapman, R. L. (1998). A phylogenetic study of the Corallinales (Rhodophyta) based on nuclear small-subunit rRNA gene sequences. *J. Phycol.* 34, 692–705. doi: 10.1046/j.1529-8817.1998.340692.x

Ballesteros, E. (1988). Composiciòn y estructura de la comunidad de *Corallina elongata* Ellis and Solander, 1786, de la Costa Brava (Mediterraneo occidental). *Inv. Pesq.* 52, 135–151.

Ballesteros, E. (2006). Mediterranean coralligenous assemblages: a synthesis of present knowledge. *Oceanogr. Mar. Biol. Ann. Rev.* 44, 123–195. doi: 10.1201/9781420006391.ch4

Barattolo, F., Bassi, D., and Romano, R. (2007). Upper Eocene larger foraminiferal–coralline algal facies from the Klokova Mountain (southern continental Greece). *Facies* 53, 361–375. doi: 10.1007/s10347-007-0108-2

Barrier, E., Vrielynck, B., Bergerat, F., Brunet, M.-F., Mosar, J., Poisson, A., et al. (2018). *Palaeotectonic Maps of the Middle East: Tectono-Sedimentary-Palinspastic Maps From Late Norian to Pliocene*. Commission for the Geological Map of the World (CGMW / CCGM), Paris, France.

Bassi, D. (1998). Coralline algal facies and their palaeoenvironments in the Late Eocene of Northern Italy (Calcare di Nago). *Facies* 39, 179–202. doi: 10.1007/BF02537016

Bassi, D., Braga, J. C., and Iryu, Y. (2009). Palaeobiogeographic patterns of a persistent monophyletic ineage: *Lithophyllum pustulatum* species group (Corallinaceae, Corallinales, Rhodophyta). *Palaeogeogr. Palaeoclimatol. Palaeoecol.* 284, 237–245. doi: 10.1016/j.palaeo.2009.10.003

Bassi, D., Braga, J. C., Zakrevskaya, E., and Radionova, E. P. (2005). Re-assessment of the type collections of corallinalean genera (Corallinales, Rhodophyta) described by Maslov (1935–1962). *Palaeontology* 48, 1–17. doi: 10.1111/j.1475-4983.2005.00503.x

Bassi, D., Simone, L., and Nebelsik, J. H. (2017). "Re-sedimented rhodoliths in channelized depositional systems", in *Rhodolith/Maërl Beds: A Global Perspective,* eds. R. Riosmena-Rodríguez, W. Nelson, and J. Aguirre (Basel: Springer International Publishing), 139–167. doi: 10.1007/978-3-319-29315-8_6

Basso, D. (1995). Living calcareous algae by a paleontological approach: the genus *Lithothamnion* Heydrich nom. cons. from the soft bottoms of the Tyrrhenian Sea (Mediterranean). *Riv. It. Paleont. Strat*. 101, 349–366.

Basso, D., Babbini, L., Ramos-Esplá, A. R., and Salomidi, M. (2017). "Mediterranean rhodolith beds" in *Rhodolith/Maërl Beds: a Global Perspective,* eds R. Riosmena-Rodriguez, W. Nelson, and J. Aguirre (Basel: Springer International Publishing), 281–298. doi: 10.1007/978-3-319-29315-8_11

Basso, D., Caronni, S., Caragnano, A., Hereu, B., Angeletti, L., and Bracchi, V. (2018). "Evidence of coralline white patch disease in a rhodolith bed of the Egadi Islands," in *Abstract Book, VI International Rhodolith Workshop (Roscoff), 60.*

Basso, D., Coletti, G., Bracchi, V. A., and Yazdi-Moghadam, M. (2019). Lower oligocene coralline algae of the Uromieh section (Qom Formation, NW Iran) and the oldest record of *Titanoderma pustulatum* (Corallinophycidae, Rhodophyta). *Riv. It. Paleontol. Stratig*. 125, 197–218.

Basso, D., Fravega, P., and Vannucci, G. (1996). Fossil and living corallinaceans related to the Mediterranean endemic species *Lithophyllum racemus* (Lamarck) Foslie. *Facies* 35, 257–292. doi: 10.1007/BF02536965

Basso, D., and Rodondi, G. (2006). A Mediterranean population of *Spongites fruticulosus* (Rhodophyta, Corallinales), the type species of *Spongites*, and the taxonomic status of *S. stalactitica* and *S. racemosa. Phycologia* 45, 403–416. doi: 10.2216/04-93.1

Basso, D., Rodondi, G., and Bressan, G. (2011). A re-description of *Lithothamnion crispatum* and the status of *Lithothamnion superpositum* (Rhodophyta, Corallinales). *Phycologia* 50, 144–155. doi: 10.2216/10-20.1

Basso, D., Rodondi, G., and Mari, M. (2004). A comparative study between *Lithothamnion minervae* and the type material of *Myllepora fasciculata* (Corallinales, Rhodophyta). *Phycologia* 43, 215–223. doi: 10.2216/i0031-8884-43-2-215.1

Bianchi, C. N., and Morri, C. (2000). Marine biodiversity of the Mediterranean Sea: situation, problems and prospects for future research. *Mar. Poll. Bull*. 40, 367–376. doi: 10.1016/S0025-326X(00)00027-8

Bittner, L., Payri, C., Maneveldt, G., Couloux, A., Cruaud, C., de Reviers, B., et al. (2011). Evolutionary history of the Corallinales (Corallinophycidae, Rhodophyta) inferred from nuclear, plastidial and mitochondrial genomes. *Mol. Phylogen. Evol*. 61, 697–713. doi: 10.1016/j.ympev.2011.07.019

Blanfuné, A. (2016). *Global change in the NW mediterranean sea: the fate of forests of Cystoseira and Sargassum, Lithophyllum rims and blooms of ostreopsis* (Ph.D. thesis). Université d'Aix-Marseille, Marseilles, France.

Bory de Saint-Vincent, J. B. G. M. (1832). "Notice sur les polypiers de la Gréce," in Expédition Scientifique de Morée (Section des Sciences Physiques). Tome III [1.re Partie, 1.re Section]. Zoologie [pl. LIV - Atlas] (Paris; Strasbourg: F.G. Levrault, imprimeur-libraire), 204-209,

Bosellini, F. R., and Perrin, C. (2008). Estimating mediterranean oligocene-miocene sea-surface temperatures: an approach based on coral taxonomic richness. *Palaeogeogr. Palaeoclimatol. Palaeoecol.* 258, 71–88. doi: 10.1016/j.palaeo.2007.10.028

Bosellini, F. R., and Russo, A. (1992). Stratigraphy and facies of an oligocene fringing reef (Castro Limestone, Salento Peninsula, Southern Italy). *Facies* 26, 145–166. doi: 10.1007/BF02539798

Bosence, D. W. J. (1976). Ecological studies on two unattached coralline algae from western Ireland. *Palaeontology* 19, 365–395.

Bosence, D. W. J., and Pedley, H. M. (1982), Sedimentology and palaeoecology of a Miocene coralline algal biostrome from the Maltese Islands. *Palaeogeog. Palaeoclimatol. Palaeoecol*. 38, 9–43. doi: 10.1016/0031-0182(82)90062-1

Boudouresque, C. F. (2004). Marine biodiversity in the Mediterranean: status of species, populations and communities. *Trav. Sci. Parc Nat. Port-Cros* 20, 97–146.

Boudouresque, C. F., and Verlaque, M. (1978). Végétation marine de la Corse (Méditerranée). Documents pour la flore des algues. *Bot. Mar*. 21, 265–275. doi: 10.1515/botm.1978.21.5.265

Bover-Arnal, T., Ferràndez-Cañadell, C., Aguirre, J., Esteban, M., Fernández-Carmona, J., Albert-Villanueva, E., et al. (2017). Late Chattian platform carbonates with benthic foraminifera and coralline algae from the SE Iberian Plate. *Palaios* 32,61–82. doi: 10.2110/palo.2016.007

Bracchi, V. A., Angeletti, L., Marchese, F., Taviani, M., Cardone, F., Hajdas, I., et al. (2019a). A resilient deep-water rhodolith bed off the Egadi Archipelago (Mediterranean Sea) and its actuopaleontological significance. *Alp. Medit. Quat.* 32, 1–20. doi: 10.26382/AMQ.2019.09

Bracchi, V. A., and Basso, D. (2012). The contribution of calcareous algae to the biogenic carbonates of the continental shelf: Pontian Islands, Tyrrhenian Sea, Italy. *Geodiversitas* 34, 61–76. doi: 10.5252/g2012n1a4

Bracchi, V. A., Basso, D., Savini, A., and Corselli, C. (2019b). Algal reefs (Coralligenous) from glacial stages: origin and nature of a submerged tabular relief (Hyblean Plateau, Italy). *Mar. Geol*. 411, 119–132. doi: 10.1016/j.margeo.2019.02.008

Braga, J. C. (2017). "Neogene rhodoliths in the Mediterranean basins", in *Rhodolith/Maërl Beds: A Global Perspective,* eds R. Riosmena-Rodríguez, W. Nelson, and J. Aguirre (Basel: Springer Inter. Publ.), 169–193. doi: 10.1007/978-3-319-29315-8_7

Braga, J. C., and Aguirre, J. (2001). Coralline algal assemblages in upper Neogene reef and temperate carbonates in Southern Spain. *Palaeogeogr. Palaeoclimatol. Palaeoecol*. 175, 27–41. doi: 10.1016/S0031-0182(01)00384-4

Braga, J. C., and Bassi, D. (2007). Neogene history of *Sporolithon* Heydrich (Corallinales, Rhodophyta) in the Mediterranean region. *Palaeogeogr. Palaeoclimatol. Palaeoecol*. 243, 189–203. doi: 10.1016/j.palaeo.2006.07.014

Braga, J. C., and Bassi, D. (2011). Facies and coralline algae from Oligocene limestones in the Malaguide Complex (SE Spain). *Ann. Naturhist. Mus. Wien Serie A* 113, 291–308.

Braga, J. C., Bassi, D., and Piller, W. (2010). "Palaeoenvironmental significance of Oligocene-Miocene coralline red algae - a review," in *Carbonate Systems During the Oligocene-Miocene Climatic Transition,* Vol. 42. eds M. Mutti, W. E. Piller, and C. Betzler (Oxford; Chichester; Hoboken, NJ: IAS Spec. Publ.; Wiley-Blackwell), 165–182. doi: 10.1002/9781118398364.ch10

Braga, J. C., Vescogni, A., Bosellini, F., and Aguirre, J. (2009). Coralline algae (Corallinales, Rhodophyta) in western and central Mediterranean Messinian reefs. *Palaeogeogr. Palaeoclimatol. Palaeoecol*. 275, 113–128. doi: 10.1016/j.palaeo.2009.02.022

Brandano, M. (2017). "Oligocene rhodolith beds in the central Mediterranean area", in *Rhodolith/Maërl Beds: A Global Perspective,* eds R. Riosmena-Rodríguez, W. Nelson, and J. Aguirre (Basel: Springer Inter. Publ.), 195–219. doi: 10.1007/978-3-319-29315-8_8

Bressan, G. (1974). Rodoficee calcaree dei mari italiani. *Boll. Soc. Adr. Sci Nat*. 54, 1–132.

Bressan, G., and Babbini, L. (1995). Inventario delle Corallinales del Mar Mediterraneo: considerazioni tassonomiche. *Giorn. Bot. It.* 129, 367–390. doi: 10.1080/11263509509436152

Bressan, G., and Babbini, L. (2003). Corallinales del Mar Mediterraneo: guida alla determinazione. *Biol. Mar. Medit*. 10, 1–237.

Bressan, G., and Babbini-Benussi, L. (1996). Phytoceanographical observations on coralline algae (Corallinales) in the Mediterranean Sea. *Rend. Fis. Acc. Lincei* 7, 179–207. doi: 10.1007/BF03001802

Bressan, G., and Cabioch, J. (2004). *Titanoderma trochanter* (Bory) Benhissoune, Boudouresque, Perret Boudouresque et Verlaque, et *Titanoderma ramosissimum* (Heydrich) comb. nov. (Corallinales, Rhodophytes) une redefinition. *Cah. Biol. Mar*. 45, 225–242.

Bressan, G., Chemello, R., Gravina, M. F., Gambi, M. C., Peirano, A., Cocito, S., et al. (2009). "Other types of bioconcretions" in *Italian habitats - Marine bioconstructions*, eds A. Cosentino, A. La Posta, C. Morandini, and G. Muscio (Udine: Museo Friulano di Storia Naturale), 89–150.

Bressan, G., Miniati-Radin, D., and Smundin, L. (1977). Ricerche sul genere *Fosliella* (Corallinaceae - Rhodophyta): *Fosliella cruciata* sp.nov. *Giorn. Bot. It*. 111, 27–44. doi: 10.1080/11263507709426571

Brodie, J., Walker, R. H., Williamson, C., and Irvine, L. M. (2013). Epitypification and redescription of *Corallina officinalis* L., the type of the genus, and *C. elongata* Ellis et Solander (Corallinales, Rhodophyta). *Cryptog. Algol*. 34, 49–56. doi: 10.7872/crya.v34.iss1.2013.49

Brodie, J., Williamson, C., Barker, G. L., Walker, R. H., Briscoe, A., and Yallop, M. (2016). Characterising the microbiome of *Corallina officinalis*, a dominant calcified intertidal red alga. *FEMS Microbiol. Ecol.* 92:fiw110. doi: 10.1093/femsec/fiw110

Bucur, I. I. (1994). Algues calcaires de la zone de Resita-Moldova Noua (Carpathes meridionales, Roumanie). *Rev. Paléobiol.* 13, 147–209.

Bucur, I. I. (2008). Barremian-Aptian calcareous algae from Romania: an overview. *Boll. Soc. Geol. It.* 127, 245–255.

Bucur, I. I., and Baltres, A. (2002). Cenomanian microfossils in the shallow water limestones from Babadag Basin: biostratigraphic significance. *Stud. Univ. Babes-Bolyai, Geol.* 1, 79–95.

Bucur, I. I., Onac, B. P., and Todoran, V. (1989). *Algues Calcaires dans les Dépôts Oligocènes Inférieurs de la Région Purcâret-Mesteacân-Valea Chioarului (NW du Bassin de Transylvanie).* The Oligocene from the Transylvanian Basin (Petrescu-Iustinian Editions, Univ. Cluj-Napoca, Cluj-Napoca), 141–148.

Bustamante, D. E., Calderon, M. S., and Hughey, J. R. (2019). Conspecifity of the Peruvian Corallina ferreyrae with *C. caespitosa* (Corallinaceae, Rhodophyta) inferred from genomic analysis of the type specimen. *Mitochondrial DNA* 4, 1285–1286. doi: 10.1080/23802359.2019.1591203

Cabioch, J., and Mendoza, M. L. (1998). Mesophyllum alternans (Foslie) comb. nov. (Corallinales, Rhodophyta), a mediterraneo-atlantic species, and new considerations on the Lithothamnion philippii Foslie complex. *Phycologia* 37, 208–221. doi: 10.2216/i0031-8884-37-3-208.1

Cabioch, J., and Mendoza, M. L. (2003). *Mesophyllum expansum* (Philippi) comb. nov. (Corallinales, Rhodophytes), et mise au point sur les *Mesophyllum* des mers d'Europe. *Cah. Biol. Mar.* 44, 257–273.

Canals, M., and Ballesteros, E. (2007). Production of carbonate particles by phytobenthic communities on the Mallorca-Menorca shelf, northwestern Mediterranean Sea. *Deep Sea Res.* 44, 611–629. doi: 10.1016/S0967-0645(96)00095-1

Catra, M., Alongi, G., Serio, D., Cormaci, M., and Furnari, G. (2006). The benthic algal flora on rocky substrata of the Egadi islands, a marine protected archipelago off the western coast of Sicily (Italy, Mediterranean Sea). *Nova Hedwigia* 82, 489–538. doi: 10.1127/0029-5035/2006/0082-0489

Cavalcanti, G. S., Gregoracci, G. B., dos Santos, E. O., Silveira, C. B., and Meirelles, P. M. (2014). Physiologic and metagenomic attributes of the rhodoliths forming the largest $CaCO_3$ bed in the South Atlantic Ocean. *ISME J.* 8, 52–62. doi: 10.1038/ismej.2013.133

Cebrián, E., Ballesteros, E., and Canals, M. (2000). Shallow rocky bottom benthic assemblages as calcium carbonate producers in the Alboran Sea (southwestern Mediterranean). *Oceanol. Acta* 23, 311–322. doi: 10.1016/S0399-1784(00)00131-6

Cecere, E., Cormaci, M., Furnari, G., Petrocelli, A., Saracino, O., and Serio, D. (1996). Benthic algal flora of Cheradi Islands (Gulf of Taranto, Mediterranean Sea). *Nova Hedwigia* 62, 191–214.

Celis-Plá, P. S. M., Martínez, B., Quintano, E., García-Sánchez, M., Pedersen, A., et al. (2014). Short-term ecophysiological and biochemical responses of *Cystoseira tamariscifolia* and *Ellisolandia elongata* to environmental changes. *Aquat. Biol.* 22, 227–243. doi: 10.3354/ab00573

Cerrano, C., Bavestrello, G., Bianchi, C. N., Cattaneo-Vietti, R., Bava, S., Morganti, C., et al. (2000). A catastrophic mass-mortality episode of gorgonians and other organisms in the Ligurian Sea (NW Mediterranean), summer 1999. *Ecol. Lett.* 3, 284–293. doi: 10.1046/j.1461-0248.2000.00152.x

Chamberlain, Y. M. (1985). The typification of *Melobesia membranacea* (Esper) Lamouroux (Rhodophyta, Corallinaceae). *Taxon* 34, 673–677. doi: 10.2307/1222213

Chamberlain, Y. M. (1997). Observations on *Lithophyllum lichenoides* Philippi (Rhodophyta, Corallinaceae) and its reproductive structures. *Cryptog. Algol.* 18, 139–149.

Chatalov, A., Bonev, N., and Ivanova, D. (2015). Depositional characteristics and constraints on the mid-Valanginian demise of a carbonate platform in the intra-Tethyan domain, Circum-Rhodope Belt, northern Greece. *Cret. Res.* 55, 84–115. doi: 10.1016/j.cretres.2015.02.001

Checconi, A. (2006). *Le Associazioni ad Alghe Calcaree Corallinacee (Corallinales, Rhodophyta) delle Successioni Carbonatiche d'acqua Bassa del Miocene Inferiore-Medio dell'Appennino Meridionale (Formazione di Cusano): analisi paleoecologica e paleoambientale* (Ph.D. thesis). Università degli Studi di Perugia, Perugia, Italy.

Checconi, A., Bassi, D., Passeri, L., and Rettori, R. (2007). Coralline red algal assemblage from the Middle Pliocene shallow-water temperate carbonates of the Monte Cetona (Northern Apennines, Italy). *Facies* 53, 57–66. doi: 10.1007/s10347-006-0085-x

Coletti, G., Basso, D., and Corselli, C. (2018a). Coralline algae as depth indicators in the Sommières Basin (early Miocene, southern France). *Geobios* 51, 15–30. doi: 10.1016/j.geobios.2017.12.002

Coletti, G., Bracchi, V. A., Marchese, F., Basso, D., Savini, A., Vertino, A., et al. (2018b). Quaternary build-ups and rhodalgal carbonates along the Adriatic and Ionian coasts of the Italian Peninsula: a review. *Riv. It. Paleontol. Stratig.* 124, 387–406. doi: 10.13130/2039-4942/10269

Coll, M., Piroddi, C., Steenbek, J., Kaschner, K., Lasram, F. B. R., Aguzzi, J., et al. (2010). The biodiversity of the Mediterraneran Sea: estimates, patterns and threats. *PLoS ONE* 5:e11842. doi: 10.1371/journal.pone.0011842

Coma, R., Ribes, M., Serrano, E., Jiménez, E., Salat, J., and Pascual, J. (2009). Global warming-enhanced stratification and mass mortality events in the Mediterranean. *Proc. Nat. Acad. Sci U.S.A.* 106, 6176–6181. doi: 10.1073/pnas.0805801106

Conrad, M. A., and Masse, J. P. (1989). Les algues calcaires des formations carbonatées de l'Hauterivien-Barrémien pro partedu Jura vaudois et neuchâtelois (Suisse). *Mém. Soc. Neuchâteloise Sci. Nat.* 11, 277–290.

Conti, S. (1950). Alghe Corallinacee fossili. *Pubbl. Ist. Geol. Univ. Genova, Quad.* 4 ser. A, 1–156.

Coppejans, E. (1978). Sur les propagules de *Fosliella farinosa* (Lamouroux) Howe var. *farinosa* (Rhodophyceae - Cryptonemiales). *Bull. Soc. Roy. Bot. Belg.* 111, 55–61.

Cormaci, M., and Furnari, G. (1988). Sulla presenza nell'Italia meridionale di alcune alghe marine bentoniche rare per il Mediterraneo. *Giorn. Bot. Ital.* 122, 215–226. doi: 10.1080/11263508809429401

Cormaci, M., Furnari, G., and Alongi, G. (2017). Flora marina bentonica del Mediterraneo: Rhodophyta (*Rhodymeniophycidae* escluse). *Boll. Acc. Gioenia Sci. Nat.* 50, 1–391.

Cormaci, M., Furnari, G., Alongi, M., Catra, M., and Serio, D. (2000). The benthic algal flora on rocky substrata of the Tremiti Islands (Adriatic Sea). *Plant Biosyst.* 134, 133–152. doi: 10.1080/11263500012331358404

Cormaci, M., Lanfranco, E., Borg, J. A., Buttigieg, S., Furnari, G., Micallef, S. A., et al. (1997). Contribution to the knowledge of benthic marine algae on rocky substrata of the Maltese Islands (Mediterranean Sea). *Bot. Mar.* 40, 203–215. doi: 10.1515/botm.1997.40.1-6.203

Cornwall, C. E., Comeau, S., and McCulloch, M. T. (2017). Coralline algae elevate pH at the site of calcification under ocean acidification. *Glob. Change Biol.* 23, 4245–4256. doi: 10.1111/gcb.13673

Cox, T. E., Díaz-Castañeda, V., Martin, S., Alliouane, S., Mahacek, P., Le Fur, A., et al. (2017a). Effects of in situ CO_2 enrichment on epibiont settlement on artificial substrata within a *Posidonia oceanica* meadow. *J. Exp. Mar. Biol. Ecol.* 497, 197–211. doi: 10.1016/j.jembe.2017.10.003

Cox, T. E., Nash, M., Gazeau, F., Déniel, M., Legrand, E., Alliouane, S., et al. (2017b). Effects of in situ CO_2 enrichment on *Posidonia oceanica* epiphytic community composition and mineralogy. *Mar. Biol.* 164:103. doi: 10.1007/s00227-017-3136-7

Cox, T. E., Schenone, S., Delille, J., Díaz-Castañeda, V., Alliouane, S., Gattuso, J. P., et al. (2015). Effects of ocean acidification on *Posidonia oceanica* epiphytic community and shoot productivity. *J. Ecol.* 103, 1594–1609. doi: 10.1111/1365-2745.12477

Cumani, F., Bradassi, F., Di Pascoli, A., and Bressan, G. (2010). Marine acidification effects on reproduction and growth rates of Corallinaceae spores (Rhodophyta), Rapp. *Comm. Int. Mer Medit.* 39:735.

De Clerck, O., Guiry, M. D., Leliaert, F., Samyn, Y., and Verbruggen, H. (2013). Algal taxonomy: a road to nowhere? *J. Phycol.* 49, 215–225. doi: 10.1111/jpy.12020

De Jode, A., David, R., Haguenauer, A., Cahill, A., Erga, Z., Guillemain, D., et al. (2019). From seascape ecology to population genomics and back. Spatial and ecological differentiation among cryptic species of the red algae *Lithophyllum stictiforme/L.* cabiochiae, main bioconstructors of coralligenous habitats. *Mol. Phylogen. Evol.* 137, 104–113. doi: 10.1016/j.ympev.2019.04.005

de Lamarck, J. B. (1801). *Systeme des Animaux Sans Vertebres*. Libraire Derteville, Paris.

Di Geronimo, R. (1998). *Le Corallinales del quaternario dell'Italia meridionale (sistematica, paleoecologia e paleobiogeografia)* (Ph.D. thesis). Università di Messina, Messina, Italy.

Diaz-Pulido, G., Nash, M. C., Anthony, K. R. N., Bender, D., Opdyke, B. N., Reyes-Nivia, C., et al. (2014). Greenhouse conditions induce mineralogical changes

and dolomite accumulation in coralline algae on tropical reefs. *Nat. Commun.* 5:3310. doi: 10.1038/ncomms4310

Donnarumma, L., Lombardi, C., Cocito, S., and Gambi, M. C. (2014). Settlement pattern of *Posidonia oceanica* epibionts along a gradient of ocean acidification: an approach with mimics. *Medit. Mar. Sci.* 15, 498–509. doi: 10.12681/mms.677

Egan, S., Harder, T., Burke, C., Steinberg, P., Kjellenberg, S., and Thomas, T. (2012). The seaweed holobiont: understanding seaweed-bacteria interactions. *FEMS Microbiol. Rev.* 37, 462–476. doi: 10.1111/1574-6976.12011

Egilsdottir, H., Noisette, F., Laure, M. L. N., Olafsson, J., and Martin, S. (2013). Effects of pCO_2 on physiology and skeletal mineralogy in a tidal pool coralline alga, *Corallina elongata*. *Mar. Biol.* 160, 2103–2112. doi: 10.1007/s00227-012-2090-7

El Haikali, B., Bensoussan, N., Romano, J. C., and Bousquet, V. (2004). Estimation of photosynthesis, and calcification rates of *Corallina elongata* Ellis et Solander, 1786, by measurements of dissolved oxygen, pH and total alkalinity. *Sci. Mar.* 68, 45–56. doi: 10.3989/scimar.2004.68n145

El Maghraby, D. M., and Fakhry, E. M. (2015). Lipid content and fatty acid composition of Mediterranean macro-algae as dynamic factors for biodiesel production. *Oceanologia* 57, 86–92. doi: 10.1016/j.oceano.2014.08.001

Ellis, J. (1768). Extract of a letter from John Ellis, Esquire, F.R.S. to Dr. Linnaeus of Upsala, F.R.S. on the animal nature of the genus of zoophytes, called Corallina. *Phil. Trans. Roy. Soc. London* 57, 404–425. doi: 10.1098/rstl.1767.0042

Ellis, J., and Solander, D. (1786). *The Natural History of Many Curious and Uncommon Zoophytes, Collected From Various Parts of the Globe*. London: Benjamin White and Son.

Esper, E. J. C. (1796). *Fortsetzungen der Pflanzenthiere in Abbildungen nach der Natur mit Farben erleuchtet nebst Beschreibungen*. Nuremberg: Lieferung 5.

Falace, A., Kaleb, S., Orlando-Bonaca, M., Mavrič, B., and Lipej, L. (2011). First contribution to the knowledge of coralline algae distribution in the Slovenian circalittoral zone (Northern Adriatic). *Ann. Ser. Hist. Nat.* 21, 27–40.

Feldmann, J. (1939). Les algues marines de la Côte des Albères. IV. Rhodophycées. *Rev. Algol.* 11, 247–330.

Figueroa, F. L. (1993). Photoregulation of nitrogen metabolism and protein accumulation in the red alga *Corallina elongata* Ellis et Soland. *Z. Naturforsch.* 48, 788–794. doi: 10.1515/znc-1993-9-1017

Figueroa, F. L., Barufi Bonomi, J., Malta, E. J., Conde-Álvarez, R., Nitschke, U., Arenas, F., et al. (2014a). Short-term effects of increasing CO_2, nitrate and temperature on three Mediterranean macroalgae: biochemical composition. *Aquat. Biol.* 22, 177–193. doi: 10.3354/ab00610

Figueroa, F. L., Domínguez-González, B., and Korbee, N. (2014b). Vulnerability and acclimation to increased UVB radiation in three intertidal macroalgae of different morpho-functional groups. *Mar. Environ. Res.* 97, 30–38. doi: 10.1016/j.marenvres.2014.01.009

Fine, M., Tsadok, R., Meron, D., Cohen, S., and Milazzo, M. (2017). Environmental sensitivity of *Neogoniolithon brassica-florida* associated with vermetid reefs in the Mediterranean Sea. *ICES J. Mar. Sci.* 74, 1074–1082. doi: 10.1093/icesjms/fsw167

Flecha, S., Pérez, F. F., García-Lafuente, J., Sammartino, S., Ríos, A. F., and Huertas, I. E. (2015). Trends of pH decrease in the Mediterranean Sea through high frequency observational data: indication of ocean acidification in the basin. *Sci. Rep.* 5:16770. doi: 10.1038/srep16770

Fravega, P., Giammarino, S., Piazza, M., Russo, A., and Vannucci, G. (1987). Significato paleoecologico degli episodi coralgali a Nord di Sassello. Nuovi dati per una ricostruzione paleogeografica-evolutiva del margine meridionale del Bacino Terziario del Piemonte. *Atti Soc. Tosc. Sc. Nat. Mem. Ser.* 94, 19–76.

Friedrich, O., Richard, D., Norris, R. D., and Erbacheret, J. (2012). Evolution of middle to Late Cretaceous oceans - A 55 m.y. record of Earth's temperature and carbon cycle. *Geology* 40, 107–110. doi: 10.1130/G32701.1

Furnari, F., Cormaci, G., and Alongi, G. (1996). *Lithophyllum frondosum* (Dufour) comb. nov. (Corallinaceae, Rhodophyta): the species to which Mediterranean "*Pseudolithophyllum expansum*" should be referred. *Eur. J. Phycol.* 31, 117–122. doi: 10.1080/09670269600651281

Gabrielson, P. W., Hughey, J. R., and Diaz-Pulido, G. (2018). Genomics reveals abundant speciation in the coral reef building alga *Porolithon onkodes* (Corallinales, Rhodophyta). *J. Phycol.* 54, 429–434. doi: 10.1111/jpy.12761

Galli, G., Solidoro, C., and Lovato, T. (2017). Marine heat waves hazard 3D maps and the risk for low motility organisms in a warming Mediterranean Sea. *Front. Mar. Sci.* 4:136. doi: 10.3389/fmars.2017.00136

Garrabou, J., and Ballesteros, E. (2000). Growth of *Mesophyllum alternans* and *Lithophyllum frondosum* (Corallinales, Rhodophyta) in the northwestern Mediterranean. *Eur. J. Phycol.* 35, 1–10. doi: 10.1080/09670260010001735571

Gómez-Garreta, A. (1981). *Estudio fenologico de la vegetation marina de la isla de Mallorca* (Ph.D. thesis). Universitat de Barcelona, Barcelona, Spain.

Gómez-Garreta, A., Ribera Siguan, A., and Seoane Camba, J. A. (1982). Aportacion al estudio fenologico de las algas de la isla de Mallorca. *Boll. Soc. Hist. Nat. Balears* 26, 37–62.

Goyet, C., Hassoun, A. E. R., Gemayel, E., Touratier, F., Saab, M. A. A., and Guglielmi, V. (2016). Thermodynamic forecasts of the mediterranean sea acidification. *Mediterr. Mar. Sci.* 17, 508–518. doi: 10.12681/mms.1487

Graham, L. E., Graham, J. M., Wilcox, L. W., and Cook, M. E. (2018). *Algae. 3rd Edn*. Madison, WI: LJLM Press, LLC.

Guiry, M. D. (1990). "Sporangia and spores" in *Biology of the Red Algae,* eds K. M. Cole and R.G. Sheath (Cambridge: Cambridge University Press), 347–376.

Guiry, M. D., and Guiry, G. M. (2019). AlgaeBase. *World-wide electronic publication, National University of Ireland, Galway.* Available online at http://www.algaebase.org (last accessed July 30, 2019).

Guy-Haim, T., Silverman, J., Raddatz, S., Wahl, M., Israel, A., and Rilov, G. (2016). The carbon turnover response to thermal stress of a dominant coralline alga on the fast warming Levant coast. *Limnol. Oceanogr.* 61, 1120–1133. doi: 10.1002/lno.10279

Häder, D.-P., Herrmann, H., Schafer, J., and Santas, R. (1996). Photosynthetic fluorescence induction and oxygen production in corallinacean algae measured on site. *Bot. Acta* 109, 285–291. doi: 10.1111/j.1438-8677.1996.tb00575.x

Häder, D.-P., Lebert, M., Flores-Moya, A., Jiménez, C., Mercado, J., Salles, S., et al. (1997). Effects of solar radiation on the photosynthetic activity of the red alga *Corallina elongata* Ellis et Soland. *J. Photochem. Photobiol.* 37, 196–202. doi: 10.1016/S1011-1344(96)07402-7

Hale, R., Calosi, P., McNeill, L., Mieszkowska, N., and Widdicombe, S. (2011). Predicted levels of future ocean acidification and temperature rise could alter community structure and biodiversity in marine benthic communities. *Oikos* 120, 661–674. doi: 10.1111/j.1600-0706.2010.19469.x

Halfar, J., and Mutti, M. (2005). Global dominance of coralline red algal facies: a response to Miocene oceanographic events. *Geology* 33, 481–484. doi: 10.1130/G21462.1

Hall-Spencer, J. M., Rodolfo-Metalpa, R., Martin, S., Ransome, E., Fine, M., Turner, S. M., et al. (2008). Volcanic carbon dioxide vents show ecosystem effects of ocean acidification. *Nature* 454, 96–99. doi: 10.1038/nature07051

Hamel, G., and Lemoine, M. (1953). "Corallinacées de France e d'Afrique du Nord," in *Arch Mus. Nat. Hist. Nat. Paris* 1, 15–136.

Harley, C. D. G., Anderson, K. M., Demes, K. W., Jorve, J. P., Kordas, R. L., Coyle, T. A., et al. (2012). Effects of climate change on global seaweed communities. *J. Phycol.* 48, 1064–1078. doi: 10.1111/j.1529-8817.2012.01224.x

Harzhauser, M., and Piller, W. E. (2007). Benchmark data of a changing sea - Palaeogeography, palaeobiogeography and events in the Central Paratethys during the Miocene. *Palaeogeogr. Palaeoclimatol. Palaeoecol.* 253, 8–31. doi: 10.1016/j.palaeo.2007.03.031

Hassoun, A. E. R., Gemayel, E., Krasakopoulou, E., Goyet, C., Saab, M. A. A., Gugliemi, V., et al. (2015). Acidification of the Mediterranean sea from anthropogenic carbon penetration. *Deep Sea Res.* 102, 1–15. doi: 10.1016/j.dsr.2015.04.005

Hereu, B., and Kersting, D. K. (2016). Diseases of coralline algae in the Mediterranean Sea. *Coral Reefs* 35:713. doi: 10.1007/s00338-016-1428-x

Hernández, R. Y. S., Zucchetti, M., Aumento, F., Gual, M. R., Cozzella, M. L., and Hernández, C. M. A. (2011). Measurement of plutonium pollution in sediments and algae in marine environment: cienfuegos bay and la Maddalena Islands. *Fresenius Environ. Bull.* 20, 802–809.

Hernandez-Kantun, J. J., Gabrielson, P. W., Hughey, J. R., Pezzolesi, L., Rindi, F., Robinson, N. M., et al. (2016). Reassessment of branched *Lithophyllum* spp. (Corallinales, Rhodophyta) in the Caribbean Sea with global implications. *Phycologia* 55, 609–635. doi: 10.2216/16-7.1

Hernandez-Kantun, J. J., Rindi, F., Adey, W. A., Heesch, S., Peña, V., Le Gall, L., et al. (2015a). Sequencing type material resolves the identity and distribution of the generitype *Lithophyllum incrustans*, and related European species *L. hibernicum* and *L. bathyporum* (Corallinales, Rhodophyta). *J. Phycol.* 51, 791–807. doi: 10.1111/jpy.12319

Hernandez-Kantun, J. J., Riosmena-Rodriguez, R., Hall-Spencer, J. M., Peña, V., Maggs, C. A., and Rindi, F. (2015b). Phylogenetic analysis of rhodolith formation in the Corallinales (Rhodophyta). *Eur. J. Phycol.* 50, 46–61. doi: 10.1080/09670262.2014.984347

Hind, K. R., Gabrielson, P. W., Jensen, C., and Martone, P. T. (2016). *Crusticorallina* gen. nov., a nongeniculate genus in the subfamily Corallinoideae (Corallinales, Rhodophyta). *J. Phycol.* 52, 929–941. doi: 10.1111/jpy.12449

Hind, K. R., Gabrielson, P. W., and Saunders, G. W. (2014). Molecular-assisted alpha taxonomy reveals pseudocryptic diversity among species of *Bossiella* (Corallinales, Rhodophyta) in the eastern Pacific Ocean. *Phycologia* 53, 443–456. doi: 10.2216/13-239.1

Hind, K. R., Starko, S., Burt, J. M., Lemay, M. A., Salomon, A. K., and Martone, P. T. (2019). Trophic control of cryptic coralline algal diversity. *Proc. Nat. Acad. Sci. U.S. A.* 116, 15080–15085. doi: 10.1073/pnas.1900506116

Howes, E. L., Stemmann, L., Assailly, C., Irisson, J.-O., Dima, M., Bijma, J., et al. (2015). Pteropod time series from the North Western Mediterranean (1967–2003): impacts of pH and climate variability. *Mar. Ecol. Prog. Ser.* 531, 193–206. doi: 10.3354/meps11322

Hrabovský, J., Basso, D., and Doláková N. (2016). Diagnostic characters in fossil coralline algae (Corallinophycidae: Rhodophyta) from the Miocene of southern Moravia (Carpathian Foredeep, Czech Republic). *J. Syst. Paleontol.* 14, 499–525. doi: 10.1080/14772019.2015.1071501

Hsü, K. J., Montadert, L., Bernoulli, D., Cita, M. B., Erickson, A., Garrison, R. E., et al. (1977). History of the Messinian salinity crisis. *Nature* 267, 399–403. doi: 10.1038/267399a0

Hughey, J. R., Braga, J. C., Aguirre, J., Woelkerling, W. J., and Webster, J. M. (2008). Analysis of ancient DNA from fossil corallines (Corallinales, Rhodophyta). *J. Phycol.* 44, 374–383. doi: 10.1111/j.1529-8817.2008.00462.x

Huvé, H. (1962). Taxonomie, écologie et distribution d'une mélobesiée méditerraneenne: *Lithophyllum papillosum* (Zanardini) comb. nov., non Lithophyllum (Dermatolithon) papillosum (Zanard.) Foslie. *Bot. Mar.* 4, 219–240. doi: 10.1515/botm.1962.4.3-4.219

Huvé, P. (1954). Etude expérimentale de la réinstallation d'un "trottoir à *Tenarea*," en Méditerranée occidentale. *C.R. Acad. Sci. Fr.* 239, 323–325.

Huvé, P. (1956a). Sur la réinstallation d'un "trottoir à *Tenarea*" en *Méditerranée occidentale*. *C.R. Acad. Sci. Fr.* 243, 2157–2158.

Huvé, P. (1956b). Résultats sommaires de l'étude expérimentale de la réinstallation d'un "trottoir à *Tenarea*" en Méditerranée occidentale. Rapp. P.V. Commiss. internation. *Explor. Sci. Mer Médit.* 14, 429–448.

Huvé, P. (1970). *Recherches sur la genèse de quelques peuplements algaux marins dela roche littorale dans la région de Marseille* (Ph.D. thesis). Comité National de la Recherche Scientifique, Paris, France.

Ingrosso, G., Abbiati, M., Badalamenti, F., Bavestrello, G., Belmonte, G., Cannas, R., et al. (2018). Mediterranean bioconstructions along the Italian coast. *Adv. Mar. Biol.* 79, 61–136. doi: 10.1016/bs.amb.2018.05.001

Irvine, L. M., and Chamberlain, Y. M. (1994). *Seaweeds of the British Isles. Vol. 1, Rhodophyta, Part 2B. Corallinales, Hildenbrandiales.* London: The Natural History Museum.

Ismail-Ben Ali, A., El Bour, M., Ktari, L., Bolhuis, H., Ahmed, M., Bouddabous, A., et al. (2012). *Jania rubens*-associated bacteria: molecular identification and antimicrobial activity. *J. Appl. Phycol.* 24, 525–534. doi: 10.1007/s10811-011-9758-0

Kaleb, S., Falace, A., Sartoni, G., and Woelkerling, W. J. (2011). Morphology-anatomy of *Mesophyllum macroblastum* (Hapalidiaceae, Corallinales, Rhodophyta) in the Northern Adriatic Sea and a key to Mediterranean species of the genus. *Cryptog. Algol.* 32, 223–242. doi: 10.7872/crya.v32.iss3.2011.223

Kaleb, S., Falace, A., and Woelkerling, W. J. (2012). *Phymatolithon lamii* (Hapalidiaceae, Corallinales, Rhodophyta): a first report for the Mediterranean Sea. *Bot. Mar.* 55, 377–386. doi: 10.1515/bot-2012-0141

Kamenos, N. A., Burdett, H. L., Aloisio, E., Findlay, H. S., Martin, S., Longbone, C., et al. (2013). Coralline algal structure is more sensitive to rate, rather than the magnitude, of ocean acidification. *Glob. Change Biol.* 19, 3621–3628. doi: 10.1111/gcb.12351

Kamenos, N. A., Cusack, M., and Moore, P. G. (2008). Coralline algae are global palaeothermometers with bi-weekly resolution. *Geochim. Cosmochim. Ac.* 72, 771–779. doi: 10.1016/j.gca.2007.11.019

Kamenos, N. A., Perna, G., Gambi, M. C., Micheli, F., and Kroeker, K. J. (2016). Coralline algae in a naturally acidified ecosystem persist by maintaining control of skeletal mineralogy and size. *Proc. R. Soc. B.* 283:20161159. doi: 10.1098/rspb.2016.1159

Kapsenberg, L., Alliouane, S., Gazeau, F., Mousseau, L., and Gattuso, J.-P. (2017). Coastal ocean acidification and increasing total alkalinity in the northwestern Mediterranean Sea. *Ocean Sci.* 13, 411–426. doi: 10.5194/os-13-411-2017

Kato, A., Baba, M., and Suda, S. (2013). Taxonomic circumscription of heterogeneous species *Neogoniolithon brassica-florida* (Corallinales, Rhodophyta) in Japan. *Phycol. Res.* 61, 15–26. doi: 10.1111/j.1440-1835.2012.00665.x

Kerrison, P., Hall-Spencer, J. M., Suggett, D. J., Hepburn, L. J., and Steinke, M. (2011). Assessment of pH variability at a coastal CO_2 vent for ocean acidification studies. *Estuar. Coast. Shelf Sci.* 94, 129–137. doi: 10.1016/j.ecss.2011.05.025

Khairy, H. M., and El-Sheikh, M. A. (2015). Antioxidant activity and mineral composition of three Mediterranean common seaweeds from Abu-Qir Bay, Egypt. *Saudi J. Biol. Sci.* 22, 623–630. doi: 10.1016/j.sjbs.2015.01.010

Kiessling, W. (2010). Geologic and biologic controls on the evolution of reefs. *Ann. Rev. Ecol. Evol. Syst.* 40, 173–192. doi: 10.1146/annurev.ecolsys.110308.120251

Koch, M., Bowes, G., Ross, C., and Zhang, X. H. (2013). Climate change and ocean acidification effects on seagrasses and marine macroalgae. *Glob. Change Biol.* 19, 103–132. doi: 10.1111/j.1365-2486.2012.02791.x

Korbee, N., Navarro, N. P., García-Sánchez, M., Celis-Plá, P. S. M., Quintano, E., Copertino, M. S., et al. (2014). A novel *in situ* system to evaluate the effect of high CO_2 on photosynthesis and biochemistry of seaweeds. *Aquat. Biol.* 22, 245–259. doi: 10.3354/ab00594

Kroeker, K. J., Micheli, F., and Gambi, M. C. (2012). Ocean acidification causes ecosystem shifts via altered competitive interactions. *Nat. Clim. Change* 3, 156–159. doi: 10.1038/nclimate1680

Kuffner, I. B., Andersson, A. J., Jokiel, P. L., Rodgers, K. S., and Mackenzie, F. T. (2008). Decreased abundance of crustose coralline algae due to ocean acidification. *Nat. Geosci.* 1, 114–117. doi: 10.1038/ngeo100

Laborel, J. (1987). Marine biogenic constructions in the Mediterranean, a review. *Sci. Rep. Port-Cros Nat. Park* 13, 97–126.

Laborel, J., Morhange, C., and Laborel-Denguen, F. (1993). Dégradation récente des formations construites superficielles à *Lithophyllum lichenoides* Philippi dans la Réserve marine de Scandola. *Trav. Sci. Parc Nat. Rég. Rés. Nat. Corse.* 41, 19–23.

Laib, E., and Legouchi, E. (2012). Cd, Cr, Cu, Pb, and Zn concentrations in *Ulva lactuca*, *Codium fragile*, *Jania rubens*, and *Dictyota dichotoma* from Rabta Bay, Jijel (Algeria). *Environ. Monitor. Assess.* 184, 1711–1718. doi: 10.1007/s10661-011-2072-0

Langar, H., Bessibes, M., Djellouli, A., Pergent-Martini, C., and Pergent, G. (2011). The *Neogoniolithon brassica-florida* (Harvey) Setchell and LR Mason (1943) Reef of Bahiret el Bibane Lagoon (Southeastern Tunisia). *J. Coast. Res.* 27, 394–398. doi: 10.2112/JCOASTRES-D-10-00082.1

Legrand, E., Riera, P., Lutier, M., Coudret, J., Grall, J., and Martin, S. (2017). Species interactions can shift the response of a maerl bed community to ocean acidification and warming. *Biogeosciences* 14, 5359–5376. doi: 10.5194/bg-14-5359-2017

Lejeusne, C., Chevaldonné, P., Pergent-Martini, C., Boudouresque, C.-F., and Pérez, T. (2010). Climate change effects on a miniature ocean: the highly diverse, highly impacted Mediterranean Sea. *Tr. Ecol. Evol.* 25, 250–260. doi: 10.1016/j.tree.2009.10.009

Lemoine, M. P. (1939). Algues calcaires fossiles de l'Algérie. Matériaux pour la Carte Géologique de L'Algérie. *1re Série Paléontol.* 9, 1–128.

Lemoine, M. P. (1970). Les algues floridées calcaires du Crétacé du sud de la France. *Arch. Mus. Nat. d'Hist. Nat.* 7, 129–240.

Lemoine, M. P. (1977). Étude d'une collection d'algues corallinacées de la région de Skopje (Yougoslavie). *Rev. Micropaléont.* 20, 10–42.

Linnaeus, C. (1758). *Systema Naturae per Regna Tria Naturae, Secundum Classes, Ordines, Genera, Species, Cum Characteribus, Differentiis, Synonymis, Locis.* Holmiae: Impensis direct. Laurentii Salvi.

López-Figueroa, F., and Niell, F. X. (1990). Effects of light quality on chlorophyll and biliprotein accumulation in seaweeds. *Mar. Biol.* 104, 321–327. doi: 10.1007/BF01313274

López-Figueroa, F., Perez, R., and Niell, F. X. (1989). Effects of red and far-red light pulses on the chlorophyll and biliprotein accumulation in the red alga *Corallina elongata*. *J. Photochem. Photobiol.* 4, 185–193. doi: 10.1016/1011-1344(89)80004-1

Lopez-Horgue, M. A., Owen, H. G., Aranburu, A., Fernandez-Mendiola, P. A., and Garcia-Mondéjar, J. (2009). Early late Albian (Cretaceous) of the central region of the Basque-Cantabrian Basin, northern Spain: biostratigraphy based on ammonites and orbitolinids. *Cret. Res.* 30, 385–400. doi: 10.1016/j.cretres.2008.08.001

Lüning, K. (1990). *Seaweeds. Their Environment, Biogeography, and Ecophysiology*. London: Wiley Interscience.

Marbà, N., and Duarte, C. M. (2010). Mediterranean warming triggers seagrass (*Posidonia oceanica*) shoot mortality. *Glob. Change Biol.* 16, 2366–2375. doi: 10.1111/j.1365-2486.2009.02130.x

Marchini, A., Ragazzola, F., Vasapollo, C., Castelli, A., Cerrati, G., Gazzola, F., et al. (2019). Intertidal Mediterranean coralline algae habitat is expecting a shift toward a reduced growth and a simplified associated fauna under climate change. *Front. Mar. Sci*. 6:106. doi: 10.3389/fmars.2019.00106

Mariotti,. A., Struglia, M. V., Zeng, N., and Lau, K. M. (2002). The hydrological cycle in the Mediterranean region and implications for the water budget of the Mediterranean Sea. *J. Climate* 15, 1674–1690. doi: 10.1175/1520-0442(2002)015<1674:THCITM>2.0.CO;2

Martin, C. S., Giannoulaki, M., De Leo, F., Scardi, M., Salomidi, M., Knittweis, L., et al. (2014). Coralligenous and maerl habitats: predictive modeling to identify their spatial distributions across the Mediterranean Sea. *Sci. Rep*. 4:5073. doi: 10.1038/srep06646

Martin, S., Castets, M. D., and Clavier, J. (2006). Primary production, respiration and calcification of the temperate free-living coralline alga *Lithothamnion corallioides*. *Aquat. Bot*. 85, 121–128. doi: 10.1016/j.aquabot.2006.02.005

Martin, S., Charnoz, A., and Gattuso, J. P. (2013b). Photosynthesis, respiration and calcification in the Mediterranean crustose coralline alga *Lithophyllum cabiochae* (Corallinales, Rhodophyta). *Eur. J. Phycol*. 48, 163–172. doi: 10.1080/09670262.2013.786790

Martin, S., Cohu, S., Vignot, C., Zimmerman, G., and Gattuso, J. P. (2013a). One-year experiment on the physiological response of the Mediterranean crustose coralline alga, *Lithophyllum cabiochae*, to elevated pCO_2 and temperature. *Ecol. Evol*. 3, 676–693. doi: 10.1002/ece3.475

Martin, S., and Gattuso, J. P. (2009). Response of Mediterranean coralline algae to ocean acidification and elevated temperature. *Glob. Change Biol*. 15, 2089–2100. doi: 10.1111/j.1365-2486.2009.01874.x

Martin, S., and Hall-Spencer, J. M. (2017). "Effects of ocean warming and acidification on rhodolith/maërl beds" in *Rhodolith/maërl beds: a global perspective,* eds R. Riosmena-Rodríguez, W. Nelson, and J. Aguirre (Basel: Springer International Publishing), 55–85. doi: 10.1007/978-3-319-29315-8_3

Martin, S., Rodolfo-Metalpa, R., Ransome, E., Rowley, S., Buia, M. C., Gattuso, J. P., et al. (2008). Effects of naturally acidified seawater on seagrass calcareous epibionts. *Biol. Lett.* 4, 689–692. doi: 10.1098/rsbl.2008.0412

Maslov, V. P. (1956). Fossil Calcareous Algae of USSR (in Russian). *Trudy Inst. Geol. Nauk Akad. Nauk SSSR* 160, 1–301.

Mastrorilli, V. I. (1968). Nuovo contributo allo studio delle Corallinacee dell'Oligocene Ligure-Piemontese: i reperti della tavoletta Ponzone. *Atti Ist. Geol. Univ. Genova* 5, 153–406.

McCoy, S. J., and Kamenos, N. A. (2015). Coralline algae (Rhodophyta) in a changing world: integrating ecological, physiological, and geochemical responses to global change. *J. Phycol*. 51, 6–24. doi: 10.1111/jpy.12262

Miller, K. G., Mountain, G. S., Wright, J. D., and Browning, J. V. (2011). A 180-million-year record of sea level and ice volume variations from continental margin and deep-sea isotopic records. *Oceanography* 24, 40–53. doi: 10.5670/oceanog.2011.26

Morse, J. W., Arvidson, R. S., and Lüttge, A. (2007). Calcium carbonate formation and dissolution. *Chem. Rev*. 107, 342–381. doi: 10.1021/cr050358j

Moussavian, E. (1993). "Eocene corallinacean-dominated localities of the Helvetic zone / Upper Bavaria," in *Facial Development of Algae-Bearing Carbonate Sequences in the Eastern Alps. Field Trip Guidebook, Munich. Excursion B1,* eds R. Höfling, E. Moussavian, and W.E. Piller (Munich: Alpine Algae, International Symposium on Fossil Algae), 1–11.

Nalin, R., Basso, D., and Massari, F. (2006). "Pleistocene coralline algal build-ups (coralligéne de plateau) and associated bioclastic deposits in the sedimentary cover of Cutro marine terrace (Calabria, southern Italy)", in *Cool-water carbonates: depositional systems and palaeoenvironmental controls,* eds H.M. Pedley, and G. Carannante (London: Geol. Soc. Spec. Publ. 255), 11–22. doi: 10.1144/GSL.SP.2006.255.01.02

Nannini, M., De Marchi, L., Lombardi, L., and Ragazzola, F. (2015). Effects of thermal stress on the growth of an intertidal population of *Ellisolandia elongata* (Rhodophyta) from N-W Mediterranean Sea. *Mar. Environ. Res*. 112, 11–19. doi: 10.1016/j.marenvres.2015.05.005

Nash, M. C., Martin, S., and Gattuso, J. P. (2016). Mineralogical response of the Mediterranean crustose coralline alga *Lithophyllum cabiochae* to near-future ocean acidification and warming. *Biogeosciences* 13, 5937–5945. doi: 10.5194/bg-13-5937-2016

Nash, M. C., Uthicke, S., Negri, A. P., and Cantin, N. E. (2015). Ocean acidification does not affect magnesium composition or dolomite formation in living crustose coralline algae, *Porolithon onkodes* in an experimental system. *Biogeosciences* 12, 5247–5260. doi: 10.5194/bg-12-5247-2015

Nebelsick, J., Rasser, M., and Bassi, D. (2005). Facies dynamics in Eocene to Oligocene circumalpine carbonates. *Facies* 51, 197–216. doi: 10.1007/s10347-005-0069-2

Nelson, W. A., Sutherland, J. E., Farr, T. J., Hart, D. R., Neill, K. F., Kim, H. J., et al. (2015). Multi-gene phylogenetic analyses of New Zealand coralline algae: *Corallinapetra novaezelandiae* gen. et sp. nov. and recognition of the Hapalidiales ord. nov. *J. Phycol.* 51, 454–468. doi: 10.1111/jpy.12288

Norris, D., Turner, S. K., Hull, P. M., and Ridgwell, A. (2013). Marine ecosystem responses to Cenozoic global change. *Science* 341, 492–498. doi: 10.1126/science.1240543

Norton, T. A. (1992). Dispersal by macroalgae. *Br. Phycol. J.* 27, 293–301. doi: 10.1080/00071619200650271

Nykjaer, L. (2009). Mediterranean Sea surface warming 1985-2006. *Climate Res*. 39, 11–17. doi: 10.3354/cr00794

O'Brien, C. L., Robinson, S. A., Pancost, R. D., Damsté, J. S. S., Schoutten, S., Lunt, D. J., et al. (2017). Cretaceous sea-surface temperature evolution: Constraints from TEX_{86} and planktonic foraminiferal oxygen isotopes. *Earth-Sci. Rev*. 172, 224–247. doi: 10.1016/j.earscirev.2017.07.012

Olgunoglu, M. P., and Polat, S. (2008). Trace metals in marine macroalgae samples from the Iskenderun Bay, Turkey. *Fres. Environ. Bull*. 17, 589–595.

Palmiéri, J., Orr, J. C., Dutay, J.-C., Béranger, K., Schneider, A., and Beuvier, J. (2015). Simulated anthropogenic CO_2 storage and acidification of the Mediterranean Sea. *Biogeosciences* 12, 781–802. doi: 10.5194/bg-12-781-2015

Parages, M. L., Figueroa, F. L., Conde-Álvarez, R. M., and Jiménez, C. (2014). Phosphorylation of MAPK-like proteins in three intertidal macroalgae under stress conditions. *Aquat. Bot*. 22, 213–226. doi: 10.3354/ab00592

Pardo, C., Peña, V., Barreiro, R., and Barbara Criado, I. (2015). A molecular and morphological study of *Corallina* sensu lato (Corallinales, Rhodophyta) in the Atlantic Iberian Peninsula. *Cryptog. Algol*. 36, 31–54. doi: 10.7872/crya.v36.iss1.2015.31

Pascual, M., Rives, B., Schunter, C., and Macpherson, E. (2017). Impact of life history traits on gene flow: a multispecies systematic review across oceanographic barriers in the Mediterranean Sea. *PLoS ONE* 12:e0176419. doi: 10.1371/journal.pone.0176419

Patarnello, T., Volckaert, F., and Castilho, R. (2007). Pillars of Hercules: is the Atlantic-Mediterranean transition a phylogeographical break? *Mol. Ecol.* 16, 4426–4444. doi: 10.1111/j.1365-294X.2007.03477.x

Peña, V., Adey, W. H., Riosmena-Rodriguez, R., Jung, M. Y., Afonso-Carillo, J., Choi, H. G., et al. (2011). *Mesophyllum sphaericum* sp. nov. (Corallinales, Rhodophyta): a new maerl-forming species from the northeast Atlantic. *J. Phycol*. 47, 911–927. doi: 10.1111/j.1529-8817.2011.01015.x

Peña, V., De Clerck, O., Afonso-Carrillo, J., Ballesteros, E., Bárbara, I., Barreiro, R., et al. (2015a). An integrative systematic approach to species diversity and distribution in the genus *Mesophyllum* (Corallinales, Rhodophyta) in Atlantic and Mediterranean Europe. *Eur. J. Phycol*. 50, 20–36. doi: 10.1080/09670262.2014.981294

Peña, V., Hernández-Kantun, J. J., Adey, W. H., and Le Gall, L. (2018). Assessment of coralline species diversity in the European coasts supported by sequencing of type material: the case study of *Lithophyllum nitorum* (Corallinales, Rhodophyta). *Cryptog. Algol*. 39, 123–337. doi: 10.7872/crya/v39.iss1.2018.123

Peña, V., Hernández-Kantún, J. J., Grall, J., Pardo, C., López, L., Bárbara, I., et al. (2014). Detection of gametophytes in the maerl-forming species

*Phymatolithon calcareum (*Melobesioideae, Corallinales*)* assessed by DNA barcoding. *Cryptog., Algol.* 35, 15–25. doi: 10.7872/crya.v35.iss1.2014.15

Peña, V., Pardo, C., López, L., Hernandez-Kantun, J. J., Adey, W. H., Bárbara, I., et al. (2015b). *Phymatolithon lusitanicum* sp. nov. (Hapalidiales, Rhodophyta): the third most abundant maerl-forming species in the Atlantic Iberian Peninsula. *Cryptog. Algol.* 36, 429–459. doi: 10.7872/crya/v36.iss4.2015.429

Perrin, C., and Kiessling, W. (2010). "Latitudinal trends in Cenozoic reef patterns and their relationship to climate" in *Carbonate Systems During the Oligocene-Miocene Climatic Transition,* eds M. Mutti, W.E. Piller, and C. Betzler (Oxford; Chichester; Hoboken, NJ: IAS Spec. Publ.; Wiley-Blackwell) 42, 17–34. doi: 10.1002/9781118398364.ch2

Pezzolesi, L., Falace, A., Kaleb, S., Hernandez-Kantun, J. J., Cerrano, C., and Rindi, F. (2017). Genetic and morphological variation in an ecosystem engineer, *Lithophyllum byssoides* (Corallinales, Rhodophyta). *J. Phycol.* 53, 146–160. doi: 10.1111/jpy.12488

Pezzolesi, L., Peña, V., Le Gall, L., Gabrielson, P. W., Kaleb, S., Hughey, J. R., et al. (2019). Mediterranean *Lithophyllum stictiforme* is a genetically diverse species complex: implications for species circumscription, biogeography and conservation of coralligenous habitats. *J. Phycol.* 55, 473–492. doi: 10.1111/jpy.12837

Piazzi, L., Balata, D., and Ceccherelli, G. (2015). Epiphyte assemblages of the Mediterranean seagrass *Posidonia oceanica*: an overview. *Mar. Ecol.* 37, 3–41. doi: 10.1111/maec.12331

Pickett-Heaps, J. D., West, J. A., Wilson, S. M., and McBride, D. L. (2001). Time-lapse videomicroscopy of cell (spore) movement in red algae. *Eur. J. Phycol.* 36, 9–22. doi: 10.1080/09670260110001735148

Poignant, A. F. (1968). Les algues des calcaires Aptiens et Albiens d'Aquitaine méridionale. *Rev. Micropaléontol.* 10, 271–276.

Poignant, A. F. (1978). Les algues rouges crétacées. Relations mer Boréale-Téthys. Aspekte der Kreide Europas. *IUGS Ser. A* 6, 273–278.

Poignant, A. F. (1981). Sur des formes nouvelles d'algues rouges crétacées. *Cret. Res.* 2, 187–195. doi: 10.1016/0195-6671(81)90008-2

Polat, S., and Ozogul, Y. (2009). Fatty acid, mineral and proximate composition of some seaweeds from the northeastern Mediterranean coast. *Ital. J. Food Sci.* 21, 317–324.

Polat, S., and Ozogul, Y. (2013). Seasonal proximate and fatty acid variations of some seaweeds from the northeastern Mediterranean coast. *Oceanologia* 55, 375–391. doi: 10.5697/oc.55-2.375

Popov, S. V., Rögl, F., Rozanov, A. Y., Steininger, F. F., Shcherba, I. G., and Kováè, M. (2004). Lithological-paleogeographic maps of Paratethys 10 Maps Late Eocene to Pliocene. *Cour Forsch Senckenberg* 250, 1–46.

Porzio, L., Buia, M. C., and Hall-Spencer, J. M. (2011). Effects of ocean acidification on macroalgal communities. *J. Exp. Mar. Biol. Ecol.* 400, 278–287. doi: 10.1016/j.jembe.2011.02.011

Porzio, L., Garrard, S. L., and Buia, M. C. (2013). The effect of ocean acidification on early algal colonization stages at natural CO_2 vents. *Mar. Biol.* 160, 2247–2259. doi: 10.1007/s00227-013-2251-3

Quéré, G., Intertaglia, L., Payri, C., and Garland, P. E. (2019). Disease specific bacterial communities in a coralline alga of the northwestern Mediterranean Sea: a combined culture dependent and -independent approach. *Front. Microbiol.* 10:1850. doi: 10.3389/fmicb.2019.01850

Ragazzola, F., Caragnano, A., Basso, D., Schmidt, D. N., and Fietzke, J. (2019). Establishing temperate crustose early Holocene coralline algae as archives for palaeoenvironmental reconstructions of the shallow water habitats of the Mediterranean Sea. *Palaeontology* 1–16. doi: 10.1111/pala.12447

Rasser, M., and Nebelsick, J. (2003). Provenance analysis of Oligocene autochthonous and allochthonous coralline algae: a quantitative approach towards reconstructing transported assemblages. *Palaeogeogr Palaeoclimatol. Palaeoecol.* 201, 89–111. doi: 10.1016/S0031-0182(03)00512-1

Rasser, M. W. (2000). Coralline red algal limestones of the late Eocene Alpine Foreland Basin in Upper Austria: component analysis, facies and palecology. *Facies* 42, 59–92. doi: 10.1007/BF02562567

Richards, J. L., Gabrielson, P. W., Hughey, J. R., and Freshwater, D. W. (2018). A re-evaluation of subtidal *Lithophyllum* species (Corallinales, Rhodophyta) from North Carolina, USA, and the proposal of *L. searlesii* sp. nov. *Phycologia* 57, 318–330. doi: 10.2216/17-110.1

Richards, J. L., Sauvage, T., Schmidt, W. E., Fredericq, S., Hughey, J. R., and Gabrielson, P. W. (2017). The coralline genera *Sporolithon* and *Heydrichia* (Sporolithales, Rhodophyta) clarified by sequencing type material of their generitypes and other species. *J. Phycol.* 53, 1044–1059. doi: 10.1111/jpy.12562

Rindi, F., and Cinelli, F. (2000). Phenology and small-scale distribution of some rhodomelacean red algae on a western Mediterranean rocky shore. *Eur. J. Phycol.* 35, 115–125. doi: 10.1080/09670260010001735701

Rodriguez-Prieto, C. (2016). Light and temperature requirements for survival, growth and reproduction of the crustose coralline *Lithophyllum stictaeforme* from the Mediterranean Sea. *Bot. Mar.* 59, 95–104. doi: 10.1515/bot-2015-0070

Rögl, F. (1998). Palaeogeographic considerations for Mediterranean and Paratethys seaways (Oligocene to Miocene). *Ann. Natur. Mus. Wien* 99, 279–310.

Rohling, E. J., Foster, G. L., Grant, K. M., Marino, G., Roberts, A. P., Tamisiea, M. E., et al. (2014). Sea-level and deep-sea-temperature variability over the past 5.3 million years. *Nature* 508, 477–482. doi: 10.1038/nature13230

Rosales, I. (1995). *La plataforma carbonatada de castro urdiales (Aptiense-Albiense, Cantabria)* (Ph.D. thesis). Universidad del País Vasco, Bilbao, Spain.

Rosas-Alquicira, E. F., Riosmena-Rodriguez, R., and Neto, A. I. (2010). Typification and status of *Amphiroa cryptarthrodia* Zanardini (Lithophylloideae, Corallinales, Rhodophyta). *Phycol Res.* 58, 248–257. doi: 10.1111/j.1440-1835.2010.00584.x

Rösler, A., Perfectti, F., Peña, V., Aguirre, J., and Braga, J. C. (2017). Timing of the evolutionary history of Corallinaceae (Corallinales, Rhodophyta). *J. Phycol.* 53, 567–576. doi: 10.1111/jpy.12520

Rösler, A., Perfectti, F., Peña, V., and Braga, J. C. (2016). Phylogenetic relationships of Corallinaceae (Corallinales, Rhodophyta): taxonomic implications for reef-building corallines. *J. Phycol.* 52, 412–431. doi: 10.1111/jpy.12404

Sakalli, A. (2017). Sea surface temperature in the Mediterranean Sea under climate change: a linear model simulation of the sea surface temperature up to 2100. *Appl. Ecol. Environ. Res.* 15, 707–716. doi: 10.15666/aeer/1501_707716

Scheibner, C., and Speijer, R. P. (2008). Late Paleocene–early Eocene Tethyan carbonate platform evolution—a response to long- and short-term paleoclimatic change. *Earth Sci. Rev.* 90, 71–102. doi: 10.1016/j.earscirev.2008.07.002

Scotese, C. R. (2014a). *Atlas of Early Cretaceous Paleogeographic Maps, PALEOMAP Atlas for ArcGIS,* Vol. *2,* The Cretaceous, Maps 23-31, Mollweide Projection, PALEOMAP Project, Evanston, IL.

Scotese, C. R. (2014b). *Atlas of Paleogene Paleogeographic Maps (Mollweide Projection), Maps 8-15,* Vol. 1, *The Cenozoic, PALEOMAP Atlas for ArcGIS, PALEOMAP* Project, Evanston, IL.

Siboni, N., Abrego, D., Evenhuis, C., Logan, M., and Motti, C. A. (2015). Adaptation to local thermal regimes by crustose coralline algae does not affect rates of recruitment in coral larvae. *Coral Reefs* 34, 1243–1253. doi: 10.1007/s00338-015-1346-3

Sneed, J. M., Ritson-Williams, R., and Paul, V. J. (2015). Crustose coralline algal species host distinct bacterial assemblages on their surfaces. *ISME J.* 9, 2527–2536. doi: 10.1038/ismej.2015.67

Soliman, R. M., Younis, S. A., El-Gendy, N. S., Mostafa, S. S. M., El-Temtamy, S. A., and Hashim, A. I. (2018). Batch bioethanol production via the biological and chemical saccharification of some Egyptian marine macroalgae. *J. Appl. Microbiol.* 125, 422–440. doi: 10.1111/jam.13886

Solms-Laubach, H. (1881). Die Corallinenalgen des Golfes von Neapel und der angrenzenden Meeres-Abschnitte. *Fauna Fl. Neapel* 4, 1–64.

Soto, J., and Conde, F. (1989). Sobre la fenologia reproductora de las algas rojas en el litoral de Sudeste de España (Alboran oriental). *Acta Bot. Malacitana* 14, 5–12.

Stengel, D. B., Conde-Álvarez, R., Connan, S., Nitschke, U., Arenas, F., Abreu, H., et al. (2014). Short-term effects of CO_2, nutrients and temperature on three marine macroalgae under solar radiation. *Aquat. Biol.* 22, 159–176. doi: 10.3354/ab00576

Stockar, R. (2000). Fossil coralline algae from the Paleocene Montorfano Member type-section (Tabiago Formation, northern Italy). *Ecol. Geol. Helvet.* 93, 409–427.

Tomás, S., Aguirre, J., Braga, J. C., and Martín-Closas, C. (2007). Late Hauterivian coralline algae (Rhodophyta, Corallinales) from the Iberian Chain (E Spain). Taxonomy and the evolution of multisporangial reproductive structures. *Facies* 53, 79–95. doi: 10.1007/s10347-006-0088-7

Turland, N. J., Wiersema, J. H., Barrie, F. R., Greuter, W., Hawksworth, D. L., Herendeen, P. S., et al. (2018). International Code of Nomenclature for algae, fungi, and plants (Shenzhen Code) Adopted by the Nineteenth International Botanical Congress Shenzhen, China, July 2017. Regnum Vegetabile 159. Glashütten: Koeltz Botanical Books.

Vannucci, G., Piazza, M., Fravega, P., and Abate, C. (1996). Litostratigrafia e paleoecologia di successioni a rodoliti della "Pietra da Cantoni" (Monferrato orientale, Italia nord-occidentale). *Atti Soc. Tosc. Sc. Nat. Mem. Ser. A* 103, 69–86.

Vatova, A. (1948). Fenologia delle alghe marine di Rovigno. *Nova Thalassia* 1, 43–69.

Verbruggen, H. (2014). Morphological complexity, plasticity, and species diagnosability in the application of old species names in DNA-based taxonomy. *J. Phycol*. 50, 26–31. doi: 10.1111/jpy.12155

Verlaque, M. (2001). Checklist of the macroalgae of Thau Lagoon (Hérault, France), a hot spot of marine species introduction in Europe. *Oceanol. Acta* 24, 29–49. doi: 10.1016/S0399-1784(00)01127-0

Verlaque, M. (2010). Field-methods to analyse the condition of Mediterranean *Lithophyllum byssoides* (Lamarck) Foslie rims. *Sci. Rep. Port-Cros Natl. Park* 24,185–196.

Walker, R. H., Brodie, J., Russell, S., Irvine, L. M., and Orfanidis, S. (2009). Biodiversity of coralline algae in the Northeastern Atlantic including *Corallina caespitosa* sp. nov. *(Corallinoideae, Rhodophyta). J. Phycol*. 45, 287–297. doi: 10.1111/j.1529-8817.2008.00637.x

Williamson, C. J., Walker, R. H., Robba, L., Yesson, C., Russell, S., Irvine, L. M., et al. (2015). Towards resolution of species diversity and distribution in the calcified red algal genera *Corallina* and *Ellisolandia* (*Corallinales*, *Rhodophyta*) and related genera. *Phycologia* 54, 2–11. doi: 10.2216/14-024.1

Woelkerling, W. J. (1983). A taxonomic reassessment of *Lithophyllum* (*Corallinaceae, Rhodophyta*) based on studies of R.A. Philippi's original collections. *Br. Phycol. J*. 183, 299–328. doi: 10.1080/00071618300650301

Woelkerling, W. J. (1985). A taxonomic reassessment of *Spongites* (Corallinaceae, Rhodophyta) based on studies of Kützing's original collections. *Br. Phycol. J*. 20, 123–153. doi: 10.1080/00071618500650151

Woelkerling, W. J., Chamberlain, Y. M., and Silva, P. C. (1985). A taxonomic and nomenclatural reassessment of *Tenarea*, *Titanoderma* and *Dermatolithon* (*Corallinaceae, Rhodophyta*) based on studies of type and other critical specimens. *Phycologia* 24, 317–337. doi: 10.2216/i0031-8884-24-3-317.1

Woelkerling, W. J., Granier, B., and Dias-Brito, D. (2014). *Heydrichia* (?) *poignantii*, sp. nov. (*Sporolithaceae*, Sporolithales, *Rhodophyta*), a 100 million year old fossil coralline alga from north-eastern Brazil, and a new Hauterivian record of *Sporolithon* from Switzerland. *Carnéts Geol*. 14, 139–158. doi: 10.4267/2042/53736

Woelkerling, W. J., Gustavsen, G., Myklebost, H. E., Prest,ø, T., and Såstad, S. M. (2005). The coralline red algal herbarium of Mikael Foslie: revised catalogue with analyses. *Gunneria* 77, 1–625.

Woelkerling, W. J., and Irvine, L. M. (1986). The neotypification and status of *Phymatolithon* (Corallinaceae, Rhodophyta). *Br. Phycol. J*. 21, 55–80. doi: 10.1080/00071618600650071

Wolf, M. A., Falace, A., Kaleb, S., and Moro, I. (2016). Molecular data confirm the existence of attached crustose tetrasporangial thalli in *Phymatolithon calcareum* (*Melobesioideae*, Hapalidiaceae, *Rhodophyta*) from the Mediterranean Sea. *Aquat. Bot*. 134, 75–81. doi: 10.1016/j.aquabot.2016.07.006

Wolf, M. A., Maneveldt, G. W., Kaleb, S., Moro, I., and Falace, A. (2015). Morphological and molecular characterization of *Hydrolithon rupestre* (Corallinaceae, Corallinales, Rhodophyta): first report from the Mediterranean Sea. *Phytotaxa* 224, 59–71. doi: 10.11646/phytotaxa.224.1.4

Zachos, J., Pagani, M., Sloan, L., Thomas, E., and Billups, K. (2001). Trends, rhythms, and aberrations in global climate 65 Ma to Present. *Science* 292, 686–693. doi: 10.1126/science.1059412

Zachos, J. C., Dickens, G. R., and Zeebe, R. E. (2008). An early Cenozoic perspective on greenhouse warming and carbon-cycle dynamics. *Nature* 451, 279–283. doi: 10.1038/nature06588

Žuljević, A., Kaleb, S., Pena, V., Despalatović, M., and Cvitković, I., De Clerck, O., et al. (2016). First freshwater coralline alga and the role of local features in a major biome transition. *Sci. Rep*. 6:19642. doi: 10.1038/srep19642

Conflict of Interest: The authors declare that the research was conducted in the absence of any commercial or financial relationships that could be construed as a potential conflict of interest.

The reviewer AC declared a past co-authorship with one of the authors LG to the handling editor.

Copyright © 2019 Rindi, Braga, Martin, Peña, Le Gall, Caragnano and Aguirre. This is an open-access article distributed under the terms of the Creative Commons Attribution License (CC BY). The use, distribution or reproduction in other forums is permitted, provided the original author(s) and the copyright owner(s) are credited and that the original publication in this journal is cited, in accordance with accepted academic practice. No use, distribution or reproduction is permitted which does not comply with these terms.

frontiers in Marine Science

ORIGINAL RESEARCH
published: 13 March 2019
doi: 10.3389/fmars.2019.00106

Intertidal Mediterranean Coralline Algae Habitat Is Expecting a Shift Toward a Reduced Growth and a Simplified Associated Fauna Under Climate Change

Agnese Marchini[1†], Federica Ragazzola[2†], Claudio Vasapollo[3], Alberto Castelli[4], Gabriella Cerrati[5], Federica Gazzola[1], Chulin Jiang[6], Joachim Langeneck[4], Maria Chiara Manauzzi[1], Luigi Musco[7], Matteo Nannini[4,5], Jurgita Zekonyte[6] and Chiara Lombardi[5]*

[1] Department of Earth and Environmental Sciences, University of Pavia, Pavia, Italy, [2] Institute of Marine Sciences, University of Portsmouth, Portsmouth, United Kingdom, [3] National Research Council, Institute of Marine Sciences of Ancona, Ancona, Italy, [4] Department of Biology, University of Pisa, Pisa, Italy, [5] ENEA Marine Environment Research Centre, La Spezia, Italy, [6] School of Engineering, University of Portsmouth, Portsmouth, United Kingdom, [7] Stazione Zoologica Anton Dohrn, Integrative Marine Ecology Department, Naples, Italy

Coralline algae represent the most important bioconstructors in the Mediterranean Sea and are currently impaired by the effects of climate change (CC), particularly by global warming and ocean acidification (OA). We studied the effects of these two drivers on *Ellisolandia elongata*, an intertidal coralline algae that is known to host a rich biodiversity of associated fauna. We cultured turfs of *E. elongata* in experimental conditions of increased temperature and OA (using the values of the IPCC scenario RCP- 8.5 expected for 2100: actual mean temperature +3°C and pH = 7.78), and estimated alteration of algal linear growth and community structure, focusing especially on peracarid crustaceans and annelids. Our findings revealed a decrease in linear growth, yet with no significant changes on structural integrity, and a simplification of associated community, in particular for peracarids. Our study contributes to understand community-level response to CC drivers, highlighting the vulnerability of the fauna associated to an important Mediterranean marine habitat.

Keywords: climate change, intertidal ecosystem, coralline algae, bioconstruction, biodiversity, peracarid crustaceans, polychaetes

OPEN ACCESS

Edited by:
Julio Aguirre, University of Granada, Spain

Reviewed by:
Tamar Guy-Haim, Israel Oceanographic and Limnological Research, Israel
Jason Michael Hall-Spencer, University of Plymouth, United Kingdom
Sophie Martin, Station Biologique de Roscoff, France

***Correspondence:**
Federica Ragazzola
federica.ragazzola@port.ac.uk

† These authors have contributed equally to this work

Specialty section:
This article was submitted to Marine Ecosystem Ecology, a section of the journal Frontiers in Marine Science

Received: *29 October 2018*
Accepted: *21 February 2019*
Published: *13 March 2019*

Citation:
Marchini A, Ragazzola F, Vasapollo C, Castelli A, Cerrati G, Gazzola F, Jiang C, Langeneck J, Manauzzi MC, Musco L, Nannini M, Zekonyte J and Lombardi C (2019) Intertidal Mediterranean Coralline Algae Habitat Is Expecting a Shift Toward a Reduced Growth and a Simplified Associated Fauna Under Climate Change. Front. Mar. Sci. 6:106. doi: 10.3389/fmars.2019.00106

INTRODUCTION

Current increase in carbon dioxide due to anthropogenic forcing (Collins et al., 2013) is dramatically affecting the oceans. The increase in greenhouse gasses has led to a rise of the global temperature average on Earth's surface by 0.7°C during the last century and according to scenario RCP – 8.5 (IPCC, 2014), it is expected to rise by 3°C by 2100. About 93% of the excess heat accumulated in the Earth system ends up in the ocean, causing ocean warming (Bindoff et al., 2013; Rhein et al., 2013). The ocean's capacity to act as an important sink for anthropogenic carbon over the past few decades has also caused a decrease in ocean pH, with major changes

in the seawater chemistry, namely an increase of bicarbonate and a decrease of carbonate ions as well as of the saturation state of calcium carbonate. Among marine ecosystems, bioconstructions are especially vulnerable to CC, and in particular to the decrease in pH driven by the ongoing carbon uptake from the atmosphere to the ocean (Martin and Gattuso, 2009; Bijma et al., 2013; Kamenos et al., 2013). Structurally complex, bioconstructions host macroinvertebrate communities characterized by remarkable abundance and species richness (Crowder and Cooper, 1982). In fact, they increase benthic diversity by providing hard substrates with a complex architecture for the species to settle on, hide and protect, thus the resulting assemblages are highly diverse and taxonomically complex (Jokiel et al., 2008). Previous studies showed that the physical characteristics of habitats affect community structure (MacArthur and MacArthur, 1961; Lawton, 1983; Ellner et al., 2001), with several studies demonstrating the linear relationship between increase in habitat complexity and increase in the diversity and abundance of its associated fauna (Kohn and Leviten, 1976; Heck and Wetstone, 1977; Downes et al., 1998). The reasons of this linear relationship are multiple: the complexity of the structure increases the number of possible refuge areas and niches (MacArthur and MacArthur, 1961; Schoener, 1974) and the structure itself can also affect biological processes and environmental factors such as competitive interactions (Fletcher and Underwood, 1987) and impact of disturbances (e.g., mitigation of wave action) (Dommasnes, 1968; Whorff et al., 1995). Bioconstructional organisms provide the bases for many other ecosystem processes, making them pivotal for conservation (Crain and Bertness, 2006; Ingrosso et al., 2018).

On rocky intertidal shores around the world, one of the main group of bioconstructional organisms is represented by articulated coralline algae (Stewart, 1982; Dye, 1993; Benedetti-Cecchi and Cinelli, 1994), which often form complex, extremely dense and highly branched turfs that are considered the apex of algal structural complexity (Davenport et al., 1999). Even though the coralline turf is highly variable, with the fronds length and density differing at small spatial scale, they still can host high-densities of macrofaunal organisms, up to 250,000 individuals per m^2 (Kelaher et al., 2001), with annelid polychaetes and crustaceans peracarids representing the dominant macrofaunal groups (Musco, 2012).

Coralline algae not only do support high biodiversity (Jones et al., 1997; Gattie et al., 2003; Kuffner et al., 2008), but they contribute to the global inorganic carbon budgets in shallow water ecosystems (Foster, 2001; Martin and Gattuso, 2009), hence they are receiving renewed attention across the ecological and geological sciences, mainly owing to the threat of CC. This is mainly due to the mineralogical composition of their thalli, based on high Mg-Calcite, the most soluble $CaCO_3$ polymorph compared to calcite and aragonite. Several studies have analyzed the effect of pH and temperature on coralline algae, showing a stronger effect of temperature if compared with that of CO_2 concentration (Martin and Gattuso, 2009; Martin et al., 2013). Previous studies have shown a negative effect of global warming (GW) on recruitment (Kuffner et al., 2008), growth (Jokiel et al., 2008), and calcification (Gao et al., 1993; Semesi et al., 2009) of coralline algae leading to an increasing susceptibility to grazing by bioeroders (Steneck, 1986). Thus, GW and OA could have a dramatic consequence on species distributions (Harley et al., 2012; Bijma et al., 2013), possibly causing shifts in their abundance and geographical boundaries (Díez et al., 2012). Most of the studies so far have been focusing on the effect of CC on the physiology of the algae, often neglecting the organisms living within their fronds. In fact, synergism between acidification and warming exacerbates the negative effects on ecosystem associated communities, and is expected to cause a shift toward a less diverse ecosystem in terms of species richness and spatial heterogeneity, directly affecting the lower levels of the food web and eventually reducing productivity and trophic energy (Kleypas et al., 2006; Smale et al., 2011; Bijma et al., 2013; Sunday et al., 2017).

This experimental study was designed to mimic the environmental conditions predicted for the year 2100 by the RCP 8.5 (IPCC, 2014) and to analyze the responses of the coralline alga *Ellisolandia elongata* (Rodophyta, Corallinales) and its associated fauna. *Ellisolandia elongata*, formerly known under the name *Corallina elongata* (see Cormaci et al., 2017 for an appraisal of synonymies) is widely distributed in the North-Eastern Atlantic and in the whole Mediterranean Sea (Bressan and Babbini, 2003), where it represents one of the most important bioconstructors. It can create tridimensional biogenic structures which are developed on vertical shady rock faces, from the surface to one meter deep, in high energy areas (i.e., rocky bottoms exposed to waves and currents) (Bressan and Babbini, 2003).

In particular, we analyzed the combined effects of GW and OA on: (1) *E. elongata* linear extension; (2) *E. elongata* structural integrity; (3) community structure of the associated fauna.

This study aimed to approach the responses to climate change (CC) at the community level, and highlighted the vulnerability to the dominant combination of climate drivers occurring at specific habitats. Despite its importance, the response to global changes at community level has been still poorly investigated, thus, the need for field observations and long-term experiments to understand the emergence of different levels of biological responses and their feedbacks is a priority, in order to design appropriate mitigation actions (Pörtner et al., 2014).

MATERIALS AND METHODS

Target Algal Species

Ellisolandia elongata (J. Ellis and Solander) K. R. Hind and G. W. Saunders is a red alga belonging to the order Corallinales, family Corallinaceae. Reddish-lilac to whitish-pink in color, it has branching, pinnate flexible fronds and an erect thallus attached to the rocky substrate by a crustose holdfast (**Figure 1**). The fronds are made of small calcified segments (intergenicula), which are separated from one another by uncalcified nodes (genicula) (Babbini and Bressan, 1997; Bressan and Babbini, 2003).

Being adapted to variable habitats (e.g., the intertidal rocky pools of the northeastern Atlantic), this species can experience

FIGURE 1 | (A) *Ellisolandia elongata* fronds; **(B)** *E. elongata* at Palmaria island.

large fluctuations in the physico-chemical factors, and therefore it has been suggested to have advantages, under the current GW and OA scenario, over other coralline algae adapted to more stable environments (Egilsdottir et al., 2013).

Study Site

The study area is located in the Gulf of La Spezia (North-West Mediterranean Sea), within the Natural Regional Park of Portovenere and the Islands (Palmaria, Tino, and Tinetto). The presence of vertical rocky walls as well as sandy shoals, exposed and sheltered sites, make the Gulf an important source of marine biodiversity promoted and maintained by several ecosystem engineers, including seagrass such as *Posidonia oceanica* and calcifying bioconstructors such as coralline algae, corals and bryozoans (Cocito et al., 2000, 2002; Peirano et al., 2005; Nannini et al., 2015). The sampling site is located in the Palmaria Island (surface area: 1.89 km^2), at the locality 'Cala Grande' (north-western side of the island: 44° 2.366′ N, 9° 50.519′ E; **Figure 2**). This area is characterized by an extremely limited tidal range, around 10–40 (up to 50) cm. The salinity in this area is rather constant, around 36.8–36.9 PSU (Gasparini et al., 2009), whereas surface temperatures range between 12 and 13°C in winter (minimum values) and the maximum value of 26–27°C in summer (maximum values). The minimum–maximum values recorded in March–April 2015 were 13–15°C; in the end of September–October 2015 20–24°C. Mean pH value was 8.1. Due to seawater circulation, current intensity (velocity: 4 cm s^{-1}), and wave actions (height: 20–100 cm), this site is one of the most exposed to seawater physical forces (Ciuffardi et al., 2013).

Sampling and Sample Preparation

The experiment was carried out between July and October 2015. In July, four areas, approximately 10 m far from each other, were randomly allocated on vertical rocks at 50 cm of depth. Using hammer and chisel, we collected 84 samples (5 cm × 5 cm each) of substrate covered by *E. elongata* turfs. The collected turfs were then placed in separate bags filled with seawater and transported to the laboratory inside a thermal-box. Out of the 84 samples originally collected, 12 (3 per area, haphazardly chosen) were preserved in ethanol for the identification of the associated fauna, while 72 samples were placed into a thermal bath (150 L) for the acclimatization to the laboratory condition (1 week). At the end of the week, the turfs were stained using Alizarin Red S (Andrake and Johansen, 1980), which has been used for many decades for *in vivo* labeling (Holcomb et al., 2013; Bensimon-Brito et al., 2016), by placing them in aerated (airstone pump -Mouse Air Pump 4, Delta, United States) plastic bags with a solution of 0.25 g L^{-1} Alizarin Red S staining (Fluka, Sigma-Aldrich) for 24 h at 20°C in 12:12 h light-dark cycle. At the end of the staining period, eight experimental aquaria (four for control condition, C1–C4, and four for treatment conditions, T1–T4; **Figure 3**) were set up with nine *E. elongata* turfs each by placing the bags straight into the aquaria, in order to avoid the loss of the alga-associated fauna. The alizarin was progressively washed out by in conditions of continuum water exchange, up to its complete removal from the aquaria. Once cleaned, the aquaria were progressively set up to the following experimental conditions: control – current temperature and pH conditions of the Gulf of La Spezia (24.76 ± 0.83°C in August, 23.15 ± 0.90°C in September and 20.57 ± 0.83°C in October; 385 ppmv/pH 8.1; see **Supplementary Table S1**); treatment – increased temperature (mean monthly temperature +3°C) and decreased pH (pH = 7.75) according to the 2100 scenario (IPCC – scenario RCP- 8.5). For details on the experimental design, system set-up and environmental conditions within the system see **Supporting Information S1, S2** and **Table S1**.

Linear Growth

From each of the four control aquaria and each of the four treatment aquaria, three *E. elongata* turfs were sampled after 1 month (on August 24th), three after 2 months (September 22nd), and the last three after 3 months (October 22nd). For each aquarium and each sampling event, 20 fronds were randomly selected from the three turfs and measured to estimate *E. elongata* linear extension. In particular, after collection the fronds were rinsed with deionized water, dried naturally for 24 h, and then photographed under the stereomicroscope (AZ 100, Nikon, Japan; lens 1x with camera DS-U1, Nikon, Japan), then the distance between the red band left after the staining and the new frond apex was measured using ImageJ® software (**Figure 4a**).

Structural Integrity

Nanoindentation on all samples was performed using Nanotest (Platform 3) indentation instrument (Micromaterials, Ltd., Wrexham, United Kingdom). Instrument description and its working principle is in detailed explained in Beake and Leggett (2002), Beake et al. (2002). Indents were done using standard Berkovich diamond indenter in a load-controlled mode. Maximum force was set to 5 mN, loading and unloading rates were set each to 0.01 mN/s, holding time of 30 s at maximum load was set to minimize the influence of creep. Measurements were performed on the top of three genicula of each algae branch (three branches per set). A matrix of 60 to 120 indents with 50 μm space between each indent was set on each geniculum to measure the distribution of mechanical properties, such as hardness and elastic modulus (see section "Statistical Analyses"). To identify the position of an indent, an integrated optical microscope was used before and after indentation experiments.

Associated Fauna

From each of the four control (C) aquaria and four treatment (T) aquaria, three turfs were sampled on August 24th, three

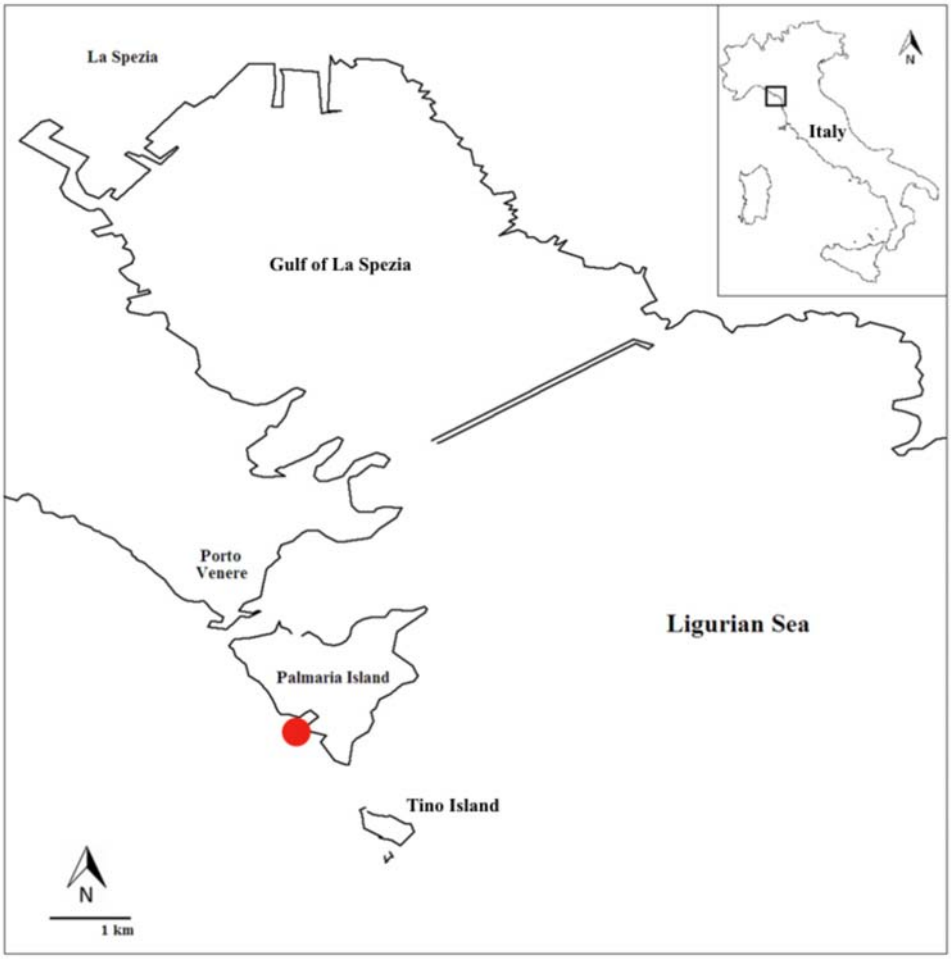

FIGURE 2 | Map of the Gulf of La Spezia showing the sampling site (red dot).

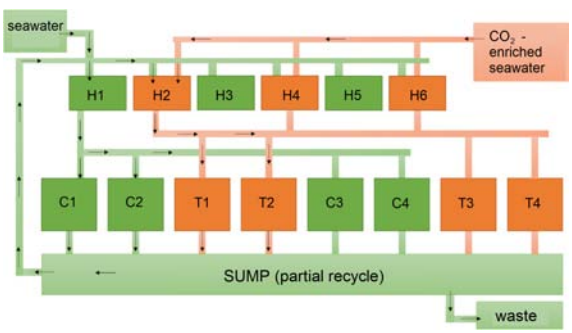

FIGURE 3 | Scheme of the experimental system. Green: control, orange: treatment; H: header tanks; C: control aquaria; T: treatment aquaria. Arrows indicate flow direction.

on September 22nd and finally, three on October 22nd, 2015, meaning that at each month 24 turfs were collected in total (12 C + 12 T). Each sample was put into a separate container and preserved in ethanol. To remove the associated macrofauna from the algal fronds, the sample was washed with tap water, while being gently rubbed, and subsequently sieved (0.5 mm mesh size). The sequence of rubbing-washing-sieving was repeated at least three times to ensure the removal of all the vagile fauna associated to *E. elongata*. After this, the sample was observed under a stereoscope (AZ100, Nikon, Japan) to ensure the complete removal of all individuals.

When each turf sample was cleared by the fauna, the volume of the sample was used as standard unit to compare samples with different size (i.e., tridimensional structures of different size = difference in habitat availability = difference in abundance of associated taxa) created by each algal turf. Each sample was immersed in a 1000 cm^3 beaker, filled with tap water, and the volume was calculated as difference between final and initial volume (Pereira et al., 2006; Izquierdo and Guerra-García, 2011).

Samples of associated vagile fauna were preserved in 70% ethanol and analyzed under a stereomicroscope (WILD M5A, Heerbrugg); individuals were counted and divided in different higher-rank taxonomic groups, including both calcifying (i.e., molluscs, crustaceans, echinoderms) and non-calcifying organisms (i.e., polychaetes, nematodes). The only exception

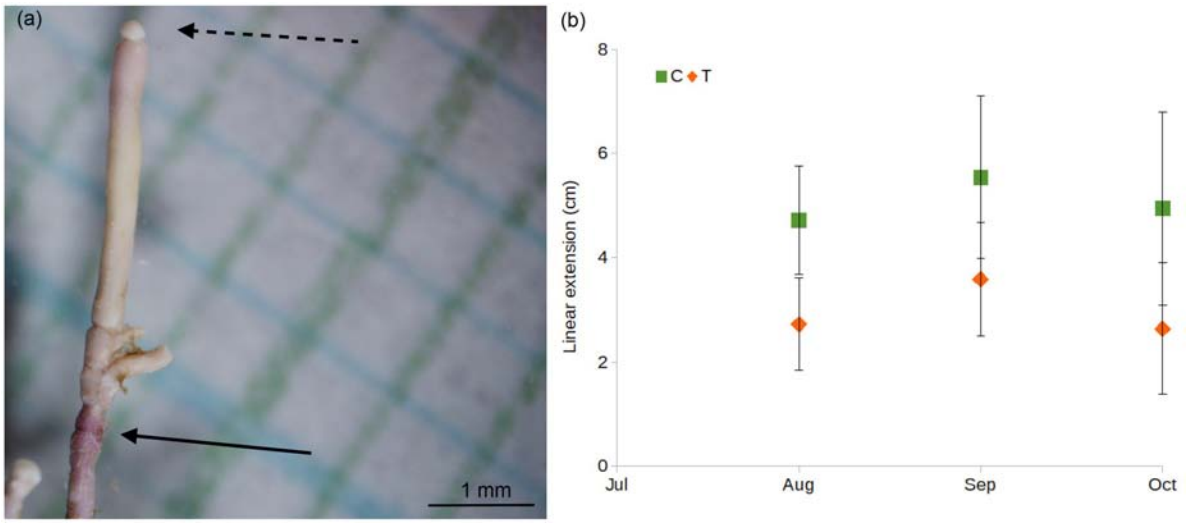

FIGURE 4 | (a) Frond of *E. elongata* stained with Alizarin Red. Continuous arrow indicates red line of the staining. Dotted arrow indicates the frond tip. Linear extension (i.e., portion of frond grown after the staining) is comprised between dotted and continuous arrow. **(b)** Linear growth of *E. elongata* (mean ± SD; *N* = 80: 20 fronds × 4 aquaria) measured after 1 month (August), 2 months (September), and 3 months (October).

was represented by the bivalve *Mytilus galloprovincialis* Lamarck 1819, a semi-sessile species representing the most abundant mollusc in natural conditions, which was included within mollusc counting. Peracarid crustaceans and polychaete annelids, representing the dominant component of the vagile assemblage, were identified at species level and counted. The abundance of each taxon was standardized to the volume of the sample to obtain relative abundance values.

Statistical Analyses

An orthogonal design was employed to test the null hypotheses that (1) linear extension of *E. elongata* fronds and (2) their structural integrity and (3) the abundance and diversity of the fauna associate to *E. elongata* turfs did not vary at different spatial and temporal scales under different experimental conditions (control: current monthly mean temperature and pH = 8.10; treatment: the monthly mean temperature +3°C and pH = 7.75) through time (3 months). Each experimental condition has been replicated four times (e.g., four aquaria for control and four for treatment). For the structural integrity analysis only three replicates were used.

Linear Extension

Differences in linear extension between the levels of the factors 'condition' (fixed; two levels: C and T) and 'time' (random; three levels: August, September, October) were estimated using the generalized linear mixed model (GLMM). The factor 'aquaria' (e.g., random) had been tested separately and excluded from the analyses due to the non-significant differences encountered.

Normality and homoscedasticity were assessed by visually checking the residuals distributions and relation versus predicted values (Zuur et al., 2007). A more formal Levene's test was also used to assess the variance homogeneity. When the test was significant ($p < 0.05$), transformations (square root, logarithmic) were applied. In the case of failure of the transformation, the more stringent criterion of $\alpha < 0.01$ was applied (Underwood, 1997). *Post hoc* Student-Newman-Keuls (SNK) tests were performed whenever a significant difference was found. These analyses were performed using Statistica® v.7.

Nano Indentation

During nanoindentation experiments a series of force vs. displacement curves were recorded. The analysis was performed using analytical software provided by MicroMaterials, where the unloading portion of the curve was fitted to a power law function to determine hardness and elastic modulus of algae samples (Oliver and Pharr, 1992).

Sample hardness (H) was calculated from the maximum load ($F_{\max}$) and projected area of contact, A_c, determined through a series of indentations at different loads on calibration sample of fused silica, by:

$$H = \frac{F_{\max}}{A_c} \tag{1}$$

Young's modulus (or elastic modulus), E, of the sample was determined from

$$\frac{1}{E_r} = \frac{1-\nu^2}{E} + \frac{1-\nu_i^2}{E_i}, \tag{2}$$

where ν is the Poisson's ratio of the sample, E_r is the reduced modulus of the sample derived from the load vs. displacement curves (Oliver and Pharr, 1992), ν_i is the Poisson's ratio of the indenter (0.07) and E_i is the Young's modulus for the indenter (1141 GPa). As Poisson's ratio of algae are not known, reduced indentation modulus (E_r) will be reported in this paper.

Maps of elastic modulus and hardness were generated to determine the distribution of the mechanical properties. These maps were further processed by eliminating values obtained on

epoxy resin as well as where surface defects interfered with points of measurement. Statistical histograms of modulus and hardness were also obtained, and mean values were calculated (**Figure 5**).

Associated Fauna

Relative abundances of taxonomic groups were compared for the two factors 'condition' and 'time' (see section "Linear Extension") by using multifactorial ANOVA (Underwood, 1997). Rare taxonomic groups were excluded from the analysis. Prior the application of multifactorial ANOVA, a data exploring protocol (Zuur et al., 2010) was applied to test for presence of anomalous values, heterogeneity of variance and dependence among observations. In case of violation of ANOVA assumptions, generalized least squares (GLSs) method (Aitken, 1935) based on restricted maximum likelihood (REML) was applied according to Zuur et al. (2009) protocol. The method allowed the corrections of the heterogeneity of residuals respect to the factors, thus respecting normality and homoscedastic assumptions.

The model selection was based on Akaike Information Criterion (AIC; Akaike, 1974) and the model with lower AIC value was selected. These analyses were performed with R © (R Core Team, 2016).

The effects of the experimental conditions on the vagile fauna community structure were also tested *via* permutational multivariate analysis of variance (PERMANOVA; Anderson, 2001), based on a Bray–Curtis similarity matrix. Rare species were removed from the data matrix. Data were transformed via square root, then zero-Adjusted Bray–Curtis method (Clarke et al., 2006) was applied to create a dissimilarity matrix. This approach was necessary in order to avoid indefinite values caused by the presence of double zero in the main matrix. The PERMANOVA test was applied to clarify differences between treatments and among months, and when a significant factor was found, a pairwise test was applied to identify the source of the differences. The SIMPER test was used to identify species mostly contributing to the dissimilarity between the significant factors obtained by PERMANOVA. A non-metric multi-dimensional scaling (nMDS) was plotted for each of the two groups, showing the variation in time of the peracarids and polychaetes under C and T conditions. These analyses were carried out on Primer 6.1.13 (Clarke and Gorley, 2006, 2015).

RESULTS

Linear Extension

The measurement of 480 *E. elongata* fronds [20 fronds × 8 aquaria (4C + 4T) × 3 months] showed that the species maintained a positive growth trend after 1 month (July–August) as well as after 2 months (July–September) in both C and

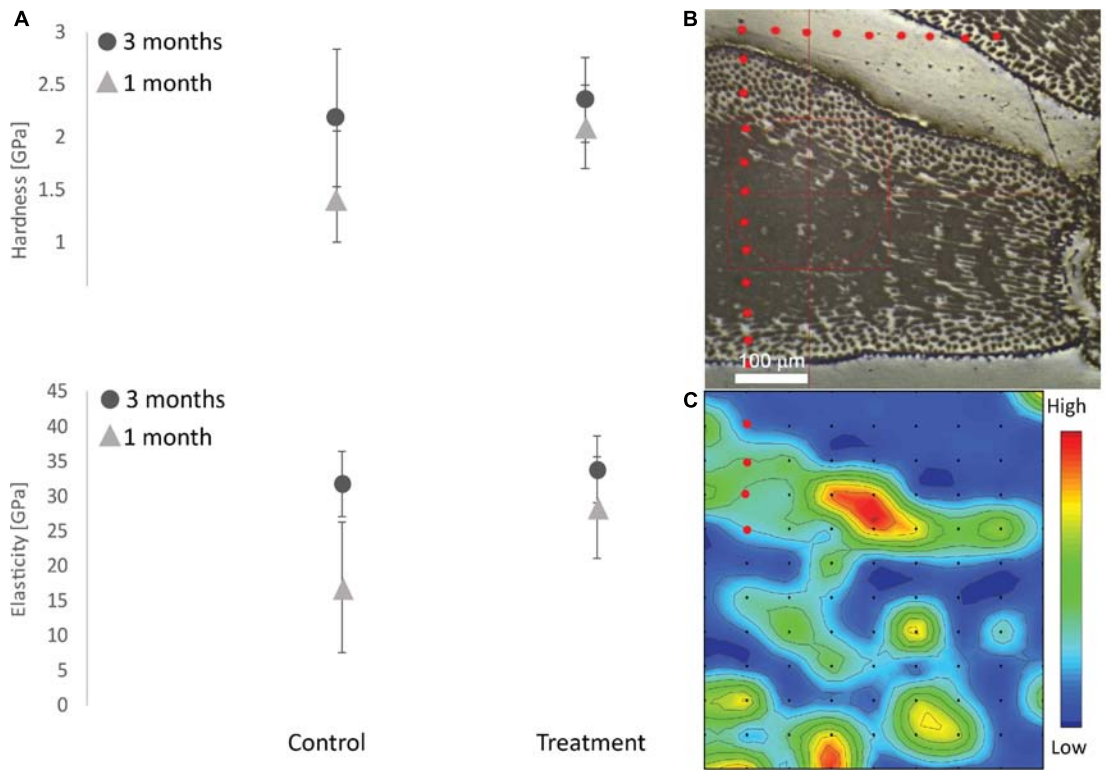

FIGURE 5 | Structural analysis of the *E. elongata* skeleton. **(A)** Elastic modulus and hardness on thalli growing under different conditions and times (H: C1month = 1.41 ± 1.4; C3months = 2.18 ± 0.69; T1month = 2.41 ± 1.1; T3months = 2.4 ± 0.7; E: C1month = 19.9 ± 16.2; C3months = 31.7 ± 8.09; T1month = 28.4 ± 12.5; T3months = 33.8 ± 8.3; *N* = 3 fronds, 60 × 120 indents each). **(B)** Optical images of a section of the skeleton. Red dots represent the frame of the indents. **(C)** Example of the distribution of the hardness within the skeleton. Red dots represent the frame of the indents.

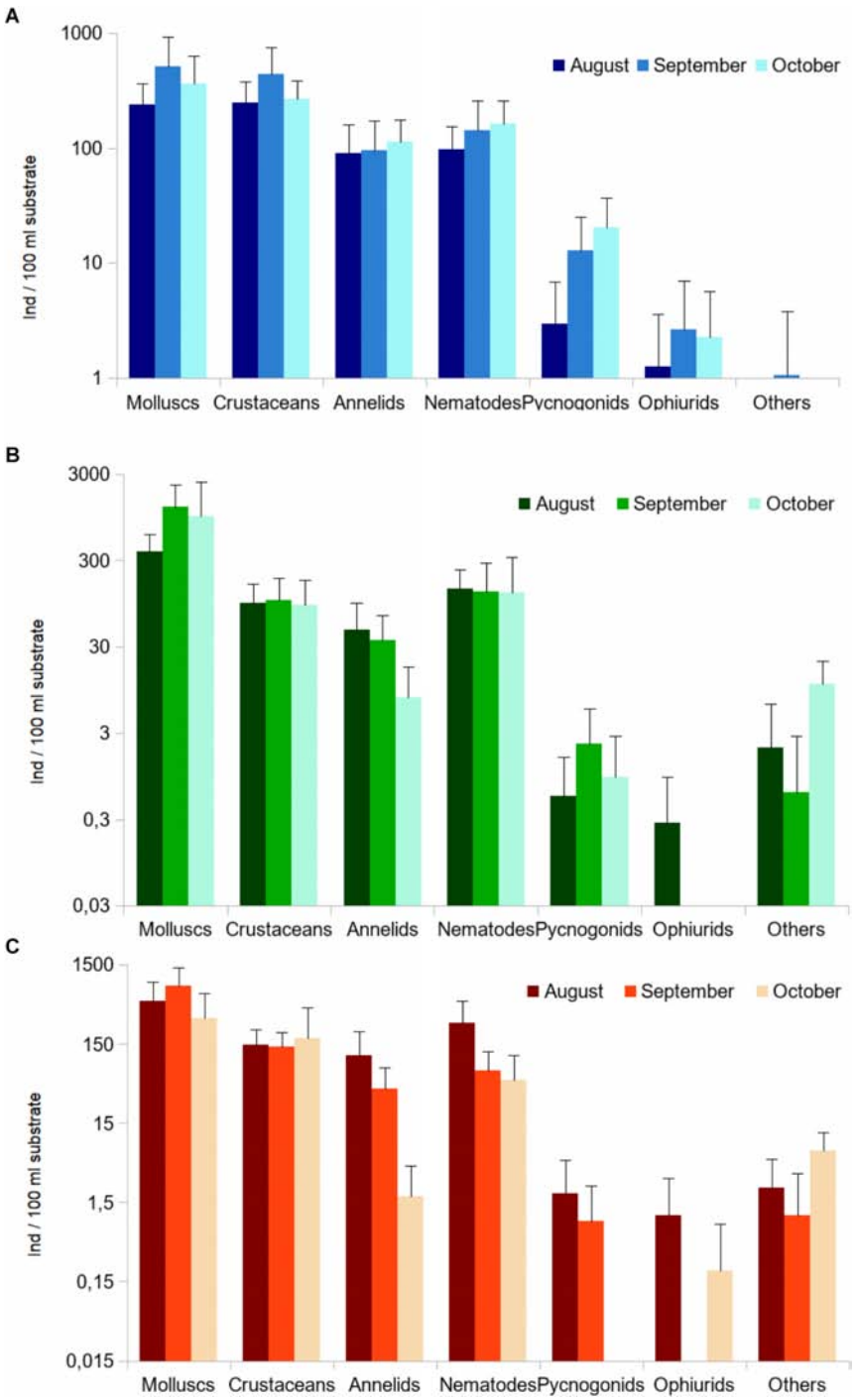

FIGURE 6 | Relative abundance (mean ± SD) of the main taxa associated to *E. elongata*, from August to October 2015 (on a logarithmic scale; please note that scales differ among graphs); **(A)** Palmaria island (*N* = 15: 5 sites × 3 replicates), **(B,C)** laboratory aquaria (*N* = 12: 4 aquaria × 3 replicates), under **(B)** control and **(C)** treatment conditions. Number of individuals standardized over a 100 ml volume of substrate. The category "others" includes nemerteans, sipunculids, and platyhelmints.

T conditions (**Figure 4b**), with an increase from August to September of $\Delta_{Aug-Sept}$ = 0.84 cm and $\Delta_{Aug-Sept}$ = 0.87 cm, respectively. At the end of the experiment (October), after 3 months of exposure, the linear extension was 4.94 ± 1.85 cm (C) and 2.64 ± 1.26 cm (T). Compared to the beginning of the experiment (July), in October the fronds maintained a positive growth in C conditions ($\Delta_{Aug-Oct}$ = 0.22) whereas a decrease under T condition was shown ($\Delta_{Aug-Oct}$ = −0.08 cm).

Data analyses revealed significant differences between conditions (F_1 = 177.48, $p < 0.01$) and among months (F_2 = 11.99, $p < 0.01$), and *post hoc* (SNK) showed significant differences after 1 and 2 months of exposure, in August and September ($p < 0.01$).

Structural Integrity

For the structural integrity analysis of the algal thallus, only the second genicula of each branch were analyzed in order to have full calcified cells. The hardness (H) and the elastic modulus (E) of the thallus in C condition after 1 month were 1.41 ± 1.4 SD GPa and 19.86 ± 16.92 SD Gpa, respectively, while after 3 months they were 2.18 ± 0.70 SD GPa and 31.80 ± 8.09, respectively (**Figure 5A**). Paired *t*-test showed no significant difference between 1 and 3 months of culturing (H: p = 0.31, df = 2; E: p = 0.19, df = 2) in C conditions. No significant difference was also found in the algae cultured in T conditions (Paired *t*-test-H: p = 0.69, df = 2; E: p = 0.52, df = 2): H and E of the thallus after 1 month were 2.41 ± 1.1 SD GPa and 28.40 ± 12.50 SD Gpa, respectively, while after 3 months they were 2.36 ± 0.70 SD GPa and 33.86 ± 8.30 SD GPa. No significant difference in the overall structural integrity (E and H) was found between C and T after both 1 and 3 months (Paired *t*-test-H 1 month: p = 0.64, df = 2; H 3 months: p = 0.81, df = 2; Paired *t*-test-E 1 month: p = 0.66, df = 2; H 3 months: p = 0.82, df = 2).

Associated Fauna

The macrofauna found on *E. elongata* turfs at Palmaria was characterized by dominance of molluscs and crustaceans over other groups (**Figure 6A**).

A similar pattern could be observed in the laboratory aquaria, both in C (**Figure 6B**) and T conditions (**Figure 6C**), although prominence of molluscs was more striking in the laboratory than in the field. For most groups, relative abundance was much higher in C than in T aquaria.

When looking at the species composition, peracarid crustaceans associated to *E. elongata* at Palmaria island were highly diverse, exhibiting 23 different species (see **Supplementary Table S2**; see also **Supporting Information S3** for an appraisal on some interesting faunal entities found in the samples).

In each sample, composed by a single turf of *E. elongata*, we found 22 ± 14 species on average per sample (values standardized over 100 cm^3 volume; **Figure 7A**). In the laboratory samples, the total number of peracarid species was lower than in the field, namely 7.5 ± 6.0 species on average (over 100 ml), but with differences among months, both in C and T aquaria (**Figures 7B,C**). As regards annelids, the analysis to species level showed that each sample had 14.5 ± 9.0 species on average (over 100 ml volume; **Figure 7A**; see also **Supplementary Table S3**). The laboratory aquaria hosted a notably high richness of polychaete species (30), with 7.5 ± 7.0 species on average per sample, yet with differences among months (**Figures 7B,C**).

Analysis of variance based on abundance values of the macro-groups revealed only two significant responses of single taxa to treatment (C vs. T conditions) and months (August vs. September vs. October). The abundance of crustaceans differed significantly between C and T aquaria, and polychaetes decreased significantly their abundance with time (**Table 1**). No significant differences emerged for molluscs and nematodes; other groups were not tested due to insufficient number of specimens.

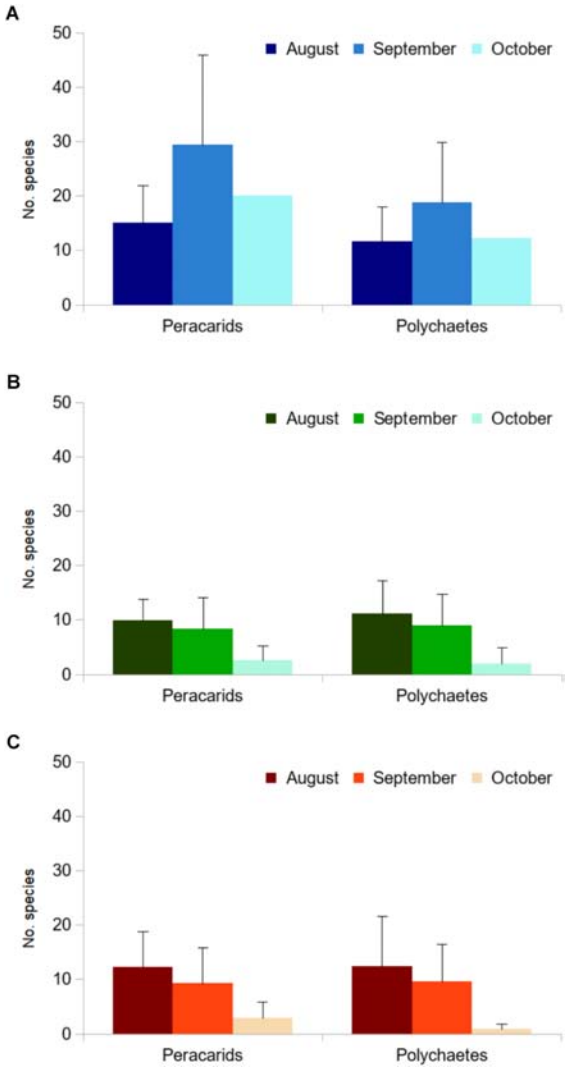

FIGURE 7 | Number of peracarid and polychaete species (mean ± SD) associated to *E. elongata*, from August to October 2015. **(A)** Palmaria island (N = 15: 5 sites × 3 replicates), **(B,C)** laboratory aquaria (N = 12: 4 aquaria × 3 replicates), under **(B)** control and **(C)** treatment conditions. Number of species standardized over a 100 ml volume of substrate.

The PERMANOVA analysis on the community structure of macro-groups, based on the Bray–Curtis similarity index, showed no significant response to the experimental conditions (C vs. T), yet highlighting differences in the abundance of the taxa along the 3 months of experiment (**Table 2**).

A different picture emerged when analyzing more in depth the species composition of peracarids and polychaetes assemblages with PERMANOVA. The interaction between condition and month was significant in shaping the community structure of peracarids (**Table 3**). The pairwise test applied to the

TABLE 1 | Results of linear multifactorial ANOVA (method GLS and REML) based on abundance values of the four major benthic groups investigated, tested for two orthogonal factors: *condition* (two levels: control and treatment) and *month* (three levels: August, September, October).

	df	Log likelihood ratio	*p*-value		df	Log likelihood ratio	*p*-value
Molluscs				Annelids			
Treatment	1	0.066	0.797	*Treatment*	1	1.872	0.171
Month	2	3.582	0.167	*Month*	2	14.546	**0.0007**
*Condition * Month*	2	2.511	0.285	*Condition * Month*	2	2.564	0.278
Crustaceans				Nematodes			
Condition	1	4.217	**0.040**	*Condition*	1	1.443	0.229
Month	2	0.409	0.815	*Month*	2	4.175	0.124
*Condition * Month*	2	0.138	0.931	*Condition * Month*	2	3.899	0.142

Here, only results of the best models are reported, after selection of the minimum AICc value and ΔAIC < 2. Significant p-values in bold font.

TABLE 2 | Results of PERMANOVA based on Bray–Curtis similarities for macro-groups, tested for two orthogonal factors: *condition* (two levels: control and treatment) and *month* (three levels: August, September, October).

	df	Pseudo-F	*p*-value
Condition	1	0.50684	0.6977
Month	2	3.0155	**0.0135**
*Condition * Month*	2	0.49837	0.8229

Significant p-value in bold font.

interaction factor showed clear differences between all the considered pairs of months, indicating a shift in the peracarid community along the period, under both conditions. The SIMPER analysis identified the species providing the highest contributions to the dissimilarity among months and between experimental conditions: the amphipods *Elasmopus pocillimanus* and *Jassa marmorata*, and the isopod *Paranthura costana*. In particular, *E. pocillimanus* gave the highest contribution (up to 44.0%) to the dissimilarity between C and T conditions across months, while *J. marmorata* and *P. costana* contributed up to 20.6 and 36.7%, respectively. However, the two latter ones decreased in abundance under T conditions, showing a negative response to the simulated conditions of reduced pH and increased temperature. Conversely, the average abundance of *E. pocillimanus* was higher in T than in C aquaria.

For polychaetes, instead, the interaction did not appear significant, despite significant differences observed for both factors (condition and month; **Table 4**). The pairwise test applied to the month factor showed significant differences between all the considered pairs of months, reflecting the progressive reduction in the polychaete abundances along the experiment period (they were absent from 11 replicates out of 24 at the end of the experiment, in October). According to the SIMPER test, the species mostly contributing to the dissimilarity among months were *Syllis gracilis* (19.7% between August and September and 24.7% between August and October), *Amphiglena mediterranea* (18.0% between August and September and 19.3% between August and October) and *Perinereis cultrifera* (15.0% between August and September and 18.6% between August and October). In fact, their average abundance progressively decreased with time. The nMDS revealed some separation between control and treatment samples for the peracarid assemblage (**Figure 8A**), with their dissimilarity increasing with time, thus confirming that the interaction between the two factors (condition × month) is important in shaping the peracarid assemblages. This pattern is less clear when the polychaetes assemblage is taken into account, possibly because of the low number of specimens recorded in the majority of replicates (**Figure 8B**).

DISCUSSION

In the Mediterranean Sea, previous studies on the effects of either warming or acidification on benthic communities have focused on very specific study-cases, reporting mass mortality events after heat wave events (e.g., Garrabou et al., 2009) and simplification of

TABLE 3 | Results of PERMANOVA based on Bray–Curtis similarities for peracarids: main test (left) and pairwise test (right), tested for two orthogonal factors: *condition* (two levels: 'control' and 'treatment') and *month* (three levels: August, September, October).

Main test				**Pairwise tests**	**Within level 'control' of factor *condition***		**Within level 'treatment' of factor *condition***	
	df	**Pseudo-F**	***p*-value**		***t***	***p*-value**	***t***	***p*-Value**
Condition	1	14,705	**0.0002**	August, September	3.0528	**0.0004**	1.9173	**0.008**
Month	2	14.164	**0.0002**	August, October	5.2885	**0.0002**	3.2571	**0.0002**
*Condition * Month*	2	6,7028	**0.0002**	September, October	2.1855	**0.0016**	2.5668	**0.0002**

Significant p-values in bold font.

TABLE 4 | Results of PERMANOVA based on Bray–Curtis similarities for polychaetes: main test (left) and pairwise test (right), tested for two orthogonal factors: *condition* (two levels: 'control' and 'treatment') and *month* (three levels: August, September, October).

Main test				**Pairwise tests**		
	df	**Pseudo-F**	***p*-value**		***t***	***p*-value**
Condition	1	3.1167	**0.0222**	August, September	2.307	**0.0002**
Month	2	15.551	**0.0002**	August, October	5.3404	**0.0002**
*Condition * Month*	2	1.2078	0.313	September, October	3.9718	**0.0002**

Significant p-values in bold font.

community structure along gradients of decreasing pH observed at volcanic CO_2 vent habitats (e.g., Cigliano et al., 2010; Kroeker et al., 2011; Porzio et al., 2011). Our study instead explores the combined effect of both pH and temperature alterations, experimentally exposing the organisms to values expected for 2100 (IPCC, 2014 –RCP- 8.5). We target the habitat-forming alga *E. elongata* and its associated fauna, finding that high CO_2 and high temperature conditions are responsible for the decreased linear growth rate in the alga and of structural changes in the benthic community; this effect is even more evident when taking into account the specific composition of selected taxonomic groups.

Physiological and structural responses withstanding the effects of ocean acidification have been already identified in coralline algae (Ragazzola et al., 2013, 2016; McCoy and Ragazzola, 2014), but little is still known on the algal structural responses in high CO_2 and high temperature environments.

In this study *E. elongata* showed a decrease in linear growth rates under high CO_2 and high temperature but, interestingly with no significant changes in the structural integrity of the skeleton. Due to their very densely packed and highly branched fronds, coralline algae represent the extreme end of algal structural complexity (Coull and Wells, 1983; Davenport et al., 1999). The unchanged structural integrity of the skeleton could represent a strong selective advantage allowing *E. elongata* to survive in changing environments. The partial preservation of the structural complexity, although hindered by the reduction in linear growth rate, could still provide a suitable habitat for the associated fauna.

However, the ecological costs of a possible shift in the energy budget from growth extension to maintaining structural integrity, like in *Lithothamnion glaciale* (Ragazzola et al., 2016), will need further investigations. For instance, during this experiment we were not able to assess if the decrease in linear growth rates was related to a decrease in the branching of the algae, which would in turn reduce the space availability for the macrofauna.

We verified that in the Palmaria island, the habitat-creator species *E. elongata* hosts a diverse and highly abundant community of small mobile invertebrates, as observed in similar habitats elsewhere (e.g., see Cowles et al., 2009; Guerra-García et al., 2009, 2012; Izquierdo and Guerra-García, 2011; Zakhama-Sraieb et al., 2011; Berthelsen et al., 2015). Besides the high number of individuals recorded from field turfs, belonging to various taxa (up to several 1000 individuals per 100 cm^3 of substrate), our samples host peculiar communities of crustacean peracarids and polychaetes and possibly even endemic species (see **Supporting Information S3** and **Tables S2, S3**).

When exposed to high CO_2 and high temperature environment, the whole associated community, when identified at a low taxonomic level, did not show a clearly discernible response, but the two rich assemblages of peracarids and polychaetes were used as models to study the effects of CC drivers. In fact, the analysis of the species composition within at least one selected taxon (peracarids) did prove that reduced pH and increased temperature can affect community structure, thus providing empirical evidence to the predictions made by Sunday et al. (2017) regarding the effects of GW and OA on communities associated to habitat-forming species, based on a literature review. In particular, here peracarid crustaceans exhibited significant changes in species composition under treatment conditions, also depending on the exposure time to altered pH and temperature. In almost all treatment samples, the species dominating the assemblages until the end of the experiment (October) was the amphipod *E. pocillimanus*, which has already been reported to withstand stressful environmental conditions (Sparla et al., 1993; Zakhama-Sraieb et al., 2011), including low pH (Scipione et al., 2017). Under a control condition, instead, different species were dominant: the isopod *P. costana*, a predator, and the amphipod *J. marmorata*, a suspension feeder. Interestingly, most isopods that occurred in the control aquaria (the herbivorous *Dynamene* spp., *Ischyromene lacazei*, the fish parasite *Gnathia* sp., the predator *Kupellonura serritelson*), were very rare or absent under treatment conditions. This could be possibly explained by the fact that the exoskeleton of isopods is characterized by high magnesium calcite (Munguia and Alenius, 2013), thus more soluble to OA (Andersson et al., 2008), possibly confirming previous findings on isopods vulnerability to CC (Munguia and Alenius, 2013; Garrard et al., 2014; Wood et al., 2014; Turner et al., 2016). In particular, Turner et al. (2016) observed that some isopod species alter their metabolism to regulate the internal acid–base balance under natural low pH conditions (at CO_2 vents), but it has also been suggested that indirect effects of acidification, such as changes in food quality, or competition and predation interactions (Garrard et al., 2014) may affect the isopods' response to OA. Given the large number of isopod species inhabiting marine ecosystems and the wide range of trophic functions they express (Poore and Bruce, 2012), as well as their role in transferring energy from the benthic to the pelagic compartment (as food item for fish), it would be important to better elucidate their response to changing environmental conditions.

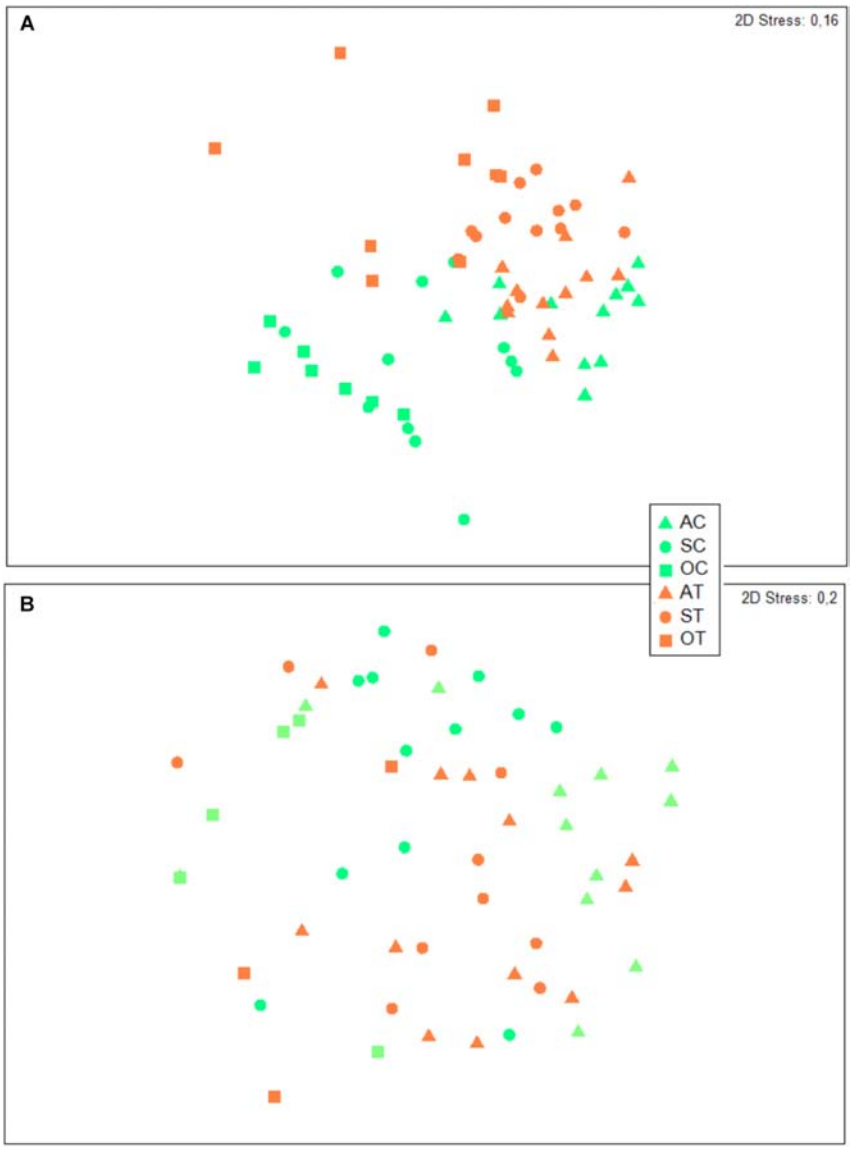

FIGURE 8 | Non-metric multidimensional scaling plots of peracarids **(A)** and polychaetes **(B)** assemblages associated to *E. elongata* in experimental aquaria. A = August; S = September; O = October; C = Control; T = Treatment.

As regards polychaetes, it was shown that under natural low pH conditions (CO_2 vents) they exhibit species-specific responses to OA, which are related to their functional traits (Gambi et al., 2016). However, in our study it was not possible to quantify the response of this taxon to the treatment conditions, since the aquarium effect covered the possible effects of lowered pH – increased temperature. In fact, although PERMANOVA highlighted significant differences between controls and treatments, at the end of the 3-month experiments, too few individuals survived both in the control and treatment aquaria to highlight any clear pattern.

Possible explanations could be related to the effect of Alizarine Red S staining treatment, which has been shown to negatively affect the growth of corals (Holcomb et al., 2013), or type of feeding provided in the aquaria (*Chlorella* sp. mix, see **Supporting Information S1**), which may not have been suitable for the carnivorous polychaete species (e.g., syllids and phyllodocids) included in the assemblage. Moreover, while the majority of peracarid crustaceans reported in this study have direct development with parental care, which allows for a successful recruitment under experimental conditions, the majority of the reported polychaetes are characterized by pelagic reproductive phases (epitoke stages, pelagic larvae, or both), and a natural mortality under experimental conditions would not be compensated by the recruitment. Different reproductive strategies might then account for the different response of the two taxonomic groups.

Our results partially overlap with those obtained by Hale et al. (2011) with a similar experiment, yet we acknowledge that in our case community responses are less obvious. In Hale et al. (2011), however, the treatment conditions may have been exacerbated by the fact that invertebrates had been grown on artificial substrates (nylon pan scourers), whereas the natural substrate (living algal turfs) used in the present experiment could have mitigated the effect of acidification, through local alteration of the water chemistry at the micro-habitat scale. Further testing is required to clarify this aspect, as well as to test whether reduced pH and increased temperature, when combined, exert an additive, antagonistic, or synergistic effect (Crain et al., 2008).

CONCLUSION

Our study shows that the species-rich Mediterranean assemblages associated to *E. elongata* should be considered at risk. The combined effect of low pH and high temperature that are expected for the future can impair algal growth and generate structural changes at the level of the associated benthic community, especially concerning selected taxonomic groups. Under future CC scenario, a rich and diverse mobile associated fauna shifts to a more simplified and depleted community. Despite preliminary and subject to the limitations of experimental conditions, our results show (i) that *E. elongata* is able to somewhat counter-act the effect of combined stressors (acidification and increased temperature); and (ii) that these stressors cause shifts in the associated assemblages toward a less diverse structure, with possible dominance of the more opportunistic species. These conclusions suggest two important pathways of further investigation: (1) the loss of some species and the resilience of others, at different trophic levels, need to be better understood in order to clarify the potential of species interactions in mediating the effects of CC; (2) analogously to seagrass meadows (Koweek et al., 2018), plastic and metabolic responses of calcareous, habitat-forming algae are key elements that need to be explored for studying mitigation strategies at local scale.

AUTHOR CONTRIBUTIONS

FR, AM, and CL designed the study. MN carried out the experimental work with help from GC and CL. AM, MCM, FG, JL, AC, and LM did the taxonomical work. CJ and JZ performed the analyses on structural integrity. CL, MN, CV, and AM performed statistical analyses with help from JL and LM. FR and AM drafted the first version of this manuscript assisted by CL. All authors contributed to the later versions of the manuscript and approved the final version for publication.

FUNDING

The present project was supported by internal funding of ENEA, University of Pavia and University of Portsmouth.

ACKNOWLEDGMENTS

The authors would like to thank students who contributed to the project: Tirzah Bottomley, Maurizio Florio, Maria Murcia Diaz, Lorenzo Pasculli. CL would like to thank her colleagues at ENEA: G. Raiteri, A. Bordone, A. Peirano, and S. Cocito for the technical and scientific support. Three reviewers have provided significant inputs to this work through constructive criticism.

SUPPLEMENTARY MATERIAL

The Supplementary Material for this article can be found online at: https://www.frontiersin.org/articles/10.3389/fmars.2019.00106/full#supplementary-material

REFERENCES

Aitken, A. C. (1935). On least squares and linear combinations of observations. *Proc. R. Stat. Soc.* 55, 42–48.

Akaike, H. (1974). A new look at the statically model identification. *IEEE Trans. Automation Control* 19, 716–723. doi: 10.1109/TAC.1974.1100705

Anderson, M. J. (2001). A new method for non-parametric multivariate analyses of variance. *Aust. J. Ecol.* 26, 32–46.

Andersson, A. J., Mackenzie, F. T., and Bates, N. R. (2008). Life on the margin: implications of ocean acidification on Mg-calcite, high latitude and cold-water marine calcifiers. *Mar. Ecol. Prog. Ser.* 373, 265–273. doi: 10.3354/meps07639

Andrake, W., and Johansen, H. W. (1980). Alizarin red dye as marker for measuring assemblages: an experimental study from Mediterranean rocky shore. *J. Exp. Mar. Biol. Ecol.* 215, 271–290.

Babbini, L., and Bressan, G. (1997). Recensement des corallincées de la Mer Mediteranée et consideration sphytogeographiques. *Bibl. Phycol.* 1, 103–121.

Beake, B., and Leggett, G. J. (2002). Nanoindentation and nanoscratch testing uniaxially and biaxially drawn poly (ethylene terephtalate) film. *Polymer* 43, 319–327. doi: 10.1016/S0032-3861(01)00600-0

Beake, B., Leggett, G. J., and Alexander, M. R. (2002). Characterization of the mechanical properties of plasma-polymerized coatings by nanoindentation and tribology. *J. Mater. Sci.* 37, 4919–4927. doi: 10.1023/A:1020830717653

Benedetti-Cecchi, L., and Cinelli, F. (1994). Recovery of patches in an assemblage of geniculate coralline algae: variability at different successional stages. *Mar. Ecol. Prog. Ser.* 110:9. doi: 10.3354/meps110009

Bensimon-Brito, A., Cardeira, J., Dionísio, G., Huysseune, A., Cancela, M. L., and Witten, P. E. (2016). Revisiting in vivo staining with alizarin red S-a valuable approach to analyse zebrafish skeletal mineralization during development and regeneration. *BMC Dev. Biol.* 16:2. doi: 10.1186/s12861-016-0102-4

Berthelsen, A. K., Hewitt, J. E., and Taylor, R. B. (2015). Coralline turf-associated fauna are affected more by spatial variability than by host species identity. *Mar. Biodivers.* 45, 689–699. doi: 10.1007/s12526-014-0270-z

Bijma, J., Pörtner, H. O., Yesson, C., and Rogers, A. D. (2013). Climate change and the oceans–What does the future hold? *Mar. Pollut. Bull.* 74, 495–505. doi: 10.1016/j.marpolbul.2013.07.022

Bindoff, N. L., Stott, P. A., AchutaRao, K. M., Allen, M. R., Gillett, N., Gutzler, D., et al. (2013). "Detection and attribution of climate change: from global to regional," in *Climate Change 2013: The Physical Science Basis. Contribution of Working Group I to the Fifth Assessment Report of the Intergovernmental Panel on Climate Change*, eds T. F. Stocker, D. Qin, G.-K. Plattner, M. Tignor,

S. K. Allen, J. Boschung, et al. (Cambridge, MA: Cambridge University Press), 867–952.

Bressan, G., and Babbini, L. (2003). Biodiversità marina delle coste italiane: corallinales del mediterraneo: guida alla determinazione. *Biol. Mar. Mediterr.* 10(Suppl. 2), 1–237.

Cigliano, M., Gambi, M. C., Rodolfo-Metalpa, R., Patti, F. P., and Hall-Spencer, J. M. (2010). Effects of ocean acidification on invertebrate settlement at volcanic CO2 vents. *Mar. Biol.* 157, 2489–2502. doi: 10.1007/s00227-010-1513-6

Ciuffardi, T., Giuliani, A., Barsanti, M., Bordone, A., Cerrati, G., Di Nallo, G., et al. (2013). *Quarant'anni di Dati Oceanografici a Cura Del Centro Ricerche Ambiente Marino ENEA S. Teresa: Il Quadro Del Golfo di La Spezia. Distribuzione Storica Dei Dati Dal 1973 al 2013*. ENEA Technical Report No. 19. Kista: ENEA.

Clarke, K. R., and Gorley, R. N. (2006). *PRIMER v6: User Manual/Tutorial*. Plymouth: PRIMER-E, 192.

Clarke, K. R., and Gorley, R. N. (2015). *Getting Started with PRIMER v7*. Plymouth: PRIMER-E.

Clarke, K. R., Somerfield, P. J., and Chapman, M. G. (2006). On resemblance measures for ecological studies, including taxonomic dissimilarities and a zero-adjusted bray-curtis coefficient for denuded assemblages. *J. Exp. Mar. Biol. Ecol.* 330, 55–80. doi: 10.1016/j.jembe.2005.12.017

Cocito, S., Bedulli, D., and Sgorbini, S. (2002). Distribution patterns of the sublittoral epibenthic assemblages on a rocky shoal in the Ligurian Sea (NW Mediterranean). *Sci. Mar.* 66, 175–181. doi: 10.3989/scimar.2002.66n2175

Cocito, S., Ferdeghini, F., Morri, C., and Bianchi, C. N. (2000). Patterns of bioconstruction in the cheilostome bryozoan *Schizoporella errata*: the influence of hydrodynamics and associated biota. *Mar. Ecol. Prog. Ser.* 192, 153–161. doi: 10.3354/meps192153

Collins, M., Knutti, R., Arblaster, J., Dufresne, J.-L., Fichefet, T., Friedlingstein, P., et al. (2013). "Long-term climate change: projections, commitments and irreversibility," in *Climate Change 2013: The Physical Science Basis. Contribution of Working Group I to the Fifth Assessment Report of the Intergovernmental Panel on Climate Change*, eds T. F. Stocker, D. Qin, G.-K. Plattner, M. Tignor, S. K. Allen, J. Boschung, et al. (Cambridge: Cambridge University Press), 1029–1136.

R Core Team (2016). *R: A Language and Environment for Statistical Computing*. Vienna: R Foundation for Statistical Computing.

Cormaci, M., Furnari, G., and Alongi, G. (2017). Flora marina bentonica del Mediterraneo Rhodophyta (Rhodymeniophycidae escluse). *Bollettino Accademia Gioenia di Scienze Naturali in Catania* 50, 1–391.

Coull, B. C., and Wells, J. B. J. (1983). Refuges from fish predation: experiments with phytal meiofauna from the New Zealand rocky intertidal. *Ecology* 64, 1599–1609. doi: 10.2307/1937513

Cowles, A., Hewitt, J. E., and Taylor, R. B. (2009). Density, biomass and productivity of small mobile invertebrates in a wide range of coastal habitats. *Mar. Ecol. Prog. Ser.* 384, 175–185. doi: 10.3354/meps08038

Crain, C. M., and Bertness, M. D. (2006). Ecosystem engineering across environmental gradients: implications for conservation and management. *AIBS Bull.* 56, 211–218.

Crain, C. M., Kroeker, K., and Halpern, B. S. (2008). Interactive and cumulative effects of multiple human stressors in marine systems. *Ecol. Lett.* 11, 1304–1315. doi: 10.1111/j.1461-0248.2008.01253.x

Crowder, L. B., and Cooper, W. E. (1982). Habitat structural complexity and the interaction between bluegills and their prey. *Ecology* 63, 1802–1813. doi: 10.2307/1940122

Davenport, J., Butler, A., and Cheshire, A. (1999). Epifaunal composition and fractal dimensions of marine plants in relation to emersion. *J. Mar. Biol. Assoc.* 79, 351–355. doi: 10.1017/S0025315498000393

Díez, I., Muguerza, N., Santolaria, A., Ganzedo, U., and Gorostiaga, J. M. (2012). Seaweed assemblage changes in the eastern Cantabrian Sea and their potential relationship to climate change. *Estuar. Coast. Shelf Sci.* 99, 108–120. doi: 10.1016/j.ecss.2011.12.027

Dommasnes, A. (1968). Variations in the meiofauna of *Corallina officinalis L.* with wave exposure. *Sarsia* 34, 117–124. doi: 10.1080/00364827.1968.10413376

Downes, B. J., Lake, P. S., Schreiber, E. S. G., and Glaister, A. (1998). Habitat structure and regulation of local species diversity in a stony, upland stream. *Ecol. Monogr.* 68, 237–257. doi: 10.1890/0012-9615(1998)068[0237:HSAROL]2.0.CO;2

Dye, A. H. (1993). Recolonization of intertidal macroalgae in relation to gap size and molluscan herbivory on a rocky shore on the east coast of southern Africa. *Mar. Ecol. Prog. Ser.* 95, 263–263. doi: 10.3354/meps095263

Egilsdottir, H., Noisette, F., Noël, L., Olafsson, J., and Martin, S. (2013). Effects of pCO2 on physiology and skeletal mineralogy in a tidal pool coralline alga *Corallina elongata*. *Mar. Biol.* 160, 2103–2112. doi: 10.1007/s00227-012-2090-7

Ellner, S. P., McCauley, E., Kendall, B. E., Briggs, C. J., Hosseini, P. R., Wood, S. N., et al. (2001). Habitat structure and population persistence in an experimental community. *Nature* 412, 538–543. doi: 10.1038/35087580

Fletcher, W. J., and Underwood, A. J. (1987). Interspecific competition among subtidal limpets: effect of substratum heterogeneity. *Ecology* 68, 387–400. doi: 10.2307/1939270

Foster, M. S. (2001). Rhodoliths: between rocks and soft places. *J. Phycol.* 37, 659–667. doi: 10.1046/j.1529-8817.2001.00195.x

Gambi, M. C., Musco, L., Giangrande, A., Badalamenti, F., Micheli, F., and Kroeker, K. J. (2016). Distribution and functional traits of polychaetes in a CO2 vent system: winners and losers among closely related species. *Mar. Ecol. Prog. Ser.* 550, 121–134. doi: 10.3354/meps11727

Gao, K., Aruga, Y., Asada, K., Ishihara, T., Akano, T., and Kiyohara, M. (1993). Calcification in the articulated coralline alga *Corallina pilulifera*, with special reference to the effect of elevated CO2 concentration. *Mar. Biol.* 117, 129–132. doi: 10.1007/BF00346434

Garrabou, J., Coma, R., Bensoussan, N., Bally, M., Chevaldonné, P., Cigliano, M., et al. (2009). Mass mortality in Northwestern Mediterranean rocky benthic communities: effects of the 2003 heat wave. *Glob. Chang. Biol.* 15, 1090–1103. doi: 10.1111/j.1365-2486.2008.01823.x

Garrard, S., Gambi, M. C., Scipione, M. B., Lorenti, M., Zupo, V., Paterson, D. M., et al. (2014). Indirect effects may buffer negative responses of seagrass invertebrate communities to ocean acidifcation. *J. Exp. Mar. Biol. Ecol.* 461, 31–38. doi: 10.1016/j.jembe.2014.07.011

Gasparini, G. P., Abbate, M., Bordone, A., Cerrati, G., Galli, C., Lazzoni, E., et al. (2009). Circulation and biomass distribution during warm season in the Gulf of La Spezia (north-western Mediterranean). *J. Mar. Syst.* 78, 48–62. doi: 10.1016/j.jmarsys.2009.01.010

Gattie, D. K., Smith, M. C., Tollner, E. W., and McCutcheon, S. C. (2003). The emergence of ecological engineering as a discipline. *Ecol. Eng.* 20, 409–420. doi: 10.1073/pnas.1102712108

Guerra-García, J. M., Cabezas, P., Baeza-Rojano, E., Espinosa, F., and García-Gómez, J. C. (2009). Is the north side of the Strait of Gibraltar more diverse than the south side? A case study using the intertidal peracarids (Crustacea: Malacostraca) associated to the seaweed *Corallina elongata*. *J. Mar. Biol. Assoc.* 89, 387–397. doi: 10.1017/S0025315409002938

Guerra-García, J. M., Ros, M., Izquierdo, D., and Soler-Hurtado, M. M. (2012). The invasive *Asparagopsis armata* versus the native *Corallina elongata*: differences in associated peracarid assemblages. *J. Exp. Mar. Biol. Ecol.* 416, 121–128. doi: 10.1016/j.jembe.2012.02.018

Hale, R., Calosi, P., McNeill, L., Mieszkowska, N., and Widdicombe, S. (2011). Predicted levels of future ocean acidification and temperature rise could alter community structure and biodiversity in marine benthic communities. *Oikos* 120, 661–674. doi: 10.1111/j.1600-0706.2010.19469.x

Harley, C. D., Anderson, K. M., Demes, K. W., Jorve, J. P., Kordas, R. L., Coyle, T. A., et al. (2012). Effects of climate change on global seaweed communities. *J. Phycol.* 48, 1064–1078. doi: 10.1111/j.1529-8817.2012.01224.x

Heck, K. L. Jr., and Wetstone, G. S. (1977). Habitat complexity and invertebrate species richness and abundance in tropical seagrass meadows. *J. Biogeogr.* 4, 135–142. doi: 10.2307/3038158

Holcomb, M., Cohen, A. L., and McCorkle, D. C. (2013). An evaluation of staining techniques for marking daily growth in scleractinian corals. *J. Exp. Mar. Biol. Ecol.* 440, 126–131. doi: 10.1016/j.jembe.2012.12.003

Ingrosso, G., Abbiati, M., Badalamenti, F., Bavestrello, G., Belmonte, G., Cannas, R., et al. (2018). Mediterranean bioconstructions along the italian coast. *Adv. Mar. Biol.* 79, 61–136. doi: 10.1016/bs.amb.2018.05.001

IPCC (2014). *Climate Change 2014: Synthesis Report. Contribution of Working Groups I, II and III to the Fifth Assessment Report of the Intergovernmental Panel on Climate Change*. Available at: https://epic.awi.de/id/eprint/37530/.

Izquierdo, D., and Guerra-García, J. M. (2011). Distribution patterns of the peracarid crustaceans associated with the alga *Corallina elongata* along the intertidal rocky shores of the Iberian Peninsula. *Helgol. Mar. Res.* 65, 233–243. doi: 10.1007/s10152-010-0219-y

Jokiel, P. L., Rodgers, K. S., Kuffner, I. B., Andersson, A. J., Cox, E. F., and Mackenzie, F. T. (2008). Ocean acidification and calcifying reef organisms: a mesocosm investigation. *Coral Reefs* 27, 473–483. doi: 10.1371/journal.pone.0154844

Jones, C. G., Lawton, J. H., and Shachak, M. (1997). Positive and negative effects of organism as physical ecosystem engineers. *Ecology* 78, 1946–1957. doi: 10.1890/0012-9658(1997)078[1946:PANEOO]2.0.CO;2

Kamenos, N. A., Burdett, H. L., Aloisio, E., Findlay, H. S., Martin, S., Longbone, C., et al. (2013). Coralline algal structure is more sensitive to rate, rather than the magnitude, of ocean acidification. *Glob. Chang. Biol.* 44, 3621–3628. doi: 10.1111/gcb.12351

Kelaher, B. P., Chapman, M. G., and Underwood, A. J. (2001). Spatial patterns of diverse macrofaunal assemblages in coralline turf and their associations with environmental variables. *J. Mar. Biol. Assoc.* 81, 917–930. doi: 10.1017/S0025315401004842

Kleypas, J., Feely, R., Fabry, V., Langdon, C., Sabine, C. L., and Robbins, L. L. (2006). impacts of ocean acidification on coral reefs and other marine calcifiers: a guide for future research. *Atmospher. Res.* 18:88.

Kohn, A. J., and Leviten, P. J. (1976). Effect of habitat complexity on population density and species richness in tropical intertidal predatory gastropod assemblages. *Oecologia* 25, 199–210. doi: 10.1007/BF00345098

Koweek, D. A., Zimmerman, R. C., Hewett, K. M., Gaylord, B., Giddings, S. N., Nickols, K. J., et al. (2018). Expected limits on the ocean acidification buffering potential of a temperate seagrass meadow. *Ecol. Appl.* 28, 1694–1714. doi: 10.1002/eap.1771

Kroeker, K. J., Micheli, F., Gambi, M. C., and Martz, T. R. (2011). Divergent ecosystem responses within a benthic marine community to ocean acidification. *Proc. Natl. Acad. Sci. U.S.A.* 108, 14515–14520. doi: 10.1073/pnas.1107789108

Kuffner, I. B., Andersson, A. J., Jokiel, P. L., Rodgers, K. S., and Mackenzie, F. T. (2008). Decreased abundance of crustose coralline algae due to ocean acidification. *Nat. Geosci.* 1, 114–117. doi: 10.1038/ngeo100

Lawton, J. H. (1983). Plant architecture and the diversity of phytophagous insects. *Annu. Rev. Entomol.* 28, 23–39. doi: 10.1146/annurev.en.28.010183.000323

MacArthur, R. H., and MacArthur, J. W. (1961). On bird species diversity. *Ecology* 42, 594–598. doi: 10.2307/1932254

Martin, S., Cohu, S., Vignot, C., Zimmerman, G., and Gattuso, J. P. (2013). One-year experiment on the physiological response of the Mediterranean crustose coralline alga, *Lithophyllum cabiochae*, to elevated pCO2 and temperature. *Ecol. Evol.* 3, 676–693. doi: 10.1002/ece3.475

Martin, S., and Gattuso, J. P. (2009). Response of Mediterranean coralline algae to ocean acidification and elevated temperature. *Glob. Chang. Biol.* 15, 2089–2100. doi: 10.1002/ece3.475

McCoy, S. J., and Ragazzola, F. (2014). Skeletal trade-offs in coralline algae in response to ocean acidification. *Nat. Clim. Change* 4:719. doi: 10.1038/nclimate2273

Munguia, P., and Alenius, B. (2013). The role of preconditioning in ocean acidification experiments: a test with the intertidal isopod *Paradella dianae*. *Mar. Freshw. Behav. Physiol.* 46, 33–44. doi: 10.1080/10236244.2013.788287

Musco, L. (2012). Ecology and diversity of Mediterranean hard-bottom Syllidae (Annelida): a community-level approach. *Mar. Ecol. Prog. Ser.* 461, 107–119. doi: 10.3354/meps09753

Nannini, M., De Marchi, L., Lombardi, C., and Ragazzola, F. (2015). Effects of thermal stress on the growth of an intertidal population of *Ellisolandia elongata* (Rhodophyta) from N-W Mediterranean Sea. *Mar. Environ. Res.* 112, 11–19. doi: 10.1016/j.marenvres.2015.05.005

Oliver, W. C., and Pharr, G. M. (1992). An improved technique for determining hardness and elastic modulus using load and displacement sensing indentation experiments. *J. Mater. Res.* 7, 1564–1583. doi: 10.1557/JMR.1992.1564

Peirano, A., Abbate, M., Cerrati, G., Difesca, V., Peroni, C., and Rodolfo-Metalpa, R. (2005). Monthly variations in calix growth, polyptissue, and density banding of the Mediterranean scleractinian *Cladocora caespitosa* (L.). *Coral Reefs* 24, 404–409. doi: 10.1007/s00338-005-0020-6

Pereira, S. G., Lima, F. P., Queiroz, N. C., Ribeiro, P. A., and Santos, A. M. (2006). Biogeographic patterns of intertidal macroinvertebrates and their association with macroalgae distribution along the Portuguese coast. *Hydrobiologia* 555, 185–192. doi: 10.1007/s10750-005-1115-3

Poore, G. C., and Bruce, N. L. (2012). Global diversity of marine isopods (except Asellota and crustacean symbionts). *PLoS One* 7:e43529. doi: 10.1371/journal.pone.0043529

Pörtner, H. O., Karl, D. M., Boyd, P. W., Cheung, W., et al. (2014). "Ocean systems," in *Climate Change 2014: Impacts, Adaptation, and Vulnerability. Part A: Global and Sectoral Aspects. Contribution of Working Group II to the Fifth Assessment Report of the Intergovernmental Panel on Climate Change*, eds C. Field, V. Barros, D. Dokken, K. Mach, M. Mastrandrea, T. Bilir, et al. (Cambridge, MA: Cambridge University Press).

Porzio, L., Buia, M. C., and Hall-Spencer, J. M. (2011). Effects of ocean acidification on macroalgal communities. *J. Exp. Mar. Biol. Ecol.* 400, 278–287. doi: 10.1016/j.jembe.2011.02.011

Ragazzola, F., Foster, L. C., Form, A. U., Büscher, J., Hansteen, T. H., and Fietzke, J. (2013). Phenotypic plasticity of coralline algae in a high CO 2 world. *Ecol. Evol.* 3, 3436–3446. doi: 10.1002/ece3.723

Ragazzola, F., Foster, L. C., Jones, C. J., Scott, T. B., Fietzke, J., Kilburn, M. R., et al. (2016). Impact of high CO2 on the geochemistry of the coralline algae *Lithothamnion glaciale*. *Sci. Rep.* 6:20572. doi: 10.1038/srep20572

Rhein, M., Rintoul, S. R., Aoki, S., Campos, E., Chambers, D., Feely, R. A., et al. (2013). "Observations: ocean," in *Climate Change 2013: The Physical Science Basis. Contribution of Working Group I to the Fifth Assessment Report of the Intergovernmental Panel on Climate Change*, eds T. F. Stocker, D. Qin, G.-K. Plattner, M. Tignor, S. K. Allen, J. Boschung, et al. (Cambridge, MA: Cambridge University Press), 255–316.

Schoener, T. W. (1974). Resource partitioning in ecological communities. *Science* 185, 27–39. doi: 10.1126/science.185.4145.27

Scipione, M. B., Kroeker, K. J., Ricevuto, E., and Gambi, M. C. (2017). Amphipod assemblages along shallow water natural pH gradients: data from artificial substrata (Island of Ischia. Italy). *Biodivers. J.* 8, 469–470.

Semesi, I. S., Beer, S., and Björk, M. (2009). Seagrass photosynthesis controls rates of calcification and photosynthesis of calcareous macroalgae in a tropical seagrass meadow. *Mar. Ecol. Prog. Ser.* 382, 41–47. doi: 10.3354/meps07973

Smale, D. A., Wernberg, T., Peck, L. S., and Barnes, D. K. A. (2011). Turning on the heat: ecological response to simulated warming in the sea. *PLoS One* 6:e16050. doi: 10.1371/journal.pone.0016050

Sparla, M. P., Scipione, M. B., and Riggio, S. (1993). Peracarid Crustacea inhabiting aegagropylae of the red algae *Rytiphloa tinctoria* (Clemente) C. Ag. in the Stagnone Sound, western Sicily, Italy. *Crustaceana* 64, 1–17. doi: 10.1163/156854093X00018

Steneck, R. S. (1986). The ecology of coralline algal crusts: convergent patterns and adaptive strategies. *Annu. Rev. Ecol. Syst.* 17, 273–303. doi: 10.1146/annurev.es.17.110186.001421

Stewart, J. G. (1982). Anchor species and epiphytes in intertidal algal turf. *Pacific Sci.* 36, 45–59.

Sunday, J. M., Fabricius, K. E., Kroeker, K. J., Anderson, K. M., Brown, N. E., Barry, J. P., et al. (2017). Ocean acidification can mediate biodiversity shifts by changing biogenic habitat. *Nat. Clim. Chang.* 7, 81–85. doi: 10.1038/nclimate3161

Turner, L. M., Ricevuto, E., Gallucci, A. M., Lorenti, M., Gambi, M. C., and Calosi, P. (2016). Metabolic responses to high pCO2 conditions at a CO2 vent site in juveniles of a marine isopod species assemblage. *Mar. Biol.* 163:211. doi: 10.1007/s00227-016-2984-x

Underwood, A. J. (1997). *Experiments in Ecology. Their Logical Design and Interpretation Using Analysis of Variance*. Cambridge, MA: Cambridge University Press.

Whorff, J. S., Whorff, L. L., and Sweet, M. H. (1995). Spatial variation in an algal turf community with respect to substratum slope and wave height. *J. Mar. Biol. Assoc.* 75, 429–444. doi: 10.1017/S0025315400018282

Wood, H. L., Sköld, H. N., and Eriksson, S. P. (2014). Health and population-dependent effects of ocean acidification on the marine isopod *Idotea balthica*. *Mar. Biol.* 161, 2423–2431. doi: 10.1007/s00227-014-2518-3

Zakhama-Sraieb, R., Sghaier, Y. R., Guesmi, S., and Charfi-Cheikhrouha, F. (2011). Peracarid crustaceans associated with the red alga *Corallina elongata* in Rafraf, Tunisia (Mediterranean Sea). *Crustaceana* 84, 69–80. doi: 10.1163/001121610X538868

Zuur, A., Ieno, E. N., and Smith, G. M. (2007). *Analyzing Ecological Data*. New York, NY: Springer. doi: 10.1007/978-0-387-45972-1

Zuur, A., Ieno, E. N., Walker, N., Saveliev, A. A., and Smith, G. M. (2009). *Mixed Effects Models and Extensions in Ecology With R*. New York, NY: Springer.

Zuur, A. F., Ieno, E. N., and Elphick, C. S. (2010). A protocol for data exploration to avoid common statistical problems. *Methods Ecol. Evol.* 1, 3–14. doi: 10.1111/j.2041-210X.2009.00001.x

Conflict of Interest Statement: The authors declare that the research was conducted in the absence of any commercial or financial relationships that could be construed as a potential conflict of interest.

Copyright © 2019 Marchini, Ragazzola, Vasapollo, Castelli, Cerrati, Gazzola, Jiang, Langeneck, Manauzzi, Musco, Nannini, Zekonyte and Lombardi. This is an open-access article distributed under the terms of the Creative Commons Attribution License (CC BY). The use, distribution or reproduction in other forums is permitted, provided the original author(s) and the copyright owner(s) are credited and that the original publication in this journal is cited, in accordance with accepted academic practice. No use, distribution or reproduction is permitted which does not comply with these terms.

frontiers in Marine Science

ORIGINAL RESEARCH
published: 28 February 2019
doi: 10.3389/fmars.2019.00081

Colonization, Growth and Productivity of Crustose Coralline Algae in Sunlit Reefs in the Atlantic Southernmost Coral Reef

Frederico T. S. Tâmega[1] and Marcia A. O. Figueiredo[2]*

[1] Programa de Pós-Graduação em Oceanografia Física, Química e Geológica, Instituto de Oceanografia, Universidade Federal do Rio Grande, Rio Grande, Brazil, [2] Instituto de Pesquisas Jardim Botânico do Rio de Janeiro, Rio de Janeiro, Brazil

One of the most important contributions of crustose coralline algae (CCA) to some coral reefs is their structural role in sunlit habitats, but in the Atlantic southernmost coral reef, Abrolhos, these algae are also important components of living communities covering larger areas than corals. Little is known about their competence in occupying reef space and consequently their ecological role. This work compared two CCA species along reef sites and habitats and their responses to different irradiance levels. To study colonization, epoxy disks were placed at four sites and three habitats (reef base, reef flat, and reef edge). Crustose coralline individual pieces were glued onto epoxy disks and their relative growth was estimated. Productivity responses to irradiance levels found on reef habitats was measured on incubated samples. In general, CCA were less abundant than filamentous algae and non-calcareous crusts. Crustose algae showed no seasonal or spatial pattern in cover, contrasting with erect algae that differed in biomass among sites depending on season. Differences among habitats were only found for CCA. The dominant coralline *Porolithon onkodes* was more productive and grew faster than *Lithophyllum stictaeforme* at high irradiance level and both species were inhibited at low light. Dominance of *P. onkodes* in shallow and sunlit reefs was explained by its preference for high-light environments.

Keywords: reef habitats, irradiance levels, Abrolhos, Brazil, crustose coralline algae, growth rates, colonization, productivity

OPEN ACCESS

Edited by:
Nadine Schubert, Federal University of Santa Catarina, Brazil

Reviewed by:
Mirta Teichberg, Leibniz Centre for Tropical Marine Research (LG), Germany
Bonnie Lewis, University of Glasgow, United Kingdom

****Correspondence:***
Frederico T. S. Tâmega
fredtamega@gmail.com

Specialty section:
This article was submitted to Marine Ecosystem Ecology, a section of the journal Frontiers in Marine Science

Received: *05 October 2018*
Accepted: *12 February 2019*
Published: *28 February 2019*

Citation:
Tâmega FTS and Figueiredo MAO (2019) Colonization, Growth and Productivity of Crustose Coralline Algae in Sunlit Reefs in the Atlantic Southernmost Coral Reef. Front. Mar. Sci. 6:81. doi: 10.3389/fmars.2019.00081

INTRODUCTION

The crustose coralline algae (CCA, Corallinales Rhodophyta) on coral reefs can cover large areas, such as in the Africa (McClanahan et al., 2001b), Australia (Fabricius and De'ath, 2001), Caribbean (Adey and Vassar, 1975; McClanahan et al., 2001a; Williams and Polunin, 2001), Fiji (Littler and Littler, 1997), Hawaii (Vroom et al., 2005), and Brazil (Figueiredo, 1997; Gherardi and Bosence, 2001; Villas-Bôas et al., 2005). Studies have confirmed that together with corals, CCA are important components of the reef framework in shallow environments exposed to strong wave action in the Caribbean (Macintyre, 1997) and Brazilian reefs (Kikuchi and Leão, 1997; Leão and Dominguez, 2000; Gherardi and Bosence, 2001; Leão and Kikuchi, 2001; Lei et al., 2018). The cementation of reefs by CCA maintains reef complexity, reduces erosion (Littler, 1972; Steneck, 1986) and increases resistance to herbivore action due to calcium carbonate deposited in the cell walls (Pitlik and Paul, 1997).

According to models of seaweed (algal) form and function, proposed to describe the distribution and abundance of seaweeds, CCA are classified as a unique functional group that dominates highly productive environments with exposure to high levels of disturbance (Littler and Littler, 1980, 1984; Steneck, 1988; Steneck and Dethier, 1994; Mariath et al., 2013). Morphological characteristics of coralline algae indicate adaptations to many environmental and biological factors, such as wave exposure, light intensity, sediment deposition, competition, and herbivory (Steneck, 1986, 1988; Steneck and Dethier, 1994).

Herbivory is regarded as one of the main processes maintaining the structure and diversity of tropical reefs (Bellwood et al., 2004). In tropical coral ecosystems, herbivorous fishes play key roles in the carbon and energy flux of food webs and are considered some of the primary determinants of the benthic structure (Clements et al., 2009). Herbivorous fish assemblages, dominated by surgeonfishes (Acanthuridae) and parrotfishes (Labridae: Scarini), are widely regarded for their importance in the control of the settlement, growth, and spread of benthic seaweeds (Steneck, 1988; Horn, 1989).

Several descriptive studies have related patterns of distribution and abundance of these algae to environmental parameters that influence coral reefs (Adey and Vassar, 1975; Littler et al., 1995; Steneck, 1997; Fabricius and De'ath, 2001; Figueiredo and Steneck, 2002). The biological limits of CCA were analyzed for a few temperate and subtropical species, showing influence of temperature and light intensity (Adey, 1970; Edyvean and Ford, 1987; Matsuda, 1989; Leukart, 1994), competition and herbivory (Steneck et al., 1991; Keats et al., 1994; Figueiredo et al., 1996). In contrast, experimental studies that test the effect of environmental factors on growth and production of CCA on coral reefs are less common and consist of studies of irradiance (Littler, 1973), sediments (Kendrick, 1991), and herbivory (Steneck and Adey, 1976; Figueiredo, 1997).

Among the most important reef builders on the Atlantic Ocean are the CCA *Porolithon onkodes* (Heydrich) Foslie and *Lithophyllum stictaeforme* (J.E. Areschoug) Hauck, which form algal crests on reefs edges (Adey, 1975; Steneck and Adey, 1976; Tâmega et al., 2014; Spotorno-Oliveira et al., 2015). These two coralline species have distinct growth forms: *P. onkodes* is encrusting and *L. stictaeforme* has branched thalli. Both species are commonly found on shallow reefs of the Abrolhos Archipelago in Brazil (Figueiredo and Steneck, 2002; Tâmega and Figueiredo, 2007; Tâmega et al., 2014). This study aims to describe the early colonization and growth of CCA on the reef flat, edge and base of sheltered and exposed sites in summer and winter, testing the responses of the two most common coralline species to different light levels.

Preliminary observations of seaweeds on the reef community of Abrolhos Archipelago generated three hypotheses that were tested in field and laboratory experiments:

H1: CCA are more abundant than other form-functional seaweeds groups in early stages of colonization in any of the studied reef habitats, sites and seasons.

H2: Encrusting CCA have faster marginal growth than branched CCA in any of the studied reef habitats, sites, and seasons.

H3: Encrusting CCA are more productive than branched CCA in environments under high irradiance.

MATERIALS AND METHODS

Study Sites

The present study was conducted in Abrolhos Archipelago (17° 57′–17° 59′S and 38° 41′–38° 43′W; **Figure 1**) about 70 km off North-eastern Brazil. This archipelago is composed by five volcanic islands bordered by fringing reefs and is included in the Abrolhos Marine National Park. The average seawater temperature ranges from 23 to 27°C (Muehe, 1988) and salinity from 36.5 to 36.7 (Muehe, 1988). In autumn and winter (from March to September), winds are mostly from the south. In spring and summer (September to February), winds are from the east to north. Tides range from ± 2.4 to 0.1 m in the north (Porto de Ilhéus) and ± 1.8 to 0.0 m in the south (Barra do Riacho) (Muehe, 1988).

Study sites at Santa Barbara Island were selected according to reef orientation: Porto Norte (N), Caldeiros (NW), Mato Verde (SW), and Porto Sul (S) (**Figure 1**). Studies were run during two periods: December 2001 to March 2002 (austral summer) and July 2002 to October 2002 (austral winter and spring). Three habitats were studied: reef flat, edge, and slope base in Mato Verde, during austral winter. Reef flats are usually exposed to air on extreme spring low tides. Reef bases are at 4 to 5 m depth. Reefs have a gradual slope on Porto Norte and Porto Sul, while at Caldeiros and Mato Verde they have steep slopes from 50°. Sites were compared only at the reef edge in both seasons, where corallines are more abundant (Figueiredo, 1997; Tâmega and Figueiredo, 2007).

Colonization

The colonization of CCA and erect seaweeds was followed at all study sites, 10 replicate disks made of epoxy (Tubolit), 75 mm diameter, were fixed by epoxy to the substratum at each study site. After 3 months each disk was recovered and stored in a plastic bag with formalin solution (4% in seawater). The cover of colonizing seaweeds was analyzed using a Petri dish marked with 47 random points, placed on the surface of each disk. Seaweeds were separated in functional form groups (Littler and Littler, 1984; Steneck and Dethier, 1994) and also identified to species level when possible. Sorted samples were oven dried at 60°C for 72 h until their mass was constant (not changing with time).

Colonizing seaweeds can be limited by herbivores such as parrotfishes (Labridae: Scarini), that are able to excavate calcified thalli with their fused teeth (Steneck, 1986).

Growth Rates

Growth was compared between two CCA, *L. stictaeforme* and *P. onkodes*. CCA were collected with a hammer and chisel and shaped by cutting pliers to obtain 20 mm diameter and 3 ml volume disks. A single disk naturally free of epiphytes

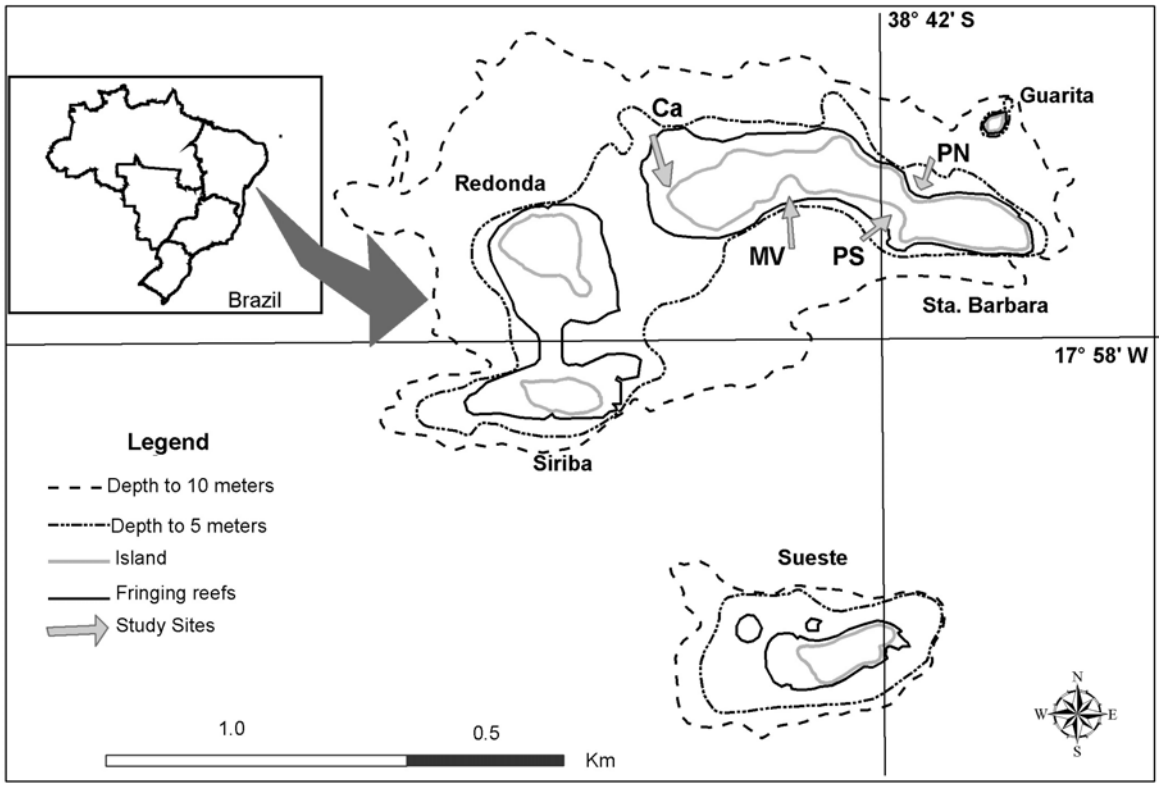

FIGURE 1 | Study sites in the Abrolhos Marine National Park: Porto Norte (PN), Caldeiros (Ca), Mato Verde (MV), and Porto Sul (PS).

was fixed onto an epoxy disk of 30 mm diameter (for each crustose coralline species, n = 10 per location). Disks of both CCA species were interspersed, fixed to the reef with epoxy and left for the same period as colonization disks. The initial and final sizes of CCA were estimated by averaging two perpendicular diameters measured with calipers. The formula used to calculate the marginal relative growth rate (RGR) was:

$$\mathrm{RGR} = \left(\ln \mathrm{D_t} - \ln \mathrm{D_0}\right)/\mathrm{t}$$

which is based on the difference between the logarithms of final and initial average diameter (D) over time (t), following recommendations of Kain (1987). *L. stictaeforme* also had thickness (vertical) growth measured but in *P. onkodes* only marginal (horizontal) growth was measured as it was considered that vertical growth was not sufficient to be detected in this species during such a short deployment time. CCA species were identified following Tâmega et al. (2014).

Productivity

To estimate the competence of the two most abundant CCA species under different irradiance levels, oxygen produced by CCA through net photosynthesis was measured at different levels of light intensities naturally found at each habitat. The irradiance at each site was measured with a Li-Cor light meter (LI-1000) linked to a terrestrial and submersible sensor to estimate the percentage of incident irradiance reduced by the water column. In the field, the irradiance was measured at midday hours in the summer on sunny days. The light levels of habitats were reproduced in the laboratory by 4, 6, or 10 fluorescent lamps (daylight, 20 watts each), and in the field by shading with 1 or 3 layers of black plastic grids, with 3 mm mesh diameter.

Fragments of the two species of CCA were collected and cleaned of epiphytes with brush and forceps. Seawater was filtered through coarse filter paper in the field or by Millipore 0.47 μm pore and sterilized at boiling point to fill 300 ml BOD bottles. Seaweed samples of standard size (diameter 20 mm) and volume of 3 ml were distributed among clear BOD bottles (with or without shades) to measure O_2 production. One clear BOD bottle with only seawater was used as an initial reference for O_2 production. Number of replicates varied between 8 and 12, in the laboratory and field experiments, respectively. In the laboratory experiments, CCA samples were acclimated to light levels lower than the ones found at the reef base, 2 weeks prior to the experiments. Dissolved oxygen readings were measured by a sensor with a stirrer linked to an oximeter (YSI 5000). Net photosynthesis was calculated to estimate primary productivity using the modified formula of Thomas (1988):

$$\text{Net photosynthesis} = [\left(\text{BOD bottle} - \text{initial bottle}\right)] / \text{incubation time}$$

At the end of experiments, CCA were decalcified by a solution of 10% nitric acid and oven dried at 60°C to adjust

O_2 production readings to sample weight. Incubation time (4 h) was previously tested and showed no difference from either 2 or 6 h, though shorter times resulted in negative readings at some light levels. Pigment concentration of CCA species was assumed to be similar because only sunlit specimens were used in experiments. Nutrients and carbon depletion did not interfere with results. Similar levels of nitrate, phosphate, and alkalinity between incubated samples and surrounding seawater were found for *P. onkodes* after 4 h of incubation (pers. comm. S. M. Ribeiro). Levels of irradiance used in field tests corresponded to ones mentioned for CCA in shallow reefs (Littler and Littler, 1984), being close to saturated photosynthesis (623 and 408 μmol m^{-2} s^{-1}), photo-inhibition (1093 and 716 μmol m^{-2} s^{-1}), or to levels below those that might limit photosynthesis (218 and 143 μmol m^{-2} s^{-1}). In the laboratory, irradiance levels corresponded to those found at the reef base and within cryptic habitats (218, 107, and 68 μmol m^{-2} s^{-1}).

Statistical Analysis

Variance homogeneity was tested using Cochrans test before performing analysis of variance (ANOVA) and, when necessary, data were transformed (Underwood, 1997). Uni or bi-factorial orthogonal ANOVAs were used to test differences between treatments in experiments. Multiple comparison of means was performed using Tukey's test.

RESULTS

Colonization

The most common erect seaweeds found on colonization disks were filamentous algae (*Cladophora dalmatica*, *Sphacelaria tribuloides*, *Polysiphonia scopulorum*, *Ceramium byssoides*), foliose algae (*Enteromorpha flexuosa*, *Padina gymnospora*, *Colpomenia sinuosa*, *Dictyota ciliolata*, *Dictyota mertensii*, *Dictyota menstrualis*), non-calcareous crusts (cyanobacteria, crusts) and calcareous coralline crusts.

The abundance of coralline crusts was different among sites independent of seasons (**Figures 2A,B**). These groups of algae were abundant at all sites, except Caldeiros. Foliose algae showed similar distribution pattern. A significant interaction between seasons and sites was found for filamentous algae and non-calcareous crusts (**Figures 2A,B**, ANOVA $F = 2.99$; $p \leq 0.05$ and $F = 2.99$; $p \leq 0.05$, respectively). The filamentous algae were abundant in almost all sites during both seasons, except in Caldeiros (ANOVA $p \leq 0.0001$ and $p \leq 0.01$). In contrast, non-calcareous crusts were more abundant in Caldeiros in both seasons (ANOVA $p \leq 0.0001$ and $p \leq 0.0001$).

A significant interaction was observed for biomass of colonizing algae between sites and seasons (**Figures 3A,B** and **Table 1**). Total biomass was different among sites in summer and in winter (ANOVA $F = 5.68$; $p \leq 0.05$ and $F = 7.11$; $p \leq 0.001$, respectively). There was less biomass on Caldeiros than on most sites in summer and higher biomass in Porto Sul than on most sites in winter. In relation to total cover of algae, there were no significant interactions or differences in colonization among sites or seasons, in summer the total cover ranged from 90 to 97%, and in winter from 90 to 99%.

There was a significant difference in the total macroalgal biomass among habitats (**Figure 4A**, $F = 4.85$, $p \leq 0.05$), which was higher at the reef base and lower at both reef flat and edge. Similarly, total algae cover did not differ significantly among reef habitats (ANOVA $F = 0.65$; $p > 0.05$). In relation

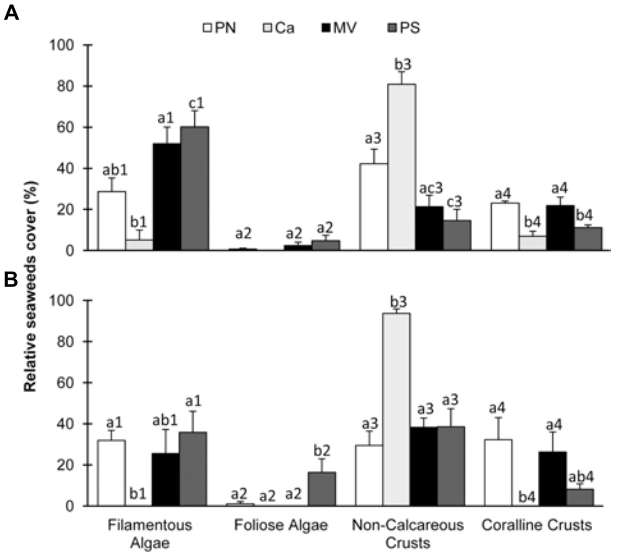

FIGURE 2 | Seaweeds cover at study sites on reef edge, in summer **(A)** and winter **(B)**. Means ± standard error. Different letters above bars indicate significant differences among means detected by Tukey's test ($p < 0.05$).

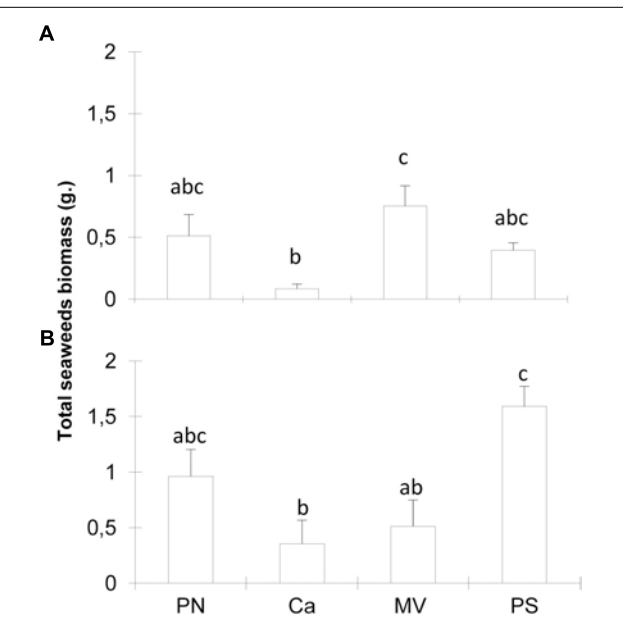

FIGURE 3 | Seaweeds biomass at study sites on reef edge, in summer **(A)** and winter **(B)**. Means ± standard error. Different letters above bars indicate significant differences among means detected by Tukey's test ($p < 0.05$).

TABLE 1 | Analysis of variance for algae colonization in relation to total cover and total biomass in study sites in summer and winter (n = 8).

	Source	*df*	MS	*F*	*P*-value
Cover	Seasons	1	0.84	0.01	$P>0.05$
	Sites	3	11.16	0.17	$p>0.05$
	Interaction	3	151.74	2.39	$p>0.05$
	Error	40	63.24		
Biomass	Seasons	1	1.62	11.59	$p\leq0.001$
	Sites	3	1.89	13.52	$p\leq0.0001$
	Interaction	3	1.42	10.16	$p\leq0.0001$
	Error	40	0.14		

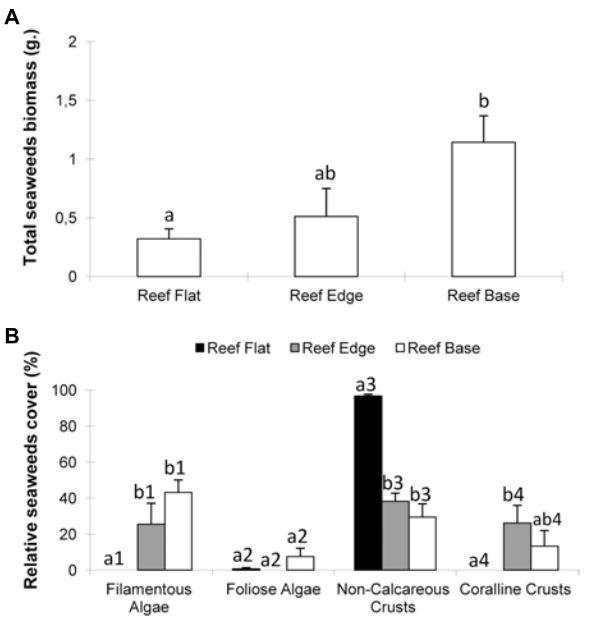

FIGURE 4 | Seaweeds biomass **(A)** and seaweeds cover **(B)** in different habitats at Mato Verde. Means ± standard error. Different letters above bars indicate significant differences among means detected by Tukey's test ($p < 0.05$).

to algae functional groups, coralline crusts were present at the reef base and edge, but absent on the reef flat (**Figure 4B**, ANOVA $F = 5.37$; $p \leq 0.01$). Filamentous algae were abundant at the reef base and edge and absent on the reef flat (ANOVA $F = 10.74$; $p \leq 0.001$). Foliose algae were present only at the reef base (ANOVA $F = 3.38$; $p \leq 0.05$). Non-calcareous crusts were abundant in all habitats, and were dominant at the reef flat (ANOVA $F = 38.56$; $p \leq 0.0001$).

Growth Rates

The absolute marginal growth ranged from 0.01 to 0.28 mm for *P. onkodes* and 0.01 to 0.13 mm for *L. stictaeforme*. The vertical growth of this second species varied from 0.02 to 0.23 mm. Marginal relative growth of *P. onkodes* between seasons and among sites though was not significantly different, a small growth was observed at Caldeiros in winter (**Figures 5A,B** and **Table 2**). Marginal relative growth of *L. stictaeforme*, had a strong

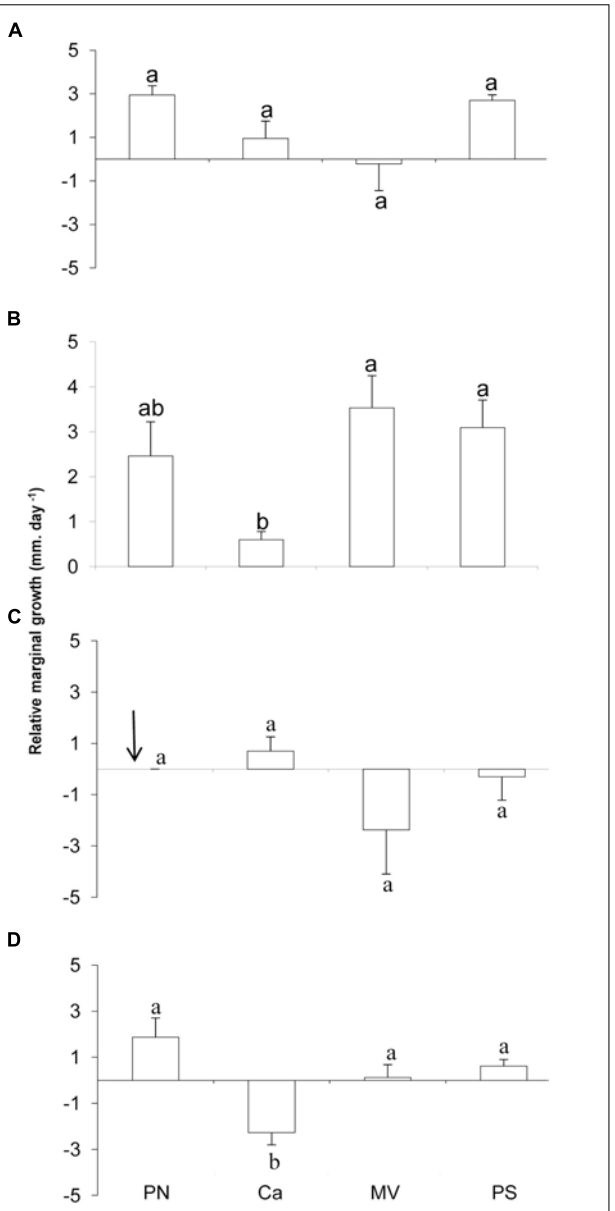

FIGURE 5 | Relative marginal growth of *Porolithon onkodes* at study sites on reef edge, in summer **(A)** and winter **(B)**, and *Lithophyllum stictaeforme* in summer **(C)** and winter **(D)**. Arrow indicates missing data. Means ± standard error. Different letters above bars indicate significant differences among means detected by Tukey's test ($p < 0.05$).

significant interaction among sites and seasons, growth was negative in Caldeiros differing from all other sites only in winter, (**Figures 5C,D** and **Table 2**). Comparing seasons in Caldeiros, growth was positive in summer and negative in winter (ANOVA $F = 30.35$; $p \leq 0.001$). In Mato Verde and Porto Sul growth was negative in summer and positive in winter, but differences between seasons were not significant (ANOVA $F = 2.10$; $p > 0.05$ and $F = 1.70$; $p > 0.05$, respectively). In summer growth could not be measured at Porto Norte because samples were lost due to strong wave surge.

TABLE 2 | Analysis of variance for marginal growth rate of *Porolithon onkodes* and *Lithophyllum stictaeforme* and vertical growth of *L. stictaeforme* in study sites in summer and winter.

	Source	*df*	MS	*F*	*P*-value
P. onkodes (marginal growth)					
	Season	1	3.49×10^{-6}	1.18	$p>0.05$
	Sites	3	4.39×10^{-6}	1.48	$p>0.05$
	Interaction	3	6.49×10^{-6}	2.19	$p>0.05$
	Error	24	2.96×10^{-6}		
L. stictaeforme (marginal growth)					
	Season	1	8.98×10^{-7}	0.23	$p>0.05$
	Sites	2	4.34×10^{-6}	1.14	$p>0.05$
	Interaction	2	1.96×10^{-5}	5.16	$p\leq0.01$
	Error	18	3.80×10^{-6}		
L. stictaeforme (vertical growth)					
	Season	1	0.0002	9.73	$p\leq0.05$
	Sites	2	4.61×10^{-5}	2.10	$p>0.05$
	Interaction	2	0.0001	7.67	$p\leq0.05$
	Error	18	2.19×10^{-5}		

Relative growth rates (RGRs) calculated from differences in initial and final $\log_e$ of average diameters over time (n = 4). Mean squares are exponential numbers ($MS \times 10^{-4}$).

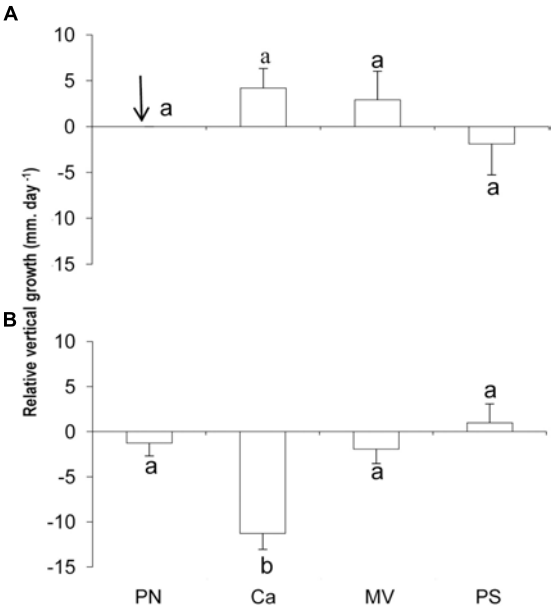

FIGURE 6 | Relative vertical growth of *L. stictaeforme* at study sites on reef edge, in summer **(A)** and winter **(B)**. Missing data (↓). Means ± standard error. Different letters above bars indicate significant differences among means detected by Tukey's test ($p < 0.05$).

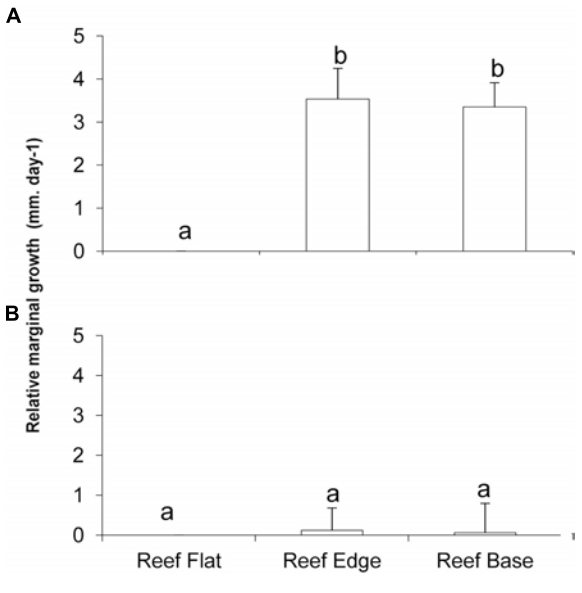

FIGURE 7 | Relative marginal growth of *P. onkodes* **(A)** and *L. stictaeforme* **(B)** in different habitats at Mato Verde. Means ± standard error. Different letters above bars indicate significant differences among means detected by Tukey's test ($p < 0.05$).

Vertical growth rate of *L. stictaeforme* showed a similar pattern as marginal growth with a significant interaction among seasons and sites. Again Caldeiros showed different growth rates from all other sites but only in winter. (**Figures 6A,B** and **Table 2**). In Caldeiros, there was a positive growth in summer and negative in winter. (ANOVA $F = 60.77$; $p \leq 0.001$). In Mato Verde and Porto Sul there was no significative difference between summer and winter (respectively, ANOVA $F = 1.49$; $p > 0.05$ and $F = 0.81$; $p > 0.05$).

Comparing marginal relative growth among habitats there was a significant difference for *P. onkodes* (**Figure 7A**, ANOVA $F = 11.76$; $p \leq 0.001$), being higher on the reef edge and reef base and zero on reef flat. However, *L. stictaeforme*, had an inconspicuous marginal growth on both edge and base and zero on the reef flat, so differences was not significant among habitats. (**Figure 7B**, ANOVA $F = 0.008$; $p > 0.05$). There was also no significant difference in vertical growth for *L. stictaeforme* among habitats (ANOVA $F = 0.67$; $p > 0.05$), since growth was negative on both edge and base and zero on the reef flat. Epiphyte algae overgrew some coralline crusts but this cover was not enough to interfere with their growth in any habitat.

Productivity

The maximum irradiance measured was 1975 μmol m^{-2} s^{-1} on the reef flat, 1125 μmol m^{-2} s^{-1} on the reef edge and 869 μmol m^{-2} s^{-1} on the reef base, at midday on a sunny day in summer. Considering light attenuation of 56% by water column on a spring tide, irradiance on reef base could reach as low as 105 μmol m^{-2} s^{-1} in late afternoon. Under the conditions of low irradiance simulated in the laboratory, it was observed that crustose coralline species presented significant differences at the three levels tested (218, 107, and 68 μmol m^{-2} s^{-1}), O_2 production being greater for *P. onkodes* than *L. stictaeforme* (**Figure 8A**, ANOVA $F = 7.81$; $p \leq 0.005$ and

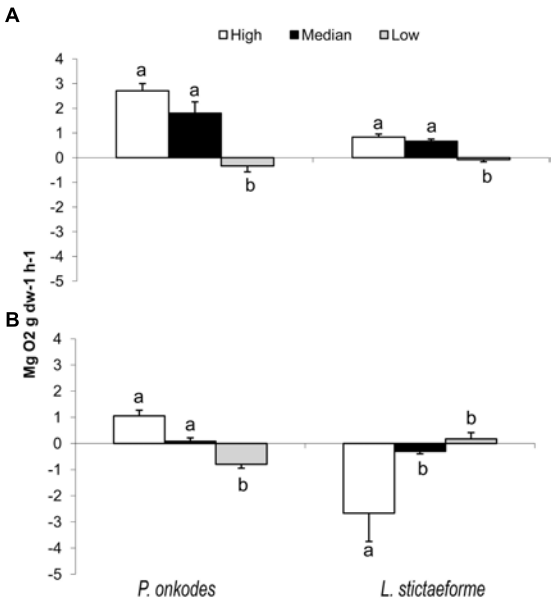

FIGURE 8 | Responses of *P. onkodes* and *L. stictaeforme* to irradiance at high, median, and low levels in the laboratory **(A)** and in the field **(B)** showing the net photosynthesis. Means ± standard error. Different letters above bars indicate significant differences among means detected by Tukey's test ($p < 0.05$).

$F = 19.42$; $p \leq 0.0001$, respectively). In contrast, exposure to the lowest irradiance level, 68 μmol m^{-2} s^{-1}, resulted in negative production in both species (**Figure 8A**).

In the field, irradiance effects on oxygen produced by *P. onkodes* presented significative difference among levels, being positive at 1093 (high), 623 (median), and negative at 218 (low light level) μmol m^{-2} s^{-1}, (**Figure 8B**, ANOVA $F = 30.75$; $p \leq 0.0001$). In contrast, *L. stictaeforme* exposed to equivalent irradiance levels, had a negative O_2 production under high irradiances of 716 and 408 μmol m^{-2} s^{-1} and positive under the lowest one of 143 μmol m^{-2} s^{-1} (**Figure 8B**, ANOVA $F = 4.79$; $p \leq 0.05$).

DISCUSSION

Colonization

In the Abrolhos Archipelago shallow reefs are mainly dominated by the CCA *P. onkodes* and *L. stictaeforme* (Figueiredo and Steneck, 2002; Tâmega and Figueiredo, 2007; Tâmega et al., 2014; Amado-Filho et al., 2018). However, during early stages of colonization erect seaweeds may smother coralline crusts. Filamentous algae generally are small in size, being less than 5 mm in height, and have low biomass (Steneck and Watling, 1982; Hackney et al., 1989), so their proliferation in summer may contribute little to final biomass, unless they form dense turfs. Nevertheless, filamentous algae were abundant colonizers covering reef edges of most sites, except during winter in Caldeiros. This absence may be related to competition by preemption of space (Olson and Lubchenco, 1990) by the non-calcareous crusts as these crusts are thinner and might have faster growth when compared to thick CCA (Dethier, 1994). Though the non-calcareous crusts were common early colonizers in all sites and seasons they were not common on the mature reef communities. These crusts occur seasonally during the development of communities but may be less successful than other fast growing ephemeral algae that may shade or sweep the substratum (Dethier, 1981). The CCA are long living crusts and are more resistant than non-calcareous crusts to consumption by grazers (Steneck and Dethier, 1994) and generally dominate in environments under moderate herbivore pressure (Steneck and Watling, 1982; Hackney et al., 1989; Figueiredo, 1997). However, intense herbivory could result in an inversion of this pattern in favor of non-calcareous crusts, which have faster growth (Steneck et al., 1991). In relation to the dominant algae groups, the colonization patterns found generally agreed with those found by others in Abrolhos' reef communities. Algae turf is one of the most abundant functional groups, ranging from 15 to 80% cover in both early colonization and in mature reef communities (Figueiredo, 1997; Villaça and Pitombo, 1997; Tâmega and Figueiredo, 2007).

Biomass of colonizing algae was higher on the reef base and edge than on the reef flat. The base and edge were covered by filamentous, foliose, non-calcareous crusts, and CCA. The absence of filamentous algae on reef flats may be related to the inability of their propagules to support prolonged desiccation during low tide, as diurnal low tides are more frequent in autumn and winter (Hackney et al., 1989). Species of *Polysiphonia* can lose 25% of water in its thallus in only 1 or 2 h and 75 up to 90% in longer periods when exposed to air (Kain and Norton, 1990). Foliose algae were present only on the reef base, which may act as a refuge from high hydrodynamic conditions as these algae are easily removed by wave action (Norton, 1991) and as refuge for fishes (mainly Acanthuridae and Labridae: Scarini) that is reduced when depth increases (Steneck, 1997; Figueiredo and Steneck, 2002; Tâmega and Figueiredo, 2007).

Coralline crusts colonized reef edges and bases but did not grow on the reef flat, similar to non-calcareous crusts. Despite both crustose groups being able to survive most disturbances (Dethier, 1994; Steneck and Dethier, 1994), coralline crusts are easily bleached when exposed to air although they can be protected from high light intensities by epiphyte cover (Figueiredo et al., 2000). The success of CCA depends not only on the capacity of recruits to resist disturbance, but also on their ability to occupy space through marginal vegetative growth.

Growth Rates

The absolute marginal growth of *P. onkodes* and *L. stictaeforme* ranged from 0.01 to 0.28 mm and 0.01 to 0.13 mm per day, respectively, the vertical growth being 0.023 to 0.23 mm per day for the latter species. These values were close to daily rates found for the first species in the Brazilian reef: Abrolhos (0.02 to 0.17 mm, Figueiredo, 1997); Rocas Atoll (0.01 to 0.05 mm, Villas-Bôas et al., 2005), and other reef forming species in the Caribbean region (0.07 mm for *P. onkodes* and 0.07–0.12 mm for *Neogonioliton megacarpum* in Adey and Vassar, 1975), but were

higher than those found in Pacific reefs (*P. onkodes* 0.02 mm, Matsuda, 1989). Coralline crust growth is comparatively slower in temperate environments (0.02 to 0.04 mm, Huvé *appud* Adey, 1970; Leukart, 1994). However, studies elsewhere have based their estimates of growth on small individuals during early colonization and thus, they proportionally detected greater marginal extension rates.

In general, marginal growth of *P. onkodes* crusts was positive at all sites in both seasons, except in Mato Verde in summer. Cover of epiphytic algae, especially non-calcareous crusts may have influenced crustose coralline growth because they were abundant when growth was reduced or absent. In contrast, marginal growth of *L. stictaeforme* crusts were negative or absent in most sites in both seasons, but significantly higher in Caldeiros in summer. This result can also be related to epiphytic cover mainly by non-calcareous crusts and articulated calcareous algae. Comparing reef habitats, lateral growth of *P. onkodes* was positive on the reef edge and base, but zero on the reef flat, which could be explained by desiccation plus high epiphytic cover of non-calcareous crusts. The minute or imperceptible marginal growth of *L. stictaeforme* might also have resulted from desiccation and epiphytes, which out-competed coralline crusts on the reef flats.

Lithophyllum stictaeforme develops well at depths around 0.3 to 4 m in regions where wave action is greater (Steneck and Adey, 1976). In shallow habitats, protected from waves, the CCA need herbivores to remove epiphytes, especially turf algae (Steneck, 1997), which may limit their growth (Williams and Carpenter, 1990; Figueiredo et al., 2000). The mechanism of sloughing epithelial cells to remove epiphytes (e.g., Masaki et al., 1984; Keats et al., 1997) is efficient in less productive environments, such as under canopies (Figueiredo et al., 1997) and probably in cryptic environments and at great depths (Steneck, 1997). In the sites at the Abrolhos, it was observed that epiphytic seaweeds were drastically reduced on *P. onkodes* on the reef edge and base, where herbivorous fishes are more frequently seen (Figueiredo and Steneck, 2002; Tâmega et al., 2016). However, epiphytes proliferated on *L. stictaeforme* in all habitats, probably because branches of these algae protect epiphytes against potential herbivory by acanthurids. In contrast, the vertical growth of *L. stictaeforme* was negative on the reef base and edge probably due to herbivory by parrotfishes, which are more adapted to consume branches and large portions of coralline crusts. The ramified forms of *L. stictaeforme* attract these fishes, resulting in a drastic loss of biomass (Steneck and Adey, 1976). Preliminary experiments with transplants of *L. stictaeforme* in Abrolhos demonstrated high consumption rates (40 to 80% of its branches to 12 h, unpublished data). Studies demonstrated that tropical seaweeds could survive and grow following ingestion by surgeonfishes and parrotfishes in the Caribbean (Vermeij et al., 2013) and Brazil (Tâmega et al., 2016), suggesting that these fishes contribute to the dispersion of seaweeds on reefs.

Productivity

In the laboratory *P. onkodes* usually responded better than *L. stictaeforme* under low irradiance, but under 68 μmol m^{-2} s^{-1} both species showed negative net O_2 production, which indicates that this level is beneath their compensation point (Bessell-Browne et al., 2017). In the field *P. onkodes* was more productive under irradiance levels up to 623 μmol m^{-2} s^{-1}, but in contrast to the lab, showed negative growth when exposed to 218 μmol m^{-2} s^{-1}.

Lithophyllum stictaeforme responded positively, as expected, to equivalent levels of irradiance (143 μmol m^{-2} s^{-1}), but was photo-inhibited under irradiance up to 408 μmol m^{-2} s^{-1}. The encrusting coralline algae *P. onkodes* not only grew better but was also more productive in environments subjected to high irradiance, when compared to *L. stictaeforme*.

Deposited sediments can limit incident light. Sediments are more easily trapped among turf algae than among other erect macroalgal thalli. In fact, sediments on disks tended to accumulate more on the reef base, where filamentous turfs are more abundant than on the reef flat (unpublished data). According to Fabricius and De'ath (2001), sedimentation increases even more with a slight reef slope, resulting in a decrease of CCA abundance. Filamentous turfs that trap sediments might also cause damage to the encrusting coralline algae because sediments create an anoxic area over the epithelial cells, suffocating these crusts (Connell and Slatyer, 1977; Kendrick, 1991; Steneck, 1997). Crustose corallines were as abundant on the reef edge as on the reef base, thus it was assumed that the deposition of sediments trapped by erect seaweeds was too low to affect CCA.

On the reef edge, crusts of *P. onkodes* are twice as abundant as branched *L. stictaeforme* (Tâmega and Figueiredo, 2007), which is apparently more common in cryptic habitats, such as reef crevices. In all experiments, flat crusts of *P. onkodes* responded better than branched crusts of *L. stictaeforme* to high irradiances, showing marginal growth rates up to four times faster in sunlit areas. In fact, fused branches of *L. stictaeforme* may indicate photoinibition of branch tips exposed directly to sunlight (Littler and Littler, 2000). Competition for space between these coralline crusts might be regulated not only by their intrinsic capacity to grow and respond to different light conditions, but also by their resistance to herbivores. It has been shown that *L. stictaeforme* is more likely to be consumed by Labridae: Scarini (Steneck and Adey, 1976); when transplanted to the reef edge the consumption was about 50 to 60% in the study area (unpublished data).

CONCLUSION

In summary, although there exist differences in biological limits between CCA, *L. stictaeforme* coexists with *P. onkodes* in habitats with high light intensity probably due to self-shading by its dense branches. *L. stictaeforme* showed high abundance only in cryptic reef habitats, such as crevices and beneath reefs with negative slopes. *P. onkodes* grew faster and was more productive under high light levels. Therefore, *P. onkodes* can be regarded as a plant adapted to high light environments and *L. stictaeforme* adapted to low light ones, where saturations levels are around 500 and 150 μmol m^{-2} s^{-1}, respectively (Lüning, 1990). These CCA are highly dependent on light, as has been demonstrated

for CCA in tropical and temperate environments (Adey, 1970; Leukart, 1994).

Coralline crusts were not the most common algae among early colonizers, rather filamentous turfs and non-calcareous crusts dominated the studied reefs. They are, however, usually more abundant in mature communities, possibly because of their greater resistance to disturbances (Steneck and Dethier, 1994). Changes in community structure in coral reefs are highly determined by a continuous gradient of grazing intensity (Hackney et al., 1989; Williams and Carpenter, 1990). Herbivory of coralline crusts in Abrolhos was lower (up to 10% of fish bite marks, unpublished data) when compared to former studies (up to 40% of fish bite marks, Figueiredo, 1997). Parrotfishes are one the most important and abundant herbivorous fish families on tropical reefs (Steneck, 1988) and form shoals with large individuals in the Abrolhos Archipelago (Ferreira and Gonçalves, 1999, 2006). In Abrolhos, *Scarus trispinosus*, one of the most abundant scarinae, has been reported to forage intensely on CCA (Ferreira and Gonçalves, 1999, 2006; Tâmega et al., 2016). We suggest that branches of *L. stictaeforme* might be preferentially consumed (Steneck and Adey, 1976) because its protruding branches seemed to attract herbivorous fishes (field observations), thus explaining the higher abundance of *L. stictaeforme* in reef refuges and its rarity on reef edges and flats. Parrotfishes are the only fish group able to excavate CCA (Steneck, 1983, 1986), but articulated calcareous, filamentous algae and a large amount of detritus are also important items in their diet (Ferreira and Gonçalves, 2006).

AUTHOR CONTRIBUTIONS

FT and MF conceived the study, conducted the analysis, and wrote the manuscript.

ACKNOWLEDGMENTS

We would like to thank the staff of the National Marine Park of Abrolhos who supported field work, Abrolhos Turismo for helping with boat transportation, Tubolit for providing epoxy putty, and the Brazilian Navy for their hospitality. Instituto Brasileiro do Meio Ambiente – IBAMA issued a research the license IBAMA 026/2000 for collecting samples. We are also grateful to Gary Andrew Kendrick from University of Western Australia for improving the English version and for their important comments. Comments and suggestions from the Editor NS and two reviewers improved the early version of the manuscript.

REFERENCES

Adey, W. H. (1970). The effects of light and temperature on growth rates in boreal-subartic crustose coralline algae. *J. Phycol.* 6, 269–276. doi: 10.1371/journal.pone.0027973

Adey, W. H. (1975). The algal ridges and coral reefs of St. Croix, their structure and Holocene development. *Atoll Res. Bull.* 187, 1–66. doi: 10.5479/si.00775630.187.1

Adey, W. H., and Vassar, J. M. (1975). Colonization, succession and growth rates of tropical crustose coralline algae (Rhodophyta, Cryptonemiales). *Phycologia* 14, 55–69. doi: 10.2216/i0031-8884-14-2-55.1

Amado-Filho, G. M., Bahia, R. G., Mariath, R., Jesionek, M. B., Moura, R. L., Bastos, A. C., et al. (2018). Spatial and temporal dynamics of the abundance of crustose calcareous algae on the southernmost coral reefs of the western Atlantic (Abrolhos Bank, Brazil). *Algae* 33, 85–99. doi: 10.4490/algae.2018.33.2.25

Bellwood, D. R., Hughes, T. P., Folke, C., and Nyström, M. (2004). Confronting the coral reef crisis. *Nature* 429, 827–833. doi: 10.1038/nature02691

Bessell-Browne, P., Negri, A. P., Fisher, R., Clode, P. L., and Jones, R. (2017). Impacts of light limitation on corals and crustose coralline algae. *Sci. Rep.* 7:11553. doi: 10.1038/s41598-017-11783-z

Clements, K. D., Raubenheimer, D., and Choat, J. H. (2009). Nutritional ecology of marine herbivorous fishes: ten years on. *Funct. Ecol.* 23, 79–92. doi: 10.1111/j.1365-2435.2008.01524.x

Connell, J. H., and Slatyer, R. O. (1977). Mechanisms of succession in natural communities and their role in community stability and organization. *Am. Nat.* 3, 1119–1144. doi: 10.1086/283241

Dethier, M. N. (1981). Heteromorphic algal life histories: the seasonal pattern and response to herbivore of the brown crust, *Ralfsia californica*. *Oecologia* 49, 333–339. doi: 10.1007/BF00347594

Dethier, M. N. (1994). The ecology of intertidal algal crusts: variation within a functional group. *J. Exp. Mar. Biol. Ecol.* 177, 37–71. doi: 10.1016/0022-0981(94)90143-0

Edyvean, R. G. J., and Ford, H. (1987). Growth rates of *Lithophyllum incrustans* (Corallinales, Rhodophyta) from south west Wales. *Br. Phycol. J.* 22, 139–146. doi: 10.1080/00071618700650161

Fabricius, K., and De'ath, G. (2001). Enviromental factors associated with the spatial distribution of crustose coralline algae on the Great Barrier Reef. *Coral Reefs* 19, 303–309. doi: 10.1007/s003380000120

Ferreira, C. E. L., and Gonçalves, J. E. A. (1999). The unique Abrolhos reef formation (Brazil): need for specific management strategies. *Coral Reefs* 18:352. doi: 10.1007/s003380050211

Ferreira, C. E. L., and Gonçalves, J. E. A. (2006). Community structure and diet of roving herbivorous reef fishes in the Abrolhos Archipelago, South Western Atlantic. *J. Fish Biol.* 69, 1–19. doi: 10.1111/j.1095-8649.2006.01220.x

Figueiredo, M. A. O. (1997). "Colonization and growth of crustose coralline algae in Abrolhos, Brazil," in *Proceedings of the 8th International Coral Reef Symposium*, Vol. 1, eds H. A. Lessios and I. G. Macintyre (Panama: Smithsonian Tropical Research Institute), 689–694.

Figueiredo, M. A. O., Kain, J. M., and Norton, T. A. (1996). Biotic interactions in the colonization of crustose coralline algae by epiphytes. *J. Exp. Mar. Biol. Ecol.* 199, 303–318. doi: 10.1016/0022-0981(96)00018-4

Figueiredo, M. A. O., Kain, J. M., and Norton, T. A. (2000). Responses of crustose coralline algae to epiphyte and canopy cover. *J. Phycol.* 36, 17–24. doi: 10.1046/j.1529-8817.2000.98208.x

Figueiredo, M. A. O., Norton, T. A., and Kain, J. M. (1997). Settlement and survival of epiphytes on two intertidal crustose coralline algae. *J. Exp. Mar. Biol. Ecol* 213, 247–260. doi: 10.1016/S0022-0981(96)02766-9

Figueiredo, M. A. O., and Steneck, R. S. (2002). "Floristic and ecological studies of crustose coralline algae on Brazil's Abrolhos reefs," in *Proceedings of the Ninth International Coral Reef Symposium*, Panama, 493–498.

Gherardi, D. F. M., and Bosence, D. W. J. (2001). Composition and community structure of the coralline algal reefs from Atol das Rocas, South Atlantic, Brazil. *Coral Reefs* 19, 205–219. doi: 10.1007/s003380000100

Hackney, J. M., Carpenter, R. C., and Adey, W. H. (1989). Characteristic adaptations to grazing among algal turfs on a Caribbean coral reef. *Phycologia* 28, 109–119. doi: 10.2216/i0031-8884-28-1-109.1

Horn, M. H. (1989). Biology of marine herbivorous fishes. *Oceanogr. Mar. Biol. Annu. Rev.* 27, 167–272.

Kain, J. M. (1987). Seasonal growth and photoinhibition in *Plocamium cartilagineum* (Rhodophyta) off the Isle of Man. *Phycologia* 26, 88–99. doi: 10.2216/i0031-8884-26-1-88.1

Kain, J. M., and Norton, T. A. (1990). "Marine ecology," in *The Biology of the Red Algae*, eds K. M. Cole and R. Sheath (Cambridge: Cambridge University Press), 377–422.

Keats, D. W., Knight, M. A., and Pueschel, C. M. (1997). Antifouling effects of epithallial shedding in three crustose coralline algae (Rhodophyta, Coralinales) on a coral reef. *J. Exp. Mar. Biol. Ecol.* 213, 281–293. doi: 10.1016/S0022-0981(96)02771-2

Keats, D. W., Mathews, I., and Maneveldt, G. (1994). Competitive relationships and coexistence in a guild of crustose algae in eullitoral zone, Cape Province, South Africa. *S. Afr. J. Bot.* 60, 108–113. doi: 10.1016/S0254-6299(16)30640-8

Kendrick, G. A. (1991). Recruitment of coralline crust and filamentous turf algae in the Galapagos archipelago: effect of simulated scour, erosion and accretion. *J. Exp. Mar. Biol. Ecol.* 147, 47–63. doi: 10.1016/0022-0981(91)90036-V

Kikuchi, R. K. P., and Leão, Z. M. A. N. (1997). "Rocas (southwestern equatorial Atlantic, Brazil): an atol built primarily by coralline algae"in *Proceedings Of The International Coral Reef Symposium*, Panama, 731–736.

Leão, Z. M. A. N., and Dominguez, J. M. L. (2000). Tropical coast of Brazil. *Mar. Pollut. Bull.* 41, 112–122. doi: 10.1016/S0025-326X(00)00105-3

Leão, Z. M. A. N., and Kikuchi, R. K. P. (2001). The Abrolhos reefs of Brazil. *Ecol. Stud.* 144, 83–96. doi: 10.1007/978-3-662-04482-7_7

Lei, X., Huang, H., Lian, J., Zhou, G., and Jiang, L. (2018). Community structure of coralline algae and its relationship with environment in Sanya reefs, China. *Aquat. Ecosyst. Health* 21, 19–29. doi: 10.1080/14634988.2018.1432954

Leukart, P. (1994). Field and laboratory studies on depth dependence, seasonality and light requirement of growth in three species of crustose coralline algae (Rhodophyta, Corallinales). *Phycologia* 33, 281–290. doi: 10.2216/i0031-8884-33-4-281.1

Littler, M. M. (1972). The crustose Corallinaceae. *Oceanogr. Mar. Biol. Ann. Rev.* 10, 311–347.

Littler, M. M. (1973). The population and community structure of Hawaiian fringing-reef crustose corallinaceae (Rhodophyta, Cryptonemiales). *J. Exp. Mar. Biol. Ecol.* 11, 103–120. doi: 10.1016/0022-0981(73)90050-6

Littler, M. M., and Littler, D. S. (1980). The evolution of thallus form and survival strategies in benthic marine macroalgae: field and laboratory tests of a functional form model. *Am. Nat.* 116, 25–44. doi: 10.1086/283610

Littler, M. M., and Littler, D. S. (1984). Relationships between macroalgal functional form groups and substrata stability in a subtropical rocky intertidal system. *J. Exp. Mar. Biol. Ecol.* 74, 13–34. doi: 10.1016/0022-0981(84)90035-2

Littler, M. M., and Littler, D. S. (1997). "Disease-induced mass mortality of crustose coralline algae on coral reefs provides rationale for the conservation of herbivorous fish stocks," in *Proceedings of the Eighth International Coral Reefs Symposium*, Panama, 719–724.

Littler, M. M., and Littler, D. S. (2000). *Caribean Reef Plant. An Identification Guide to the Reef Plants of the Caribbean*. Boca Raton, FL: Off Shore Grafics, Inc.

Littler, M. M., Littler, D. S., and Taylor, P. R. (1995). Selective herbivore increases biomass of its prey: a chiton-coralline reef-building association. *Ecology* 76, 1666–1681. doi: 10.2307/1938167

Lüning, K. (1990). *Seaweeds. Their Environmental, Biogeography, and Ecophysiology*. New York, NY: John Wiley and Sons.

Macintyre, I. G. (1997). "Reevaluating the role of crustose coralline algae in the construction of the coral reefs," in *Proceedings of the 8th International Coral Reef Symposium*, Panama, 725–730.

Mariath, R., Riosmena-Rodriguez, R., and Figueiredo, M. A. O. (2013). Succession of crustose coralline red algae (Rhodophyta) on coralgal reefs exposed to physical disturbance in the southwest Atlantic. *Helgol. Mar. Res.* 67, 687–696. doi: 10.1007/s10152-013-0354-3

Masaki, T., Fujita, D., and Hagen, N. T. (1984). The surface ultrastructure and epithallium shedding of crustose coralline algae in an "isoyake" area of southwestern Hokkaido, Japan. *Hydrobiologia* 117, 219–223.

Matsuda, S. (1989). Succession and growth rates of incrusting crustose coralline algae (Rhodophyta, Cryptonemiales) in the upper fore-reef enviromental off Ishigaki Island, Ryukyu Islands. *Coral Reefs* 7, 185–195. doi: 10.1007/BF00301597

McClanahan, T. R., McField, M., Huitric, M., Bergman, K., Sala, E., Nyström, et al. (2001a). Responses of algae, corals and fish to the reduction of macroalgae in fished and unfished patch reefs of Glovers Reef Atoll, Belize. *Coral Reefs* 19, 367–379. doi: 10.1007/s003380000131

McClanahan, T. R., Muthinga, N. A., and Mangi, S. (2001b). Coral and algal changes after the 1998 coral bleching: interaction with reef management and herbivores on Kenyan reefs. *Coral Reefs* 19, 380–391. doi: 10.1007/s003380000133

Muehe, D. (1988). O arquipélago dos Abrolhos: geomorfologia e aspectos gerais. *An. Inst. Geoc.* 11, 90–100.

Norton, T. A. (1991). Conflicting constraints on the form of intertidal algae. *Br. Phycol. J.* 26, 203–218. doi: 10.1080/00071619100650191

Olson, A. M., and Lubchenco, J. (1990). Competition in seaweeds: linking plant traits to competitive outcomes. *J. Phycol.* 26, 1–6. doi: 10.1111/j.0022-3646.1990.00001.x

Pitlik, T. J., and Paul, V. J. (1997). "Effects of toughness, calcite level, and chemistry of crustose coralline algae (Rhodophyta, Corallinales) on grazing by the parrot fish *Chorurus sordidus*," in *Proceedings of the 8th International Coral Reef Symposium*, Panama, 701–706.

Spotorno-Oliveira, P., Figueiredo, M. A. O., and Tâmega, F. T. S. (2015). Coralline algae enhance the settlement of the vermetid gastropod *Dendropoma irregulare* (d'Orbigny, 1842) in the southwestern Atlantic. *J. Exp. Mar. Biol. Ecol.* 471, 137–145. doi: 10.1016/j.jembe.2015.05.021

Steneck, R. S. (1983). Escalating herbivory and resulting adaptive trends in calcareous algal crusts. *Paleobiology* 9, 44–61. doi: 10.1017/S0094837300007375

Steneck, R. S. (1986). The ecology of coralline algal crusts: convergent patterns and adaptive strategies. *Ann. Rev. Ecol. Syst.* 17, 273–303. doi: 10.1146/annurev.es.17.110186.001421

Steneck, R. S. (1988). "Herbivore on coral reefs: a synthesis," in *Proceedings of the 8th International Coral Reef Symposium*, Panama, 37–49.

Steneck, R. S. (1997). "Crustose corallines, other algal functional grups, herbivores and sediments: complex interactions along reef productivity gradients," in *Proceedings of the 8th International Coral Reef Symposium*, Vol. 1, eds H. A. Lessios and I. G. Macintyre (Panama: Smithsonian Tropical Research Institute), 695–700.

Steneck, R. S., and Adey, W. H. (1976). The role of environment in control of morphology in *Lithophyllum congestum*, a Caribbean algal ridge builder. *Bot. Mar.* 19, 197–215. doi: 10.1515/botm.1976.19.4.197

Steneck, R. S., and Dethier, M. N. (1994). A functional group approach to the structure of algal-dominated communities. *Oikos* 69, 476–498. doi: 10.2307/3545860

Steneck, R. S., Hacker, S. D., and Dethier, M. N. (1991). Mechanisms of competitive dominance between crustose coralline algae: an herbivore-mediated competitive reversal. *Ecology* 72, 938–950. doi: 10.2307/1940595

Steneck, R. S., and Watling, L. E. (1982). Feeding capabilities and limitations of herbivorous molluscs: a functional group approach. *Mar. Biol.* 68, 299–319. doi: 10.1007/BF00409596

Tâmega, F. T. S., and Figueiredo, M. A. O. (2007). Distribution of crustose coralline algae (Corallinales, Rhodophyta) in the Abrolhos reefs, Bahia, Brazil. *Rodriguésia* 58, 941–947. doi: 10.1111/j.1529-8817.2007.00431.x

Tâmega, F. T. S., Figueiredo, M. A. O., Ferreira, C. E. L., and Bonaldo, R. M. (2016). Seaweed survival after consumption by the greenbeak parrotfish, Scarus trispinosus. *Coral Reefs* 35, 329–334. doi: 10.1007/s00338-015-1373-0

Tâmega, F. T. S., Riosmena-Rodriguez, R., Mariath, R., and Figueiredo, M. A. O. (2014). Nongeniculate coralline red algae (Rhodophyta: Corallinales) in coral reefs from Northeastern Brazil and a description of *Neogoniolithon atlanticum* sp. nov. *Phytotaxa* 190, 277–298. doi: 10.11646/phytotaxa.190.1.17

Thomas, M. L. H. (1988). "Photosynthesis and respiration of aquatic macroflora using the light and dark bottle oxygen method and dissolved oxygen analyzer," in *Experimental Phycology: a Laboratory Manual*, eds C. S. Lobban, D. J. Chapman, and B. P. Kremer (Cambridge: Cambridge University Press), 64–77.

Underwood, A. J. (1997). *Experiments in Ecology. Logical Design and Interpretation using Analysis of Variance*. Cambridge: Cambridge University Press.

Vermeij, M. J. A., van der Heijden, R. A., Olthuis, J. G., Marhaver, K. L., Smith, J. E., and Visser, P. M. (2013). Survival and dispersal of turf algae and macroalgae consumed by herbivorous coral reef fishes. *Oecologia* 171, 417–425. doi: 10.1007/s00442-012-2436-3

Villaça, R., and Pitombo, F. B. (1997). Benthic communities of shallow-water reefs of Abrolhos, Brazil. *Rev. Bras Oceanogr.* 45, 35–43. doi: 10.1590/S1413-77391997000100004

Villas-Bôas, A. B., Figueiredo, M. A. O., and Villaça, R. C. (2005). Colonization and growth of crustose coralline algae (Corallinales Rhodophyta) on the Rocas Atoll. *Braz. J. Ocean.* 53, 147–156. doi: 10.1590/S1679-87592005000200005

Vroom, P. S., Page, K. N., Peyton, K. A., and Kukea-Shultz, J. K. (2005). Spatial heterogeneity of benthic community assemblages with an emphasis on reef algae at French frigate shoals, Northwestern Hawaiian Island. *Coral Reefs* 24, 574–581. doi: 10.1007/s00338-005-0028-y

Williams, I. D., and Polunin, N. V. C. (2001). Large-scale associations between macroalgal cover and grazer biomass on mid-depth reefs in the Caribbean. *Coral Reefs* 19, 358–366. doi: 10.1007/s003380000121

Williams, S. L., and Carpenter, R. C. (1990). Photosynthesis/ photon flux density relationships among components of coral reef algal turfs. *J. Phycol.* 26, 36–40. doi: 10.1111/j.0022-3646.1990.00036.x

Conflict of Interest Statement: The authors declare that the research was conducted in the absence of any commercial or financial relationships that could be construed as a potential conflict of interest.

Copyright © 2019 Tâmega and Figueiredo. This is an open-access article distributed under the terms of the Creative Commons Attribution License (CC BY). The use, distribution or reproduction in other forums is permitted, provided the original author(s) and the copyright owner(s) are credited and that the original publication in this journal is cited, in accordance with accepted academic practice. No use, distribution or reproduction is permitted which does not comply with these terms.

frontiers in Marine Science

ORIGINAL RESEARCH
published: 07 January 2019
doi: 10.3389/fmars.2018.00495

Elevated CO_2 Leads to Enhanced Photosynthesis but Decreased Growth in Early Life Stages of Reef Building Coralline Algae

*Alexandra Ordoñez[1], Daniel Wangpraseurt[2,3,4], Niclas Heidelberg Lyndby[4,5], Michael Kühl[4,6] and Guillermo Diaz-Pulido[1,7]**

[1] School of Environment and Science, Australian Rivers Institute, Griffith University, Brisbane, QLD, Australia, [2] Department of Chemistry, University of Cambridge, Cambridge, United Kingdom, [3] Scripps Institution of Oceanography, University of California, San Diego, La Jolla, CA, United States, [4] Marine Biological Section, Department of Biology, University of Copenhagen, Helsingør, Denmark, [5] Laboratory for Biological Geochemistry, School of Architecture, Civil and Environmental Engineering, Ecole Polytechnique Fédérale de Lausanne, Lausanne, Switzerland, [6] Climate Change Cluster, University of Technology Sydney, Ultimo, NSW, Australia, [7] ARC Centre of Excellence for Coral Reef Studies, Townsville, QLD, Australia

OPEN ACCESS

Edited by:
Laurie Carol Hofmann, Max Planck Institute for Marine Microbiology (MPG), Germany

Reviewed by:
Maggy Nugues, Université de Sciences Lettres de Paris, France
Raphael Ritson-Williams, California Academy of Sciences, United States

***Correspondence:**
Guillermo Diaz-Pulido
g.diaz-pulido@griffith.edu.au

Specialty section:
This article was submitted to Marine Ecosystem Ecology, a section of the journal Frontiers in Marine Science

Received: *29 August 2018*
Accepted: *11 December 2018*
Published: *07 January 2019*

Citation:
Ordoñez A, Wangpraseurt D, Lyndby NH, Kühl M and Diaz-Pulido G (2019) Elevated CO_2 Leads to Enhanced Photosynthesis but Decreased Growth in Early Life Stages of Reef Building Coralline Algae. Front. Mar. Sci. 5:495. doi: 10.3389/fmars.2018.00495

Crustose coralline algae (CCA) are key organisms in coral reef ecosystems, where they contribute to reef building and substrate stabilization. While ocean acidification due to increasing CO_2 can affect the biology, physiology and ecology of fully developed CCA, the impacts of elevated CO_2 on the early life stages of CCA are much less explored. We assessed the photosynthetic activity and growth of 10-day-old recruits of the reef-building crustose coralline alga *Porolithon* cf. *onkodes* exposed to ambient and enhanced CO_2 seawater concentration causing a downward shift in pH of ∼0.3 units. Growth of the CCA was estimated using measurements of crust thickness and marginal expansion, while photosynthetic activity was studied with O_2 microsensors. We found that elevated seawater CO_2 enhanced gross photosynthesis and respiration, but significantly reduced vertical and marginal growth of the early life stages of *P.* cf. *onkodes*. Elevated CO_2 stimulated photosynthesis, particularly at high irradiance, likely due to increased availability of CO_2, but this increase did not translate into increased algal growth as expected, suggesting a decoupling of these two processes under ocean acidification scenarios. This study confirms the sensitivity of early stages of CCA to elevated CO_2 and identifies complexities in the physiological processes underlying the decreased growth and abundance in these important coral reef builders upon ocean acidification.

Keywords: ocean acidification, global warming, early stages, red algae, algal physiology, photosynthesis, respiration

INTRODUCTION

Crustose coralline algae (CCA) are abundant in tropical and temperate reef ecosystems, where they provide important ecosystem functions (Littler, 1972; Littler and Doty, 1975). CCA contribute to the stabilization of coral reef frameworks by consolidating and cementing loose rubble and by sealing porous dead corals skeleton against mechanical erosion (Littler, 1972; Adey, 1998). CCA also provide food and habitat for a range of reef organisms such as parrot fish and sea urchins

(Littler and Doty, 1975; Steneck, 1983) and are preferred settlement substrates for larvae of corals and other invertebrates (Heyward and Negri, 1999; Harrington et al., 2004). The presence of CCA is thus crucial for the health and recovery of coral reefs following disturbances.

The current and projected increase in atmospheric pCO_2 and the derived ocean acidification (OA) due to a decrease in seawater pH and calcium carbonate ($CaCO_3$) saturation state (Ω) is critical for the integrity and fitness of calcifying organisms (Anthony et al., 2008; Kroeker et al., 2010). CCA are among the marine organisms most sensitive to OA as their skeleton is predominantly formed by high-magnesium calcite, a highly soluble form of $CaCO_3$ (Morse et al., 2007). Rates of net calcification and growth of CCA are generally negatively affected by OA (Anthony et al., 2008; Kuffner et al., 2008; Martin and Gattuso, 2009) due to reduced availability of carbonate ions (CO_3^{2-}) for calcification (Feely et al., 2004) and increased skeletal dissolution of existing calcium carbonate (Diaz-Pulido et al., 2014). On the other hand, increased atmospheric CO_2 increases the concentration of dissolved CO_2 and bicarbonate ions (HCO_3^-) in seawater potentially alleviating inorganic carbon limitation (Larkum et al., 2003) and thus stimulating algal photosynthesis. However, the available experimental evidence shows that the responses of CCA photosynthesis to OA are highly variable, including positive (Semesi et al., 2009) or negative effects (Anthony et al., 2008; Gao and Zheng, 2010; Martin et al., 2013), as well as no significant response (Noisette et al., 2013; Johnson et al., 2014; Comeau et al., 2017). This variability in response to OA may be due to a number of reasons, including use of different experimental setups and time scales (e.g., 1 year experiment with *Lithophyllum cabiochae* vs. 3 months experiment with *Lithophyllum incrustans* Martin et al., 2013; Noisette et al., 2013), different life history stages (e.g., recruits vs. adults), and flexibility of different CCA species in their use of inorganic carbon uptake strategies, i.e., use of carbon concentrating mechanisms (CCM) vs. diffusive CO_2 uptake (Cornwall et al., 2012, 2015; Diaz-Pulido et al., 2016).

Increased availability of dissolved inorganic carbon (DIC) is expected to enhance algal photosynthesis and consequently algal growth rates (Roleda et al., 2012). However, growth responses to OA have been less explored in coralline algae compared to fleshy macroalgae (e.g., Kroeker et al., 2013), and in most studies changes in CCA growth rates have been based on changes in crust weight rather than on a direct measurement of algal growth (e.g., Anthony et al., 2008; Johnson and Carpenter, 2012). Changes in crust weight have the innate difficulty of not allowing distinction between new growth and skeletal dissolution (Lewis et al., 2017). The relationship between photosynthesis and growth rates has been previously studied in fleshy macroalgae (e.g., Koch et al., 2013), where elevated CO_2 enhanced photosynthetic activity and tissue growth in two species of red algae *Gracilaria* (Gao et al., 1993), but similar relations in CCA remain unexplored.

Existing knowledge on the physiological responses of elevated CO_2 on tropical CCA comes from studies on adult crusts (Anthony et al., 2008; Johnson et al., 2014; Comeau et al., 2017). In our previous studies using the reef building CCA *Porolithon onkodes*, we explored the impacts of OA and warming on spore germination and germling growth and found these processes to be highly sensitive to elevated CO_2 (Ordoñez et al., 2017). Roleda et al. (2015) tested the effects of OA on growth of temperate coralline algae recruits and found a direct negative response of crust size upon exposure to OA conditions. Studies of the early life stages of tropical (Kuffner et al., 2008; Fabricius et al., 2015; Ordoñez et al., 2017) and temperate (Bradassi et al., 2013; Roleda et al., 2015; Guenther et al., 2018) CCA have demonstrated a high vulnerability to elevated CO_2, as well as other environmental stressors (Santelices, 1990). However, very little is known about the effects of OA on photosynthesis and the coupling between photosynthesis and growth rates in the early life stages of CCA (but see Cornwall et al., 2013). In the present study, we explore the effect of elevated CO_2 conditions on the photosynthetic activity and growth rates of recruits of a dominant crustose coralline alga in the Great Barrier Reef, Australia. We used O_2 microsensors due to the small size of the CCA recruits (around 0.004–002 mm^2 surface area), and because microsensors can decouple light respiration from gross oxygen production, as compared to chamber based incubation measurements (Revsbech and Jorgensen, 1983; Larkum et al., 2003).

MATERIALS AND METHODS

Experimental Approach

The effects of ocean acidification on rates of growth and photosynthesis of CCA recruits were investigated by exposing *Porolithon* cf. *onkodes* spores to elevated and ambient CO_2 conditions in the laboratory during a 4 week experiment. Dynamics of O_2 concentration (measured using O_2 microsensors) and crust thickness (measured using scanning electron microscopy, SEM) of 10-day-old recruits were estimated at the end of the experiment. The experiment was conducted in an indoor laboratory at Heron Island Research Station (HIRS), Great Barrier Reef (GBR), Australia during the summer of 2014 (February–March 2014). The species *P.* cf. *onkodes* was used for this experiment due to its important role as a reef builder and cementer (Littler, 1972), and because it is a common alga in tropical reefs, especially in the Great Barrier Reef (Ringeltaube and Harvey, 2005; Dean et al., 2015). Identification of *P.* cf. *onkodes* (Heydrich) Foslie was obtained with field and laboratory observations. Microscope techniques such as Scanning Electron Microscopy and histology were used to examine morphological and anatomical characteristics. The encrusting coralline alga *P.* cf. *onkodes* used for this experiment is usually found on the reef crest (approx. 3–5 m depth), has a pink-orange color surface with granular appearance due to the presence of numerous tightly packed mega cells in horizontal fields (trichocytes fields), reproductive structures (conceptacles) are unipored, small, flush or slightly raised, cell fusions are present and thallus has a non-coaxial organization. DNA sequences of individuals of this species can be found

in GenBank (Accession No. MF979936, see Gabrielson et al., 2018).

Cultivation of Recruits and Experimental Setup

To obtain CCA spores for the experiment, spore release from reproductive *P.* cf. *onkodes* fragments was induced in the laboratory following a combination of methods described in Jones and Moorjani (1973); Ichiki et al. (2000), Roleda et al. (2012), and Ordoñez et al. (2017). Adult *P.* cf. *onkodes* fragments (3 cm × 3 cm) were collected from the reef crest (ca 5 m depth at highest tide) at Harry's Bommie (Heron Island, GBR, 23°27′631″S, 151°55′798″E) using hammer and chisel. After collection, fragments were cleaned from epiphytes with a soft brush and rinsed with filtered sterilized seawater. Seawater was filtered twice: first using a hand-made sand filter containing a cotton filter mat and then a house water filter with a 5 μm cartridge (house water filter OMNI OPAQUE), seawater was then sterilized using an aquarium ultra violet sterilizer (Pro Aqua UV sterilizer). Spore release was then induced by placing the fragments on a tray with no water and in a dark, cold (18°C) room for 30 min. Subsequently, sterilized ambient seawater was added to the tray, which was then placed under an artificial metal-halide lamp (Aqua Medic Ocean Light Plus equipped with one 150 W aqualine bulb and two 24 W T5 blue fluorescent bulbs) for 7 h. Immediately after the illumination period, adults commenced spore release and were carefully transferred to the experimental containers (1 L plastic containers) where spore release continued under experimental conditions. Three replicate containers ($n = 3$) were used for each CO_2 treatment (6 experimental containers in total, 3 for ambient CO_2 and 3 for high CO_2). One transparent polystyrene Petri dish (94 mm × 16 mm diameter) was placed on the bottom of each experimental container to provide substratum for spore settlement and growth. Three adult fragments were randomly assigned to each experimental container to obtain sufficient spores for analysis. However, adults were removed after 4 h, when the first spore attachment was detected, for the following two reasons: (1) To avoid having individuals at different growth stages and (2) to have sufficient number of spores to get a good estimate of their individual growth, but only enough spores to avoid those that had settled close to each other to coalesce. The margin of coalesced spores are difficult to distinguish making individual measurements hard to perform.

Spores were cultured for a period of 10 days in seawater under (i) ambient CO_2 (400.8–448.1 μatm) and pH 8.00–8.03 (National Bureau of Standards/National Institute of Standards and Technology) and (ii) high CO_2 (998.9–1070.6 μatm) and pH 7.67–7.70. The high CO_2 treatment corresponded to the representative concentration pathway 8.5 scenario (RCP 8.5), i.e., the worst case OA scenario predicted by the end of the century (year 2100) according to the Intergovernmental Panel on Climate Change (IPCC, 2014). To achieve the target pH for the high CO_2 treatment, analytical grade CO_2 gas (BOC Limited Australia) was injected into a 120 L mixing sump using an aquarium control system (Aquatronica, AEB Technologies, Italy). Seawater pH was monitored in the mixing sump by temperature compensated pH electrodes (inPro4501VP, Mettler-Toledo, Switzerland). When seawater pH exceeded the desired threshold, the control system opened solenoid valves to inject CO_2 into the mixing sump as previously described in Diaz-Pulido et al. (2011). CO_2 conditioned seawater was pumped continuously into experimental containers at a rate of 500 mL min^{-1}. The same set up was used for ambient CO_2 treatment, but with untreated seawater in the mixing sump. Mixing sumps were constantly fed with seawater from the Heron Island reef flat. pH probes were calibrated daily to 0.01 pH units with three NIST-certified pH buffers (Mettler-Toledo, Switzerland). Temperatures in both sumps (ambient CO_2 and high CO_2) and in one container of each treatment was constantly monitored every 30 s and recorded by the aquarium control system. In addition, pH and temperature measurements were frequently taken on experimental containers with a portable pH and temperature meter (SG98-B-SevenGo Duo Pro, Mettler-Toledo, Switzerland) to ensure the pH and temperature were kept constant. Illumination was provided with metal-halide lamps (Aqua Medic Ocean Light Plus equipped with one 150 W aqualine bulb and two 24 W T5 blue fluorescent bulbs) over a 12 h light: 12 h dark photoperiod under an irradiance of 160 μmol photons m^{-2} s^{-1}, as measured by cosine corrected quantum sensor connected to a light meter (Li-COR, United States). Total alkalinity, pH and salinity values were used to estimate the concentration of dissolved inorganic carbon (pCO_2, HCO_3^- and CO_3^{2-}) using Microsoft Excel CO_2SYS version 2.1 (Pierrot et al., 2006). The saturation state of seawater with respect to high-Mg-calcite was calculated for a 16.4 mol% $MgCO_3$, following a protocol described in (Diaz-Pulido et al., 2012). Carbonate chemistry parameters are shown in **Table 1**.

O_2 Microsensor Measurements

Microscale O_2 concentration measurements were done with Clark-type O_2 microsensors (Revsbech, 1989) connected to a pA-meter (PA2000, Unisense A/S, Aarhus, Denmark) interfaced to a PC via an A/D converter (**Figure 1**). The O_2 microsensors (OX25; Unisense, Denmark) had a measuring tip diameter of 25 μm, a t_{90} response time of <0.5 s, a stirring sensitivity of the measuring signal of <2–3%, and a detection limit of ∼0.3 μM[1]. The O_2 microsensors were linearly calibrated from signal readings in air saturated seawater and anoxic seawater (flushed with N_2). The O_2 concentration (μmol O_2 L^{-1}) in air saturated seawater at experimental temperature and salinity was determined using tabulated values of O_2 solubility in water at defined temperature and salinity[1].

The O_2 microsensors were mounted on a PC-controlled motorized micromanipulator for automatic profiling (Pyro Science GmbH, Germany) at an angle of 15° relative to the vertically incident collimated light from a fiber-optic tungsten-halogen lamp (KL-2500, Schott GmbH, Germany), equipped

[1]http://www.unisense.com

TABLE 1 | Summary of water chemistry parameters for the different CO_2 levels.

Treatment	Temperature °C	TA μmol kg^{-1}	pH	pCO_2 μatm	HCO^3 μmol kg^{-1}	$CO_3{}^2$ μmol kg^{-1}	ΩHigh Mg Calcite 16.4 mol% $MgCO_3$
Control CO_2	26.1 (±0.3) (25.0–27.2)	2323.7 (±4.8) (2319.35–2333.61)	8.01 (±0.005) (8.0–8.03)	425 (±6.4) (400.8–448.1)	1801.76 (±10.1) (1763.1–1846.1)	213.34 (±2.8) (201.7–220.9)	1.14 (±0.02) (1.06–1.19)
High CO_2	26.1 (±0.3) (25.0–27.2)	2347.4 (±8.9) (2311.55–2379.98)	7.69 (±0.004) (7.67–7.7)	1026.67 (±9.4) (998.9–1070.6)	2065.06 (±7.6) (2038–2096.9)	115.95 (±1.4) (110.1–120.6)	0.61 (±0.01) (0.58–0.65)

Values represent means (±SEM) (range) for n = 8 biological replicates.

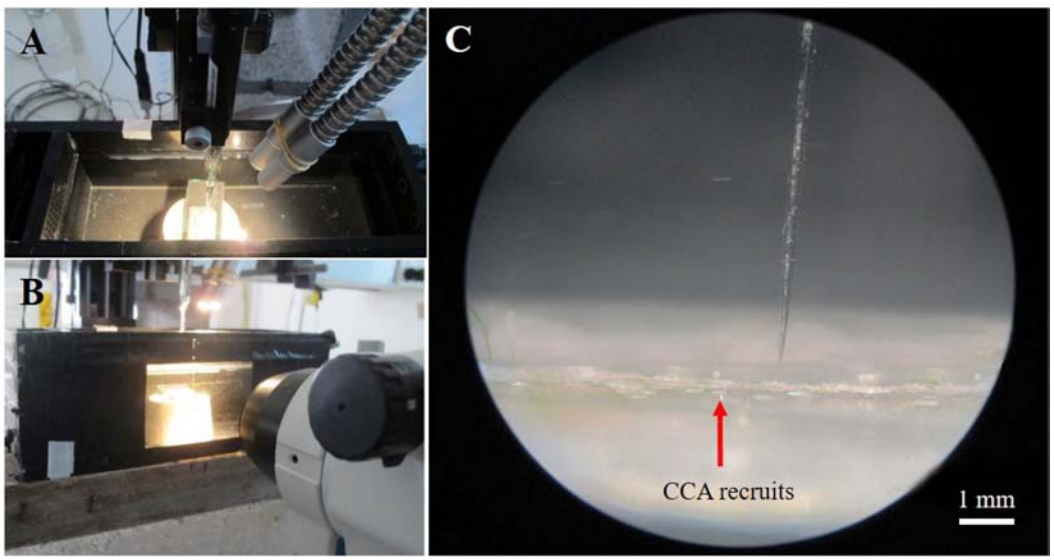

FIGURE 1 | Setup for O_2 microsensor measurements on crustose coralline algae. General overview of the set-up showing a flow-chamber with a mounted CCA sample **(A,B)**, with an O_2 microsensor mounted in a manual micromanipulator, illumination via a fiber-optic halogen lamp, and observation of the sample via a dissection microscope **(B)**. **(C)** Close up image (via the dissection microscope) of an O_2 microsensor performing O_2 measurements on CCA recruits (pink crust).

with a heat filter and a collimating lens. Positioning of the microsensor as well as data acquisition of microsensor signals was facilitated by customized software (Profix, Pyro-Science GmbH, Germany). Experiments were conducted with CCA recruits placed in a custom-made black acrylic flow chamber supplied with seawater at a flow velocity of ∼1–2 cm s^{-1} (Brodersen et al., 2014). We used the same seawater as in the different CO_2 treatments. The downwelling photon irradiance (PAR, 400–700 nm) was measured for defined lamp settings with a calibrated cosine corrected quantum sensor connected to a light meter (LI-250A, Li-COR). For the high CO_2 treatment, the seawater taken from the treatment sumps was exchanged every 20–30 min in order to account for changes in pH related to atmospheric CO_2 exchange. The pH in the water was monitored constantly with a portable pH meter (SG98-B-SevenGo Duo Pro, Mettler-Toledo, Switzerland) calibrated with NIST-certified pH buffers (Mettler-Toledo, Switzerland) to 0.01 pH units. Recruits from 3 ambient and 2 high CO_2 experimental tanks were used for O_2 microsensor measurements. Only two replicates could be used from high CO_2 treatments due to unexpected experimental constrains. However, around 6–9 measurements were taken on different spots within a single recruit with the objective of including and understanding spatial variations within the recruit.

After measurements of steady-state O_2 concentrations at the surface of CCA samples under defined photon irradiance levels, the microsensor tip was positioned at the CCA surface, where the local volume-specific gross photosynthesis rate (in units of nmol O_2 cm^{-3} s^{-1}) was measured from the immediate O_2 depletion rate during a brief 1–3 s darkening according to the microsensor light–dark shift technique (Revsbech and Jorgensen, 1983); for these measurements, microsensor signals were recorded on a fast-responding strip-chart recorder (BD25, Kipp & Zonen, Netherlands).

The diffusive flux of O_2 between CCA and the overlaying water across the diffusive boundary layer (DBL), J, was determined from steady state O_2 concentration profiles using

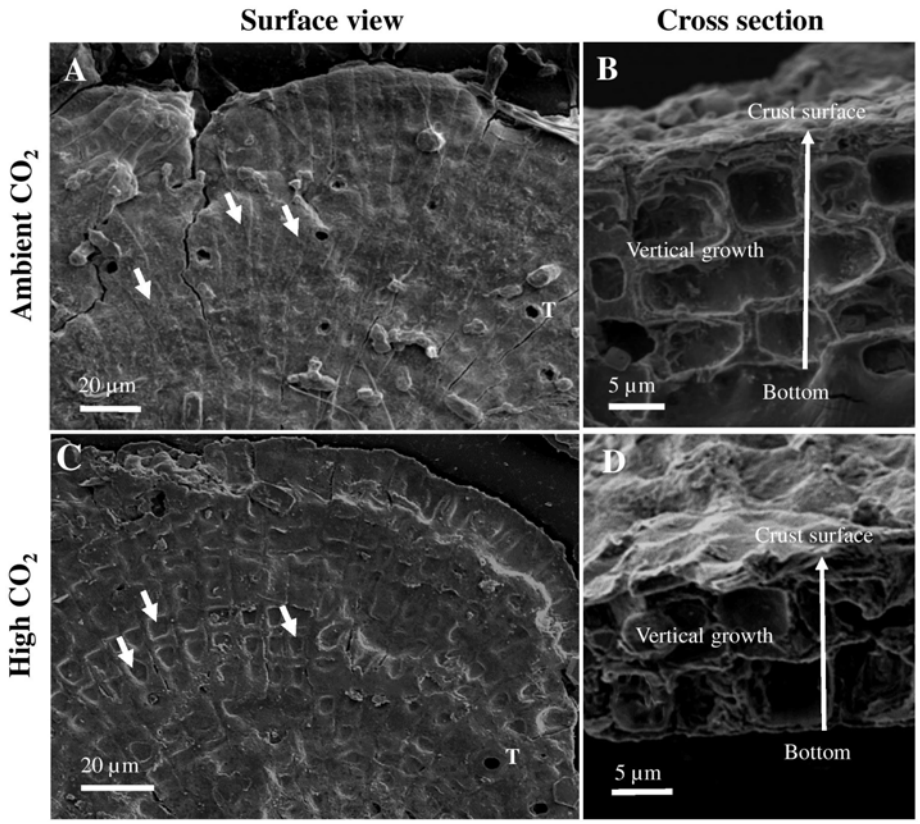

FIGURE 2 | Scanning electron microscopy images of surface view **(A,C)** and cross section **(B,D)** of 10-day-old *Porolithon* cf. *onkodes* recruits developed under ambient CO_2 (CO_2 between 400.8 and 448.1 µatm, pH 8.0–8.03) and high CO_2 (CO_2 between 998.9 and 1070.6 µatm, pH 7.67–7.70) conditions. Arrows in panels **(B,D)** indicate vertical growth direction. Short white arrows in panel **(A)** indicate non-collapsed epithallial/perithallial cells and in panel **(C)** collapsed epithallial/perithallial cells. White T in panels **(A,C)** indicate first appearance of mega cells (trichocytes).

Fick's first law of diffusion: $J = -D0^* \frac{dC}{dz}$, where dC/dz is the slope of the O_2 concentration profile in the DBL, and D_0 is the molecular diffusion coefficient of O_2 in seawater at experimental temperature and salinity (2.1707×10^{-5} cm^2 s^{-1}), as taken from tabulated values[2].

To examine the effects of elevated CO_2 on the photosynthetic performance of the CCA, we measured gross and net photosynthesis as a function of increasing photon irradiance (P-E curves). Each specimen was incubated for about 15 min at each irradiance level before microsensor measurements commenced to provide steady state O_2 conditions. Gross photosynthesis data was fitted to an exponential function (Webb et al., 1974): $P = P_{\max} * 1 - e^{-\alpha * \frac{E}{P\max}}$, where P_{max} is the maximum photosynthetic rate and α is the photosynthetic efficiency, i.e., the initial slope of the P-E curve. The saturation irradiance (E_k) was calculated as $E_k = P_{max}/\alpha$, and describes the photon irradiance above which photosynthesis approaches saturation. Net photosynthesis data were fitted to the modified exponential function used in Roberts et al. (2002): $P = P_{\max} * 1 - e^{-\alpha * \frac{E}{P\max}} + R$. This function considers the term of respiration (R) and assumes absence of photoinhibition.

Vertical and Marginal Growth Measurements

Vertical growth of the juvenile CCA samples was estimated at the end of the experiment by measuring the crust thickness using a scanning electron microscope (JSM-6510 series, JEOL). To obtain cross sections, recruits attached to the petri dish were carefully detached from the substrate and sliced into sections using a razor blade. The resulting fragments were mounted on a metal stub with adhesive. Samples were carbon coated using a sputter coater (JFC-1600 auto fine coater, JEOL) for SEM analyses. Images were taken with a magnification of ×3000 at a high voltage of 5 kV with a spot size of 50 nm and a working distance (WD) of 12–16 mm. We measured a total of 15 points along the crust from different fragments. To estimate thickness of the crust, the distance from the surface of the crust to the bottom was measured using the SEM software (JEOL Scanning electron microscope software) (**Figures 2B,D**). Growth rates in units of µm crust increment day^{-1} were obtained by normalizing crust thickness to the duration of

[2]http://www.unisense.com

the experiment, i.e., 10 days. Marginal growth was estimated by measuring the change in surface area. Final and initial photographs of individual recruits were taken and images were analyzed using Image J software (University of Wisconsin-Madison).

Statistical Analyses

Photosynthetic parameters were compared between treatments using one-way ANOVA. Pearson correlation was used to test the relationships between vertical growth and gross photosynthesis. Normal distribution of data and homogeneity of variances were tested using Kolmogorov-Smirnov and Cochran's test and data was arc-sin transformed when needed. All statistical analyses were performed using SPSS (version 25).

RESULTS

Photosynthesis and Respiration

The measured P-E curves showed a significant difference between recruits growing under elevated CO_2 and recruits growing under ambient CO_2 conditions (**Figures 3A,B**). Maximum gross photosynthesis was 50% higher under elevated CO_2 [mean P_{max} = 75.36 nmol O_2 cm^{-3} s^{-1} (±9.7 SE)] as compared to ambient CO_2 conditions [mean P_{max} = 37.36 nmol O_2 cm^{-3} s^{-1} (±7.8 SE)], ANOVA p = 0.044). Photosynthetic efficiency and saturation irradiance were slightly higher under high CO_2 when compared to ambient CO_2, but the difference was not statistically significant (ANOVA, α: p = 0.22, E_k: p = 0.12). At the maximum photon irradiance used in the experiment (340 μmol photons m^{-2} s^{-1}), gross photosynthesis was 39% higher under high CO_2 than under ambient CO_2 conditions but the difference was not significant (ANOVA p = 0.081, **Figure 4A**).

The responses of net photosynthetic rates to the CO_2 treatments followed a similar trend as the gross photosynthesis, with increased P_{max}, and slightly higher α and E_k values under elevated CO_2 than under ambient CO_2 conditions. However, the difference across CO_2 treatments was less pronounced and not statistically significant (ANOVA, p = 0.12, p = 0.78, p = 0.35, for P_{max}, α and E_k, respectively, **Figure 3B**).

Dark respiration was significantly enhanced by elevated CO_2, with recruits showing a 48.7% increase in respiration rates compared to recruits from ambient CO_2 (ANOVA, p = 0.0001, **Figure 4B**). In addition, surface dynamics of O_2 concentration during experimental dark-light shifts showed higher O_2 production and faster response of CCA recruits under elevated CO_2 compared to measurements under ambient CO_2 (**Figure 5**).

Growth Rates

Vertical and marginal growth rates were significantly affected by high CO_2 (ANOVA, p = 0.01 and 0.03, respectively). *P.* cf. *onkodes* recruits grown under ambient CO_2 conditions showed thicker and larger crusts as compared to recruits exposed to high CO_2 conditions (**Figures 6A,B**). Crust vertical growth rates were reduced from 2.8 ± 0.24 μm d^{-1} under ambient CO_2 to 2.05 μm d^{-1} (±0.04 SE) under high CO_2, i.e., a 28.7% change. Marginal growth rates were also reduced by 19%. Structural damage of the cells under high CO_2 was observed on the crust surface, where epithallial/perithallial cells seemed to have collapsed (**Figure 2C**) as opposed to observations of the crust surface of germlings growing under ambient conditions where cells seem to preserve their structure (**Figure 2A**). Furthermore, cross sections of CCA recruits showed cells with irregular shapes and thinner cell walls in samples exposed to elevated CO_2 (**Figure 2D**) compared to those under ambient conditions (**Figure 2B**).

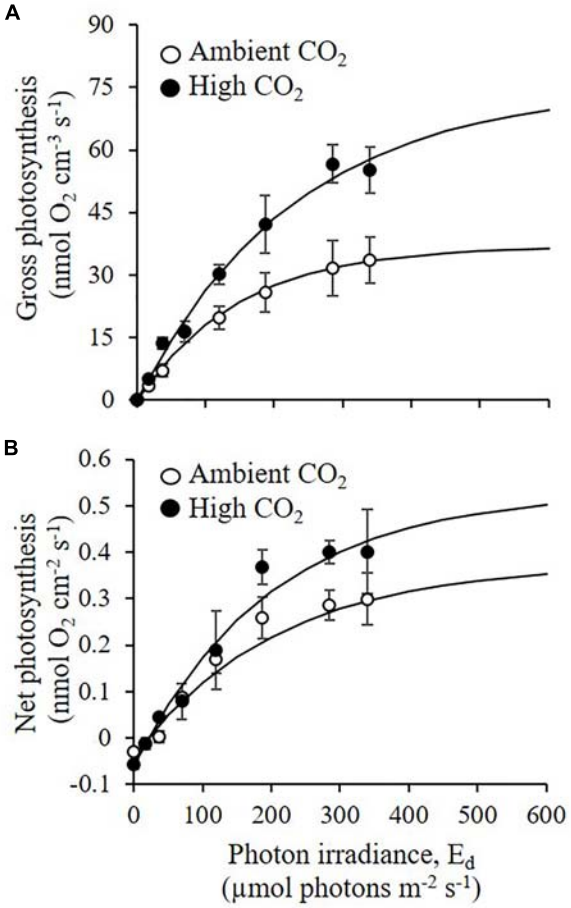

FIGURE 3 | Effects of elevated CO_2 on net and gross photosynthesis of CCA recruits. **(A)** Gross photosynthesis (nmol O_2 cm^{-3} s^{-1}), and **(B)** net photosynthesis (nmol O_2 cm^{-2} s^{-1}) were measured under ambient CO_2 (CO_2 between 400.8 and 448.1 μatm, pH 8.0–8.03) and high CO_2 (CO_2 between 998.9 and 1070.6 μatm, pH 7.67–7.70) conditions, for a range of incident downwelling photon irradiance regimes (E_d: μmol photons m^{-2} s^{-1}). Symbols with error bars represent means ± SE (n = 3 for ambient CO_2 and n = 2 for High CO_2; biological replicates). Solid lines represent curve fits ($R^2 > 0.9$) of the equation $P = P_{max} * 1 - e^{-\alpha * \frac{E}{P_{max}}}$ for gross photosynthesis and the equation $P = P_{max} * 1 - e^{-\alpha * \frac{E}{P_{max}}} + R$ for net photosynthesis.

Growth vs. Photosynthesis

We found a negative correlation between gross photosynthesis and crust thickness of *P.* cf. *onkodes* recruits at an incident

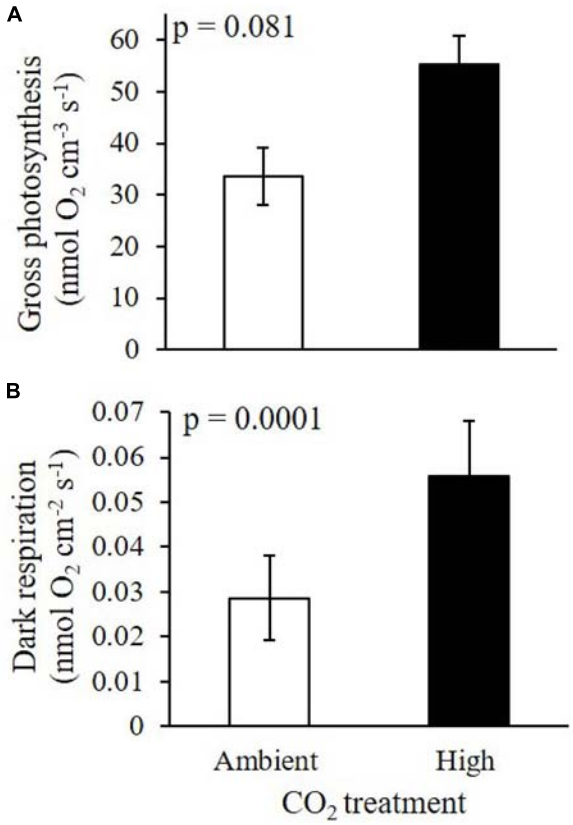

FIGURE 4 | Effects of elevated CO_2 on **(A)** surface gross photosynthesis, and **(B)** dark respiration of 10-day-old CCA recruits under two treatments: ambient CO_2 (CO_2 between 400.8 and 448.1 μatm, pH 8.0–8.03) and high CO_2 (CO_2 between 998.9 and 1070.6 μatm, pH 7.67–7.70). Gross photosynthesis was measured at the CCA surface at a photon irradiance of 340 μmol photons m^{-2} s^{-1}. Data on panel **(A)** are means ± SE (n = 3 for ambient CO_2 and n = 2 for high CO_2; biological replicates). Data on panel **(B)** are means ± SE (n = 9 for each CO_2 treatment).

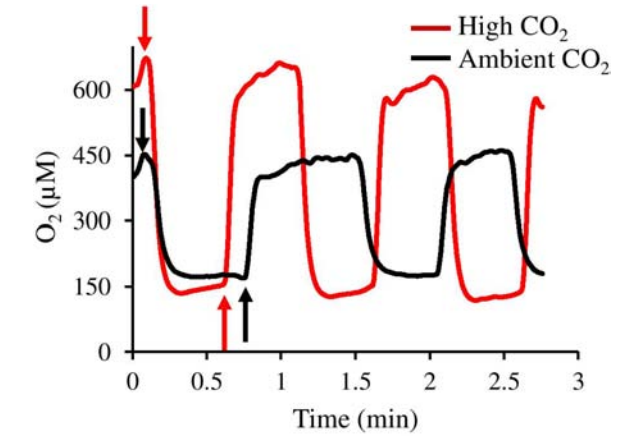

FIGURE 5 | Surface O_2 concentration dynamics of CCA recruits during light-dark shifts under ambient CO_2 (black line, CO_2 between 400.8 and 448.1 μatm, pH 8.0–8.03) and high CO_2 (red line, CO_2 between 998.9 and 1070.6 μatm, pH 7.67–7.70). Upward arrows and downward arrows exemplify onset of light and dark periods, respectively.

irradiance of 340 μmol photons m^{-2} s^{-1} (Pearson correlation coefficient 0.89, p = 0.01, n = 5, **Figure 7**). The highest gross photosynthetic rate (55.16 nmol O_2 cm^{-3} s^{-1}) was found on thinnest recruits (1.93 μm d^{-1}) growing under elevated CO_2, whereas the lowest gross photosynthetic rate (3.29 nmol O_2 cm^{-3} s^{-1}) was measured on the thickest recruits (3.35 μm d^{-1}) from ambient CO_2 condition.

DISCUSSION

The impacts of ocean acidification (OA) on adult coralline algae have been relatively well documented (Hofmann and Bischof, 2014), and there is a growing body of evidence supporting the sensitivity of the early life history stages of coralline algae to OA. In particular, recent studies have shown reduced spore germination (Bradassi et al., 2013; Ordoñez et al., 2017) and attachment (Guenther et al., 2018) and declined germling abundance [e.g., % cover, Kuffner et al. (2008); Ordoñez et al. (2014); Fabricius et al. (2015); Ordoñez et al. (2017)] and growth (Roleda et al., 2015; Ordoñez et al., 2017) under elevated CO_2 conditions. However, whether metabolic processes such as photosynthesis and respiration of early life stages of CCA also show a negative response to elevated CO_2 has not been well documented. Our study tests for the first time the effects of elevated CO_2 on the photosynthesis and respiration of recruits of a major reef building coralline alga. We demonstrate that increased CO_2 can potentially enhance gross photosynthesis and dark respiration, but can reduce the growth of *P.* cf. *onkodes* recruits. Our findings also reveal a possible decoupling between photosynthesis and growth rates in CCA recruits, suggesting that the carbon fixed during the photosynthetic process does not necessarily translate into enhanced algal growth. Understanding the relationships between physiological and vital processes under OA, in particular on vulnerable early life stages, is essential to improve our understanding of OA impacts on coral reef organisms and the important ecosystem services they support.

Effects of Elevated CO_2 on Photosynthesis

Porolithon cf. *onkodes* recruits growing under high CO_2 conditions showed significantly higher maximum gross photosynthetic rates at the thallus surface compared to those under ambient CO_2 conditions, suggesting that photosynthesis in our experimental CCA was carbon limited under ambient CO_2 conditions, in line with, e.g., measurements on epilithic algal layers on coral tiles (Larkum et al., 2003). The photosynthetic responses of coralline algae to elevated CO_2 (reduced pH) documented in the literature are highly variable and depend on the nature of the experiments, the techniques employed to quantify O_2 dynamics, and the species of algae considered in the experiments. For example, two studies using adult *Porolithon onkodes* from French Polynesia found no effect of elevated CO_2 on gross photosynthesis and respiration (Johnson et al., 2014;

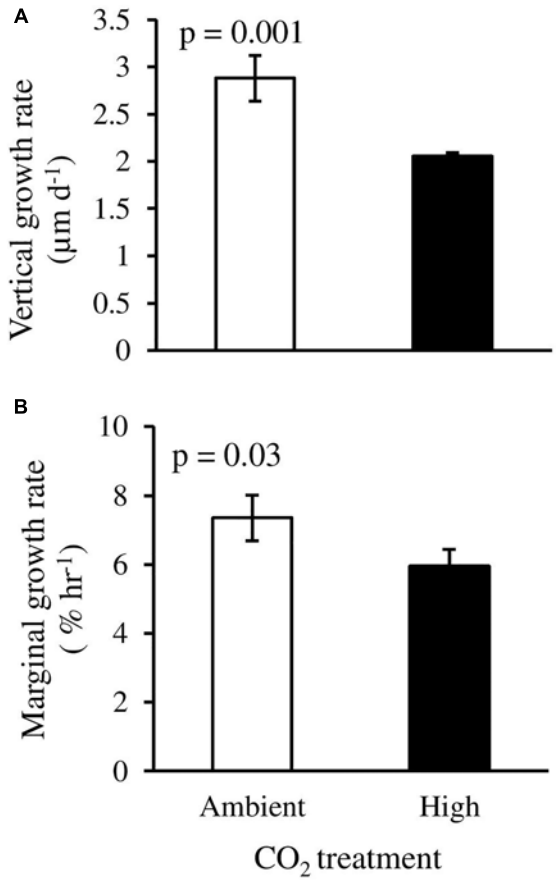

FIGURE 6 | Effects of elevated CO_2 on **(A)** vertical growth rate, and **(B)** marginal growth rate of CCA recruits in response to two treatments: ambient CO_2 (CO_2 between 400.8 and 448.1 μatm, pH 8.0–8.03) and high CO_2 (CO_2 between 998.9 and 1070.6 μatm, pH 7.67–7.70). Columns with error bars represent means ± SE [**(A)**: $n = 3$ for ambient CO_2 and $n = 2$ for high CO_2; **(B)** $n = 6$, biological replicates].

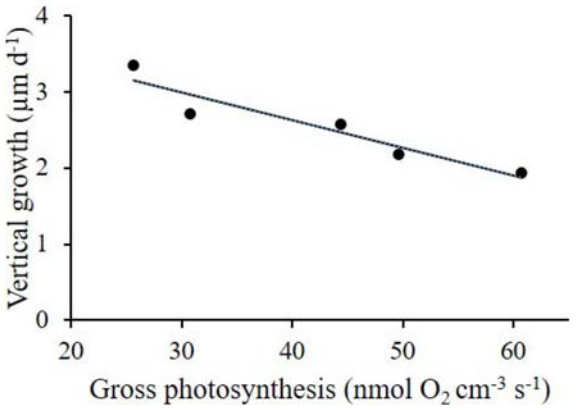

FIGURE 7 | Negative linear correlation ($R^2 = 0.89$; $p = 0.016$) between vertical growth (μm d^{-1}) and gross photosynthesis (nmol O_2 cm^{-3} s^{-1}) of CCA recruits grown under ambient CO_2 (CO_2 between 400.8 and 448.1 μatm, pH 8.0–8.03) and high CO_2 (CO_2 between 998.9 and 1070.6 μatm, pH 7.67–7.70).

Comeau et al., 2017), although in the Johnson et al. (2014) study, high CO_2 decreased net photosynthesis, similar to results from the Great Barrier Reef using the same CCA species (Anthony et al., 2008). Studies using different taxa from temperate regions found gross photosynthesis to remain constant under elevated CO_2 [e.g., articulated algae *Corallina officinalis* (Hofmann et al., 2012), *Corallina elongata* (Noisette et al., 2013), CCA *Lithophyllum incrustans*, *Lithothamnion corallioides* (Noisette et al., 2013), *Lithothamnion glaciale* (Kamenos et al., 2013)]. Enhanced productivity in response to elevated CO_2 has been observed for some adult tropical corallines (Semesi et al., 2009; Yildiz et al., 2014). Using O_2 microsensors on adult CCA, Hofmann et al. (2016) found elevated photosynthetic rates under reduced pH, similar to the findings in our study.

Enhanced photosynthesis in response to elevated CO_2 concentrations may indicate that photosynthesis in early life stages of *P. onkodes* is limited by intracellular inorganic carbon availability. There are two main mechanisms by which algae acquire CO_2 for carbon fixation within the cell: (1) the active uptake of HCO_3^- via a number of carbon concentrating mechanisms (CCMs), and (2) the diffusive uptake of CO_2 (Giordano et al., 2005; Raven et al., 2005). These mechanisms could be altered by elevated seawater CO_2 concentrations. Coralline algae have CCMs that facilitate active transport of HCO_3^- across cellular membranes leading to higher concentrations of CO_2 at the site of RuBisCO (Comeau et al., 2013; Hofmann and Heesch, 2018) and given the high availability of HCO_3^- in seawater, enhanced CO_2 may thus not significantly enhance DIC transport to the site of photosynthesis. However, since CCM activity is energetically costly, it is likely that elevated seawater CO_2 alleviates the use of CCMs, effectively downregulating CCM activity upon enhanced and energetically less costly diffusive CO_2 uptake under OA conditions. Flexibility in the use of carbon acquisition strategies under OA has been suggested for a number of articulated coralline algae including *C. officinalis* (Cornwall et al., 2012) and *Arthrocardia corymbosa* (Cornwall et al., 2013). Our study cannot discern the mechanistic basis for the increased rates of photosynthesis observed in our recruits under OA, but could suggest that photosynthesis in our early life stages of CCA is carbon limited. The majority of studies examining the effects of elevated CO_2 on CCA photosynthesis have used incubation chambers with larger O_2 sensors and have shown negative or no response of OA on photosynthetic activity (Anthony et al., 2008; Gao and Zheng, 2010; Hofmann et al., 2012; Cornwall et al., 2013; Martin et al., 2013; Noisette et al., 2013; Johnson et al., 2014; Comeau et al., 2017). However, when microsensors have been used to test CO_2 effects on coralline algae photosynthesis, increased O_2 production has been detected (e.g., Hofmann et al., 2016, but see Cornwall et al., 2013). Microsensors measure O_2 dynamics directly at the surface of the CCA, with minimum interference from epiphytic algae (e.g., diatoms, Roleda et al., 2015) or bacteria, or endolithic algae (e.g., Anthony et al., 2008), presumably providing a more local and direct measurement of the effects of CO_2 on CCA physiology.

Declined Growth and Relationship With Photosynthesis

Photosynthesis is the major source of carbon for CCA algal tissue construction, therefore, it is generally expected that increased photosynthetic rates and consequently the amount of fixed carbon would be positively correlated with algal growth. As detailed earlier, photosynthetic rates of the experimental recruits increased with increased CO_2 concentration, however, this increase in CO_2 did not translate directly in enhanced algal growth. On the contrary, both vertical and marginal growthrates of the algal crusts were depressed under high CO_2 (a 28 and 19% decrease under high compared to ambient CO_2, **Figures 6A,B**), and we additionally observed a significant inverse relationship between algal photosynthesis and growth (Pearson correlation $R^2 = 0.89$, $p = 0.01$, **Figure 7**). The decreased growth of CCA under elevated CO_2 shown in our study agrees with findings from several studies using both adult and early life stages of CCA (Kuffner et al., 2008; Bradassi et al., 2013; Ordoñez et al., 2017). The decoupling between increased photosynthetic rates and algal growth rates may be explained by two key processes. First, and perhaps the most important process, high CO_2 enhances skeletal dissolution of the coralline algal crusts. In fact, SEM images showed distorted crust tissues, collapsed epithelial cells (**Figure 2C**), and apparently a thinning of calcified cell walls (**Figure 2D**), similar to observations on *Lithothamnion glaciale* from the Mediterranean (Ragazzola et al., 2012) and *Hydrolithon samoense* from Japan exposed to high CO_2 (Kato et al., 2014). Several studies have attributed such reduction in growth of CCA recruits (e.g., Bradassi et al., 2013; Roleda et al., 2015) and adults (Diaz-Pulido et al., 2014) to increased skeletal dissolution due to undersaturation of seawater with respect to the dominant form of calcium carbonate in the CCA, i.e., high-magnesium-calcite. **Table 1** shows a high Mg-calcite saturation state <1 in the high CO_2 treatment, indicating undersaturation of seawater calcium carbonate and hence conditions for skeletal dissolution. Undersaturation may also affect deposition of new calcium carbonate in the algal skeleton. Secondly, since algal growth is a function of photosynthesis minus algal respiration and excretion of photosynthates, this suggest that carbon losses due to respiratory and excretion/secretion processes are higher than carbon gains from the photosynthetic process (Falkowski and Raven, 2013). In this regard, respiration rates were indeed higher under high CO_2, which may explain the observed reduced growth, albeit net photosynthesis was also slightly higher under elevated CO_2. It is also likely that a significant fraction of photosynthetically fixed carbon is excreted/secreted as dissolved organic carbon (DOC) to the external environment, leaving less carbon readily available for algal growth (e.g., Iñiguez et al., 2016, 2017) and potentially for calcification. This situation may be particularly important when nutrients limit algal growth, as shown in symbiotic algae (Yellowlees et al., 2008) and polar algae (Iñiguez et al., 2016). Recent work shows that high CO_2 concentrations stimulated the release of DOC in a range of tropical reef algae, particularly red algae (Diaz-Pulido and Barron, personal observation). The mechanisms explaining the decoupling of algal photosynthesis and growth under OA conditions require further investigations.

Although our study did not directly quantify the calcification rate of the early life stage of *P.* cf. *onkodes*, we expect that the observed reduction in both vertical and marginal crust growth is associated with a lowering in the amount of calcium carbonate deposited by the algal crusts. On the other hand, a direct positive relationship between photosynthesis and calcification has also been postulated (Borowitzka, 1981; Hofmann et al., 2016), although decoupling between photosynthesis and calcification on adult coralline algae has also been shown (Semesi et al., 2009). Our finding of increased photosynthetic rate under elevated CO_2 does not seem to be coupled with elevated rates of calcification, given the reduced growth observed when exposed to high CO_2, and the considerable alterations in crust thickness and ultrastructure. Any positive effect of elevated DIC (both CO_2 and HCO_3^-) on CCA photosynthesis and potentially on calcification may thus not be sufficient to compensate for the reduction in high-Mg-calcite saturation state and resulting skeletal dissolution, as discussed by Comeau et al. (2013) and Bradassi et al. (2013). The very thin crusts of the early life stages of *P.* cf. *onkodes* could contribute to some extent to the high vulnerability of these recruits to OA, thus CCA recruits may represent one of the most sensitive life stages to OA. A further understanding of the metabolic processes underpinning decreased growth and calcification is fundamental for understanding the underlying causes for decreased abundance in key reef building coralline algae.

DATA AVAILABILITY STATEMENT

Data are available at the Australian Rivers Institute – Coast and Estuaries repository system at Griffith University.

AUTHOR CONTRIBUTIONS

AO and GD-P designed the experiments, collected and analyzed the growth data, and drafted the manuscript. AO performed the experiments. DW and NL collected and analyzed the photosynthesis data. All authors contributed with manuscript writing and gave final approval for publication.

FUNDING

This project was supported by the Australian Research Council (DP-120101778), the Great Barrier Reef Foundation, a Sapere-Aude Advanced grant from the Independent Research Fund Denmark (MK), and the Carlsberg Foundation (DW). Samples for this study were collected under the permit G12/34877.1 granted by Great Barrier Reef Marine Park Authority.

ACKNOWLEDGMENTS

We thank P. Gartrell, C. Barron, B. Lewis, L. Gomez, E. Kennedy, and HIRS staff who assisted with the experiments.

REFERENCES

Adey, W. H. (1998). Coral reefs: algal structured and mediated ecosystems in shallow, turbulent, alkaline waters. *J. Phycol.* 34, 393–406. doi: 10.1046/j.1529-8817.1998.340393.x

Anthony, K. R. N., Kline, D. I., Diaz-Pulido, G., Dove, S., and Hoegh-Guldberg, O. (2008). Ocean acidification causes bleaching and productivity loss in coral reef builders. *Proc. Natl. Acad. Sci. U.S.A.* 105, 17442–17446. doi: 10.1073/pnas.0804478105

Borowitzka, M. A. (1981). Photosynthesis and calcification in the articulated coralline red algae *Amphiroa anceps* and *A. foliacea*. *Mar. Biol.* 62, 17–23. doi: 10.1007/BF00396947

Bradassi, F., Cumani, F., Bressan, G., and Dupont, S. (2013). Early reproductive stages in the crustose coralline alga *Phymatolithon lenormandii* are strongly affected by mild ocean acidification. *Mar. Biol.* 160, 2261–2269. doi: 10.1007/s00227-013-2260-2

Brodersen, K. E., Lichtenberg, M., Ralph, P. J., Kühl, M., and Wangpraseurt, D. (2014). Radiative energy budget reveals high photosynthetic efficiency in symbiont-bearing corals. *J. Royal Soc. Interface* 11:20130997. doi: 10.1098/rsif.2013.0997

Comeau, S., Carpenter, R. C., and Edmunds, P. J. (2013). Coral reef calcifiers buffer their response to ocean acidification using both bicarbonate and carbonate. *Proc. R. Soc. B* 280:1753. doi: 10.1098/rspb.2012.2374

Comeau, S., Carpenter, R. C., and Edmunds, P. J. (2017). Effects of pCO_2 on photosynthesis and respiration of tropical scleractinian corals and calcified algae. *ICES J. Mar. Sci.* 74, 1092–1102. doi: 10.1093/icesjms/fsv267

Cornwall, C. E., Hepburn, C. D., McGraw, C. M., Currie, K. I., Pilditch, C. A., Hunter, K. A., et al. (2013). Diurnal fluctuations in seawater pH influence the response of a calcifying macroalga to ocean acidification. *Proc. R. Soc. B* 280:1772. doi: 10.1098/rspb.2013.2201

Cornwall, C. E., Hepburn, C. D., Pritchard, D., Currie, K. I., McGraw, C. M., Hunter, K. A., et al. (2012). Carbon-use strategies in macroalgae: differential responses to lowered pH and implications for ocean acidification. *J. Phycol.* 48, 137–144. doi: 10.1111/j.1529-8817.2011.01085.x

Cornwall, C. E., Revill, A. T., and Hurd, C. L. (2015). High prevalence of diffusive uptake of CO_2 by macroalgae in a temperate subtidal ecosystem. *Photosynth. Res.* 124, 181–190. doi: 10.1007/s11120-015-0114-0

Dean, A. J., Steneck, R. S., Tager, D., and Pandolfi, J. M. (2015). Distribution, abundance and diversity of crustose coralline algae on the Great Barrier Reef. *Coral Reefs* 34, 581–594. doi: 10.1007/s00338-015-1263-5

Diaz-Pulido, G., Anthony, K. R. N., Kline, D. I., Dove, S., and Hoegh-Guldberg, O. (2012). Interactions between ocean acidification and warming on the mortality and dissolution of coralline algae. *J. Phycol.* 48, 32–39. doi: 10.1111/j.1529-8817.2011.01084.x

Diaz-Pulido, G., Cornwall, C., Gartrell, P., Hurd, C., and Tran, D. V. (2016). Strategies of dissolved inorganic carbon use in macroalgae across a gradient of terrestrial influence: implications for the Great Barrier Reef in the context of ocean acidification. *Coral Reefs* 35, 1327–1341. doi: 10.1007/s00338-016-1481-5

Diaz-Pulido, G., Gouezo, M., Tilbrook, B., Dove, S., and Anthony, K. R. N. (2011). High CO_2 enhances the competitive strength of seaweeds over corals. *Ecol. Lett.* 14, 156–162. doi: 10.1111/j.1461-0248.2010.01565.x

Diaz-Pulido, G., Nash, M. C., Anthony, K. R. N., Bender, D., Opdyke, B. N., Reyes-Nivia, C., et al. (2014). Greenhouse conditions induce mineralogical changes and dolomite accumulation in coralline algae on tropical reefs. *Nat. Commun.* 5:3310. doi: 10.1038/ncomms4310

Fabricius, K. E., Kluibenschedl, A., Harrington, L., Noonan, S., and De'ath, G. (2015). In situ changes of tropical crustose coralline algae along carbon dioxide gradients. *Sci. Rep.* 5:9537. doi: 10.1038/srep09537

Falkowski, P. G., and Raven, J. A. (2013). *Aquatic Photosynthesis*. Princeton, NJ: Princeton University Press. doi: 10.1515/9781400849727

Feely, R. A., Sabine, C. L., Lee, K., Berelson, W., Kleypas, J., Fabry, V. J., et al. (2004). Impact of anthropogenic CO_2 on the $CaCO_3$ system in the oceans. *Science* 305, 362–366. doi: 10.1126/science.1097329

Gabrielson, P. W., Hughey, J. R., and Diaz-Pulido, G. (2018). Genomics reveals abundant speciation in the coral reef building alga *Porolithon onkodes* (Corallinales, Rhodophyta). *J. Phycol.* 54, 429–434. doi: 10.1111/jpy.12761

Gao, K., Aruga, Y., Asada, K., and Kiyohara, M. (1993). Influence of enhanced CO_2 on growth and photosynthesis of the red algae *Gracilaria* sp. and *G. chilensis*. *J. Appl. Phycol.* 5, 563–571. doi: 10.1007/BF02184635

Gao, K., and Zheng, Y. (2010). Combined effects of ocean acidification and solar UV radiation on photosynthesis, growth, pigmentation and calcification of the coralline alga *Corallina sessilis* (Rhodophyta). *Glob. Change Biol.* 16, 2388–2398. doi: 10.1111/j.1365-2486.2009.02113.x

Giordano, M., Beardall, J., and Raven, J. A. (2005). CO_2 concentrating mechanisms in algae: mechanisms, environmental modulation, and evolution. *Annu. Rev. Plant Biol.* 56, 99–131. doi: 10.1146/annurev.arplant.56.032604.144052

Guenther, R., Miklasz, K., Carrington, E., and Martone, P. T. (2018). Macroalgal spore dysfunction: ocean acidification delays and weakens adhesion. *J. Phycol.* 54, 153–158. doi: 10.1111/jpy.12614

Harrington, L., Fabricius, K., De'Ath, G., and Negri, A. (2004). Recognition and selection of settlement substrata determine post-settlement survival in corals. *Ecology* 85, 3428–3437. doi: 10.1890/04-0298

Heyward, A. J., and Negri, A. P. (1999). Natural inducers for coral larval metamorphosis. *Coral Reefs* 18, 273–279. doi: 10.1007/s003380050193

Hofmann, L. C., and Bischof, K. (2014). Ocean acidification effects on calcifying macroalgae. *Aquat. Biol.* 22, 261–279. doi: 10.3354/ab00581

Hofmann, L. C., and Heesch, S. (2018). Latitudinal trends in stable isotope signatures and carbon concentrating mechanisms of northeast *Atlantic rhodoliths*. *Biogeosciences* 15, 6139–6149. doi: 10.5194/bg-2017-399

Hofmann, L. C., Koch, M., and de Beer, D. (2016). Biotic control of surface pH and evidence of light-induced H^+ pumping and Ca^{2+}-H^+ exchange in a tropical crustose coralline alga. *PLoS One* 11:e0159057. doi: 10.1371/journal.pone.0159057

Hofmann, L. C., Yildiz, G., Hanelt, D., and Bischof, K. (2012). Physiological responses of the calcifying rhodophyte, *Corallina officinalis* (L.), to future CO_2 levels. *Mar. Biol.* 159, 783–792. doi: 10.1007/s00227-011-1854-9

Ichiki, S., Mizuta, H., and Yamamoto, H. (2000). Effects of irradiance, water temperature and nutrients on the growth of sporelings of the crustose coralline alga *Lithophyllum yessoense* Foslie (Corallinales, Rhodophyceae). *Phycol. Res.* 48, 115–120. doi: 10.1046/j.1440-1835.2000.00193.x

Iñiguez, C., Carmona, R., Lorenzo, M. R., Niell, F. X., Wiencke, C., and Gordillo, F. J. L. (2016). Increased CO_2 modifies the carbon balance and the photosynthetic yield of two common Arctic brown seaweeds: *Desmarestia aculeata* and *Alaria esculenta*. *Polar Biol.* 39, 1979–1991. doi: 10.1007/s00300-015-1724-x

Iñiguez, C., Heinrich, S., Harms, L., and Gordillo, F. J. L. (2017). Increased temperature and CO_2 alleviate photoinhibition in *Desmarestia anceps*: from transcriptomics to carbon utilization. *J. Exp. Bot.* 68, 3971–3984. doi: 10.1093/jxb/erx164

IPCC (2014). "Climate change 2013: the physical science basis," in *Contribution of Working Group I to the Fifth Assessment Report of the Intergovernmental Panel on Climate Change*, eds T.F. Stocker, D. Qin, G.-K. Plattner, M. Tignor, S. K. Allen, J. Boschung et al. (Cambridge: Cambridge University Press).

Johnson, M. D., and Carpenter, R. C. (2012). Ocean acidification and warming decrease calcification in the crustose coralline alga *Hydrolithon onkodes* and increase susceptibility to grazing. *J. Exp. Mar. Biol. Ecol.* 43, 94–101. doi: 10.1016/j.jembe.2012.08.005

Johnson, M. D., Moriarty, V. W., and Carpenter, R. C. (2014). Acclimatization of the crustose coralline alga *Porolithon onkodes* to variable pCO_2. *PLoS One* 9:e87678. doi: 10.1371/journal.pone.0087678

Jones, W. E., and Moorjani, A. S. (1973). *Attachment and Early Development of the Tetraspores of Some Coralline Red Algae*. Cochin: MBAI Special Publication dedicated to Dr. N K Panikkar 1, 293–304.

Kamenos, N. A., Burdett, H. L., Aloisio, E., Findlay, H. S., Martin, S., Longbone, C., et al. (2013). Coralline algal structure is more sensitive to rate, rather than the magnitude, of ocean acidification. *Glob. Change Biol.* 19, 3621–3628. doi: 10.1111/gcb.12351

Kato, A., Hikami, M., Kumagai, N. H., Suzuki, A., Nojiri, Y., and Sakai, K. (2014). Negative effects of ocean acidification on two crustose coralline species using genetically homogeneous samples. *Mar. Environ. Res.* 94, 1–6. doi: 10.1016/j.marenvres.2013.10.010

Koch, M., Bowes, G., Cliff, R., and Xing-Hai, Z. (2013). Climate change and ocean acidification effects on seagrasses and marine macroalgae. *Glob. Change Biol.* 19, 103–132. doi: 10.1111/j.1365-2486.2012.02791.x

Kroeker, K. J., Kordas, R. L., Crim, R., Hendriks, I. E., Ramajo, L., Singh, G. S., et al. (2013). Impacts of ocean acidification on marine organisms: quantifying sensitivities and interaction with warming. *Glob. Change Biol.* 19, 1884–1896. doi: 10.1111/gcb.12179

Kroeker, K. J., Kordas, R. L., Crim, R. N., and Singh, G. G. (2010). Meta-analysis reveals negative yet variable effects of ocean acidification on marine organisms. *Ecol. Lett.* 13, 1419–1434. doi: 10.1111/j.1461-0248.2010.01518.x

Kuffner, I. B., Andersson, A. J., Jokiel, P. L., Rodgers, K. U. S., and Mackenzie, F. T. (2008). Decreased abundance of crustose coralline algae due to ocean acidification. *Nat. Geosci.* 1, 114–117. doi: 10.1038/ngeo100

Larkum, A. W. D., Koch, E.-M. W., and Kühl, M. (2003). Diffusive boundary layers and photosynthesis of the epilithic algal community of coral reefs. *Mar. Biol.* 142, 1073–1082. doi: 10.1007/s00227-003-1022-y

Lewis, B., Kennedy, E. V., and Diaz-Pulido, G. (2017). Seasonal growth and calcification of a reef-building crustose coralline alga on the Great Barrier Reef. *Mar. Ecol. Prog. Ser.* 568, 73–86. doi: 10.3354/meps12074

Littler, M. M. (1972). The crustose corallinaceae. *Oceanogr. Mar. Biol. Annu. Rev.* 10, 103–120.

Littler, M. M., and Doty, M. S. (1975). Ecological components structuring the seaward edges of tropical pacific reefs: the distribution, communities and productivity of *Porolithon*. *J. Ecol.* 63, 117–129. doi: 10.2307/2258846

Martin, S., Cohu, S., Vignot, C., Zimmerman, G., and Gattuso, J. P. (2013). One-year experiment on the physiological response of the Mediterranean crustose coralline alga, *Lithophyllum cabiochae*, to elevated pCO_2 and temperature. *Ecol. Evol.* 3, 676–693. doi: 10.1002/ece3.475

Martin, S., and Gattuso, J. P. (2009). Response of Mediterranean coralline algae to ocean acidification and elevated temperature. *Glob. Change Biol.* 15, 2089–2100. doi: 10.1111/j.1365-2486.2009.01874.x

Morse, J. W., Arvidson, R. S., and Lüttge, A. (2007). Calcium carbonate formation and dissolution. *Chem. Rev.* 107, 342–381. doi: 10.1021/cr050358j

Noisette, F., Egilsdottir, H., Davoult, D., and Martin, S. (2013). Physiological responses of three temperate coralline algae from contrasting habitats to near-future ocean acidification. *J. Exp. Mar. Biol. Ecol.* 448, 179–187. doi: 10.1016/j.jembe.2013.07.006

Ordoñez, A., Doropoulos, C., and Diaz-Pulido, G. (2014). Effects of ocean acidification on population dynamics and community structure of crustose coralline algae. *Biol. Bull.* 226, 255–268. doi: 10.1086/BBLv226n3p255

Ordoñez, A., Kennedy, E. V., and Diaz-Pulido, G. (2017). Reduced spore germination explains sensitivity of reef-building algae to climate change stressors. *PLoS One* 12:e0189122. doi: 10.1371/journal.pone.0189122

Pierrot, D., Lewis, E., and Wallace, D. W. R. (2006). *MS Excel Program Developed for CO_2 System Calculations. ORNL/CDIAC-105a*. Oak Ridge, TN: Carbon Dioxide Information Analysis Center. doi: 10.3334/CDIAC/otg.CO2SYS_XLS_CDIAC105a

Ragazzola, F., Foster, L. C., Form, A., Anderson, P. S. L., Hansteen, T. H., and Fietzke, J. (2012). Ocean acidification weakens the structural integrity of coralline algae. *Glob. Change Biol.* 18, 2804–2812. doi: 10.1111/j.1365-2486.2012.02756.x

Raven, J. A., Ball, L. A., Beardall, J., Giordano, M., and Maberly, S. C. (2005). Algae lacking carbon-concentrating mechanisms. *Can. J. Bot.* 83, 879–890. doi: 10.1139/b05-074

Revsbech, N. P. (1989). An oxygen microsensor with a guard cathode. *Limnol. Oceanogr.* 34, 474–478. doi: 10.4319/lo.1989.34.2.0474

Revsbech, N. P., and Jorgensen, B. B. (1983). Photosynthesis of benthic microflora measured with high spatial resolution by the oxygen microprofile method: capabilities and limitations of the method. *Limnol. Oceanogr.* 28, 749–756. doi: 10.4319/lo.1983.28.4.0749

Ringeltaube, P., and Harvey, A. (2005). Non-geniculate coralline algae (Corallinales, Rhodophyta) on heron reef, Great Barrier Reef (Australia). *Bot. Mar.* 43, 409–498.

Roberts, R. D., Kühl, M., Glud, R. N., and Rysgaard, S. (2002). Primary production of crustose coralline red algae in a high artic fjord. *J. Phycol.* 38, 273–283. doi: 10.1046/j.1529-8817.2002.01104.x

Roleda, M. Y., Cornwall, C. E., Feng, Y., McGraw, C. M., Smith, A. M., and Hurd, C. L. (2015). Effect of ocean acidification and pH fluctuations on the growth and development of coralline algal recruits, and an associated benthic algal assemblage. *PLoS One* 10:e0140394. doi: 10.1371/journal.pone.0140394

Roleda, M. Y., Morris, J. N., McGraw, C. M., and Hurd, C. L. (2012). Ocean acidification and seaweed reproduction: increased CO_2 ameliorates the negative effect of lowered pH on meiospore germination in the giant kelp *Macrocystis pyrifera* (Laminariales. Phaeophyceae). *Glob. Change Biol.* 18, 854–864. doi: 10.1111/j.1365-2486.2011.02594.x

Santelices, B. (1990). Patterns of reproduction dispersdal and recruitment in seaweeds. *Oceanogr. Mar. Biol. Annu. Rev.* 28, 177–276.

Semesi, I. S., Kangwe, J., and Björk, M. (2009). Alterations in seawater pH and CO_2 affect calcification and photosynthesis in the tropical coralline alga, *Hydrolithon* sp. (Rhodophyta). *Estuar. Coast. Shelf Sci.* 84, 337–341. doi: 10.1016/j.ecss.2009.03.038

Steneck, R. S. (1983). Escalating herbivory and resulting adaptive trends in calcareous algal crusts. *Paleobiology* 9, 44–61. doi: 10.2307/2400629

Webb, W. L., Newton, M., and Starr, D. (1974). Carbon dioxide exchange of *Alnus rubra*. *Oecologia* 17, 281–291. doi: 10.1007/bf00345747

Yellowlees, D., Rees, T. A. V., and Leggat, W. (2008). Metabolic interactions between algal symbionts and invertebrate hosts. *Plant Cell Environ.* 31, 679–694. doi: 10.1111/j.1365-3040.2008.01802.x

Yildiz, G., Hofmann, L. C., Bischof, K., and Dere, S. (2014). *Ultraviolet Radiation Modulates the Physiological Responses of the Calcified Rhodophyte Corallina officinalis to Elevated CO_2*. Washington, DC: USDA. doi: 10.1594/PANGAEA.831729

Conflict of Interest Statement: The authors declare that the research was conducted in the absence of any commercial or financial relationships that could be construed as a potential conflict of interest.

Copyright © 2019 Ordoñez, Wangpraseurt, Lyndby, Kühl and Diaz-Pulido. This is an open-access article distributed under the terms of the Creative Commons Attribution License (CC BY). The use, distribution or reproduction in other forums is permitted, provided the original author(s) and the copyright owner(s) are credited and that the original publication in this journal is cited, in accordance with accepted academic practice. No use, distribution or reproduction is permitted which does not comply with these terms.

frontiers in Plant Science

ORIGINAL RESEARCH
published: 25 September 2018
doi: 10.3389/fpls.2018.01416

Arctic Coralline Algae Elevate Surface pH and Carbonate in the Dark

Laurie C. Hofmann[1], Kathryn Schoenrock[2†] and Dirk de Beer[1]*

[1] Max Planck Institute for Marine Microbiology, Microsensor Group, Bremen, Germany, [2] Department of Geographical and Earth Science, University of Glasgow, Glasgow, United Kingdom

Red coralline algae are projected to be sensitive to ocean acidification, particularly in polar oceans. As important ecosystem engineers, their potential sensitivity has broad implications, and understanding their carbon acquisition mechanisms is necessary for making reliable predictions. Therefore, we investigated the localized carbonate chemistry at the surface of Arctic coralline algae using microsensors. We report for the first time carbonate ion concentration and pH measurements ($[CO_3^{2-}]$) at and above the algal surface in the microenvironment. We show that surface pH and $[CO_3^{2-}]$ are higher than the bulk seawater in the light, and even after hours of darkness. We further show that three species of Arctic coralline algae have efficient carbon concentrating mechanisms including direct bicarbonate uptake and indirect bicarbonate use via a carbonic anhydrase enzyme. Our results suggest that Arctic corallines have strong biological control over their surface chemistry, where active calcification occurs, and that net dissolution in the dark does not occur. We suggest that the elevated pH and $[CO_3^{2-}]$ in the dark could be explained by a high rate of light independent carbon fixation that reduces respiratory CO_2 release. This mechanism could provide a potential adaptation to ocean acidification in Arctic coralline algae, which has important implications for future Arctic marine ecosystems.

Keywords: calcification, carbon concentrating mechanism, carbonate chemistry, light-independent carbon fixation, microenvironment, microsensor, rhodolith

OPEN ACCESS

Edited by:
Benoit Schoefs, University of Maine, France

Reviewed by:
Jonas Collén, Université Pierre et Marie Curie, France
Christopher Edward Cornwall, Victoria University of Wellington, New Zealand
Fanny Noisette, Institute for Marine and Antarctic Studies (IMAS), Australia

****Correspondence:***
Laurie C. Hofmann
laurie.c.hofmann@awi.de

†Present address:
Kathryn Schoenrock, Department of Botany, National University of Ireland, Galway, Ireland

Specialty section:
This article was submitted to Plant Physiology, a section of the journal Frontiers in Plant Science

Received: *09 February 2018*
Accepted: *06 September 2018*
Published: *25 September 2018*

Citation:
Hofmann LC, Schoenrock K and de Beer D (2018) Arctic Coralline Algae Elevate Surface pH and Carbonate in the Dark. Front. Plant Sci. 9:1416. doi: 10.3389/fpls.2018.01416

INTRODUCTION

Red coralline algae play key roles as ecosystem engineers in global oceans (Foster, 2001; Nelson, 2009), and contribute significantly to carbonate deposition (Amado-Filho et al., 2012; Van Der Heijden and Kamenos, 2015). Some coralline algae, particularly crustose coralline algae, have shown sensitivity to ocean acidification in many laboratory and field studies (Hofmann and Bischof, 2014; McCoy and Kamenos, 2015), but it remains to be determined if they will have the capacity to adapt to the pH decrease and associated decrease in carbonate ion saturation states expected in future surface oceans due to higher dissolved CO_2 concentrations. In the polar oceans, especially the Arctic, where the carbonate buffering capacity is weak and the system is vulnerable to environmental change (Steinacher et al., 2009; Shadwick et al., 2013), coralline algae may be less resistant to ocean acidification than in lower latitudes, particularly during the dark Arctic winters (Büdenbender et al., 2011). However, recent studies have shown that some coralline algae alter their skeletal structure and composition (Nash et al., 2013; Ragazzola et al., 2013, 2016;

McCoy and Ragazzola, 2014; Kamenos et al., 2016) under elevated CO_2, perhaps in an effort to reduce skeletal dissolution, and they can have strong biotic control over calcification and inorganic carbon uptake (Comeau et al., 2013; Hofmann et al., 2016; Cornwall et al., 2017). It is becoming clear that Arctic coralline algae, particularly rhodoliths (free-living coralline red algal nodules), are more abundant than previously believed. For example, the existence of rhodoliths in eastern Greenland was first reported last year, where several rhodolith beds along the eastern Greenlandic coast were found (Jørgensbye and Halfar, 2017). The authors of this study suggest that there are likely many more beds in remote areas that are not close to research stations or settlements. Because rhodolith bed discoveries have been made around the world recently, the current estimates of the contribution of coralline algae to the global carbonate budget are likely severely underestimated, including their contribution to carbon storage (Van Der Heijden and Kamenos, 2015). Therefore, understanding the mechanism of calcification in polar coralline algae is necessary for making reliable predictions and subsequent policy decisions.

Coralline algae deposit high-Mg calcite in their cell walls, which cement filaments of cells together. They occur as either a thin crust on hard substrata (crustose coralline algae, CCA), as free-living rhodoliths, or as a flat thallus with articulated branches. The surface chemistry of dissolved inorganic carbon (DIC) in calcifying algae can be controlled by several processes. Photosynthesis, dominant in the light, leads to an increase of the pH and carbonate ion concentration [CO_3^{2-}] and thus favors calcification, while net respiration has the opposite effect on calcification (McConnaughey, 1989). Calcification induces the liberation of protons (as $Ca^{2+} + HCO_3^- \rightarrow CaCO_3 + H^+$), and thus buffers the pH shift induced by photosynthesis, while dissolution can buffer the pH decrease by respiration (Gattuso et al., 1999). Active transport, mostly proton pumping or active uptake of HCO_3^- can induce pH shifts that are independent, and often of different time scales, as the metabolic processes (Borowitzka and Larkum, 1976; McConnaughey, 1991; de Beer and Larkum, 2001; Al-Horani et al., 2003). The latter can be considered as expression of biotic control of calcification (Borowitzka and Larkum, 1977). These ion pumps transport HCO_3^- and H^+ into the tissue in the light (Borowitzka and Larkum, 1987), where the enzyme carbonic anhydrase speeds up the dehydration of HCO_3^- to CO_2. Due to photosynthesis and the transport of protons away from the surface, the pH at the coralline algal surface (pH_S) is elevated compared to the bulk seawater pH (pH_B) (Hurd et al., 2011; Cornwall et al., 2013, 2015; Hofmann et al., 2016), which favors the surface calcification, due to higher CO_3^{2-} concentration. In the dark, the reverse process occurs, and the protons released are buffered by the CO_3^{2-} to form HCO_3^- (Comeau et al., 2013). Further evidence of elevated surface pH at the site of calcification in coralline algae has been shown in recent studies using boron isotopes (Cornwall et al., 2017; Donald et al., 2017). However, the dynamics of CO_3^{2-} and pH in response to light have never been measured at the surface of a coralline alga. Hence, no data on active processes that control the surface chemistry, like light-induced proton pumps, are available. To elucidate the possible presence of such pumps, we measured the chemistry dynamics at the surface in response to illumination, using microsensors to achieve high-spatial resolution. For describing the complete carbonate system at the surface of coralline algae data on at least two parameters of the carbonate system are needed, assuming equilibrium. Therefore, we measured surface [CO_3^{2-}] and pH using microsensors at the surface of polar coralline algae in response to light dynamics. Although these are not the ideal parameters to use for calculating the remaining parameters of the seawater carbonate system, we do so as a first attempt to provide a glimpse of what the surface chemistry of Arctic coralline algae may look like, considering it is not yet possible to measure DIC or total alkalinity (TA) directly at the algal surface. We hypothesized that surface [CO_3^{2-}] would depend on light, being elevated in the light and reduced in the dark.

MATERIALS AND METHODS

Algae Sampling and Maintenance

Samples of the crustose coralline *Phymatolithon tenue* (Rosenvinge) Düwel & Wegeberg (**Figures 1a,b**) were collected between 10 and 12 m depth at Hansneset, off the southwestern coast of the island Bloomstrand in Kongsfjord, Svalbard, where temperatures range from −2 to 7°C during the year at 20 m depth (Laudien et al., 2014). High sediment deposition from surrounding glaciers results in high freshwater input and high turbidity in Kongsfjord during summer (Hajime and Kudoh, 1997; Hanelt et al., 2001), which strongly attenuates the solar radiation at depth in the fjord (Hanelt et al., 2001). The photosynthetically active radiation (PAR) available at 10 m depth is less than 10% of surface radiation (Cui et al., 2013). Algal samples were transported to the Max Planck Institute for Marine Microbiology (MPIMM), where they were maintained at 4°C in custom-made re-circulating aquaria (20 L) with natural seawater (34 psu) on an 18:6 h day/night cycle at 10 μmol photons m^{-2} s^{-1} for 1 year prior to the experiments. One-third of the seawater in the recirculating tanks was replaced every 2 weeks. Two species of *Lithothamnion* rhodoliths, *L. glaciale* Kjellman (**Figures 1c,d**) and *L. tophiforme* (Esper) Unger (**Figures 1e,f**), were collected using SCUBA from two sites off the southwestern coast of Greenland: Købbe Fjord (*L. glaciale*: 64.14, −51.59) and Akia Penninsula (*L. tophiforme*: 64.193210, −51.908612). Surface currents in the Nuuk region exceed 1 m s^{-1} shortly before and after slack tide, therefore water flow in coralline habitats is due to tidal flux year round. The site at Akia Peninsula experiences flushing from Godthåbsfjord to the marine environment through small channels, while Købbefjord has an influx and outflux of primarily marine water. Currents at the benthos have not been measured due to logistical constraints, but the site at Akia Peninsula specifically has a great deal of sedimentation (**Figure 1e**), indicating flow significantly decreases with depth. The site at Akia Penninsula has high canopy cover of *Saccharina longicruris* (**Figure 1e**), while there is almost no defined canopy cover in Købbefjord, only spotty cover of *Agarum clathratum* (**Figure 1c**). Average mid-day summer light intensities at 10 m depth range measured with an Odyssey PAR logger (Dataflow

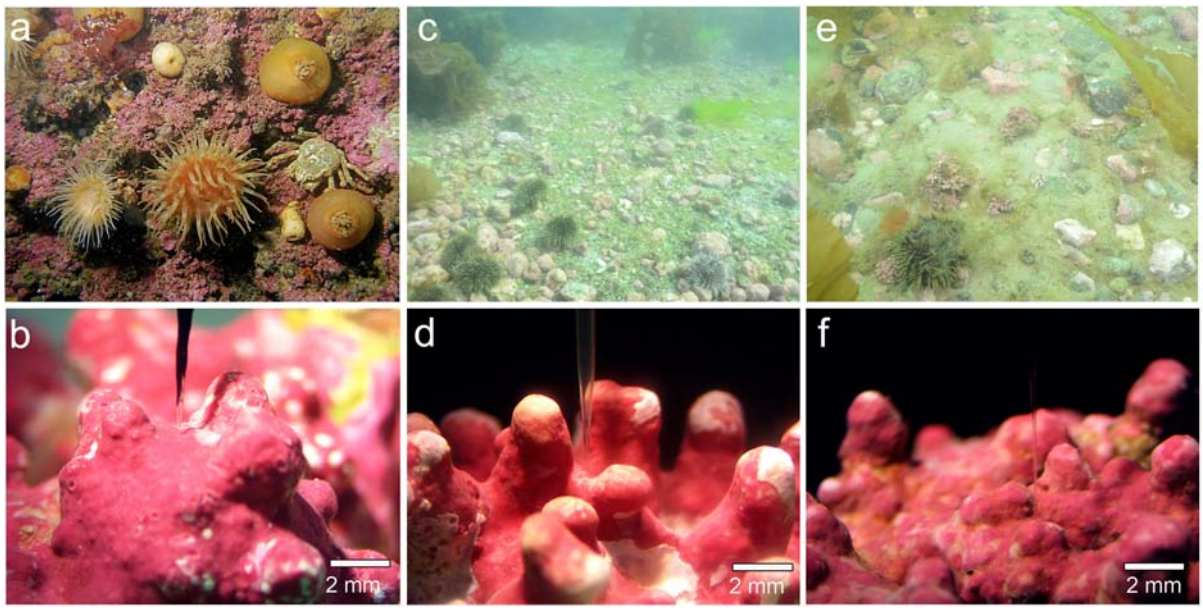

FIGURE 1 | Images from collection sites and examples of specimens investigated: **(a,b)** Kongsfjord, *P. tenue*; **(c,d)** Købbefjord, *L. glaciale*; and **(e,f)** Akia Penninsula, *L. tophiforme*. In **(c)**, high cover of the crustose coralline *Clathromorphum* sp. is apparent. The microsensors used. In **(c,d)**, the microsensor is positioned between nodes/branches. In **(f)**, the microsensor is positioned at the tip of a node. *In situ* photographs are from M. Schwanitz and K. Schoenrock. Microscopic photos taken by L. Hofmann.

Systems Ltd, Christchurch, NZ) ranged between 101 and 196 μmol photons m^{-2} s^{-1} at midday. After collection, these specimens were transported to the MPIMM via the University of Glasgow in ambient seawater at 4°C, and then maintained in custom-made recirculating aquaria in the same conditions as Svalbard collections for 9 months prior to the experiments.

Microsensor Construction

O_2 microsensors were made and used as described by Revsbech (1989), liquid ion exchange (LIX) pH and CO_3^{2-} microelectrodes were constructed according to de Beer et al. (2008). The O_2 optode was calibrated with 0 and 100% air saturated seawater obtained by bubbling with nitrogen gas and compressed air, respectively. All calibrations were conducted at 4°C. The CO_3^{2-} microelectrode was calibrated following the continuous titration method from Han et al. (2014) using natural seawater. To reduce air exposure, the calibration was conducted in a glass Schott bottle with a Teflon-sealed lid with custom made holes for the pH electrode, microelectrode, and reference electrode. The HCl titration solution was added by inserting a needle syringe through the Teflon membrane. The pH microelectrode was calibrated using pH_{NST} 7.0 and 9.0 buffers (Fluka Analytical, Buchs, Switzerland). The measured pH values were then corrected to the total pH scale by subtracting 0.1 pH units for the seawater chemistry calculations. We acknowledge that certified reference material is preferred for calibrating pH, but the extreme sensitivity of our LIX pH microelectrodes and their incompatibility with some calibration standards did not allow this. Because of the uncertainty associated with NBS buffers and the resulting calculations of the seawater system, we report the profiles of CO_3^{2-} as ratios rather than absolute concentrations. The oxygen and pH electrodes had average tip diameters between 10 and 20 μm, and therefore minimal influence on the diffusional boundary layer (DBL) of the coralline algae measured.

Microprofiling

The experimental set-up used for microprofiling was the same described in Hofmann et al. (2016). Seawater was pumped through a plexiglass flow cell (19 cm × 9 cm × 9.5 cm) attached to a temperature-controlled reservoir at approximately 2 cm s^{-1} (judged by particle movement) and passed through a perforated wall at the entrance and exit of the flow chamber to create laminar flow at the algal surface. All experiments were conducted at 7°C. pH and CO_3^{2-} microelectrodes and an oxygen optode were used to measure depth microprofiles from the surface of the algae into the overlying seawater under both saturating light (100 μmol photons m^{-2} s^{-1}) and dark conditions. Microprofiles of the three species were measured under steady state conditions. Up to four individuals from each species were measured on multiple occasions at multiple branch tips (due to variations in DBL thickness depending on morphology, only branch tips were used; see Results below), but complete datasets for all three parameters (pH, O_2, and CO_3^{2-}) could only be obtained on three replicates of each species due to broken/faulty sensors. In the light, a steady state signal was achieved after several minutes, while a dark adaptation period of at least 30 min was necessary before obtaining a steady signal with no noticeable change. In order to determine when the dark steady state was reached, O_2, pH, and CO_3^{2-} at the surface of the algae were monitored continuously overnight (see Light dynamics subsection below).

Microprofiles of O_2, pH, and CO_3^{2-} for each individual were obtained by first positioning the sensors at the surface of the algal specimen by hand using a micromanipulator (Pyroscience, Aachen, Germany) with the aid of a stereomicroscope. Using the software Profix (Pyroscience, Aachen, Germany), the microelectrodes were then programed to run four consecutive profiles from the surface of the alga (position 0) into the overlying water column (position 800 μm) at 50 μm intervals. Microprofiles were conducted first under saturating light and steady state conditions. Microprofiles in the dark were then obtained following a dark adaptation period of at least 30 min, after which there was no noticeable change in the sensor signal. Because light and dark profiles were measured at the same location on the same individual at different time points, light was treated as a repeated factor with two levels (light, dark) for statistical analysis in this case (see below). Oxygen fluxes were calculated from the concentration profiles according to Fick's Law [see Hofmann et al. (2016)] using the diffusion coefficient 1.34×10^{-9} m^2 s^{-1} for seawater at 7°C and 35‰ salinity. The delta pH was calculated by subtracting the surface pH from the bulk seawater pH ($\Delta pH = pH_S - pH_B$), and surface ratios of CO_3^{2-} were calculated by dividing the surface concentration by the bulk seawater concentration.

Microprofiles of pH at the branch tip and base of rhodoliths showed that branch bases have thicker DBL than branch tips, and consequently, the pH between branches is slightly higher than in the bulk seawater above branch tips (**Supplementary Table S1**). In order to reduce the variation in profile data driven by morphological characteristics, we measured all profiles on branch tips of individual rhodoliths. By standardizing the location of profile measurements, we observed that there was no difference in the boundary layer thickness between the crustose or branched forms investigated (**Supplementary Table S1**).

Inhibition Experiments

The extracellular carbonic anhydrase inhibitor, acetazolamide (AZ), was used to test for carbonic anhydrase activity and its effect on surface chemistry of one of the species investigated in this study (*L. glaciale*). By inhibiting carbonic anhydrase, we could determine if surface pH was directly coupled to photosynthesis. Prior the addition of the inhibitor, a gross photosynthesis versus irradiance curve was generated to determine limiting and saturating light levels. Gross photosynthesis measurements were conducted using the light–dark shift method (Revsbech and Jørgensen, 1983, 1986), and the preparation of AZ was conducted following the methods by Hofmann et al. (2016). The curve was fit using the nonlinear least squares (nls) command in R with the equation from Eilers and Peeters (1988) that considers potential photoinhibition

$$GP = \frac{I}{aI^2 + bI + c}$$

where GP is gross photosynthesis, I is the irradiance, and a, b, and c are the parameters estimated by the model. After fitting the model to the data, the light saturation point could be estimated by calculating the light intensity at which photosynthesis was saturating. pH profiles and gross photosynthesis were measured at three and five light conditions, respectively, prior to and after the addition of AZ (final concentration 280 μM). The addition of AZ was made to the seawater reservoir while the pH sensor remained on the surface of the alga. Measurements were made after a steady state was reached. Unfortunately, we could only successfully complete this experiment on a single individual, and therefore the figures can be found in the **Supplementary Material**.

Statistical Analysis

The parameters of the seawater carbonate system were calculated from the pH (total scale) and CO_3^{2-} concentrations measured at the algal surface and in the bulk seawater using the package seacarb in R. To test for an effect of site/species and light on O_2 flux, ΔpH and $[CO_3^{2-}]_S$:$[CO_3^{2-}]_B$, a nonparametric test for repeated measures data in factorial designs was conducted in RStudio (version 0.98.1087) using the nparLD package (nonparametric analysis of longitudinal data in factorial experiments). This test was appropriate because more than one group of subjects (groups = species) was observed repeatedly over time (Noguchi et al., 2012). Light and dark profiles were measured on the same individual at the same location at different time points. Results of the ANOVA-type statistic are reported. To determine if surface $[CO_3^{2-}]$ and $[O_2]$ differed from bulk $[CO_3^{2-}]$ and $[O_2]$, independent t-tests were conducted separately for each response variable for each species and light condition.

RESULTS

Oxygen, pH, and CO_3^{2-} Microprofiles

Microprofiles of O_2, CO_3^{2-}, and pH showed that despite reduced O_2 concentrations due to respiration in the dark, surface pH, and CO_3^{2-} concentrations both remained higher than the bulk seawater under both light and dark conditions (**Figures 2A–C**). This was observed on all three algal species. These trends are further shown by the ratio of $[CO_3^{2-}]_S$:$[CO_3^{2-}]_B$ and the delta pH (**Figures 3A,B**). There was no significant effect of site/species on either oxygen flux, ΔpH or $[CO_3^{2-}]_S$:$[CO_3^{2-}]_B$, but all parameters were significantly higher in the light than in the dark (O_2 flux: ANOVA-type statistic (ATS) = 62.5, $p = 2.7e-15$ ΔpH: ATS = 18.5, $p = 1.7e-5$; $[CO_3^{2-}]_S$:$[CO_3^{2-}]_B$: ATS = 5.9, $p = 0.01$; see Statistical Analysis above).

The O_2 concentration at the surface was not significantly different from that of seawater in the dark, indicating that respiration rates (oxygen flux in the dark) were very low (**Figure 3C** and **Supplementary Table S2**). In the light, the surface concentration of O_2 significantly increased due to photosynthesis and a small efflux into the bulk seawater was observed (**Figure 3D** and **Supplementary Table S2**).

Surface Carbonate Chemistry

To assess the effect of light and darkness on the surface chemistry, we measured the dynamics of surface pH and $[CO_3^{2-}]$ in response to saturating light and darkness. Both surface pH

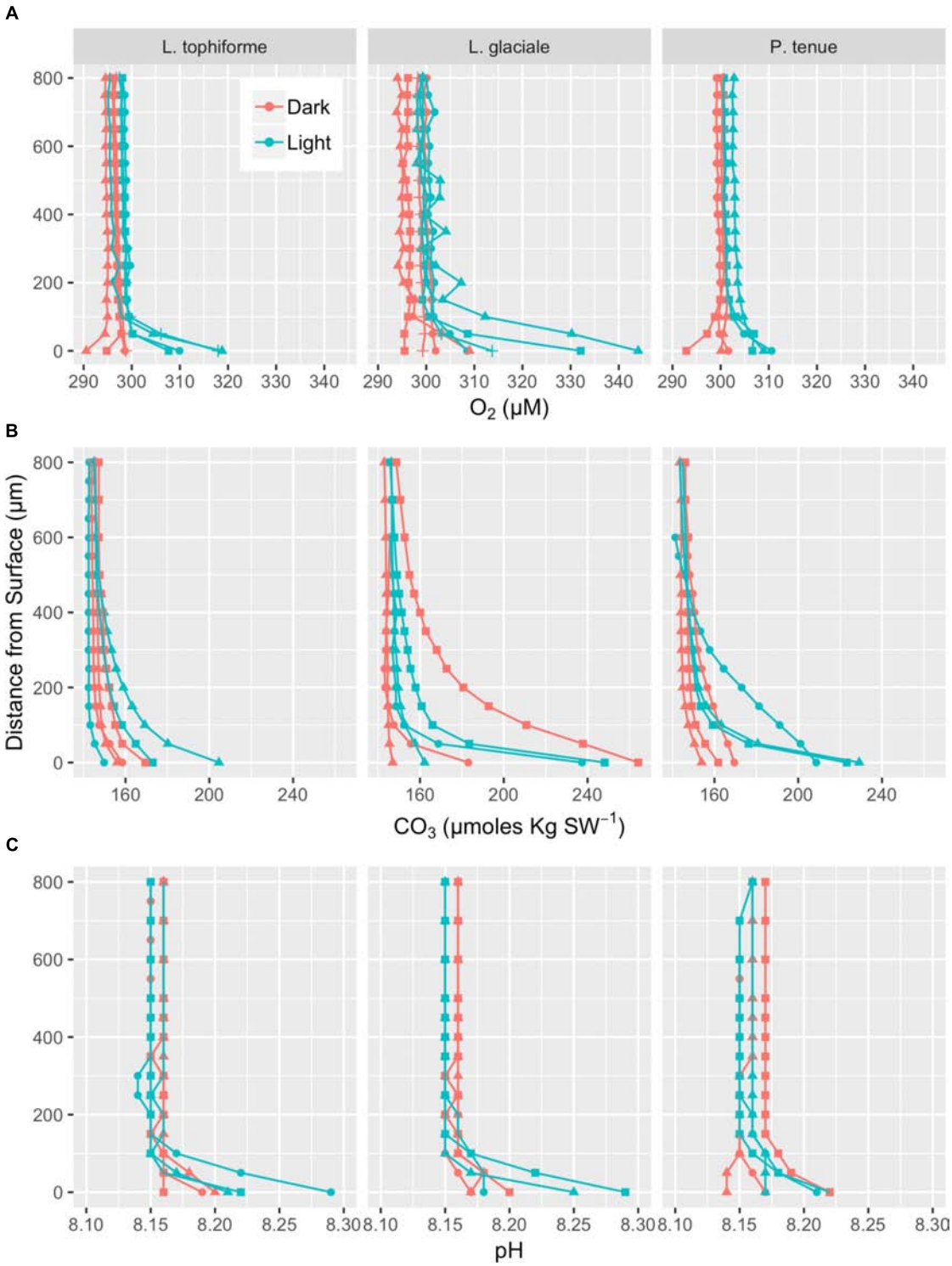

FIGURE 2 | Microprofiles of oxygen concentration **(A)**, carbonate ion concentration **(B)**, and pH **(C)** measured with microsensors under saturating light (blue) and dark (red) conditions. Each profile is an average of four replicate profiles ± SE. The symbols represent measurements conducted on different individual algae.

and $[CO_3^{2-}]$ increased in the light and decreased in the dark at the surface of *L. glaciale* from Købbe Fjord (**Figure 4**). Upon illumination, the $[CO_3^{2-}]_S$ increased sharply, and then slowly decreased before reaching steady state at a level that always remained above the levels in darkness (**Figure 4**). However, after darkening, the pH slightly increased before

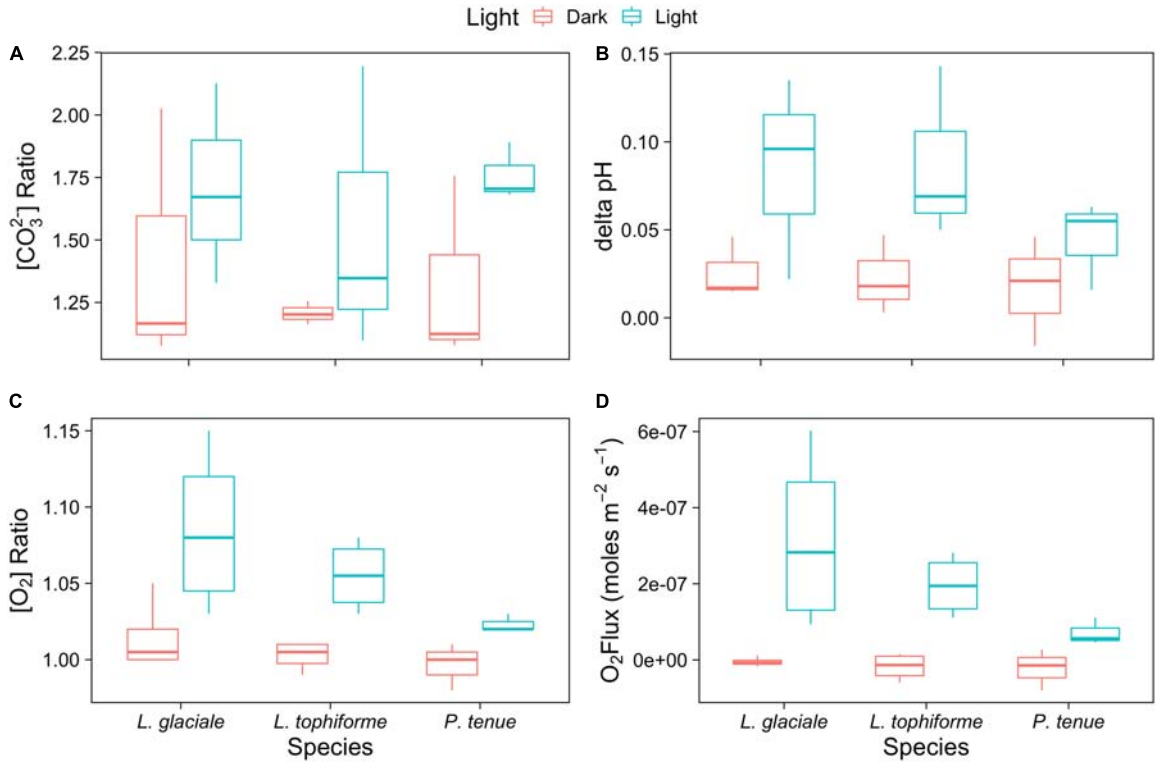

FIGURE 3 | Boxplot of **(A)** carbonate ion concentration ratios (surface:bulk), **(B)** delta pH, and **(C)** oxygen concentration ratios at the algal surface to the concentration in the bulk seawater under saturating light and dark conditions for the coralline algae investigated. **(D)** Oxygen fluxes at the surface of the algae under saturating light and dark conditions.

beginning to decrease and reaching a steady state. The opposite pattern was seen when the light was switched on, showing a slight dip in pH before it started increasing, and reaching a steady state. Regardless of whether the alga was in the light or dark, the pH_S, and $[CO_3^{2-}]_S$ always remained above the bulk seawater levels. Similar trends in light/dark dynamics were found for *P. tenue* and *L. tophiforme* (**Supplementary Figures S1**, **S2**). In order to determine when the $[O_2]_S$, pH_S, and $[CO_3^{2-}]_S$ reached steady state in the dark and to determine if they reach levels below the bulk seawater at any point, we monitored each parameter in the dark for up to 15 h. In *P. tenue* from Spitsbergen, the pH_S never dropped below pH_B in the dark, and the $[CO_3^{2-}]_S$ remained above $[CO_3^{2-}]_B$ for over 13 h, despite lower $[O_2]_S$ compared to $[O_2]_B$ (**Figure 5**). Similar patterns were found during extended periods of darkness for additional individuals of *P. tenue* and for *L. tophiforme* (**Supplementary Figures S3**, **S4**), although the pH_S dipped slightly below the pH_B in one specimen of *P. tenue* after 7 h (**Supplementary Figure S3**). From the pH and CO_3^{2-}, we calculated the remaining parameters of the carbonate system at the algal surface and in the bulk seawater using the package seacarb in R (see Materials and Methods). **Figure 6** shows that the surface DIC, pCO_2, HCO_3^-, and TA remained lower than the bulk seawater, while the aragonite saturation state remained higher than the bulk seawater.

Inhibition of Carbonic Anhydrase

The addition of AZ resulted in a slight decrease in surface O_2 and in surface pH of *L. glaciale* (**Supplementary Figure S5**). The inhibition of carbonic anhydrase only inhibited delta pH at 85 μmol photons m^{-2} s^{-1} (**Supplementary Figure S6**), which was below light saturation. The light at which gross photosynthesis was saturating before AZ addition was 130 μmol photons m^{-2} s^{-1} (**Supplementary Figure S7**). Carbonic anhydrase inhibition resulted in the inhibition of gross photosynthesis, which showed different patterns depending on light intensity. CA inhibition was constant above 10 μmol photons m^{-2} s^{-1} at approximately 50–75%. Only at the lowest light level (2 μmol photons m^{-2} s^{-1}), no inhibition was observed. This indicates that at only very low light intensities, the supply of CO_2 by transport from the seawater (13 μM) and non-catalyzed conversion of HCO_3^- is sufficient. However, at higher light intensities, and thus at higher photosynthetic capacity, CO_2 supply from the seawater limits the photosynthetic rate, and CA is needed to enhance the CO_2 supply (**Supplementary Figure S7**).

DISCUSSION

Our results show the carbonate chemistry conditions in the microenvironment of Arctic coralline algae. We did not observe

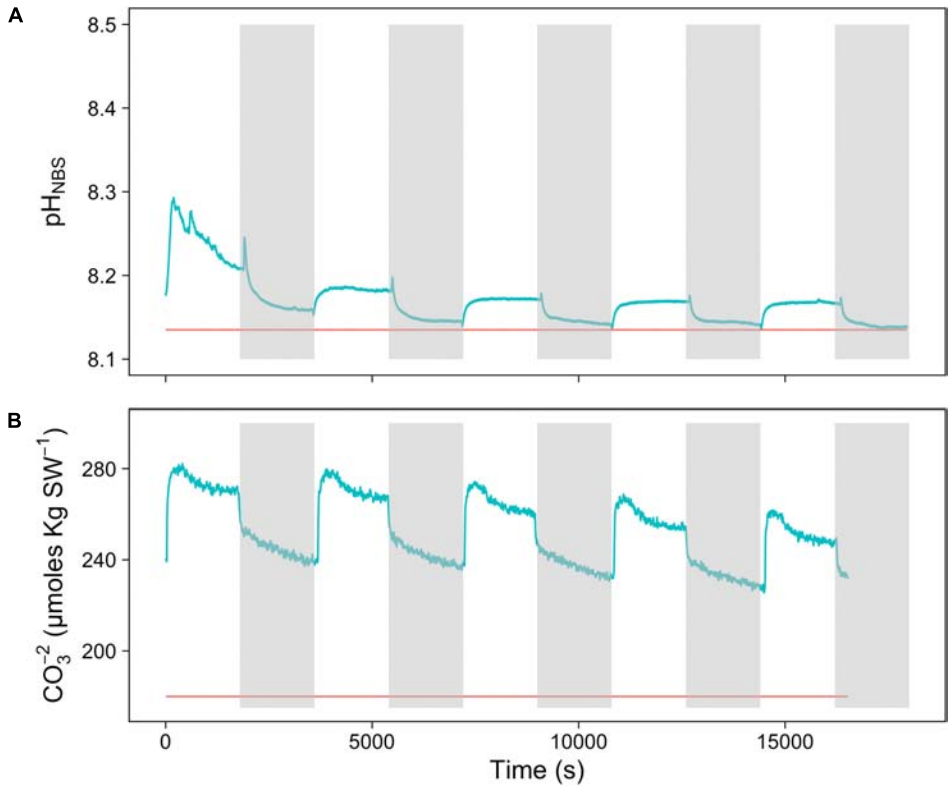

FIGURE 4 | Surface **(A)** carbonate ion concentration and **(B)** pH of a *L. glaciale* rhodolith from Købbefjord measured in 30-min light/dark intervals. The gray shaded areas indicate periods of darkness. The blue lines represent values measured at the surface of the alga, and the red lines indicate bulk seawater concentrations.

strong differences in pH_S or $[CO_3^{2-}]_S$ between the three species, indicating that in this case, the rhodolith versus crustose morphology did not have a strong influence on surface chemistry. Also, it suggest that our observations may hold generally for Arctic rhodoliths. The saturation state of calcite and aragonite remained greater than 1 under all conditions, despite respiration in the dark. Dark dissolution did not likely occur under our experimental conditions, even after hours of darkness, because TA at the algal surface was lower than in the bulk seawater, suggesting that dissolution was not the source of elevated CO_3^{2-} ions. The lower alkalinity at the surface in the dark could be due to nutrient uptake, as the uptake of phosphate and ammonium ions results in a decrease in alkalinity (Wolf-Gladrow et al., 2007). These results support the growing evidence that coralline algae have strong biotic control over their skeletal structure (Kamenos et al., 2013, 2016; Nash et al., 2015) and microenvironments where active calcification is occurring (Hofmann et al., 2016; Cornwall et al., 2017).

Arctic rhodoliths and crustose coralline algae control their surface chemistry actively. The surface pH dynamics upon illumination and darkening were rapid (within seconds), showing the presence of a light-driven proton pump. Further evidence for the presence of a proton pump was provided by the inhibition experiment with *L. glaciale*, which showed that despite inhibition of gross photosynthesis, there was no significant change in delta pH. Therefore, a process independent of photosynthesis also influences the surface pH. Our observation differs from the recently proposed mechanism (Chrachri et al., 2018) in the marine diatom *Odontella sinensis*, whose surface pH was strongly inhibited by AZ, suggesting that surface pH is directly dependent on the rate of photosynthesis in this organism. Although photosynthesis in *L. glaciale* is strongly dependent on CA, it has an additional mechanism, a light-induced proton pump, that influences surface pH independently from photosynthesis. The same result has been reported for a tropical crustose coralline alga (Hofmann et al., 2016) and the calcifying green alga *Halimeda discoidea* (de Beer and Larkum, 2001). This photosynthesis independent, light-triggered proton pump may have been responsible for the rapid pH spikes we observed after turning off the light.

The surface carbonate ion dynamics were slower than the pH dynamics, suggesting that the carbonate dynamics were not only driven by pH. Because carbonate and bicarbonate are in almost instant equilibrium, the peaks in the carbonate dynamics likely represent rapid bicarbonate uptake by a carbon concentrating mechanism before a steady state is reached. The presence of a carbon concentrating mechanism in these algae has been recently supported by a separate study (Hofmann and Heesch, 2017). Additional support for the presence of a carbon concentrating mechanism utilizing HCO_3^-/H^+ co-transport was provided by our measurements during extended darkness. Despite the higher surface pH and CO_3^{2-} that we measured, the calculated TA

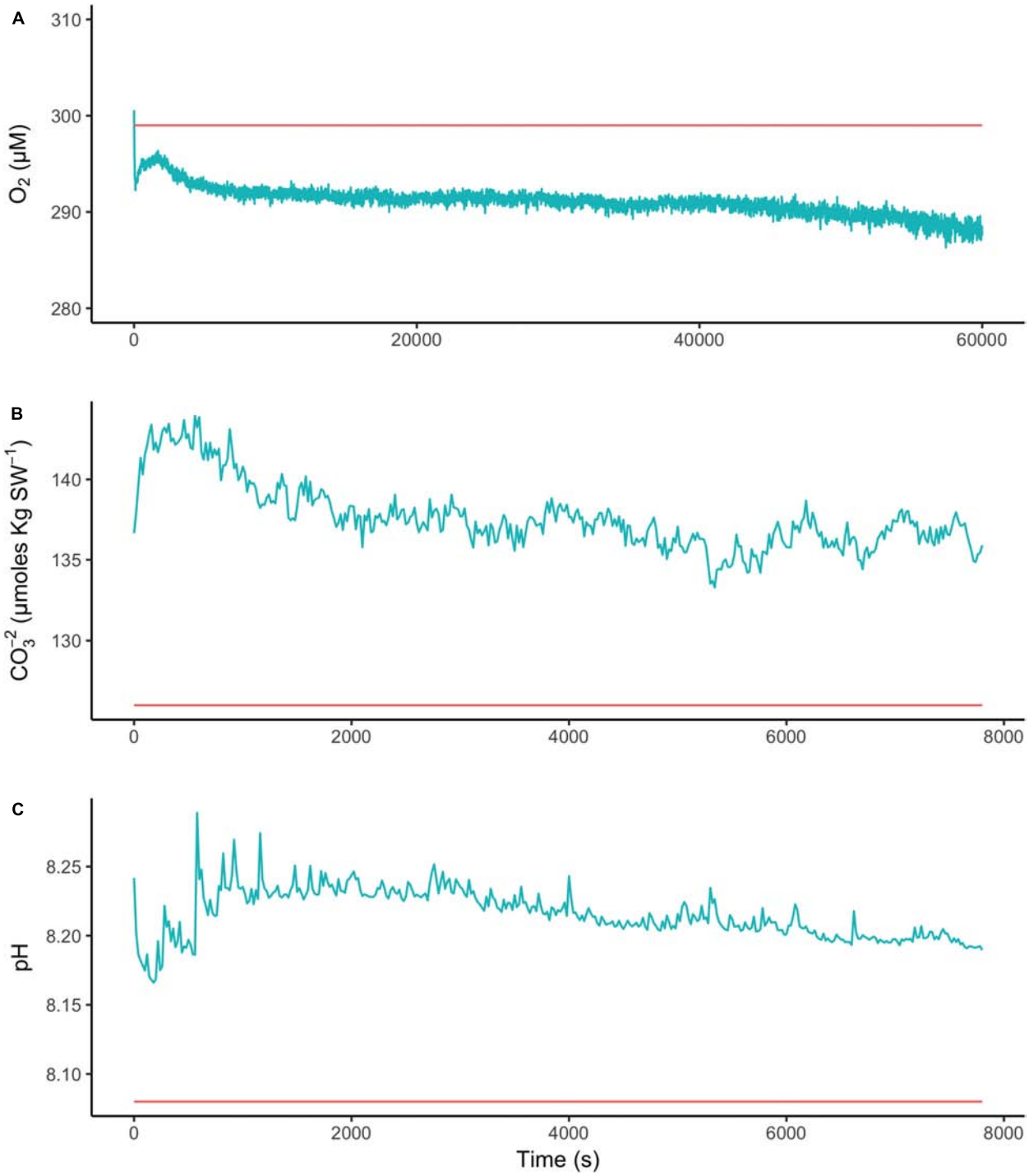

FIGURE 5 | Surface (blue) and bulk seawater (red) concentrations of **(A)** oxygen, **(B)** carbonate ion, and **(C)** pH measured during a period of extended darkness on a *P. tenue* individual from Spitsbergen. Note that time axis for oxygen is longer than for pH and carbonate.

at the algal surface during extended darkness was lower than the bulk seawater. This was explained by a strong reduction (ca. 75%) in the concentration of surface HCO_3^-, which was comparable to the reduction in protons (ca. 69%) associated with the elevated surface pH. Further evidence of HCO_3^- uptake can be provided by modeling the seawater carbonate system. If we assume a photosynthetic quotient (O_2 released: CO_2 fixed) of 1 (but note that Chisholm (2000) reported a photosynthetic quotient of 1.05–1.48 for tropical coralline alga), we would expect the surface DIC concentration to decrease the same

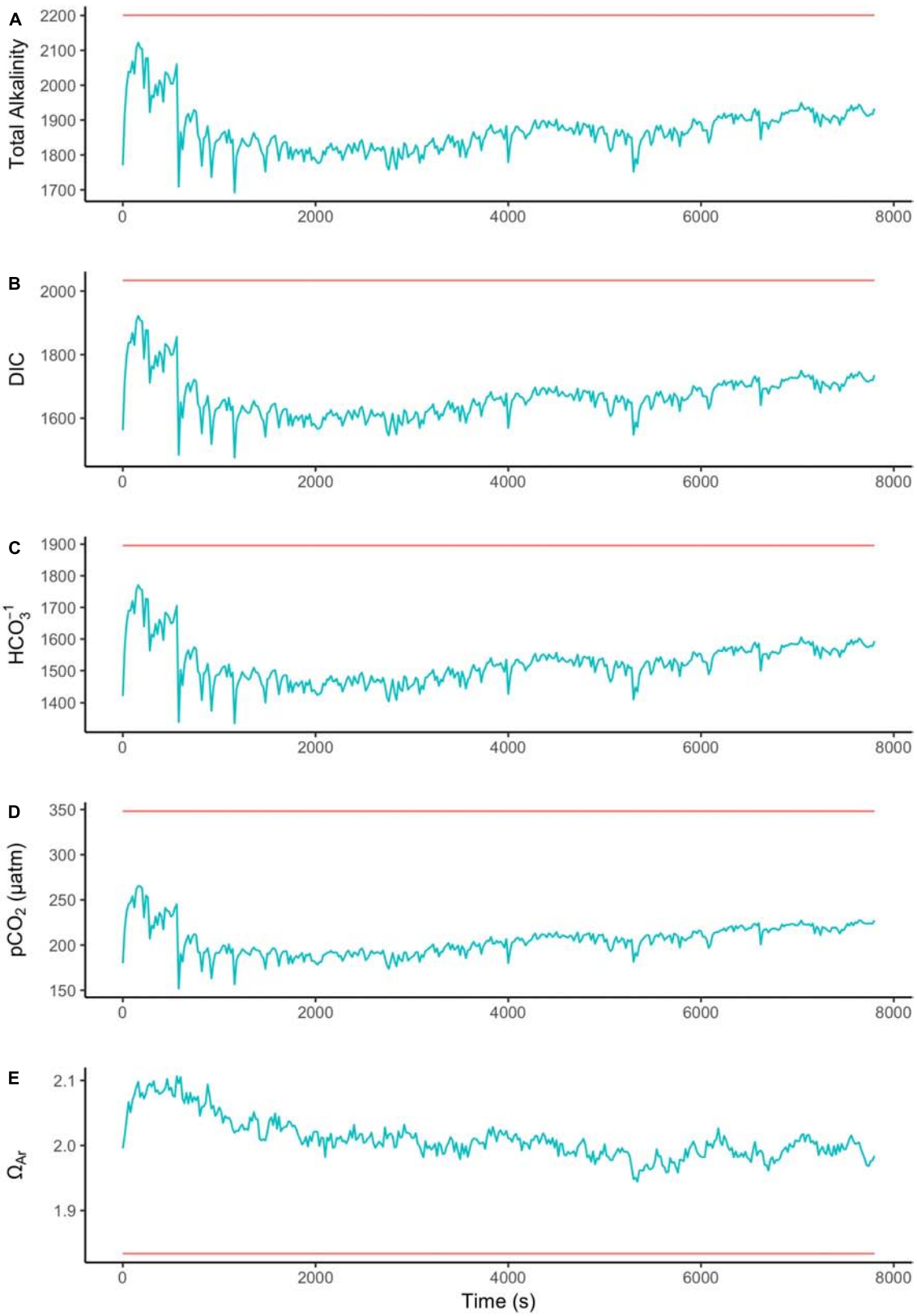

FIGURE 6 | Surface (blue) and bulk seawater (red) concentrations of **(A)** total alkalinity (TA), **(B)** total dissolved inorganic carbon (DIC), **(C)** bicarbonate (HCO_3^-), **(D)** pCO_2, and **(E)** aragonite saturation state calculated from the values measured in **Figure 5**. The units for TA, DIC, and HCO_3^- are in µmoles Kg SW^{-1}.

magnitude as the surface O_2 concentration increased. On average, the O_2 concentration at the surface increased 10 μM under saturating light. Therefore, if we consider the bulk seawater has a pH of 8.15 and TA of 2200, the [CO_3^{2-}] is 139 μM. An increase in pH to 8.2, which we observed, accompanied by a 10 μM decrease in DIC as CO_2 would result in a [CO_3^{2-}] of 50 μM. On the other hand, a decrease in DIC as HCO_3^- would result in a [CO_3^{2-}] of 159 μM, which is comparable to the concentrations we observed at the surface of all the coralline algae investigated. Therefore, it is highly likely that the changes in surface chemistry are due to HCO_3^- uptake coupled to H^+ co-transport or OH^- exchange. Our data, along with those from Comeau et al. (2013) and Hofmann et al. (2016) support the hypothesis by Borowitzka and Larkum (1987) that there is a H^+/HCO_3^- symporter or HCO_3^-/OH^- antiporter in coralline algae. Co-transport of HCO_3^- and protons away from the calcifying surface and into the cell results in optimal conditions for calcification at the cell surface under both light and dark conditions, and elevated HCO_3^- concentrations inside the cell neutralize the protons, providing an inorganic carbon source for photosynthesis in the light. This mechanism is in stark contrast to the mechanism proposed in some non-calcifying macroalgae, Characean algae, and freshwater flowering plants, where HCO_3^- use is coupled to H^+ extrusion, producing acidic zones where the concentration of CO_2 is elevated due to the low pH and therefore diffuses into the cell (Moulin et al., 2011; Raven and Hurd, 2012). The H^+ extrusion must be accompanied by OH^- extrusion in alkaline zones. Our microsensor measurements do not support the presence of acidic or alkaline zones in coralline algae, although these zones are hypothesized to be much smaller than the diameter of a microsensor, and therefore cannot be accessed. Nevertheless, our results strongly suggest that HCO_3^- is taken up directly, with either a net H^+ co-transport or net OH^- efflux, which results in a net increase in surface pH.

While this mechanism is easily explained under light conditions, it remains to be determined why and how Arctic coralline algae maintain elevated pH_S and [CO_3^{2-}]$_S$ in darkness. We hypothesize that these observations are a result of high rates of light independent carbon fixation, which is a common adaptation in polar macroalgae that facilitates their survival through the polar winter (Wiencke et al., 2009). Light independent carbon fixation (or β-carboxylation) is an anaplerotic pathway that involves the enzymes phosphoenol pyruvate carboxylase (PEPC) or phosphoenol pyruvate carboxykinase (PEPCK) to fix carbon dioxide (or bicarbonate) to the β-carbon of PEP or pyruvate. This process reduces carbon loss under darkness and produces important metabolites, such as amino acids. High rates of light independent carbon fixation would explain the continued inorganic carbon uptake (in this case as HCO_3^-) and elevated surface pH in the dark, despite oxygen consumption resulting from dark respiration. Further evidence for this hypothesis can be seen in the data from Hofmann and Heesch (2017), who reported the total and organic ^{13}C:^{12}C fractionation in Atlantic rhodoliths. The organic fraction $\partial^{13}C$ signatures of Arctic rhodoliths, including specimens from the same collection sites used in this study, deviated from the linear trend with latitude. The Arctic rhodoliths had organic material more enriched in ^{13}C than would be expected based on the latitudinal trend, which may be due to higher rates of anaplerotic reactions that result in ^{13}C enriched carboxyl carbons (Savidge and Blair, 2004). Although the CO_2 concentration at the algal surface (based on the measured pH and CO_3^{2-} concentrations) was lower than the bulk seawater and hence suggests CO_2 uptake by the alga in the dark, our hypothesis is at this time speculative, as we did not directly measure CO_2 uptake in the dark. Additional possibilities for dark CO_2 uptake [e.g., carbamoyl phosphate synthase (Raven et al., 1990)] cannot be excluded. Further studies measuring direct CO_2 fluxes would be necessary to confirm our hypothesis.

CONCLUSION

In conclusion, our results suggest that Arctic corallines have strong biological control over their surface chemistry, where active calcification occurs. High rates of light independent carbon fixation are likely an adaptive strategy in Arctic coralline algae for limiting carbon loss during long periods of darkness, and additionally create a microenvironment that prevents dissolution in the dark. Our results suggest that net dissolution in the dark is not currently a threat to Arctic coralline algae during the summer. However, long exposure to darkness resulted in a surface pH below seawater pH, suggesting that dissolution could still occur during winter. These unique physiological mechanisms likely play an important role in facilitating the survival of Arctic coralline algae under harsh conditions, but further studies will be needed to determine if these mechanisms could facilitate adaptation to ocean acidification in the future, which would have important implications for Arctic marine ecosystems.

DATA AVAILABILITY

The datasets generated during and/or analyzed during the current study are available from the corresponding author upon reasonable request.

AUTHOR CONTRIBUTIONS

LH designed and carried out the experiment and wrote the manuscript. KS collected the samples from Greenland and edited the manuscript. DdB edited the manuscript.

FUNDING

This research was funded by the National Science Foundation Ocean Sciences International Postdoctoral Research Fellow program awarded to Dr. L. C. Hofmann (Grant No. 1521610): "Plasticity of Inorganic Carbon Use in Marine Calcifying Macroalgae Across a Latitudinal Gradient and Consequences of Global Change." Funding for KS to travel to and participate in this project at the Max Planck Society for Marine Microbiology was provided by a Federation of European Microbiological

Societies (FEMS) Research Grant (Grant No. FEMS-RG-2015-0111).

ACKNOWLEDGMENTS

The authors would like to thank Max Schwanitz for collecting the *P. tenue* specimens used in this study.

SUPPLEMENTARY MATERIAL

The Supplementary Material for this article can be found online at: https://www.frontiersin.org/articles/10.3389/fpls.2018.01416/full#supplementary-material

FIGURE S1 | Light/dark dynamics of [CO_3^{2-}] in *P. tenue*.

FIGURE S2 | Light/dark dynamics and extended darkness [CO_3^{2-}] in *L. tophiforme*.

FIGURE S3 | Surface pH and [O_2] of *P. tenue* during extended darkness.

FIGURE S4 | Surface [CO_3^{2-}] and pH of *L. tophiforme* during extended darkness.

FIGURE S5 | Surface [O_2] and pH before and after AZ addition.

FIGURE S6 | Delta pH at the surface of *L. glaciale* before and after AZ addition.

FIGURE S7 | Effect of AZ on gross photosynthesis in *L. glaciale*.

TABLE S1 | Thickness of the diffusional boundary layer at different locations on the thalli.

TABLE S2 | *T*-tests comparing surface and bulk [O_2] for each species.

REFERENCES

Al-Horani, F. A., Al-Moghrabi, S. M., and De Beer, D. (2003). The mechanism of calcification and its relation to photosynthesis and respiration in the scleractinian coral *Galaxea fascicularis*. *Mar. Biol.* 142, 419–426. doi: 10.1007/s00227-002-0981-8

Amado-Filho, G. M., Moura, R. L., Bastos, A. C., Salgado, L. T., Sumida, P. Y., Guth, A. Z., et al. (2012). Rhodolith beds are major CaCO 3 BIO-factories in the tropical south West Atlantic. *PLoS One* 7:e35171. doi: 10.1371/journal.pone.0035171

Borowitzka, M. A., and Larkum, A. W. D. (1976). Calcification in the green alga Halimeda: III. The sources of inorganic carbon for photosynthesis and calcification and a model of the mechanism of calcification. *J. Exp. Bot.* 27, 879–893. doi: 10.1093/jxb/27.5.879

Borowitzka, M. A., and Larkum, A. W. D. (1977). Calcification in the green alga Halimeda. I. An ultrastructure study of thallus developement. *J. Phycol.* 13, 6–16. doi: 10.1111/j.1529-8817.1977.tb02879.x

Borowitzka, M. A., and Larkum, A. W. D. (1987). Calcification in algae: mechanisms and the role of metabolism. *CRC. Crit. Rev. Plant Sci.* 6, 1–45. doi: 10.1080/07352688709382246

Büdenbender, J., Riebesell, U., and Form, A. (2011). Calcification of the Arctic coralline red algae *Lithothamnion glaciale* in response to elevated CO 2. *Mar. Ecol. Prog. Ser.* 441, 79–87. doi: 10.3354/meps09405

Chisholm, J. R. M. (2000). Calcification by crustose coralline algae on the northern great barrier reef, Australia. *Limnol. Oceanogr.* 45, 1476–1484. doi: 10.4319/lo.2000.45.7.1476

Chrachri, A., Hopkinson, B. M., Flynn, K., Brownlee, C., and Wheeler, G. L. (2018). Dynamic changes in carbonate chemistry in the microenvironment around single marine phytoplankton cells. *Nat. Commun.* 9:74. doi: 10.1038/s41467-017-02426-y

Comeau, S., Carpenter, R. C., and Edmunds, P. J. (2013). Coral reef calcifiers buffer their response to ocean acidification using both bicarbonate and carbonate. *Proc. R. Soc. B* 280:20122374. doi: 10.1098/rspb.2012.2374

Cornwall, C. E., Comeau, S., and McCulloch, M. T. (2017). Coralline algae elevate pH at the site of calcification under ocean acidification. *Glob. Chang. Biol* 23, 4245–4256. doi: 10.1111/gcb.13673

Cornwall, C. E., Hepburn, C. D., Pilditch, C. A., and Hurd, C. L. (2013). Concentration boundary layers around complex assemblages of macroalgae: implications for the effects of ocean acidification on understory coralline algae. *Limnol. Oceanogr.* 58, 121–130. doi: 10.4319/lo.2013.58.1.0121

Cornwall, C. E., Pilditch, C. A., Hepburn, C. D., and Hurd, C. L. (2015). Canopy macroalgae influence understorey corallines' metabolic control of near-surface pH and oxygen concentration. *Mar. Ecol. Prog. Ser.* 525, 81–95. doi: 10.3354/meps11190

Cui, S., He, J., He, P., Zhang, F., Lin, L., and Ma, Y. (2013). The adaptation of Arctic phytoplankton to low light and salinity in Kongsfjorden (Spitsbergen). *Adv. Polar Sci.* 23, 19–24. doi: 10.3724/SP.J.1085.2012.00019

de Beer, D., Bissett, A., de Wit, R., Jonkers, H., Köhler-Rink, S., Nam, H., et al. (2008). A microsensor for carbonate ions suitable for microprofiling in freshwater and saline environments. *Limnol. Oceanogr. Methods* 6, 532–541. doi: 10.4319/lom.2008.6.532

de Beer, D., and Larkum, A. W. D. (2001). Photosynthesis and calcification in the calcifying algae *Halimeda discoidea* studied with microsensors. *Plant Cell Environ.* 24, 1209–1217. doi: 10.1046/j.1365-3040.2001.00772.x

Donald, H. K., Ries, J. B., Stewart, J. A., Fowell, S. E., and Foster, G. L. (2017). Boron isotope sensitivity to seawater pH change in a species of *Neogoniolithon coralline* red alga. *Geochim. Cosmochim. Acta* 217, 240–253. doi: 10.1016/j.gca.2017.08.021

Eilers, P., and Peeters, J. (1988). A model for the relationship between light intensity and the rate of photosynthesis in phytoplankton. *Ecol. Modell.* 42, 199–215. doi: 10.1016/0304-3800(88)90057-9

Foster, M. S. (2001). Rhodoliths: between rocks and soft places. *J. Phycol.* 37, 659–667. doi: 10.1046/j.1529-8817.2001.00195.x

Gattuso, J. P., Allemand, D., and Frankignoulle, M. (1999). Photosynthesis and calcification at cellular, organismal and community levels in coral reefs: a review on interactions and control by carbonate chemistry. *Am. Zool.* 39, 160–183. doi: 10.1093/icb/39.1.160

Hajime, I., and Kudoh, S. (1997). Characteristics of water in Kongsfjorden, Svalbard. *Proc. NIPR Symp. polar Meteorol. Glaciol.* 11, 211–232. doi: 10.1016/j.scitotenv.2011.03.015

Han, C., Cai, W.-J., Wang, Y., and Ye, Y. (2014). Calibration and evaluation of a carbonate microsensor for studies of the marine inorganic carbon system. *J. Oceanogr.* 70, 425–433. doi: 10.1007/s10872-014-0243-7

Hanelt, D., Tüg, H., Bischof, K., Groß, C., Lippert, H., Sawall, T., et al. (2001). Light regime in an Arctic fjord: a study related to stratospheric ozone depletion as a basis for determination of UV effects on algal growth. *Mar. Biol.* 138, 649–658. doi: 10.1007/s002270000481

Hofmann, L. C., and Bischof, K. (2014). Ocean acidification effects on calcifying macroalgae. *Aquat. Biol.* 22, 261–279. doi: 10.3354/ab00581

Hofmann, L. C., and Heesch, S. (2017). Latitudinal trends in stable isotope signatures and carbon concentrating mechanisms of northeast Atlantic rhodoliths. *Biogeosci. Discuss.* doi: 10.5194/bg-2017-399

Hofmann, L. C., Koch, M., and De Beer, D. (2016). Biotic control of surface pH and evidence of light-induced H^+pumping and Ca^{2+}-H^+exchange in a tropical crustose coralline alga. *PLoS One* 11:e0159057. doi: 10.1371/journal.pone.0159057

Hurd, C. L., Cornwall, C. E., Currie, K., Hepburn, C. D., McGraw, C. M., Hunter, K. A., et al. (2011). Metabolically induced pH fluctuations by some coastal calcifiers exceed projected 22nd century ocean acidification: a mechanism for differential susceptibility? *Glob. Chang. Biol.* 17, 3254–3262. doi: 10.1111/j.1365-2486.2011.02473.x

Jørgensbye, H. I. Ø, and Halfar, J. (2017). Overview of coralline red algal crusts and rhodolith beds (Corallinales, Rhodophyta) and their possible ecological

importance in Greenland. *Polar Biol* 40, 517–531. doi: 10.1007/s00300-016-1975-1

Kamenos, N. A., Burdett, H. L., Aloisio, E., Findlay, H. S., Martin, S., Longbone, C., et al. (2013). Coralline algal structure is more sensitive to rate, rather than the magnitude, of ocean acidification. *Glob. Chang. Biol.* 19, 3621–3628. doi: 10.1111/gcb.12351

Kamenos, N. A., Perna, G., Gambi, M. C., Micheli, F., and Kroeker, K. J. (2016). Coralline algae in a naturally acidified ecosystem persist by maintaining control of skeletal mineralogy and size. *Proc. R. Soc. London B Biol. Sci.* 283:20161159. doi: 10.1098/rspb.2016.1159

Laudien, J., Sahade, R. J., and Schwanitz, M. (2014). *Water Temperature at Time Series Station Kongsfjordneset-2, Spitsbergen, Kongsfjorden, Arctic in 2012/2013*. Bremerhaven: Alfred Wegener Institute, Helmholtz Center for Polar and Marine Research, doi: 10.1594/PANGAEA.830142

McConnaughey, T. (1991). Calcification in Chara corallina: CO 2 hydroxylation generates protons for bicarbonate assimilation. *Limnol. Oceanogr.* 36, 619–628. doi: 10.4319/lo.1991.36.4.0619

McConnaughey, T. A. (1989). "Biomineralization Mechanisms," in *Origin, Evolution, and Modern Aspects of Biomineralization in Plants and Animals*, ed. R. E. Crick (Boston, MA: Springer), 57–73. doi: 10.1007/978-1-4757-6114-6

McCoy, S. J., and Kamenos, N. A. (2015). Coralline algae (Rhodophyta) in a changing world: integrating ecological, physiological, and geochemical responses to global change. *J. Phycol.* 51, 6–24. doi: 10.1111/jpy.12262

McCoy, S. J., and Ragazzola, F. (2014). Skeletal trade-offs in coralline algae in response to ocean acidification. *Nat. Clim. Chang.* 4, 719–723. doi: 10.1038/nclimate2273

Moulin, P., Andría, J. R., Axelsson, L., and Mercado, J. M. (2011). Different mechanisms of inorganic carbon acquisition in red macroalgae (Rhodophyta) revealed by the use of TRIS buffer. *Aquat. Bot.* 95, 31–38. doi: 10.1016/j.aquabot.2011.03.007

Nash, M. C., Opdyke, B. N., Troitzsch, U., Russell, B. D., Adey, W. H., Kato, A., et al. (2013). Dolomite-rich coralline algae in reefs resist dissolution in acidified conditions. *Nat. Clim. Chang.* 3, 268–272. doi: 10.1038/nclimate1760

Nash, M. C., Uthicke, S., Negri, A. P., and Cantin, N. E. (2015). Ocean acidification does not affect magnesium composition or dolomite formation in living crustose coralline algae, *Porolithon onkodes* in an experimental system. *Biogeosci. Discuss* 12, 1373–1404. doi: 10.5194/bgd-12-1373-2015

Nelson, W. A. (2009). Calcified macroalgae critical to coastal ecosystems and vulnerable to change: a review. *Mar. Freshw. Res.* 60, 787–801. doi: 10.1071/MF08335

Noguchi, K., Gel, Y. R., Brunner, E., and Konietschke, F. (2012). nparLD: an R software package for the nonparametric analysis of longitudinal data in factorial experiments. *J. Stat. Softw* 50, 1–23. doi: 10.18637/jss.v050.i12

Ragazzola, F., Foster, L. C., Form, A. U., Büscher, J., Hansteen, T. H., and Fietzke, J. (2013). Phenotypic plasticity of coralline algae in a high CO world. *Ecol. Evol.* 3, 3436–3446. doi: 10.1002/ece3.723

Ragazzola, F., Foster, L. C., Jones, C. J., Scott, T. B., Fietzke, J., Kilburn, M. R., et al. (2016). Impact of high CO2 on the geochemistry of the coralline algae *Lithothamnion glaciale*. *Sci. Rep.* 6:20572. doi: 10.1038/srep20572

Raven, J. A., and Hurd, C. L. (2012). Ecophysiology of photosynthesis in macroalgae. *Photosynth. Res.* 113, 105–125. doi: 10.1007/s11120-012-9768-z

Raven, J. A., Johnston, A. M., and Macfarlane, J. J. (1990). "Carbon Metabolism," in *Biology of the Red Algae*, eds K. M. Cole and R. G. Sheath (Cambridge: Cambridge University Press), 171–202.

Revsbech, N. P. (1989). An oxygen microsensor with a guard cathode. *Limnol. Oceanogr.* 34, 474–478. doi: 10.4319/lo.1989.34.2.0474

Revsbech, N. P., and Jørgensen, B. B. (1983). Photosynthesis of benthic microflora measured with high spatial resolution by the oxygen microprofile method: Capabilities and limitations of the method. *Limnol. Oceanogr.* 28, 749–756. doi: 10.4319/lo.1983.28.4.0749

Revsbech, N. P., and Jørgensen, B. B. (1986). "Microelectrodes: their use in microbial ecology," in *Advances in Microbial Ecology*, ed. K. Marshall (New York, NY: Springer), 293–352.

Savidge, W. B., and Blair, N. E. (2004). Patterns of intramolecular carbon isotopic heterogeneity within amino acids of autotrophs and heterotrophs. *Oecologia* 139, 178–189. doi: 10.1007/s00442-004-1500-z

Shadwick, E. H., Trull, T. W., Thomas, H., Gibson, J. A. E., Stouffer, R. J., Manabe, S., et al. (2013). Vulnerability of polar oceans to anthropogenic acidification: comparison of arctic and antarctic seasonal cycles. *Sci. Rep.* 3, 660–662. doi: 10.1038/srep02339

Steinacher, M., Joos, F., Frölicher, T. L., Plattner, G.-K., and Doney, S. C. (2009). Imminent ocean acidification in the Arctic projected with the NCAR global coupled carbon cycle-climate model. *Biogeosciences* 6, 515–533. doi: 10.5194/bg-6-515-2009

Van Der Heijden, L., and Kamenos, N. A. (2015). Reviews and syntheses: calculating the global contribution of coralline algae to total carbon burial. *Biogeosciences* 12, 6429–6441. doi: 10.5194/bg-12-6429-2015

Wiencke, C., Gó Mez, I. N., and Dunton, K. (2009). Phenology and seasonal physiological performance of polar seaweeds. *Bot. Mar.* 52, 585–592. doi: 10.1515/BOT.2009.078

Wolf-Gladrow, D. A., Zeebe, R. E., Klaas, C., Körtzinger, A., and Dickson, A. G. (2007). Total alkalinity: the explicit conservative expression and its application to biogeochemical processes. *Mar. Chem.* 106, 287–300. doi: 10.1016/J.MARCHEM.2007.01.006

Conflict of Interest Statement: The authors declare that the research was conducted in the absence of any commercial or financial relationships that could be construed as a potential conflict of interest.

Copyright © 2018 Hofmann, Schoenrock and de Beer. This is an open-access article distributed under the terms of the Creative Commons Attribution License (CC BY). The use, distribution or reproduction in other forums is permitted, provided the original author(s) and the copyright owner(s) are credited and that the original publication in this journal is cited, in accordance with accepted academic practice. No use, distribution or reproduction is permitted which does not comply with these terms.

Advantages of publishing in Frontiers

OPEN ACCESS
Articles are free to read for greatest visibility and readership

FAST PUBLICATION
Around 90 days from submission to decision

HIGH QUALITY PEER-REVIEW
Rigorous, collaborative, and constructive peer-review

TRANSPARENT PEER-REVIEW
Editors and reviewers acknowledged by name on published articles

Frontiers
Avenue du Tribunal-Fédéral 34
1005 Lausanne | Switzerland

Visit us: www.frontiersin.org
Contact us: info@frontiersin.org | +41 21 510 17 00

REPRODUCIBILITY OF RESEARCH
Support open data and methods to enhance research reproducibility

DIGITAL PUBLISHING
Articles designed for optimal readership across devices

FOLLOW US
@frontiersin

IMPACT METRICS
Advanced article metrics track visibility across digital media

EXTENSIVE PROMOTION
Marketing and promotion of impactful research

LOOP RESEARCH NETWORK
Our network increases your article's readership